About Gandhinagar Institute of Technology

Gandhinagar Institute of Technology is established by Platinum Foundation in 2006. It offers under graduate programs in Mechanical Engineering, Information Technology, Computer Engineering, Electronics and Communication Engineering, Electrical Engineering and Civil Engineering and Post graduate program in MBA (Finance, Human Resource Development, and Marketing) and M.E. in Mechanical Engineering with specialization in Thermal Engineering and Computer Aided Design & Computer Aided Manufacturing.

All these programs are approved by AICTE, New Delhi and affiliated to Gujarat Technological University. We have elaborate laboratory facilities and highly motivated and qualified faculty members. We are also arranging technical seminars, conferences, industry-institute interaction programs, workshops and expert lectures of eminent dignitaries from different industries and various reputed educational institutes.

Our students are innovative and have excellent acceptability to latest trends and technologies of present time. Our students have also participated in various technical activities as well as sports activities and have achieved various prices at state level. We have two annual publications, a National level research journal 'GIT-Journal of Engineering and Technology (ISSN 2249–6157)' and 'GIT-a Song of Technocrat' (college magazine).

Editorial Board

Editorial Chief	**Gandhinagar Institute of Technology** **Moti Bhoyan, Ta. Kalol Gandhinagar - 382721.**

Disclaimer

Views expressed in the papers are solely from respective authors. Editorial board has no responsibility of their authentication.

Message from Director

It is indeed a matter of great pleasure that the sixth issue of our National journal 'GIT-Journal of Engineering and Technology' is being published with ISSN 2249 – 6157 for sixth successive year. The aim of the journal is to publish peer reviewed research articles in rapidly developing field of engineering and technology. The issue is a result of imaginative and expressive skill and talent of GIT family. Research papers were invited from the researcher of all domains of engineering and technology. More than 120 research papers were received. After peer review, about 50 papers have been selected and published in this issue of the journal. The objectives of imparting added education, combined with creation, dissemination and application of knowledge, are being met in an integrated form, to create a synergetic impact. To fulfill its mission in new and powerful ways, each member of GIT community strives to achieve excellence in every endeavour – be it education, research, consulting or training – by making continuous improvements in curricula and pedagogical tools.

Being a part of GIT, it fills my heart with immense pride and sense of gratitude to state that GIT is whole-heartedly carrying out the chief objective of Educational Process- to equip the students as the best professionals. I'm extremely delighted to witness that GIT is working admirably well to prepare the students for their successful career so that they bring crowning glory to themselves and to the institute. Keeping in mind the inevitable need of providing educational atmosphere to the students, our institute tries its best to develop their skill and impart knowledge of all domains to enhance their horizons and create more and more opportunities in the field of Technology and Research. In the world where change is a buzzword and innovation is the basic necessity, GIT teaches its students to ingrain innovativeness as a way of thinking that governs every aspects of life thereby to foster growth of technology.

During a short span of six years; GIT has accomplished the mission effectively and remarkably well for which it was established. Institute has been constantly achieving the glory of excellence in the field of curricular, co-curricular and extra-curricular activities. Through dedicated efforts of our faculty members and students, it is attempted to translate the vision into action to achieve our mission. "Success is empty if it arrives at the finish line alone. The best reward is to get there surrounded by winners. The more winners you can bring with you the more gratifying the victory you have." For the fourth consecutive year, an annual technical symposium TechXtreme-2013 was successfully organized by the institute. More than 1400 students of various technical institutions across the Gujarat participated in the TechFest. Prizes worth Rs 2 lacs and trophies were given to the winners of total 36 events. During the year institute has organized Spoken tutorial on Linux, Latex, Scilab, and Python in association with IIT Bombay, seminar on Cisco Networking, Robotics and CAD/CAM workshops for students. The institute has been successfully organized Debate Competition, Rangoli Competition, Kite Flying competition, Ratri B4 Navaratri, and Sports activities. Institute has also arranged two blood donation drives and more than 400 units were collected from the students and staff members. Students have also participated and won prizes in various sports events organized by other Institutions including that of GTU. Students of the institutes won prizes in many technical symposiums organized at various engineering colleges of Gujarat. Institute has organized many

industrial visits and expert lectures for the students for supplementing the class room teaching. I am extremely happy to mention that throughout the year the faculty members have worked very hard to achieve all kinds of curricular, co-curricular and extra-curricular activities.

The Institute also puts emphasis on academic development of its faculty members. During the year, 20 International and 24 National papers were presented by the faculty members at various conferences organized across India. The faculty members were also deputed to attend total 154 seminars/workshops/training programs/symposiums. The institute has organized many state level seminars and workshops on current trends of Engineering and Management. Spoken tutorial on Linux, Latex, Scilab, and Python in association with IIT Bombay, CAD/CAM/CAE workshop and AutoCAD 2011 Professional Certificate examination by Auto Desk are a few of them.

Publication of the journal of national level is not possible without whole-hearted support of committed and experienced Trustees of Platinum Foundation Mr. Hareshbhai Rohera, Mr. Ghanshyambhai Thakkar, Mr. Deepakbhai Ravani, Mr. Pravinbhai Shah and Smt. Varshaben M. Pandhi. I take an opportunity to express my deep feelings of gratitude to all the trustees of Platinum Foundation and Mr. Mahendrabhai Pandhi, member of Governing body of the trust for their constant motivational support.

It's my privilege to compliment the staff members and the students for showing high level of liveliness throughout the year. Mere thanks in a few words are not enough to offer my sincere appreciation and congratulate the team of the 'GIT-Journal of Engineering and Technology' for their untiring effort to give final shape to the sixth issue of the journal. I am heartily thankful to each and every member of the institute for providing active participation and best motivational support in the thorough development of the institute.

Dr N M Bhatt
Director

MECHANICAL ENGINEERING

Sr. No.	Paper Title	Author Name	Institute Detail	Author E_Mail Id	Co-Authors Name
1	Heat Transfer Coefficient and Pressure Drop over Inline Pitch Variation using CFD	Prof.Nirav R. Bhavsar	Parul Institute of Engineering & Technology	er_niravbhavsar@yahoo.co.in	Mr.Rupen R. Bhavsar
2	Thermal Analysis of Liquid Nitrogen Storage Vessel	Prof. Vimalkumar P Salot	L.J.Institute of Engineering & Technology, Ahmedabad	salot.vimal@gmail.com	
3	Employment of Advanced Materials for Boilers and Steam Turbines	Prof.Chintan T. Barelwala	Gandhinagar Institute of Technology	barelwala_chintan2004@yahoo.co.in	
4	Effect of target frequency, bias voltage, bias frequency and deposition temperature on tribological properties of pulsed DC CFUBM sputtered TiN coating	Prof. Arpan P.Shah	BITS Education Campus, Varnama	apskarjan@gmail.com	Dr. Soumitra Paul
5	Prevention Methods for reduce welding leakages in Aluminium using TIG and MIG welding	Prof.Vyomesh R Buch	BITS Education Campus, Varnama	vyomdhar_19@yahoo.co.in	Prof.K. Baba.Pai
6	Parametric Study of Tube Hydroforming Process	Prof.Vijaykumar R Parekh	Shri S'ad Vidya Mandal Institute Of Technology	parekh_saiaerovij@yahoo.co.in	Prof.B. C. Patel Prof. J. R. Shah
7	Effect of Applying HPC JET in Machining of 42CrMo4 Steel Using Uncoated Carbide Inserts	Prof.Mayur S Modi	Shree Swami Atmanand Saraswati Institute of Technology, SURAT	maymodi@gmail.com	Mr.Sandip G. Patel
8	Experimental analysis of heat pump used for simultaneous heating and cooling utilities	Mr. Rahulbhai P Patel	Shri S'ad Vidya Mandal Institute Of Technology	rahulpatel2985@gmail.com	Dr. Ragesh G Kapadia
9	Design and Analysis of a High Pressure vessel using ASME code	Prof. Mitesh Mungla	Gandhinagar Institute of Technology	mitesh.mungla@git.org.in	Mr.K N Srinivasan Prof. V R Iyer
10	Studies on effect of process parameters on tensile properties and failure behavior of friction stir welding of Al alloy	Prof. Bhavesh R.Rana	Indus University, Rancharda Via Thaltej Ahemedabad	bhavesh.ind.met@gmail.com	Prof. L.V.Kasmble Dr.S.N.Soman
11	Review on The Energy Savings And Economic Viability Of Heat Pump Water Heaters In The Residential Sectors – A Comparison With Solar Water Heating System	Mr.Vinod P Rajput	Gandhinagar Institute of Technology	rajputvinodp@gmail.com	Mr.Ankit K. Patel Prof.Nimesh Gajjar
12	Effect of PWHT soaking time on Mechanical & metallurgical properties of 9Cr-1Mo-V steel	Mr. Naishadh Patel	Indus University, Rancharda Via Thaltej Ahemedabad	naishadh.patel27@gmail.com	Mr. Pavan Maniar Prof. M.N. Patel
13	Heat Transfer Coefficient and Pressure Drop over Staggered Pitch Variation using CFD	Prof.Nirav R. Bhavsar	Parul Institute of Engineering & Technology	er_niravbhavsar@yahoo.co.in	Mr. Rupen R. Bhavsar
14	Application of Porous Medium Technology to Internal Combustion Engine for Homogeneous Combustion- A Review	Prof.Ratnesh T Parmar	L D College of Engineering	parmar.ratnesh93@gmail.com	Prof.Vimal Patel
15	Fabrication and Characterization of Cast Aluminium Fly Ash Composite	Dr. Vandana J Rao	The Maharaja Sayajirao University of Baroda	vandana11866@yahoo.co.in	Prof.Hemant N. Panchal Ms.Sonam M. Patel

16	Review on CO2 Laser Cutting Process Parameter	Prof. Dhaval P Patel	Gandhinagar Institute of Technology	dhaval.patel@git.org.in	
17	Effect of Silicon addition in LM25 Aluminium Alloy	Prof. Hitesh H. Patel	Gandhinagar Institute of Technology	hitesh.patel1@git.org.in	
18	Numerical Investigation of Flow over cylinder for the study of different flow pattern	Prof. Hardik R Gohel	Gandhinagar Institute of Technology	hardik.gohel@git.org.in	Prof. Absar M Lakdawala
19	Development of Test Rig for Vibration Monitoring of Bearing	Prof. Amit R Patel	Gandhinagar Institute of Technology	amit.er1984@gmail.com	
20	Secondary Refrigerant System for Water Ice Candy Manufacturing Process with Calcium Chloride Brine	Prof. Keyur C Patel	Gandhinagar Institute of Technology	keyur.patel6786@gmail.com	Dr. Vikas J. Lakhera
21	Development of Typical sample holder with Cryostat for the Measurement of Hall Effect and Magnetic Susceptibility at LN2 Temperature.	Mr. Shaival R Parikh	L D College of Engineering	shaival01@gmail.com	Prof. Hardik Shukla
22	A Review on Heat-pipe Oven for Plasma Wakefield Accelerator (PWFA) Experiment	Mr. Milind A. Patel	Gandhinagar Institute of Technology	milindpatel@rocketmail.com	Prof. Krunal Patel
23	Cryostat for Measurement of Thermal Conductivity, Electrical Resistivity and Thermoelectric Power of LaBa2Cu3O7-δ	Mr. Ruchir Parikh	L D College of Engineering	ruchir.parikh@git.org.in	Dr. J M Patel
24	Enhancement in mapping capability of Feature Replace command in NX CAD software	Mr.Pankaj Sharma	Nirma University	11mmcc14@nirmauni.ac.in	Prof.Girish Deshmukh Prof.Reena trivedi
25	Waste Heat Recovery from VCR Systems – A Review	Mr. Ankit Patel	Gandhinagar Inst. of Technology	patelankit27789@gmail.com	Dr N M Bhatt Prof. Nimesh Gajjar

COMPUTER SCIENCE

Sr. No.	Paper Title	Author Name	Institute Detail	Author E_Mail Id	Co-Authors Name
1	**Skinput Technology**	Mr. Nirav K. Shah	Shree swaminarayan college of computer science, Bhavnagar (Affiliated to M.K. Bhavnagar University, Bhavnagar)	nkshah.mca@gmail.com	Mr. Madhav K. Dave Mr. Parag B. Makwana
2	**Privacy - Preserving Data Stream Classfication: An approach Using MOA Framework**	Prof. Kirankumar S Patel	Gandhinagar Institute of Technology	kiran.patel@git.org.in	
3	**Comparative Study of Web Page Classification Techniques**	Prof. Anirudhdha M Nayak	Gandhinagar Institute of Technology	anirudhdha.nayak@git.org.in	
4	**Explain Use Case Point Effort Estimation Method Taking the Case of University Registration System Use Case Diagram**	Prof. Svapnil Vakharia	Gandhinagar Institute of Technology	svapnil.vakharia@git.org.in	
5	**Essential Aspects of Security, Privacy and Challenges in Cloud**	Ms. Leena B.Patel	Gandhinagar Institute of Technology	leena.patel@git.org.in	
6	**System Description Formation for University Blackboard Tool**	Prof. Birendrasinh K Zala	Gandhinagar Institute of Technology	birendra.zala@git.org.in	
7	**A Survey On Recommending Tags Methodologies**	Prof. Brinda R. Parekh	Gandhinagar Institute of Technology	brinda.parekh@git.org.in	
8	**Study and Review of Various Identity and Privacy Management Techniques in Consumer Cloud Computing**	Ms. Archana N Mahajan	SSBT'S College Of Engg and Technology	archanamagare@gmail.com	Mr. Sandip S. Patil

ELECTRONICS & COMMUNICATION

Sr. No.	Paper Title	Author Name	Institute Detail	Author E_Mail Id	Co-Authors Name
1	Performance Analysis of a Sub-Optimum Transmit Antenna Selection Scheme with M-PSK and M-QAM Constellations.	Prof. Jatin M. Chakravarti	Gandhinagar Institute Of Technology	jatin.chakravarti@git.org.in	Prof. Mitul P. Maniar
2	Comparision of Different Edge Based Active Contour Models and Their Solution for Image Segmentation	Prof. Dhaval Rajeshbhai Sathawara	U.V. Patel College of Engineering, Ganpat University, Kherva	dhaval_sathawara@yahoo.co.in	Prof. Margam K. Suthar Mr.Bharat P. Solanki
3	BER Performance of Equalized Signal in Wireless Communication Architecture of Smart Grid	Prof. Vineeta Nishad	Gandhinagar Institute of Technology	vineeta.nishad@gmail.com	Prof. Jitendra Thathagar
4	High Speed CMOS Comparator Design	Prof. Megha Maulesh Desai	Gandhinagar Institute of Technology	meghnow@yahoo.co.in	
5	Simulation & Performance Analysis of DVB-T System Using Efficient Wireless Channels	Prof. Nirali Kotak	Gandhinagar Institute of Technology	nirali.kotak@git.org.in	
6	Technique for Non Distractive Quality Evaluation of Cuminum Cyminum L(Cumin) Seeds Using Colorization	Prof. Jalpa Patel	Gandhinagar Institute of Technology	jalpa.patel@git.org.in	
7	Portable WirelessVibrationMonitoringSystem for Measurement	Prof. Pratik Gohel	Gandhinagar Institute of Technology	pratik.gohel@git.org.in	Prof. Gunjan Jani Prof. Dhiren Vaghela

Skinput Technology

Mr. Nirav K. Shah, Mr. Madhav K. Dave, Mr. Parag B. Makwana

(nkshah.mca@gmail.com, dave.madhav@gmail.com, paragmakwana@ymail.com)

Abstract—**This is a technology that appropriates the human body for acoustic transmission, allowing the skin to be used as an input surface. In particular, resolves the location of finger tips on the arm and hand by analyzing mechanical vibrations that propagate through the body. We collect these signals using a novel array of sensors worn as an armband. This approach provides an always available, naturally portable, and on-body finger input system. We assess the capabilities, accuracy and limitations of our technique through a two-part, twenty-participant user study. So in a few years time, with Skinput, computing is always available: A person might walk toward their home, tap their palm to unlock the door and then tap some virtual buttons on their arms to turn on the TV and start flipping through channels.**

Index Terms—Microsoft Technology, Skinput, Acoustic Handson

I. INTRODUCTION

The primary goal of *Skinput* is to provide an always available mobile input system - that is, an input system that does not require a user to carry or pick up a device. A number of alternative approaches have been proposed that operate in this space. Techniques based on computer vision are popular these, however, are computationally expensive and error prone in mobile scenarios (where, e.g., non-input optical flow is prevalent). Speech input is a logical choice for always-available input, but is limited in its precision in unpredictable acoustic environments, and suffers from privacy and scalability issues in shared environments. Other approaches have taken the form of wearable computing.

This typically involves a physical input device built in a form considered to be part of one's clothing. For example, glove-based input systems allow users to retain most of their natural hand movements, but are cumbersome, uncomfortable, and disruptive to tactile sensation. Post and Orth present a "smart fabric" system that embeds sensors and conductors into abric, but taking this approach to always-available input necessitates embedding technology in all clothing, which would be prohibitively complex and expensive. The Sixth Sense project proposes a mobile, always available input/output capability by combining projected information with a color-marker-based vision tracking system. This approach is feasible, but suffers from serious conclusion and accuracy

limitations. For example, determining whether, a finger has tapped a button, or is merely hovering above it, is extraordinarily difficult.

II. BIO-SENSING

Skinput leverages the natural acoustic conduction properties of the human body to provide an input system, and is thus related to previous work in the use of biological signals for computer input. Signals traditionally used for diagnostic medicine, such as heart rate and skin resistance, have been appropriated for assessing a user's emotional state. These features are generally subconsciously driven and cannot be controlled with sufficient precision for direct input. Similarly, brain sensing technologies such as electroencephalography (EEG) & functional near-infrared spectroscopy (fNIR) have been used by HCI researchers to assess cognitive and emotional state; this work also primarily looked at involuntary signals. In contrast, brain signals have been harnessed as a direct input for use by paralyzed patients, but direct brain computer interfaces (BCIs) still lack the bandwidth required for everyday computing tasks, and require levels of focus, training, and concentration that are incompatible with typical computer interaction.
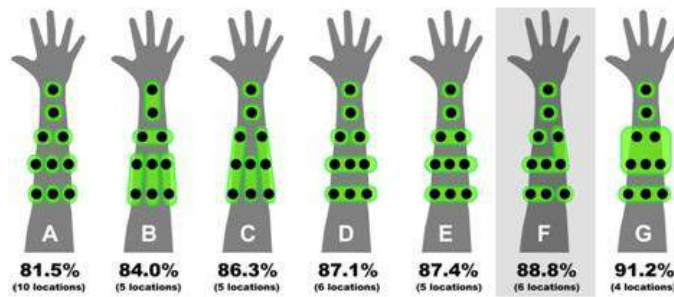
Fig 1.0 Hand sensing

There has been less work relating to the intersection of finger input and biological signals. Researchers have harnessed the electrical signals generated by muscle activation during normal hand movement through electromyography (EMG). At present, however, this approach typically requires expensive amplification systems and the application of conductive gel for effective signal acquisition, which would limit the acceptability of this approach for most users. The input technology most related to our own is that of Amen to et al who placed contact microphones on a user's wrist to assess finger movement. However, this work was never formally evaluated, as is constrained to finger motions in one hand.

The Hambone system employs a similar setup, and through an HMM, yields classification accuracies around 90% for four gestures (e.g., raise heels, snap fingers). Performance of false positive rejection remains untested in both systems at present. Moreover, both techniques required the placement of sensors near the area of interaction (e.g., the wrist), increasing the degree of invasiveness and visibility. Finally, bone conduction microphones and headphones - now common consumer technologies - represent an additional bio-sensing technology that is relevant to the present work. These leverage the fact that sound frequencies relevant to human speech propagate well through bone.

Bone conduction microphones are typically worn near the ear, where they can sense vibrations propagating from the mouth and larynx during speech. Bone conduction headphones send sound through the bones of the skull and jaw directly to the inner ear, bypassing transmission of sound through the air and outer ear, leaving an unobstructed path for environmental sounds.

III ACOUSTIC INPUT

Our approach is also inspired by systems that leverage acoustic transmission through(non-body) input surfaces. Paradise et al. measured the arrival time of a sound at multiple sensors to locate hand taps on a glass window. Ishii et al. use a similar approach to localize ball hitting a table, for computer augmentation of a real-world game. Both of these systems use acoustic time-of-flight for localization, which we explored, but

found to be insufficiently robust on the human body, leading to the fingerprinting approach described in this paper frequencies propagate more readily through bone than through soft tissue, and bone conduction carries energy over larger distances than soft tissue conduction. While we do not explicitly model the specific mechanisms of conduction, or depend on these mechanisms for our analysis, we do believe the success of our technique depends on the complex acoustic patterns that result from mixtures of these modalities. Similarly, we also believe that joints play an important role in making tapped locations acoustically distinct. Bones are held together by ligaments, and joints often include additional biological structures such as fluid cavities. This makes joints behave as acoustic filters. In some cases, these may simply dampen acoustics; in other cases, these will selectively attenuate specific frequencies, creating location specific acoustic signatures.

IV. SENSING

To capture the rich variety of acoustic information described in the previous section, we evaluated many sensing technologies, including bone conduction microphones, conventional microphones coupled with stethoscopes and accelerometers. However, these transducers were engineered for very different applications than measuring acoustics transmitted through the human body. As such, we found them to blacking in several significant ways. Foremost, most mechanical sensors are engineered to provide relatively flat response curves over the range of frequencies that is relevant to our signal. This is a desirable property for most applications where a faithful representation of an input signal uncolored by the properties of the transducer is desired. However, because only a specific set of frequencies is conducted through the arm in response to tap input, a flat response curve leads to the capture of irrelevant frequencies and thus to a high signal-to-noise ratio. While bone conduction microphones might seem a suitable choice for Skinput. These devices are typically engineered for capturing human voice, and filter out energy below the range of human speech(whose lowest frequency is around 85Hz). Thus most sensors in this category were not especially sensitive to lower-frequency signals (e.g., 25Hz), which we found in our empirical pilot studies to be vital in characterizing finger taps. To overcome these challenges, the idea of a single sensing element with a flat response curve, to an array of highly tuned vibration sensors was dropped. Specifically, employed a small, cantilevered piezo films MiniSense100, Measurement Specialties, Inc.).By adding small weights to the end of the cantilever, we are able to alter the resonant frequency, allowing the sensing element to be responsive to a unique, narrow, low-frequency band of the acoustic spectrum. Adding more mass lowers the range of excitation to which sensor responds; we weighted each element such that it aligned with particular frequencies that pilot studies showed to be useful in characterizing bio-acoustic input. Figure shows the response curve for one of our sensors,

tuned to a resonant frequency of 78Hz. The curve shows a ~14dB drop-off ±20Hz away from the resonant frequency. Additionally, the cantilevered sensors were naturally insensitive to forces parallel to the skin (e.g., shearing motions caused by stretching). Thus, the skin stretch induced by many routine movements (e.g., reaching for a doorknob) tends to be attenuated. However, the sensors are highly responsive to motion perpendicular to the skin plane perfect for capturing transverse surface waves and longitudinal waves emanating from interior structures Finally, our sensor design is relatively inexpensive and can be manufactured in a very small form factor (e.g., MEMS), rendering it suitable for inclusion in future mobile devices (e.g., an arm-mounted audio player).

ARMBAND PROTOTYPE

In five sensing elements, incorporated into an armband form factor. The decision to have two sensor packages was motivated by our focus on the arm for input. In particular, when placed on the upper arm (above the elbow), we hoped to collect acoustic information from the fleshy bicep area in addition to the firmer area on the underside of the arm, with better acoustic coupling to the Hummers the main bone that runs from shoulder to elbow. When the sensor was placed below the elbow, on the forearm, one package was located near the Radius , the bone that runs from the lateral side of the elbows the thumb side of the wrist, and the other near the Ulna , which runs parallel to this on the medial side of the arm closest to the body. Each location thus provided slightly different acoustic coverage and information, helpful in disambiguating input location. Based on pilot data collection, we selected a different set of resonant frequencies for each sensor package. We tuned the upper sensor package to be more sensitive to lower frequency signals, as these were more prevalent in fleshier areas. Conversely, we tuned the lower sensor array to be sensitive to higher frequencies, in order to better capture signals transmitted though (denser)bones.

PROCESSING

In this prototype system, each channel was sampled at 5.5kHz, a sampling rate that would be considered too low for speech or environmental audio, but was able to represent the relevant spectrum of frequencies transmitted through the arm. This reduced sample rate (and consequently low processing bandwidth) makes our technique readily portable to embedded processors. For example, the ATmega168 processor employed by the Adriano platform can sample analog readings at 77 kHz with no loss of precision, and could therefore provide the full sampling power required for Skinput (55 kHz total).Data was then sent from our thin client over a local socket to our primary application, written in Java. This program performed three key functions. First, it provided a live visualization of the data from our ten sensors, which was useful in identifying acoustic features. Second, it segmented inputs from the DataStream into independent instances (taps). Third, it classified these input instances. The audio stream was segmented into individual taps using an absolute exponential average of all ten channels. When an intensity threshold was exceeded, the program recorded the timestamp as a potential start of a tap. If the intensity did not fall below a second, independent closing" threshold between 100ms and 700ms after the onset crossing (a duration we found to be the common for finger impacts), the event was discarded. If start and end crossings were detected that satisfied these criteria, the acoustic data in that period (plus a 60ms buffer on either end)was considered an input event .Although simple, this heuristic proved to be highly robust, mainly due to the extreme noise suppression provided by sensing approach. After an input has been segmented, the waveforms are analyzed. The highly discrete nature of taps (i.e. point impacts) meant acoustic signals were not particularly expressive over time (unlike gestures, e.g., clenching of the hand). Signals simply diminished in intensity overtime. Thus, features are computed over the entire input window and do not capture any temporal dynamics. Brute force machine learning approach is employed, computing 186 features in total, many of which are derived combinatorial. For gross information, the average amplitude, standard deviation and total(absolute) energy of the waveforms in each channel (30 features) is included. From these, average amplitude ratios between channel pairs (45 features) are calculated. An average of these ratios (1 feature) is also included. A 256-point FFT for all ten channels, although only the lower ten values are used (representing the acoustic power from 0Hz to 193Hz), yields100 features. These are normalized by the highest-amplitude FFT value found on any channel. Also the center of mass of the power spectrum within the same 0Hz to 193Hz range for each channel, a rough estimation of the fundamental frequency of the signal displacing each sensor(10 features) are included. Subsequent feature selection established the all-pairs amplitude ratios and certain bands of the FFT to be the most predictive features. These 186 features are passed to a Support Vector Machine (SVM) classifier. A

full description of SVMs is beyond the scope of this paper. Our software uses the implementation provided in the Weka machine learning toolkit. It should be noted, however, that other, more sophisticated classification techniques and features could be employed. Thus, the results presented are to be considered a baseline. Before the SVM can classify input instances, it must first be trained to the user and the sensor position. This stage requires the collection of several examples for each input location of interest. When using Skinput to recognize live input, the same 186 acoustic features are computed on-the fly for each segmented input. These are fed into the trained SVM for classification. Once an input is classified, an event associated with that location is instantiated. Any interactive features bound to that event are fired.

CONCLUSION

We conclude approach to appropriating the human body as an input surface. It describes a novel, wearable bio-acoustic sensing array that we built into an armband in order to detect and localize finger taps on the forearm and hand. These include single-handed gestures, taps with different parts of the finger, and differentiating between materials and objects. We conclude with descriptions of several prototype applications that demonstrate the rich design space we believe Skinput enables.

References

[1] Harrison Chris, " Skinput:Appropriating the body as an input surface"
     ACM conference 2010.

[2] Hope, Dan "Skinput turns body into touch screen interface"

[3] W. D. Doyle, "Magnetization reversal in films with biaxial anisotropy,"
     in *1987 Proc. INTERMAG Conf.*, pp. 2.2-1–2.2-6.

[4] Hornyak Tom, "Turn your arm into a phone with Skinput"

Privacy-Preserving Data Stream Classification: An approach using MOA framework

Mr.Kirankumar Patel

(kiran.patel@git.org.in)

Abstract— **Data stream can be conceived as a continuous and changing sequence of data that continuously arrive at a system to store or process. Examples of data streams include computer network traffic, phone conversations, web searches and sensor data. These data sets need to be analyzed for identifying trends and patterns which help us in isolating anomalies and predicting future behavior. However, data owners or publishers may not be willing to exactly reveal the true values of their data due to various reasons, most notably privacy considerations. Hence, some amount of privacy preservation needs to be done on the data before it can be made publicly available. To preserve data privacy during data mining, the issue of privacy- preserving data mining has been widely studied and many techniques have been proposed. However, existing techniques for privacy-preserving data mining are designed for traditional static databases and are not suitable for data streams. So the privacy preservation issue of data streams mining is a very important issue. This paper is about describing a Method which extends the process of data perturbation on dataset to achieve privacy preservation. We can compare the classification characteristics in terms of less information loss, response time, and more privacy gain so get better accuracy of data stream algorithms**

Index Terms— **Decision trees, Hoeffding Tree**

I. INTRODUCTION

In the field of information processing, data mining refers to the process of extracting the useful knowledge from the large volume of data. There is plenty of area where the data mining is widely applied such as Healthcare which includes Medical diagnostics, insurance claims analysis, drug development, Business, finance, education, sports and gambling, insurance, stock market, retail, telecommunication, transportation etc. Widely used data mining techniques in such area of application includes Clustering of data, Classification, Regression Analysis, Association rule / pattern mining.

The data stream paradigm has recently emerged in response to the continuous data problem [2]. Mining data streams is concerned with extracting knowledge structures represented in models and patterns in non-stopping, continuous streams (flow) of information. Algorithms written for data streams can naturally cope with data sizes many times

greater than memory, and can extend to challenging real-time applications not previously tackled by machine learning or data mining. The assumption of data stream processing is that training examples can be briefly inspected a single time only, that is, they arrive in a high speed stream, and then must be discarded to make room for subsequent examples. The algorithm processing the stream has no control over the order of the examples seen, and must update its model incrementally as each example is inspected. An additional desirable property, the so-called anytime property, requires that the model is ready to be applied at any point between training examples.

Traditional data mining approaches have been used in applications that have persistent data available and generated learning models are static in nature. Since whole data available before we make it available to our machine learning algorithm, statistical information of the data distribution can be known in advance. The task performed by the mining process are centralized, produce the static learning model. There is no way of incremental processing of data if the available larger dataset are sampled in order to accommodate with the memory which smaller in size with respect to larger size of data. For each sample the learning model start processing from the scratch. There is no way of intermediately analysis of the result.

But nowadays, in the field of information processing, an emergence of applications that do not fit this data model [3] Instead, information naturally occurs in the form of a sequence (stream) of data values. A data stream is a real-time, continuous, and ordered sequence of items. It is not possible to control the order in which items arrive, nor feasible to locally store a stream in its entirety. Likewise, queries over streams run continuously over a period of time and incrementally return new results as new data arrive.

II. PRIVACY CONSERN

Examples of data streams include computer network traffic, phone conversations, web searches and sensor data. These data sets need to be analyzed for identifying trends and patterns which help us in isolating anomalies and predicting future behavior. However, data owners or publishers may not be willing to exactly reveal the true values of their data due to various reasons, most notably privacy considerations. Hence, some amount of privacy preservation needs to be done on the data before it can be made publicly available. The interpretation of data is important and it is conjoined with the

need to maintain privacy using suitable algorithms. Various methods have been proposed for this purpose like data perturbation and encryption and masking, k-anonymity, association rule mining etc. However these methods cannot be applied on data streams directly. Moreover, in data streams applications, there is a need to offer strong guarantees on maximum allowed delay between incoming data and its anonymous output. Also less data losses and more privacy gain.

Verykios et al. [4] classified privacy- preserving data mining techniques based on five dimensions, which are data distribution, data modification, data mining algorithms, data or rule hiding, and privacy preservation, respectively.

In the dimension of data distribution, some approaches have been proposed for centralized data and some for distributed data. Du and Zhan [5] utilized the secure union, secure sum and secure scalar product to prevent the original data of each site from revealing during the mining process. At the end of the mining process, every site will obtain the final result of mining the whole data. The disadvantage is that the approach requires multiple scans of the database and hence is not suitable for data streams, which flows in fast and requires immediate response.

In the dimension of data modification, the confidential values of a database to be released to the public are modified to preserve data privacy. Adopted approaches include perturbation, blocking, aggregation or merging, swapping, and sampling. Agrawal and Srikant [6] used the random data perturbation technique to protect customer data and then constructed the decision tree. For data streams, because data are produced at different time, not only data distribution will change with time, but also the mining accuracy will decrease for modified data.

Privacy preservation techniques can be classified into three categories, which are heuristic-based techniques, cryptography-based techniques, and reconstruction-based techniques. From the review of previous research, we can see that existing techniques for privacy-preserving data mining are designed for static databases with an emphasis on data security. These existing techniques are not suitable for data streams.

In [7], considered the classification problem where the training data are several private data streams. Joining all streams violates the privacy constraint of such applications and suffers from the blow- up of join. In that presented a solution based on Naive Bayesian Classifiers. The main idea is rapidly obtaining the essential join statistics without actually computing the join. With this technique, they can build exactly the same Naive Bayesian Classifier as using the join stream without exchanging private information. The processing cost is linear in the size of input streams and independent of the join size. But there are some drawback related time and data arrival rate that is Having a much lower processing time per input tuple, the proposed method is able to handle much higher data arrival rate and deal with the general many-to-many join relationships of data streams.

In [8], proposed the method for privacy-preserving classification of data streams, which consists of two stages: date streams pre-processing and data streams mining. In the stage of data streams pre-processing, proposed the data streams pre-processing (DSP) algorithm to perturb data streams. Experimental results of security measurement showed that the DSP algorithm has higher .security. Experimental results of data error measurement showed that DSP algorithm has less data error. In the stage of data streams mining, proposed the WASW algorithm to mine perturbed data streams. Experiment results of accuracy measurement showed that the error rate of the VFDT algorithm increases constantly along with continuous arrival of the data stream but the error rate of the WASW algorithm is kept under the predetermined threshold value. Therefore, the WASW algorithm has higher accuracy. In conclusion, the PCDS method not only can preserve data privacy but also can mine data streams accurately.

III. RELATED WORK

Motivated by the privacy concerns on data mining tools, a research area called privacy-preserving data mining. The initial idea of it was to extend traditional data mining techniques to work with the stream data modified to mask sensitive information. The key issues were how to modify the data and how to recover the data stream mining result from the modified data. The solutions were often tightly coupled with the data stream mining algorithms under consideration.

In this paper introduce a new data perturbation algorithm for perturb the dataset. And then apply the Hoeffding tree algorithm on perturbed dataset. Two step process: in the first step applying the perturbation algorithm on dataset. In the second step applying the Hoeffding tree algorithm on that perturbed dataset.

The goal is to transform a given data set D into modified version D' that satisfies a given privacy requirement and preserves as much information as possible for the intended data analysis task.

We can compare the classification characteristics in terms of less information loss, response time, and more privacy gain so get better accuracy of different data stream algorithms against each other and with respect to the following benchmarks:

- Original, the result of inducing the classifier on unperturbed training data without randomization.
- Randomized, the result of inducing the classier on perturbed data (Perturbation based methods for privacy preserving perturb individual data values or the results of queries by swapping, condensation, or adding noise.) but without making any corrections for randomization.

IV. DATA PURTURBATION ALGORITHM

The stage of data streams pre-processing uses perturbation algorithm to perturb confidential data. Users can flexibly

adjust the data attributes to be perturbed according to the security need. Therefore, threats and risks from releasing data can be effectively reduced.

Algorithm: Data Perturbation (perturbation algorithm use for perturb confidential data and provide Data Privacy)
Input: An Original Dataset S (.ARFF or .CSV file)
Output: A perturbed Dataset S' (perturb dataset .ARFF or .CSV file)
Algorithm Step:
1. Read Original Dataset S file.(fie extension must be .ARFF or .CSV file)
2. Display set of attribute name and total number of attribute that are in the dataset S (.ARFF or .CSV file). Also With data types of that attribute
3. Display total number of tuples in dataset S.
4. Select sensitive attribute from step 3.
5. If suppose selected attribute is F* then
   a) Assign window to F* attribute (window store received dataset according to order of arrival)
   b) Suppose size of window is W(selection of size at run time) than it contain only W tuples of selected attribute F* values
   c) Then find mean of that W tuples that are in the window.
   d) Replace first tuple of window by mean that we find in above step 5c.
   e) Remaining tuples are as it is.
   f) Apply Sliding window means remove first tuple of window and insert next tuple from original dataset to end of window.so sliding window size remain same.
6. Again find mean of modified window so go to step 5(a) to 5(f) until all the values of attribute F* is changed.
7. Then modified dataset save in .CSV or .ARFF file. Also called perturbed dataset S'.

Fig.1 Data Perturbation Algorithm

See following sample table I sample dataset, in this table selected attribute F* is Salary, and table contain before and after perturbation values.so compare both salary attribute those contain salary attribute original data and perturbed data.

TABLE I
SAMPLE DATASET

Record No.	Age	Education level	Salary (Before perturbation)	Salary (After perturbation)
1	23	15	**53**	**57.5**
2	31	14	**55**	**52.0**
3	33	18	**62**	**57.5**
4	36	11	**49**	**52.0**
5	42	15	**63**	**62.0**
6	48	18	**70**	**71.5**

See Figure 2 and following step 1 to step 3 are for basic concept of sliding window.

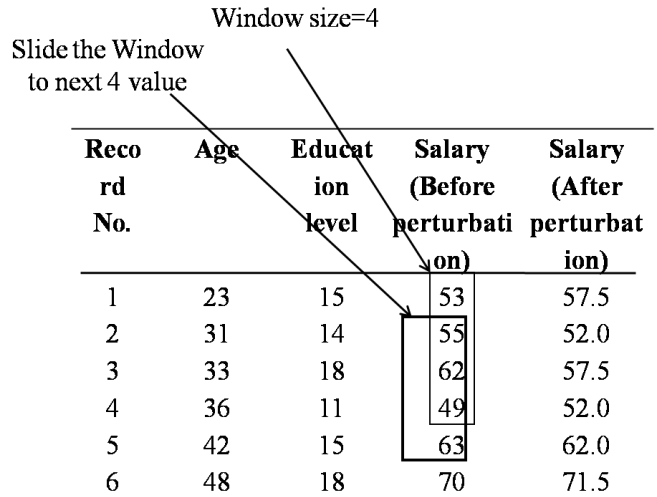| Record No.	Age	Education level	Salary (Before perturbation)	Salary (After perturbation)
1	23	15	53	57.5
2	31	14	55	52.0
3	33	18	62	57.5
4	36	11	49	52.0
5	42	15	63	62.0
6	48	18	70	71.5

Fig. 2 sliding window concepts

1. Apply window to selected attribute F*(here selected attribute is Attribute salary(before perturbation) contain window size is 4 Tuple1 to tuple4)
2. Find mean of this attribute (mean of tuple1 to tuple4) and replace first value of window that is 53 by mean. And remaining tuple values are as it is.
3. Suppose mean is 57.5 than replace first value from window by mean values 57.5. And remaining as it is. And sliding window by 1 tuple so new window is from tuple2 to tuple5. Then again find modified wind mean and replace until all values of attribute salary(before perturbation) is change and we save in new column that is salary(after perturbation) .

V.   CLASSIFICATION ALGORITHM: HOEFFDING TREE

Before starting a Hoeffding algorithm, first of all we define classification problem is a set of training examples of the form (x, y), where x is a vector of d attributes and y is a discrete class label. Our goal is to produce from the examples a model y=f(x) that predict the classes y for future examples x with high accuracy. Decision tree learning is one of the most effective classification methods. a Decision tree is learned by recursively replacing leaves by test nodes, starting at the root. Each node contains a test on the attributes and each branch from a node corresponds to a possible outcome of the test and each leaf contains a class prediction. All training data stored in main memory so it's expensive to repeatedly read from disk when learning complex trees so our goal is design decision tree learners than read each example at most once, and use a small constant time to process it.

So key observation is find the best attribute at a node. So for that consider only small subset of training examples that pass through that nodes. Choose the root attribute. Then expensive examples are passed down to the corresponding leaves, and used to choose the attribute there, and so on recursively. so use Hoeffding bound to decide, how many examples are enough at each node???

Consider a random variable a contain range is R. suppose we have n observation of a. so find mean of a ($\bar{r}$).so Hoeffding bound states that "with probability 1-δ, the true mean of a is at least $\bar{r}$- ε. where Hoeffding bound ε

$$\varepsilon = \sqrt{\frac{R^2 \ln (1/\delta)}{2n}}$$

(1)

Algorithm Hoeffding tree induction algorithm.
1: *HT* be a tree with a single leaf (the root)
2: **for all** training examples **do**
3:   Sort example into leaf *l* using *HT*
4:   Update sufficient statistics in *l*
5:   Increment *nl* , the number of examples seen at *l*
6:   **if** *nl mod Nmin* = 0 **and** examples seen at *l* not all of same Class **then**
7:     Compute $\bar{G}_1 (X_l)$ for each attribute
8:     Let X_a be attribute with highest $\bar{G}_1$
9:     Let X_b be attribute with second-highest $\bar{G}_1$
10: Compute Hoeffding bound $\varepsilon = \sqrt{\frac{R^2 \ln (1/\delta)}{2n}}$
11: **if** $X_a \neq X_\emptyset$; **and** ($\bar{G}_1 (X_a) - \bar{G}_1 (X_b) > \varepsilon$ **or** $\varepsilon < \tau$) **then**
12: Replace *l* with an internal node that splits on X_a
13:     **for all** branches of the split **do**
14:       Add a new leaf with initialized sufficient statistics
15:     **end for**
16:   **end if**
17:   **end if**
18: **end for**

Figure 4 Hoeffding tree algorithm [9]

In Line 1 initializes the tree data structure, which starts out as a single root node. Lines 2-18 form a loop that is performed for every training example. Every example is filtered down the tree to an appropriate leaf, depending on the tests present in the decision tree built to that point (line 3). This leaf is then updated (line 4)—each leaf in the tree holds the sufficient statistics needed to make decisions about further growth. The sufficient statistics that are updated are those that make it possible to estimate the information gain of splitting on each attribute. Line 5 simply points out that nl is the example count at the leaf, and it too is updated. Technically nl can be computed from the sufficient statistics. Lines 7-11 perform the test described in the previous section, using the Hoeffding bound to decide when a particular attribute has won against all of the others. G is the splitting criterion function (information gain) and $\bar{G}$ is its estimated value. In line 11 the test for $X_\emptyset$, the null attribute, is used for pre-pruning. The test involving τ is used for tie-breaking. If an attribute has been selected as the best choice, lines 12-15 split the node, causing the tree to grow. [9]

VI.   EXPERIMENT SETUP AND RESULT

We have conducted experiments to evaluate the performance of data perturbation method. We choose generated Database. Generate a dataset from MOA (massive online analysis) Framework [11]. And use the Agraval dataset generator. We use WEKA (Waikato Environment for Knowledge Analysis) [10] software that is integrated with MOA to test the accuracy of Hoeffding tree algorithm. The data perturbation algorithm implemented by a separate Java programme. In Hoeffding tree algorithm taken parameter are Split Criterion is InfoGain, Tie Threshold: 0.05, Split Confidence: 0and training set to test option to obtain the classification results.

TABLE II
EXPERIMENTAL RESULT OF AGRAVAL DATASET

	Original dataset (Agraval Dataset)	Perturbed Dataset (Agraval Dataset)		
Window Size		W=2	W=3	W=4
Time taken to build model (In second)	0.12	0.13	0.2	0.19
correctly classified (In %)	94.60	66.82	67.34	67.42

For experiment we take two dataset. First is Agraval dataset that is generated by using MOA Framework that contain 5000 instances and 10 attributes. And second dataset is Bank Marketing dataset [12] that is taken from UCI dataset repository it is related with direct marketing campaigns of a Portuguese banking institution, and it contain 45211 instances and 17 attribute. We apply data perturbation algorithm on both dataset and generate the dataset for window size W=2, W=3, and W=4.then after applying Hoeffding tree algorithm to all perturbed dataset and generate result. See the following table II and table III for experiment result.

TABLE III
EXPERIMENTAL RESULT OF BANK MARKETING DATASET

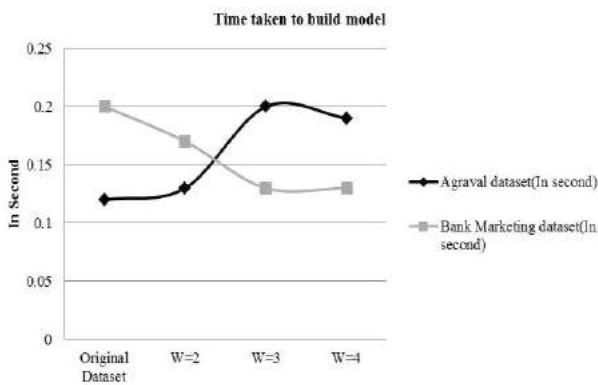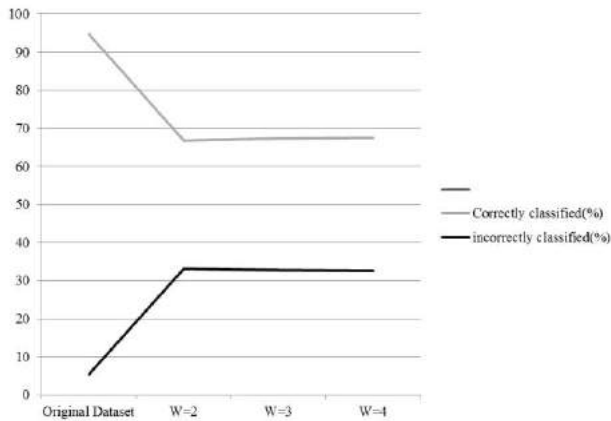|	Original dataset (bank marketing)	Perturbed Dataset (bank marketing Dataset)		
Window Size		W=2	W=3	W=4
Time taken to build model (In second)	0.2	0.17	0.13	0.13
correctly classified (In %)	89.04	88.48	82.32	86.12

Fig.3 Time taken to build Model

Fig. 4 comparison of different perturbed Agraval dataset classification model (in terms of correctly classified instances)
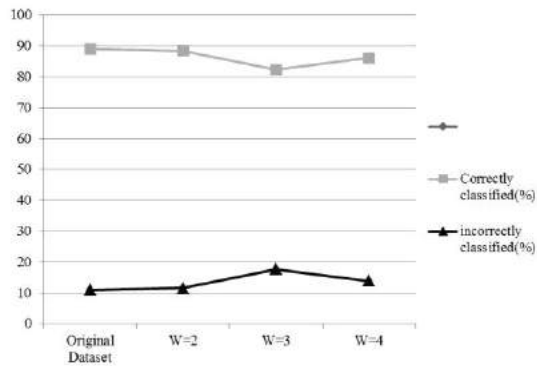

Fig. 5 comparison of different perturbed Bank Marketing dataset classification model (correctly classified instances)

See the following Fig.3 for time that taken for building the classification model.in Fig.4 that describe the comparison of different perturbed Agraval dataset in terms of correctly classified instance. And in Fig.5 that describe the comparison of different perturbed Agraval dataset in terms of correctly classified instance.

VII. CONCLUSION

We proposed the data perturbation method for privacy-preserving classification of data streams, which consists of two steps: date streams preprocessing and data streams mining. In the step of data streams preprocessing, we proposed algorithms for data perturbation that are the data perturbation using sliding window concept. And in the second step we apply the Hoeffding tree algorithm on perturbed dataset. We have done experiment to generate classification model of original dataset and perturbed dataset. We evaluate the experiment result in terms of correctly classified instance, Misclassification error. The classification result of perturb dataset shows minimal information loss from original dataset classification.

REFERENCES

[1] Chaudhry, N.A., Show, K., and Abdelgurefi, M. "Stream Data Management," *Advances in Database system*. Vol. 30. Springer(2005).

[2] A. Bifet, G. Holmes, R. Kirkby and B. Pfahringer, "Data Stream Mining-A Practical approach," 2011.

[3] L. Golab, M. Tamer Ozsu," Data Stream Management Issues -A Survey Technical Report", 2003.

[4] Verykios, V. S., Bertino, K., Fovino, I. N., Provenza, L. P., Saygin, Y. and Theodoridis, Y., "State-of-the-Art in Privacy Preserving Data Mining," ACM SIGMOD Record, Vol. 33, pp. 50-57 (2004).

[5] Du, W. and Zhan, Z., "Building Decision Tree Classifier on Private Data," Proceedings of *IEEE International Conference on Privacy Security and Data Mining*, pp. 1-8 (2002).

[6] Agrawal, R. and Srikant, R., "Privacy-Preserving Data Mining," *Proceedings of ACM SIGMOD International Conference on Management of Data*, pp. 439-450 (2000).

[7] Yabo Xu, Ke Wang, Ada Wai-Chee Fu,Rong She, and Jian Pei, "Privacy-Preserving Data Stream Classification," springer,pp.489-510(2008).

[8] Ching-Ming Chao, Po-Zung Chen and Chu-Hao Sun, "Privacy-Preserving Classification of Data Streams," *Tamkang Journal of Science and Engineering*, Vol. 12, No. 3, pp. 321-330(2009).

[9] Albert Bifet, Geoff Holmes, Richard Kirkby and Bernhard Pfahringer, "Data Stream Mining A Practical Approach."(2011)

[10] The Weka Machine Learning Workbench. http://www.cs.waikato.ac.nz/ml/weka.

[11] Albert Bifet, Richard Kirkby,Philipp Kranen, Peter Reutemann,"Massive Online Analysis Manual", May 2011. http://moa.cs.waikato.ac.nz/.

[12] S. Moro, R. Laureano and P. Cortez. "Using Data Mining for Bank Direct Marketing: An Application of the CRISP-DM Methodology." In P. Novais et al. (Eds.), *Proceedings of the European Simulation and Modelling Conference - ESM'2011*, pp. 117-121, Guimarães, Portugal, October, 2011. EUROSIS (http://hdl.handle.net/1822/14838).

A Comparative Study of Web Page Classification Techniques

Mr. Anirudhdha Nayak

(anirudhdha.nayak@git.org.in)

Abstract— Internet provides millions of web pages for each and every search term and it is a powerful medium for communication between computers and accessing online documents but tools like search engines assist users in locating and organizing information. Classification is a data mining technique used to predict group membership for data instances. In Web classification, web pages are assigned to pre-defined categories mainly according to their content (content mining). In this paper, we present the some basic classification techniques like decision trees, k-nearest neighbor, naïve bayes and support vector machine. Web page classification is one of the essential techniques for Web mining because classifying Web pages of an interesting class is often the first step of mining the Web. The goal of this paper is to provide a comprehensive review of different classification techniques.

Index Terms— Data Mining, Web Mining, Web page classification, Classification Techniques.

I. Introduction

The growth of information sources available on the World Wide Web has made it necessary for users to utilize automated tools in finding the desired information resources. There is a necessity of creating intelligent systems for servers and clients that can effectively mine for knowledge. Web mining can be broadly defined as the discovery and analysis of useful information from the World Wide Web by the extraction of interesting and potentially useful patterns and implicit information from artifacts or activity related to the World Wide Web.

There are roughly three knowledge discovery domains that pertain to web mining: Web Content Mining, Web Structure Mining, and Web Usage Mining. Web content mining is the process of extracting knowledge from the content of documents or their descriptions. Web structure mining is the process of inferring knowledge from the World Wide Web organization and links between references and referents in the Web. Finally, web usage mining is the process of extracting interesting patterns in web access logs [1].

Web content mining is an automatic process that goes beyond keyword extraction. Since the content of a text document presents no machine readable semantic, some approaches have suggested restructuring the document content in a representation that could be exploited by machines. The usual approach to exploit known structure in documents is to use techniques to map documents to some data model. There are two web content mining strategies: those that directly mine the content of documents and those that improve on the content search of other tools. From a Data Mining point of view, Web mining, has three areas of interest: clustering (finding natural groupings of users, pages etc.), associations (which URLs tend to be requested together), and classification (characterization of documents).

Web page classification is the process of assigning a Web page to one or more predefined category labels [2]. Classification can be understood as a supervised learning problem in which a set of labelled data is used to train a classifier which can be applied to label future examples. The general problem of Web page classification can be divided into more specific problems. Subject classification is concerned about the subject or topic of a Web page. Functional classification cares about the role that the Web page plays. Sentiment classification focuses on the opinion that is presented in a Web page, that is, the author's attitude about some particular topic. Other types of classification include genre classification, search engine spam classification. This paper focuses on subject and functional classification.

II. The Web Data: Features Of Web Pages

Web pages are what make up the World Wide Web. A Web page is a document or information resource written usually in HTML (hypertext markup language) and translated by your Web browser. Web pages are formed by a variety of information, such as: images, videos or other digital assets that are addressed by a common URL (Uniform Resource Locator). These pages are typically written in scripting languages such as PHP, Perl, ASP, or JSP. The scripts in the pages run functions on the server that return things like the date and time, and database information. All the information is returned as HTML code, so when the page gets to your browser, all the

browser has to do is translate the HTML, interpreting it and displaying it on the computer screen. Since all pages share the same language and elements it is possible to characterize each of them accurately in an automatic way. All web pages are different, in order to classify them, data extracted from the HTML code will be used. Pages can then be classified according to multiple categories. Throughout this document, the following labels have been used: blog, video, images and news.

- Blogs: short for weblog is a personal online journal with reflections, comments provided by the writer. Blogs are frequently updated and intended for general public consumption. Blogs generally represent the personality of the author or reflect the purpose of the Web site that hosts the blog. Blogs can be distinguished by their structure: a series of entries posted to a single page in reverse-chronological order. Blogs contents are basically text, occasionally images and videos are included.
- Video: these web pages provide a venue for sharing videos among friends and family as well as a showcase for new and experienced videographers. Videos are streamed to users on the web site or via blogs and other Web sites. Specific codes for playing each video are embedded on the Web page.
- Image: a photo gallery on a website is collection of images or photos that is uploaded to a website and available for website visitors to view. These web pages hardly have any text and generally carry a navigator that allows the visitor to move around the images.
- News: an online newspaper is a web site which provides news on a basis which is close to real time. A good news site updates its content every few minutes.

III. CLASSIFICATION TECHNIQUES

Classification means given a collection of records called training set, and each record contains a set of attributes, one of the attributes is the class. The technique is to find a model for class attribute as a function of the values of other attributes. It will assign a class as accurately as possible from the previously unknown records. The several classification techniques, summarized as follows:

A. *Decision Trees*

Decision trees are trees that classify instances by sorting them based on feature values. Each node in a decision tree represents a feature in an instance to be classified, and each branch represents a value that the node can assume. Instances are classified starting at the root node and sorted based on their feature values.

The basic algorithm for decision tree induction is a greedy algorithm that constructs decision trees in a top-down recursive divide-and-conquer manner.
The algorithm, summarized as follows:

1. create a node N;
2. if samples are all of the same class, C then
3. return N as a leaf node labeled with the class C;

4. if attribute-list is empty then
5. return N as a leaf node labeled with the most common class in samples;
6. select test-attribute, the attribute among attribute-list with the highest information gain;
7. label node N with test-attribute;
8. for each known value ai of test-attribute
9. grow a branch from node N for the condition test-attribute= ai;
10. let si be the set of samples for which test-attribute= ai;
11. if si is empty then,
12. attach a leaf labeled with the most common class in samples;
13. else attach the node returned by Generate_decision_tree.

Decision trees are usually unvaried since they use based on a single feature at each internal node. Most decision tree algorithms cannot perform well with problems that require diagonal partitioning. Decision trees can be significantly more complex representation for some concepts due to the replication problem. A solution is using an algorithm to implement complex features at nodes in order to avoid replication.

To sum up, one of the most useful characteristics of decision trees is their comprehensibility. People can easily understand why a decision tree classifies an instance as belonging to a specific class. Since a decision tree constitutes a hierarchy of tests, an unknown feature value during classification is usually dealt with by passing the example down all branches of the node where the unknown feature value was detected, and each branch outputs a class distribution. The output is a combination of the different class distributions that sum to 1. The assumption made in the decision trees is that instances belonging to different classes have different values in at least one of their features. Decision trees tend to perform better when dealing with discrete/categorical features.

Wen-Chen Hu [3] has performed a modified decision trees for web page classification, which facilitates web page search. By choosing keywords and descriptions for the web pages and keywords for web categories, the level of accuracy can be improved significantly. V. Estruch et. al. [4] have proposed web categorization using distance-based decision trees. It can be seen as a general and flexible web categorization framework which is potentially able to deal with any kind of information (belonging to the content, the structure or the usage of the Web pages) in a uniform way.

B. *K-Nearest Neighbor*

Nearest neighbor classifiers are based on learning by analogy. The training samples are described by n dimensional numeric attributes. Each sample represents a point in an n-dimensional space. In this way, all of the training samples are stored in an n-dimensional pattern space. When given an unknown sample, a k-nearest neighbor classifier searches the pattern space for the k training samples that are closest to the unknown sample. "Closeness" is defined in terms of Euclidean

distance, where the Euclidean distance, where the Euclidean distance between two points, X=(x1,x2,……,xn) and Y=(y1,y2,….,yn) is

$$d(x,y) = \sqrt{\sum_{i=1}^{n}(x_i - y_i)^2}$$

(1)

The unknown sample is assigned the most common class among its k nearest neighbors. When k=1, the unknown sample is assigned the class of the training sample that is closest to it in pattern space.

The *k-nearest neighbors' algorithm* is amongst the simplest of all machine learning algorithms. An object is classified by a majority vote of its neighbors, with the object being assigned to the class most common amongst its *k* nearest neighbors. *k* is a positive integer, typically small. If *k* = 1, then the object is simply assigned to the class of its nearest neighbor. In binary (two class) classification problems, it is helpful to choose *k* to be an odd number as this avoids tied votes.

The neighbors are taken from a set of objects for which the correct classification is known. This can be thought of as the training set for the algorithm, though no explicit training step is required. In order to identify neighbors, the objects are represented by position vectors in a multidimensional feature space. It is usual to use the Euclidian distance, though other distance measures, such as the Manhattan distance could in principle be used instead. The *k*-nearest neighbor algorithm is sensitive to the local structure of the data.

Juan Zhang et. al. [5] has proposed web document classification based on fuzzy k-NN algorithm to increase the accuracy in the classification results. They used TF/IDF for select features of a document. Performance was better than k-NN and SVM but speed was bit slow than k-NN.

C. *Support Vector Machine*

The Support Vector Machine (SVM) is a classification technique based on statistical learning theory that was applied with great success in many challenging non-linear classification problems and on large data sets. Support Vector Machines (SVM) is a classification technique for finding a decision boundary that separates the labeled data set with the widest margin. For simplicity, the assumption is that the data set is composed of data points and each data point is made up of a set of attribute-value pairs. Furthermore, each data point is assigned a label for the purpose of training the SVM. We distinguish two cases of data set in this section.

SVM was first bought forward by Cortes and Vapnik [6] as a learning algorithm for classification and regression. It tried to maximize the margin of confidence of classification on the training data set, which could use the linear, polynomial or radial basis function (RBF) kernels. In the case of support vector machine, an object is viewed as n-dimensional vector and we want to separate such objects with n-1 dimensional hyper-plane. This is called a linear classifier. There are many hyper-planes that might classify the data. The goal of SVM is try to address the nearest distance between a point in one class

and a point in the other class being maximized and draw a hyper-plane to classify two categories as clearly as possible.

D. *Naïve Bayes*

The Naïve Bayes classifiers (Lewis 1992) are known as a simple Bayesian classification algorithm. Under the Bayes independent assumption premise, it simulates each kind of class condition joint probability distribution separately, and then constructs posterior classifier with Bayes theorem. Regarding web document categorization problem, a document $d \in D$ corresponds to a data instance, where *D* denotes the training document set. Each document *d* is associated with a class label $c \in C$, where C denotes the class label set [7].

A Bayesian Network (BN) is a graphical model for probability relationships among a set of variables features. The Bayesian network structure *S* is a directed acyclic graph (DAG) and the nodes in *S* are in one-to-one correspondence with the features *X*. Typically, the task of learning a Bayesian network can be divided into two subtasks: initially, the learning of the directed cyclic graph (DAG) structure of the network, and then the determination of its parameters. Probabilistic parameters are encoded into a set of tables, one for each variable, in the form of local conditional distributions of a variable given its parents. Given the independences encoded into the network, the joint distribution can be reconstructed by simply multiplying these tables.

The methods for learning Bayesian belief network (BN) based predictive models for classification was investigated by Jie Cheng and Russell Greiner [8]. They studied two types of unrestricted BN classifiers – general Bayesian networks and Bayesian multi-nets. The results show that BN learning algorithms are very efficient, and the learned BN classifiers can give really good prediction accuracy. By checking and modifying the learned BN predictive models, domain experts can study the relationships among the attributes and construct better BN predictive models. The most interesting feature of BNs, compared to decision trees or neural networks, is most certainly the possibility of taking into account prior information about a given problem, in terms of structural relationships among its features. This prior expertise, or domain knowledge, about the structure of a Bayesian network can take the following forms:

1. Declaring that a node is a root node, i.e., it has no parents.
2. Declaring that a node is a leaf node, i.e., it has no children.
3. Declaring that a node is a direct cause or direct effect of another node.
4. Declaring that a node is not directly connected to another node.
5. Declaring that two nodes are independent, given a condition-set.
6. Providing partial nodes ordering, that is, declare that a node appears earlier than another node in the ordering.
7. Providing a complete node ordering.

IV. Evaluations Measures

A. *Precision & Recall*

For classification tasks, the terms **true positives**, **true negatives**, **false positives**, and **false negatives** compare the results of the classifier under test with trusted external judgments. The terms *positive* and *negative* refer to the classifier's prediction (sometimes known as the *observation*), and the terms *true* and *false* refer to whether that prediction corresponds to the external judgment (sometimes known as the *expectation*).

B. *F-measure*

A measure that combines precision and recall is the harmonic mean of precision and recall, the traditional F-measure or balanced F-score. This is also known as the F_1 measure, because recall and precision are evenly weighted.

V. Conclusion

We have surveyed some existing classification techniques. The goal of classification result integration algorithms is to generate more certain, precise and accurate system results. Decision trees and Bayesian Network generally have different operational profiles, when one is very accurate the other is not and vice versa. Classification methods are typically strong in modeling interactions. However, a straightforward application of classification methods to large numbers of markers has a potential risk picking up randomly associated markers. Although or perhaps because many methods of web page classification have been proposed, there is yet no clear picture of which method is best.

References

[1] Dunham M. H., "Data Mining: Introductory and Advanced Topics", Prentic Hall, New Jersey, 2003.

[2] Qi X and Davison B.D., "Web Page Classification: Features and Algorithms ACM Computing Surveys", Vol. 41, No. 2, Article 12, 2009.

[3] Wen-Chen Hu, "WebClass: Web document classification using modified decision- trees", The Fifth International Conference on Computer Science and Informatics, September 1999.

[4] V. Estruch, C. Ferri, J. Hernandez-Orallo and M.J. Ramirez-Quintana, "Web Categorisation Using Distance-Based Decision Trees", Published by Elsevier Science B. V., 2005.

[5] Juan Zhang, Yi Niu and Huabei Nie, "Web Document Classification Based on Fuzzy k-NN Algorithm", International Conference on Computational Intelligence and Security, pp. 193-196, 2009.

[6] C. Cortes and V. Vapnik, "Support Vector Networks," Machine Learning, vol. 30 No. 3, pp. 273-297, 1995.

[7] Jensen, F., "An Introduction to Bayesian Networks", Springer, 1996.

[8] Cheng, J. & Greiner, R., "Learning Bayesian Belief Network Classifiers: Algorithms and System", In Stroulia, E. & Matwin, S. (ed.), *AI 2001*, 141-151, LNAI 2056, 2001.

[9] Bernhard E. B., Isabelle M. G., Vladimir N. V., "A Training Algorithm for Optimal Margin Classifiers", In Proceedings of International Conference on Computational Learning Theory, pp. 144-152, 1992.

[10] E. Glover, K. Tsioutsiouliklis, S. Lawrence, D. Pennock, and G. Flake, "Using web structure for classifying and describing web pages", In Proc. of the WWW2002, Hawaii, USA, May 2002.

Explain Use Case Point Effort Estimation Method Taking the Case of University Registration System Use Case Diagram

Prof. Svapnil M Vakharia

svapnil.vakharia@git.org.in

Abstract — Use case point (UCP) method has been proposed to estimate software development effort in early phase of software project and used in a lot of software organizations naturally, UCP is measured by counting the number of actors and transactions included in use case models. Several tools to support calculating UCP have been developed. However, they only extract actors and use cases and the complexity classification of them are conducted manually.
In this paper I am using the case of university registration system to explain use case point effort estimation method.

Index Terms — Use Case, Actor, Unadjusted Use Case Points, Technical Complexity Factor, Environment Complexity Factor.

I. INTRODUCTION

Effort estimation is a challenge in every software project.

The Estimates will impact costs and expectations on schedule, functionality and quality. While expert estimates are widely used, they are difficult to analyze and the estimation quality depends on the experience of experts from similar projects. Alternatively, more formal estimation models can be used. Traditionally, software size estimated in the number of Source Lines of Code (SLOC), Function Points (FP) and Object Points (OP) are used as input to these models, e.g. COCOMO and COCOMO II.
Because of difficulties in estimating SLOC, FP or OP, and because modern systems are often developed using the Unified Modeling Language (UML), UML-based software sizing approaches are proposed. Examples are effort estimation methods based on use cases and software size estimation in terms of FP from various UML diagrams
The Use Case Points (UCP) estimation method introduced in 1993 by Karner estimates effort in person-hours based on use cases that mainly specify functional requirements of a system
Use cases are assumed to be developed from scratch, be sufficiently detailed and typically have less than 10-12 transactions. The method has earlier been used in several industrial software development projects (small projects compared to this study) and in student projects.

II INTRODUCTION OF USE CASE DIAGRAM OF UNIVERSITY REGESTATION SYSTEM
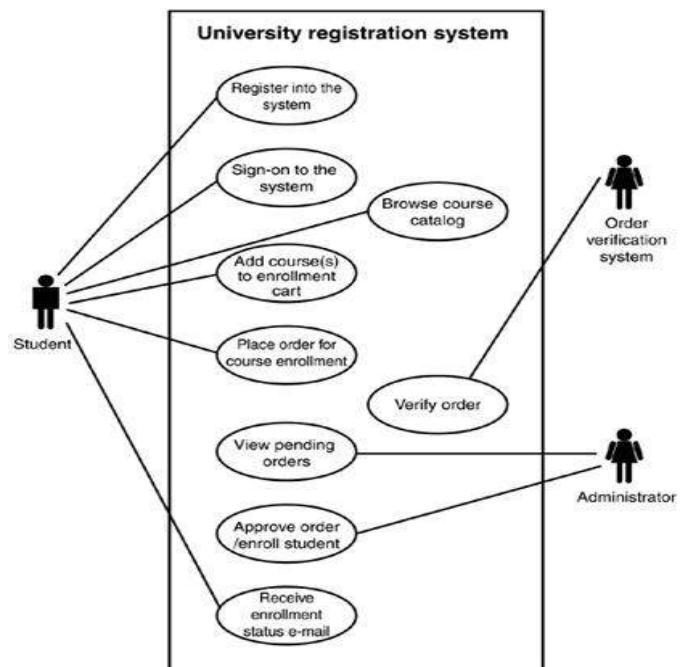

Fig 1 Use Case Diagram

The use case diagram in this case consists of actors, such as student, administrator, and order verification system. The following describes the use cases:

- New students register with the system.
- Existing students log on to the system and can browse the course catalog.
- A student can select courses and add them to the enrollment cart.
- A student places an order for the enrollment cart contents.
- The system verifies the order in the background.
- An administrator can view the verified orders that need approval for enrollment.
- An administrator approves the order and enrolls the student in the courses.
- The system notifies the student of enrollment via e-mail.

III THE USE CASE POINTS ESTIMATION METHOD

The Use Case Points (UCP) method provides the ability to estimate the man-hours a software project requires from its use cases.
The UCP equation is composed of three variables:

1. Unadjusted Use Case Points (UUCP).
2. The Technical Complexity Factor (TCF).
3. The Environment Complexity Factor (ECF).

Each variable is defined and computed separately using weighted values, subjective values, and constraining constants. The subjective values are determined by the development team based on their perception of the project's technical complexity and efficiency.
Additionally, when productivity is included as a coefficient that expresses time, the equation can be used to estimate the number of man-hours needed to complete a project. Here is the complete equation with a Productivity Factor (PF) included:

$$UCP = UUCP * TCF * ECF * PF$$

The necessary steps to generate the estimate based on the UCP method are the following:

1. Determine and compute the UUCPs.
2. Determine and compute the TCFs.
3. Determine and compute the ECFs.
4. Determine the PF.
5. Compute the estimated number of
   Hours

A. UUCPs

UUCPs are computed based on two computations:

1. The Unadjusted Use Case Weight (UUCW) based on the total number of activities (or steps) contained in all the use case scenarios.

2. The Unadjusted Actor Weight (UAW) based on the combined complexity of all the actors in all the use cases

1. UUCW

The UUCW is derived from the number of use cases in three categories: simple, average, and complex (see Table 1). Each use case is categorized by the number of steps its scenario contains, including alternative flows.
The UUCW is calculated by tallying the number of use cases in each category, multiplying each total by its specified weighting factor, and then adding the products.

Table 1: Use Case Categories

Use Case Category	Description	Weight
Simple	Simple user interface. Touches only a single database entity. Its success scenario has three steps or less. Its implementation involves less than Five classes.	5
Average	More interface design. Touches two or more database entities. Between four and seven steps. Its implementation involves between five and 10 classes.	10
Complex	Complex user interface or processing. Touches three or more database entities. More than seven steps. Its implementation involves more than 10 classes.	15

Table 2: Computing UUCW

Use Case Category	Description	Weight	Number of Use Cases	Result
Simple	Simple user interface. Touches only a single database entity. Its success scenario has three steps or less. Its implementation involves less than five classes.	5	2	10
Average	More interface design. Touches two or more database entities. Between four and seven	10	3	30

	steps. Its implementation involves between five and 10 classes.			
Complex	Complex user interface or processing. Touches three or more database entities. More than seven steps. Its implementation involves more than 10 classes.	15	2	30
Total UUCW				70

2. UAW

In a similar manner, the Actor Types are classified as simple, average, or complex as shown in Table 3.
The UAW is calculated by totaling the number of actors in each category, multiplying each total by its specified factor, and then adding the products.

Table 3: Use Case Categories

Actor Type	Description	Weight
Simple	The actor represents another system with a defined application programming interface.	1
Average	The actor represents another system interacting through a protocol, like Transmission Control Protocol/Internet Protocol	2
Complex	The actor is a person interacting via a graphical user interface.	3

Table 4: Computing UAW

Actor Type	Description	Weight	Number of Actors	Result
Simple	The actor represents	1	0	0

	another system with a defined application programming interface.			
Average	The actor represents another system interacting through a protocol, like Transmission Control Protocol/Internet Protocol	2	1	2
Complex	The actor is a person interacting via a graphical user interface.	3	2	6
Total UAW				7

B. TCFs

Thirteen standard technical factors exist to estimate the impact on productivity that various technical issues have on a project Each factor is weighted according to its relative impact.

For each project, the technical factors are evaluated by the development team and assigned a perceived complexity value between zero and five. The perceived complexity factor is subjectively determined by the development team's perception of the project's complexity – concurrent applications, for example, require more skill and time than single-threaded applications. A perceived complexity of 0 means the technical factor is irrelevant for this project, 3 is average, and 5 is strong influence.

Two constants are computed with the Technical Total Factor to produce the TCF. The constants constrain the effect the TCF has on the UCP equation from a range of 0.60 (perceived complexities all zero) to a maximum of 1.30 (perceived complexities all five).

TCF values less than one reduce the UCP because any positive value multiplied by a positive fraction decreases in magnitude: $100 * 0.60 = 60$ (a reduction of 40 percent).

TCF values greater than one increase the UCP because any positive value multiplied by a positive mixed number increases in magnitude: $100 * 1.30 = 130$ (an increase of 30 percent).

Since the constants constrain the TCF from a range of 0.60 to 1.30, the TCF can impact the UCP equation from - 40 percent (.60) to a maximum of +30 percent (1.30).

For the mathematically astute, the complete formula to compute the TCF is:

$$TCF = C_1 + C_2$$
$$\cdot \sum_{i=1}^{13} W_i * F_1$$

where,
Constant 1 (C1) = 0.6
Constant 2 (C2) = .01
W = Weight
F = Perceived Complexity Factor

For the rest of us, a more digestible equation is:

TCF = 0.6 + (.01 * Technical Total Factor)

   = 0.6 + (.01*26)

   = 0.6 + 0.26

   = 0.86

Table 5: Technical Complexity Factors

Technical Factor	Description	Weight
T1	Distributed System	2
T2	Performance	1
T3	End User Efficiency	1
T4	Complex Internal Processing	1
T5	Reusability	1
T6	Easy to Install	0.5
T7	Easy to Use	0.5
T8	Portability	2
T9	Easy to Change	1
T10	Concurrency	1
T11	Special Security Features	1
T12	Provides Direct Access for Third Parties	1
T13	Special User Training Facilities Are Required	1

Table 6: Calculating the Technical Complexity Factors

Technical Factor	Description	Weight	Perceived Complexity	Calculated Factor (Weight* Perceived Complexity)
T1	Distributed System	2	0	0
T2	Performance	1	3	3
T3	End User Efficiency	1	3	3
T4	Complex Internal Processing	1	1	1
T5	Reusability	1	4	4
T6	Easy to Install	0.5	4	2
T7	Easy to Use	0.5	4	2
T8	Portability	2	2	4
T9	Easy to Change	1	3	3
T10	Concurrency	1	2	2
T11	Special Security Features	1	1	1
T12	Provides Direct Access for Third Parties	1	1	1
T13	Special User Training Facilities Are Required	1	0	0
Technical Total Factor				26

C. ECF

The ECF provides a concession for the development team's experience. More experienced teams will have a greater impact on the UCP computation than less experienced teams. The development team determines each factor's perceived impact based on its perception the factor has on the project's success. A value of 1 means the factor has a strong, negative impact for the project; 3 is average; and 5 means it has a strong, positive impact. A value of zero has no impact on the project's success. For example, team members with little or no motivation for the project will have a strong negative impact (1) on the project's success while team members with strong object-oriented experience will have a strong, positive impact (5) on the project's success.

To produce the final ECF, two constants are computed with the Environmental Total Factor. The constants, "based on interviews with experienced Objectors users at Objective Systems. Constrain the impact the ECF has on the UCP equation from 0.425 (Part-Time Workers and Difficult Programming Language = 0, all other values = 5) to 1.4 (perceived impact all 0).

Therefore, the ECF can reduce the UCP by 57.5 percent and increase the UCP by 40 percent.

The ECF has a greater potential impact on the UCP count than the TCF. The formal equation is:

$$ECF = C_1 + C_2 \sum_{i=1}^{8} W_i * F_1$$

where,
Constant 1 (C1) = 1.4
Constant 2 (C2) = -0.03
W = Weight
F = Perceived Impact
Informally, the equation works out to be:

ECF = 1.4 + (-0.03 * Environmental Total Factor)

$= 1.4 + (-0.03* 16)$

$= 1.4 - 0.48$

$= 0.92$

Table 7: Environmental Complexity Factors

Environmental Factor	Description	Weight
E1	Familiarity With UML*	1.5
E2	Part-Time Workers	-1
E3	Analyst Capability	0.5
E4	Application Experience	0.5
E5	Object-Oriented Experience	1
E6	Motivation	1
E7	Difficult Programming Language	-1
E8	Stable Requirements	2

Table 8: Calculating the Environmental Total Factor

Environmental Factor	Description	Weight	Perceived Impact	Calculated Factor (Weight* Perceived Complexity)
E1	Familiarity With UML*	1.5	3	4.5
E2	Part-Time Workers	-1	2	-2
E3	Analyst Capability	0.5	2	1
E4	Application Experience	0.5	3	1.5
E5	Object-Oriented Experience	1	3	3
E6	Motivation	1	3	3
E7	Difficult Programming Language	-1	2	-2
E8	Stable Requirements	2	4	8
Environmental Total Factor				16

Calculating the UCP
As a reminder, the UCP equation is:

UCP = UUCP * TCF * ECF

$= 77* 0.86 * 0.92$

$= 60.92$

D. PF

The Productivity Factor (PF) is a ratio of the number of man hours per use case point based on past projects. If no historical data has been collected, a figure between 15 and 30 is suggested by industry experts. A typical value is 20.

Estimated Hours
The total estimated number of hours for the project is determined by multiplying the UCP by the PF.

Total Estimate = UCP * PF

$= 60.92 * 20$

$= 1218$ hours for the project

If no historical data has been collected, consider two possibilities:
1. Establish a baseline by computing the UCP for previously completed projects (as was done with the sample case study in this article).
2. Use a value between 15 and 30 depending on the development team's overall experience and past accomplishments (Do they normally finish on time? Under budget? etc.). If it is a brand-new team, use a value of 20 for the first project.
After the project completes, divide the number of actual hours it took to complete the project by the number of UCPs.
The product becomes the new PF.

IV CONCLUSION

An effort estimation method based on use cases has been adapted and tested on a large industrial system with incremental changes in use cases. One main assumption is that use cases may be used as a measure of the size of a system, and that changes in these may be used as a measure of changes in functionality between releases. Generally, predicting the size of a software system in SLOC or FP in early phases is as difficult as predicting the needed effort..
The method does not depend on any tools (although there are tools for the original UCP method), paradigms or programming languages, and can promote high quality use cases. The method is cheap, transparent and easy to understand. The method is also suitable when development is being outsourced.

REFERENCES

1. Karner, Gustav. "Resource Estimation for Objectory Projects." Objective Systems SF AB, 1993.
2. Albrecht, A.J. Measuring Application Development Productivity. Proc. Of IBM Applications Development Symposium, Monterey, CA, 14-17 Oct. 1979: 83.
3. Jacobson, I., G. Booch, and J. Rumbaugh. The Objectory Development Process. Addison-Wesley, 1998.

4. [Nageswaran, Suresh. "Test Effort Estimation Using Use Case Points." June 2001 <www.cognizant.com/cog community/presentations/Test_ Effort_Estimation.pdf>.

5. Anda, Bente. "Improving Estimation Practices By Applying Use Case Models." June 2003 <www.cognizant. com/cogcommunity/presentations/Test_Effort_Estim ation.pdf

6. Ashman, R. Project estimation: a simple use-case-based model". *IT Pro*, 6, 4 (July/August 2004), 40-44.

Essential Aspects of Security, Privacy and Challenges in Cloud

Ms. Leena Patel

Lecturer, Computer Engineering, Gandhinagar Institute Of Technology, Gandhinagar

Email ID: leena.patel@git.org.in

Abstract –

   Cloud Computing is one of the powerful technology to be established within network for the benefits and profits of the enterprises and government too. This paper describes categories of cloud architectures (cloud service delivery models), security and privacy concerns with challenges. It seeks to contribute a better understanding of emerging in trends and issues arise along with security and privacy for cloud infrastructures with key findings having attributions about cloud computing security.

Keywords: Cloud computing, Cloud, security, privacy, challenges

1. Introduction:

   Cloud computing is defined as a model which is based on internet that enable convenient, on demand and pay per user access to gain access to applications and data in a web-based environment on demand [3]. It satisfies user's requirement for computing resources like networks, storage, servers, services and applications, without physically acquiring them [1]. Cloud service delivery models are "Software as a Service" (SaaS), Platform as a Service (PaaS) and Infrastructure as a Service (IaaS) [2].

1.1 The Definition of Cloud Computing

   Cloud computing is a model for enabling convenient, on-demand network access to a shared pool of configurable computing resources such as networks, servers, storage, applications, and services which can be frequently provisioned and released with less management efforts or service provider interaction. This cloud model is composed of five essential characteristics, three service models, and four deployment models [4]. A cloud is incorporated with routers, firewalls, bridges, servers, modems and all other network devices.

1.2 CATEGORIES OF CLOUD SERVICES
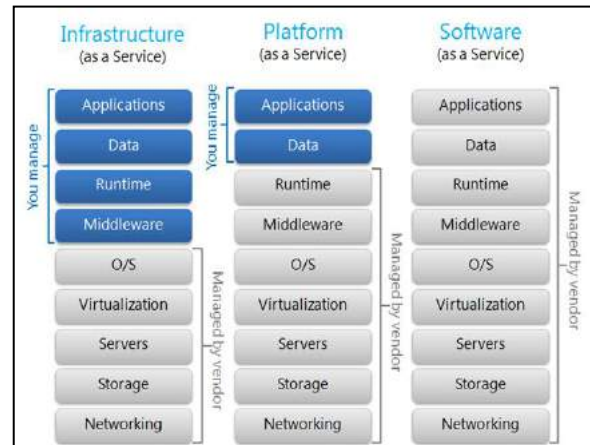
   David C. Chau's self portrait is-

Figure.1 Cloud Service Models [7].

1. Infrastructure as a Service (IaaS) is the foundation of cloud services which provides clients with access to server hardware, storage, bandwidth and fundamental computing resources. E.g; Amazon EC2 allows individuals and businesses to rent machines preconfigured with selected operating system on which to run their own applications [3]. The capability provided to the consumer is to utilize the provider's applications running on a cloud infrastructure. The applications are accessible from various client devices through a thin client interface such as web-based email [5].

2. Platform as a Service (PaaS), builds upon IaaS and provides clients with access to the basic operating software and optional services to develop and use software applications within cloud [5].

3. Software as a Service (SaaS), builds upon the underlying IaaS and PaaS provides clients with integrated access to software applications. For example, Oracle SaaS Platform allows independent software vendors to build, deploy and manage SaaS and cloud-based applications using a licensing economic model [3].The capability provided to the consumer is to provision processing, storage,

networks and other fundamental computing resources where the consumer is able to deploy and run arbitrary software, which can include operating systems and applications [5].
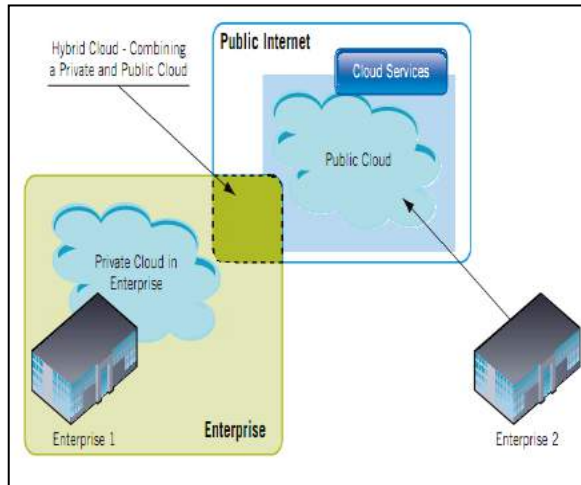
1.3 TYPES OF CLOUDS

Figure.2 Public, Private and Hybrid Cloud Deployment Example [11].

1. Private cloud- The cloud infrastructure is operated for a specific organization. It may be managed by the organization or a third party and may be in house [11].
2. Community cloud- The cloud infrastructure is shared by several organizations and supports a specific community that has shared concerns to the mission, security requirements, policy, and compliance considerations [5].
3. Public cloud- The cloud infrastructure is made available to the general public or large industry group and is owned by an organization selling cloud services [6].
4. Hybrid cloud- Hybrid cloud is a private cloud linked to one or more external cloud services, centrally managed, provisioned as a single unit, and circumscribed by a secure network [14]. It provides virtual IT solutions through a mix of both public and private clouds. Hybrid Cloud provides more secure control of the data and applications and allows various parties to access information over the Internet [13].

2. Security

A number of the current applications of cloud computing involve consumer services, including e-mail, and social networks. The protection of personal data and management of privacy issues may well determine the success or failure of many cloud services [5].

As an OECD (Organization for Economic Cooperation and Development) paper has noted:

Companies that wish to provide Cloud services globally must adopt leading-edge security and auditing technologies and best-in-class practices. If they fail to earn the trust of their customers by adopting clear and transparent policies on how their customers' data will be used, stored, and protected, governments will come under increasing pressure to regulate privacy in the Cloud. And if government policy is poorly designed, it could stymie the growth of the Cloud and commercial Cloud services [8].

2.1 Securing information within a cloud computing environment requires three levels of security:
a) Network security
b) Host security
c) Application security.

Encryption for the information security is not a complete solution because data needs to be decrypted in certain situations – so that computation can occur and the usual data management functions of indexing and sorting can be carried out. Thus although data in transit and data at rest are effectively encrypted, the need to decrypt, generally by the cloud service provider, can be a security concern. Nevertheless cloud services can be augmented by email filtering (including back-up, and spam), Web content filtering, and vulnerability management, all of which improve security [5].

2.2. SECURITY ON DEMAND

The Cloud Computing systems are secured if users can depend on them (i.e. DaaS, SaaS, PaaS,IaaS, and so on) to behave as users expect. Traditionally, it contains 5 goals, say availability, confidentiality, data integrity, control and audit, to achieve adequate security. They are integrated systematically, and none of them could be forfeited to achieve the adequate security [16].

A. Availability

The goal of availability for Cloud Computing systems is to ensure its users can use them at any time, at any place [16].

B. Confidentiality

Confidentiality means keeping users' data secret in the Cloud systems. The confidentiality in Cloud systems is a big obstacle for users to step into it, as many users said "My sensitive corporate data will never be in the Cloud" in the article named "Above the Cloud" [16].

C. Data Integrity

Data integrity in the Cloud system means to preserve information integrity (i.e., not lost or modified by unauthorized users). As data is the base for providing Cloud Computing services, keeping data integrity is a fundamental task [16].

3. Privacy

Email, Instant messaging, business softwares and web content management are applications of the cloud environment. Many of them have been used remotely through internet. E.g. *Microsoft* recognizes privacy policies and protections to obtain trust of customers. Even secured systems and datacenters help to protect privacy and support [9].

3.1 Privacy Questions in Cloud Computing

 Are hosted data and applications within the cloud protected by suitably robust privacy policies?

 Are the cloud computing provider's technical infrastructure, applications, and processes secure?

 Are processes in place to support appropriate action in the event of an incident that affects privacy or security?

Security is an essential component of strong privacy safeguards in all online computing environments, but security alone is not sufficient. Consumers and businesses are willing to use online computing only if they trust that their data will remain private and secure [9].

4. Legal and Regulatory Challenges

Cloud services can thrive when companies are able to provide cloud services in an efficient way and assure customers that their data will remain private and secure [9].

4.1 Challenges

The following are some of the notable challenges associated with cloud computing, some of them lead to the delay in services and some give the opportunity to be resolved with due care and focus [10] :

• **Security and Privacy** —these challenges can be addressed, for example, by storing the information internal to the organization, but allowing it to be used in the cloud. For this to occur, though, the security mechanisms between organization and the cloud need to be robust and a Hybrid cloud could support such a deployment [10].

• **Lack of Standards** — Clouds have documented interfaces; however, no standards are associated with these, and thus it is unlikely that most clouds will be interoperable. The Open Grid Forum is developing an Open Cloud Computing Interface to resolve this issue and the Open Cloud Consortium is working on cloud computing standards and practices. The findings of these groups will need to mature, but it is not known whether they will address the needs of the people deploying the services [10].

• **Continuously Evolving** — User requirements are continuously evolving, as are the requirements for interfaces, networking, and storage. This means that a "cloud," especially a public one, does not remain static and is also continuously evolving [10].

• **Compliance Concerns** —these challenges typically result in Hybrid cloud deployment with one cloud storing the data internal to the organization [10].

5. Key Findings with Attributions about cloud computing security

Bar Chart 1 reports cloud providers' agreement with three attributions about cloud computing security. These findings indicate that respondents overwhelmingly believe it is the responsibility of users of cloud computing to ensure the security of cloud resources they provide. The majority does not believe their cloud services include the protection of sensitive data. Further, only 19 percent of US cloud providers and 18 percent of European cloud providers strongly agree or agree that their organization perceives security as a competitive advantage in the cloud marketplace [2].

Bar Chart 1: Cloud providers' attributions about cloud computing security [2].
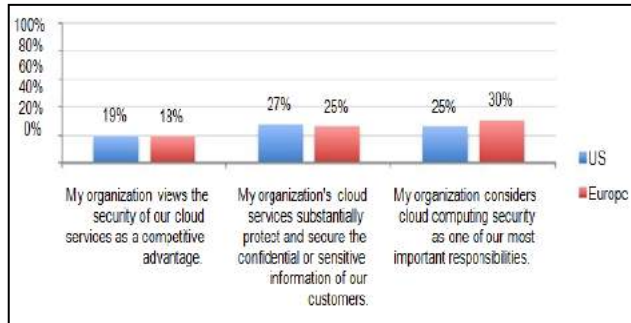
As shown below in Bar Chart 2, the majority of cloud providers (79 percent) say their organizations allocate 10 percent or less of IT resources or efforts to
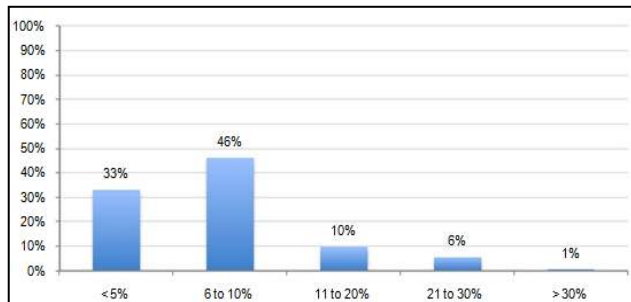
security and control-related activities [2].

Bar Chart 2: Percent of resources dedicated to security and control-related activities [2].
US & Europe results combined
As shown in Bar Chart 5, when asked why companies purchase cloud computing services, the top choices are reduced cost, faster deployment time, improved customer service and increased efficiency. The least cited reasons are improved security and compliance with contractual agreements or policies [2].

Bar Chart 3: Reasons customers migrate to the cloud computing environment [2].
US & Europe results combined
This concludes that the focus on cost and speed and not on security or data protection creates a security hole. This may explain why 62 percent of US and 63 percent of European providers are not confident or unsure that cloud applications are sufficiently secured. As noted in Bar Chart 4, two thirds of US cloud providers and 61 percent of European cloud providers are not confident or are unsure that their customer's security requirements are met. Similarly,
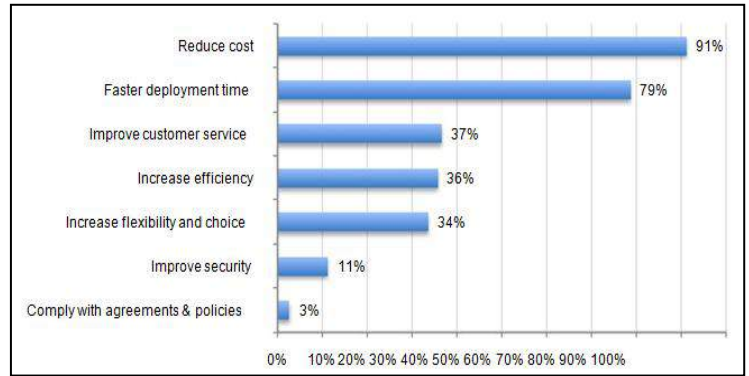
there is a lack of confidence that their cloud applications and other resources are secure [2].

Bar Chart 4: Lack of confidence in the security of cloud resources provided [2]. Not confident & unsure response combined
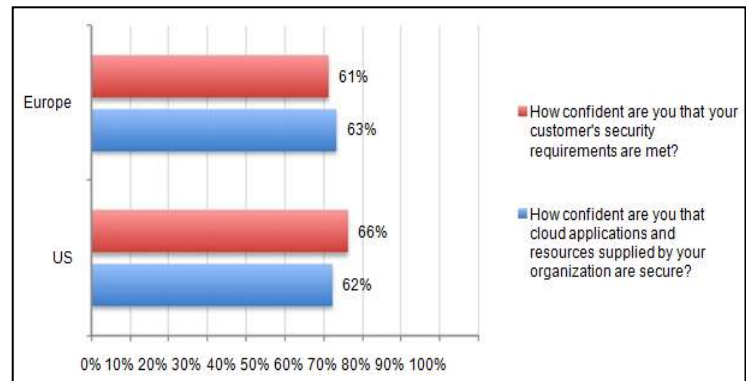
Bar Chart 5 provides responses to two separate but related questions about the provisioning of IT security services as a possible product offering. Most cloud providers (91 percent) do not provide security as a service from the cloud today, but about one-third are considering offering this type of service at some point in the next two years [2].

Bar Chart 5: Security as a service from the cloud
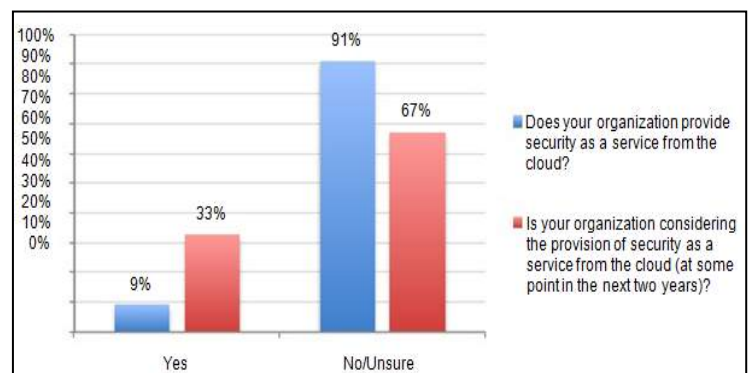
5. **Conclusion**

The study of research determines the aspects and dimensions for establishing security and privacy with challenges which would be leading-edge to more efficient and secured cloud services in the cloud infrastructures. By using a cloud system, your company's sensitive data and information will be stored on third-party servers. This article will be helpful to establish a future's powerful and efficient plus secured network through internet using cloud services. It will be the advanced new technology to the new era and future enhancement. This paper will lead IT professionals to conduct high quality, empirical studies on critical issues affecting the management and security of sensitive information about people and organizations.

References

[1] Choubey, 2011. *A survey on cloud computing security, challenges and threats.* Bhopal, India: IJCSE.

[2] *Security of Cloud Computing Providers study*. Ponemon Institute, Researched report. Sponsored by CA Technologies.April, 2011.

[3] Kim-Kwang Raymond Choo, (2010). Cloud computing: *Challenges and future directions. Australian Government*,. Australian Institute of Criminology (Trends and Issues in crime and criminal justice). Page No.400.

[4] National Institute of Standards and Technology, December 2009, *Guidelines on security and privacy in public cloud comuting*. [online]. US, special publication 800-144, US department of commerce. Standard from Information Technology Laboratory (NIST), accessed on 14 May 2012 at http://csrc.nist.gov/groups/SNS/cloud-computing/cloud-def-v15.doc

[5] Mudge, J C. (2010). CLOUD COMPUTING: Opportunities and Challenges for Australia.[online] Executive summery by *The australian academy of Technological sciences and engineering (ATSE).* Last accessed on 15 May 2012 at http://www.egov.vic.gov.au/trends-and-issues/information-and-communications technology/cloud-computing/cloud-computing-opportunities-and-challenges-for-australia-in-pdf-format-1367kb.html

[6] Wyld, D C, (2010). The cloudy future of government IT: *Cloud computing and the public sector around the world.* [online] International Journal of Web & Semantic Technology (IJWesT), Vol 1, Num 1, January 2010, Last accessed on 22 June 2010 at http://airccse.org/journal/ijwest/papers/0101 w1.pdf

[7] Chou D C, 16th August 2010. Figure-1, self portrait. [Online image]. Last accessed at 9th May, 2012 at: http://blogs.msdn.com/b/johnalioto/archive/ 2010/08/16/10050822.aspx

[8] Nelson M R, (2009). Organization for Economic Cooperation and Development. Briefing paper for the ICCP Technology Foresight Forum: *Cloud computing and public policy,* Last accessed on 22 June 2010 at http://www.oecd.org/dataoecd/39/47/439337 71.pdf

[9] Microsoft. (2009). Privacy in the Cloud Computing Era; *A Microsoft Perspective*, page.no.9 [online]. Lasr accessed on 16 May 2012 at http://download.microsoft.com/download/3/ 9/1/3912e37e-5d7a-4775-b677-b7c2baf10807/cloud_privacy_wp_102809.p df

[10] Dialogic Corporation, (2010). White Paper: *Introduction to cloud computing.* [Online]. Last accessed on 14 May 2012 at *www.dialogic.com.*

[11] Machi J., 2010. Figure-2., Dialogoc Exchange Network, Corporate Blog [online image]. Last accessed on May 15, 2012 at http://blog.tmcnet.com/industry-insight/

[12] Department for Culture, Media and Sport (DCMS) and Department for Business, Innovation and Skills (DBIS), 2009, Digital Britain: Final Report, London.

[13] Kuyoro S. O., Ibikunle F. & Awodele O., 2011. Cloud Computing Security Issues and Challenges International Journal of Computer Networks (IJCN), Volume (3) : Issue (5) : 2011,p249.

[14] Global Netoptex corporated."Demystifying the cloud. Important opportunities, crucial choices." pp4-14[online].Last accessed on May 15,2012 at:
http://www.gni.com

[15] Minqi Zhou,Rong Zhang, Wei Xie, Weining Qian, Aoying Zhou, (2010). Security and Privacy in Cloud Computing [online]. In: *Sixth International Conference on Semantics, Knowledge and Grids*. Software Engineering Institute, East China Normal University, Shanghai 200062, p106. Last accessed on May 16, 2012 at {mqzhou,wxie,wnqian,ayzhou}@sei.ecnu.edu.cn, rongzhang@nict.go.jp.

[16] M. Armbrust, A. Fox, R. Griffith, A. Joseph, R. Katz, A. Konwinski, G. Lee, D. Patterson et al., "Above the clouds: A Berkeley view of cloud computing," University of California, Berkeley,Tech. Rep, 2009.

System Description Formation for University Blackboard Tool

Birendrasinh.K.Zala, Gandhinagar Institute of Technology, Gandhinagar

birendra.zala@git.org.in

Abstract: **A major challenge, and thus opportunity, in the field of usability engineering is developing effective system description for system which has no fixed guidelines. I present an exemplar system description report on University Blackboard Tool which is developed to establish effective channel of communication and collaboration to next phases of usability engineering are called system redesign and system evaluation. This paper will discuss all steps of system description for University Blackboard in a very general manner. The research method used is Formative Evaluation.**

Index terms: User Centered System Design (UCSD), Human Computer Interaction (HCI), Information and Communication Technology (ICT).

Keywords: Formative Evaluation, Mapping, System Domain, Usability, Task Characteristics.

I INTRODUCTION

HCI focus on verifying three main things like system is self learnable for users [1], complexity of interaction and filling the gap between the system image and user' model. To get success in all three factors we don't need to look around we already have one approach called User Centred System Design (UCSD) [2]. Domain area for this study includes University Blackboard Tool which specifies target system for users

➔ *SYSTEM DOMAIN*

Organizing and facilitating group work can be a daunting experience for students. They may be paired with students who have quite different timetables and work/study arrangements. Finding time to schedule meetings and effective methods of collaborating on work can be very frustrating. One thing all the students have in common is Blackboard. Blackboard has a number of features which try to support group work and organization independently. Firstly, there is the Group Area where tutors can create a private area for each group of students to carry out their own discussions and post

files. Secondly, there are the calendar and task tools. Students can add events and tasks to their own Blackboard calendars. In addition, lecturers can also add tasks for all students in their unit. The aim of this project is to develop an add-on for Blackboard (known as a Building Block) that will help students manage the process of group work. UCSD approach includes System Description phase which gather, identifies and specifies all basic requirements to produce a base for system redesign phase.

This paper discusses steps which performed during the system description formation of University Blackboard Tool. Formative Evaluation (both formal and informal) is an observational, empirical evaluation method that assesses user interaction by iteratively placing representative users in task-based scenarios in order to identify usability problems, as well as to assess the design's ability to support user exploration, learning, and task performance[3].

II CASE STUDY: A USER-BASED STUDY EXAMINING UNIVERSITY BLACKBOARD TOOL

One of the three phases of usability engineering will be explained in this part of paper with respect to one example system which is a Blackboard tool for a university they are developing for the faculty members and students.

➔ *SYSTEM DESCRIPTION*

The Group Work Tool (Blackboard Add-on) shall support students, lectures and tutors for academic purposes where group[4] or team work is involved. This is a type of groupware tailored suit the existing academic environment. Blackboard tool relies on the Internet. Also group related data can only be accessed by relevant group members. However, in some subjects the convener or tutor needs to assess each group member's contribution by viewing the group area. Assigned

staff members for the subject should be able to carry out this assessment as well.

This groupware should be able to provide non-collocated users to interact in synchronous or asynchronous manner. This product has to cater groups of varied interaction styles as group composition changes from one to another and it changes from assessment item to another. Therefore different communication mechanisms need to be present in this tool.

- Share messages among members, replying messages.
- Email facilities
- Instant messaging.

Moreover product shall support sharing documents via a central repository of documents and versioning of progressive documents. This product shall support setting appointments, managing events and calendar capabilities to setup meeting times so that students can perform their task in a timely and informed manner. In addition it allows task allocation for individual students so that group as a whole knows what the responsibilities of each student students

➔ CONCEPT MAPPING

The blackboard building block is tool, useful for the student in their course of study where he/she can store the files; communicate with the staff, student and the group mates. They can access the assessment, view the message board, messaging and email with this tool. The calendar that enables students to add events setup reminders on specific dates.
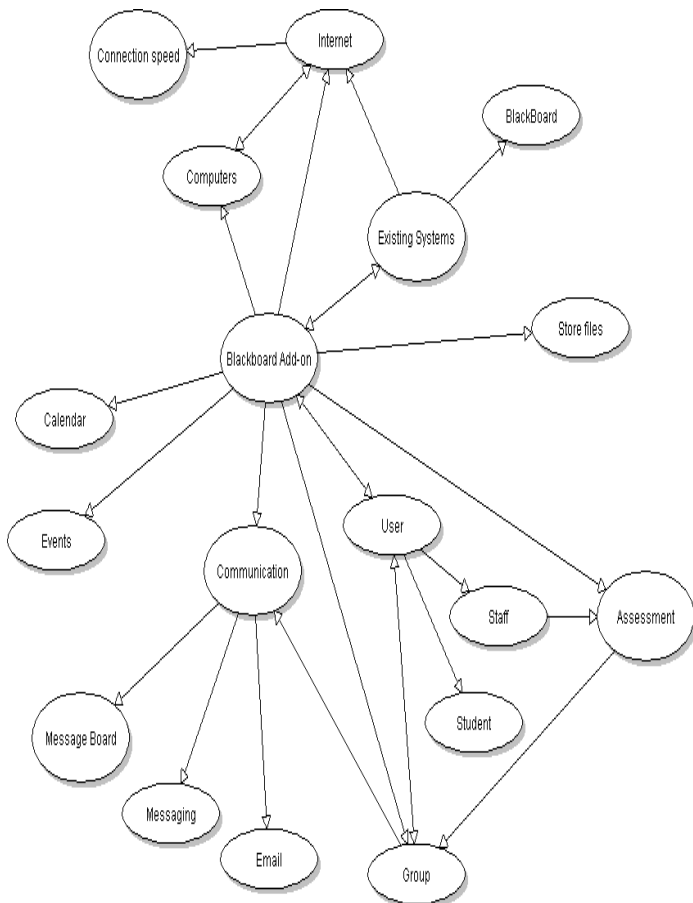

Figure.1. Concept mapping Design for Blackboard tool.

➔ USER DESCRIPTION

The primary users[4] if this system will be students. And Lecturers and tutors can be considered secondary users as they may use this product less frequently than students.

Table 1. User Profile: Student (primary user)

Attribute	User Characteristics
Age	18 – 35
Gender	Male (60%)/female (40%)
Physical abilities and disabilities:	Probably have small number of less-able students Vision – average - good (May have students with low level.) Hearing –good
Educational Background	Secondary (25%), Bachelors(55%)/ Masters (20%)/
Computing and IT experience	Novice/Intermediate/Experienced (Novice:0 to 3 months Intermediate : more than three months, less than one year Experience :more than one year) **Basic Computer skills** Generally good. Able to use office software. But new students may find it difficult at the beginning. ICT students tend to be more comfortable. **Experience with blackboard/ blackboard Group area** After few weeks into the studies at university, students can become comfortable. **Experience with other groupware tools (e.g. Outlook Express, Lotus Notes)** Novice, Intermediate Less likely to use full featured collaborative software.
Motivation	High (eg. they find it difficult to manage group assessments. Help of a tool is appreciated, some motivated by group environment) Moderate Low: some may not even like the idea of group work due to bad experiences.
Attitude	Positive (80%): As enabling tools for studies. Use of similar tools makes them comfortable.

	Quick learning ability. Can do attitude. May have confidence (20%): Impression of hard to learn may not like group work at all.

➔ *USER GOALS*

1. Lecturer
   - Form a group of students.
   - Communicate the student about updates of the assignment.
2. Student
   - Share a file with group members.
   - Send a message to the group members
   - Reply to a message sent by a group member.

➔ *TASK CHARACTESTICS*

Following are goals are represented as a sequence of tasks and the characteristics tasks involved.

Form a group of students.
1. Lecturer selects to create a group.
2. Select a student to join the group.
3. Add this student to the group.
4. Add more students to the group until desired number of students per group are reached.

➔ *ANALYSIS OF CURRENT SYSTEM*

According to our system domain primary user, Student had goals like according to previous analysis; Communication with students who are in the same group is one of the goals. Based on interviews conducted, we were able to find out the following problems. Interviews/observations were targeted on group activities

1. **Reluctance to use group area emailing facility**.
   Instead they use Web mail (Through Blackboard/directly) Reasons as per users
   - Does not look appealing.
   - More used to web mail as they use it more often.
2. **Lack of integration**
   When using web mail for communication with group members lack integration between backboard and web mail causes inconvenience. Instant switching from blackboard to web mail requires login with different credentials.

3. **Security.**
   In addition web mail credentials cannot be changed. It stays as student Id (username) and date of birth.

As students use web a mail for group work we will discuss the issues of web mail in relation to "Lack of integration and security".

➔ *USASBILITY METRICS*

Developers using Usability metrics to identified the problems in the system domain before the system releases.

Efficiency
- Time to learn on a specified task.
- Time to complete a specified task
- Time spent on errors
- Number of bugs

Based on the observations
- Time to learn on a specified task.
  User had good experience before using the web mail, like hotmail, MsOutlook. Not difficult to learn.
- Time to complete a specified task
  In relation to the selected goal, based on our observation, real user would have thought few steps to be unnecessary. Login twice, address book tasks. Completed fairly quickly took around (40-50s it was a short message)
- Time spent on errors
  The user had fairly good knowledge of the domain and knew how to fulfill the goal using web mail.
- Number of bugs
  During the observation did not come across any bugs/errors

Effectiveness
- Number of tasks completed (percentage)
- Workload of the specified tasks
- Ratio of success to failure

Based on the observations
- Number of tasks completed
  Completed around 7 for the selected goal, but user feels that can be reduces
- Workload of the specified tasks
  User felt it was a simple set of tasks, but can refine it more
- Ratio of success to failure
  Did not fail to complete the task

Satisfaction
- Rating scale of the usefulness of system domain
- Rating scale of the satisfaction of features
- Number of times real users express frustration and less satisfaction

Based on the observations
- On a scale of 1-5
- Rating scale of the usefulness of system domain: 4
- Rating scale of the satisfaction of features: 3
- Number of times real users express frustration and less satisfaction: 2

III CONCLUSION

At the end of system analysis some of the problems uncovered like Student feel lack of integration between two systems (blackboard and web mail). They find it inconvenient to login to web mail, switch back to blackboard to do some work and again to mail and so on even though it is link to blackboard. And Users can't change their default password which is a concern for the students. Security wise they have concerns. System description phase provides input to the next phase called system design report to help developers implement system better.

IV REFERENCES

[1] C. Abras, D. Maloney-Krichmar, and J. Preece, "User-Centered Design," In W. Bainbridge (Ed.), Encyclopedia of Human-Computer Interaction, Thousand Oaks, Sage Publications, 2004.

[2] J. Gulliksen, B. Goransson, I. Boivie, S. Blomkvist, J. Persson, and A. Cajander, "Key principles for user-centred systems design," Behaviour and Information Technology, 22(6), 2003, pp. 397-409.

[3] S. Sade, M. Nieminen, and S. Riihiaho," Testing usability with 3D paper prototypes—Case Halton system," Applied Ergonomics, 29 (1), 1998, pp. 67-73.

[4] C. Courage and K. Baxter," Understanding your users: A practical guide to user requirements, methods, tools and techniques," 2005, pp. 25.

[5] D. Bowman, J. Gabbard, and D. Hix, "A Survey of Usability Evaluation in Virtual Environments: Classification and Comparison of Methods," Presence: Teleoperators and Virtual Environments, vol. 11, no. 4, 2002, pp. 404-424

A SURVEY ON RECOMMENDING TAGS METHODOLOGIES

Prof. Brinda Parekh

(brinda.parekh@git.org.in)

Abstract—**With the Internet usage gaining fame and the stable growth of users, the World Wide Web has become a huge repository of data. The increasing volume of information on the Web is the main motivation for recommender systems: they support users while they interact with large information spaces, directing them toward the information they need.**

Social tagging is an innovative and powerful mechanism introduced with Web 2.0: it shifts the task of classifying resources from a reduced set of knowledge engineers to the wide set of Web users.

This paper is a survey which discusses the role of tags in recommender systems. The aim of this paper is to analyze the state of the art related to the role of tags in social tagging systems, specifying how tags are actually used by users, how recommender systems use tags for suggesting resources and how the process of tagging is supported by tag recommendations.

Index Terms— **Tag, social tagging, recommender system, personalization, Web 2.0.**

I. INTRODUCTION

Each day, the Internet grows by roughly a million electronic pages, adding to the hundreds of millions pages already online. As a result, Web users are always drowning in an "ocean" of information and facing the problem of information overload when interacting with the web. Because of speedy growth of the information, the resulting arrangement of information lacks of organization and structure. Users often feel confused and get lost in that information overload that continues to expand. Therefore, the crucial need nowadays is that of predicting the user needs in order to improve the usability and user retention of a web site. It is necessary for a Web developer or designer to know what the user really wants to do, predict which pages the user is potentially interested in, and present the customized Web pages to the user [2].

Web personalization is a strategy, a marketing tool, and an art [2]. The objective of a Web personalization system is to "provide users with the information they want or need, without expecting from them to ask for it explicitly" [3].

Web 2.0 applications are based on a set of technologies which provide users with tools for creating, sharing and promoting new content: users can easily leave the role of passive consumers of resources and become active producers of information. This trend increases both the knowledge on the Web and the number of available resources. Actually, the growing number of resources prevents an effective access to knowledge: a user needs to read the content of resources for evaluating if it is what she really wants to know. An effective classification of the resources can improve the access to knowledge.

Social tagging applications [4] allow users to freely associate labels (known as tags) to resources, distributing the task of classifying document over the set of Web 2.0 users. Social tagging systems do not require significant efforts: human classifiers do not have to follow specific rules and may classify only the set of resources they consider interesting.

Social tagging applications have both private and public aspects [4]:

• Users apply tags for personal aims: typically they associate labels to resources in order to find them again.

• Each user can enjoy the classification applied by other users. A user can browse available documents following classifications provided by other users.

However, due to the freedom of social tagging systems the classification process is not precise. This means that the classification applied by a user may be not useful to other users. In order to improve the access to resource classified in social tagging systems we needs of technologies able to overcome this limitation adapting the available classification to the specific user [1].

Recommender systems have been proposed for supporting users in social tagging system to sort resources which appear related to target users according to their interests and their tagging habits.

The aim of this paper is to analyze the state of the art related to the role of tags in social tagging systems, specifying how tags are actually used by users, how recommender systems use tags for suggesting resources and how the process of tagging is supported by tag recommendations.

The rest of this paper is organized as follows: Section II introduces social tagging and recommender systems; Section III deepens the discussion on the use of tags for recommending *content*, while Section IV illustrates the use of tags for recommending *tags*. Final considerations and a look to the future close the paper.

II. BACKGROUND

In this section we present an overview of social tagging and recommender systems, describing in particular how tags are applied by users, what are limitations connected to the tagging process, and how the recommender systems.

A. Social tagging systems

Social tagging is an innovative and powerful mechanism introduced with Web 2.0: it shifts the task of classifying resources from a reduced set of knowledge engineers to the wide set of Web users.

A *tag* is a term freely chosen by a user as significant for a resource; it represents a metadata describing the item, so it can be useful as a keyword to identify or to find again later a document. Tags are also the main mechanism used to browse and search new resources in social tagging systems.

The collection of all the tag assignments performed by a user constitutes her *personomy*, while the collection of all personomies constitutes a *folksonomy*.

Nevertheless, tags contain very useful, social/semantic information, and their nature can be better understood by analyzing the various motivations/goals that lead a user to perform tagging [5,6,7].

Common purposes are [1]:

- **Describe the content**. Tags may be used for summarizing the content of the resource.
- **Describe the type of the document**. Some users use tags for identifying the kind of document. A document may be classified according to its MIME type (for example pdf, doc) or taking into account the publication form (article, blog, book).
- **Describe features and qualities**. Adjectives (such as 'interesting', 'good', and so on) may be used for expressing opinions, emotions or qualitative judges.
- **Associate people to documents**. Tags can report the authors of a document or people involved in a particular task or event. Moreover, tags such as 'my', 'mycomments', 'mystuff', and so on are used to define a relationship between the resources and the tagger.
- **Associate events to documents**. Locations, dates, conferences acronyms are widely used for associating an event to a document.
- **Associate tasks to documents**. Some tags, such as 'mypaper', 'to read', 'jobsearch' reveal personal matters or engagements.

These possible motivations should be considered together with the following two further factors:

1. **Heterogeneity of users**. Taggers have different levels of expertise and goals. This has several consequences: classifications exploited by some users may be not understandable (or acceptable) for other users; different users may describe the content of a resource using distinct vocabularies; different users may have different opinions about a topic; users may not have knowledge about people, events or tasks associated to a resource by other users.

2. **Temporal changes**. Users' knowledge, motivations, and opinions may change over the time. A tag used today for describing an item can be useless in the future: emotions and opinions of people may change; reputation of people evolves; a topic may be not any more interesting to the user.

B. Recommender systems

The increasing volume of information on the Web is the main motivation for recommender systems: they support users while they interact with large information spaces, directing them toward the information they need [8]; these systems model user interests, goals, knowledge and tastes, monitoring and modeling some implicit and/or explicit feedback. User feedback can be acquired by means of ratings for quantifying a relation between the user and an item: the ratings may be explicit, when they require the user evaluation, or implicit when they are automatically generated by the system in terms of measures, such as, for example, the time spent by a user on a Web page. By taking in consideration the ratings provided by a user, a recommender system defines a personalized order of importance for the set of available resources.

According to the strategy used for collecting and evaluating ratings, recommender system can be classified into three main classes [1]:

1. **Collaborative filtering recommender systems**. Collaborative filtering recommender systems [9] implement the idea that a user, that shares interests, knowledge and goals with a community, with good probability may be interested in the documents which appear relevant to that community. For this reason, a collaborative filtering recommender system builds and maintains a profile for each user and computes similarities among users: similar users, known as *neighbors*, are the bridge which allows the user to receive suggestions for new potentially interesting content. In turn, collaborative filtering approaches can be classified into two classes [10]:

• *Model-based* approaches, which build a probabilistic model for predicting, on the basis of user history, her future rating assignments.

• *Memory-based* approaches, which use statistical techniques for identifying users with common behaviour. When the neighborhood has been defined, neighbors'feedbacks are combined for generating a list of recommendations.

2. **Content-based recommender systems**. Contentbased recommender systems [11] analyze the past user activities looking for resources she liked; they model resources extracting some features from documents. The user profile is then defined describing what features are interesting for the user. The relevance of a new resource for a user is calculated matching the representation of the resource to the user profile.

3. **Hybrid recommender systems**. The results returned by collaborative and content-based recommender systems can be combined in a hybrid recommender system [12], applying several different strategies:

• A *weighted* hybrid recommender system merges results of different techniques. The score of an item is defined as a

weighted sum of scores calculated by different recommender systems.

• A *cascade* hybrid recommender system filters a starting set of resources using a first recommender system. The ranking of these resources is then refined by a second recommender system.

• A *switching* hybrid recommender system uses one of the available recommender system according to some criterion.

• A *feature combination* hybrid recommender system considers collaborative data as the features used in content-based approaches.

III. RECOMMENDING TAGS

Recommender systems can suggest to the user not only content, by also tags for labeling for a resource: this typology of recommendation aims to improve the usage of social tagging applications [13]:

- Tag suggestions can *increase* the probability of having *tagged resources*. Users just select one or more suggested tags instead of summarizing a resource in order to find representative tags.

- Tag suggestions can promote a *common vocabulary* among users. Proposing a well defined set of tags it is possible to reduce problems connected to the absence of both guidelines and supervised methodologies to the tagging process.

The methodologies can be classified by means of three classes [14]:

• *Content-based tag recommender systems*. These systems look to the content of resources for suggesting relevant terms to the user.

• *Collaborative tag recommender systems*. Collaborative approaches analyze metadata associated by users to resources inferring the relevance of tags for the specific resource.

• *Graph based tag recommender systems*. These systems build a graph representation of a folksonomy which can be explored for finding tags to be recommended.

Different tag recommender systems use different criteria for evaluating the relevance of tags to be suggested. According to the relevance criteria tag recommender systems can be divided into two classes:

1. Not personalized tag recommender systems. These systems select for each document the best tags to describe the specific resource, ignoring user's tagging habits. Different users will receive the same suggestions for the same resource.

2. Personalized tag recommender systems. These systems suggest the set of the most relevant tags for a resource according to the specific user and her personal way to classify resources.

IV. FINAL CONSIDERATIONS

In this paper we described some important limitations of current social tagging systems, discussing the different methodologies applied by recommender systems for improving the access and the classification of resources. Summarizing, collaborative approaches model the user's tagging behavior

and look for users with similar tagging habits: these systems are based on the idea that users with similar interests search and bookmark similar resources. On the other hand, content-based approaches use tags to build a user profile and then suggest resources which appear relevant for the specific user profile. Both collaborative and content approaches have limitations mainly due to ambiguity of tags.

REFERENCES

[1] Antonina Dattolo, Felice Ferrara, Carlo Tasso," The role of tags for recommendation: a survey", Rzeszow, Poland, May 13-15, 2010.

[2] A.Jebaraj Ratnakumar ,"An Implementation of Web Personalization Using Web Mining Techniques". Journal of Theoretical and Applied Information Technology. Page 1, 2005.

[3] Brinda R. Parekh, Pooja Mehta, Prof. Kirit J. Modi, Prof. Paresh S. Solanki, "Web Personalization Using Web mining: Concept & Research Issues", International Journal of Information and Education Technology, Mumbai, 2012.

[4] Mathes, A.: Folksonomies cooperative classification and communication through shared metadata. computer mediated communication - lis590cmc. http://www.adammathes.com/academic/ computer-mediatedcommunication/folksonomies.html (2004)

[5] Golder, S., Huberman, A.: The structure of collaborative tagging systems. Journal of Information Science **32**(2) (2006)198-208.

[6] Dattolo, A., Tomasi, F., Vitali, F. In: Towards disambiguating social tagging systems. Volume 1, Chapter 20. IGI-Global (2010) 349–369.

[7] Xu, Z., Fu, Y., Mao, J., Su, D.: Towards the semantic web: Collaborative tag suggestions. In: Proceedings of the Collaborative Web Tagging Workshop at the World Wide Web Conference. (2006).

[8] Adomavicius, G., Tuzhilin, A.: Toward the next generation of recommender systems: A survey of the state-of-the-art and possible extensions. IEEE Transaction on Knowledge andData Engeneering **17**(6) (2005) 734–749.

[9] Schafer, J., Frankowski, D., Herlocker, J., Sen, S.: Collaborative filtering recommender systems. In Brusilovsky, P., Kobsa, A., Nejdl,W., eds.: The AdaptiveWeb. LNCS (4321).Springer-Verlag, Berlin, Germany (May 2007) 291–324

[10] Breese, J., Heckerman, D., Kadie, C.: Empirical analysis of predictive algorithms for collaborative filtering. In: Proceeding of the Fourteenth Conference on Uncertainty in Artificial Intelligence (UAI), Morgan Kaufmann (1998) 43–52.

[11] Pazzani, M.J., Billsus, D.: Content-based recommendation systems. In Brusilovsky, P., Kobsa, A., Nejdl, W., eds.: The Adaptive Web. LNCS (4321). Springer-Verlag, Berlin, Germany(May 2007) 325–341

[12] Burke, R.: Hybrid web recommender systems. In Brusilovsky, P., Kobsa, A., Nejdl, W., eds.: The Adaptive Web. LNCS (4321). Springer-Verlag, Berlin, Germany (May 2007) 377–408

[13] J¨aschke, R., Marinho, L., Hotho, A., Schmidt-Thieme, L., Stumme, G.: Tag recommendations in social bookmarking systems. AI Commununications **21**(4) (2008) 231–247

[14] Musto, C., Narducci, F., De Gemmis, M., Lops, P., Semeraro, G.: Star : a social tag recommender system. In: Proceedings of the ECML/PKDD 2009 Discovery Challenge Workshop.(2009)

Study and Review of Various Identity and Privacy Management Techniques in Consumer Cloud Computing

Archana N. Mahajan[#], Sandip S. Patil[*]

[#]*Research Scholar,* *Computer Engg Department* *S.S.B.T.'s College of Engg.& Tech.,*

North Maharashtra University Bambhori,Jalgaon(M.S.)
[1]*archanamagare@gmail.com*

[*] *Associate Professor in Computer Engg Department*
S.S.B.T.'s College of Engg. and Technology Bambhori, Jalgaon(M.S.)
[2] *san_78004@yahoo.co.in*

Abstract— **Consumer cloud computing is the result of expected evolution and integration of advances in several areas such as distributed computing, service oriented architecture, and last but not the least consumer electronics. We can say that integration of consumer electronics that is home networks with cloud computing is known as consumer cloud computing. In this paper we are presenting abstractive study of identity and privacy management in consumer cloud computing. In the consumer cloud environment, all attention and energy is given to distribution of information and heterogeneity of clouds but less attention is given to security and identity management challenges in this context.**

Keywords— **Consumer cloud computing, Identity Management, SAMLv2, dynamic federation establishment,Privacy.**

I. INTRODUCTION

Cloud computing is a large scale distributed computing model in which computing resources are available to cloud consumers via Internet. The key characteristics of the cloud are the ability to scale and provision computing power dynamically in a cost efficient way and the ability of the consumer (end user, organization or IT staff) to make the most of that power without having to manage the underlying complexity of the technology. The cloud architecture itself can be private (hosted within an organization's firewall) or public (hosted on the Internet). The consumer cloud computing platform is a networked collection of servers, storage systems, and devices in order to combine software, data, and computing power scattered in multiple locations across the network. Consumer cloud computing offers resources as services that are more flexible, scalable, affordable and attractive to customers and technology investors. Thus consumer cloud computing enables different applications related to consumer electronics (CE), such as virtualization of consumer storage, CloudTV platforms that provide access to a number of Web applications such as social networking, user generated video games, etc[1].

II. IMPORTANCE OF IDENTITY MANAGEMENT IN CONSUMER CLOUD ENVIRONMENT

Service providers use infrastructure provided by Cloud Computing provider to provide their services to their customers. While using these services, consumers provide the service providers with sensitive data such as civil ID (name), SSN number, credit card information in order to have access to these online services. Current privacy laws require cloud computing service providers to implement varied security measures depending on the nature of the information. However, consumers can not verify that a provider of a service conform to the privacy laws and protect their digital identity. Given this, a consumer has to decide as what type of personal information they could provide.

For example, a "Twitter breach of information stored on Google Apps" shows the implications of leakage of private information in cloud security. The July 15 disclosure by Twitter exposed that a hacker had accessed a substantial amount of company data stored on Google Apps. First the hacker hijacked a Twitter employee's official e-mail account. Then, he took advantage of poor password practices, Hotmail's inactive account feature and personal information on the Web to access hundreds of Twitter documents. This probes the weakness of the username/password security token used by most service providers to authenticate consumers, which leaves the consumer susceptible to phishing attacks. [2] Many organizations are uncomfortable with storing their data and applications on systems they do not control. Migrating workloads to a shared infrastructure increases the potential for unauthorized exposure. Consistency around authentication, identity management, compliance, and access technologies will become increasingly important. To reassure their customers, cloud providers must offer a high degree of transparency into their operations.

A. *Identity management and authentication in consumer cloud computing*

In the consumer cloud environment, all attention and energy is given to distribution of information and heterogeneity of clouds: private, community, public, and hybrid but less attention is given to security and identity management challenges in this context. For example, users in a private cloud should be able to access applications hosted in a

community cloud as long as a trust relationship exists between cloud domains, which represents different forms of their identities. This is due to cloud scenarios are multi-provider and multi-service. Also applications in cloud computing may combine data from multiple cloud-based sources, which hold different conditions of service, privacy policies, and location.

Thus, because of the distributed and open nature of cloud environments, it is necessary to dynamically propagate trust for managing digital identity related to access control, reputation, anonymity and privacy in different domains in a protected and flawless manner.

For this purpose, federated Identity Management (IdM) has developed. This helps for enabling global scalability which is required for the successful implantation of cloud technologies. Federated identities are based on the user-centric profiles, which protect consumers from cloud computing services.

In the context of consumer electronics, federations of clouds have right to alter how CE device applications are developed, deployed or used while simultaneously removing constraints on device functionality; into home private clouds, public clouds, etc. For example, consider a consumer cloud scenario, in which cloud federation allows Alok to build different layers in his car navigation map to get recommendations for the best routes (CSP1); as well as consult relevant information on sites close to his position, in a Cloud Tourist Information Provider (CSP2), by means of the cooperation between his mobile and the car navigator. In addition, Alok can connect to his Social Network (CSP3) to see if some friends have been on that site and share information with them without compromising his privacy [1]. However, federated IdM systems not have mechanisms to achieve agile and dynamic federation, which is one of the most significant architectural issues. Dynamic federation requires allowing agile decision making without requiring static pre-configuration. There are various standards for federated IdM which include privacy considerations, but they do not cover all aspects related to anonymity, pseudonyms or tracking.

In addition, current IdM specifications support partial anonymity, define poor privacy policies or they are complex to implement. A similar situation can be found in the case of audit mechanisms.

B. Existing identity management tools

Some known identity management tools are as follows: -
1. OpenID[May 2005]
The original OpenID authentication protocol was developed in May 2005 by Brad Fitzpatrick, creator of popular community website LiveJournal. Initially referred to as Yadis (an acronym for "Yet another distributed identity system"), it was named OpenID after the openid.net domain name was given to use for the project. With OpenID a user uses one username and one password to access many web applications. The user authenticate to an OpenID server to get his/her OpenID and use the token to authenticate to web applications. A user of OpenID does not need to provide a service provider with his credentials or other sensitive information such as an email

address. OpenID is a decentralized authentication protocol. No central authority must approve or register service providers or OpenID Providers. An end user can freely choose which OpenID Provider (OP) (OpenID Authentication server on which a service provider relies to assert the authenticity of the identity of the consumer) to use, and can preserve their Identifier if they switch OpenID Providers.

OpenID is highly at risk to phishing attacks, as the whole OpenID structure hinge on the URL routing to the correct machine on the Internet i.e. the OpenID Provider. A user who visits an evil site (through conventional phishing or DNS cache poisoning), sends the fraud service provider her URL. The provider consults the URL's content to determine the location of her OP (OpenID provider). Instead of redirecting the user to the legitimate OP, it redirects her to the Evil Scooper site. The Evil Scooper contacts the legitimate OP and pulls down an exact replica of its login experience (it can even simply become a "man in the middle"). Convinced she is talking to her OP, the user posts her credentials (username and password) which can now be used by the Evil Scooper to get tokens from the legitimate OP. These tokens can then be used to gain access to any legitimate Service Provider. [2]

2.Zero-Knowledge Proof [Selective Disclosure and Anonymous Credential][1985]
Zero-knowledge proofs were first conceived in 1985 by Shafi Goldwasser, Silvio Micali, and Charles Rackoff in a draft of "The Knowledge Complexity of Interactive Proof-Systems".

In an identity management system, two parties negotiate to establish trust through sensitive data exchange. The negotiation process should protect user's private information. The private data could be personal data pertaining to the user, certificates, unspecified credentials of the user, or private keys. Traditional certificates and tokens offer a weak trust model. The negotiation and data exchange process should protect the user's real identity by using a more advanced cryptographic private-certificate-based mechanism such as selective disclosure and zero knowledge proofs (ZKPs) [2].

The ZKP approach allows proving a claim or assertion without actually disclosing any credentials. A solution using a ZKP works as follows: a service requires a user to be over 18. The user wants to satisfy the relying party's technical policy but tell the party nothing or as little as possible. He need not to reveal his date of birth, just needs to somehow prove being over 18. [2] The purpose of ZKP protocols is to help a prover convince a verifier that she holds some knowledge (usually secret), without leaking any information about the knowledge during the verification process (zero-knowledge). The concept of ZKP has been working in many authentication and identification protocols. [4]

3. Federated Identity Management [2003]
Federation allows sharing and distributing attributes and identity information across different administrative domain according to certain established policies. Current frameworks are not suitable for dynamic environments because the trust model are poorly defined or out of the specifications scope.

Current framework dependents on pre-configuration between Service Providers and Identity Providers. [3]

III. REVIEW OF IDM AND PRIVACY IN CONSUMER CLOUD COMPUTING

An Enhanced Client Profile (ECP) [1] which is an extension to SAMLv2 for providing an efficient identity management in consumer cloud computing as well as dynamic, autonomic, and user-centric establishment of cloud federations.

Even though current works allows sharing media, cloud services and personalized content by means of a user-centric approach using different authentication and authorization mechanisms, none of the earlier works deals with dynamic federated identity management along with privacy tools in the consumer cloud computing scenarios. The existing work presents an authentication framework for consumer electronic devices, in order to share personal cloud services allowing users for the time being to transfer their services and content rights within trusted environments. The main idea is that "the home network experience must become mobile and the means to achieve this is to authenticate people, rather than devices".
A zero-knowledge proof technique is used for preserving user's privacy in the process of providing his identity. Zero knowledge proof technique is one which achieves the cloud service provider's robustness against attempting to gain knowledge about user's privacy.

However, this approach only deals with privacy concerning services and dynamism in the management of trust relationships is not taken into considerations. A zero-knowledge proof mechanism also helps for authentication of an entity in a virtual machine.

PRIVACY: - Privacy management is an important factor for consumer cloud computing. But the solution for privacy management should be compliant with laws passed by a government. This enhances user's trust when accessing to this kind of environments through their CE devices. Pearson[1] suggests various guidelines and techniques on designing privacy-aware IdM architectures for cloud services. They are as follows:-

1. Minimizing customer personal information sent to and stored in the cloud.
2. Protecting sensitive customer information.
3. Maximizing user control.
4. Allowing user choice.
5. Specifying and limiting the purpose of data usage.
6. Providing the customer with privacy feedback.

A. Dynamic Federation between Cloud Providers

The Dynamic trust establishment is the fundamental and mandatory issue in order to achieve usability and scalability in consumer cloud computing. Nowadays there is still not much work done in this field.

The related work in this area defines a three-phase cross-cloud federation model based on SAML and agent technologies, but it does not specify how to carry out trust establishment between unknown cloud providers.

Moreover, approaches related to trust management in distributed environments can be found for peer to-peer systems only. This form the foundation for emerging next generation computer applications. The related work uses reputation based on global scope and local scope according to the familiarity-based personal relationships on a community to assign trust values.

B. SAMLv2

Secure Assertion Markup Language (SAML) version 2, X.509 and OAuth are the standards which the first come forward for the federation are now coming to undertake cloud security challenges posed by identity management.

SAMLv2 defines an XML-based framework to allow the exchange of security assertions between entities. These security assertions are about authentication, authorization decision, and attributes. This specification is based on ID-FF (Identity Federation Framework) from Liberty Alliance. The aim behind this is to establish open standards to easily carry out online transactions while protecting the privacy and security of identity information. These standards allow identity federation and management through attributes such as account linkage, and profiles, particularly for the simple session management such as Single Sign-On (SSO) and Single LogOut (SLO).

In such Identity Federation there are
Service Providers (SPs):- Entities using identity data issued by a trusted third party (TTP),
Identity Providers (IdPs):- Entities which give asserting information about a subject,
Users: - that are the subjects of the assertions.

Creation of Identity federation is the establishment of trust relationships between SPs and IdPs through the formal contracts. The identity federation establishment is without input from consumers. It also creates the circles-of-trust (i.e. a trust domain). The federation establishment requires exchange of metadata by metadata's providers. This metadata contains identifiers, public key certificates, service attributes, etc. These all are needed for the location and secure communication between providers' services. This metadata is available only to IdP (Identity Provider). Due to this IdPs can support many SPs in a distributed fashion. They can also focus on managing identities, access control policies, security token issuing, etc. In addition, enhanced users (ECPs) could be introduced in order to take part of a federation. In this, the user acts as a mediator between providers. ECP also helps to authorize the user's role respect to the privacy, because user makes decisions over data control.

C. X.509

X.509 is the well-known key management infrastructure through digital certificates for authentication. It is widely deployed as security standard currently. SAML and ID-FF take over and balance the static vision of trust from PKI(Primary key Infrastructure), because trust relationships are also derived by formal contracts between Certification

Authorities (CAs), Registration Authorities (RAs), and end users. Such relationships are managed by the creation of trusted anchor lists, similar to the circles-of-trust (CoT) in federated environments.

D. OAUTH

OAuth 2.0 Authorization Protocol is an open protocol which allows using any underlying authentication system. OAuth allows users sharing verifiable assertions (i.e. security tokens) about themselves instead of sharing any personal information. This protocol simplifies access to protected data while protecting the owner's account credentials. It also includes SSO scenarios between SPs. OAuth and SAML together form primary federation. They allow mechanism for token management between the actors involved in a transacti*on.*

IV. TRUST AWARE IDM ARCHITECHURE [1]

This IdM infrastructure has the functionality to allow Identity Providers (IdPs), Service Providers (SPs), and enhanced clients to share common knowledge. The ECP (Enhanced Client Profile) has been defined especially for consumer cloud computing. This ECP gives the required user-centric approach needed for consumer electronics. The ECP is a software element which minimizes direct interactions between SPs and IdPs, and provides full control to users over their identities, thereby improving mainly privacy.
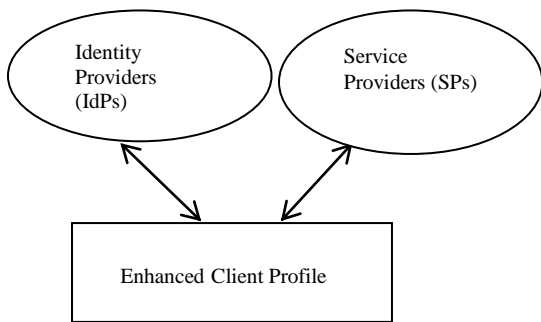
Figure 1: Role of ECP

The planned architecture for the dynamic IdM system is represented in Figure 2.
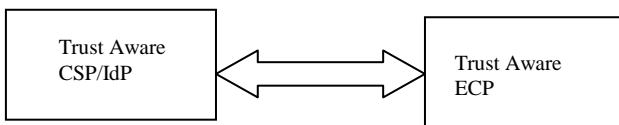
Figure 2: Enhanced Privacy and IdM Architecture for Consumer cloud

The layered architecture of Trust aware CSP/IdP is shown in figure 3.
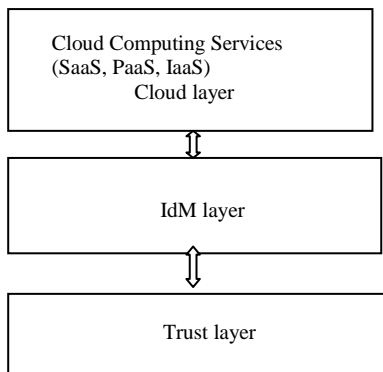
Figure 3: Trust aware CSP/IdP

The layered architecture for trust aware ECP is as shown in figure 4.
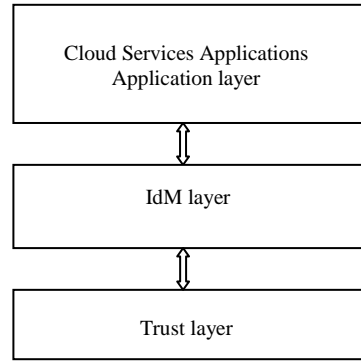
Figure 4: Trust aware ECP

At the top of the architecture for CSP/IdP or ECP there is the Cloud or the Apps layers. The first one contains cloud services offered by cloud providers (SPs or IdPs). The second one is located on the ECPs, containing client applications.

The second layer is the IdM layer, which gives the basic functionality of each role defined in the SAMLv2 specification. In addition, such basic functionality is extended by adding the Privacy Engine module.

Finally, there is the Trust layer*,* focusing on the reputation manager in order to allow secure interaction between unknown parties. This last layer combines reputation information with other related data, for instance, historical interactions. So the user can request access, through the ECP installed on his mobile, to services provided by SPs and IdPs. IdM Layer.
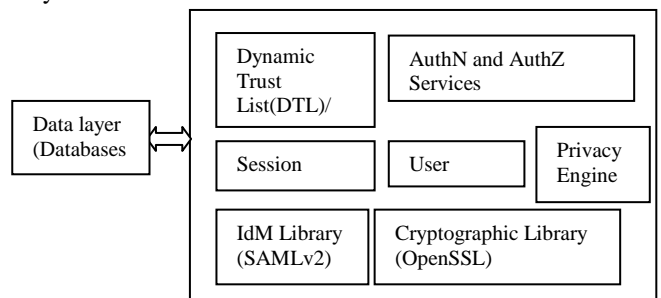
Figure 5: The IdM layer of Trust Aware
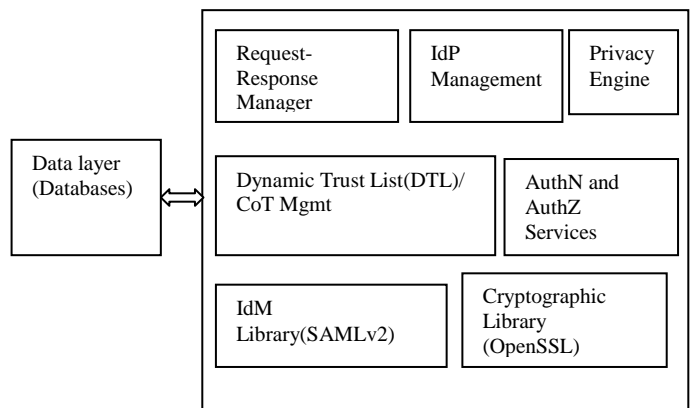
Figure 6: The IdM layer of ECP

The figures 5 and 6 show the IdM layer of CSP/IdP and ECP respectively.

The common core modules of IdM layer to both CSP/IdP and ECP are as follows:-

1) Dynamic Trust List (DTL)/CoT Management:-The function of this module is to maintain an Updated circle of trust, which contains more complete information than traditional certificate lists, such as trust level, previous interaction results, reputation scores, keys, etc. This trust information is automatically updated through modules in the Trust layer.

2) AuthN and AuthZ Service Management:- The function of this module depends on its location. So, it receives and processes the <AuthnRequest> messages from either the SP or the ECP, regarding to the ECP or IdP, respectively. In the CSP, it issues such authentication and authorization request. The modules in each unit i.e. either in ECP, IdP, CSP interacts to verify the user requesting a service is really who he claims. For this purpose, it supports multiple authentication mechanisms including PKI, username/password, etc.

For authorization process, the security assertions and the attributes exchanged informs about authentication decisions, profiles and attributes to cloud services providers which help them to decide what services or resources the user can access. For that, this module issues (IdP) or verifies (SP), and manages SAML authentication assertions and attribute statements. The aim is to assist authentication and user management to users and cloud services. Thus improving user experience while reducing complexity and management costs.

3) Privacy Engine:-The functionality of this module is managing user identifiers (e.g. pseudonymous) and monitoring how user data is being accessed without compromising user's identity. For this purpose, the fields that are logged by monitoring tools and verified by audit tools show the auditor what information about the user is being accessed without exposing the actual information. Thus, this module provides multiple and partial identities, which allows users to access cloud services and share digital content without revealing their name and true identity to everyone. The use of different pseudonyms enables to support differing ranges of identification and authentication strengths.

These modules are supported by basic libraries such as IdM and cryptographic, which implement SAMLv2/ID-FF functionalities and cryptographic algorithms and protocols, respectively.

In the user's side, these libraries implement the minimal functionality, taking into account limited devices. Thus, ECP incorporates "lite" library versions.

At the provider's side, there are also other two additional modules whose functionality is specific to service provision:

1) Session Management (SM):- This module has the responsibility of managing user identifiers, as well as the session data of those users accessing CSPs or IdPs services. The CSP together with IdP checks when user's session is active. The CSP creates session identifiers for every user once user has already been authenticated and registered in the service. Such session identifiers are linked to users' profile. SM also may check several user profiles and select the most proper content for a specific service (e.g. video on demand). Thus, the SM communicates with other modules managing authentication and attribute exchange. It also interacts with the User Management module to request the user's profile, related to the cloud services, and matches it with the cloud profile policy and any other imposed IdP policies. Finally, this module may also request information about the device profile in order to support multi-device SSO.

2) User Management (UM):- This module is used for storing credential, management users' profiles according to their preferences and policy enforcement. Regarding credential management, the user can store his credentials (e.g. username/passwords, digital certificates, etc.) that are required by cloud applications that can be accessed from the Personal Cloud (PC): TV services, social networks, payment services, etc.

The ECP also contains other two additional modules whose functionalities are:

1) IdP Management: - This module coordinates with the DTL/CoT Management and the trust layer to configure trust relationships with the IdPs in a dynamic and secure manner. Also, it is responsible for determining the most satisfactory identity provider depending on the requested service, the user's preferences related to privacy and security (e.g. type of credential) and the context. For example, in some contexts the user may not want to disclose any personal information, whereas in other contexts he may wish for partial or full disclosure of identity. To accomplish these tasks, this module collaborates with the Request-Response Manager and the Privacy Engine.

2) Request-Response Manager:- This module receives authentication, authorization or attribute requests from the applications. This module provides the interface between Authn and Authz Service and applications. These requests can be initiated by authentication request statements from the SP.

V. TRUST LAYER IN BOTH CSP/IDP AND ECP[1]
The Trust Layer consists of three components: The Reputation Manager (RM), the Evidence and Risk Manager (ERM), and the Trust Manager (TM) as shown in the figure 4.7.
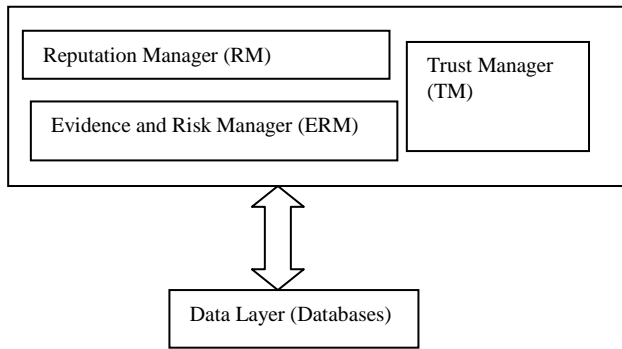
Figure 7 Trust Layer in CSP/IdP and ECP

1) RM (Reputation Manager):- The RM is responsible for distributing, collecting and managing requests and responses of reputation to federate. The protocol is explained in the next section. The RM is connected to the ERM module to analyze the risk factors associated with each transaction and keep a history of past interactions.

2) ERM (Evidence and Risk Manager):- It calculates the trust value associated to each entity, and includes the trust evolution, as this will change over time.

3) TM (Trust Manager):- It organizes the communications and operations of the described modules, and manages the trust data repository. It is responsible for managing dynamically trust information, negotiating the trust relationship establishment, and providing trust data to other layers. The trust information contains data related to the entities' behaviour and external trust information from trusted third parties, thus it takes advantage of the common knowledge in the federation. Finally, the TM is also augmented with more complex functionality, such as context and policy management for making richer decisions depending on the actions defined by policies and context in each specific situation.

VI.DYNAMIC FEDERATION ESTABLISHMENT

Reputation can be considered as a collective measure of trustworthiness based on the referrals or ratings from members in a community [1]. Adding reputation support to SAML implies modifications to both Assertions and Protocols. Here a new assertion is defined. Such assertion is a custom statement type, called [1] <ReputationStatement>, which is conveyed in a response message. The structure of such reputation assertion has an initial part (i.e. header), whose content is the same defined in the standard. This common section includes the assertion identifier (ID), the names of the issuer and the subject, and information about the instant in which the assertion was issued. The <Subject> tag, in our case, indicates the identifier of the entity for which reputation data has been requested.

Apart from this information, the statement contains
a body section, which contains all the related data to the reputation metric.

These include the following attributes:
ReputationInstant, to ensure data freshness;
ReputationScore that corresponds to the reputation value;
DistributionFunction, for the reputation to be aggregatable;
Context, to illustrate for what situation the reputation was made.

This <ReputationStatement> is exchanged using the SAML "Assertion Query and Request Protocol". So query/response formats are as per the rules defined.

The communication flow has the following steps:

1. Alok accesses a service offered by a CSP2. The CSP2 needs to authenticate Alok, so it performs IdP discovery for determining who should be asked for user authentication. This checks local configuration data to see if the discovered IdP is known (i.e. metadata stored).

2. As CSP2 determines IdP1 is unknown, the RM executes the logic to gather reputation information about it. This sends a <ReputationRequest> acting as a Reputation Requester.

3. The IdP2 and CSP1 returns a <ReputationResponse> containing a <ReputationStatement> in case of success, or an error message in case of failure. These entities would be a Reputation Responder. As IdP1 is trusted in accordance with the reputation information received, then the CSP2 downloads IdP1 metadata and initiates SSO as usually.

4. The CSP2 requests Alok's authentication to IdP1.

5.I dP1 authenticates Alok and sends the successful authentication response to the CSP2.

6. Finally, the CSP2 grants service access to Alok.

Here the aim is to demonstrate that collecting external information allows flawless trust establishment and facilitates this kind of interactions, otherwise impossible or insecure. We have worked with a simple SAML-based SSO scenario: a user, two CSPs, and two IdPs. In this situation, CSP2 and IdP1 are unknown, so CSP2 requests information about IdP1 to trusted providers such as IdP2 and CSP1. This same situation using SAML without the proposed extension, CSP2 and IdP1 will not interact, or they will require manual intervention from administrators to configure both ones.

VI.CONCLUSION

A privacy enhanced and trust-aware IdM architecture compliance with SAMLv2/ID-FF standards is used to provide an efficient identity management and access control, as well as dynamic, autonomic, and user-centric system for better scalability in consumer cloud computing services. With the addition of reputation information and the introduction of the Trust-Aware ECP, mobile users may take part in the cloud federation in a more active way. Similarly, the presented reputation extensions allow the cloud providers to make richer trust decisions when interacting with unknown entities. In regard to privacy, the privacy enhanced and trust-aware IdM system allows users to access cloud services and share digital content without essentially revealing their true identity to everyone. Besides, privacy enhanced and trust-aware IdM provides a framework that facilitates to keep to a trace-off

between user's privacy and degree of tracking to obtain an enough personalization degree in the different services. Finally, privacy engine enables users to have enhanced awareness over their online identity use by introducing monitoring tools and an audit service focused on data sharing through the Personal Cloud. In future the optimal values of parameters of reputation model can be validated.

REFERENCES

[1] Rosa Sánchez, Florina Almenares, Daniel Díaz-Sánchez, and Andrés Marín, "Enhancing Privacy and Dynamic Federation in IdM for Consumer Cloud Computing", IEEE Transactions on Consumer Electronics, Vol. 58, No. 1, pp.95-103, February 2012.

[2] Bharat Bhargava, Noopur Singh, and Asher Sinclair, "Privacy in Cloud Computing Through Identity Management" ,Computer Science, Purdue University, Electrical and Computer Engineering, Purdue University, pp.25-31, December 2011.

[3] Patricia Arias, Florina Almenárez, Andrés Marín and Daniel Díaz-Sánchez "Enabling SAML for Dynamic Identity Federation Management", Second Joint IFIP Wireless and Mobile Networking Conference, pp.1-21, September, 2009.

[4] Li Lu, Jinsong Han, Yunhao Liu, Lei Hu, Jinpeng Huai, Lionel M. Ni, and Jian Ma Ab "Pseudo Trust: Zero-Knowledge Authentication in Anonymous P2Ps", *IEEE Transactions On Parallel And Distributed Systems,* VOL. 19, NO. 10, pp.1325-1337, October 2008.

Performance Analysis of a Sub-Optimum Transmit Antenna Selection Scheme with M-PSK and M-QAM Constellations

Jatin M. Chakravarti, Mitul P. Maniar

(Email: jatin.chakravarti@git.org.in, mitul.maniar@git.org.in)

Abstract—We consider a sub-optimum transmit antenna selection (TAS) scheme in multiple input single output (MISO) systems equipped with N transmit antennas. We keep one antenna fixed and select the best among the remaining $N-1$ antennas. We assume spatially independent flat fading channel with perfect channel state information (CSI) at receiver and an ideal feedback link. We use Alamouti transmit diversity and derive the closed-form expressions of symbol error rate (SER) for M-ary Phase Shift Keying (M-PSK) and M-ary Quadrature Amplitude Modulation (M-QAM) constellation.

Index Terms—Alamouti transmit diversity (ATD), symbol error rate (SER), M-ary Phase Shift Keying (M-PSK), M-ary Quadrature Amplitude Modulation (M-QAM), transmit antenna selection (TAS).

I. INTRODUCTION

Space-time block codes (STBC) [1] have been used in multiple input multiple output (MIMO) systems to eliminate the effects of fading by providing diversity gain. However, each antenna requires one RF chain, which increases the cost and complexity of the overall wireless communication system.. Therefore, Antenna selection (AS) [3]-[7] has been proposed and discussed in the literature. AS helps in retaining the full diversity order of the MIMO systems with reduced RF chains [6].

In the above-mentioned papers, optimum AS algorithms have been used which are of full complexity. To remove this complexity, some sub-optimum AS algorithms have also been proposed and analyzed in the literature. Three sub-optimum schemes have recently been proposed in [4], [5] and [9] to reduce feedback rate compared to the optimum TAS scheme [3].

The evolution of wireless communication systems follows the need for high data rates, measured in bits/sec (bps) and with a high spectral efficiency, measured in bps/Hz. This can be achieved by using M-PSK and M-QAM digital modulation schemes. In this paper, we have derived the closed form expression of SER of M-PSK and M-QAM constellation for the sub-optimum scheme given in [9]. In [9], the authors have derived the closed form expression of BER for BPSK constellation.

The remainder of the paper is organized as follows. The system and channel models are explained in Section II. In Section III we present closed form expression of SER for M-PSK and M-QAM constellation. Section IV deals with simulations and results. Finally, we present conclusions in Section V.

II. SYSTEM AND CHANNEL MODELS

We consider a wireless link in a flat Rayleigh fading environment equipped with N transmit antennas and one receive antenna. A block diagram of the considered system is shown in Fig. 1. The channel fading coefficients h_i between transmit antenna i and the receive antenna is denoted by $1 \leq i \leq N$, are spatially and timely independent identically distributed (i.i.d.) circularly symmetric complex Gaussian random variables with zero mean and unit variance.

We assume that the channel remains constant for at least two consecutive instants. We use Alamouti transmit diversity [2] for which the received symbols can be represented as

$$\begin{bmatrix} y_1 \\ y_2^* \end{bmatrix} = \begin{bmatrix} h_m & h_f \\ h_f^* & -h_m^* \end{bmatrix} \begin{bmatrix} x_1 \\ x_2 \end{bmatrix} + \begin{bmatrix} n_1 \\ n_2^* \end{bmatrix} \quad (1)$$

where the superscript $*$ denotes the complex conjugate. x_1 and x_2 are transmitted data symbols for BPSK modulation scheme with an average power of $E_s/2$, i.e. $x_1, x_2 \in \{-\sqrt{E_s/2}, \sqrt{E_s/2}\}$ and $n_i \sim \mathcal{CN}(0, N_0)$ for $1 \leq i \leq 2$ is AWGN noise. y_1 and y_2 are received symbols.

In (1) h_f is the channel between the fixed transmit antenna and receive antenna, whereas h_m is the channel between the selected antenna among the remaining $N-1$ transmit antennas. The selection of antenna is based on the maximization of received SNR, which can be expressed as

$$m = \arg \max_{1 \leq i \leq N-1} \{|h_i|^2\}$$

The receiver feeds back the index (m) via a dedicated ideal link. Here, ideal link denotes zero delay and noiseless.

At the receiver, the resulting decision variables for both symbols are denoted as [2]

$$\widehat{x_1} = [h_m^* \quad h_f] \begin{bmatrix} y_1 \\ y_2^* \end{bmatrix}$$

$$\widehat{x_2} = [h_f^* \quad -h_m] \begin{bmatrix} y_1 \\ y_2^* \end{bmatrix}$$

where $\widehat{x_1}$ and $\widehat{x_2}$ are the decision variables for data symbols x_1 and x_2 respectively.

III. Performance analysis

In this section, using closed form expression of received SNR in [9], we obtain exact expression of SER for M-PSK and M-QAM constellations.

We assume that both x_1 and x_2 are equally probable. Hence, we can express the instantaneous SNR (γ) per bit as

$$\gamma = \|\mathbf{H}\|^2 \gamma_c \qquad (2)$$

where $\mathbf{H} = [h_m \ h_f]^T$ and $\gamma_c = E_s/2N_o$. Now, the pdf of γ is derived in [9] as

$$p_\gamma(\gamma) = \frac{N-1}{\gamma_c}\left[\frac{\gamma}{\gamma_c}e^{-\frac{\gamma}{\gamma_c}} + \sum_{k=1}^{N-2}(-1)^k\left(\frac{1}{k}\right)\binom{N-2}{k}\right.$$
$$\left.\left\{e^{-\frac{\gamma}{\gamma_c}} - e^{-\frac{\gamma(1+k)}{\gamma_c}}\right\}\right] \qquad (3)$$

A. SER for M-ary PSK Modulation

The SER for M-PSK constellation can be represented as [13]

$$P_e = \frac{1}{\pi}\int_{\theta=0}^{\frac{\pi(M-1)}{M}}\int_{\gamma=0}^\infty p_\gamma(\gamma)e^{-\frac{\sin^2(\pi/M)\gamma}{\sin^2(\theta)}}d\gamma.d\theta \qquad (4)$$

where M is the number of symbols transmitted. SER can be derived by substituting (3) in (4)

$$P_e = N-1\left[\frac{M-1}{M} - \frac{1}{\pi}\sqrt{\frac{C_1}{1+C_1}}\left\{\left(\frac{\pi}{2}+\tan^{-1}(\alpha_1)\right)\right.\right.$$
$$\times\left(1+\frac{1}{2(1+C_1)}\right) - \frac{\sin(2\tan^{-1}(\alpha_1))}{4(1+C_1)}\right\} + \sum_{k=1}^{N-2}$$
$$\times\frac{(-1)^k}{k}\binom{N-2}{k}\left(\frac{M-1}{M}\right)\left[1-\sqrt{\frac{C_2}{1+C_2}}\right.$$
$$\times\left(\frac{M}{(M-1)\pi}\right)\left(\frac{\pi}{2}+\tan^{-1}(\alpha_2)\right)\right] - \sum_{k=1}^{N-2}$$
$$\times\frac{(-1)^k}{k(1+k)}\binom{N-2}{k}\left(\frac{M-1}{M}\right)\left[1-\sqrt{\frac{C_3}{1+C_3}}\right.$$
$$\left.\left.\times\left(\frac{M}{(M-1)\pi}\right)\left(\frac{\pi}{2}+\tan^{-1}(\alpha_3)\right)\right]\right], \qquad (5)$$

where

$$C_1 = C_2 = \gamma_c\sin^2(\pi/M);$$
$$C_3 = \frac{\gamma_c}{1+k}\sin^2(\frac{\pi}{M});$$
$$\alpha_i = \sqrt{\frac{C_i}{1+C_i}}\cot(\frac{\pi}{M}), \quad 1\le i\le 3.$$

For the special case of $M = 2$ (BPSK), the above expression matches the equation no. (9) of [9]
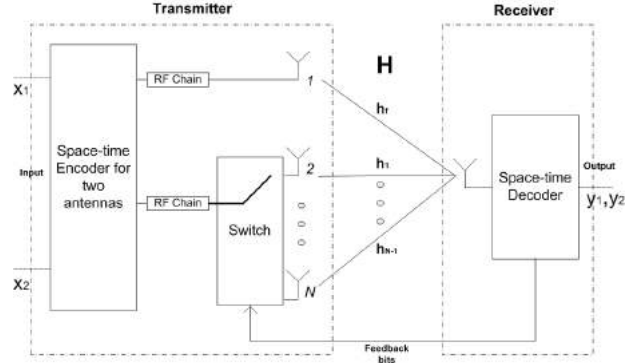
Fig. 1. Block diagram of an Alamouti transmit diversity system with sub-optimum $(N, 2; 1)$ TAS scheme

B. SER for M-ary QAM Modulation

The SER for M-QAM constellation can be represented as [13]

$$P_e = \frac{4}{\pi}\left(1-\frac{1}{\sqrt{M}}\right)\int_0^{\frac{\pi}{2}}\int_0^\infty p_\gamma(\gamma)e^{-\frac{3\gamma}{2(M-1)\sin^2(\theta)}}d\gamma d\theta$$
$$-\frac{4}{\pi}\left(1-\frac{1}{\sqrt{M}}\right)^2\int_0^{\frac{\pi}{4}}\int_0^\infty p_\gamma(\gamma)e^{-\frac{3\gamma}{2(M-1)\sin^2(\theta)}}d\gamma d\theta \qquad (6)$$

where M is the number of symbols. SER can be derived by substituting (3) in (6)

$$P_e = D - E, \qquad (7)$$

where D is shown as below

$$D = 4(N-1)\left(1-\frac{1}{\sqrt{M}}\right)\left[\frac{1}{2}-\frac{1}{\pi}\sqrt{\frac{C_1}{1+C_1}}\right.$$
$$\times\left\{\left(\frac{\pi}{2}+\tan^{-1}(\alpha_1)\right)\left(1+\frac{1}{2(1+C_1)}\right)\right.$$
$$\left.-\frac{\sin(2\tan^{-1}(\alpha_1))}{4(1+C_1)}\right\} + \sum_{k=1}^{N-2}\frac{(-1)^k}{2k}\binom{N-2}{k}$$
$$\times\left[1-\sqrt{\frac{C_2}{1+C_2}}\left(\frac{2}{\pi}\right)\left(\frac{\pi}{2}+\tan^{-1}(\alpha_2)\right)\right]$$
$$-\sum_{k=1}^{N-2}\frac{(-1)^k}{2k(1+k)}\binom{N-2}{k}\left[1-\sqrt{\frac{C_3}{1+C_3}}\right.$$
$$\left.\left.\times\left(\frac{2}{\pi}\right)\left(\frac{\pi}{2}+\tan^{-1}(\alpha_3)\right)\right]\right],$$

where

$$C_1 = C_2 = \frac{3\gamma_c}{2(M-1)};$$
$$C_3 = \frac{3\gamma_c}{2(M-1)(1+k)};$$
$$\alpha_i = \sqrt{\frac{C_i}{1+C_i}}\cot(\frac{\pi}{2}), \quad 1\le i\le 3,$$

and E is shown as below

$$E = 4(N-1)\left(1 - \frac{1}{\sqrt{M}}\right)^2 \left[\frac{1}{4} - \frac{1}{\pi}\sqrt{\frac{C_1}{1+C_1}}\right.$$

$$\left\{\left(\frac{\pi}{2} + \tan^{-1}(\alpha_1)\right)\left(1 + \frac{1}{2(1+C_1)}\right)\right.$$

$$\left. - \frac{\sin(2\tan^{-1}(\alpha_1))}{4(1+C_1)}\right\} + \sum_{k=1}^{N-2}\frac{(-1)^k}{4k}\binom{N-2}{k}$$

$$\times \left[1 - \sqrt{\frac{C_2}{1+C_2}}\left(\frac{2}{\pi}\right)\left(\frac{\pi}{2} + \tan^{-1}(\alpha_2)\right)\right]$$

$$- \sum_{k=1}^{N-2}\frac{(-1)^k}{2k(1+k)}\binom{N-2}{k}$$

$$\left. \times \left[1 - \sqrt{\frac{C_3}{1+C_3}}\left(\frac{2}{\pi}\right)\left(\frac{\pi}{2} + \tan^{-1}(\alpha_3)\right)\right]\right],$$

where

$$C_1 = C_2 = \frac{3\gamma_c}{2(M-1)};$$

$$C_3 = \frac{3\gamma_c}{2(M-1)(1+k)};$$

$$\alpha_i = \sqrt{\frac{C_i}{1+C_i}}\cot(\frac{\pi}{2}), \quad 1 \le i \le 3.$$

IV. RESULTS

In this section, we show the analytical results obtained in section III. We denote the considered sub-optimum system as $(N, 2; 1)$, which indicates that two transmit antennas are selected from N with one receive antenna. Fig. 2 shows the SER for $N = 3, 4$ and 5 using M-PSK constellation. We have carried out the simulation for $M = 2$ and 4, also known as BPSK and QPSK respectively. It can be seen that the SER performance of BPSK is better than that of QPSK, but spectral efficiency can be achieved in the latter case. It can also be observed that performance has been improved for larger values of N.

Fig. 3 shows the SER for $N = 3, 4$ and 5 using M-QAM constellation. We have carried out the simulation for $M = 16$ and 64, also known as 16-QAM and 64-QAM respectively. It can be seen that the SER performance of 16-QAM is better than that of 64-QAM, but spectral efficiency can be achieved in the latter case. It can also be observed that performance has been improved for larger values of N.

V. CONCLUSION

We have considered the sub-optimum transmit antenna selection scheme given in [9]. In this scheme we have N transmit antennas in MISO systems, wherin one antenna is fixed and the other is selected out of the remaining $N - 1$ antennas. We have derived the closed-form expressions of SER of M-PSK and M-QAM constellation
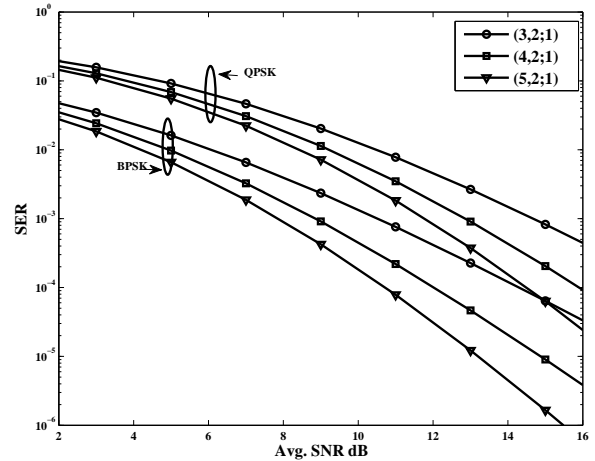
Fig. 2. SER Vs Avg. SNR for M-PSK constellation
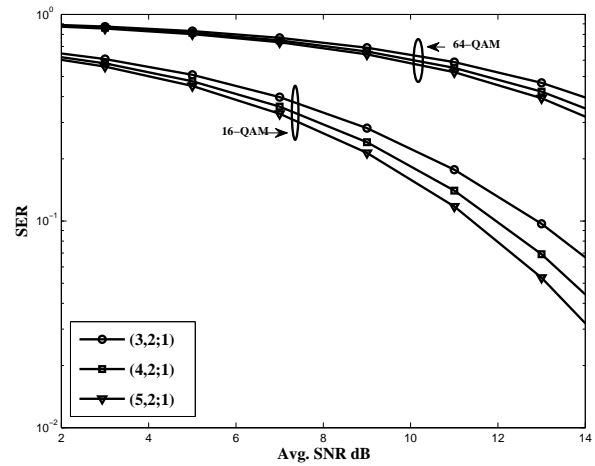
Fig. 3. SER Vs Avg. SNR M-QAM constellation

for Alamouti transmit diversity. We have compared our analytical results for higher values of M for M-PSK and M-QAM constellation. We achieve spectral efficiency as the value of M increases with some performance degradation in terms of SER.

REFERENCES

[1] V Tarokh, H. Jafarkhani and A.R.Calderbank, "Space-time block codes from orthogonal designs," *IEEE Trans. Inform. Theory*, vol 45, pp. 1456-1467, July 1999.

[2] S. M. Alamouti, "A simple transmit diversity technique for wireless communications," *IEEE J. Selected Areas Communications*, vol. 16, pp. 1451-1458, October 1998.

[3] Z. Chen, J. Yuan, B. Vucetic and Z. Zhou, "Performance of Alamouti scheme with transmit antenna selection," *Electronics Letters*, vol. 39, No. 23, pp. 1666-1668, November 2003.

[4] Z. Chen, I. B. Collings, Z. Zhuo and B. Vucetic, "Transmit Antenna Selection Schemes with Reduced Feedback Rate," *IEEE Trans. Wireless Communications*, vol. 8, No. 2, pp 1006-1016, February 2009.

[5] Y N Trivedi , A K Chaturvedi, "Performance analysis of Alamouti Scheme with Transmit Antenna Selection in MISO Systems," *National Conference on Communications (NCC), IIT Madras*,2010.

[6] D. A. Gore and A. Paulraj, "MIMO antenna subset selection with space-time coding," *IEEE Trans. Signal Processing*, vol 50, No. 10, pp. 2580-2588, October 2002.

[7] D. J. Love, "On the Probability of Error of Antenna-Subset Selection With Space-Time Block Codes," *IEEE Trans. Communications*, vol. 53, No. 11, pp. 1799-1803, November 2005.

[8] "Physical layer procedures (FDD)," 3rd Generation Partnership Project (3GPP), Tech. Rep. 25.214, 2005.

[9] J. M. Chakravarti, Y. N Trivedi, "Performance Analysis of Alamouti Transmit Diversity with Transmit Antenna Selection for Reduced Feedback Rate," *ICDeCom-11, BIT Mesra (Ranchi), India*, February 2011.

[10] A. Papoulis and S. U. Pillai, *Probability, Random Variables and Stochastic Processes*, 4th ed. MH.

[11] J G Proakis, *Digital Communication*, 4th ed. MH, 2001.

[12] H. A. David, *Order statistics*, New York Wiley, 1970.

[13] M K Simon and M S Alouini, *Digital communication over fading channels -A unified approach to performance analysis*, John Wiley & Sons, 2000.

COMPARISION OF DIFFERENT EDGE BASED ACTIVE CONTOUR MODELS AND THEIR SOLUTION FOR IMAGE SEGMENTATION

[1]Asst. Prof. Dhaval R. Sathawara, [2] Asst. Prof. Margam K. Suthar, [3]Mr.Bharat P. Solanki

[1]Department of Electronic and Communication Engineering
U.V.Patel collage of engineering, Ganpat university Kherva (Mehsana), India
dhaval_sathawara@yahoo.co.in

[2]Department of Electronic and Communication Engineering,
Sankalchand Patel collage of engineering, visnagar (Mehsana), India
mksuthar.19ec@gmail.com

[3]Department of Electronic and Communication Engineering,
Student M.Tech [L. D. collage of engineering, Gujarat Technological university (Ahmedabad), India
bharat69solanki@yahoo.co.in

Abstract—**Image segmentation is one of the most important steps in the image analyses. Its aim is to divide image in some parts which correlate strongly by objects. Segmentation is difficult task because of big variety of object, shape as well as different quality. In t h i s paper various models of finding active contour is discussed. First two methods of image segmentation are based on principle paradigm of edge or gradient by minimizing the energy of an image. Later section discuss about the practical limitation of the models. Another paradigm is that the detection of active contour whose stopping term does not depend on the gradient. Later on we discuss how this method is advantageous or more beneficial in finding the interested regions from an image.**

I. INTRODUCTION

Active contours are used in the domain of image processing to locate the contour of an object. Trying to locate an object contour purely by running a low level image processing task such as canny, sobel and prewitt edge detections are not particularly successful. Often the edge is not continuous, i.e. edges are broken or not connected, and spurious edges can be present because of noise. An active contour tries to improve on this by imposing desirable properties such as continuity and smoothness to the contour of the object.

In section II, discussion of the basic active contour method which is introduced in "*international journal of computer vision*". How image is segmented based on minimizing energy terms and how it can be formulated in different energy terms. Section III, introduce new model to overcome limitations of previous model. Section IV, involve model of active contour detection which is not depend on edge rather than depending on level set function. Section V, experimental results are discussed for selecting the model which satisfy requirement for application.

II. SNAKE OR CLASSICAL ACTIVE CONTOUR BY KASS

The concept of active contours models was first introduced in 1987 [1] and has later been developed by different researchers. An active contour is an energy minimizing that detects specified features within an image. It is a flexible curve which can be dynamically adapted to required edges or objects in the image.
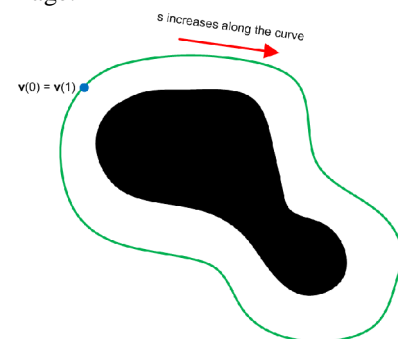
Figure 1. Illustration of a parametric snake curve v(s). The blue dot marks the starting point and end point of the snake curve [2].

The position of the snake is given by the parametric curve v(s) = $[x(s); \; y(s)]^T$ with Sϵ [0; 1],in practice the curve is often closed which means that v(0) = v(1). Furthermore the curve is assumed to be parameterized by arc length. A closed parametric snake curve is illustrated in Fig. 1. Each point along the curve is under the influence of both internal and external forces [2]. Fitting active contours to shapes in image is an interactive process. The contour will then be attracted to Features in the image extracted by internal energy creating an attractor image [3].

The active contour model that Kass et al. introduced was further developed by Laurent D. Cohen in the paper\On Active Contour Models and Balloons". The snake model that Cohen

presents in the paper works on the same principles as the Kass et al. snake, but where the Kass et al. snake would shrink when not under the influence of image forces the Cohen snake Expands. The expansion of the snake bears some resemblance to a balloon being inflated in 2D, which is why this snake model is usually called the balloon snake [6].

A. The Original Snake by Kass, Witkin & Terzopoulos

Snakes, developed by Kass et al. [1], is a method of molding a closed contour to the boundary of an object in an image. The snake model is a controlled continuity closed contour that deforms under the influence of internal forces, image forces, and external constraint forces. The internal contour forces provide a piecewise smoothness constrain [4]. Kass et al. introduced the following energy functional for calculating the snake energy

$$E_{snake}^{\bullet} = \int_0^1 E_{snake}(V(s))\,ds$$

$$= \int_0^1 E_{int}(V(s)) + E_{ext}(V(s))\,ds$$

$$= \int_0^1 E_{int}(V(s)) + E_{img}(V(s)) + E_{con}(V(s))\,ds \qquad (1)$$

The snake energy consists of three terms. The first term E_{int} represents the internal energy of the snake while the second term E_{img} denotes the image forces; the last term E_{con} Gives rise to external constraint forces [2]. The sum of the image forces E_{img} And the external constraint forces E_{con} is also simply known as the external snake forces, denoted by E_{ext}. The internal energy of the snake is written

$$E_{int} = \frac{1}{2}\left(\alpha(s)\|V_s(s)\|^2 + \beta(s)\|V_{ss}(s)\|^2\right) \qquad (2)$$

Where, the first-order term $\|V_s(s)\|^2$ gives a measure measure of the curvature. This means that in parts of the snake where the curve is stretched, the elasticity term will have a high value, while in parts of the snake where the curve is kinked; the curvature term will have a high value. The influence that these terms have on the overall snake energy is controlled by the confidents $\alpha(s)$ and $\beta(s)$. The image forces E_{img} attract the snake to the desired features in the image. If the snake should settle on edges in the image, then the image energy can be defined as $E_{img} = -\|\nabla I(x,y)\|^2$, with I being the image function. Thus the snake will position itself in parts of the image with high gradient values. The external constraint forces E_{con} are attributed to some form of high level image understanding, most likely defined by human interaction [2]. The external energy E_{ext} consists of both the image energy $E_{int}(V(s))$ and the external constraint forces $E_{con}(V(s))$, however in order to simplify the analysis we will disregard the external constraint forces.

B. The image energy forces $E_{img}(V(s))$

Let us take closer look at the image energy $E_{img}(V(s))$. A crucial step in the Snake model is finding a suitable term for the image energy; this is because the snake will try to position itself in areas of low energy. Often the snake should be attracted to edges in the image and when this is the case a suitable energy term is $E_{img} = -\|\nabla I(x,y)\|^2$, where I is the image function. In order to remove noise from the image and increase the capture range of the snake. The image can be convolved with a Gaussian kernel before computing the gradients. This gives the following image energy term

$$E_{img} = -\|\nabla[G_\sigma(x,y) * I(x,y)]\|^2 \qquad (3)$$

Where $G_\sigma(x,y)$ is a two dimensional Gaussian with standard deviation σ. When strong edges in the image are blurred by the Gaussian the corresponding gradient is also smoothed which results in the snake coming under the influence of the gradient forces from a greater distance, hereby increasing the capture range of the snake

C. The internal energy of the sanake $E_{int}(V(s))$

The internal energy of the snake is defined as in (2). As The first order term $\|V_s(s)\|^2$ measures the elasticity of the snake, while the second order term $\|V_{ss}(s)\|^2$ measures the curvature energy. The influence of each term is controlled by the coefficients $\alpha(s)$ and $\beta(s)$. The more the snake is stretched at a point v(s) the greater the magnitude of the first order term, whereas the magnitude of the second order term will be greater in places where the curvature of the curve is high. It should be noted that if the snake is not under the influence of any image energy, and only moves to minimize its own internal energy. Then, for a closed curve, it will take the form of a circle that keeps shrinking and for a open curve the snake will position itself to form a straight line that also shrinks. The internal forces of the snake are however necessary in order to preserve desirable properties such as continuity and smoothness of the curve [2].

III. THE GREEDY SNAKE ALGORITHM

To improve and correct some of the problems associated with the Kass et al. snake model D. J. Williams and M. Shah developed a snake algorithm dubbed the Greedy snake. One of the problems is that the snake control points in the Kass et al. snake model are not always evenly spaced. Sometimes the snake control points bunch up in areas of the contour where the image energy has high negative values. This behaviour causes problems with calculating the curvature since the assumption that the snake parameter is arc length will not hold if the snake points are not equally spaced. The Greedy snake algorithm also introduce the problem of numerical instability that might occur if the temporal step size of the Kass et al. snake is too large. Furthermore, problems arising from the finite difference approximations for the elasticity and curvature terms are evaluated and new discrete approximations are suggested

A. *Evaluating the image energy*

The image energy of the Greedy snake is calculated same as the image energy is calculated in snake by Kass with a quite different

$$E_{img} = \|\nabla[G_\sigma(x,y) * I(x,y)]\|^2 \qquad (4)$$

Which is almost the same energy term as in the Kass et al. snake except that there is missing a minus in front of the term. The Greedy snake algorithm works by examining the neighbourhood around each snake point and then moving to the position with the lowest energy. Therefore the image energy in the neighbourhood of the snake control point $V(S_i)$ has to be normalized in a manner which assigns large negative values to pixels with high gradient values, while assigning lower negative values to pixels with a lower gradient value. The gradient magnitudes are all in the interval [0; 255]. The normalization of the neighbourhood is calculated as

$$location(x,y) = \frac{(min - mag(x,y))}{(max - min)} \qquad (5)$$

min is the minimum gradient value in the neighborhood. max is the maximum and $mag(x,y)$ the gradient magnitude of the current point. This normalization sets the highest gradient magnitude in the neighbourhood to -1 and the lowest to 0. One problem with this method is that if the neighbourhood is nearly uniform in gradient magnitude we get large difference in the normalized values [2].

B.   *Elastic term of greedy snake*

As mentioned by Kass et al. snake the elasticity term $\|V_s(s)\|^2$ has the effect of causing the curve to shrink upon itself. The Greedy snake utilizes a different way of calculating the elasticity term. Thus reducing the shrinking effect and also making sure that the snake control points does not bunch up in places with high image energy. The elasticity term in the Greedy snake is calculated in the neighbourhood of each snake control point as

$$d - \|V(S_i) - V(S_{i-1})\|$$
$$= d - \sqrt{(x(s_i) - x(s_{i-1}))^2 + (y(s_i) - y(s_{i-1}))^2} \quad (6)$$

Where d is the average distance between all the points in the snake. Once the above term has been calculated for each pixel in the neighbourhood of a snake control point all the values are divided by the largest value in the neighbourhood. Which means that the neighbourhood is normalized so, it only contains elasticity term values between [0; 1]. The minimum energy will be achieved when

$$d - \|V(S_i) - V(S_{i-1})\| = 0 \qquad (7)$$

Equation (7) will be true for all points where, the average distance equals the distance between the current and previous point on the snake.

IV.   ACTIVE CONTOUR USING LEVEL SET FUNCTION

All these classical snakes and active contour models rely on the edge function, depending on the image gradient, to stop the curve evolution; these models can detect only objects with edges defined by gradient. In practice, the discrete gradients are bounded and then the stopping function is never zero on the edges, and the curve may pass through the boundary, especially for the model in [1], [8]-[10]. If the image is very noisy, then the isotropic smoothing Gaussian has to be strong which will smooth the edges. In this section, we propose a different active contour model, without a stopping edge function, i.e. a model which is not based on the gradient of the image for the stopping process. The stopping term is based on Mumford–Shah segmentation techniques. In this way, we obtain a model which can detect contours both with and without gradient, for instance objects with very smooth boundaries or even with discontinuous boundaries. In addition, our model has a level set formulation, interior contours are automatically detected, and the initial curve can be anywhere in the image [7].

A. *Energy function and Lipschitz dunction*

Our method is the minimization of an energy based-segmentation. Let us first explain the basic idea of the model in a simple case. Assume that the image u_0 is formed by two regions of approximately piecewise-constant intensities, of distinct values u_0^i and u_0^o. Assume further that the object to be detected is represented by the region with the value u_0^i. Let denote its boundary by C_0. Then we have $u_0 = u_0^i$ inside the object and $u_0 = u_0^o$ outside the object. Now let us consider the following "fitting" term:

$$F_1(C) + F_2(C) = \int_{inside\,(c)} |u_0(x,y) - c_1|^2\, dx\, dy$$

$$+ \int_{outside\,(C)} |u_0(x,y) - c_2|^2\, dx\, dy \quad (8)$$

This can be seen easily. For instance, if the curve C is outside the object, then $F_1(C) > 0$ and $F_2(C) \approx 0$. If the curve C is inside the object, then $F_1(C) \approx 0$ but $F_2(C) > 0$. If the curve C is both inside and outside the object, then $F_1(C) > 0$ and $F_2(C) > 0$. Finally, the fitting energy is minimized if $C = C_0$, i.e., if the curve C is on the boundary of the object. These basic remarks are illustrated in figure 2.
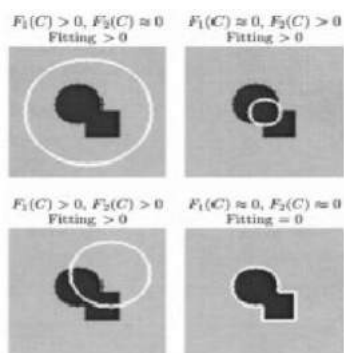
Figure 2. All possible cases in the position of the curve. The fitting term is minimized only in the case when the curve is on the boundary of object [7].
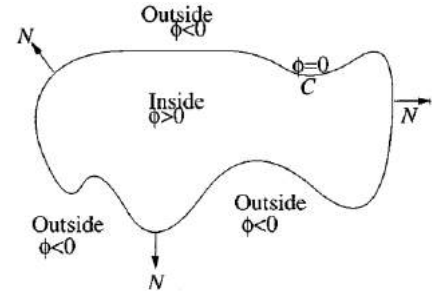
In the Level set method, $C \subset \omega$ is represented by the zero Level set of a Lipschitz function $\emptyset$, $\Omega \rightarrow R$ such that

$$C = \partial\omega = \{(x,y) \in \Omega : \emptyset(x,y) = 0\}$$
$$inside\,(C) = \omega = \{(x,y) \in \Omega : \emptyset(x,y) > 0\}$$
$$outside\,(C) = \Omega \backslash \bar{\omega} = \{(x,y) \in \Omega : \emptyset(x,y) < 0\} \quad (9)$$

For the Level set formulation of our variation active contour model, we replace the unknown variable C by the unknown variable $\emptyset$. Using the Heaviside function H, and the one-dimensional Dirac measure δ_0, and defined, respectively, by

$$H(z) = \begin{cases} 1, & if\ z \geq 0 \\ 0, & if\ z < 0 \end{cases} \quad (10)$$

$$\delta_0(z) = \frac{d}{dz} H(z) \quad (11)$$

Then, the energy $F(c_1, c_2, \emptyset)$ can be written as

$$F(c_1, c_2, \emptyset) = \mu \cdot \int_\Omega \delta_0(\emptyset(x,y)) |\nabla\emptyset(x,y)|\, dx\, dy +$$

$$v \cdot \int_\Omega H(\emptyset(x,y))\, dx\, dy$$

$$+\lambda_1 \int_\Omega |u_0(x,y) - c_1|^2 H(\emptyset(x,y))\, dx\, dy$$

$$+\lambda_2 \int_\Omega |u_0(x,y) - c_2|^2 (1 - H(\emptyset(x,y)))dx\, dy \quad (12)$$

We note that, u as defined earlier, solution of our model as a particular case of the Mumford–Shah minimal partition problem, can simply be written using the Level set formulation as

$$u(x,y) = c_1 H(\emptyset(x,y)) + c_2(1 - H(\emptyset(x,y))), (x,y) \in \bar{\Omega} \quad (13)$$

Keeping $\emptyset$ fixed and minimizing the energy $F(c_1, c_2, \emptyset)$ with respect to the constants c_1 and c_2, it is easy to express these constants function of $\emptyset$ by

$$c_1(\emptyset) = \frac{\int_\Omega u_0(x,y) H(\emptyset(x,y))\, dx\, dy}{\int_\Omega H(\emptyset(x,y))\, dx\, dy} \quad (14)$$

If $\int_\Omega H(\emptyset(x,y))\, dx\, dy > 0$ (i.e. if the curve has a nonempty interior in Ω), and

$$c_2(\emptyset) = \frac{\int_\Omega u_0(x,y)(1 - H(\emptyset(x,y)))\, dx\, dy}{\int_\Omega (1 - H(\emptyset(x,y)))\, dx\, dy} \quad (15)$$

Here, c_1 and c_2 are the average intensity within the objects and outside the objects respectively .Thus we can define boundary of objects by function rather than the edge of an image.

B. Algorithm for evaluating contour

In this model first we have to select initial region for better and fast result. Steps for evolving the contours are as follows:

- Select Initial mask to calculate Initial $\emptyset$.
- Compute $C_1(\emptyset^n)$ and $C_2(\emptyset^n)$.
- Calculate Image force by image energy function.
- Evaluate $\emptyset$ as:

$$\emptyset_{new} = \emptyset_{old} + \Delta t * Image\ Force$$

- Check whether the solution is stationary. If not then increase n by $n=n+1$ and Repeat these steps.

V. EXPERIMENTAL RESULTS

We conclude this paper by analyze different models and their response for different types of Images. Sample image of a leaf is take to evaluate the contour by different models. Kass model is first step of field of contour evolving models but it does not have smooth curve. In greedy snake model, curvature is smooth but it not enough to exactly match the boundary of objects. Their model which is depend on Lipchitz function rather than edge provide complete boundary as well as it is less sensitive to high bending curvature as shown in Fig. 4.
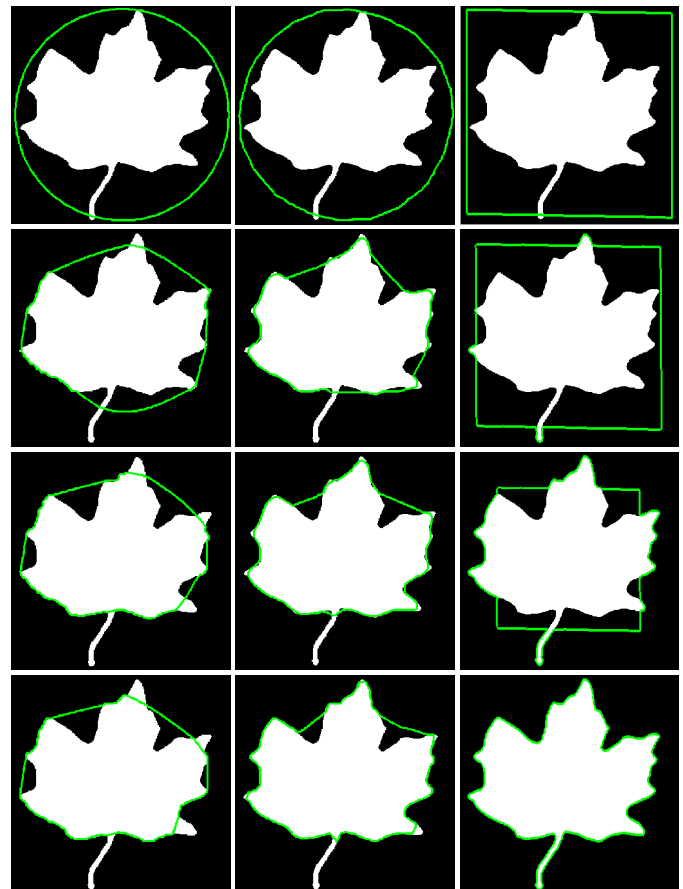
Figure 4. Evaluating contour of binary Image by Kass, Greedy and Active contour using Lipchitz function column wise respectively.
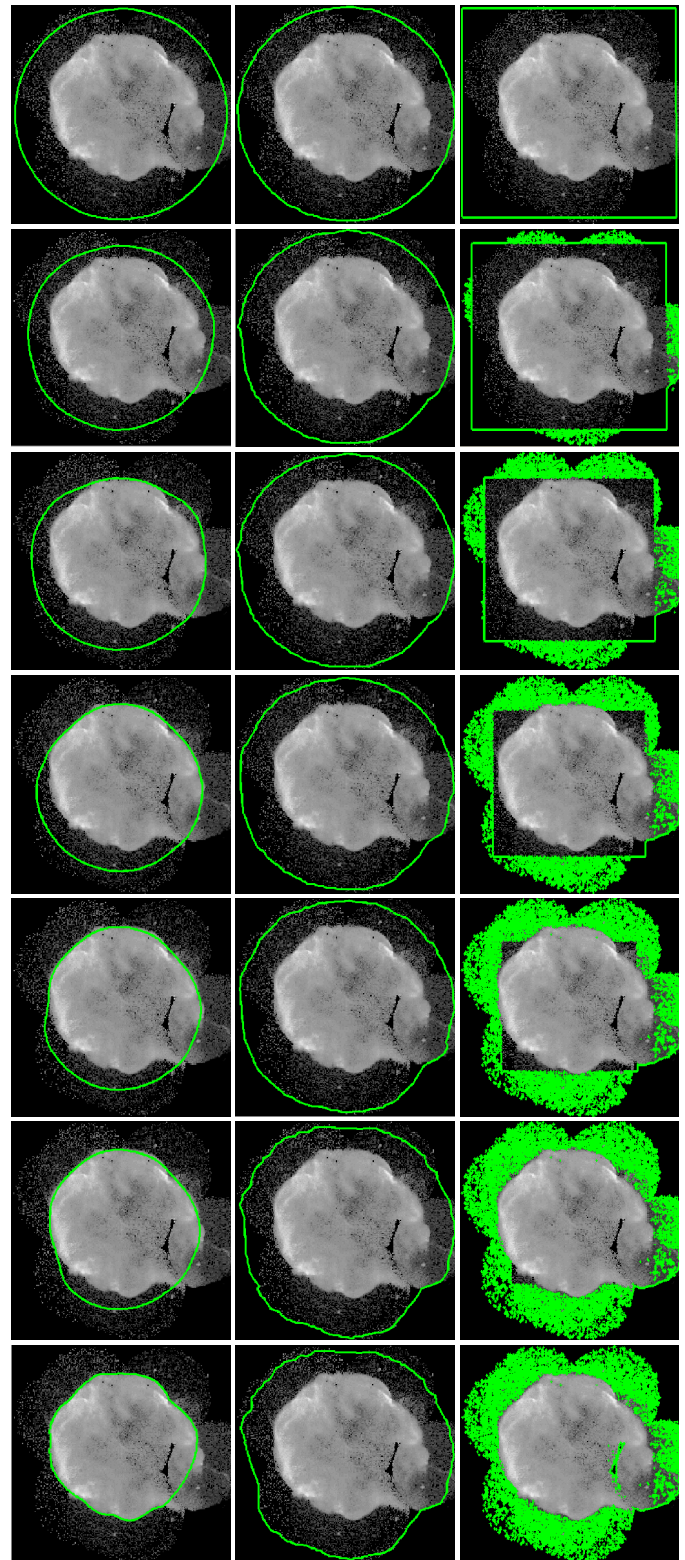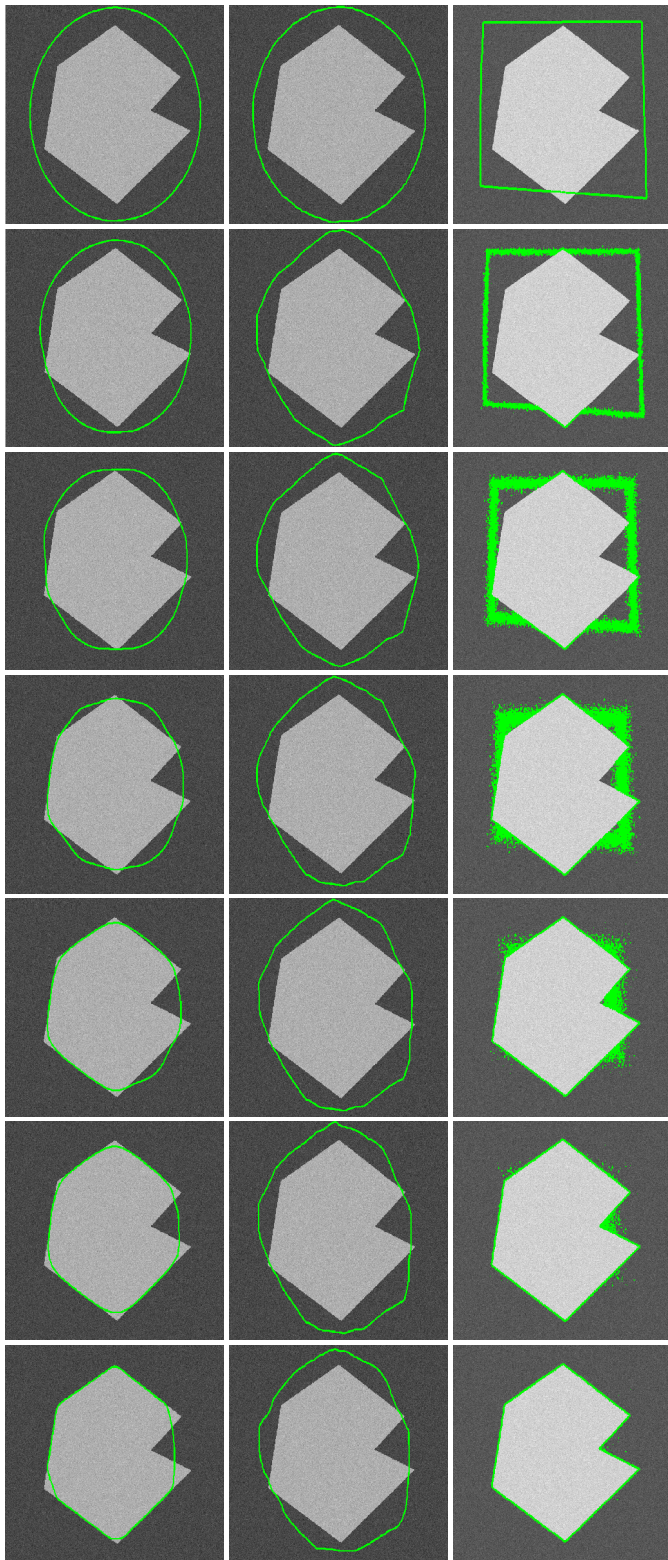
Figure 5. Evaluating contour of Noisy gray scale Imageof std. dev=10 by Kass, Greedy and Active contour using Lipchitz function column wise respectively.

Figure 5 shows different response of AWGN corrupted iamge. Greedy is less sensitive to noise rather than Kass and third model takes higher iteration to compote but it provide higher accuracy compared to other two models.

Figure 6. Evaluating contour of Cygnusloop Xray image by Kass, Greedy and Active contour using Lipchitz function column wise respectively.

Figure 6 shows that Kass model will neglect small objects and attract toward the larger object where in greedy model, small objects are grouped and consider as a one object and in third model all objects are consider separately rather than grouping.
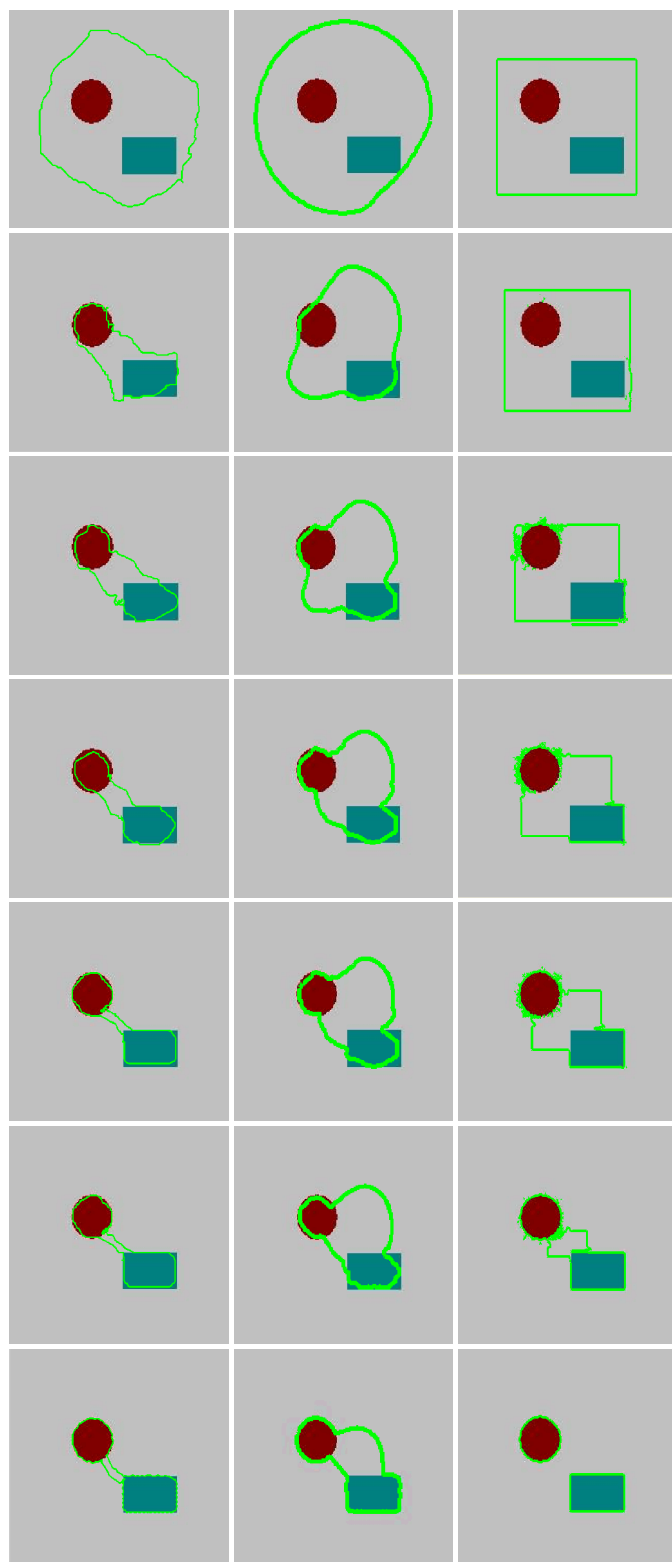
Figure 7. Evaluating contour of two object RGB image by Kass, Greedy and Active contour using Lipchitz function column wise respectively.

Figure 7 shows nature of response of different models under influence of image which contain two objects. Both Kass and Greedy models are not able to find boundary of those object

separately where in third model separate boundary are extracted. And both contour are well separated not linked in one contour.

VI. CONCLUSION

In this paper we discuss about need of segmentation in image processing then we describe one domain of segmentation that is active contour detection. There are two approaches for detecting active contours, first two models (Ksaa and Greedy) are based on edge and third is independent of edge. A model of detecting active contour whose fitting term depends on the edge or gradient is very sensitive to noise. In such cases a model, which's fitting term depend on the function rather than gradient will provide better and reliable results. Third model uses Lipchitz function to evaluate contour and gives better result with high accuracy as discussed in previous section. Thus active contour without gradient is better way to segment an image rather than gradient based model.

REFERENCES

[1] M. Kass, A. Witkin, and D. Terzopoulos, "Snakes: Active contour models," Int. J. Comput. Vis., vol. 1, pp. 321–331, 1988.
[2] Nikolas Petteri Tiilikainen, "A Comparative Study of Active Contour Snakes", 2007.
[3] Marian Bakos, "Active Contours and their Utilization at Image", 5th Slovakian-Hungarian Joint Symposium on Applied Machine Intelligence and Informatics January 25-26, 2007.
[4] William K. Pratt, "Digital Image Processing", PIKS Inside, Third Edition.
[5] R. C. Gonzalez and R. E. Wood, "digital image processing", third edition.
[6] Chenyang Xu and Jerry Prince," an example of balloon model on the room object", 1996-97.
[7] Tony F. Chan and Luminita A. Vese, " Active Contours Without Edges", IEEE transactions on image processing, vol. 10, no. 2, february 2001.
[8] S. Kichenassamy, A. Kumar, P. Olver, A. Tannenbaum, and A. Yezzy, "Gradient flows and geometric active contour models," in Proc. Int.Conf. Computer Vision, Cambridge, MA, 1995, pp. 810–815.
[9] M.-S. Lee and G. Medioni, "Inferred descriptions in terms of curves, regions and junctions from sparse, noisy binary data," in Proc. IEEE Int. Symp. Computer Vision, Coral Gables, FL, 1995, pp. 73–78.
[10] R. Malladi, J. A. Sethian, and B. C. Vemuri, "Shape modeling with front propagation: A level set approach," IEEE Trans. Pattern Anal. Machine Intell., vol. 17, pp. 158–175, Feb. 1995.
[11] Dhaval R. sathawara and Assist. Prof. Amrut N. Patel, "Image Segmentation Using Active Contour" International Conference on Information, Knowledge & Research in Engineering, Technology & Sciences-2012, Amoghsiddhi Education Society journal.
[12] Junmo Kim, Member, IEEE, John W. Fisher, III, Member, IEEE, Anthony Yezzi, Member, IEEE, Müjdat Çetin, Member, IEEE, and Alan S. Willsky, Fellow, IEEE, "A Nonparametric Statistical Method for Image Segmentation Using Information Theory and Curve Evolution", IEEE Transactions On Image Processing, Vol. 14, No. 10, October 2005.
[13] Xavier Bresson, Selim Esedoḡlu, Pierre Vandergheynst, Jean-Philippe Thiran, Stanley Osher, "Fast Global Minimization of the Active Contour/Snake Model", Journal of Mathematical Imaging and Vision, Volume 28, Issue 2, pp 151-167, June 2007.
[14] Chunming Li, Chenyang Xu, Senior Member, IEEE, Changfeng Gui, and Martin D. Fox, Member, IEEE, "Distance Regularized Level Set Evolution and Its Application to Image Segmentation", IEEE Transactions On Image Processing, Vol. 19, No. 12, December 2010.

BER Performance of Equalized Signal in Wireless Communication Architecture of Smart Grid

VineetaNishad ,JitendraThathagar

(vineeta.nishad@gmail.com, jkt1428571@gmail.com)

Abstract—**Smart grid is a next-generation electrical grid which set up a high-speed, fully integrated, two way communication technological frameworks having network features of dynamic interaction, real-time information and power exchange. This paper represents an end-to-end baseband model of the physical layer of a WiMAX communication network according to the IEEE® 802.16 standard. The model supports all mandatory and optional data rates 27 Mb/s. The model also illustrates adaptive modulation and coding over a flat-fading and dispersive multipath fading channel, whereby the simulation varies the data rate dynamically The channel estimation technique uses training sequence inserted at the beginning of each transmission. Theory and methods are presented in details. The system model is designed for WiMAX IEEE 802.16 transceiver in MATLAB Simulink and the performances are evaluated using software Matlab.**

Index Terms— **Adaptive modulation, Multipath Fading, OFDM, Smart Grid,WiMAX.**

I. Introduction

The conventional centrally controlled electrical grid is facing challenges such as rising energy demand, aging infrastructure, renewable energy sources, reliability and security which necessitate it to evolve towards intelligence, autonomy, improved efficiency, easy control, and high security. *The smart grid* will be the next-generation electricity grid and integrates emerging technologies in the areas of embedded sensing, broadband wireless communication, pervasive computing, and adaptive control. Cognitive Radio is an efficient and reliable communication technology to establish two-way information transmission between customers and utilities.

In recent years, Mobile WiMAX has received wide interest for next generation wireless communications. Two key technologies, Multiple Input Multiple Output (MIMO) and Orthogonal Frequency Division Multiplexing (OFDM) have been adopted in Mobile WiMAX standard, IEEE 802.16e (Mobile WiMAX) which is an extension of the IEEE 802.16-2004, which enable high data rate transmission over multipath and frequency selective fading channels Accurate channel state information (CSI) is required to perform coherent detection of OFDM signals and estimating mobile channels

for high data rate communications has proved to be very challenging [10].

Channel estimation of MIMO-OFDM systems has been widely investigated by researchers and two kinds of approaches have been introduced, frequency and time domain channel estimation. In these methods, a complete OFDM frame composed of training symbols is first sent in order to estimate the channel parameters. The channel is therefore assumed to be constant for the next OFDM blocks until a new estimation is performed. In fast fading environment, performances degradation would be noticed due to the outdated channel estimation. Normally, estimation performed in time domain would be more appropriate as impulse responses contain fewer parameters than frequency responses.

Simulations were conducted based on the specifications given in the IEEE 802.16e standard for WiMAX and under Stanford University Interim (SUI) channel models.

II. Communication Architecture In Smart Grid

Three fundamental functionalities are desirable for the communications infrastructure of the smart grid: sensing, transmission, and control. Embedded sensing is carried out by a large number of smart meters or sensors to detect the states of the various points of the grid in a real-time manner. Two-way transmission links should be established for data transport between the sensors and the control centers. To fulfill these purposes, the smart grid communications infrastructure has to integrate enabling networking technologies. The smart grid is usually deployed in a considerably large geographical field to connect a large set of nodes. Therefore, the communication infrastructure is envisioned to be a multilayer structure that extends across whole smart grid from the home area to the neighborhoodarea and the wide area (Fig. 1). In particular, home area networks (HANs) communicate with various smart devices to provide energy efficiency managementand demand response. Neighborhood area networks (NANs)connect multiple HANs to local access points. Wide area networks (WAN) provide communication links between theNANs and the utility systems to transfer information.

A.Proposed Three-Layered Structure

Fig.1 shows the proposed communication architecturebased on cognitive radio (CR) for the smart grid. The communication architecture adopts the three-tiered hierarchical structure, including HAN, NAN, and WAN. On one hand, cognitive communications that operate in the license-free bands are appliedin the HAN to coordinate the heterogeneous wireless technologies; on the other hand, cognitivecommunications thatoperate in the licensed band are applied in the NAN andWAN to dynamically access the unoccupied spectrum opportunities.

B.Cognitive Communications in Home Area Networks

Topology — The HAN consists of a cognitive home gateway (HGW), smart meters, sensors, actuators, and other intelligent devices. A networked smart meter system is a typical instance in a HAN to offer an energy-efficient and reliable next-generation power grid. The presented HAN uses a star topology with either wired technologies (e.g., power line communications) or different wireless technologies (e.g., Zigbee, Bluetooth, WiMAX and WiFi). Consequently, HAN is an essentially heterogeneous networkwith a number of complementary technologies, which calls for a very flexible service gateway to manage the communications within the HAN and the communications between different HANs in a NAN service range.

Dynamic Spectrum Sharing in Cognitive HANs — In this sense, the HGW is able to intelligently interact with the radio surroundings, adaptively connect, and change their transmitters' parameters. The radioagility capacity in the HGW is able to sense unused frequencies in the surroundings and can utilize them subject to interference constraints. In addition, the HGW will connect to the HAN, which in turn will connect to external networks (e.g., the Internet, NAN, or a utility). The HGW enables two-way communications in the HAN. In the forward direction, the HGW periodically collects power-related data (e.g. metered data, sensed data, and load and control information) from various machines/devices/terminals within the HAN, and then transfers the collected data outside of the NAN. In the opposite direction, the HGW acts as a central node within the cognitive NAN to receive data (e.g., pricing, demand response) from the NAN and then distribute the received data to the smart meters or display to the customers. Within a HAN, the HGW manages the license-free spectrum bands to provide optimal data rate with low interference. An efficient solution to spectrum sharing among networked smart meters is necessary. Apart from spectrum sharing management, the HGW enables other devices and sensors to join the network, assigns channel and network addresses to each device, and coordinates the communications between thedevices within the HAN.
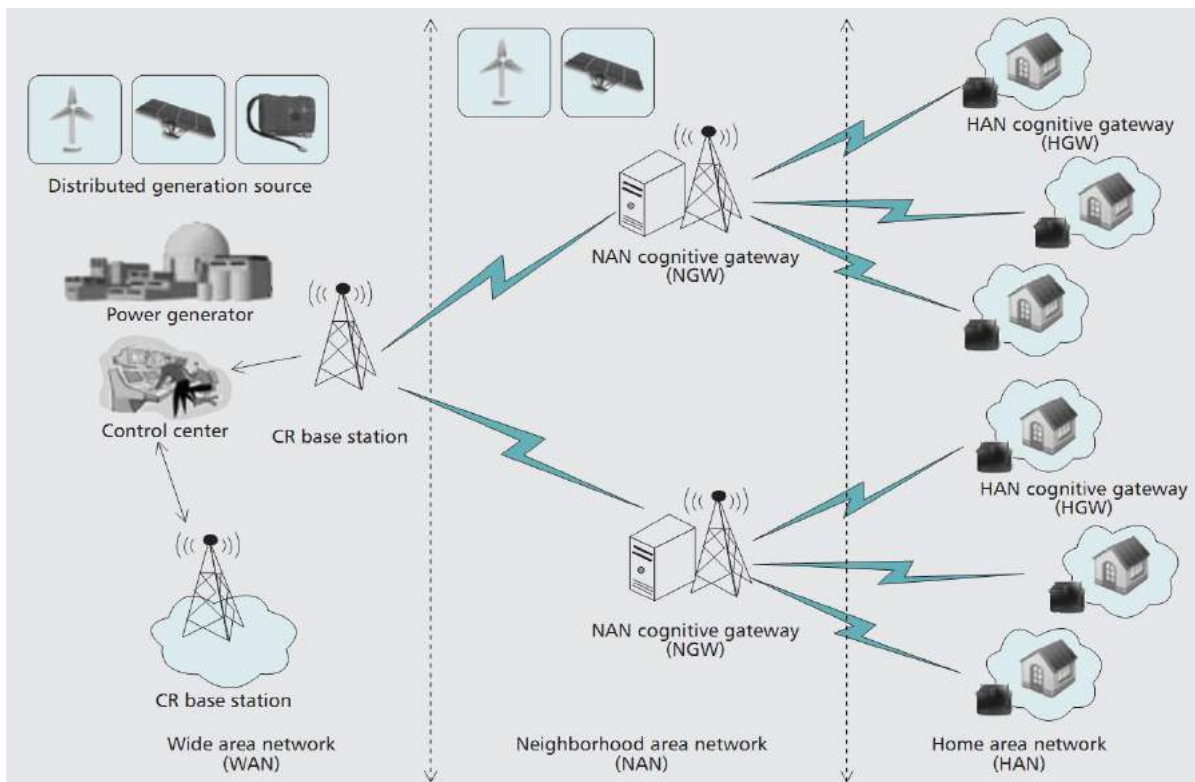
Fig 1. Cognitive radio based hierarchical communications architecture in the smart grid.

C.Cognitive Communications in Neighborhood Area Networks

Topology — In smart grid applications, the NANs will collect energy consumption information from households in a neighborhood and deliver the information to a utility company through either open or private WANs. NANs typically comprise multiple utility meters, each of which is installed on or outside of a house. In the proposed cognitive communication architecture, a NAN is the next immediate tier of a HAN. In a NAN, a cognitive gateway (NGW) connects several HGWs from multiple HANs together, as shown in Fig. 1. The HGWs are the data access points of the HANs to the outside NAN, and they also act as the cognitive nodes located in the NAN.

D. Cognitive Communications in Wide Area Networks

Topology — Fig.1 shows that multiple NANs constitute a WAN, andeach NAN exchanges information with the utility control center through the WAN. In the WAN, each NGW is no longeran access point, but a cognitive node with the capability tocommunicate with the control center through frequency spaceunused by a licensed PU. The control center is connected withcognitive radio base stations that are dispersed over a largearea (e.g., a city). In conjunction with the control center, thereis a spectrum broker that plays an important role in sharingthe spectrum resources among different NANs to enablecoexistence of multiple NANs. The cognitive radio base stations manage the communications of the NGW. In a largegeographical distribution of NANs, several NGWs may not bewithin the geographic area covered by base stations. TheseNGWs have to communicate in an ad hoc mode to shareunoccupied spectrum bands by themselves.To improve the spectrum efficiency and reduce the cost ofbuying spectrum bands, licensed and unlicensed accessmodes are intelligently scheduled and seamlessly switched.The smart grid user (or service) is not aware of the actualaccess mode it is using.

E. Cross-Layer Spectrum Sharing in HAN

Smart meters and intelligent sensors and actuators in homeareas are networked for information collection and delivery toconstitute the HAN of the smart grid. As mentioned before,different wireless technologies may be adopted by variousmeters/sensors/actuators, and hence coexist in a HAN. Thespectral overlay between these wireless systems may causesevere interference to each other and deteriorate systemcapacity. Thus, cognitive spectrum sharing is necessary tocoordinate the spectrum access of the heterogeneous wirelesssystems. Here, an HGW-assisted cross-layer cognitive

spectrum sharing mechanism is proposed.The mechanism has two main components: the spectrumaccess controller and power coordinator, which operate at themedium access control (MAC) and physical (PHY) layers,respectively. Each wireless node in a HAN is allowed toaccess the spectrum only if it is permitted by the access controller.

F. Power Coordination

Consider a HAN with Iwireless nodes (e.g., smart meters,sensors, or actuators) intending to transmit data. The achievable rate of the ith node is given by Shannon's formula,

$$R_i = \int_0^{B_i} \log\left(1 + \frac{p_i(f)}{N_0 + \sum_{j \neq i} p_j(f)}\right) df,$$

(1)

where B_i is the channel bandwidth, and $p_i(f)$ and N_0 arethe power spectral density (PSD) function of system i and noise in receivers, respectively. The utility function of the ith node is defined by

$$U_i = R_i - \alpha_i \int_{B_i} p_i(f) df,$$

(2)

G. Spectrum Access Control

Within the HAN, the cognitive HGW manages thespectrum bands allocation and sharing to provide optimal data rate with low interference. The spectrumaccess controller aims to guarantee the QoS of all in-servicewireless nodes (i.e., players) by controlling the number of newplayers. If the presence of a new player significantly degradesthe achievable rate of one or more existing players, the newplayer shall be blocked. Fig.2 shows four phases in thespectrum access control:
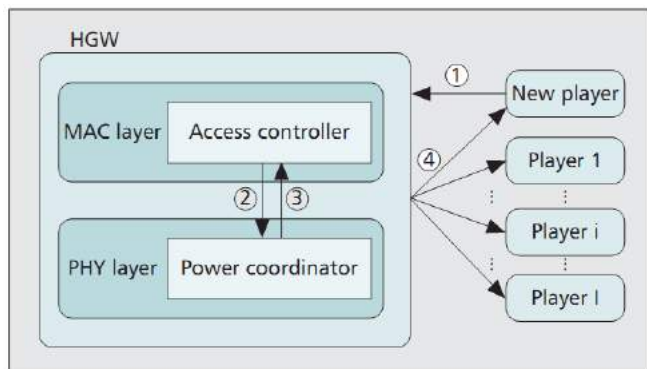
Fig.2 HGW-assisted cross-layer spectrum sharing in a HAN.

Phase 1: The access control procedure is launched by the new player that sends an access request to the HGW.

Phase 2: The access controller passes the profile of the new player to the power coordinator. The profile contains the information of the specific parameters of the utility function and the PSD function of the new players.

Phase 3: The power coordinator analyzes and obtain the optimal power control of all players (including the new one) The resulting power control and achievable rate are fed back to the access controller.

Phase 4: If one or more players reach an undesirable rate the new player is denied; otherwise, it is admitted. The access controller informs the new player of the admission/rejection decision, and all the players about whether to update the transmitting power. Denied players may retry to access later.

H. Joint WAN/NAN Spectrum Management

The spectrum management of the WAN and NANs should be jointly optimized for the following main reasons:

• In most situations, all the NANs in the same WAN operate in the same range of spectrum bands. There are underlying competitions on spectrum resource among the NANs, which need overall coordination.

• Different NANs have diverse demands on the amount of spectrum bands, due to the difference in the total number of HANs and traffic flows of HANs caused by the diversity in quantity and category of smart meters/sensors/actuators.

We consider a WAN with k NANs. Let $N^l_{G,k}$, $N^u_{G,k}$, $N^l_{C,k}$, and $N^u_{C,k}$ denote the number of licensed and unlicensed guard channels (GCs), and licensed and unlicensed common channels of the k_{th} NAN. Let $P_{d,k}$, $P_{b,k}$ denote the dropping probability and blocking probability of the k_{th} NAN, and N_k the number of allocated total channels of the k_{th}NAN. The joint WAN/NAN spectrum management could be formulated as the following optimization problem:

$$\min \ \max_k \left\{ P_{d,1} \cdots, P_{d,k}, \cdots P_{d,K} \right\}$$
$$\text{s.t.} \ \sum_k N^l_{G,k} + N^l_{C,k} = N_L$$
$$P_{b,k} \left(N^l_{G,k}, N^u_{G,k}, N^l_{C,k}, N^u_{C,k} \right) \le P^0_b, k = 1, \cdots, K$$
$$N^l_{G,k} + N^u_{G,k} + N^l_{C,k} + N^u_{C,k} = N_k, k = 1, \cdots, K$$
$$\sum_k N_k \le N$$

(3)

The target is to find the optimal spectrum allocation scheme with parametric tuples {N_k, $N^l_{G,k}$, $N^u_{G,k}$, $N^l_{C,k}$, $N^u_{C,k}$} for all NANs. Fig.3 shows the performance gain of the proposed cognitive communications infrastructure at the NAN and WAN level. It is observed that the proposed scheme achieves much lower dropping probability than the traditional solution. By using joint NAN/WAN spectrum management, the cognitive infrastructure is aware of the diversity of traffic load in different NANs, and consequently is able to intelligently allocate the spectrum bands. As a consequence, spectrum resources (both licensed and unlicensed) are utilized in a highly efficient manner.
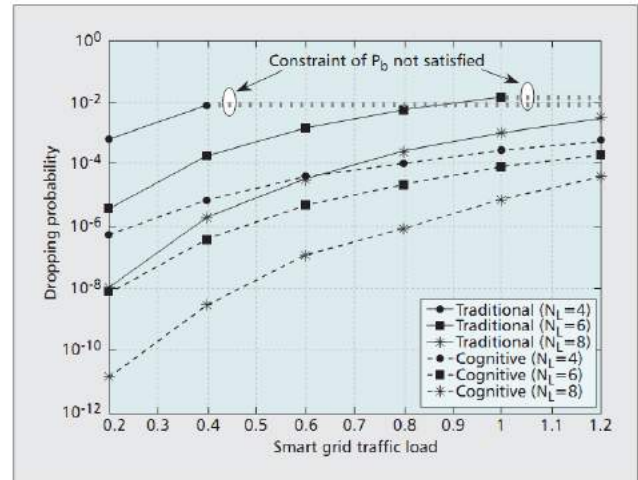
Fig.3 Performance comparison in a NAN between traditional and proposed CR communications infrastructures for the smart grid.

III. WIRELESS COMMUNICATION SYSTEM MODEL

OFDM system works on the principle of division of the available frequency spectrum into several subcarrier channel frequencies. The subcarriers are orthogonal in nature and hence overlapping is possible to achieve better spectral efficiency. Even though the signal passes through a time dispersive fading channel, orthogonality can be completely maintained with a small price in a loss in SNR[11].

A block diagram of a WiMAX OFDM PHY system is shown in Fig. 4[4]. The random binary signal information is first generated and grouped in symbols, then coded for error correction. Adaptive modulation system is used because different modulation scheme is needed for different data rates. After that guard band is inserted and the Inverse Fast Fourier Transform (IFFT) block transforms the data sequence into time domain. If multiple antennas are used, then space-time diversity encoder is also implemented. Then a cyclic prefix is used which is chosen larger than the expected delay spread to avoid inter-symbol and inter-carrier interferences (ISI and ICI). The D/A converter contains low-pass filters withbandwidth $1/T_S$, where T_S is the sampling interval. The channel is considered to be a multipath fading channel followed by addition of white Gaussian noise.

At the receiver, after passing through the analog-to-digital converter (ADC) and removing the CP, the FFT is used to transform the data back to frequency domain. Adaptive filtering technique is used for channel estimation. Lastly, the binary information data is obtained back after the demodulation and channel decoding.

1.1 Forward Error Correction Code

Digital communications need forward error correction (FEC) code for reducing errors due to noise, fading, interference, and other channel impairments. It is also called channel coding or error control coding. It introduces controlled redundancies to a transmitted signal so that they may be exploited at the receiver. The redundancy of the

encoded data is quantified by the ratio of b_d data bits per b_c encoded bits

$$R_c = \frac{b_d}{b_c} \text{ where } (b_d < b_c) \quad (1)$$

This ratio is known as the code rate, which basically means for every b_d data bits input into the encoder, there will be b_c code bits output from the encoder. Generally, correction codes are categorized into two main types: block codes and

convolutional codes. Block coding is basically generating a "codeword" of b_c coded bits that would be algebraically related to a sequence of b_d data bits. Convolutional coding is generated by the discrete-time convolution of a continuous sequence of input data bits. Both block code and convolutional code are employed in wireless systems. However, convolutional codes have proven superiority over block codes for a given degree of decoding complexity[14].
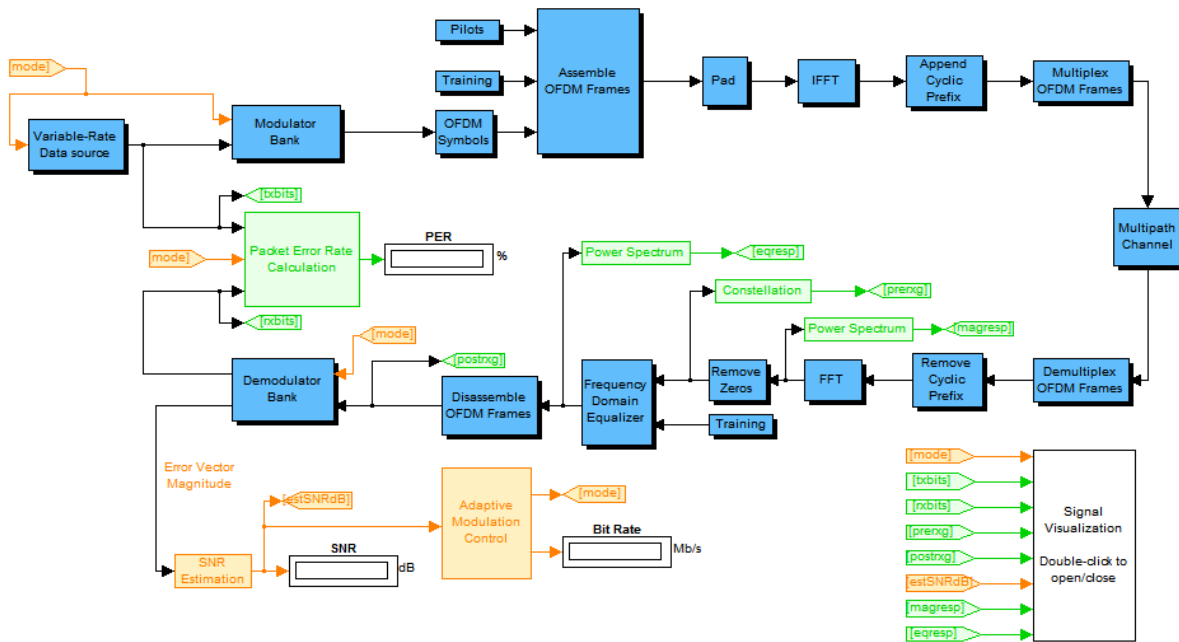
Fig. 4 IEEE 802.16 WiMAX - OFDM PHY system model in MATLAB Simulink[4].

1.2 Block Interleaving

The decoder operates under the assumption that the errors will be random or spaced apart. However, in fading channels, deep fades may cause a long sequence of errors, which may render the decoder ineffective. In order to alleviate bit correlation, the encoded bits are scrambled with a block interleaver (fig.5). Interleaving can either be done before symbol mapping, and is known as bit interleaving, or it can be done after symbol mapping, and is known as symbol interleaving . The purpose of interleaving is to minimize the bit correlation, while data symbols are essentially groups of bits. Maintaining the bits in groups, in a sense, adds to the bit correlation, especially when using larger constellations[11].

1.3 Modulation Schemes

Adaptive modulation systems improve the rate of transmission. The implementation of adaptive modulation isaccording to the channel information that is present at the transmitter.
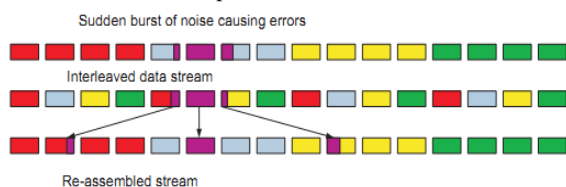
Fig. 5 Transmission with a burst error and interleaving.

TABLE I.
IEEE 802.16 TRANSMISSION MODES

Mode or Rate_ID	Modul-ation	Interlea-ving	Code Rate	Data Rate (Mbps)	Simulation-Threshold SNR (dB)
0	BPSK	6 x 8	1/2	3	0
1	BPSK	6 x 8	3/4	4.5	10
2	QPSK	12 x 8	1/2	6	11
3	QPSK	12 x 8	3/4	9	14
4	16-QAM	12 x 16	1/2	12	18
5	16-QAM	12 x 16	3/4	18	22
6	64-QAM	18 x 16	2/3	24	26
7	64-QAM	18 x 16	3/4	27	28

The method of making adaptive modulation in this model is according to the estimated SNR, a bit rate will be specified and then data source generates binary data according to the specified data rate in adaptive modulation control. The transmission modes supported in the IEEE 802.16 standard are described in the Table 1.

1.4 OFDM Transmitter

OFDM converts serial data stream into parallel blocks of size N and modulates these blocks using inverse fast Fourier

transform (IFFT). Time domain samples of an OFDM symbol can be obtained from frequency domain data symbols [15] as

$$x(i,n) = IFFT_N[X(i,k)] = \frac{1}{N}\sum_{k=0}^{N-1} X(i,k)\exp\left\{\frac{j2\pi nk}{N}\right\}$$

$$(2)$$

where X(i,k) is the transmitted data symbol at the kth subcarrier of the ith OFDM symbol, N is the fast Fourier transform (FFT) size. After the addition of cyclic prefix (CP) and D/A conversion, the signal is passed through the radio channel. The channel is assumed to be constant over an OFDM symbol, but time-varying across OFDM symbols.

At the receiver, the signal is received along with noise. After synchronization, down-sampling, and removal of the CP, the simplified baseband model of the received samples can be formulated[15] as

$$y(n) = \sum_{l=0}^{L-1} x(n-l)h(l) + w(n),$$

$$(3)$$

where L is the number of sample-spaced channel taps, w (n) is the additive white Gaussian noise (AWGN) sample with zero mean and variance of σ^2 , and the time domain channel impulse response (CIR) for the current OFDM symbol, h (l), is given as a time-invariant linear filter. Note that perfect time and frequency synchronization is assumed. In this case, after taking FFT of the received signal y(n), the samples in frequency domain can be written as

$$Y(i,k) = X(i,k)H(i,k) + W(i,k) \qquad (4)$$

where H and W are FFTs of h and w respectively.

1.5 Pilot Insertion

An OFDM system is equivalent to a transmission of data over a set of parallel channels. At the receiver, there are equalizers for compensation of channel characteristics which is achieved by sending pilot symbols from transmitter. Two types of methods can be used for this as shown in fig.6.The fading channel of the OFDM system can be viewed as a 2D lattice in a time-frequency plane, which is sampled at pilot positions and the channel characteristics between pilots are estimated by using pilot information by the channel estimator algorithm. The art in designing channel estimators is to solve this problem with a good trade-off between complexity and performance. The first one, block-type pilot channel estimation, is developed under the assumption of slow fading channel, and it is performed by inserting pilot tones into all subcarriers of OFDM symbols within a specific period. The second one, comb-type pilot channel estimation, is introduced to satisfy the need for equalizing when the channel changes even from one OFDM block to the subsequent one[11].

1.6 Training Sequence Preamble

The first symbol of each downlink subframe is dedicated as a preamble in OFDMA mode of 802.16 standard. The preamble is generated by modulating each third subcarrier using boosted binary phase shift keying (BPSK) with a specific pseudo noise (PN) sequence. Hence, the time domain

preamble consists of three repeating parts. This preamble is used for initial estimation of time-varying channel[15].
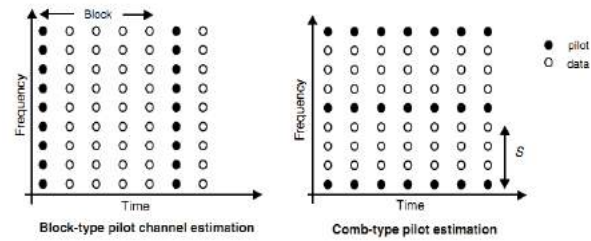
Fig. 6 Two Basic Types of Pilot Arrangement for OFDM Channel Estimations

1.7 Equalization

A symbol-spaced linear equalizer consists of a tapped delay line that stores samples from the input signal. Once per symbol period, the equalizer outputs a weighted sum of the values in the delay line and updates the weights to prepare for the next symbol period. This class of equalizer is called *symbol-spaced* because the sample rates of the input and output are equal. Below is a schematic of a symbol-spaced linear equalizer with N weights, where the symbol period is T.
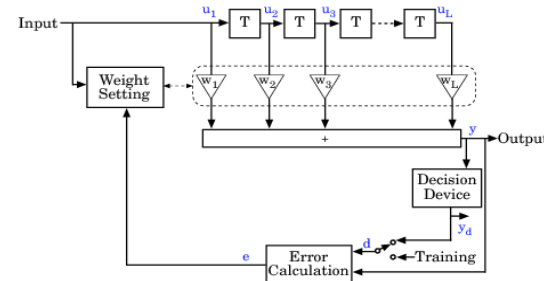
Fig. 7 A linear equalizer with tapped delay line and N weights.

1.8 Radio Channel

There are three basic types of channels considered for this work. Performance of three channels, viz., AWGN, Rayleigh Fading Channel, Rician Fading Channel in communication environment is evaluated through simulation. Multipath fading is a significant problem in communications. In a fading channel, signals experience fades (i.e., they fluctuate in their strength). When the signal power drops significantly, the channel is said to be in a fade. This gives rise to high bit error rates (BER)[7].

1.9 Channel Estimation

Time-dispersive channels can cause inter-symbol interference (ISI), a form of distortion that causes symbols to overlap and become indistinguishable by the receiver. For example, in a multipath scattering environment, the receiver sees delayed versions of a symbol transmission, which can interfere with other symbol transmissions. An equalizer based on LMS channel estimation algorithm attempts to mitigate ISI and improve receiver performance.

IV. SIMULATIONS

In the realistic scenario where the channel state information is not known at the receiver, this has to be extracted from the received signal. We assume that the channel estimator performs this using orthogonal pilot signals that are prepended to every packet. It is assumed that the channel remains unchanged for the length of the packet (i.e., it undergoes slow fading).

Scatter plots of the received signal before and after equalization are shown in each simulation. From the plot of the equalized signal, modulation type the system can be recognized, because the plot resembles a signal constellation of 2, 4, 16, or 64 points. The power spectrum of the received signal before and after equalization, in dB. The dynamics of the signal's spectrum before equalization depend on the fading mode parameter in the Multipath Channel block. The estimate of the SNR based on the error vector magnitude. The bit rate of the transmission is shown. Table II shows parameter values for different simulations.

TABLE II

SIMULATION PARAMETERS IN ACCORDANCE WITH WIMAX 802.16 STANDARD

Carrier Frequency	2.3, 2.5, 3.5 GHz
Channel Model	LOS/Non-LOS
Raw Bit Rate	1.0-75.0 Mbps
Modulation	BPSK, QPSK, 16QAM, 64QAM
OFDM subcarriers	256
Channel Bandwidth	1.75, 3.5, 3, 7, 5.5, 10, 20 MHz
Frame Duration	5 ms
Number of Frames (per second)	200
IFFT/FFT	256 point
Data Tone	192
Pilot tone	8
Cyclic Prefix	64
Guard Interval/Symbol Interval	1/4, 1/8, 1/16, 1/32 (or 64, 32, 16,8 samples)
Decoder	Viterbi
Fading Channel	No fading; flat-fading; and Rayleigh or Rician Multipath fading
Noise	AWGN

TABLE III

SIMULATION RESULTS FOR VARYING PARAMETERS IN WIMAX SYSTEM MODEL

Case No.	OFDM symbols/block	OFDM symbols/training sequence	SNR (dB)	Doppler Shift (Hz)	Fading Mode	Bit Rate (Mb/s)	PER (%)
1.	200	8	20.44	200	No Fading	18	0
2.	200	8	19.67	50	Flat Fading	18	4
3.	200	8	4.119	200	Flat Fading	6	18
4.	50	8	13.89	200	Dispersive	12	14
5.	200	20	17.73	50	Dispersive	18	20
6.	500	8	15.89	50	Dispersive	12	34
7.	200	8	4.334	200	Dispersive	6	74

Fig. 8 shows the signal constellation and power spectrum of received and equalized signal when there is no fading due to channel. The SNR chosen is 20 dB and resultant bit rate is 18 Mbps but there are no packet errors. The received signal is having distortion in amplitude only.

Fig. 9 shows the effect of flat fading channel with maximum Doppler shift of 50 Hz. The signal is distorted in amplitude as well as in phase but after equalization we can recognize the signal. The power spectrum of received signal is flat. As we vary the SNR values, bit rate is changed and error is generated at 0 dB. Fig. 10 also shows the effect of flat fading channel but maximum Doppler shift (200 Hz) is more than fig. 9 which

increases the packet error (18%), so BER performance is relatively poor.

Fig. 11 through fig. 14 are having dispersive channel, which means there is a multipath fading effect introduced in these simulations. In fig. 8, the number of OFDM symbols/block (50) is less as compared to other cases (200), so the number of bits which are erroneous is least in this case because each burst is having separate fading and noise effects. When the length of block increases, a noise can deteriorate whole burst block, so more number of data bits become erroneous.
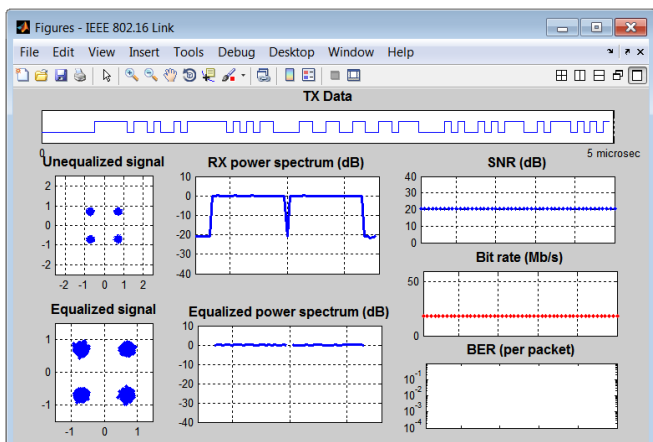
Fig.8 Effect on received and equalized signal when there is no fading.

Fig.9 Effect of flat-fading channel on received and equalized signal
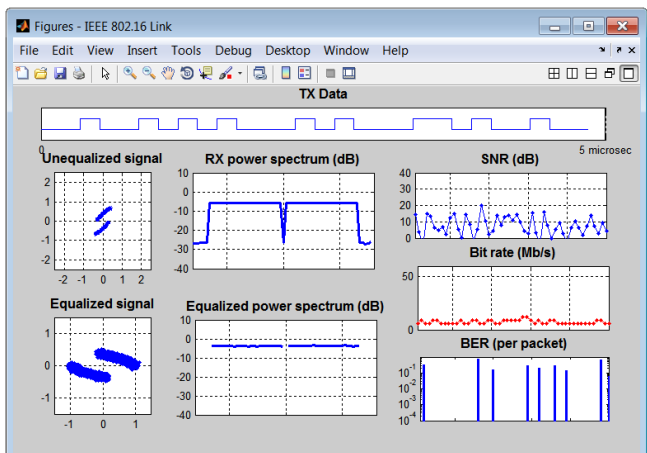
Fig.10 Effect on received and equalized signal when there is flat- fading channel with more Doppler shift.

.

Fig.11 Effect of dispersive channel on received and equalized signal

In fig. 12 and 13, the received signal is distorted in amplitude and phase due to multipath fading effects and the received power spectrum is also varying. But after equalization, signal constellation can be recognized and power spectrum is balanced. Due to dispersive channel, SNR values continuously changes, so bit rate is also changed. Number of training symbols are more in case 5 (20) as compared to case 6 (8),so equalization is better in case 5 and resultant erroneous bits are less here.
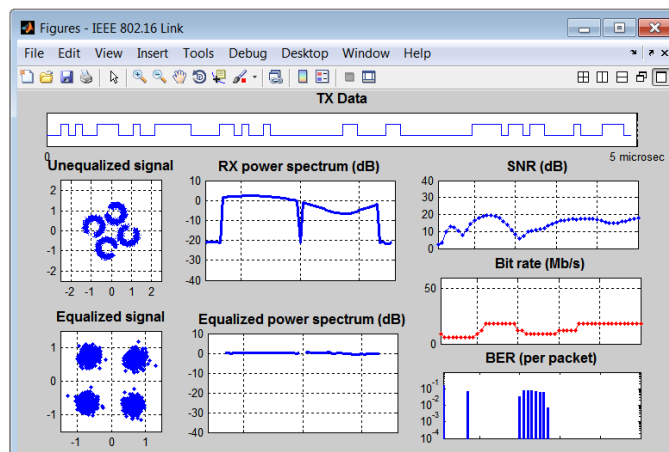
Fig.12 Effect of multipath-fading channel on received and equalized signal with more training symbols.

Fig. 14 shows the effect of signal to noise ratio upon bit rate and packet error. When the SNR value of the signal goes below a threshold level, the modulation scheme is changed for a transmission with relatively lower bit rate. If the SNR value of the received signal is too low, even after equalization the packet error rate is very high as shown in the figure. The SNR value (4.334 dB) is minimum in case 7, so packet error (74%) is maximum here.
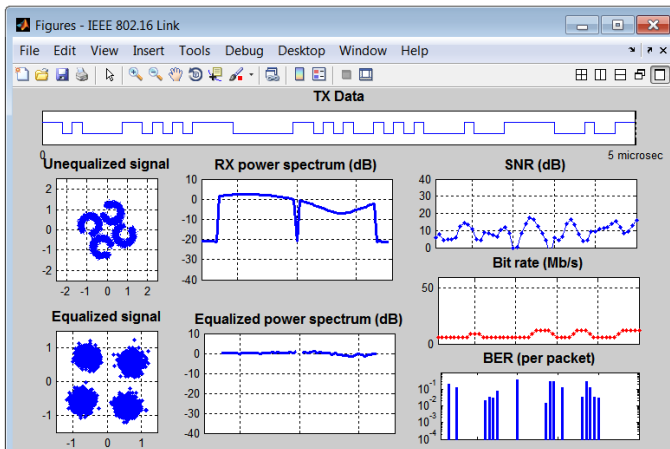
Fig: 13 Effect of multipath-fading channel on received and equalized signal with more OFDM symbols per block.
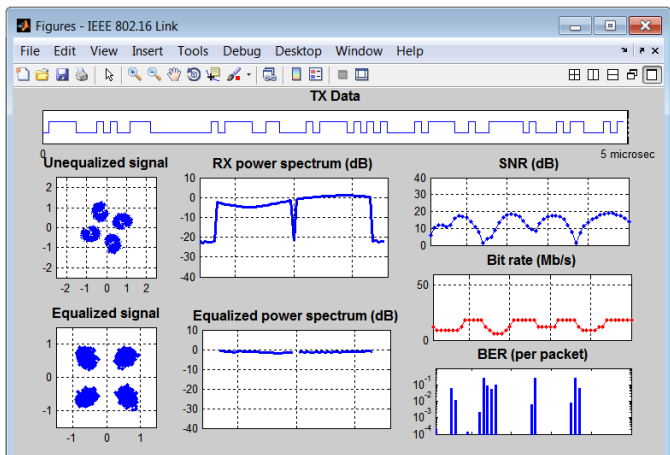
Fig: 14Effect of signal to noise ratio upon bit rate and packet error.

V. CONCLUSIONS

A MATLAB simulation is carried out in order to analyze baseband processing of the transceiver. For this, IEEE 802.16 standard is applied which allows transmission data rates from 3 up to 27 Mbps. Channel behavior is analyzed in terms of BER performance for radio environments having flat and multipath fading effects. Simulation results are compared for analyzing system behavior in terms of error probability. For channel estimation, the received signal is splitted up into the training symbols and data symbols.The following blocks display numerical results:

1. The PER block shows the packet error rate as a percentage.
2. The SNR block at the top level of the model shows an estimate of the SNR based on the error vector magnitude. The SNR block in the Multipath Channel subsystem shows the SNR based on the received signal power.

3. The Bit Rate block shows which of the bit rates specified in the standard is currently in use.

As a conclusion, it can be said that channel estimation and equalization are necessary for multipath fading channels so that the packet error rate can be reduced. Using more training symbols give better results in terms of accuracy but also increases the overhead.

REFERENCES

[1]S. Haykin, "Adaptive Filter Theory", Prentice Hall, Englewood Cliffs, NJ,Fourth Edition, 2002.
[2] J. G. Proakis, "Digital Communications", McGraw-Hill Book Co., New York Fourth Edition, 2001.
[3] T. S. Rappaport, "Wireless Communications: Principles and Practice", IEEE Press, Piscataway, NJSecond Edition, 2002.
[4]http://www.mathworks.com/matlabcentral/fileexchange/ "IEEE 802.16 OFDM PHY link model."
[5] IEEE Standard for Local and Metropolitan area networks Part 16, *The Institute of Electrical and Electronics Engineering*, Inc. Std.IEEE 802.16E-2005.
[6] IEEE Standard for Local and Metropolitan area networks Part 16, *The Institute of Electrical and Electronics Engineering*, Inc. Std.IEEE 802.16D-2004.
[7] Tirthankar Paul, Priyabratakarmakar and SouravDhar, "Comparative Study of Channel Estimation Algorithms under Different Channel Scenario", *International Journal of Computer Applications (0975 – 8887)*Vol 34– No.7, Nov, 2011.
[8] Phuong Thi Thu PHAM and Tomohisa WADA, "Pilot-Aided Channel Estimation for WiMAX 802.16e Downlink Partial Usage of Subchannel System using least Squares Line Fitting", *IEICE Trans. COMMUN.*, Vol E93-B, No.6, June2010.
[9] SudhakarReddy.P and RamachandraReddy.G, "Design and FPGA Implementation of Channel Estimation Method and Modulation Technique for MIMO System Su", *European Journal of Scientific Research,* Vol.25, No2, pp.257-265,2009.
[10] F.Delestre and Y.Sun, "A Channel Estimation Method for MIMO-OFDM Mobile WiMaxSystems ", *ISWCS*,2010.
[11] YushiShen and Ed Martinez, "Channel Estimation in OFDM Systems", *Freescale Semiconductor*, AN3059, Rev. 0, 1/2006.
[12] F.Delestre and Y.Sun, "Pilot Aided Channel Estimation for MIMO-OFDM Systems", *London Communications Symposium* 2009.
[13] AzadehBabapour, VahidTabatabaVakili, MahdiehRahmani and Zohre Mohades, "Effective Method of Channel Estimation for Mobile WiMAX DL-PUSC systems", *International Conference on Communications Engineering*, Dec 2010.
[14]G.L. Stuber, Principles of Mobile Communication Second Edition . Kluwer Academic Publishers, Norwell, Massachusetts 02061, 2000.
[15]T. Yucek, M. K. Ozdemir, H. Arslan, F. E. Retnasothie, "A Comparitive study of initial downlink channel estimation algorithms for Mobile WiMAX", Mobile WiMAX Symposium, pp. 32-37, 2007.
[16] Rong Yu, Yan Zhang, Stein Gjessing, Chau Yuen, ShengliXie, and Mohsen Guizani, "Cognitive Radio Based Hierarchical Communications Infrastructure for Smart Grid", IEEE Network, Sept /Oct 2011, pp. 6-14.
[17] KranthimanojNagothu, Brian Kelley, Mo Jamshidi, and Amir Rajaee, "Persistent Net-AMI for Microgrid Infrastructure using Cognitive Radio on Cloud Data Centers", IEEE Systems Journal, 2011.
[18] AshwinAlurSreesha, ShashankSomal, and I-Tai Lu, "Cognitive radio Based Wireless Sensor Network Architecture for Smart Grid Utility", IEEE conference paper, 2011.
[19] Fu Chuan, and Liu Anqing, "Key Techniques in Green Communication", IEEE Journal, 2011, pp. 1360-1363.
[20]Jianfeng Wang, MonishaGhosh, and KiranChallapali, "Emerging Cognitive Radio Applications: A Survey", IEEE Communications Magazine, March 2011, pp. 74-81.

High Speed CMOS Comparator Design

Megha M. Desai

(meghnow@yahoo.co.in)

Abstract **- Nowadays, demand for portable battery operated device increases. These mobile devices require data convertor. The heart of the converter is comparator. The accuracy of such comparators, which is defined by its offset, along with power consumption, speed is of keen interest in achieving overall higher performance of convertor. This paper includes different types of comparators such as Basic comparator, Two-stage comparator, Conventional (Three stage) comparator, Track and latch comparator and their parameters comparison. Also Auto zeroing technique for offset minimization is mention. These analog modules are implemented in LTspice 0.18μm CMOS technology.**

I. INTRODUCTION

This work focuses on the design of different comparator circuits. The schematic symbol and basic operation of a voltage comparator are shown in   Fig 1.The comparator can be thought of as a decision making circuit.

$$Vp > Vn \quad then$$
$$Vo = V_{DD} = logic\ 1$$

$$Vp < Vn \quad then$$
$$Vo = V_{SS} = logic\ 0$$
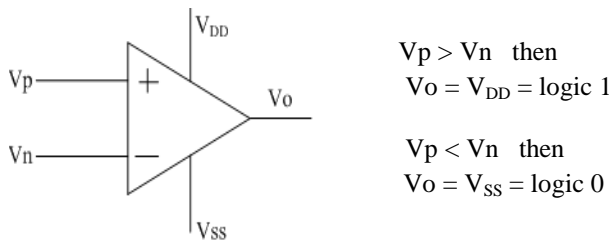
Fig. 1 Comparator Operation.

The comparators are classified on the basis of configuration [1] as follows:

1. Open-Loop Comparator: It consists of Operational Amplifiers without Compensation.
2. Regenerative Comparator: It uses positive feedback to accomplish the comparison of the magnitude between two signals.
3. High Speed Comparator: It is combination of Open-Loop and Regenerative Comparator.

Open-loop comparators are too slow because of its limited gain-bandwidth product. To overcome this, the regenerative and the High Speed Comparators (pre-amplifier based latched comparators) are design which provides fast speed and low input referred latch offset voltage.

This paper is organized as follows: Section II describes theory, design and implementation of analog comparators. Simulation results are included in section III. Finally section IV represents conclusions.

II. COMPARATORS DESIGN

A. Basic Comparator

It is an open loop comparator. The differential amplifier will work as a comparator if its input signal amplitude exceeds above the saturation limit. The transfer characteristic (Fig.2) [1] shows that such differential amplifier having large transition region.

Fig.2 Transfer Characteristic of Basic Comparator.

All transistors are of 10/1 size.

Fig. 3. Basic Comparator (Differential Amplifier)

Consider Fig. 3, the current through M1 is I_1, I_2 is current through M2, I is the load current and Iss is the current M5. Here two cases,

Case: 1   Vp > Vn $\therefore$ I1 > I2 $\Rightarrow$ Vo$\rightarrow$V$_{DD}$.
Case: 2   Vp < Vn $\therefore$ I1 < I2 $\Rightarrow$ Vo$\rightarrow$V$_{SS}$.

B.   Two stage comparator

It is a combination of the basic differential amplifier stage and the inverter. The circuit diagram of comparator is shown in Fig. 4. This comparator [1] has high gain and good signal swing compare to differential amplifier base comparator. The inverter will gives the full swing output.

All transistors are of 10/1 size.

Fig. 4 Two Stage Comparator

C.   Conventional three stage comparator

The Basic comparator and two stage comparator have less speed. The conventional three stage comparator [2] improves the speed and output swing. The input stage, first stage, is a differential amplifier with diode connected active loads which convert   input voltage into current.

Fig.5 Equivalent circuit when Vo+ < Vo-

The second stage, decision stage, is a bistable cross coupled circuit. It is in one state or another. The state is determined by the magnitude of the input currents. If $i_{o-} \gg i_{o+}$, M7 and M9 are off and M8 and M10 are on, which is shown in Fig. 5. Similarly if

$i_{o-} \ll i_{o+}$ then M7 and M9 are on but M8 and M10 are in off condition.

The output stage is third stage. Which is used to convert the output voltage of the decision circuit into digital logic signal (0 or 5V). In addition it must not be slew rate limited. One such circuit is the complementary self-biased CMOS differential amplifier (CSDA) [3]. Fig. 6 shows the whole circuit diagram of Conventional Three Stage Comparator.

Fig. 6 Conventional Three Stage Comparator

D.   Track and Latch Comparator:

The track and latch comparator [5] [6], shown in Fig. 7, is collected by an NMOS input differential pair M1-M2, inverters M3-M8 and M4-M9 in positive feedback configuration, pre-charge transistors M6-M7, and by the current source controlled(*phi1*) M5.

Fig. 7 Track and latch comparator

In an instant before active semi-cycle phi1, the input signals Vin- and Vin+ have to be defined and then, initiating at rising edge of the clock phi1, the pre-charge transistors are "open" and the differential pair is activated, initiating the comparison.

In the pre-charge phase (inactive semi-cycle), the current of M5 (Itail) is turned off and the input drivers are reset. The outputs Vo+ and Vo- are pre-charged to V_{DD}. It has the advantage of low power- dissipation, since it shuts down current consumption after the clocked comparison. The speed of this type of comparator is strongly dependent on the Itail current, that is, speed is directly proportional to the current in M5 This operation is shown in Fig.8
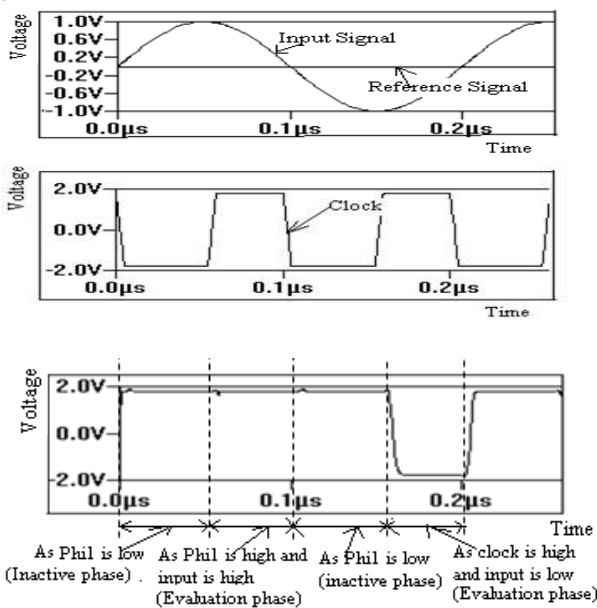
Fig. 8 Overall operations of Track and Latch.

Table 1: Transistor sizing of Track and Latch Comparator

Transistor	W (µm)	L (µm)
M1-M2	6	1
M3-M4	46	0.3
M5	3	3
M6-M7	2	1
M8-M9	2	1

Table 1 show the sizing of transistors which are selected on basis of satisfactory output with minimum area.

E.   Auto zeroing techniques

There are two areas in which the performance of an open-loop, high-gain comparator can be improved. These areas are the input-offset voltage and a single transition of the comparator in a noisy environment. The first problem can be solved by auto zeroing and the second can be solved by the introduction of hysteresis using a bistable circuit. Here the auto zeroing method is implemented. Input-offset voltage can be a particularly difficult problem   in comparator design. In precision applications, such as high-resolution anolog to digital converters, large input-offset voltages cannot be tolerated. As a result, offset

voltages can be measured, stored on capacitors, and summed with the input so as to cancel the offset. [2]
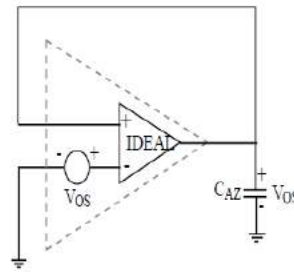
Fig. 9(a) First Half Cycle.   Fig. 9(b) Second Half Cycle
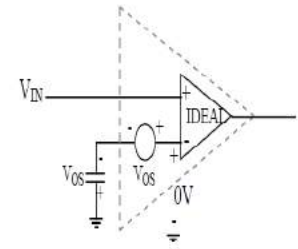
As shown in Fig. 9(a) during the first half cycle the comparator connected in the unity-gain configuration so that the input offset is available at the output. For the proper work, it is necessary that the comparator should be stable in the unity-gain configuration. This implies that only self compensated high-gain amplifiers would be suitable for auto zeroing. In the second half cycle Fig. 9(b) of the auto zero algorithms C_{AZ} is placed at the input of the comparator in series with Vos. The voltage across $C_{AZ \ adds}$ to Vos, resulting in zero volts at the inverting input of the comparator. Since there is no path to discharge the auto zero capacitor, the voltage across it remains indefinitely (in the ideal case). In reality, there are leakage paths in shunt with C_{AZ} that can discharge it over a period of time. The solution to this problem is to repeat the auto zero cycle periodically.
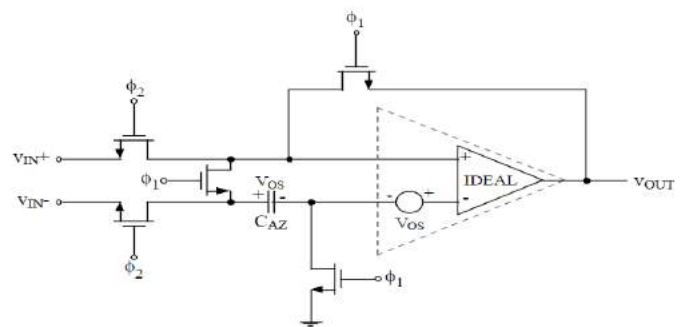
All   transistors have size i.e. (W/L)=10/1

Fig.10 Auto zeroing implementation.

Fig. 10 shows the implementation of the auto zeroing method for offset minimisation. Here the area under the dashed part is the two stage comparator, whose offset is minimised using auto zeroing.

III. SIMULATION RESULTS

The simulation result of conventional three stage comparator is shown in Fig.11.
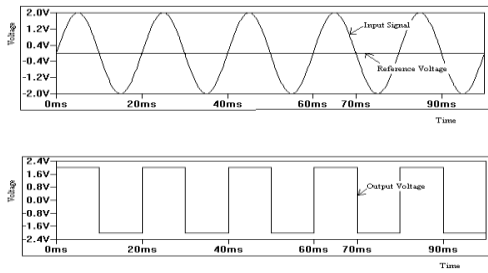
Fig. 11 Conventional Three Stage Comparator.

Fig. 12 shows the overall measured performance of the track and latch comparator with an input frequency of 1MHz and   phi 1 (clock) frequency of 51 MHz.

Fig. 13 shows the measured plot of the current of M5 (I_{tail}), It indicates that current is flow only during rising edge of clock and for rest of the clock period, this tail current is almost zero. So power consumption is reduced.
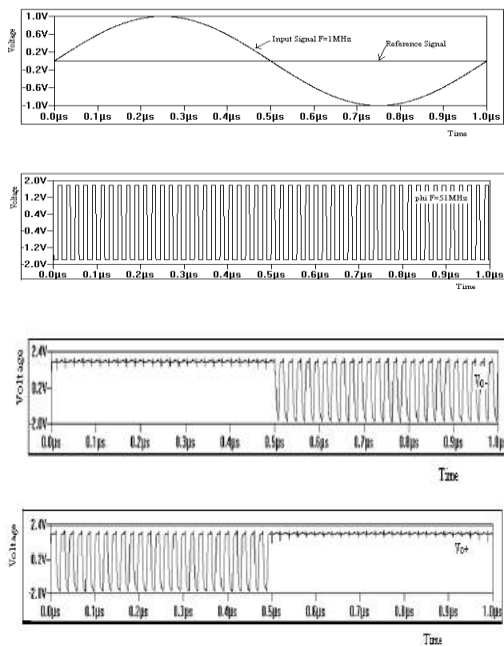
Fig. 12 Measured overall performance of the Track and Latch comparator – Fin=1000 KHz and phi1=51MHz.
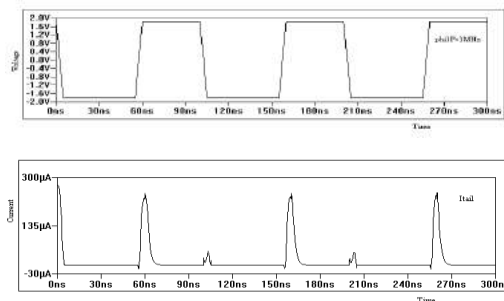
Fig. 13 Measured switched tail current of the Track and Latch comparator – *Fin*=100 kHz and *phi1*=1MHz.

TABLE 2: COMPARISON OF TRACK AND LATCH COMPARATOR WITH THE PREVIOUS WORK.

Parameters	This work	Previous Work [4]
I_{tail}	331μA	288 μA
Slew rate	0.6700V/nS	-
Delay	8.83nS	80 nS
Speed	51.2 MHz	18 MHz
Area	56.6 um^2	-
Power Supply	±1.8V	±1.65V
Technology	0.18 μm	0.35μm

TABLE 3: COMPARISON OF DIFFERENT COMPARATOR PARAMETERS.

Parameters	Differential comparator	Two Stage comparator	Three Stage comparator	Track and latch comparator
Power Dissipation	1.43mW	1.43mW	2mW	0.44833mV
Slew rate	0.133V/nS	0.290 V/ns	0.660V/ns	0.6700V/nS
Delay	0.55μS	0.425 μS	0.0322 μS	0.00883 μS
Speed	1.81MHz	2.35MHz	31.05MHz	51.2MHz
Area	50 μm^2	70 μm^2	428 μm^2	56.6 μm^2
Offset Voltage	45.4mV	1.65mV	0.498mV	275.488mV

Table 2 shows the simulation results of the Track and Latch Comparator with the previous work. The speed and area are improved at the cost of power dissipation.

Table 3 shows the comparisons of the comparator parameters.
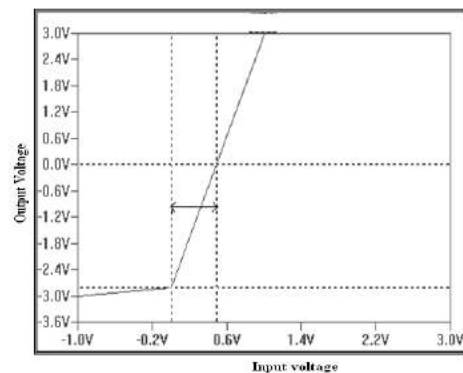
Fig. 14   Offset Voltage= 486.5mV without Minimisation Technique
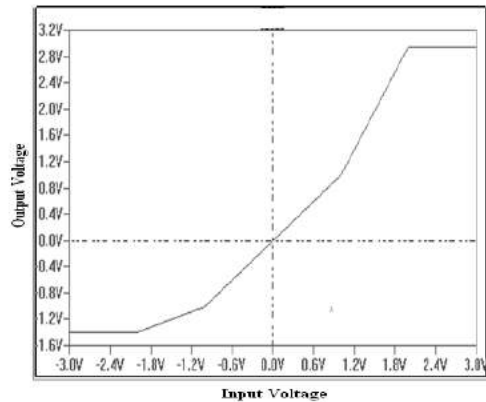
Fig.15 Offset Voltage = 1.465mV with Minimisation Technique

Fig.14 and 15 shows the simulation of offset voltage without and with minimization technique respectively.

IV.   CONCLUSIONS

Here the different comparator modules are designs and discuss. From the simulation results it shows that among all the comparator modules the Track and Latch Comparator provides the high speed, low power dissipation at the expense of the larger offset voltage.

V.   REFERENCES

[1]   P.E. Allen and D.R. Holberg, CMOS Analog Circuit
         Design – 2nd Ed., Oxford.
[2]   Debasis Parida," A Novel High Speed Cmos Comparator With Low
         Power Disipation And Low Offset".
[3]   M. Bazes, "Two Novel Fully Complementary Self- Biased CMOS
         Differential Amplifiers", IEEE - Journal of Solid-State Circuits, vol.
         26, NO. 2, Feb 1991.
[4]   Track-and-Latch Comparator Design Using associations of MOS
         Transistors and Characterization by Fernando Paixão Cortes,
         Alessandro Girardi, Sergio Bampi,IEEE 20006.
[5]   J. H. Choi, "Mixed-Signal Design of Sigma-Delta Modulators on the
         Pre-Diffused Array Using Trapezoidal Association of Transistors",
         Ph.D. Thesis, UFRGS, 2001
[6]   P. Cortes, E. Fabris, S. Bampi, "Analysis and design of amplifiers and
         comparators in CMOS 0.35μm technology", in Microelectronics
         Reliability, Eselvier Ltd., April 2004, vol. 44, p. 657 – 664.

Simulation & Performance Analysis of DVB-T System Using Efficient Wireless Channels

Nirali A. Kotak

nirali.kotak@git.org.in

Abstract: This paper presents the critical comparative analysis of efficient wireless channels using the modeling of Digital Video Broadcasting (DVB) system. In the last few years, the telecommunication industries' development has focused on an intensive use of broadband systems, which are characterized by high quality features. For this issue, new technologies with lower Bit Error Rate abilities have been designed. That is the fundamental of the wireless communication system that allows a fast deployment as well as efficient channel modeling. As wireless communication is in great demand for different personal communication, effective channel modeling becomes imperative. Digital Video Broadcasting (DVB), is a set of internationally accepted open standards for digital television, maintained by the DVB Project. This system is much more than a simple replacement for existing analogue transmission. This system has many advantages such as picture quality and allows you a range of new features and services including subtitling, multiple audio tracks, interactive content, multimedia content, etc. The paper helps to understand the concept of effective modeling of a DVB-T system with the proper use of various types of wireless channels under appropriate circumstances. In this paper, we build up a DVB-T simulator which is designed for digital terrestrial television services to operate within the existing VHF (Very High Frequency) and UHF (Ultra High Frequency) spectrum allocations for analog transmissions, 50-230 MHz and 470-870 MHz respectively including digital modulation, OFDM modulator and demodulator, different channel models such as AWGN, Rayleigh and Rician fading channels. In the first phase the modeling and simulation of DVB-T system has been presented along with different types of channels. In the second phase the comparative analysis of AWGN, Rayleigh and Rician channel has been done under practical scenario by taking the various values of Bit Error Rate and S/N ratio as well as Doppler shift. The whole model includes the basic mechanism of OFDM system so as to have effective communication by saving the required value of bandwidth.

Index Terms - DVB-T System, OFDM, AWGN Channel, Rayleigh Channel, Rician Channel, BER & SNR .

I. INTRODUCTION

The wireless networks have experienced massive growth and commercial success in the recent years. A new kind of "wireless video" is currently entering consumer's homes – digital television. The term digital video broadcasting is used as a synonym for digital television. Digital Video Broadcasting is a transmission scheme based on moving pictures expert group MPEG-2 video compression. DVB provides superior picture quality with the opportunity to view pictures in standard format or wide screen (16:9) format along with mono, stereo and surround sound. The three key DVB standards concern the delivery of digital TV to the consumer via the traditional broadcast networks are:

- DVB – S for satellite network
- DVB – C for cable network
- DVB – T for terrestrial network.

In the ETSI 300 744 standard, the DVB-T system is defined as the functional block of equipment performing the adaptation of the baseband TV signals from the output of the MPEG-2 transport multiplexer, to the terrestrial channel characteristics. The system is designed for digital terrestrial television services to operate within the existing VHF (Very High Frequency) and UHF (Ultra High Frequency) spectrum allocations for analog transmissions, 50-230 MHz and 470-870 MHz respectively. The DVB-T standard is based on the Orthogonal Frequency Division Multiplexing (OFDM) multi carrier modulation scheme. The transmission

data stream is distributed over a set of orthogonal subcarriers, equally spaced in pre-assigned VHF and UHF channels, characterized by a bandwidth equal respectively to 7 MHz and 8 MHz. Each subcarrier is then digitally modulated according to a QPSK, 16-QAM or 64-QAM scheme. The number of subcarriers can be set according to two modes of operation: *2K mode* and *8K mode*.

However, the radio channels in mobile radio systems are usually not amiable as the wired one. Unlike wired channels that are stationary and predictable, wireless channels are extremely random and time-variant. It is well known that the wireless multi-path channel causes an arbitrary time dispersion, attenuation, and phase shift, know as fading, in the received signal. Fading is caused by interference between two or more versions of the transmitted signal which arrived at the receiver at slightly different times.

In general, the need for communication channel are for providing faith full mobility, capable of higher data rate, better integrated interoperable with wide range of equipment, easier to configure and use. Hence effective modeling and diverting the multiple paths to the receiver is extremely important for the performance of the overall systems. In this paper, the simulation of DVB – T system has been discussed with the implementation of three wireless channels. For wireless communication system, different parameters such as modulation technique, bandwidth, frequency range, bit rate, etc in some sense or the other depends up on the channel modeling. Therefore, it is very important to look forward for effective channel modeling. The paper is divided into two parts. First part deals with the modeling and simulation of DVB – T system with different wireless channels and second part is regarding their comparative analysis.

II. ORTHOGONAL FREQUENCY MULTIPLEXING

In real-life transmission environments, multipath propagation and echoes from objects lead to the received signals arriving at the destination in a time-delayed fashion. These signals suffer frequency selective fading as a result of the multipath propagation effects. When single carrier is used to carry high data rates (i.e., a short symbol time), the received signals have enough delay spread to fall into the slots of other symbols thereby causing intersymbol

interference. In the case of a single carrier modulation, this type of propagation limits the data rates that can be used in non-line-of-sight (NLOS) environments. The technology of OFDM is based on the use of a large number of carriers spread in the allocated bandwidth, with each carrier being modulated by a proportionately lower data rate than would be the case in a single-carrier scenario.

OFDM can be viewed as a form of frequency division multiplexing (FDM) with the special property that each tone is orthogonal with every other tone, but it is different from FDM in several ways. On one hand, **FDM requires, typically, the existence of frequency guard bands between the frequencies so that they do not interfere with each other.** On the other hand, **OFDM allows the spectrum of each tone to overlap, and because they are orthogonal, they do not interfere with each other.** Furthermore, the overall amount of required spectrum is reduced due to the overlapping of the tones.
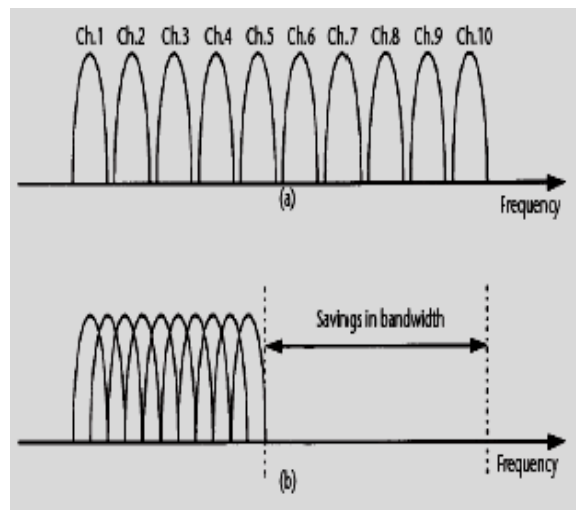
Figure-1 orthogonal frequency-division multiplexing

In OFDM systems, each carrier is orthogonal with respect to the other carriers, so that the sidebands of the carrier cancel out rather than interfering with the next carrier. OFDM is a common technology used in achieving high bit rates in all wireless and wireline systems, which may be subject to frequency selective fading or intersymbol interference from reflected signals. OFDM systems provide a very robust transmission technique for NLOS environments.

III. DVB-T SYSTEM WITH AWGN CHANNEL

The simplest type of channel is the Gaussian channel. It is often referred to the additive white Gaussian noise (AWGN) channel. Basically, it is the noise generated in the receiver side if we assume that the transmitter is ideal and noiseless. This type of noise is assumed to have a constant power spectral density over the whole channel bandwidth and its amplitude probability density function (PDF) obeys the statistics of a Gaussian distribution. The classical AWGN channel is always considered as the starting point to develop basic systems performance. Also, according to central limit theorem, even when there are a larger number of non-Gaussian independent noise sources, the mobile channel noise may still be approximated with a Gaussian distribution.

The traditional model for DVB – T system is built on OFDM & 64-QAM modulation scheme. The modeling setup includes Matlab R2007a, Simulink7 and Communications Block set 3 running on Windows XP SP2. Matlab Simulink includes all the mandatory function blocks as specified by the standard documents. The Model itself consists of three main components namely transmitter, receiver and channel. Transmitter and receiver components consist of modulation/ demodulation blocks and OFDM modulation and demodulation blocks whereas channel is modeled as AWGN.

Bernoulli data generator is the first process carried out in the physical layer after the data packet is received from the higher layers. Each burst in Downlink and Uplink is randomized. The purpose of the scrambled data is to convert long sequences of O's or 1's in a random sequence to improve the coding performance. Forward Error Correction is done on both the Uplink and the Downlink bursts and consists of concatenation of Reed- Solomon Outer Code and a rate compatible convolution inner code. Convolution coders are used to correct the random error during the data transmission. The block interleaver interleaves all encoded data bits with a block size corresponding to the number of coded bits per OFDM symbol. The number of coded bits depends on the modulation technique used in the Physical layer.

The function of the IQ mapper is to map the incoming bits of data from inter-leaver onto a constellation. In the modulation phase the coded bits are mapped to the IQ constellation. To simplify transmitter and receiver designs, all symbols and data bursts are transmitted with equal power by using a normalization factor.
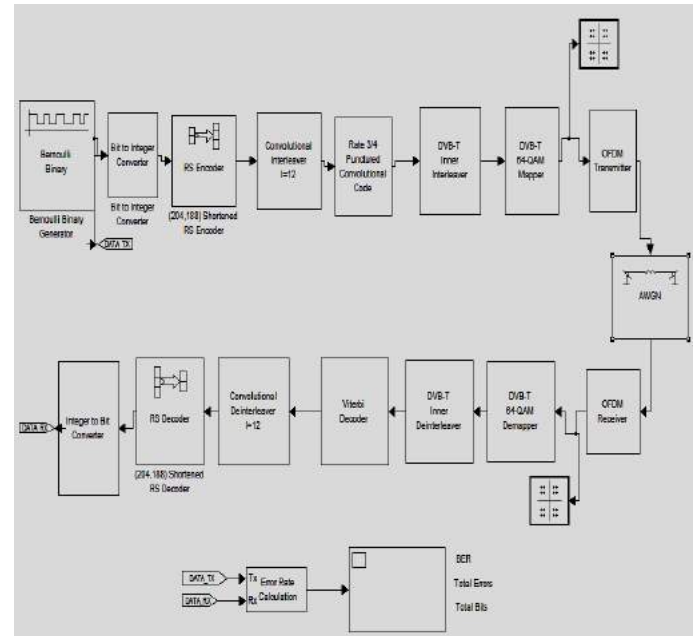
Figure 2 System model with AWGN channel

Now before transmitting this modulated data stream through the channel, it is given to the OFDM modulator block which performs the multiplexing over the data in such a manner that approximately 50% of the bandwidth can be saved because of the mechanism of bifurcating the signal in in-phase and quadrature phase components. Basically OFDM modulator and demodulator comprise of mainly IFFT and FFT blocks respectively for the orthogonal component generation.

Finally the processed data from the transmitter block is transmitted through AWGN channel which will give the different values of BER at various S/N level in the long distance communication. At higher db values of the SNR, the realization of AWGN channel gives the maximum accurate throughput about the signal variations because through the modeling of AWGN channel, the point to point variation in BER can be found out wrt SNR at longer distances. Based on the model presented in this paper, and tests carried out, the performance was established based on 10 million symbols in each case.

IV. SYSTEM MODELING USING RAYLEIGH CHANNEL

In a mobile radio communication system, one of the most devastating phenomena is fading. Fading is the direct result of multi-path propagation where radio waves propagate along different paths before arriving at the receiver antenna. These radio waves may arrive at receiver after different delays, with different amplitudes, and with different phases. Because there are so many different received signal components, constructive and destructive interference results in fading. This sort of channel is called a multi-path fading channel or Rayleigh channel. In urban areas where generally there is no line of sight component present, the analysis of the mobile radio channel can be obtained by modeling the Rayleigh channel rather than AWGN channel for mobile communication because the multipath structure can completely predicated through the modeling of this.

V. SYSTEM MODELING USING RICIAN CHANNEL

Rayleigh channel model is suitable for modeling urban areas that are characterized by many obstructions where a line of sight path does not exist between the transmitter and receiver. In suburban areas, a line of sight path may exist between the transmitter and receiver and this will give rise to Rician fading. Rician fading is characterized by a factor, which is expressed as the power ratio of the specular (los or dominant path) component to the diffused component. This ratio, k, defines how near to Rayleigh statistics the channel is. In fact when k=infinite, there is no fading at all and when k=0, this means to have Rayleigh fading. The ratio is expressed linearly, not in decibels. While the Average path gain vector parameter controls the overall gain through the channel, the **K-factor** parameter controls the gain's partition into line-of-sight and diffuses components.

We can specify the **K-factor** parameter as a scalar or a vector. If the **K-factor** parameter is a scalar, then the first discrete path of the channel is a Rician fading process (it contains a line-of-sight component) with the specified **K-factor**, while the remaining discrete paths indicate independent Rayleigh fading processes (with no line-of-sight component).
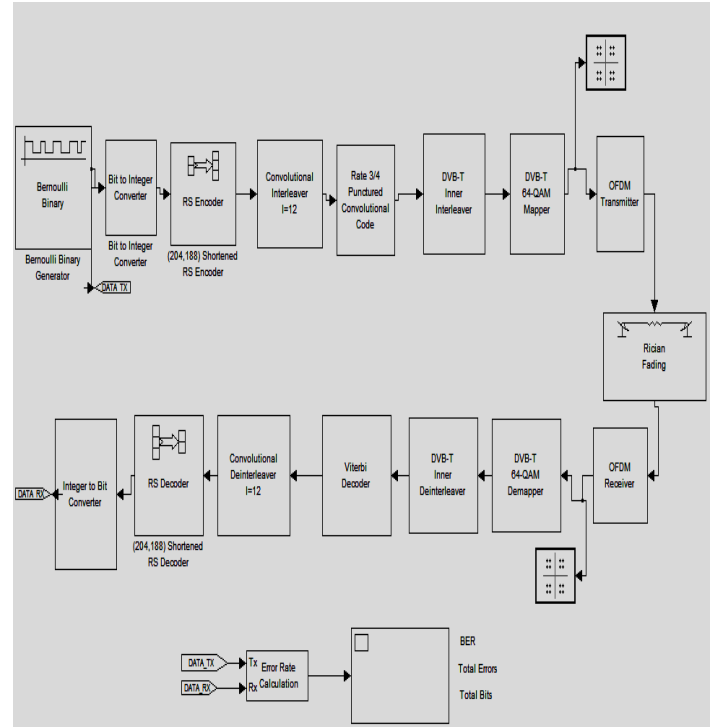
Figure 3 System model with Rayleigh channel
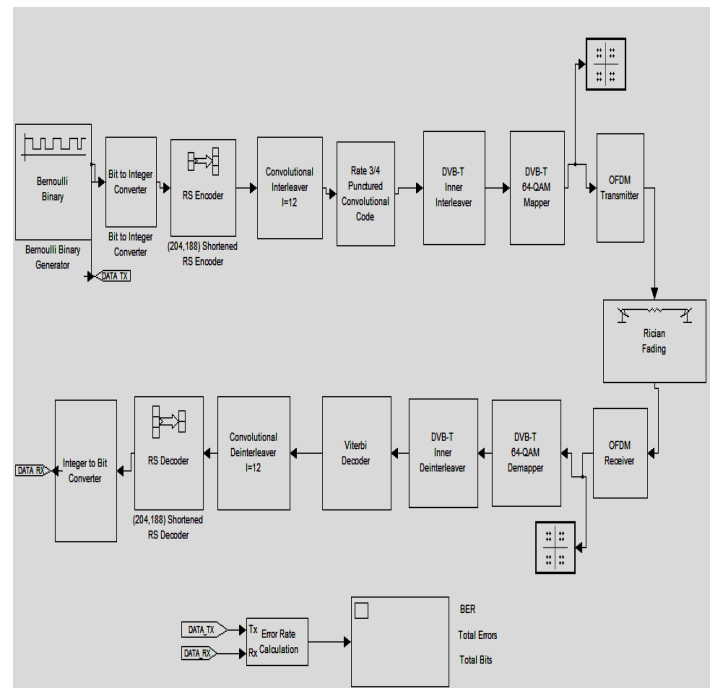
Figure 4 System model with Rician channel

If the K-factor parameter is a vector of the same size as Discrete path delay vector, then each discrete path is a Rician fading process with a K-factor given by the corresponding element of the vector.

VI. SIMULATION RESULTS

From the simulation model with AWGN channel, the time-scattered plot and BER plot can be obtained for SNR equal to 8 and 22db.

It can be seen from the figure that as the SNR of AWGN channel decreases, the fluctuation of the OFDM symbols form the mean values are changing and hence BER of system increases proportionally. It also shows that at very low SNR the symbols are very difficult to recognize. Real time signals are also transmitted through this model.

(a)

(a)

(b)

Figure 6(a) & (b) Simulation Results for Rayleigh channel with 1/1000 and 1/100 Doppler shift

In case of Rayleigh channel modeling the complete multipath structure of the transmitted signal can be analyzed by means of the variation in the amount of Doppler shift as well as path gain factor. The above simulation results show the constellation diagram of the received data under the multi path environment.

(b)

Figure 5(a) & (b) Simulation Results for AWGN channel with 8 db and 22 db SNR

(a)
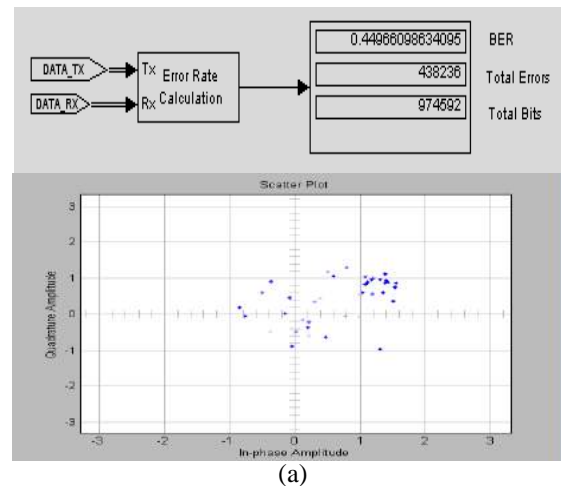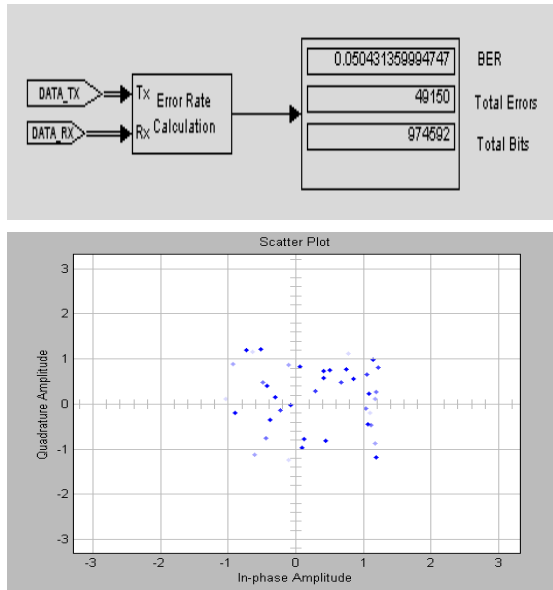
(b)

Figure 7 (a) & (b) Simulation Results for Rician channel with k=10 and k=40

From the simulation results shown in the above figure for the Rician channel modeling, it can be observed that the BER totally depends upon the value of k-factor which gives the relationship between the line of sight path and the multi paths. As k-factor increases the error rate would decrease because communication is now tending towards the line of sight communication.

VII. CONCLUSION

Based on the simulation models of DVB-T presented in this paper and the tests carried out, the comparative performance analysis of the three wireless channels i.e. AWGN, Rayleigh and Rician can be described based on various parameters. For the long distance communication, at the higher value of SNR, it is appropriate to model wireless channel as AWGN channel because through this modeling we can analyze the variations in SNR through which the BER can be calculated. While for the small scale propagation, under the multi path environment, the modeling of wireless channel as a Rayleigh channel will give the accurate analysis if no line of sight component is present. But if surrounding atmosphere supports the single line of sight component along with the multipath structure then the Rician channel realization will give the appropriate modeling scenario for the modeling of any wireless system.

VIII. FUTURE WORK

To combat with the current demands of wireless technologies, still the performance of the DVB-T system can be improved by reducing the BER at lower SNR with the implementation of various antenna diversity techniques.

IX. REFERENCES

[1] David Tse, University of California, Berkeley Pramod Viswanath, *Fundamental of Wireless Communication*, published by Cambridge University Press, 2004

[2] Jelena Mi¡si and Vojislav B. Misic, *Wireless Personal Area Networks Performance, Interconnections and Security with IEEE 802.15.,* John Wiley & Sons, Ltd

[3] Ibrahim A. Z.Qatawneh, "*Comparison of Bit Error Rate Performance of multicarrier DE-APSK system and single carrier DE-APSK system in the presence of AWGN & Rician fading channels*", IEEE Transaction

[4] Nedeljo Cvejic, Tapio Seppanen, "*Rayleigh fading Channel model v/s AWGN Channel model in Audio Watermarking*", IEEE Transaction

[5] Lei Zhou, Shidong Zhou, and Yan Yao, "*Non-coherent Mutual Information of the Multipath Rayleigh Fading Channel in the Low SNR Regime*", IEEE Transaction

[6] Muhammad Islam, M A Hannan, S. A. Samad and A. Hussain, "*Performance of RFID with AWGN and Rayleigh Fading Channels for SDR Application*", IEEE Transaction

[7]Ladislav Polák, Tomáš Kratochvíl, "*MATLAB simulation of DVB-T transmission under different transmission conditions*", IEEE Transaction.

[8] Daniele Fortin, "*Performance assessment of DVB-T and wireless communication systems*", IEEE Transaction.

[9] *Ondřej Hüttl, Tomáš Kratochvíl, "DVB-T Channel coding implementation in MATLAB*"

[10] Mark Massel, "Digital Television, DVB-T COFDM and ATSC 8-VSB."

[11] Walter Fischer, "Digital Video and Audio Broadcasting Technology"

[12] R. Van Nee, R. Prasad, "OFDM for wireless multimedia communication"

[13] ETSI EN 300 744, Digital Video Broadcasting (DVB); Framing structure, channel coding and modulation for digital terrestrial television, v. 1.5.1, June 2004

[14] www.mathworks .com

Technique for Non Distractive Quality Evaluation Of Cuminum Cyminum L (Cumin) Seeds Using Colorization

Jalpa J. Patel

jalpa.patel@git.org.in

Abstract: **Colorization based analysis is widely used in spice as well as in food industry. Using this paper we propose a technique for non destructive, efficient and novel technique of color image processing and then propose an efficient quality analysis for the spices to be exported. Prior to export, Cuminum Cyminum L(Cumin) seeds are subjected to examine for the purpose of quality control and grading. For quality grading, the cumin seeds are cleaned and screened manually hence the practice is laborious, time consuming and labor intensive. We have developed of a machine vision system for quality examine using combined measurement analysis. The methodology involves collecting the RGB images and then converting them to gray scale images based on histogram analysis. Some colorization procedures are used for image enhancement to analyze the species from the background. Then the combined measurements consisting of area, minor axis length are extracted from the ISEF applied colorized images. The quality evaluation of the specified samples is done on the basis of quality table so formed.**
Keywords: **Quality control, Machine Vision, Cuminum cyminum L (Cumin Seeds), ISEF edge detection, combined measurements.**

I.   INTRODUCTION

In the world of automation intense research is in progress on application of electronic eye and nose in food, beverages to food quality and safety, such as, the shape or color or odor of a given good.

Traditionally, in India quality inspection is performed by trained human inspectors, who approach the problem of quality assessment in two ways, observing by looking and feeling the whole bulk of cumin seeds. In addition to being costly, this method is highly variable and decisions are not always consistent between inspectors or from day to day [10]. This is, however, changing with the advent of electronic imaging systems and with the rapid decline in cost of computers [7], cameras, peripherals and other digital devices.

In this type of environment, machine vision systems are ideally suited for routine inspection and quality assurance tasks. Backed by powerful state-of-the-art electronic technologies [17], machine vision provides a mechanism in which the human thinking process is simulated artificially. Kavindra Jain et al [20],[21], developed a quality evaluation method describing two major parameters for quantification by taking a RGB image directly. The quality value computed using the method proposed in [21] is not near to the true quality values. Up till now colorization was implemented in and spice industry. Non destructive technique so used makes it possible to examine the quality of food without damaging it. In this area of food industry such type of quality evaluation is gaining more momentum. Image processing is one of the most commonly used for this purpose especially for the quality control of proteins, lipids and species etc. Indian spice industry accounts for 30% to 45% in world trade. Indian spice industry especially from Gujarat (Unjha) and Tamil Nadu provide quality species at competitive prices. To increase share in exports of the species the need of Indian manufacturers is to ensure consistency in supply, product, quality, pricing, and marketing producers are now incorporating latest methods and techniques to ensure higher quality of species and herbs.

On the basis of such large new techniques the most user friendly and best approach is with the help of image processing. Quality control is essential in the food and spice industry and efficient quality assurance is becoming increasingly important [4]. Consumers expect the best quality at a competitive and affordable price, good shelf-life and high safety while spice inspections require good manufacturing practices. In this context, machine vision technologies might prove highly relevant, providing objective measurements of relevant visual attributes related

food by Liyanage C De Silva[22] but not in spice industry. So we have combined colorization with the method proposed in [21] which results in to quality value near to true quality values.

Paper is broadly divided into six main section and various sub sections wherever required. In this paper the problem being faced by the spice industry, in particular cumin seeds exporters is discussed in Section 2. Section 3 discusses the materials and methods proposed for quantifying the quality of cumin seeds. The colorization is described in the same section. The proposed algorithm for computing cumin seeds with pedestals as well as foreign materials [9] being present (sticks, stones etc.) in the sample is also discussed in the same section. Section 4 discusses the quantification for the quality of cumin seeds based on image processing and then comparison of various results. Section 5 comprise of results and discussion based on quality analysis. Section 6 concludes the paper.

II.   PROBLEM DEFINITION

Cuminum cyminum L (Cumin) is a small and slender annual herb, which grows up to a height ranging from 40-50 cm with many branches and linear, dark green leaves. The stem has 3-5 primary and 2-3 secondary branches. Flowers are very small, mostly pink and sometimes white in color. Seeds are small elongated, oval and attain light yellowish to greyish brown in color. The seeds are mostly used as condiments in the form of an essential ingredient in all mixed spices and in curry powder for favouring vegetables, pickles, soups, sausages, cheese and other preparations and also for seasoning of breads, cakes and biscuits. It is used in many Ayurvedic and veterinary medicines as carminative, stomachic, astringent and is useful against diarrhoea and dyspepsia.

A Cuminum cyminum L (cumin) seed contains pedestals as shown in Figure 1.

Fig 1: Cumin seeds with
and without pedestals

Fig 2: Foreign Elements in the sample

If seen closely to the cumin seeds having pedestals they are of prime importance for quantifying quality. If these pedestals are incorrectly removed then it not only deteriorates the quality but it also increases its pungency. This may lead to microbial growth and blackening of kernel at that particular point. Microbial growth not only spoils the taste of food but is also unfit for consumption. Other than pedestals the presence of foreign elements in cumin seeds also reduces its quality. This foreign element basically consists of top part of the seeds, stones and only pedestals as shown in Figure 2. This problem leads us to think that if the quality of the Cuminum cyminum L (cumin) seeds can be quantified automatically using machine vision system at the initial level itself then this product would become a part of export at a higher rate. This problem also leads us to define quality of cumin seeds and different grades of quality of cumin seeds. The same strategy and method was followed by Kavindra R. Jain et al in his method the result were satisfactory and even acceptable for use but the main problem faced by the paper was they were not so close to true value as per expectation.

III.   Materials and Methods

In this section we discuss the proposed algorithms along with the definition of quality based on combined measurements technique. We have used area of cumin seeds and minor axis length of cumin seeds for counting the number of Cuminum cyminum L (cumin seeds) with long pedestals as well as foreign elements.

A. System Description, Image Pre Processing and Operating Procedure:

Colorization is a very straight forward and simple approach for quality inspection. The general block diagram as shown in figure:-3 suggest that first of all a RGB image is captured and converted to Grayscale image.
The gray scale image is applied with swatch algorithm. With help of this algorithm the image would now be represented in YUV space. Then histogram is taken and background as well as foreground images are separated. Foreground image is applied with a different color and after processing a scribbled image is obtained. This image on further processing using optimization gives a final colorized image which is then applied with ISEF edge detection algorithm and result so

TABLE I
OPERATING PROCEDURE

Sr.No.	Steps
1.	Spread the samples uniformly on the tray to avoid overlapping of seed.
2.	Capture the image with the help of digital camera
3.	Processing the Image in computer
4.	Display number of cumin seeds with pedestals and foreign elements on screen.
5	Repeat the steps 1 to 4 for 10 to 15 samples

obtained can be seen on screen. The simplicity of operation of system can be concluded from the operating procedure as in Table I.

According to the procedure the person should first of all select random samples from the bulk of cumin seeds to be packed and sent to the market. These samples are spread on tray in such a way that there is no overlapping of the seeds. Image captured is now transferred to the processing unit where according to Table II quality of cumin seeds is determined and displayed on screen [13].

B.   Proposed algorithm to detect cumin seeds with pedestals and foreign elements: According to our proposed algorithm the captured image will be a color image as shown in Figure 4. So it is converted in to gray scale image as shown in Figure 5 since to apply swatches in the image.

Swatching the image according to the histogram of the gray level image. The resultant image is a colorized image as shown in figure 6. An optimal edge detection technique, ISEF, given by Shen and Castan is applied on the colorized image [12] to separate the cumin seeds having long pedestal as well as foreign elements being present in the sample. Hysteresis thresholding is applied in the ISEF algorithm, which is detailed in Table III.

TABLE II
PROPOSED ALGORITHM TO COMPUTE QUALITY OF CUMIN
SEEDS

Sr.No.	Steps
1	Select the region of interest of the cumin seeds
2	Convert the RGB image to gray images
3	Swatches based on histogram of gray level image.
4	Resultant is scribbled image
5	Apply optimization on scribbled image to get a colorized image
6	Apply the ISEF edge detection (detailed in Table: III)on colorized image
7	Calculate the area of the cumin seeds.
8	Calculate the minor axis of the cumin seeds
8	Find the histogram of the areas of cumin seeds.
9	Compute the threshold value based on histogram
10	Classify the three different classes of cumin seeds based on the threshold value computed from the histogram
11	Display on screen a) The total number of cumin seeds in the sample b) Number of cumin seeds with pedestals c) Number of foreign materials in the sample.

Fig 4: RGB image of the sample

Fig 5: Gray Scale image
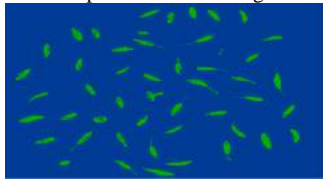
Fig 6: Colorized image

C. Swatching and colorization using optimization:

In the process of swatching based on histogram the foreground and background images are separated and a different color is assigned. A single seed out of all seeds is assigned a color and using this process a scribbled image is acquired which would finally give a swatched image displaying all seeds with a different color as shown in figure 6. The color to be assigned is totally dependent on YUV Color space. The resultant swatches / scribbled image is applied with colorization using optimization. The following equations are used for the process applying optimization in colorized image.

$$J(U) = \sum_r \left(U(r) - \sum_{s \in N(s)} WrsU(s) \right)^2 \quad \text{..........}(2.3.1)$$

$$J(V) = \sum_r \left(V(r) - \sum_{s \in N(s)} WrsV(s) \right)^2 \quad \text{..........}(2.3.2)$$

$$Wrs \propto \exp{-(Y(r) - Y(s))^2 / 2\sigma_r^2} \quad \text{..........}(2.3.3)$$

D. ISEF EDGE DETECTION: The edge can be detected by any of template based edge detector but Shen-Castan Infinite symmetric exponential filter based edge detector is an optimal edge detector like canny edge detector which gives optimal filtered image. First the whole image will be filtered by the recursive ISEF filter in X direction and in Y direction, which can be implement by using equations as written below.

Recursion in x direction:

$$y_1[i, j] = \frac{(1-b)}{(1+b)} I[i, j] + b\, y_1[i, j-1], \quad (1)$$
$$j = 1...N, i = 1..M$$

$$y_2[i, j] = b \frac{(1-b)}{(1+b)} I[i, j] + b\, y_1[i, j+1] \quad (2)$$
$$j = N...1, i = 1..M$$

$$r[i, j] = y_1[i, j] + y_2[i, j+1] \quad (3)$$

Recursion in y direction:

$$y_1[i, j] = \frac{(1-b)}{(1+b)} I[i, j] + b\, y_1[i-1, j], \quad (4)$$
$$i = 1...M, j = 1..N$$

$$y_2[i, j] = b \frac{(1-b)}{(1+b)} I[i, j] + b\, y_1[i+1, j], \quad (5)$$
$$i = M...1, j = 1..N$$

$$y[i, j] = y_1[i, j] + y_2[i+1, j] \quad (6)$$

b=Thinning Factor (0<b<1)

TABLE III
ISEF ALGORITHM

No	Steps
1	Apply ISEF Filter in X and Y direction
2	Apply Binary Laplacian Technique
3	Apply Non Maxima Suppression
4	Find the Gradient
5	Apply Hysteresis Thresholding
6	Thinning

Then the Laplacian image can be approximated by subtracting the filtered image from the original image. At the location of an edge pixel there will be zero crossing in the second derivative of the filtered image. The first derivative of the image function should have an extreme at the position corresponding to the edge in image and so the second derivative should be zero at the same position. And for thinning purpose apply non maxima suppression as it is used in canny for false zero crossing.

The gradient at the edge pixel is either a maximum or a minimum. If the second derivative changes sign from

positive to negative this is called positive zero crossing and if it changes from negative to positive it is called negative zero crossing .We will allow positive zero crossing to have positive gradient and negative zero crossing to have negative gradient, all other zero crossing we assumed to be false and are not considered to an edge.

Now gradient the simple thresholding can have only one cutoff but Shen-Castan suggests to go for Hysteresis thresholding. Spurious response to the single edge caused by noise usually creates a streaking problem that is very common in edge detection. applied image has been thinned, and ready for the thresholding.

The output of an edge detector is usually thresholded, to decide which edges are significant and streaking means the breaking up of the edge contour caused by the operator fluctuating above and below the threshold.

Streaking can be eliminated by thresholding with Hysteresis. Individual weak responses usually correspond to noise, but if these points are connected to any of the pixels with strong responses, they are more likely to be actual edge in the image. Such connected pixels are treated as edge pixels if there response is above a low threshold. Finally thinning is applied to make edge of single pixel. The ISEF algorithm is given in Table III. In Figure 7(a) cumin seed of good quality without pedestal is shown, while Figure 7(b) contains an image of a seed with

pedestal. After applying the ISEF algorithm of Table III, we get images of Figures 8 (a) and (b) respectively.
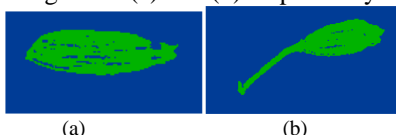
(a)   (b)
Fig 7: Colorized Cumin seed with and without pedestals
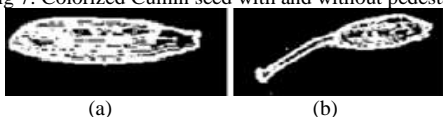
(a)   (b)
Fig 8: ISEF applied Cumin seed with and without pedestals

E. Computation of area and minor axis length of cumin seeds based on colorized image:

Area and minor Axis Length are defined as follows:

The area A of any object in an image is defined by the total number of pixels enclosed by the boundary of the object.

The minor axis length M of an image is defined as the length (in pixels) of the minor axis of the ellipse that has the same normalized second central moments as the region.

If we find the area of each cumin seeds separately and if the area of normal cumin seeds is, x, the area of cumin seeds with pedestal to be y will mostly be greater than x. While in case of foreign elements like sticks and lower quality seed (thin seed), the area z will mostly be less than x. Use of minor axis length of the seed will remove the usage of

Vernier caliper in case of human inspection system . To make the classification robust, we propose automatic threshold computation based on histogram of area discussed in next subsection.

F. Classification Of Cumin Seeds: The classification of the cumin seeds is done based on combined measurements of area and minor axis. A typical histogram of area of cumin seeds computed from a typical sample is shown in Figure 9 to identify different clusters of cumin seeds.   A typical histogram of minor axis length of cumin seeds computed from a typical sample is shown in Figure 10.
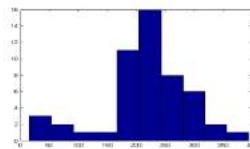
Fig 9: Histogram showing area   Fig 10: Histogram showing minor
of Cumin seed   axis length of Cumin seed
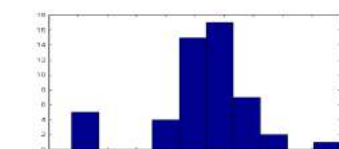
IV.   DEFINITION OF QUALITY OF CUMIN   SEEDS

The classification of cumin seeds as cumin with pedestal, without pedestal and foreign elements is based on combination of two parameters that is the area and the minor axis length of cumin seed.

The quality Q, of cumin seeds is not having any particular formula for quantification and assessment. Generally spice experts use simple formulas for analyzing the quality of Cuminum cyminum L (cumin) seeds. The quality factor Q depends on cumin seed with pedestals and foreign materials.

If these parameters increase percentage wise in the bulk of cumin seeds then as a result the quality Q would decrease. Hence the quality factor Q is inversely proportional to cumin seed with pedestals and foreign materials. So the Q factor can be defined as

$$Q = \frac{c_1 c_2}{x_1 + x_2}, \quad (7)$$

Assuming c_1 and c_2 to be 10, Q Table can be prepared defining various Q values on the basis of two parameters x_1 and x_2 . The first row and first column of Figure12 represents percentage of x_1 and x_2 present in the bulk of Cuminum cyminum L (cumin seeds). In figure 11: the top most ellipse represents Grade ”A”, the red color filled area represents grade ”B” which comprise of higher percentage of foreign elements as well as cumin seeds with pedestals. The bottom most encircled area is grade”C”. This formula would provide us same value of quality in each and every same possible combination as shown in Figure 12. So if one is having the value of cumin seeds then the grade of cumin seed could be easily analyzed based on the Figure.
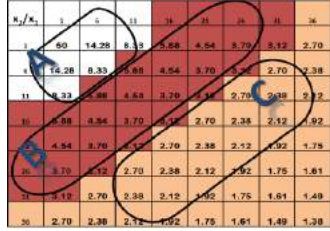
Fig 11: Q Curves according to figure 12

V. RESULT AND DISCUSSION

According to the ISEF edge detection method the gray scale image is applied with recursive filtering process in both x and y direction. The filtered image is subtracted from the original image and the binary Laplacian image is obtained as shown in Figure 13. After applying the positive and negative zero crossing on the gradient image it gets thinned. We apply Hysteresis thresholding with HT=40. The hysteresis threshold image is shown in Figure 14. The thresholded image is analyzed for computation of areas of cumin seeds with and without long pedestals and foreign elements (sticks, stones, broken seeds etc.). The area of cumin seeds which are greater than 275 in terms of pixels are the Cuminum cyminum L (cumin seeds) with pedestals. Area of Cuminum cyminum L (cumin seeds) without pedestals is between 100 and 275 pixel square. The foreign elements being present are having areas less than 100 pixel squares correspondingly. Correspondingly there are changes in minor axis length of Cuminum cyminum L (Cumin seeds).The results so obtained by the analysis of eleven such samples are given in Table IV. Table V describes the detailed (percentagewise) results of the analysis. The percentage average of x_1 is approximately 17 and that of x_2 is 6, giving the Q value as 4.54 which show that the sample under evaluation is not the best quality cumin seeds.
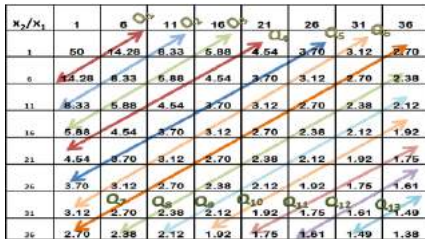
Fig 12: Symmetrical combination of Q values

Fig 13 :Gradient image of the sample
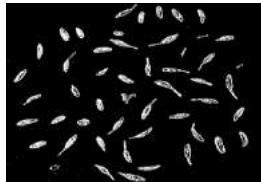
Fig 14: Hysteresis image of the sample

VI. CONCLUSION

In this paper we proposed a method for quantifying the

quality of cumin seeds by computing the number of cumin seeds with long pedestals as well as foreign elements (sticks, stones etc.) in the sample.

The method proposed in the paper gives a direction of certification of quality of cumin seeds based on non destructive machine vision based technique. The technique is simple, easy to implement and the results so obtained are good and can give better analysis of the quality as compared to human inspection sensory system. The time taken to obtain such results is also very less which clearly depicts its importance in the world of automation for machine vision and it would be also helpful for the quality inspection as customer loyalty with quality is of prime importance in the market.

TABLE IV
RESULT ANALYSIS OF VARIOUS SAMPLES

Sample	Total seeds	Number of cumin seeds with pedestal	Number of foreign elements	Number of normal cumin seeds
1	53	10	2	41
2	48	8	3	36
3	51	19	3	29
4	52	12	2	37
5	49	11	3	35
6	51	16	6	29
7	53	14	2	37
8	56	10	3	43
9	51	11	3	38
10	48	5	1	42
11	55	4	3	48

Comparison of three various tables (true values, values of the previous paper and new values) on the basis of percentage analysis are discussed as follows:-

TABLE V
PERCENTAGE WISE RESULT ANALYSIS OF VARIOUS SAMPLES OF TRUE VALUES

Sample	Total seeds	Cumin seeds with Pedestal (%) X_1	Foreign Elements (%) X_2
1	53	18.86792	3.773585
2	48	16.66667	37.5
3	51	37.2549	0
4	52	23.07692	16.66667
5	49	22.44898	27.27273
6	51	31.37255	37.5
7	53	26.41509	14.28571
8	56	17.85714	30
9	51	21.56863	27.27273
10	48	10.41667	20
11	55	7.272727	75
Average		25.72696	4.26402995

TABLE VI
PERCENTAGE WISE RESULT ANALYSIS OF VARIOUS SAMPLES OF
KAVINDRA R. JAIN ET .AL

Sample	Total seeds	Cumin seeds with Pedestal (%) X_{1K}	Foreign Elements (%) X_{2K}
1	53	20.75	3.77
2	53	13.20	7.54
3	49	38.78	0
4	52	11.54	13.46
5	48	31.25	6.25
6	51	25.41	11.76
7	55	12.72	9.09
8	51	49.01	5.88
9	48	37.5	4.16
10	51	3.92	19.6
11	56	7.14	0.125
Average		22.838	7.421364

TABLE VII
PERCENTAGE WISE RESULT ANALYSIS OF VARIOUS SAMPLES OF
COLORIZED IMAGE

Sample	Total seeds	Cumin seeds with Pedestal (%) X_{1J}	Foreign Elements (%) X_{2J}
1	53	24.528323	3.773585
2	53	9.433962	3.873585
3	49	21.454898	5.122449
4	52	13.46154	3.846154
5	48	17.66667	6.25
6	51	15.647066	13.76471
7	55	10.9090945	20
8	51	48.0196134	7.843137
9	48	10.416672	2.083333
10	51	18.647065	6.843137
11	56	3.571429	3.571429
Average		18.954934	6.98832

In all the three cases the value of Q so calculated according to the equation is 3.434335, 3.1645632 4.124583 respectively. The root mean square value of the third author and mine with true values are shown as follows in Table VIII:-

TABLE VIII
RMSE OF THREE TABLES

Sample	X_1-X_{1K}	X_2-X_{2k}	X_1-X_{1J}	X_2-X_{2J}
1	14.24497	0	19.33387	0
2	7.307516	7.307516	11.78302	3.26802
3	0	0	31.61619	6.122449
4	22.178	13.46154	21.06625	3.846154
5	11.21909	0	23.93568	0
6	14.67317	7.069708	23.52941	7.069708
7	28.16715	8.907235	28.91995	19.91718
8	34.01834	0	34.01834	5.187748
9	0	4.658475	36.0242	5.892557
10	19.21168	19.50956	8.546861	7.594085
11	0	3.992979	6.185896	3.992979
Avg.	13.72908	5.900637	22.26906	5.717353

But if factor x1 is calculated by third author's method and x2 ix calculated by color image method then the Q factor is near to true value:-3.163

VII.   FUTURE WORK

More parameters can be included for combined measurements technique which may result in to precise computation of Q values.

REFRENCES

[1] Abdullah MZ, Fathinul-Syahir AS, Mohd-Azemi BMN (2005)"Automated inspection system for color and shape grading of starfruit (Averrhoa carambola L.) using machine vision sensor." Transactions of the Institute of Measurement and Control, 27 (2), 65-87

[2] Abutaleb AS (1989)"Automatic thresholding of grey-level pictures using two-dimensional entropies." Pattern Recognition, 47 (1), 22-32.

[3] Batchelor BG (1985) "Lighting and viewing techniques In AutomatedVisual Inspection"(Batchelor BG, Hill DA, Hodgson DC, eds). Bedford:IFS Publication Ltd, pp.103-179.

[4] Blasco J, Aleixos N, Molt E (2003) "Machine vision system for automatic quality grading of fruit." Biosystems Engineering, 85 (4), 415-423.

[5]

[6] Canny J (1986) "A computational approach to edge detection." IEEETransactions on Pattern Analysis and Machine Intelligence, 8 (6), 679-698.

[7] J. M.Aguilera, A.Cipriano, M.Erana, I.Lillo, D.Mery A. Soto."Computer Vision for Quality Control in Latin American Food Industry"

[8] Du C-J, Sun D-W (2006c) "Learning techniques used in computer vision for food quality evaluation: a review." Journal of Food Engineering, 72(1), 39-55.

[9] Gan TH, Pallav P, Hutchins DA (2005) "Non-contact ultrasonic quality measurements of food products." Journal of Food Engineering, 77 (2),239-247.

[10] Ginesu G, Guisto DG, Mrgner V, Meinlschmidt P (2004)"Detection of foreign bodies in food by thermal image processing." IEEE Transactions of Industrial Electronics,51 (2), 480-490.

[11] Harmond J E, Kelin L M and Brandenburg N R.(1961)."Seed Cleaner and handling".USDA Handbook,179:38-48.

[12] R.P.Kachru et.Al."Development and testing of pedal cum power operated air screen cleaner."Agrcultural Machanization in Asia,Africa and Latin America.21(4):29-32.1990

[13] Kapur JN, Saho PK, Wong AKC (1985)" A new method for gray level picture thresholding using the entropy of the histogram." Computer Vision, Graphics, and Image Processing, 29, 273-285.

[14] Fu X, Milroy GE, Dutt M, Bentham AC, Hancock BC, Elliot JA (2005)"Quantitative analysis of packed and compacted granular systems by x-ray micro tomography." SPIE Proceedings Medical Imaging and Image Processing, 5747, 1955.

[15] Pun T (1980)"A new method for gray-level picture thresholding using the entropy of the histogram." Signal Processing, 2 (3), 223-237.

[16] Paulsen M (1990)"Using machine vision to inspect oilseeds." INFORM,1 (1), 50-55.

[17] Pearson T (1996) "Machine vision system for automated detection of stained pistachio nuts." Lebensmittel Wissenschaft and Technologie, 29 (3), 203-209.

[18] Xiaopei Hu, ParmeshwaraK.M.,DavidV."Development Of Non Destructive Methods To Evaluate Oyster Quality By Electronic Nose Technology". Springer Science Business Media, LLC2008

[19] Du CJ, Sun D-W (2004a) "Recent development in the applications of image processing techniques for food quality evaluation." Trends in Food Science and Technology, 15,230-249.

[20] Shen Castan, Sian Zhao, "A Comparitive study of Performance of Noisy roof edge detection "5th International conference on Computer analysis of Images and Patterns, volu.179,pp 170-174

[21] Kavindra R.Jain, Chintan K. Modi, Kunal J.Pithadiyaet.Al "Quality evaluation in spice industry with specific refrence to cumin seeds "MONAISH UNIVERSITY CITISIA 2009(IEEE),Malyasia, JULY 2009.

[22] Kavindra R.Jain, Chintan K. Modi, Kunal J.Pithadiya et.Al"Non destructive quality evaluation in spice industry with specific refrence to foeniculum vulgare(fennel seeds)"13th International Conference,IASTED VIIP,2009,Cambridge, UK conference in July 2009.

[23] Liyanage C De Silva, Anton Pereira, and Amal Punchihewa Institute of Information Sciences and Technology, Massey University, New Zealand

Portable Wireless Vibration Monitoring System for Measurement

Pratik J. Gohel
Electronics & communication Department,
GIT

Gunjan Jani
Electronics & communication Department,
GIT

Dhiren Vaghela
Electronics & communication Department,
GIT

Abstract—Now a days automobile industry and wireless technology is growing rapidly. For comfort and safety purpose extreme care is taken in automobile industry with the help of electronic devices. This type of devices are also used to make the user aware of some critical parameters like vibration of the system. Hence in this work we are proposing a microcontroller based cost effective wireless vibration monitoring system that can be useful in automobile industries. The system is equipped with accelerometer sensor and Bluetooth module for acquiring the vibration data and transmitting the same to other unit for wireless monitoring. This system includes transmitter and receiver sections for implementing this task. Transmitter section transmits acclerometer's sensed data which is conversed in digital form and sent to the receiver using Bluetooth module KC21. At the receiver side data is received and stored in Multi Media memory card and displayed on Graphical LCD.

Keywords: *Vibration, Wireless, measurement, Microcontroller*

I. INTRODUCTION

In today's era wireless technology is growing rapidly. Wire-less devices are used to make the system cable free and also used in remote monitoring system. With the help of integration of wireless technology with the embedded system, we can transmit data in wireless fashion for remote monitoring. For safety, security and measurement purpose, we use sensor based embedded system technology. There is rapid growth of sensor technology that enables us to measure any parameter and convert it into digital form. By advancement in sensor technology, we can measure such parameters related to the safety and security. Accelerometer is one of them, which measures amount of acceleration and converts it into electrical form representing the vibrations in any direction in form of electrical signal. There are many application in the real world based on the accelerometer in various field of engineering and medical technologies.

The recent research work has been reported about measuring and diagnosing the effect of vibration in different areas like biomedical, Automobile parts and automobile. In biomedical field, accelerometer is used to measure the body motion[1], various daily activities like walking,falling etc. for the elderly causing an extra burden on health care systems[2]. The research is conducted for the engine vibration measurement[3]. In this process they collect data from accelerometer and for the

diagnosis purpose they have used MATLAB tools and personal computer, for other parts of an automobile like gear, shaft and main retarder[4][5][6] vibration measurement and fault detection personal computer and data processing tools have been used. Main problem with this existing system is that, it require special kind of software tools and personal computer for diagnosis and fault detection. It is also difficult to realize in real time and use it online. There is need of real time Microcontroller baesd embedded system which can replace the requirement of PC and provide the online measurement directly to end user.

In this paper we are proposing the realtime wireless embedded system for monitoring the vibration information in automotive environment. The system supports multiple sensor nodes for acquiring vibration data from multiple peripheral sites in the automotive environment.

II. SYSTEM DESIGN

The system proposed here consists of transmitters as sensor nodes and a receiver for acquiring the sensor datas. Transmitter section contains battery, microcontroller, accelerometer and wireless transceiver. On the other hand receiver contains a microcontroller, wireless transceiver, power supply, SD mem- ory card and Graphical LCD. The basic work of transmitter module is to transmit measured data to receiver. If we see the detail working then, first the accelerometer sensor senses vibration of the automobile environment. Accelerometer is the sensor which measure vibration and convert it into electrical or analog signal form. The analog data of the accelerometer is gathered by the microcontroller. Controller collects the data and transmits it to the receiver module through the wireless device. The wireless device is interfaced serially with the controller. Battery is used for the power supply. The receiver module working principle is simple but very effective. The wireless device is interfaced with the receiver microcontroller and serially collects the data. Wireless device receives data that is transmitted, and it is nurtured to microcontroller. The microcontroller processes on this data. It shows the output in Graphic LCD and save same data in memory card.
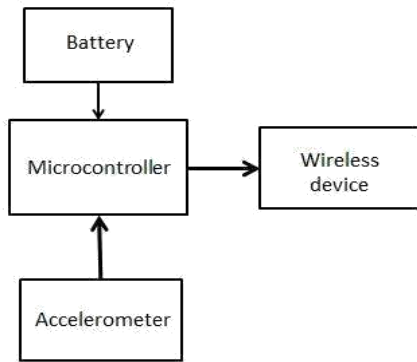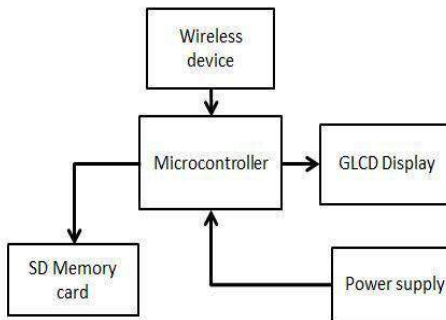
Fig. 1: Transmitter Design

Fig. 2: Receiver Design

A. Features of the System

The proposed system have the following features.

- Small, compact and highly reliable wireless embedded system to acquire an accelerometer data and to transmit wireless in automotive environment.
- It is portable, so we can use it any where at a time in any car or similar automotive vehicle for vibration measurement.
- It is wireless and battery operated so easy to move from one environment to another environment.
- The measurement and monitoring of the automobile environment is continuous and accurate.
- All the data is saved in memory card for further processing and data collection.
- It can show all data in Graphic LCD at realtime environment.
- Because it is battery operated, it requires low power consumption.
- It is also using the microcontroller and other low price device and because of that it replaces the need of personal computer so it is very cost effective.

B. Choices of the components

Choice of the system component is main key parameter because the wrong choice of the components not only affects the system work, efficiency and accuracy but also affect

the overall cost of the system. So for the best result right component must be chosen.

1) Microcontroller: Microcontroller is heart of the system. it handle all the resources and also controls the resources. it make all the necessary decision and take action according to requirement. In market so many microcontrollers are available.

Key Features	LPC2148	MSP430	8051
Operating Voltage	3.0 to 3.6v	1.8 to 3.6v	5v
Pin package	64	28	40
Architecture	32-bit	16-bit	8-bit
Timer	Two 32-bit	Three 16-bit	Two 16-bit
A/D converter	One 10-bit	Two 10-bit	-
ROM\RAM	40k\512k	256byte\8k	128byte\64k
Power down mode	Two power down mode	Five power down mode	-

Fig. 3: Comparison of Microcontrollers

Form the above table it clear that LPC2148 is best suited for our system. The key feature of LPC2148 is:

- 16/32-bit ARM7TDMI-S microcontroller in a tiny LQFP64 package.
- 8 to 40 kB of on-chip static RAM and 32 to 512 kB of on-chip flash program memory. 128 bit wide interface/accelerator enables high speed 60 MHz operation.
- EmbeddedICE RT and Embedded Trace interfaces offer real-time debugging with the on-chip RealMonitor soft- ware and high speed tracing of instruction execution.
- Two10-bit A/D converters provide a total of 14 analog inputs, with conversion times as low as 2.44 us per channel.
- Two 32-bit timers/external event counters (with four capture and four compare channels each), PWM unit (six outputs) and watchdog.
- Multiple serial interfaces including two UARTs (16C550), two Fast I2C-bus (400 kbit/s), SPI and SSP with buffering and variable data length capabilities.
- Power saving modes include Idle and Power-down.
- Single power supply chip with Power-On Reset (POR) and BOD circuits.

2) Wireless devices: Wireless devices act as communication mediator. It sends and receives data form each other. There are so many wireless devices available in market differing in range, power consumption and other parameters. From the Figure 4 we consider that Bluetooth is the best suitable module which will fulfill our requirement because of these reasons: The application focus is the cable replacement that is main requirement we want to replace the cable and make it independent. The system resources of the Bluetooth is 250kb+ and because of this we get faster data transmission and also reliable. Its battery life 1 to 7 days depends on the application. The bandwidth of the device is larger than zigbee. The range is 10+ meters which meets our requirement. At the last key attributes is cost and convenience which is the best and main plus point of this device. So we choose KC21 bluetooth module. it contains Wireless Data Communications System,

Embedded Bluetooth Serial Port Profile (SPP), Remote Command And Control, Low Power Connection Modes $< 500\mu A$, Easy To Use AT Command Interface Using UART, OEM Programmable Configuration. The KC21 offers reprogrammable,

	ZigBee™ 802.15.4	Bluetooth™ 802.15.1	Wi-Fi™ 802.11b	GPRS/GSM 1XRTT/CDMA
Application Focus	Monitoring & Control	Cable Replacement	Web, Video, Email	WAN, Voice/Data
System Resource	4KB-32KB	250KB+	1MB+	16MB+
Battery Life (days)	100-1000+	1-7	.1-5	1-7
Nodes Per Network	255/65K+	7	30	1,000
Bandwidth (kbps)	20-250	720	11,000+	64-128
Range (meters)	1-75+	1-10+	1-100	1,000+
Key Attributes	Reliable, Low Power, Cost Effective	Cost, Convenience	Speed, Flexibility	Reach, Quality

Fig. 4: Comparison of Wireless Devices

embedded firmware for serial cable replacement deploying the Bluetooth Serial Port Profile (SPP). OEM specific parameters and settings can be easily loaded into these modules. provides an easy to use AT style command interface over UART. kcSerial is capable of storing OEM default settings, and is upgradable over UART. kcSerial also provides remote control capability, where our AT commands can be issued remotely from any other Bluetooth device using SPP. Custom firmware is available.

3) Accelerometer: Many accelerometers are available In the market, but we choose sunroom 3-axial accelerometer because it is cost effective and easily available. Other features which given below:
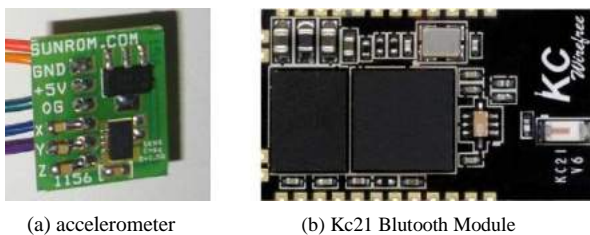
(a) accelerometer   (b) Kc21 Blutooth Module

The main feature of sunrom accelerometer is that it contain MMA7260 IC onboard with power regulating and amplifier IC. It gives Analog output for each axis, +5V operation @1ma current, Accelerometer is one of them which measures proper acceleration, High Sensitivity (800mV/g @ 1.5g), Selectable Sensitivity (+-1.5g, +- 6g), Robust design, high shock survivability and Low Cost.

4) Graphic LCD: The Nokia 3310 GLCD is very good LCD module for the display purpose. The display is 38*35 mm, with an active display surface of 30*22 mm, and a 84*48

pixel resolution. The display is easy to interface, using standard SPI communication. Logic supply voltage range VDD to VSS : 2.7 to 3.3 V respectively, Low power consumption, suitable for battery operated systems.
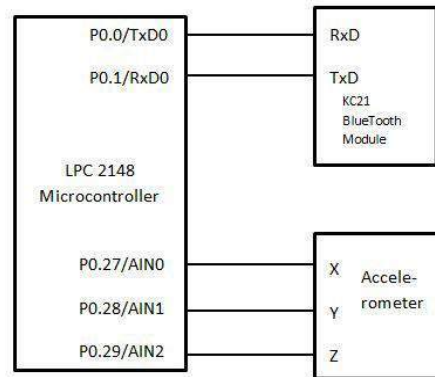
Fig. 5: Transmitter schematic
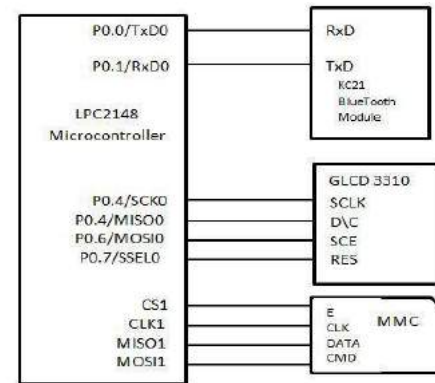
Fig. 6: Receiver schematic

C. Description of Schematic

Transmitter: As shown in Figure 6. microcontroller's UART Port pins TxD0 and RxD0 are connected to the Bluetooth's RxD and TxD pins respectively. At the other side port pins P0.27 to P0.29 which also works as the ADC, is connected to the accelerometer's X,Y and Z output axis respectively. The main design issue in real time data collection from all the three axes is the selection of the sampling frequency. It is high enough to fulfill the nyquist criteria i.e. sampling frequency should be more than double of the maximum frequency component present in the signal to avoid aliasing or overlapping while reconstructing the signal at base station. The ADC of LPC2148 can be scaled to clock 4.5Mhz so there is no issue for conversion at the sampling frequency rate.

Receiver: bluetooth and controller is connected at the receiver side same way as in transmitter section, but the connection is vice-versa. GLCD is interfaced with the SPI0, where serial clock pin of SPI is connected with GLCD's clock pin to synchronize the GLCD. The data pin of GLCD is interface with master in serial out pin of controller. Data is

stored in the memory card using SPI1 interface configuration as shown in Figure 7.

III. DESCRIPTION OF SOFTWARE

The software part plays a vital role for the better performance of the hardware and efficient use of the hardware resources. Real time model needs realtime operating system. The software part is not complex as well as it is user friendly and easy to understand for the users.
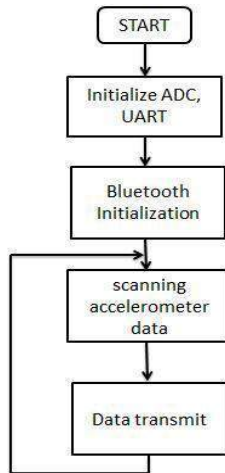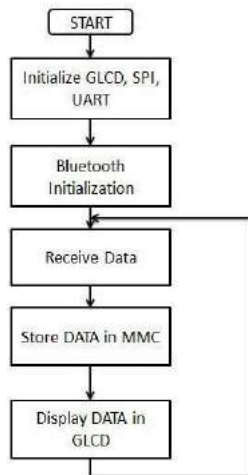

Fig. 7: Transmitter Flowchart

Fig. 8: Receiver Flowchart

A. Transmitter

The first step in operating system is to initialize the hard- ware resources and setting up parameters. UART is initialized by UART init();, while the other parameters ADC and Blue- tooth is initialized by ADC_init(); and BLUETOOTH _init(); respectively. A communication link is set between transmitter and receiver bluetooth in next step. We start ADC conversion and accelerometer data collection by Setting the start bit as high. At the end of conversion we send this data to the receiver

module via bluetooth link. Now return to the step ADC conversion and repeat both step for continuous monitoring.

Fig. 9: Transmitter Module of Wireless Monitoring System
Above Fig. 8 shows the real-time Model of portable Wireless transmitter Module.

B. Receiver

As shown in Fig. 8 of receiver flowchart in the initial step UART is initialize by UART init();, while the other parameters SPI, Bluetooth and GLCD is initialized by SPI0_init();, SPI1_init(); and BLUETOOTH_init();, GLCD_init(); respectively. A communication link is set between receiver and transmitter bluetooth in next step same like the transmitter. Reception of the data is started after setting link. Received data is stored in buffer and then it is stored in multimedia card. Same data is displayed in Graphic LCD 3310 Which is stored in MMC. Now we go to previous step and receive new data and this will continue up to the last data received.

Fig. 10 Receiver Module of Wireless Monitoring System
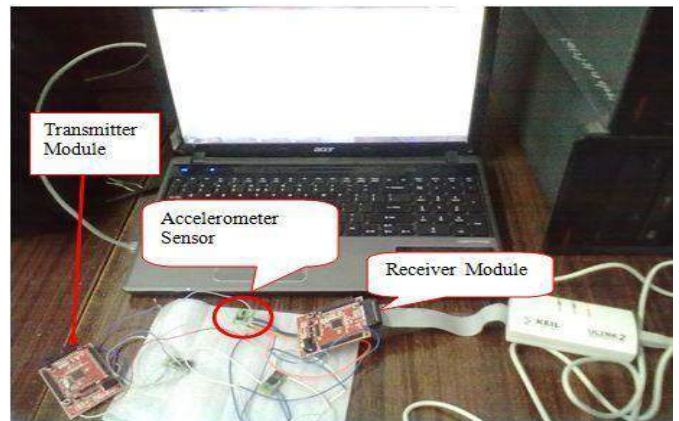
Fig. 11 Complete portable Wireless vibration Monitoring System

IV. Conclusion

Wireless vibration monitoring based on accelerometer is proposed for automobile environment. In the research area for vibration analysis such system provide excellent platform for acquiring the vibration information in wireless fashion. The data is stored in memory card for long time recording.

References

[1] P.Bifulco, M.Cesarelli, A.Fratini, M.Ruffo, G. Pasquariello and Gaetano Gargiulo, *"A wearable device for recording of biopotentials and body movements"*, IEEE Xplore, 2011.

[2] Amit Purwar, Do Un Jeong and Wan Young Chung, *"Activity Monitoring from Real-Time Triaxial Accelerometer data using Sensor Network"*, International Conference on Control, Automation and Systems, 2007.

[3] Rong-ling Shi, Ji-yun Zhao and Li-fang Kong, *"The Vibration Parameter Fault Diagnosis for Automobile Engine Based on ANFIS"*, International Conference on Computer, Mechatronics, Control and Electronic Engineering (CMCE), 2010.

[4] Dr. John Donelson III and Dr. Ronald L. Dicus, *"bearing defect detection using on-board accelerometer measurements"*, ASMEAEEE Joint Rail Conference Washington, DC, April 23-25,2002.

[5] Wilson Wang and Ofelia Antonia Jianu, *"A Smart Sensing Unit for Vibration Measurement and Monitoring"*, ieee/asme transactions on mechatronics, VOL. 15, NO.1, february 2010.

[6] Jia Huang, Jiexiong Ding and Zhenhua Tang, *"A Way to Detect the Quality of Main Retarder in Automobile Drive Shaft with Vibration Analysing"*, International Conference on Mechatronics & Automation Niagara Falls, Canada, July 2005.

[7] Chang- Ming Yang, Chih-Chung Wu, Chun-Mei Chou and Ching-Wen Yang, *"Textile-based Monitoring System for Biker"*, 9th International Conference on Information Technology and Applications in Biomedicine, ITAB, November 2009.

[8] Jennifer Healey and Beth Logan, *"Wearable Wellness Monitoring Using ECG and Accelerometer Data"*, Ninth IEEE International Symposium on Wearable Computers, 2005.

[9] Chau-Chung Song, Yin-Chieh Hsu, Chen-Fu Feng and Yu-Kai Chen, *"Construction of a Wireless Sensor Networking Platform with Vibration Sensing and GPS Positioning"*, ICROS-SICE International Joint Conference, 2009.

Heat Transfer Coefficient and Pressure Drop over Inline Pitch Variation using CFD

Nirav R. Bhavsar, Rupen R. Bhavsar

Email: er_niravbhavsar@yahoo.co.in

*Abstract-***Cross-flow over tube banks is generally encountered in heat exchangers. Steady state Navier-Stokes and the energy equations are applied for " inline" cylinders having pitch to diameter ratios of 1.75, 2.0 and 2.5 to obtain the numerical solutions of governing equations using Euler's explicit algorithm. Analyses have been done for mass flow rates ranging from 0.01 kg/s to 0.09 kg/s. The effect of change of horizontal pitch on heat transfer rate and pressure has been analyzed using CFD tool. The contours of streamlines, pressure, velocity and temperature are generated to study the effect of mass flow rate and longitudinal pitch variation. Also the local and average Nusselt numbers, pressure distributions around the cylinders are presented. Results obtained are for forced convection which suggests that with increase in the longitudinal tube distance, the range of pressure drop increases, the operating temperature range increases also the drop in the heat transfer coefficient increases. This result is helpful in predicting the performance of heat exchange equipment.**

Index Terms- Inline tube bundle, Tube Pitch

I. INTRODUCTION

Cross-flow over tube banks is generally encountered in heat transfer equipments like the evaporators and condensers of power plants, air conditioners where one fluid moves through the tubes while the other moves over the tubes in a perpendicular direction.

Number of experimental and numerical investigations has been conducted on the flow and heat transfer over a single tube or tube banks (bundles). Many previous works are found which are concerned with overall heat transfer through the banks Pierson, (1937); Huge, (1937); Grimison, 1937). Žukauskas (1972) reviewed characteristics of flow and heat transfer for a single cylinder and tube banks. Later Achenbach (1989) measured local heat transfer from one staggered tube bank at high Reynolds numbers (Re$\geq$10^5), and found boundary layer separation and transition to turbulence. Aiba et al. (1982) used Reynolds number of 1 x 10^4 to 6 x 10^4, and found the effect on the heat transfer around cylinder in the staggered tube banks. Park et al (1998), Buyruk et al. (1998) simulated the flow past a circular cylinder at low Reynolds numbers, and compared their results with the previous experimental and numerical results. Buyruk (2002) predicted the heat transfer characteristics in tube

banks with tube arrangement and flow condition below 4 x 10^2 Reynolds numbers.

When fluid passes through tube banks, different flow phenomenon are observed such as stagnation, separation, reattachment, vortex formation or recirculation which affect the local heat transfer characteristics. In such flow situations, it is difficult to measure local heat transfer coefficients by conventional heat transfer measurements. In this study, the fluid considered is water to measure the local heat transfer coefficients. The purpose of this study is to investigate the average heat transfer and pressure characteristics at various longitudinal tube distances for different mass flow rates for staggered tube bank in cross-flow.

II. METHODOLOGY

A. FUNDAMENTAL EQUATIONS

N.V. Kuznetsov's formula:

$$Nu = 0.2 \ Re^{0.64} \ Pr^{0.33} \qquad (1)$$

A.A. Zhukauskas' formula:

$$Nu = 0.27 \ Re^{0.63} \ Pr^{0.36} \qquad (2)$$

Where,
Nu = Nusselt Number,
Pr = Prandle's Number,
Re = Reynold's Number

B. PROBLEM DEFINITION

This problem considers a two dimensional section of a tube bank. A schematic of the problem is shown in Fig.1. The bank consists of uniformly spaced tubes with a diameter of 0.01 m; they are inline in the direction of cross fluid flow. Their centers are separated by a distance of 0.02 m in the X direction, and 0.02 m in the y direction. The bank has a depth of 1 m. Because of the symmetry of the tube bank geometry, only a portion of the domain needs to be modeled. A mass flow rate of 0.05 kg/s is applied to the inflow boundary of the periodic module. The temperature of the tube wall (T_{wall}) is 400 K and the bulk temperature of the cross-flow water (T_b) is 300 K. The properties of water that are used in the model are

shown in Figure. $\rho_\square$ = 998.2 kg/m³, μ= 0.001003 kg/ms, c_p = 4182 J/kgK, k = 0.6 W/mK. [6]
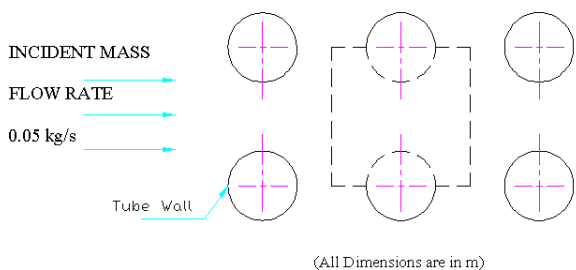

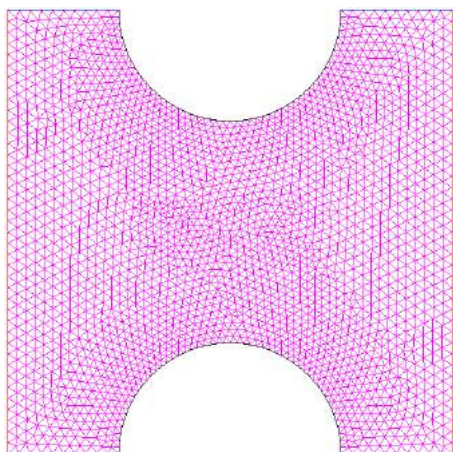Figure 1. Computational Domain Geometry

Figure 2. Meshing (6)

The analysis has been done for following Inline tube layout geometries,

TABLE.1 Inline Tube Layout Geometries; (Transverse pitch (P_T): 0.02m) [4,5]

Sr. No.	1	2	3
Longitudinal Pitch P_L (m)	0.0175	0.02	0.025

III. RESULT & DISCUSSION

A. FOR 0.02m HORIZONTAL X 0.02 VERTICAL INLINE tube LAYOUT
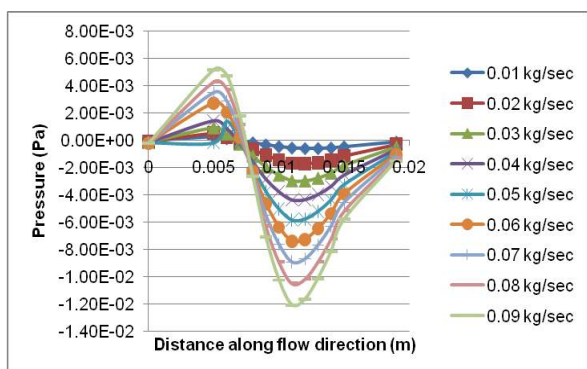
Figure 3. Pressure plot in flow direction for different mass flow
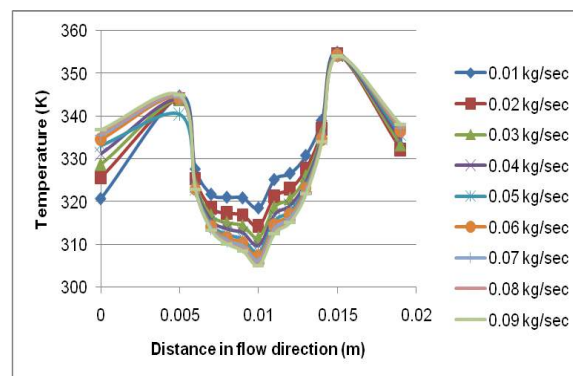
rates

Figure 4. Temperature plot in flow direction for different mass flow rates
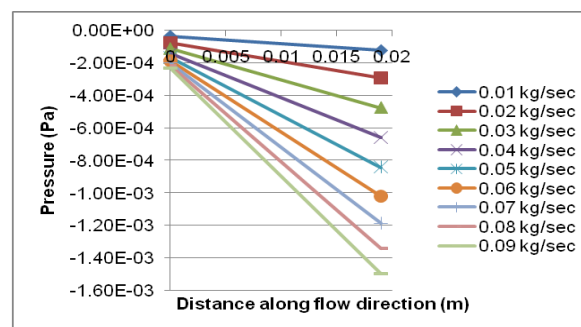
Figure 5. Pressure drop range (from Inlet to Outlet) for different mass flow rates
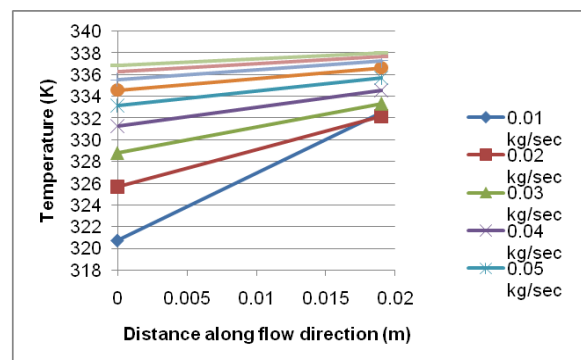
Figure 6. Temperature range from Inlet to Outlet for different mass flow rates
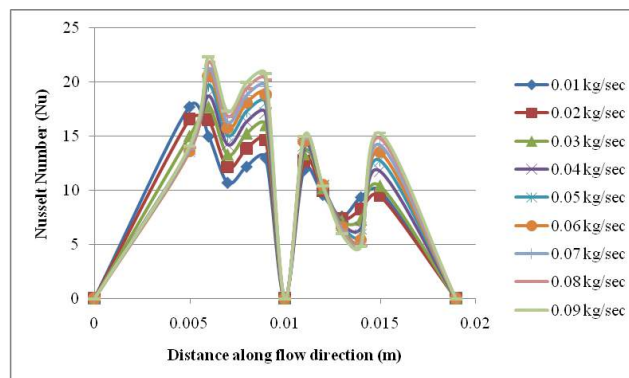
Figure 7. Nusselt Number (Nu) over tube for different mass flow rates

B. CONTOURS OF PRESSURE, VELOCITY AND TEMPERATURE IN CONTROL DOMAIN 0.02M HORIZONTAL X 0.02M VERTICAL INLINE TUBE LAYOUT.
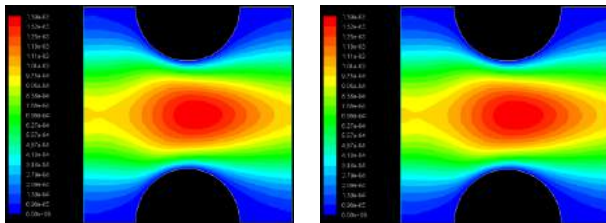
(b-1) 0.01 kg/s
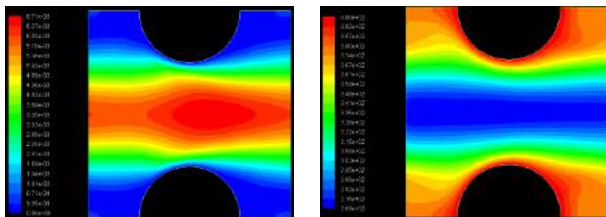
(c-1) 0.01 kg/s

(b-2) 0.05 kg/s

(c-2) 0.05 kg/s
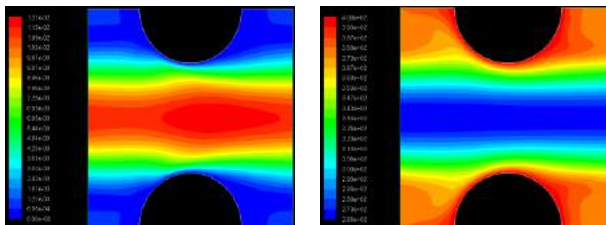
(b-3) 0.09 kg/s

(c-3) 0.09 kg/s

Figure 9. Velocity Contour

Figure 10. Temperature Contour

C. COMPARISON FOR DIFFERENT INLINE LONGITUDINAL PITCH (0.01 kg/s)

Figure.11 shows that for mass flow rate of 0.01 kg/sec the 0.02m Horizontal X 0.02m Vertical inline tube layout give the maximum pressure drop. This analysis can be useful to determine the number baffle supports required and the optimum design can be concern with rating and sizing can be determined. The Figure 12 shows that for a same mass flow rate of 0.01 kg/sec the inline tube layout of 0.025m (Horizontal) X 0.02m (Vertical) gives the maximum operating temperature range which is desirable. Moreover the graph also indicates that as the longitudinal pitch distance of inline layout increases the operating temperature range increases. This can be useful to determine the size of the heat exchanger and the number tubes and number passes required.
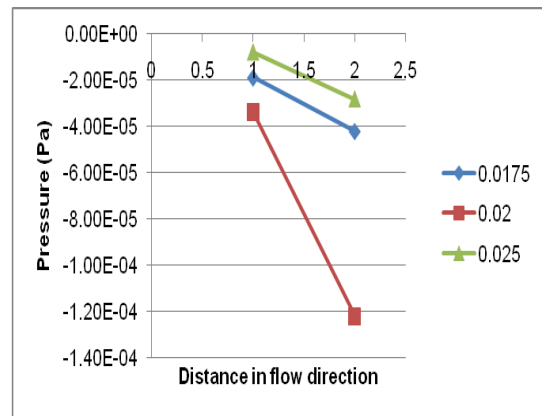
Figure 11. Comparison of Pressure drop for various Horizontal Tube Distances
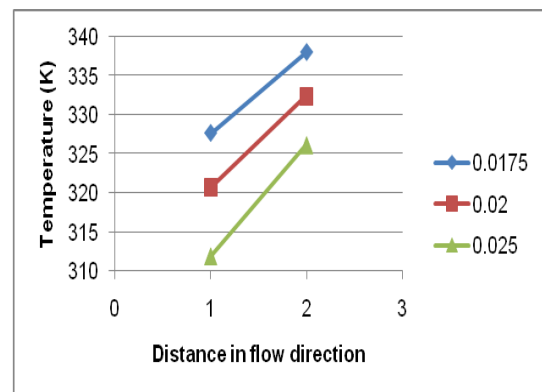
Figure 12. Comparison of Temperature Range for various Horizontal Tube Distance

IV. CONCLUSION

The analysis performed indicates that as the longitudinal tube distance increases the range of pressure drop from inlet of control volume to outlet increases which is useful to decide the number of baffles and end supports in heat exchangers. As the longitudinal tube distance increases the operating temperature range increases which can be useful to identify the number of tubes, number of passes. As the longitudinal tube distance increases the heat transfer rate increases. So the larger longitudinal tube distance in inline tube pitch within a particular range gives maximum heat transfer rate.

REFERENCES

[1]   Fluid flow and heat transfer around two circular cylinders in side-by-side arrangement, Minter Cheng, Proceedings of HT-FED04 2004 ASME Heat Transfer/Fluids Engineering Summer Conference July 11-15, 2004, Charlotte, North Carolina USA, pp. 1-3.

[2]   E. N. Pis'mennyi, Universal Relation for Calculating Convective Heat Transfer in Transversely Streamlined Bundles of Smooth Tubes, (2010), pp. 1-5

[3]   V. Yu. Semenov, A. I. Smorodin, and V. K. Orlov, Heat Exchange of a Bank of Tubes in the Transverse Flow.

[4]   Modeling Periodic Flow and Heat Transfer, Ansys Tutorial, Case-2

[5]   laitham M. S. Bahaidarah and N. K. Anand, A Numerical Study of luid flow and Heat Transfer Over a Bank of Flat Tubes, Numerical leat Transfer, Part A, 48: 359–385, 2005, ISSN: 1040-7782

[6]   Anderson, J.D., \Fundamentals of Aerodynamics", 2nd Edition

[7]   S. Jayavel and Shaligram Tiwari, Numerical Investigation of

Incompressible Flow Past Circular Tubes in Confined Channel, *Indian Institute of Technology Madras, INDIA, pp. 1-5*

Thermal Analysis of Liquid Nitrogen Storage Vessel

Salot Vimalkumar P. (Asst.Prof.)

Department of Mech.Engg., L.J.Institute of Engineering & Technology, S.G.Road, Ahmedabad.

salot.vimal@gmail.com

Abstract—**The purpose of this work is to find out boil off rate of liquid nitrogen as a function of vacuum. Heat transfer by radiation cannot be reduced for the same material and volumetric capacity, but heat transfer by residual gas conduction is a function of the pressure. This can be minimized by lowering the pressure to a such value that it enters into free molecular conduction regime. Conventional cryogenic fluid storage vessel consists of inner vessel, outer vessel and the gap between the two is filled with suitable insulation. In this work vacuum is used as insulation and its effect on boil off rate of liquid nitrogen is investigated. Here the novel concept of interposing radiation shield in between inner and outer vessel is introduced. Thus this new design consists of two insulation gaps instead of one. Theoretical analysis shows good result. The prototype of ten litre capacity is developed and it shows considerable saving of ten percent in boil off rate of liquid nitrogen, as compared to vessel without radiation shield.**

Keywords-liquid nitrogen, vacuum, radiation, heat transfer

I. INTRODUCTION

After the cryogenic fluid has been liquefied, it is necessary to store it in such a way that it results in minimum boil-off rate. Spherical vessels have most effective configuration as far as heat in leak is concerned, and they are often used for large volume storage in which the vessel is constructed on the site. Cylindrical vessels are usually required for transportable trailers and railway cars. For small laboratory vessels, cylindrical configuration is preferred for their easiness and economical fabrication. Small laboratory vessels are widely used for long time storage of cryogenic fluids, for the preservation of biological samples, for cooling of small samples and to cool detectors for space telescopes.

II. SELECTION OF MATERIAL

Some materials like carbon steel performs ductile to brittle transition when they are exposed to liquid nitrogen temperature and they become very brittle.

So this type of materials cannot be used for the construction of inner vessel. But material like Stainless Steel retains their properties even at lower temperature because of martensitic transformation[3][6]. Some other desirable properties for constructional materials are[7]:

- compatibility for high vacuum
- low emissivity
- low thermal contraction coefficient
- good weldabiity
- low out gassing rate
- available in standard shape and size
- economical

Considering all these requirements S.S. 304 is best suitable material and is selected for the construction of inner vessel, outer vessel and radiation shield.

III. PROBLEM FORMULATION

Here small laboratory vessel of 10 litre capacity is developed with radiation shield interposed between inner and outer vessel.

A. Technical specifications

Capacity: 10 litre
Ullage space: 10%
Cryogenic fluid to be stored: LN_2
Absolute design pressure: 238 kPa
Type of insulation: Vacuum
Vacuum intensity: 2 mPa

TABLE I.   PROPERTIES OF LIQUID NITROGEN

Temp.(K)	P_{sat} (kPa)	Density (kg/m^3)	Latent heat h_{fg} (kJ/kg)
75	76	818.1	202.3
77.36	101.3	807.3	199.3
80	136.7	795.1	195.8

B. Design Methodology

1) Mechanical analysis and design: It determines minimum thickness required for inner vessel and outer vessel. It is done according to ASME Boiler and Pressure Vessel Code, section VIII, Div-I.

2) Thermal analysis and design: It determines insulation requirements and heat transfer rate. In case of vacuum, heat is mainly transferred by radiation and residual gas conduction[4].

IV. DESIGN OF INNER VESSEL

A. *Height of the vessel:*

The design of inner vessel is done accrding to ASME design standards[1]. Height of the vessel is determined by the total volumetric capacity of the vessel. It is made from NPS 6 schdule 5 with following dimensions:

Inner diameter (D_{ii}) = 162.7 mm
Outer diameter (D_{oi}) = 168.3 mm
Thickness (t_i) = 2.8 mm
ASME standard 2:1 elliptical head is used as bottom cap.
The height of the vessel can be found by

$$V = V_{cyl} + V_{head} \qquad (1)$$

Where V = total volume of the vessel = 11 lit

V_{cyl} = volume of the cylindrical portion

V_{head} = volume of head

h= height of the vessel

Fig. 1 shows assembly drawing of inner vessel which includes cylindrical portion, bottom head, top flange and standard KF.
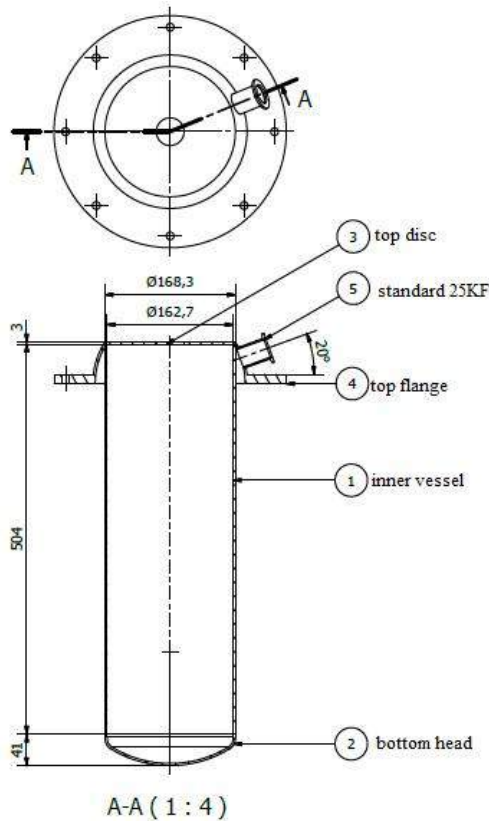
Fig.1 Inner vessel assembly drawing

V. RADIATION SHIELD

It appears that the dominant heat transfer mode is radiation in the isolating cavity[4]. This can be reduced by interposing radiation shield between inner and outer vessel.
NPS 7 schedule 5 pipe, S.S. 304 is used as radiation shield with flat bottom head. The following are dimensions:
Inside diameter (D_{is}): 189 mm
Outside diameter (D_{os}): 193 mm
Thickness (t_s): 2 mm
The gap maintained between inner vessel and radiation shield is 10 mm in order to fulfill the condition that free mean path should be larger than this gap.
Fig. 2 shows details of radiation shield which includes cylindrical portion and top flange.

VI. FREE MEAN PATH

In order for free molecular conduction to occur, the mean free path of the gas molecules must be larger than the spacing between two surfaces. To check this condition, the mean free path may be determined from
$$\lambda = (\mu_1/p) \times (\pi RT/2g_c)^{1/2} \qquad (2)$$
where
μ_1= gas visocity, Pa-s
p = vacuum pressure = 2 mPa
R = specific gas constant = 287 J/kg K

A. *check this condition for inner vessel and radiation shield:*

μ_1= 16× 10^{-6} Pa-s at 253 K
λ = 2.94 m
The gap between inner vessel and radiation shield = 10.35 mm, thus λ is geater than gap.

B. *check this condition for outer vessel and radiation shield:*

μ_1=18.47×10^{-6}Pa-s at 300K, hence λ=3.39m

VII. DESIGN OF OUTER VESSEL

It has to withstand only atmospheric pressure. So it may fail from the view point of elastic instability or buckling. It is designed by considering four times atmospheric pressure acting on it[1][2].
NPS 8 schedule 5 pipe, S.S. 304 is used as outer vessel with following are dimensions:
Inside diameter (D_{io}): 213 mm
Outside diameter (D_{oo}): 219 mm
Thickness (t_o): 3 mm
The gap maintained between outer vessel and radiation shield is 10 mm in order to fulfill the condition that free mean path should be larger than this gap.
Fig. 2 shows sectional view of assembly of the vessel which includes inner vessel, outer vessel and radiation shield with end caps.
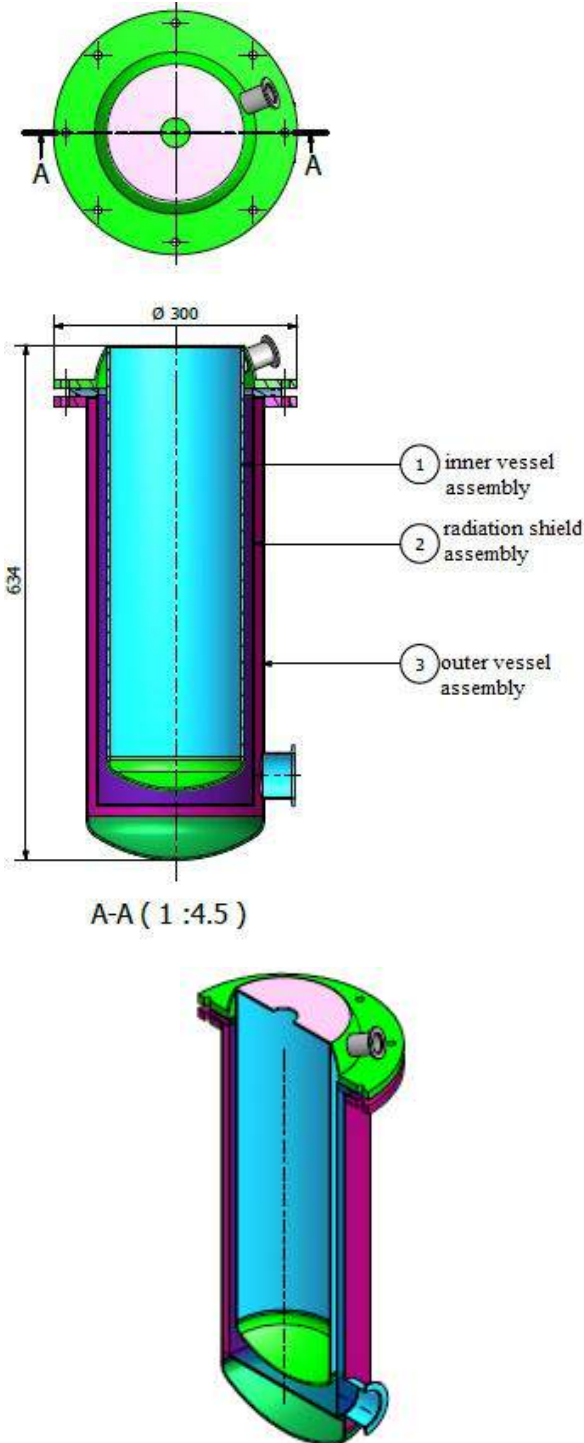
Ø 300

634

A-A (1 :4.5)

① inner vessel assembly
② radiation shield assembly
③ outer vessel assembly

Fig.2 Sectional view of assembly of vessel

VIII. HEAT TRANSFER BY RADIATION

The radiant heat transfer rate between two surfaces is given by the modified Stefan-Boltzman equation,

$$Q_r = F_e \times F_{1-2} \times \sigma \times A_1 \times (T_s^4 - T_1^4)^{[5]} \tag{3}$$

Where

F_e = emissivity factor

F_{1-2} = configuration factor

σ = Stefan-boltzman constant = 56.69×10^{-9} W/m^2 K^4

T_s = temperature of radiation shield = 252 K

T_1 = temperature of inner vessel = 78 K

Total heat transfer through cylindrical portion and head by radiation,

$Q_r = 0.4645$ W

IX. HEAT TRANSFER BY MOLECULAR GAS CONDUCTION

Heat transfer through residual gas conduction is given by

$$Q_g = G \times p \times A_1 \times (T_s - T_1) \tag{4}$$

Where

$$G = (\gamma+1)/(\gamma-1) (g_c R/8\pi T)^{1/2} \times F_a \tag{5}$$

R = specific gas constant

γ = specific heat ratio = C_p/C_v = 1.4

F_a = accommodation co-efficient

Total heat transfer through cylindrical portion and head by residual gas conduction,

$Q_g = 0.0578$ W

Total heat transfer by radiation and residual gas conduction (with radiation shield),

$Q = Q_r + Q_g = 0.4645 + 0.0578 = 0.5223$ W

Total heat transfer by radiation and residual gas conduction (without interposing radiation shield),

$Q = Q_r + Q_g = 2.3114 + 0.0784 = 2.3898$ W

X. BOIL OFF RATE

The total heat energy required to evaporate the full content of the vessel is given by,

$$E_t = \rho_f \times h_{fg} \times V \tag{6}$$

$= 807.3 \times 199.3 \times 10 \times 10^{-3} = 1608.95$ kJ

Where,

ρ_f = density of liquid nitrogen

h_{fg} = latent heat of evaporation

The total energy transfer to the vessel content during one day is,

$$E_d = Q \times t_d \tag{7}$$

$= (0.5223 \times 10^{-3}) (3600$ s/hr$) (24$ hr/day$) = 45.12$ kJ/day

The fraction of the full vessel content that is evaporated during one day is given by, E_d/E_t. Following is the summary of results.

TABLE II.　　**RESULT**

	With radiation shield	Without radiation shield
Boil off rate of liquid nitrogen	2.80% per day	12.83% per day

XI.   CONCLUSION

This experiment shows good result of using radiation shield in between inner and outer vessel. The saving achieved in boil off rate is about 10% which justifies the additional cost. For higher volume to surface area still better results may be obtained. For 25 liter capacity vessel, the boil off rate achieved is less than 2%. The performance further can be improved by providing combined insulation of MLI and vacuum.

REFERENCES

[1]   ASME Boiler and Pressure Vessel Code,Section VIII, Unfired Pressure Vessels, American Society of Mechanical Engineers, New York, 1983.

[2]   Barron R. F, "Cryogenic Systems," second edition, oxford university press, 1985.

[3]   Mohsen Botshekan, Suzanne Degallaix and Yannick Desplanques,"Influence of martensitic transformation on the low-cycle fatigue behavior of 316LN stainless steel at 77 K", 1997.

[4]   N.S. Harris, "Modern Vacuum Practice", Mcgraw-Hill Book company, 1989.

[5]   O.Khemis, M.Boumaza, M.Ait Ali and M.X.Francois,"Experimental analysis of heat transfer in a cryogenic tank without lateral insulation", Universite de constantine, constantine, Algeria,2003.

[6]   Seo Young Kim, Byung and Ha Kang,"Thermal design analysis of a liquid hydrogen vessel", Korea institute of science and technology, South Korea, 2000.

[7]   Wigley, D.A.,"The mechanical properties of Materials at Low Temperatures", Plenum Press, New York, 1971

Employment of Advanced Materials for Boilers and Steam Turbines

Chintan T. Barelwala, Asst. Prof., Mechanical Engineering Dept.,
Gandhinagar Institute of Technology

barelwala_chintan2004@yahoo.co.in

Abstract — **Advancing our science and technology, from fundamental breakthroughs in materials and chemistry to improving manufacturing processes, is critical to our energy future and to establishing new businesses that drive economic prosperity. The principal aim of this paper is development of advanced materials and components for the power industry.**

Index Terms — **Industrial Boiler, Advanced Materials, Super Alloys, Ni based Alloys, Austenitic steels.**

I.   INTRODUCTION

Since ancient times, advances in the development of materials and energy have defined and limited human social, technological and political aspirations. The modern era, with instant global communication and the rising expectations of developing nations, poses energy challenges greater than ever seen before. Materials science and engineering is certainly an old field and a new one simultaneously. The recognition of the importance of structure in determination of properties is the hallmark of the modern developments in the field.

In the 130 years since Edison, Tesla and Westinghouse installed the first primitive electricity grids; electrical technology has undergone many revolutions. From its initial use exclusively for lighting, electricity now symbolizes modern life, powering lights, communication, entertainment, trains, refrigeration and industry. In the past century, 75% of the world has gained access to this most versatile energy carrier. Such changes in our lives do not come from incremental improvements, but from groundbreaking research and development on materials that open new horizons.

These advances will require a new generation of advanced materials, including

• Battery materials for massive electrical energy storage.
• Corrosion-resistant alloys for high-temperature power conversion.
• Strong, lightweight composites for turbine blades.
• Superconducting power distribution cables.

II.   MATERIALS FOR BOILER CONSTRUCTION

Old boilers were made of best grade wrought iron, since steel was made in bulk long after boilers were. Steel is the modern material which is not better just more available and made to tighter size tolerances and composition, whereas the wrought iron would have better corrosion resistance. Gears and pistons would be of cast iron, levers wrought iron or low carbon steel and steam and water pipes of brass and/or copper. Modern boilers are made with steel and special high temperature steel containing chromium and molybdenum etc to with stand very high temperature. The vast majority of material used in boilers, steam equipment and systems is steel.

Advancing our science and technology, from fundamental breakthroughs in materials and chemistry to improving manufacturing processes, is critical to our energy future and to establishing new businesses that drive economic prosperity. The role of the materials engineer in the design and manufacture of today's highly sophisticated products is varied, complex, exciting, and always changing. The principal aim of this article is development of advanced materials and components for the power industry. Such materials and components were aimed at steam temperatures of 620 - 650ºC.

Fig.1. Steam Boilers.

Materials are selected and used as a result of a match between their properties and the needs dictated by the intended application. In this sense, the properties should be defined broadly and include fabricability, required maintenance, costs associated with the original materials and maintenance, and

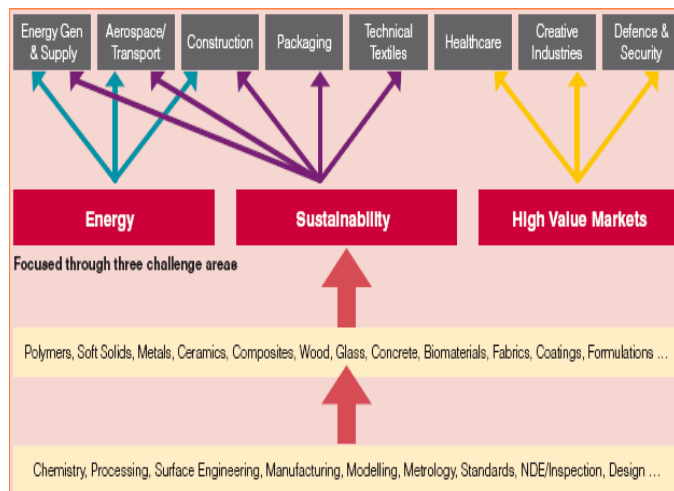the behavioural characteristics associated with the function of the item within the overall design.

Fig.2. A technology-inspired strategy focused through key challenge areas.

Specific areas covered are:
• Development and assessment of improved alloys for boiler super heaters, headers, pipe work and furnace walls.
• Development of improved alloys for steam turbine high temperature rotor forgings, castings, and bolting.

III. ADVANCED MATERIALS

Solid materials have been grouped in to three basic classifications metals, ceramics & polymers. This is primarily based on chemical and atomic structure of atoms. There are also some intermediates .In addition there are composites which are the combination of two or more than two elements. Another classification is advanced Materials which are used in high technology applications such as semiconductors, biomaterials, and nano engineered materials.

Advanced materials outperform conventional materials with superior properties such as toughness, hardness, durability and elasticity. They can have novel properties including the ability to memorize shape or sense changes in the environment and respond. Advanced materials are also amazingly versatile. The area of advanced materials research is very broad in scope and potential applications.

Advanced Materials, defined here as materials, and their associated process technologies, with the potential to be exploited in high value-added products, is both a multidisciplinary area within itself (including, for example, physics, chemistry, applied mathematics) and cross-cutting over both technology areas (e.g. electronics and photonics, biosciences) and market sectors (e.g. energy, transport, health care, packaging). Consequently, defining a core strategy for advanced materials technology is complex: it must take into account, and be consistent with, the major drivers and strategies of these related areas.

IV. SUPER ALLOYS

A Super alloy, or high-performance alloy, is an alloy that exhibits excellent mechanical strength and resistance to creep (tendency for solids to slowly move or deform under stress) at high temperatures; good surface stability; and corrosion and oxidation resistance. Super alloys typically have a matrix with an austenitic face-centered cubic crystal structure. A super alloy's base alloying element is usually nickel, cobalt, or nickel-iron.

Super alloys have contributed markedly to societal benefit. It is difficult to imagine the modern world without super alloys. These materials provide the backbone for many applications within key industries that include chemical and metallurgical processing, oil and gas extraction and refining, energy generation, and aerospace propulsion. Within this broad application space, arguably the highest visibility challenges tackled by these materials have arisen from the demand for large, efficient land-based power turbines and lightweight, highly durable aeronautical jet engines.

Fig.3. Nickel Super alloy jet engine turbine blade.

V. NICKEL BASE MATERIAL OPTIONS FOR FABRICATION OF ADVANCED COAL FIRED BOILER COMPONENTS

Current and future goals set for efficient energy production by coal-fired boilers require a stable of austenitic materials which are capable of meeting numerous stringent demands. Advanced ultra supercritical designs, possibly coming to fruition in the next few years, target very high steam temperatures, 700°C and higher, and steam pressures as high as 350 bar. Conditions in supercritical boilers coming online currently are becoming increasingly arduous as well, requiring increased utilization of austenitic materials having improved creep strength and corrosion resistance. Materials to be utilized in steam super heaters and reheaters will need a combination of exceptional strength, and corrosion resistance to combat coal ash corrosion. Resistance to steam oxidation at high temperatures will be important for steam header pipe internals and super heater and reheater internals as well. Water wall panels will continue to require overlaying with corrosion resistant materials to resist an ever more demanding environment.

Fig.4. Reheater.

Austenitic steels possess the requisite strengths at intermediate temperatures, but their physical properties (low thermal conductivity and high thermal expansion) limit their use in thick-section applications. Nickel-based super alloys must be used for components in the hottest sections and where high stresses are encountered. Ni-based based alloys are envisioned for the steam turbine casing, but they may also be applicable to other large components that connect the steam supply to the steam turbine. Nickel-base super alloys are expected to be the materials best suited for steam boiler and turbine applications above about 675° C. Nickel-based super alloys are, however, quite expensive relative to steel, and any power plant incorporating these alloys must limit their use to the most critical components.

The best commercially available steels allow the construction of boiler plant for steam conditions of 300 bar / 600°C / 620°C, for a wide range of coals, even those producing an aggressively corrosive flue gas. The various components of the boiler are employed over a range of temperatures, pressures and corrosive atmospheres, and oxidation conditions, and the range of alloys necessary to best meet the design demands covers the simple carbon manganese (CMn) steels, low alloy steels, advanced low alloy steels, the 9-12Cr martensitic family and the austenitic range with chromium varying from 18% to in excess of 25%.9-12 Cr martensitic creep resistant steels are steels designed to withstand a constant load at high temperatures. The most important application of creep resistant steels is components of steam power plants operating at elevated temperatures (boilers, turbines, steam lines). Simple carbon manganese steels are utilised at lower temperatures such as the reheater inlet but as component temperatures increase, it is necessary to move to low alloy steels such as SA213 T22 (ASME **SA 213**-**T22** is a seamless low alloy carbon steel with 2.25% Cr and 1% Mo.) which, like the CMn steels, have been employed in boiler construction for decades.

Moving to components at even higher temperatures and considering other manufacturing restrictions leads to the introduction of more modern steels that have been referred to as creep-strength enhanced ferritic (CSEF) steels4, which exhibit very high creep strength by virtue of a fine dispersion of creep strengthening precipitates. Creep strength enhanced ferritic (CSEF) steels, including Grade 91, used in the boiler tubes, piping and headers of fossil-fuel-fired and combined-cycle power plants.
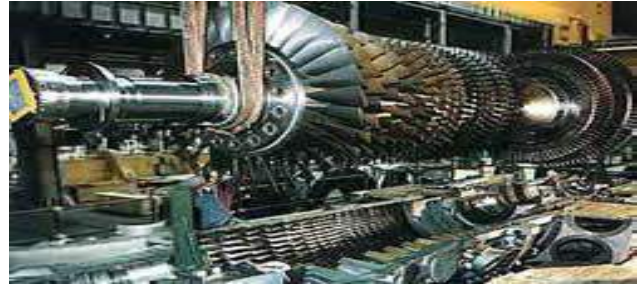
Fig.5. Large steam turbines require creep-resistant steels for safe, economical operation.

High temperature materials enable the steam conditions – and corresponding thermal efficiency – of advanced supercritical steam cycles. Ideally, materials used in steam generator pressure parts combine high temperature strength with reasonable resistance to oxidation. In addition, the workability of the materials and corrosion behavior are important attributes.

Fig.6. Membrane wall, Tubes and SH outlet header.

The increase of steam conditions primarily affects the water walls, final (SH) super heater and reheater tubing, and the thick-walled components, mainly the high pressure outlet headers and piping to the turbine. Classes of materials include conventional and advanced ferritic steel, austenitic steel, and nickel alloys. Several boiler materials with improved mechanical properties have been developed recently, and new materials still in the R&D stages will enable higher ultra-supercritical steam cycles than are today commercially available.

More than two thirds of the current and projected energy generation is from fossil fuels. Clearly this source of energy is of critical importance. Advanced materials have enabled several significant improvements in energy efficiency from systems converting fossil fuels into energy. Whether the fuel is converted to electricity in a combined cycle gas turbine or a boiler/steam turbine system, both systems produce higher efficiencies when operated at higher temperatures. Significant efforts over the past decades have resulted in advanced

materials for use in both gas turbines and boiler/steam turbine equipment.
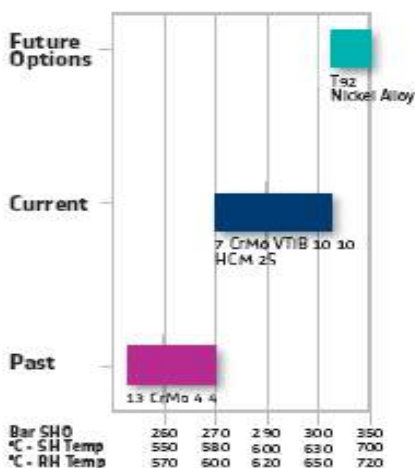
VI. COATINGS IN GAS TURBINE

Coatings applied to hot components in gas turbines have allowed higher operating temperatures thereby resulting in efficiency improvements. The newest combined cycle gas turbine plants have net plant efficiencies of 60% or greater. Advances in materials have also resulted in significant improvements in the overall efficiency of converting the energy in the fuel to electricity. Companies producing advanced materials and boiler manufacturers have worked together to develop new materials for use in supercritical boilers. These new materials and the new power cycles they enable have allowed efficiencies of coal fired power plants to be increased to 42%.Through the development of advanced coatings and new methods of applying the coatings as well as new materials, significant reductions in fuel consumption with an associated reduction in green house gas and other criteria pollutant emissions have been realized.

(b) Tubes
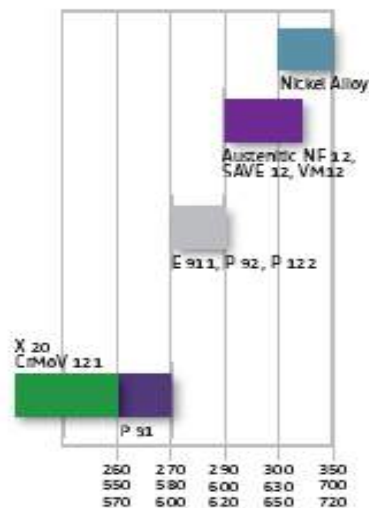
(c) SH Outlet Header

Fig.7. (a),(b),(c) Material development stages and related steam parameter limits.

(a) Membrane Wall

Two significant challenges associated with fossil energy fired power plants are cost effectively reducing carbon dioxide (CO_2) and other criteria pollutants, and taking advantage of unconventional gas reserves. Opportunities to reduce CO_2 and other pollutants in a cost effective way by:

• Development of advanced materials and coating techniques to allow operation of steam cycles at higher temperatures and pressures to continue to increase the efficiency of the power plant.

• Oxygen based processes show significant promise for yielding the lowest cost solution for carbon capture and sequestration. New methods to generate oxygen with lower power requirements are required to reduce the parasitic load on the power plant. Development of oxygen ion selective ceramic membranes has the potential to significantly reduce the cost of producing oxygen at large scales required for power production.

• Development of high temperature metals with associated welding and forming procedures will enable construction of advanced ulta-supercritical plants. Efficiency gains of at least 8–10% are anticipated, resulting in substantially reduced releases of CO_2 and other fuel-related pollutants and greenhouse gases by nearly 30%.

Fig.8. Coated turbine blades.

VII. FUTURE PARADIGM IN ALLOY DEVELOPMENT

Materials research seeks to understand fundamental physical and chemical properties, and then use that understanding to improve the technology base that we count on to meet our needs for energy, national security and defense, information technology and telecommunications, consumer products, health care, and more.

Future paradigm in alloy development focuses on reduction of weight, improving oxidation and corrosion resistance while maintaining the strength of the alloy. Furthermore, with the increasing demand for turbine blade for power generation, another focus of alloy design is to reduce the cost of super alloys.

VIII. CONCLUSION

The connection is clear between materials research and the energy technologies that we rely on today and those we need for our future. Materials research and development is a global pursuit. It covers a broad set of science and engineering disciplines and engages researchers across academia, industry and government laboratories. Advanced materials and the manufacturing techniques to make these materials can give our economy a competitive advantage for job growth.

The advanced materials technology being developed will enable construction of very high efficiency Ultra Super critical (USC) plants with greatly reduced emissions. Efficiency gains of at least 8–10 percentage points are anticipated, resulting in substantially reduced releases of carbon dioxide and other fuel-related pollutants and greenhouse gases by nearly 30 percent. The advances developed here will, at the same time, keep the cost of electricity competitive even with respect to natural gas turbine combined-cycle plants, and will also be applicable to retrofitting of existing coal-fired plants.

XI. REFERENCES

[1] ASM Handbook_ Vol 20 - Materials Selection and Design (1999)
[2] William D. Callister,Jr.,David G. Rethwisch, "Material Science and Engineering – An Introduction", John willey & Sons,Inc.VIIIth Edition.
[3] US DOE, NETL,factsheets/project, "Advanced materials for Ultra Super critical Boiler Systems".
[4] "DTI/Pub/FES 05/1687/Improved materials for Boilers and steam turbines".

Effect of target frequency, bias voltage, bias frequency and deposition temperature on tribological properties of pulsed DC CFUBM sputtered TiN coating

Arpan Shah and Dr. Soumitra Paul

(apskarjan@gmail.com, spaul@mech.iitkgp.ernet.in)

Abstract— Pulsed DC magnetron sputtering is very well known since early 1990s because of its high process stability, improved coating quality, higher plasma density and high bias current. Target frequency, bias voltage, bias frequency and deposition temperature are the four major influencing process parameters during coating deposition. Titanium nitride (TiN) has long been used as a hard, wear resistant coating material, but it has never been regarded as a low friction material. Recent results though, suggest that TiN coatings deposited by pulsed magnetron sputtering (PMS) can have significantly enhanced tribological properties, in particular, significantly lower coefficients of friction, in comparison with films deposited by continuous DC processing. This paper, therefore, reports the results to date from a detailed study of the tribological properties of TiN coatings produced by PMS. Coatings were deposited under varying conditions of bias frequency, target frequency, substrate bias (DC pulsed) and deposition temperature. In present work, the tribological performance was evaluated by ball-on-disc method at sliding speed of 12 m/min and load of 10 N, when TiN coating was deposited on 40C8 low carbon discs and the counter body was 5 mm WC-6%Co ball. Wear coefficient of less than 7.5×10^{-15} m^3/N-m was routinely obtained, with minimum of 5.6×10^{-15} m^3/N-m.

Index Terms— pulsed DC closed field unbalanced magnetron sputtering (p-DC-CFUBMS), TiN, tribological properties.

I. INTRODUCTION

TiN with its high hardness, wear and corrosion resistance, and favourable thermal, electrical and optical characteristics is widely used for applications ranging from protective coatings on cutting and forming tools to coatings for decorative and thermal diffusion barrier purposes and as a useful biomaterial for various medical needs. Mechanical properties of TiN films are the function of microstructure, morphology, density, crystallinity and stoichiometry. TiN coatings are also widely used in tribological applications to provide a wear resistance surface to protect the underlying substrate.

Titanium nitride (TiN) coatings are widely used in tribological applications to provide a wear resistant surface to protect the underlying substrate. Such coatings are produced by CVD and PVD techniques [1, 2] but, whilst the choice of technique may impact to some extent on film structures and properties, TiN is not regarded as a low friction coating material. Indeed, unlubricated tribological tests on films produced by these techniques tend to result in coefficients of friction in the range 0.3–0.9, depending on test geometry, mating face material, etc. [3]. However, recent results have shown that TiN coatings deposited by pulsed magnetron sputtering (PMS), can demonstrate significantly enhanced tribological properties, in terms of coefficient of friction (values as low as 0.09 have been recorded in unlubricated tests) compared to coatings deposited by conventional sputtering [4]. Similar results have also been obtained for TiAlN coatings [5]. The improvement in tribological properties was attributed to structural modifications arising from the enhanced deposition conditions now known to occur in the PMS process [6–8].

The parameters like bias voltage, bias frequency, target frequency and deposition temperature in p-DC-CFUBMS play significant role on coating characteristics. Kelly et. al. [9-10] have demonstrated compact featureless, non-columnar TiN and TiO$_2$ coating by suitable choice of above parameters with significant benefits in terms of coating adhesion, hardness, wear resistance and tribological properties.

Very few efforts have been made to assess the effect of pulsed target frequency, bias voltage and bias frequency on tribological properties of PVD coating, in most of the studies, only two or three of the above mentioned parameters have been varied. Moreover, bias frequency was varied within a very low range. Hence, the novelty of the present research is in investigating the effect of above three parameters along with the fourth parameter as deposition temperature over a wide domain on tribological properties of PVD TiN coating deposited on 40C8 low carbon steel substrate. Firstly, deposition temperature was varied from

150 to 250 °C at a step of 50 °C. After then bias voltage was varied from −50 to −70 V keeping the other three

parameters constant. Then bias frequency was varied from 50 to 250 kHz at a step of 50 kHz keeping the other three parameters unchanged. Finally, target frequency was varied from 50 to 250 kHz at a step of 50 kHz, keeping bias voltage, bias frequency, and deposition temperature constant. In this manner, a very wide domain of process parameters was covered. Here the tribological performance was evaluated by ball-on-disc method.

II. EXPERIMENTAL

Deposition of TiN coating:

Titanium nitride (TiN) coating was deposited by pulsed DC closed field unbalanced magnetron sputtering (CFUBMS) technique on 40C8 law carbon steel circular disc substrate in a dual cathode CFUBMS system (TOOL COATER, VTC-01A) manufactured by Milman Thin Film Systems Pvt. Ltd, Pune, India. The composition of the substrate material is furnished in Table I.

TABLE I
COMPOSITION OF SUBSTRATE MATERIAL

Elements	Compositions
C	0.40
Mn	0.7
Si	0.02
P	0.04
S	0.05
Fe	Balance

In the PVD chamber, the target separation distance was 350 mm and target to substrate distance was 130 mm. The size of each Ti (purity 99.95%) target was 125 mm × 250 mm. The substrates were polished to a roughness value of Ra = 0.05 μm and then ultrasonically cleaned with acetone, trichloroethylene and isopropyl alcohol prior to deposition. A two-fold rotation was imparted to the substrates at a speed of 3 rpm. Advanced Energy Pinnacle Plus power supply (each unit having maximum power capacity of 5 kW) was used for supplying power to both the cathodes and the substrates. The units supplying power to the cathodes were set in 'current' mode, while the one supplying power to the substrates was set in 'voltage' mode. The amount of average ion current drawn to the substrates during pulse-on time was directly displayed on the display screen of the unit dedicated for the bias power. The chamber was first pumped down to a base pressure of approximately 2×10^{-3} Pa followed by pre-sputtering of the targets in argon atmosphere with a chamber pressure of 0.2 Pa with shutters closed. In order to reduce water vapour content in the vacuum chamber, Ti was sputtered under argon during ion etching of the substrates prior to deposition with a substrate bias voltage of −500 V. Other deposition parameters are summarized in Table II.

TABLE II
DEPOSITION PARAMETERS DURING TiN COATING

Substrate bias voltage (V)	Bias(substrate) frequency with duty cycle 80 % (kHz)	Target(cathode) frequency with duty cycle 80 % (kHz)	Deposition temperature (°C)
-50	100	100	**150, 200, 250**
-50, -60, -70	100	100	250
-50	**50, 100, 150, 200, 250**	100	250
-50	100	**50, 100, 150, 200, 250**	250

III. CHARACTERIZATION OF THE TiN COATINGS

Tribological characterization is very important for cutting tool coating applications. In present work, coefficient of friction of the TiN coating deposited on 40C8 steel circular dics was measured by using tribometer TR-201-M3, DUCOM. This test is known as pin-on disc or ball-on disc test. In this research, carbide ball with 5 mm diameter was used as a counterface material.

The tests were performed at 10 N loads at a different track diameter (8 mm and 12 mm) but for same sliding distance (778 m). The tests were performed using track diameter of 12 mm for all samples with different substrate bias voltage, with different deposition temperature and with different target frequency and using track diameter of 8 mm for all samples with different substrate bias frequency. The test was continued for 65 min with linear speed of 12 m/min. All the tests were carried out at room temperature (25–27 °C) and 50±5% relative humidity. This test will give us estimation of variation of coefficient of friction along the given sliding distance. Fig. I shows the variation of coefficient of friction, friction force and depth of wear track of TiN coating deposited on 40C6 steel substrate with sliding time.

Fig. I: variation of coefficient of friction, friction force and wear
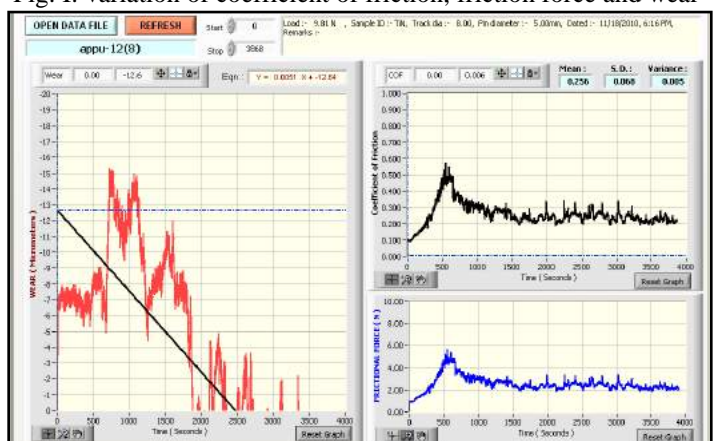
track depth with sliding distance for TiN coating.

For some selected samples (of sample id. S8, S12, S15 and S18), wear track was observed under SEM. Also EDS analysis was carried out for same samples to know the mode of failure.

The depth of the wear track was measured using Taylor-Hobson, Surtronic 3+ surface profilometer by taking at least 5 to 6 measurements at different places across the wear track to determine specific wear rate or wear coefficient. Specific wear rate or wear coefficient was calculated using the following equation,

$$W_d = \frac{V}{dL} \times 10^{-9}$$

Here W_d is the wear coefficient of the coated disc in m³/ (N·m), V is the volume of wear track in mm³, d is the sliding distance in m, L is the normal load in N.
V was determined using the following equation,

$$V = \pi A d_w$$

Here, A is the area of wear track cross-section in mm², dw is the diameter of the wear track in mm. Assuming wear scar on the disc to be a circular segment, A was calculated using the following equation,

$$\sin^{-1} A = R^2 \sqrt{\frac{h}{2R}} - \frac{1}{4}\sin\left\{4\left(\sin^{-1}\sqrt{\frac{h}{2R}}\right)\right\}$$

Here, h is the average depth of the wear track in mm (shown in Fig.3.3) and R is the radius of the ball counterpart in mm.
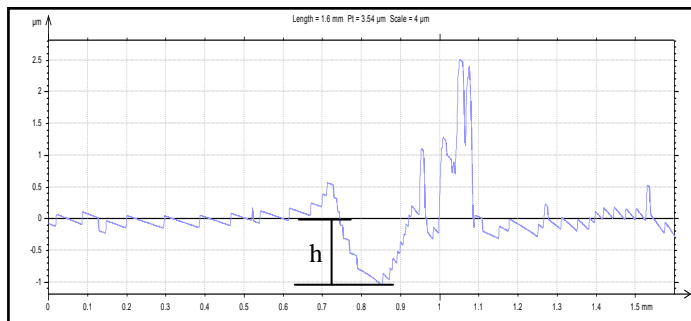
Fig. II: Representatives wear track profile

V. EFFECT OF DEPOSITION PARAMETERS ON TRIBOLOGICAL PROPERTIES OF THE COATING

Tribological performance of the coating has been evaluated by ball-on-disc test which is very important for cutting tool coatings. In ball on disc method adheso-diffusive as well as three body abrasion are prevalent wear mechanisms. Table III lists effect of different deposition parameters on coefficient of friction during ball-on-disc test. Some of the coatings provided low coefficient of friction throughout the test without coating failure. The wear coefficient should be as less as possible. The literature suggests wear coefficient less than 10×10^{-15} m³/N-m that is 10×10^{-6} mm³/N-m.
In the present case, wear coefficient as less as 5×10^{-15} m³/N-m has been obtained. Effect of deposition temperature on wear coefficient as shown from Table IV is not very systematic. But increase in negative substrate bias voltage provided increase in wear coefficient as shown in Table IV. Table IV reveal the effect of substrate bias and target frequency on wear coefficient respectively. For all most all the trials, wear coefficients were less than 7×10^{-15} m³/N-m. Table III lists effect of different

deposition parameters on coefficient of friction during ball-on-disc test. Some of the coatings provided low coefficient of friction throughout the test without coating failure.

Table III: Coefficient of friction for TiN coating deposited at various deposition parameters

Variation of parameter	Sample id	Value of parameter	coefficient of friction
Deposition temperature	S17	150	0.25-0.4
	S15	200	0.05-0.3
	S07	250	0.05
Substrate bias voltage	S07	-50	0.05
	S08	-60	0.05-0.5
	S09	-70	0.07-0.25
Substrate bias frequency	S11	50	0.1-0.35
	S07	100	0.05
	S12	150	0.1-0.5
	S13	200	0.1-0.3
	S14	250	0.05-0.3
Target frequency	S18	50	0.1
	S07	100	0.05
	S19	150	0.2-0.35
	S20	200	0.08
	S21	250	0.2-0.35

Table IV: Mechanical and tribological properties of TiN coating deposited by p-DC-CFUBMS

variation of parameter	Sample id	Value of parame-ter	Compo-site hardness (GPa)	adhesion strength (N)	Wear coefficient (×10-15) (m3/N-m)
substrate bias voltage (V)	S7	−50	24.4	59	6.1
	S8	−60	21.4	73	12.1
	S9	−70	23.2	59	14.5
substrate bias frequency (kHz)	S11	50	25.0	67	9.3
	S7	100	24.4	59	6.1
	S12	150	25.9	69	7.1
	S13	200	24.7	66	7.1
	S14	250	28.0	72	7.5
deposition temperature (0C)	S17	150	26.0	75.	10.6
	S15	200	25.1	68	20.2
	S7	250	24.4	59	6.1
Target frequency (kHz)	S18	50	23.1	68	5.6
	S7	100	24.4	59	6.1
	S19	150	25.3	65	9.3
	S20	200	24.2	54	5.8
	S21	250	25.6	61	9.1

Fig. III shows the SEM of the representative wear tracks from ball-on-disc experiment. Sample id. S18 clearly shows no coating failure even after a sliding distance of 778 m. Same sample provided a coefficient of friction of 0.1 (as given in Table III). Further, this sample yielded a wear coefficient of just

above 5×10^{-15} m³/N-m. For tool coating it is essential to have proper coverage on cutting edges.
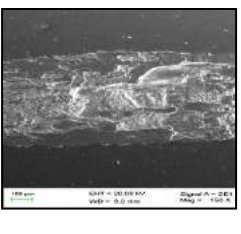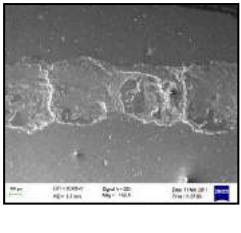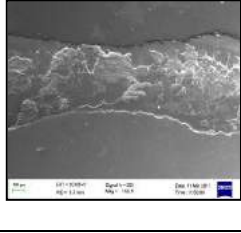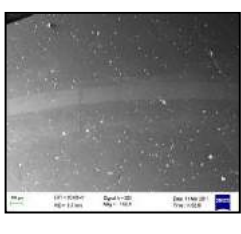
Sample id.	SEM micrographs of wear track on 40C8 steel substrate	EDS analysis (% atomic)		
		N2	Ti	Fe
Sample id. S8 Vb= −50V, ft=100 kHz, fb=100 kHz, T= 250°C		0.00	4.13	41.56
Sample id. S12 Vb= −50V, ft=100 kHz, fb=150 kHz, T= 250°C		0.00	18.03	38.20
Sample id. S15 Vb= −50V, ft =100 kHz, fb=100 kHz, T= 200 °C		0.00	5.35	42.74
Sample id. S18 Vb= −50V, ft =50 kHz, fb=100 kHz, T= 250°C		38.87	60.20	0.93

Fig. III: SEM micrographs and EDS analysis of wear track of TiN coated 40C8 steel substrate during ball-on-disc experiment.

Thus, in the present work most of the depositions have been done at −50 V. In the present work, systematic effect of deposition parameters could not be obtained but very good compact TiN coating (like sample id. S18) could be deposited with excellent wear resistance, good adhesion and low coefficient of friction. Table IV indicates mechanical and tribological properties of all deposited coatings.

VI. CONCLUSION

TiN was deposited in the present research on 40C8 low carbon steel disc substrate using pulsed DC CFUBMS technique over a very wide range of process parameters, viz. target frequency, bias voltage, bias frequency and deposition temperature.
Based on the experimental results, the following conclusions could be made:

1. Though coating deposited at low temperature provided poor wear resistance in ball-on-disc experiment but routinely wear coefficient less than 7.5×10^{-15} m³/N-m was obtained for other coatings.

2. Sample id. S7, S18, S20 (Table 3) provide low coefficient of friction. These may give relatively better machining performance in terms of lower cutting force and flank wear.

References

[1] H.A. Jehn, Surf. Coat. Technol. 131 (2000) 433.

[2] W.D. Sproul, K.O. Legg (Eds.), Opportunities for Innovation: Advanced Surface Engineering, Technomic Publishing Co., Inc., Switzerland, 1995.

[3] I. Efeoglu, R.D. Arnell, D.G. Teer, Surf. Coat. Technol. 57 (1993) 117.

[4] P.J. Kelly, C.F. Beevers, P.S. Henderson, R.D. Arnell, J.W. Bradley, H. Bäcker, Surf. Coat. Technol. 174-175 (2003) 795.

[5] C.F. Beevers, R.D. Arnell, S. Singh, P.J. Kelly, Proc. 2nd World Tribology Congress, Vienna, Sept. 2001, pp. 534–537.

[6] P.J. Kelly, J. Hisek, Y. Zhou, R.D. Pilkington, R.D. Arnell, Surf. Eng. 20 (3) (2004) 157.

[7] J.W. Bradley, H.Bäcker, P.J.Kelly,R.D.Arnell, Surf.Coat. Technol. 142-144 (2001) 337.

[8] J.W. Bradley, H. Bäcker, Y. Aranda-Gonzalvo, P.J. Kelly, R.D. Arnell, Plasma Sources Sci. Technol. 11 (2002) 165.

[9] P. J. Kelly, C. F. Beevers, P. S. Henderson, R. D. Arnell, J, W. Bradley, H. Backer, 174-175, 795-800, 2003

[10] P. J. Kelly, T. Vom Braucke, Z.Liu, R.D.Arnell, E.D.Doyle, 202, 774-780, 2007.

Prevention Methods for Reduce Welding Leakages in Aluminium using TIG and MIG Welding

Vyomesh R Buch, K.Baba.Pai

(vyomdhar_19@yahoo.co.in, kbabapai54@yahoo.co.in)

Abstract—**Intercoolers are simply air coolers, working on the same principle as radiator cooling water. The function of the radiator is to reject the coolant heat to the outside air. The cooling effect in the radiator is achieved by dispersing the heated coolant into fine streams through the radiator matrix so that relatively small quantities of coolant are brought in contact with large metal surface areas which in turn are cooled by system of air. Intercooler is made from the aluminum. So during welding of aluminum there may be chance of leakages form the pores. The welding process used for intercooler is TIG and MIG welding. By controlling the TIG and MIG welding parameter we are try to reduce the leakage and using implementation we get improvement in welding. For the inspection purpose the microstructure at different welding current and welding speeds are observed. After welding different tests like Radiography], Hardness, Microscopic examination & Depth of Heat Affected Zone is checked.**

Index Terms— *Aluminium alloy LM 6 and LM 9, Hardness Test. Leak Test, MIG welding, Radiography, TIG welding*

I. INTRODUCTION

INTERCOOLERS are air coolers, working on the same principle as radiators. The function of the radiator is to reject the coolant heat to the outside air. The cooling effect in the radiator is achieved by dispersing the heated coolant into fine streams through the radiator matrix so that relatively small quantity of coolant are brought in contact with large metal surface areas which in turn are cooled by system of air. The intercoolers are made from aluminium and having grade LM6 and LM9 composition. The intercoolers under study are used in turbocharging system of automobile engines. Intercooler is commonly made of aluminium due to the metals inherent advantages of high thermal conductivity and light weight. However the problem faced in the manufacturing unit of intercoolers is the welding of aluminium.. It is very difficult to weld aluminium because it gets high ductility at subzero temp. Pure aluminium melts at 660˚C and its alloy having melting range from 482˚C to 660˚C. Before welding of aluminium some surface cleaning is required because in open atmosphere

it reacts with oxygen and form an oxide film, so proper storage of aluminium is required. So for remove the oxide film the chemical, mechanical & washing process are done. At the manufacturing unit under consideration, for welding of aluminium the TIG and MIG welding are welding. The welding parameters considered for study are: Welding current, Polarity, Arc voltage, Welding Speed, Shielding Gases, Electrode diameter and Electrode orientation.

II. EXPERIMENTAL SETUP

An experimental set up has been made to identify the best possible welding parameters possible for the condition under study. Tests have been carried out on different samples prepared at different welding parameters. The details are given in the succeeding paragraphs. The sample material is prepared by cutting to appropriate size and then cleaned with the help to chemical. Then set appropriate current, welding speed and voltage. The test samples are prepared by using TIG & MIG welding with varying welding parameters. The various steps for making sample for observation of microstructure are as follows:

1. Cut the samples in appropriate length with the hacksaw blade.
2. Then on the belt the surface of sample is rough finished by grinding.
3. After cutting the polishing of surface is done by the different grade emery paper (0/1, 0/2, 0/3, 0/4) with the use of kerosene.
4. Then polishing is done with the use of alumina power for several minutes.
5. After polishing the sample is etched with HF.
6. Then sample is ready for observation under SEM
7. The micrographs obtained are printed at high magnification

III. RESULTS

Then the readings are obtained by considering the change in various welding parameters and welding techniques. Table I & II indicate the parameters used for TIG and MIG welding.

TABLE. I
Welding Parameter for TIG Welding

Sample No.	S1	S2	S3
Current(A)	160	170	180
Base material(mm)	4.2	4.2	4.2
Electrode Dia. (mm)	2.4	2.4	2.4
Arc Travel Speed(m/min)	0.20	0.20	0.20

TABLE. II
Welding Parameter for MIG Welding

Sample No.	S1	S2	S3
Current(A)	165	185	205
Base material(mm)	4.5	4.1	5.2
Electrode Dia. (mm)	1.2	1.2	1.2
Arc Travel Speed(m/min)	6.9	7.4	7.7
Penetration of Material	0.9	3.82	2.538
% Penetration*	20	33	44

* Allowable %Penetration is 33±1

Welding Trial: S1

Fig..1 S1 at 100X   Fig. 2 Welded Portion of
S1 with Plate 50X

1. Hydrostatic Pressure and Pneumatic Testing:

   Hydrostatic and Pneumatic Testing is done by taking the feeling water in the radiator and then air pressure is taken as 2.5 Kgf/cm^2. After this pressure we will get 50% linear leakage in the intercooler practically.

2. Radiographic Inspection:

   For radiographic inspection the film is developed taking exposure time 2min., processing time 5min at 20 ℃ by using single wall double wall technique and the time for the development taken as 5 min. For radiographic inspection Gamma rays are used.

TABLE.III
Result of Radiography for sample S1

Identification No.	Thickness	Film Size	Observation
S1	5mm	7.5"X3"	Acceptable

3. Hardness Test Report:

TABLE.IV
Result of Hardness for sample S1

Indenter	Minor Load $F0$ kgf	Major Load $F1$ kgf	Total Load F kgf	Value of E	Rockwell Hardness (HR)
1/16" steel ball	10	90	100	130	129.72

   The hardness result after the welding. The minor load is 10Kgf and the Major load is 90 kgf. The total load is 100Kgf and the hardness value which we will get is 129.72 HR.

4. Width of HAZ in sample with the use of SEM:
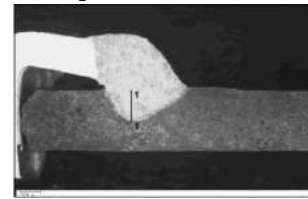
Fig. 3 Weld Penetration for sample S1

   Fig. 3 show the penetration of base metal with other metal which is indicated by 1-1 and which is equals to 786.4µ.

Welding Trial: S2

·

Fig. 4 S2 at 100X   Fig. 5 Welded portion of
S2 at 50X

1. Hydrostatic Pressure and Pneumatic Testing:

   Hydrostatic and Pneumatic Testing is done by taking the feeling water in the radiator and then air pressure is taken as 2.5 Kgf/cm^2. After this pressure we will get 40% linear leakage in the intercooler practically.

2. Radiographic Inspection:

   For radiographic inspection the film is developed taking exposure time 2min., processing time 5min at 20 ℃ by using single wall double wall technique and the time for the development taken as 5 min. For radiographic inspection Gamma rays are used.

TABLE.V
Result of Radiography for sample S2

Identification No.	Thickness	Film Size	Observation
S2	5mm	7.5"X3"	Acceptable

3. Hardness Test Report:

TABLE.V
Result of Hardness for sample S2

Indenter	Minor Load $F0$ kgf	Major Load $F1$ kgf	Total Load F kgf	Value of E	Rockwell Hardness (HR)
1/16" steel ball	10	50	60	130	129.9

   The hardness result after the welding. The minor load is 10Kgf and the Major load is 50 kgf. The total load is 60Kgf and the hardness value which we will get is 129.9 HR.

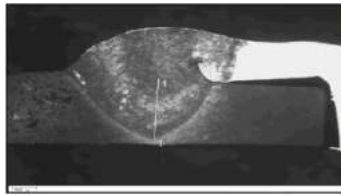**4. Width of HAZ in sample with the use of SEM:**

Fig.. 6 Weld Penetration for sample S2

Fig. 6 shows the penetration of base metal with other metal which is indicated by 1-1 and which is equals to 1541.6 µ.
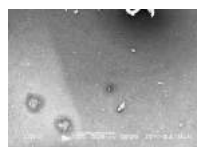
Welding Trial: S3

Fig. 7 S3 at 100X   Fig . 8 Welded portion of S3 at 50X

1. Hydrostatic Pressure and Pneumatic Testing:

Hydrostatic and Pneumatic Testing is done by taking the feeling water in the radiator and then air pressure is taken as 2.5 Kgf/cm^2. After this pressure we will get 66% linear leakage in the intercooler practically.

2. Radiographic Inspection:

For radiographic inspection the film is developed taking exposure time 2min., processing time 5min at 20 °C by using single wall double wall technique and the time for the development taken as 5 min. For radiographic inspection Gamma rays are used.

TABLE.VII
Result of Radiography for sample S3

Identification No.	Thickness	Film Size	Observation
S3	5mm	7.5"X3"	Repair

3. Hardness Test Report:

TABLE.VIII
Result of Hardness for sample S3

Indenter	Minor Load $F0$ kgf	Major Load $F1$ kgf	Total Load F kgf	Value of E	Rockwell Hardness (HR)
1/16" steel ball	10	160	170	130	129.68

The hardness result after the welding. The minor load is 10Kgf and the Major load is 160 kgf. The total load is 170Kgf and the hardness value which we will get is 129.68 HR.
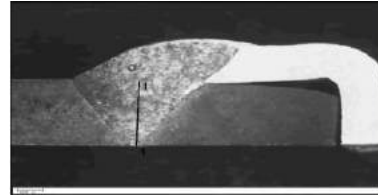
Fig. 9 Weld Penetrations for Sample S3

Fig. 9 shows the penetration of base metal with other metal which is indicated by 1-1 and which is equals to 1655.4µ.

IV. CONCLUSION

From the experimental work and consequent results and discussion we can conclude that as the welding speed is going to increase then the Welding voltage is also going to be increased so get increase in welding current, according to Ohm's law.

At lower current fine structure is observed but the penetration is 20% which is not sufficient and hence the welding leakage is 50%, whereas at higher welding speed there is higher welding current and so the metal will penetrate at faster rate and giving 44% penetration which is quite more and the welding leakage is observed is 66%..

TABLE. IX
Summary of Various types of Test

Sample No	% Leakage in Hydrostatic Pressure and Pneumatic Testing	Radiography Test	Hardness Test(HR)	Width of HAZ in µ
S1	50	Acceptable	129.72	786.4
S2	40	Acceptable	129.9	1541.6
S3	66	Repair	129.68	1655.4

So, from above conclusion it is found that in the sample S2 there is less leakage and when it is practically implemented and we will get good depth of the HAZ. It is also acceptable in Radiography test & it has good hardness after welding. For TIG and MIG welding maximum 33±1% penetration was observed. So the S2 sample fulfills all the above conditions and hence S2 parameter was recommended for in plant application. After applying these factors there is reasonable improvement in the % leakages. The recent 15 months status report of leakage problem including S2 parameter implementation is shown below:

%Status of Leakage For 2007-08

.
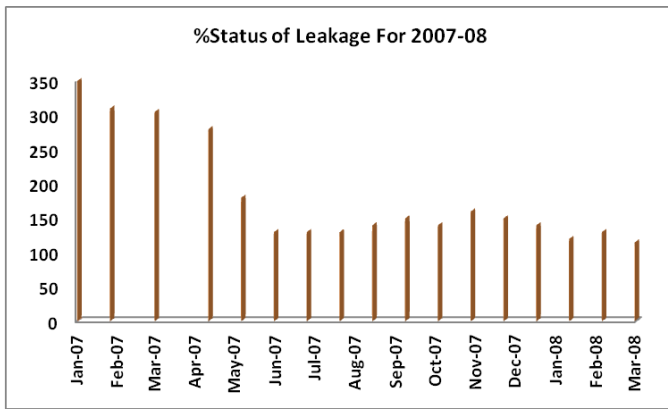
REFERENCES

[1] Balaram Gupta, Aerospace materials – Volume III, S. Chand & Company Ltd.,

[2] N.R.Mandal , Aluminum Welding

[3] Metallographic and Microstructures, ASM   Handbook, Vol-9

[4] Blunt, Jane and Nigel C. Balchin (2002). *Health and Safety in Welding and Allied Processes*. Cambridge: Woodhead. ISBN 1-   85573-538-5

[5] Cary, Howard B. and Scott C. Helzer (2005).   *Modern Welding Technology*. Upper Saddle   River, New Jersey: Pearson Education. ISBN 0-13-113029-3.

[6] Hicks, John (1999), *Welded Joint Design*.   New York: Industrial Press. ISBN 0-8311-3130-6.

[7] Lincoln Electric (1994). *The Procedure   Handbook of Arc Welding*. Cleveland: Lincoln Electric. ISBN 99949-25-82-2

[8] Weman, Klas (2003). *Welding processes   handbook*. New York: CRC Press LLC

Parametric Study of Tube Hydroforming Process

Parekh V.R.[1*], Patel B.C.[2], and Shah J.R.[3]
[1]Research Scholar, SVMIT-Bharuch
[2]Assistant Professor, SVMIT-Bharuch
[3]Assistant Professor, SVMIT-Bharuch
*Parekh_saiaerovij@yahoo.co.in

Abstract - **Tube hydroforming (THF) is one of the best & most popular unconventional metal forming processes which is widely used to form various tubular components. By this process, tubes are formed into different profile using internal pressure and axial compressive loads simultaneously to force a tubular blank to conform to the internal shape of a given die cavity. The success of a THF process is, however, dependent on a various parameters such as the loading path, lubrication conditions, and material formability & many others. In this paper, different parameters are selected for depth investigations of their effect on THF process. Most failure events in THF can be classified as wrinkling, buckling, bursting, severe thinning. These types of failures are caused by either excessive internal pressure or excessive axial end feed during the forming process. The finite element method (FEM) is a powerful method for rapidly designing both prototype and production components. The computer simulation of THF processes using the FEM has proven to be most efficient and useful, as it allows for the virtual testing and comparison of several candidate processes, thus avoiding the use of costly "trial and error" prototype tests. So a latest simulation module HYPER-FORM of HYPER-WORKS software is used to found its applicability against THF & then investigate various parametric effects on THF.**

Index Terms - **Metal forming, Hydroforming, T-shape profile & FEM.**

INTRODUCTION

Metal Forming has played central role as societies have developed [1]. [2] Metal forming is a general term, for a large group, that includes a wide variety of manufacturing processes. Metal forming processes are characteristic in that the metal being processed is plastically deformed in order to shape it into a desired geometry. The material actually gets stronger the more it is deformed plastically. This is called strain hardening or work hardening. As may be expected, strain hardening is a very important factor in metal forming processes. During a metal forming operation it is important to know the force and power that will be needed to accomplish the necessary deformation. The flow stress is the instantaneous value of the force necessary to continue the yielding and flow of the work material at any point during the process. The flow stress value can be used to analyze what is going on at any particular point

in the metal forming process. In general there are many manufacturing processes such as rolling, extrusion, forging, bending, tube bending, stamping, shearing, sheet metalworking, pressing, explosive forming, micro forming, hydroforming & many others for different types of metal forming processes the flow stress analysis may be different. The strain rate for any particular manufacturing metal forming process is directly related to the speed at which deformation is occurring. A greater rate of deformation of the work piece would mean a higher strain rate.

In all metal forming process a Tube hydroforming process is one of the best & most popular unconventional   metals forming processes which is widely used to form various tubular components. Tube Hydroforming (THF) has been called by many other names such as bulge forming of tubes (BFT's), liquid bulge forming (LBF) and hydraulic pressure forming (HPF) depending on the time and country in which it was used [3]. Establishment of process goes back to 1939 when Grey & parker [4] investigated manufacturing of Seamless copper fittings with T protrusions using a combination of internal pressure and axial load. The investigation was considered as a US patent in the 1940, which gave an indication of the coming period of tube hydroforming. By [5] define the Hydroforming process basically is a technique that uses a fluid either to form or aid in forming a part from ductile metal. The most common type of hydroforming used, tube hydroforming changes the cross-sectional shape of a tube from the normal round to other shapes that change along the part's length Hydroforming creates a much more precisely and intricately formed tube than was possible 20 years ago.

By [6] in between 1950 and 1970, researchers in the United States, United Kingdom and Japan developed related patents and application products. After 1970, researchers in Germany studied tube hydroforming and applied it to produce structural parts for automobiles. Since the early 1980's, tube hydroforming has been increasingly used in the automotive and aerospace industries, manufacturing of household appliances, and other applications. Tube hydroforming offers several advantages over conventional manufacturing via stamping and welding, such as part consolidation, weight reduction, improved structural stiffness, reduced tooling costs due to fewer parts, fewer secondary operations, tighter

dimensional tolerances and reduced distortion due to spring back and reduced scrap, since 2 trimming of excess material can be completely eliminated in THF (Dohmann and Hartl, 1996). [7] In 2000 has summarized a technological review of hydroforming process from its early years to very recent dates on various topics such as material, tribology, equipment, tooling, and many others. [8] has discussed the application of bulge forming to manufacturing near net shape components. He has also discussed about that machine & tool design & illustrates how FE simulation is playing an improving role in design of bulge forming process in 2001.[9] In 2002 have analyzed necking & bursting effect in flange & tube hydroforming by considering influence of material & process parameter, Which were applied to illustrating for tube and flange hydro-forming, bulging tests and classical stamping with good agreement with experimental knowledge.

Theoretical process window diagram (PWD) established & proposed by [10], in 2004, based on the mathematical formulations for predicting forming limits induced by buckling, wrinkling and bursting of free-expansion tube hydroforming & also validated against experimental results conducted for 6260-T4 $60\times2\times320$ (mm) aluminum tubes. Y-shape hydroforming experiments were conducted by [11], in 2004 & estimated the process parameters pressure levels, axial feeds, and initial tube length , which ware optimized" through conducting FEA simulations and verified with hydroforming experiments. In 2006 [12], was conducted an experiment and simulation techniques for investigation the influence of wrinkling behavior on formability and thickness distribution in tube hydroforming process & found different types of wrinkles in which a useful wrinkle can meet both the stress condition and the geometrical condition during calibrating. Lubricants are usually employed to increase the formability of the work piece so [13], in 2008 have use different lubrication regimes and observed along the different forming zones which vary with the lubricant layer thickness, applied load and sliding velocity. In 2010 the free bulge test for the roll-formed tubular material are carried out by [14], can be concluded that the flow stress of the tubular material should be determined from the actual free bulge test to find the practically valuable forming limit curve for the THF process. Similar formability and failures in bi-layered tube hydroforming were analyzed by [15], in 2011 using ANSYS LS-DYNA pre-processor and LS-DYNA solver in order to predict the most efficient and acceptable operating condition for certain material properties and initial blank geometry. Different sets of loading paths (relations between axial feed and internal pressure) were tested and compared with each other and analyzed that applying internal pressure in advance of the axial pushing was found to give the best formability for the process.

I.I T-Shape Profile

Since most of the parametric study for hydroforming process have been done many of the researchers by using different symmetrical or unsymmetrical sections such as T-shape, X-shape, Y-shape, Un-Equal T-shape, Bi-Layered. T-section is

one which was used by most of the researchers. In 2004 [16] have used of the finite element method in conjunction with adductive network is presented to predict an acceptable product of which the minimum wall thickness and the protrusion height fulfill the industrial demand on the T-shape tube hydroforming process. In 2005 [17] used an optimization methods along with finite element simulations were utilized to determine the optimum loading paths for closed-die and T-joint tube hydroforming processes. The objective of this study was to produce a part with minimum thickness variation while keeping the maximum effective stress below the material ultimate stress during the forming process. Similar action for T-shape part or tube using the designed adaptive system in combination with the finite element method is proposed by [18], in 2005 & found efficient way of process control & for the simulations ABAQUS/Explicit is used.

Hydroforming test machine is designed and developed by in 2006 effects of the coefficient of friction, strain hardening exponent and fillet radius on the parameters, protrusion height, thickness distribution and clamping and axial forces on unequal T joints were simulated through a code ABAQUS/EXPLICIT 6.3-1 by [19], & found different loading path. The amounts of calibration pressures and axial feedings required to produce an acceptable product in FEM were compared to better agreement with result obtained through experimentally. A hydroforming test machine with counter punch was designed and developed by [20] in 2007 & found the effects on branch height of formed product with & without a counter punch. Different process parameters like velocity and pressure profiles, and bucking system characteristics related to the finished product were studied by [21], in 2010 through copper T-shaped tube with FE simulation techniques with used codes such as LS- Dyna and ABAQUS. Single & bi-layered tube hydroforming processes were numerically simulated using the finite element method in this paper by [22] in 2011. It was found that the final bulges heights resulted from the models were in good agreement with the experimental results.

So from above of the research review THE FE techniques adopted by most of the researchers in this paper same techniques. For this Finite Element Code HYPER FORM is used for parametric study of hydroforming process. In short the overall study involves the following terms from [23] Hydroforming systems, equipment, controls and tooling ,Deformation mechanism and fundamentals of hydroforming ,Materials and their characterization for hydroforming ,Formability analysis for tubular hydroformed parts, Design and modeling of parts, process and tooling in tube hydroforming, Tribological aspects in hydroforming. In general the hydroforming techniques involved Pre-forming: tube rotary draw bending and pre-flattening/crushing in hydroforming, Hydroforming-hydro piercing , end-cutting, and welding, Hydroforming sheet metal forming components, Bending and hydroforming of aluminum and magnesium alloy tubes, Low pressure tube hydroforming ,Comparative analysis of hydroforming techniques. The Tube Hydroforming (THF)

process is a relatively new manufacturing technology, which has been used in the past decade. In 2012 an overall review on THF process is presented by [24] in which he had summarized Analytical Studies, FEM & Optimization Algorithm. This paper aims to collectively define how to various parameter affect the tube hydroforming process & different types of method used by most of the researchers to eliminate the defects with applying significant parametric value as a great success in hydroforming process.

II. THE TUBE HYDROFORMING PROCESS

The tubular blank is firstly placed between the two die halves and then filled with high-pressure liquid through holes in the plungers to remove any air bubbles trapped inside. The tube is then forced to adopt the inner contour of the tool by application of internal pressure (via high pressure liquid) and two axial forces (via plungers) simultaneously. In many cases, internal pressure can be transmitted via an elastomer (e.g. rubber or polyurethane), or a soft metal (e.g. lead). For limited applications, the tube can be formed by the increasing internal pressure only. This means that the axial plungers do not feed more material into the expansion zone. However, the axial forces acting on the tube ends must exceed a certain level to prevent leakage. This limit is known as sealing.

Fig 2 tube hydroforming sequence for T-shape
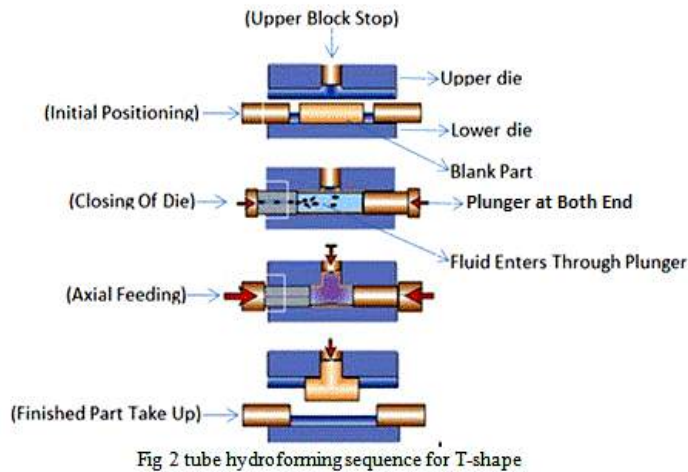
Steps for THF of T-shape profile is shown in above fig.2. Initial to final positions of T-section easily understand from fig.2.

II.I THF Advantages

The major advantage of forming processes is that they avoid the waste of material as happens in machining. Productivity can also be very high compared with machining. THF offers potential alternatives in the use of lightweight materials and hence can have a great impact in saving energy in the automotive industry. Furthermore, THF also offers potential in design of structures with high stiffness. THF offer some other advantages as compared to conventional manufacturing via stamping and welding. These advantages include: (a) part consolidation, for example stamped and welded sections to form a box section, can be formed as one single piece from a

tubular material using hydroforming, (b) weight reduction through more efficient section design and tailoring of the wall thickness in structural components, (c) improved structural strength and stiffness via optimized section geometry, (d) lower tooling costs due to fewer parts.

II.II THF Applications

The main application of this method has been found in manufacturing of reflectors, household appliances as well as components in the hygiene, aerospace, automotive and aircraft industries. Likewise, General Motors' (GM) suppliers began using hydroforming to create suspension parts. There was an eventual increase of approximately 20 percent in manufacturing productivity for GM, and the switch to hydroforming may have contributed to the gain. GM continues to use hydroforming in its production methods. In 2006, it became one of the first automakers to use this process to create structural products on vehicles (Pontiac, Chevrolet) for several of its brands. Other examples of hydroforming in the automobile industry include the making of engine cradles for various, Ford, and Chrysler models. The process has also been used by several European automobile manufacturers, such as Volkswagen, who switched from deep drawing to hydroforming in order to create unibody frames for some of their vehicles. Some of the most common applications of tube hydroforming can be found in the automobile industry. In 2002, the American automobile maker, Chrysler, began incorporating hydroforming to help reduce chassis vibration on its redesigned Dodge Ram.
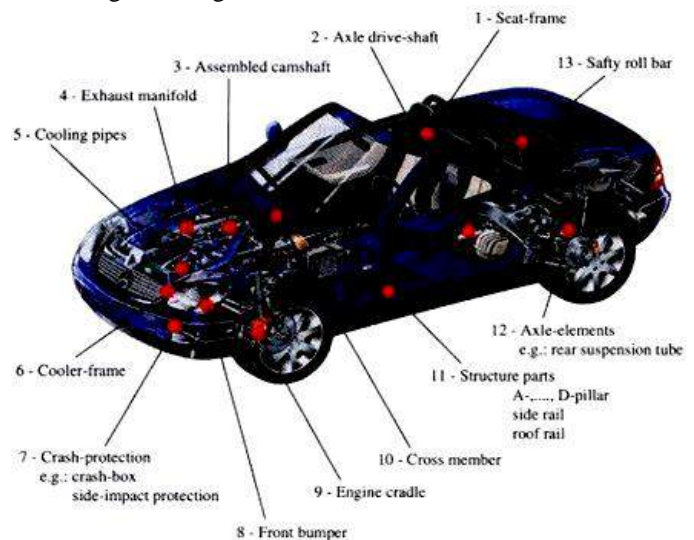

Figure 2: Examples of the automotive parts manufactured by tube hydroforming process.

II.III Tube failure in THF Process

The success of a THF process is, however, depends upon Number of process parameter such as loading path, material formability and lubrication conditions (Aue-U-Lan et al., 2004). A suitable combination of all these variables is vital to avoid part failure. Most failure modes in THF can be classified as wrinkling or buckling, bursting, or severe thinning. These

types of failures are caused by either excessive internal pressure or excessive axial end feed during the forming process.

III. SIMULATION SETUP FOR T-SECTION

A simulation set up for T-section as shown in below fig.3. All dimensions of this model taken from the experimental setup of T-section [20]. In experimental model counter punch is used to control the wrinkling & bursting effect while in case of Pro-E model A Capped ends option is utilized with fillet radius.
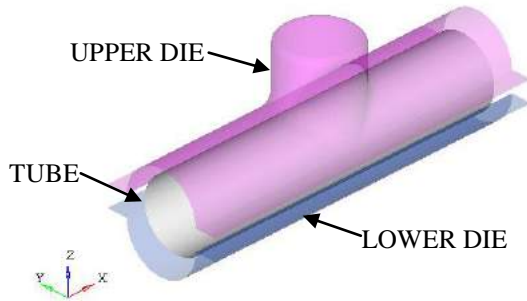

Fig.3 Model for T-section

IV FEM

For parametric analysis all kind tests of the of THF process were conducted experimentally and involved significant costs and time. The computer aided simulation of THF processes using the finite element method (FEM) has proven to be efficient and useful [6], as it allows for the virtual testing and comparison of several candidate processes, thus avoiding the use of costly "trial and error" prototype tests. The FEM was a suitable tool for the simulation of forming processes. In this paper a finite element code HYPERFORM of HYPER WORKS software adopted by me. Initial stage of parametric study of THF a simple simulation setup is used as shown in below fig.4.
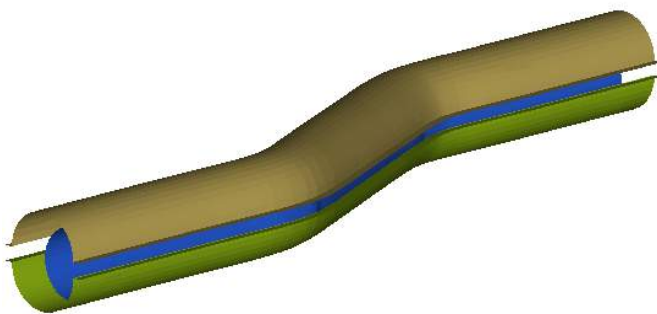
Fig.4. Simple Model of Tube with Defects

A tube with upper & lower die as IGES format imported to HYPERFORM module of manufacturing solutions. Then organize the imported model. After that meshing the individual parts, create a section, defining material, & updated to them through compos tab. A hydro setup tab used to run the process. Due to which two radios file generated as .rad000 & .rad00.Various parameters used for simple model are tabulated as below.

Sr. No	Parameter	Value
1	Tube Thickness	0.1
2	Yield Strength (6y)	185 Mpa
3	Strength Coefficient (K)	550
4	Strain Hardening	0.210
5	Material	CRDQ- Steel
6	Surface Meshing	0.5-30.0
7	Velocity	-2000mm/Sec
8	Coefficient Of .Friction	0.125
9	Initial Pressure	800 Psi
10	Final Pressure	24000 Psi

Table 1 list of parameter with value

For generating an animation file a RADIOSS SOLVER is used. With time of span total 11 number of file is generated. For analyzing the results a HYPERVIEW module is used. An animation tab is used to animate the process through which we are analyzed how to actual process is being done. Initial & final stages of animation are shown in below fig.5.
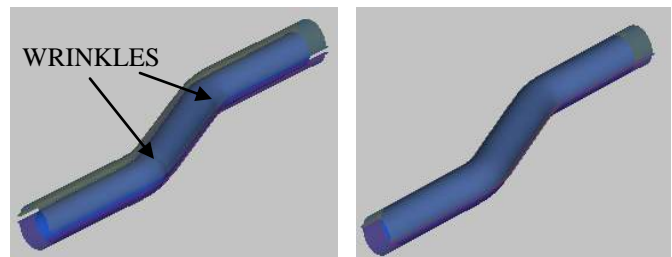

Fig.5 Initial & Final Stage of Animation.

Different results such as displacement, % of tinning thickness, stress, strain and many others can also be generated with the use of HYPERVIEW. Results for above simple model are shown in below table 2.

Sr. No	Results	Max. Value	Min. Value
1	Displacement (mm)	12.14	0
2	Strain	0.2434	0.02705
3	Stress (N/mm^2)	456.1	0
4	% of Thinning	10.26	-1.136
5	Thickness (mm)	1.315	1.167

Table 2 Results of Simple Model

A forming limit curve (FLC) & forming limit diagram (FLD) are shown in below fig.6. In spite of the fact that tube deformation can be detected, the determination of the forming severity is not straightforward using circle grid analysis by [6]. A deformed circle is manually or automatically measured at a critical location, and the corresponding surface strains are compared to a forming limit diagram (FLD).
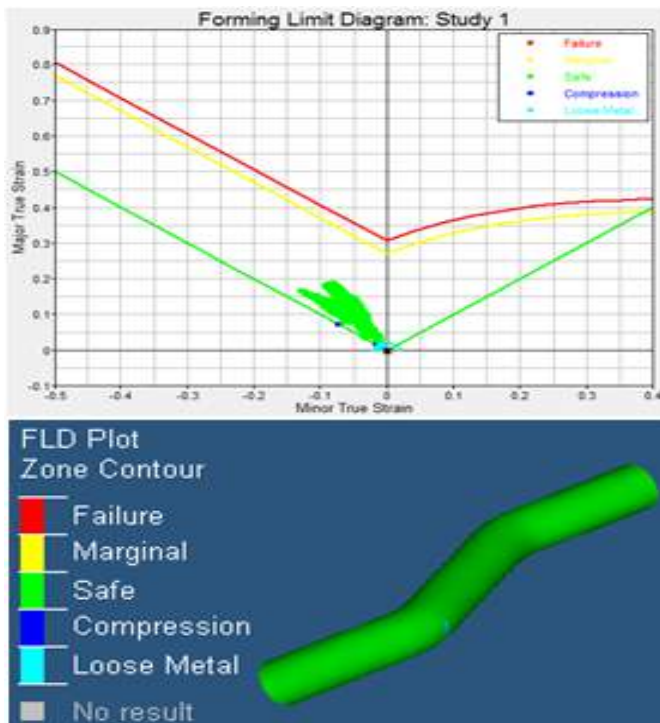
Fig.6 FLC & FLD Curve

The FLD provides information about how much a specific metal can be deformed before necking occurs.

V RESULTS & DISSCUSION

As per defined various parameter for simple tube in above table 1, different results are obtained, which is indicated in table 2. Displacement at the both ends of the tube sections quite high, while displacement at middle portion is quite low as analyzed from displacement results. In case of strain higher the value of it at middle bottom side of the tube & at the right front side of the bend portions while low value of it at left lower & right upper bend portions of the tube. In case of stress, higher the value of it at left end & middle section of the tube while low value of it at far away from the right bend portions as analyzed from the stress results. Value of thickness is quite high at the lower left & upper right portion of the tube & vice & low at upper left & lower right portion the tube as analyzed from the thickness distribution results. In case of % of thinning, higher rate of it at upper side of tube but near about the left bend portion while less value of it at left bend front portion of the tube. % of thinning is an important parameter that should be analyzed for any section of tube. As per shown in above fig.6 Forming limit curve (FLC) denotes that up-to these limit tube will be deformed but after that it will be break. From the forming limit diagram (FLD) the different zonal results are obtained as loose metal, compression, safe, marginal & failure as indicated as sky blue, blue, green, yellow & red color respectively. Most of the portion of the tube is indicated with green color so whole deformation of the tube is under safe zone. Significant parametric results of the deformed tube in terms of specific value defined in above table 2. Same thing adopted for T-shape profile, but at initial stage of my

study different results obtained in which value of % of thinning within to 90-95% which quite high by taking the value initial & final pressure limit in between (100- 10000) psi for CRDQ-Steel material so further investigation in these regard will be done by me in future with altering the parameters. Further investigation in case of T-shape profile will be carrying by me with different material such as AA6063-T5 & 6011A.

VI CONCLUSIONS

Metal Forming has played central role as societies have developed. Tube hydroforming (THF) is best & most popular unconventional metal forming processes which is widely used to form various tubular components. Most failure modes in THF can be classified as wrinkling or buckling, bursting, or severe thinning. So Selection of different parameter plays an important role for the success of the any process of the hydroforming. Axial feed with applied force selected in such a way that process has to be completed without defects & achieved best product as per requirement. A The Tube Hydroforming (THF) process is a relatively new manufacturing technology, which has been adopted by most of automotive industries. THF offers potential alternatives in the use of lightweight materials and hence can have a great impact in saving energy in the automotive industry. The finite element method (FEM) is a powerful method for rapidly designing both prototype and production components. HYPERFORM a module of HYPERWORKS software is applicable for tube hydroforming process.

REFERENCES

[1] J. Jeswiet , M. Geiger , U. Engel , M. Kleiner , M. Schikorra , J. Duflou , R. Neugebauer , P. Bariani , S. Bruschi "Review - Metal forming progress since 2000", CIRP Journal of Manufacturing Science and Technology,Vol 1, pp. 2008.

[2] Groche, P., Fittshe, D., Tekkaya, E.A., Allwood, `J.M., Hirt, G., Neugebauer, R, Incremental Bulk Forming, Annals of CIRP, Vol. 55/2, pp. 2007.

[3] Koc Muammer, Altan Taylan. "An overall review of the tube hydroforming (THF) technology", Journal of Material Process Technology, Vol.108, pp. 2001.

[4] Grey JE, Devereaux AP, Parker WN. Ing for making   wrought metal T's. US Patent; 1939.

[5] http://www.thefabricator.com/article/hydroforming/hydroforming-introduction-to-tube hydroforming.

[6] Honggang An,"Multi-objective Optimization of Tube Hydroforming Using Hybrid Global and Local Search", Electronic Theses and Dissertations, University of Windsor Scholarship at UWindsor, T.S. Jan. 2010. Muammer Koc, Taylan Altan"An overall review of the tube hydroforming (THF) technology", Journal of Materials Processing Technology, vol.108, pp. Sep 2000.

[7] Muammer Koc, Taylan Altan"An overall review of the tube hydroforming (THF) technology", Journal of Materials Processing Technology, vol.108, pp. Sep 2000.

[8] B.J. Mac Donald, M.S.J Hasmi "near net shape manufacturing of engineering components using bulge forming process: a review", Journal of Materials Processing Technology, vol.120, pp. Sep 2001.

[9] N.Boudeau, A. Lejeune, J.C. Gelin, "Influence of material and process parameters on the Development of necking and bursting in flange and

tube hydroforming", Journal of Materials Processing Technology, vol. 125, pp. Feb 2002.

[10] E Chu, Yu Xu,"Hydroforming of aluminum extrusion tubes for automotive applications. Part II: process window diagram", International Journal of Mechanical Sciences, vol. 46, pp. Feb 2004.

[11] Suwat Jirathearanat, Christoph Hartl, Taylan Altan," Hydroforming of Y-shapes—product and process design using FEA simulation and experiments", Journal of Materials Processing Technology, vol. 146, pp. 2004.

[12] Shijian Yuan , Wenjian Yuan, Xiaosong Wang," Effect Of Wrinkling Behavior On Formability And Thickness Distribution In Tube Hydroforming", Journal Of Materials Processing Technology vol. 177 pp. 2006.

[13] Mariela Luege, Bibiana M. Luccioni," Numerical simulation of the lubricant performance in tube hydroforming", journal of materials processing technology, vol.198, pp. July 2008.

[14] Woo-JinSong, Seong-ChanHeo Tae-WanKu , JeongKim , Beom-SooKang, "Evaluation of effect of flow stress characteristics of tubular material on forming limit in tube hydroforming process", International Journal of Machine Tools & Manufacture, vol. 50 pp. May 2010.

[15] A.G. Olabi, A. Alaswad, "Experimental and finite element investigation of formability and failures in bi-layered tube hydroforming process", Advances in Engineering Software, vol. 42 pp. May 2011.

[16] F C.Lin, C.T.Kwan,"Application of abductive network and FEM to predict an acceptable product on T-shape tube hydroforming process", Computers and Structures, vol.82, pp. March 2004.

[17] M. Imaninejad, G. Subhash, A. Loukus
 "Loading path optimization of tube hydroforming process", International Journal of Machine Tools & Manufacture, Vol.45 pp. March 2005.
P. Ray, B.J. Mac Donald"

[18] A. Aydemir , J.H.P. de Vree , W.A.M. Brekelmans , M.G.D. Geers ,W.H. Sillekens , R.J. Werkhoven " An adaptive simulation approach designed for tube hydroforming processes", Journal of Materials Processing Technology, vol. 159, pp. 2005.

[19] Hossein Kashani Zadeh, Mahmoud Mosavi Mashhadi," Finite Element Simulation and Experiment in Tube Hydroforming of Unequal T Shapes", Journal of Materials Processing Technology, vol. 177, pp.2006.

[20] Y.M. Hwang , T.C. Lin, W.C. Chang, " Experiments on T-shape hydroforming with counter punch", Journal of Materials Processing Technology, vol. 192–193, pp. 2007.

[21] J.Crapps, E.B.Marin, M.F.Horstemeyer R.Yassar, P.T.Wang, "Internal state variable plasticity-damage modeling of the copper tee-shaped tube hydroforming process", Journal of Materials Processing Technology, vol. 210 pp. June 2010.

[22] Abed Alaswad, K.Y. Benyounis, A.G. Olabi ,"Finite element comparison of single and bi-layered tube Hydroforming processes", Simulation Modeling Practice and Theory, Vol.19, pp. March 2011.

[23] http://www.woodheadpublishing.com/en/book.aspx?bookID=1359.

[24] A. Alaswad, K.Y. Benyounis, A.G. Olabi "Review Tube hydroforming process: A references   guide" Materials and Design, Vol. 33, pp. July 2011.

Effect of Applying HPC Jet in Machining Of 42CrMo4 Steel Using Uncoated Carbide Inserts

Prof. Mayur S. Modi[1*], Mr. Sandip G. Patel[2]*

[1, 2] Shree Swami Atmanand Saraswati Institute of Technology,
Surat-395006, Gujarat, India
(E-mail: maymodi@gmail.com[1*], patelsandip1990@rediffmail.com[2*])

Abstract— **To avoid surface distortion and to improve tool life, machining of alloy steel and other hard materials under high speed-feed condition requires instant heat transfer from the work-tool interface where the intensity of cutting temperature is the maximum. Conventional cooling is completely unable and other special techniques like MQL and cryogenic cooling are not suitable in context of product quality and cost effectiveness. Supply of high-pressure coolant (HPC) with high velocity may provide the best control to reduce cutting temperature and tool wear as well as increase tool life. This paper deals with an experimental investigation on the effect of high-pressure coolant on temperature, tool wear, surface roughness and dimensional deviation in turning 42CrMo4 steel by uncoated carbide inserts and comparing it with dry condition. It is observed that the cutting temperature and tool wear is reduced, tool life is increased, surface finish is improved, and dimensional deviation is decreased with the use of high-pressure coolant.**

Keywords— **High-pressure coolant (HPC), Alloy steel, Temperature, Wear and Product quality.**

I. INTRODUCTION

During machining, a tool penetrates into the work piece because of the relative motion between the tool and the work piece, deforms the work material plastically and removes the material in the form of chips. Plastic deformation of the work material, rubbing of the tool flank with the finished surface and friction between tool rake face and flowing chips produces huge amount of heat and intense temperature at the chip-tool interface. A major portion of the energy is consumed in the formation and removal of chips. Energy consumption increases with the increase in cutting velocity, feed and depth of cut as well as strength and hardness of work material. During machining, especially of hard materials, much heat is generated by the friction of the cutter against the work piece, which is one of the major causes of reduction in tool hardness and rapid tool wear [1]. However, the main problem with conventional coolant is that it does not reach the actual chip-tool interface where the maximum temperature attains [2]. The extensive heat generated evaporates the coolant before it can reach the cutting area, makes a semi conductive vapor barrier and consequently prevents heat conduction. Hence, heat generated during machining is not removed and is one of the main causes of the reduction in tool life.

The concept of high-pressure coolant may be a possible solution for high speed machining in achieving intimate chip-tool interaction, low cutting temperature and slow tool wear while maintaining cutting forces/power at reasonable levels, if the high pressure cooling parameters can be strategically tuned. With the use of high-pressure coolant during machining under normal cutting conditions, the tool life and surface finish are found to improve significantly, which is due to the decrease in heat and cutting forces generated[9-11]. Mazurkiewicz[11] reported that a coolant applied at the cutting zone through a high-pressure jet nozzle can reduce the contact length and coefficient of friction at chip-tool interface and thus can reduce cutting forces and increases tool life to some extent. High-pressure coolant injection technique not only provides reduction in cutting forces and temperature but also reduces the consumption of cutting fluid by 50% [12, 13]

II. EXPERIMENTAL INVESTIGATIONS

Experiments have been carried out by plain turning of 42CrMo4 steel rod (Ø 220x520 mm) in a powerful and rigid lathe at different cutting velocities (V) and feeds (f) under both dry and high-pressure coolant (HPC) conditions. The experimental set-up used for the present purpose has been shown in Figure 1. The machinability characteristics of that work material mainly in respect of cutting temperature, tool wear, tool life, surface roughness and dimensional deviation have been investigated to study the role of high-pressure coolant. The ranges of the cutting velocity (V) and feed (f) were selected based on the tool manufacturer's recommendation and industrial practices. Depth of cut (d), being less significant parameter, was kept fixed. The following cutting parameters have been chosen for the present

experiment: Use an automatic spell-checker. You have to send black-and-white texts and figures, preferably.
Cutting speed, V: 93,133,186,266 and 193 m/min, Feeds,   f: 0.10, 0.14, 0.18 and 0.22 mm/rev , Depth of cut, d: 1.0 and 1.5 mm Standard Sandvik PSBNR 2525M12 tool holder was used to hold indexable Sandvik cutting inserts SNMG and SNMM so that the geometry becomes (-6°, -6 °, 6 °, 15 °, 75 °, 0. 8 mm).

Figure 1: Photographic View of the Experimental Setup

Figure 2: Photographic View of the Calibration Setup

The average cutting temperature was measured by simple but reliable tool-work thermocouple technique with proper calibration [14]. Figure 2 shows the photographic view of the calibration setup. Figure 3 shows the calibration curve obtained for the tool-work pair with tungsten carbide as the tool material and steel undertaken as the work material. Machining has been interrupted at regular interval and the tool has unclamped to measure width of wear land on the principal and auxiliary flank.
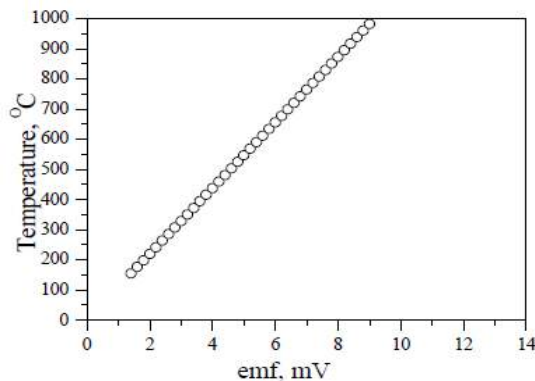
Figure 3: Temperature calibration curve for carbide and 42CrMo4 steel

Tool wear is monitored under optical microscope fitted with micrometer of least count 10 μm. As per ISO standard tool rejection criteria is selected as the growth of wear VB=300 μm on its principal flank. When the tool wear reaches to its limiting value, it is inspected under scanning electron microscope (Philips XL30) to study the wear mechanism. Surface roughness is measured along the longitudinal direction of the turned job with the help of a Talysurf roughness checker. A complete pass is performed with a fresh edge of the tool and deviation in dimension was measures with the help of a digital dial gauge of least count 10 μm.

A.   Results and Discussion

Reduction of friction between the chip-tool and work- tool interface is very important in cutting operation, as reduction in kinetic coefficient of friction not only decreases frictional work, but also decreases the shear work as well. Usually cutting temperature increases with the increase in process parameters causing decrease in hardness of the contact layer of the work piece and also the tool material. The effect of HPC on average chip-tool interface temperature at different cutting speed and feeds under both dry and HPC conditions has been shown in Figure 4. It is clear from Figure 4 that during machining at lower cutting speed the cooling effect is more as the nature of chip-tool contact is plastic-elastic. Initially the chip tool contact is plastic but when the chip leaves the tool the nature of contact is elastic. With an increase in cutting speed the chip makes fully plastic or bulk contact with the tool rake surface which prevents from entering of jet into the hot chip-tool interface. As a result, under higher speed, rate of reduction of temperature is less in comparison with lower speed. HPC cooling effect also improved to some extent with the decrease in feed particularly at lower cutting speed. At lower chip velocity, the thinner chips are pushed up by the HPC jet coming from opposite direction of chip flow and enable it come closer to the hot chip-tool contact zone to remove heat more effectively. With an increase in feed curl radius of the thick chip is increased.
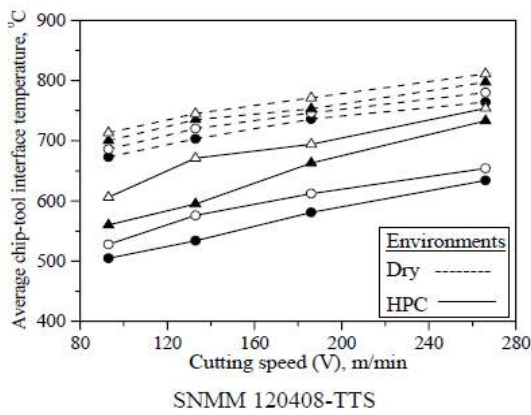

SNMG 120408-TTS

SNMM 120408-TTS
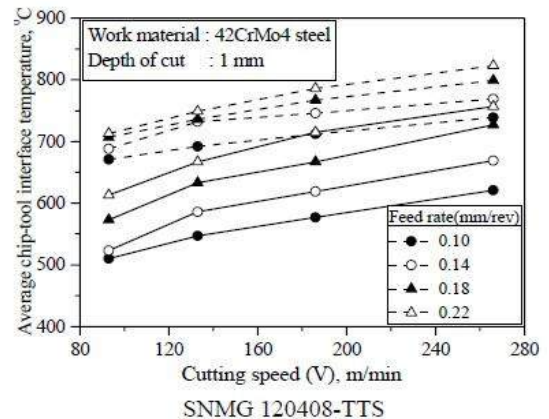
Figure 4: Variation in temperature with cutting speeds at different feeds under dry and HPC conditions
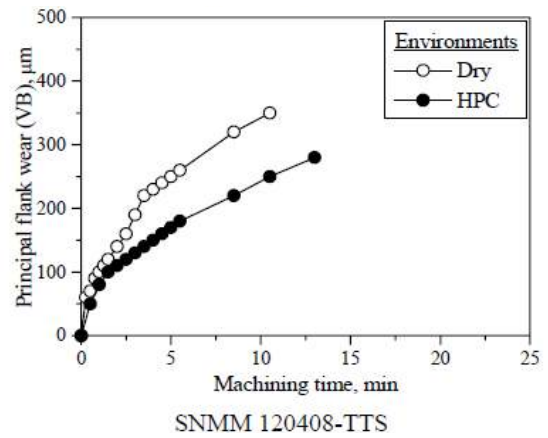

SNMM 120408-TTS

Figure 5: Growth of average principal flank wear (VB) with machining time under dry and HPC conditions

Under usual cutting conditions the cutting edge of a form stable cutting tool is wear out due to continuous interaction and rubbing between the chip and the tool and between the work and the tool. After the tool has been used for some times, wear land is appeared at the flank of the tool below the cutting edge extending approximately parallel to the cutting edge. The maximum or predominant wear is taken place in the zone where the energy input is greater. The principal concern of metal cutting research has been to investigate the basic mechanism of wear by which the life of the tool is governed. The life of carbide tools, which mostly fail by wearing, is assessed by the actual machining time after which the average value (VB) of its principal flank wear reaches a limiting value, like 300 μm. Cost of manufacturing product is affected by life of the cutting tools. Therefore, attempts should be made to reduce the rate of growth of flank wear (VB) in all possible ways without much sacrifice in MRR.

The growth of average principal flank wear, VB and average auxiliary flank wear, VS with machining time at high cutting velocity (193 m/min) and depth of cut (1.5 mm) by both the inserts under dry and high-pressure coolant conditions have been shown in Figure 5 and Figure 6 respectively.

SNMG 120408-TTS

SNMM 120408-TTS

Figure 6: Growth of average auxiliary flank wear (VS) with machining time under dry and HPC conditions

It is observed that while dry cutting principal flank wear and auxiliary flank wear is more than that of HPC condition. Tool wear reduces due to substantial reduction in cutting zone as well as flank temperature and lubrication in the interface by HPC jet. Under both the condition initially the wear rate is more for both SNMG and SNMM insert because of sharp edge of the insert rapidly break down due to plastic deformation and consequential temperature rise. After some time the wear process is more or less uniform. For both the cases, severe sparking is observed and the insert wear out rapidly in the last pass. Before the appearance of spark, the wear data taken is plotted shown in Figure 5.

Principal and auxiliary flank surfaces of the tool tip have

been observed under SEM to see the actual effects of different environments on wear of the carbide insert after being used for machining steel over reasonably long period. At the starting of last pass severe sparking is observed and the tool wears out rapidly. The SEM views principal and auxiliary flank of the worn out SNMG insert after about 14 minutes of dry machining and 20 minutes machining under HPC conditions have been shown in Figure 7 and Figure 8 respectively. Machining under dry condition with SNMM insert shown in Figure 9 and Figure 10, welding of work material over principal flank of the insert and scratching mark due to re-cutting of the chips is observed. No groove or notch wear is found under both the environments. Under all the environments, scratch marks appears in the flanks. Some plastic deformation and micro chipping are found to occur under dry and HPC machining. Effective temperature control by HPC almost reduces the growth of notch and groove wear on the main cutting edge. It has also enabled the reduction in the auxiliary notch wear. Further the figure clearly shows reduced average flank wear, average auxiliary flank wear and crater wear under High Pressure Coolant condition. The major causes behind development of surface roughness in continuous machining processes like turning, particularly of ductile metals are (i) regular feed marks left by the tool tip on the finished surface (ii) irregular deformation of the auxiliary cutting edge at the tool-tip due to chipping, fracturing and wear (iii) vibration in the machining system and (iv) built-up edge formation, if any. Figure 11 shows the variation in surface roughness with cutting velocity under dry and HPC conditions. As HPC reduces average auxiliary flank wear and notch wear on auxiliary cutting edge, surface roughness is observed comparatively lower under High Pressure Coolant conditions. However, it is evident that HPC improves surface finish depending upon the work-tool materials and mainly through controlling the deterioration of the auxiliary cutting edge by abrasion, chipping and built-up edge formation.

Dry condition, 14 min   HPC condition, 20 min
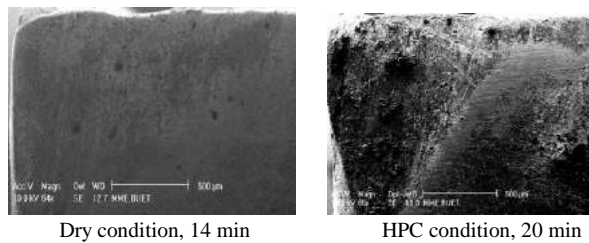
Figure 7: SEM views of principal flank of worn out tip of SNMG insert

Dry condition, 14 min   HPCcondition,20 min
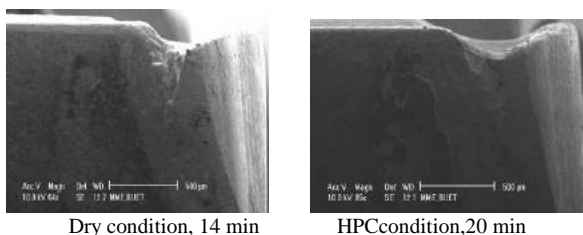
Figure 8: SEM views of auxiliary flank of worn out tip of SNMG insert

Surface roughness gradually increases as usual with the machining time as can be seen in Figure 12, due to gradual increase in auxiliary flank wear (VS). Again it is observed that the rate of increase in surface roughness decreases to some extent when machining is done under HPC condition which not only reduces the auxiliary flank wear but also possibility of built-up edge formation due to reduction in temperature. It appears from Figure 12 that surface roughness grows quite fast under dry machining due to more intensive temperature and stresses at the tooltips. High Pressure Coolant appeared to be effective in reducing surface roughness.
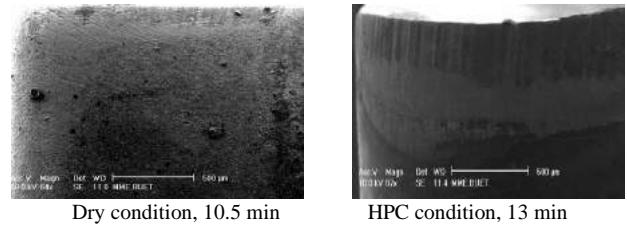

Dry condition, 10.5 min   HPC condition, 13 min

Figure 9: SEM views of principal flank of worn out tip of SNMM insert

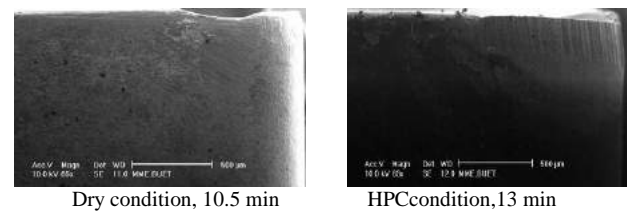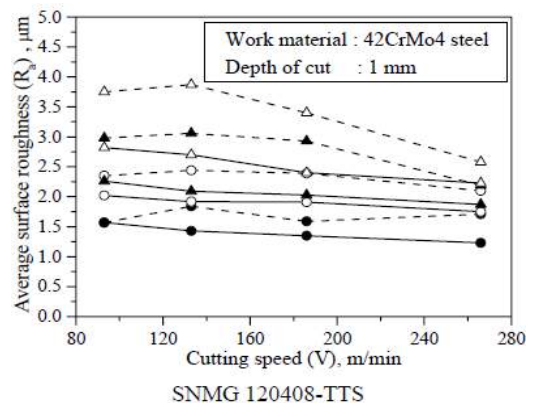Dry condition, 10.5 min   HPCcondition,13 min

Figure 10: SEM views of auxiliary flank of worn out tip of SNMM insert
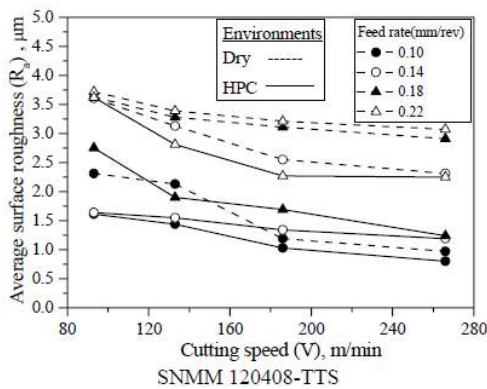

SNMG 120408-TTS

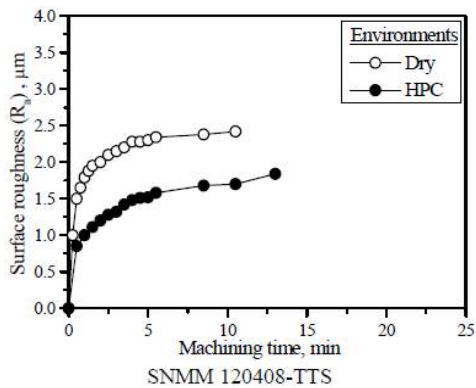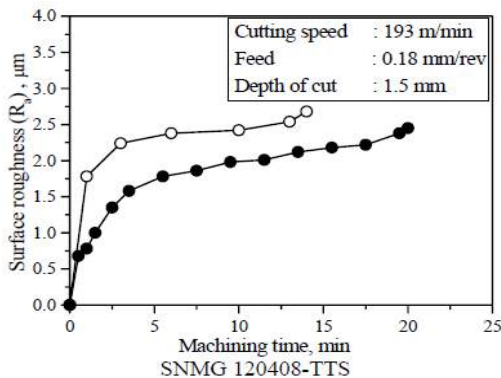Figure 11: Variation in surface roughness with cutting speeds at different feeds under dry and HPC conditions

Figure 12: Surface roughness developed with progress of Machining under dry and HPC conditions
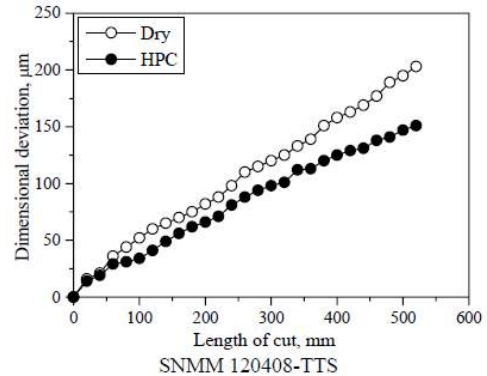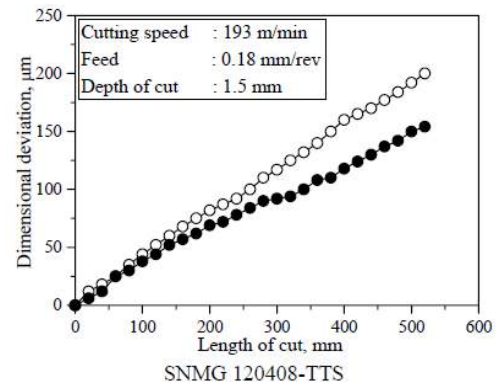

Figure 13: Dimensional deviation observed after one full Pass turning under dry and HPC conditions

After machining 14 and 20 minutes with SNMG insert under dry and HPC condition respectively, severe spark is observed and cutting tools undergo severe plastic deformation as well as rapid tool wear. Surface finish improves under high-pressure coolant condition in turning 42CrMo4 steel. Also surface roughness grows slowly with machining time under HPC condition. HPC takes away the major portion of heat and provides remarkable benefit in respect of controlling the thermal expansion of the job as a result decrease in dimensional deviation desirably with machining time.

III. CONCLUSIONS

High-pressure coolant jet not only reduces chip-tool and work-tool interface temperature but also reduces the heat generation by its effective oil film lubrication under all the investigated speed-feed combinations. High-pressure coolant has significantly reduced flank wears as a result improved tool life.

IV. REFERENCES

[1] Othani, T. and Yokogawa, H., "The Effects of Work Piece Hardness on Tool Wear Characteristics", Bulletin Japan Society of Precision Engineering, 22(3), September 1988.

[2] Wertheim, R. and Rotberg, J., "Influence of High- Pressure Flushing through the Rake Face of the Cutting Tool", Annals of CIRP, 41(1), 1992, pp. 101–106.

[3] Farook, A., Varadarajan, A.S. and Philip, P.K., "Machinability Studies on Steel Using Hard Metal Inserts with Soft Material Deposit", *Proceedings of the 18th AIMTDR*, 1998, pp.152-155.

[4] Thoors, H., Chandrasekaran, H., "Influence of the Cutting Medium on Tool Wear During Turning", Report No. IM-3118, Swedish Institute for Metal Research, 1994.

[5] Dhar, N.R., Paul, S., Chattopadhyay, A.B., "On Effects of Cryogenic Cooling on Cutting Forces and Temperature in Turning of C-40 Steel", Journal of Engineering Manufacture, Proceedings of IMechE (Part-B).

[6] Dhar, N.R., Paul, S., Chattopadhyay, A.B., "Role of Cryogenic Cooling onCutting Temperature in Turning Steel", International Journal Manufacturing Science and Engineering, ASME, 1999.

[7] Dhar, N. R., Kamruzzaman, M. and Ahmed, Mahiuddin,. "Effect of Minimum Quantity Lubrication (MQL) on Tool Wear and Surface Roughness in Turning AISI 4340 Steel", Journal of Material Processing Technology, 172, 2006, pp.299-304.

[8] Dhar, N. R., Islam, M. W., Islam, S. and Mithu, M. A. H., "The Influence of Minimum Quantity of Lubrication (MQL) on Cutting Temperature, Chip and Dimensional Accuracy in Turning AISI 1040 Steel", Journal of Material Processing Technology, 171, 2006, pp.93-99.

[9] Kovacevic, R., Cherukuthota, C. and Mohan, R., "Improving the Surface Quality by High Pressure Water Jet Cooling Assistance", Geomechanics, 93, 1994, pp. 305–310.

[10] Lindeke, R.R, Schoeing, Jr. F.C., Khan, A.K. and Haddad, J., "Cool Your Jets", Cutting Tool Engineering, October 1991, pp. 31–37.

[11] Mazukiewicz, M., Kubala, Z. and Chow, J., "Metal Machining with High Pressure Water-Jet Cooling Assistance", Journal of Engineering for Industry, 111, 1989, pp.7

[12] Lindeke, R. R., Schoening, Jr. F. C., Khan, A. K. and Haddad, J.,"Machining of Titanium with Ultra-High Pressure through Insert Lubrication/Cooling", Transaction of NAMRI/SME, 1991, pp. 154–161.

[13] Aronson, R. B., 2004. "Using High-Pressure Fluids, Cooling and Chip Removal are Critical", Manufacturing Engineering, 132 (6), June 2004.

Experimental analysis of heat pump used for simultaneous heating and cooling utilities

Rahul P.Patel*, Dr. R. G. Kapadia

(email ID of correspondence*:- rahulpatel2985@gmail.com)

Abstract— **In this research work, the performance of heat pump for simultaneous heating and cooling with R22 and R134a refrigerant studied. An experimental setup is fabricated with tube-tube water cooled heat exchanger (condenser and evaporator). The performance is carried out by varying the water flow rate through condenser and evaporator. It was found that at low water flow rate (2 LPM) maximum heating and cooling can be achieved and at high water flow rate(10 LPM) maximum coefficient of performance is there and R134a has a higher COP than R22.**

Index Terms— **COP, Heat pump, R22, R134a, tube-tube heat exchanger.**

1. INTRODUCTION

A heat pump is a thermal machine that pumps heat from a lower temperature to a higher temperature, the goal being the heating effect provided; if the goal is the cooling, the device is a refrigerator; in special cases, the goal is at the same time the cooling and heating effect, and then the device is also named heat pump.

Many food industries, textiles industries require both refrigeration and water heating. In case of textile mill, it requires central air conditioning plant which requires chilled water (all water central air conditioning system) and hot water for steam generation and heating purpose, while in food industries, refrigeration required for product preservation and hot water required for cleaning, sterilization or process heating.

It is common for the refrigeration and water heating systems to be separate and unconnected, and both consuming purchased energy. This approach wastes considerable energy, contributing to the depletion of fossil fuel reserves and the release of greenhouse gases. In vapour compression refrigeration system, heat energy is rejected in case of refrigeration and air conditioning while in heat pump cooling effect is rejected. By utilizing those rejected energy simultaneous cooling and heating effect can be achieved by saving the energy and by improving the performance of the system.[1]

The air conditioning and refrigeration industry is undergoing significant changes as it continues to replace the ozone depleting substances (ODSs) commonly used as refrigerants. According to the Montreal Protocol and its subsequent amendments and regional regulations, CFCs (chlorofluorocarbons) are banned since 1996 and the phase-out deadlines for HCFCs (hydro chlorofluorocarbons) are approaching (2030). Consequently, new fluids with zero ozone depleting potential (ODP), such as HFCs (hydro fluorocarbons) and natural refrigerants are being tested as substitutes for the ODSs. HCFC-22 has been widely used as working fluid in air conditioning and in medium and low-temperature applications within the commercial and industrial refrigeration. Nowadays, the replacement of HCFC-22 in existing and new systems without significant changes in equipment or lubricants constitutes a crucial challenge for the refrigeration industry.

At present alternative refrigerants available for R22 in residential air conditioning (A/C) and heat pumps can be categorized into three types. First, HFC (Hydro-Fluorocarbons) represented by R410A, R407C and R134a. Second, HC (Hydro-carbons) represented by R290 and R717. HC has excellent thermal performance and causes low green house effect. But its safety performance is not acceptable. It is usually flammable or toxic, which limits its use in residential A/C and heat pumps. Third, natural substances represented by CO_2. However, when working under supercritical cycle, CO_2 systems have extremely high working pressure (reaching 130 bar and above), low operation efficiency, and high manufacturing and operation cost. Hence it is hard to be widely accepted by A/C industry. As a result, it is generally considered practical and feasible to replace R22 with HFC refrigerants. HFCs are synthetic fluids entirely harmless to the ozone layer since they do not contain chlorine. These fluids are the most used substitutes for CFCs and HCFCs.[19]

2. EXPERIMENTAL APPARATUSES AND PROCEDURES

2.1 Experimental apparatus

The experimental measurements in this study were conducted in a fabricated test rig with tube-tube water cooled heat exchanger. The heat pump used in this study is with 1 tone capacity, originally designed to work with R22 refrigerant. The measurement unit consists of thermocouples, a pressure gauge and rotameter. The K-type thermocouples were

used to measure temperature. A total of 8 measurement points were used, including points for measuring inlet and outlet temperatures of each refrigeration component. Two rotameter is used to measure and control the water flow rate through heat exchanger (condenser, evaporator).

2.2 Experimental procedures

The performance was conducted with R22 by varying the water flow rate through condenser and evaporator. By three mode water flow rate is varied and test was conducted in which first mode is condenser water flow rate varied from 2 LPM to 10 LPM and evaporator water flow rate is constant at 2 LPM, second mode is evaporator water flow rate varied from 2 LPM to 10 LPM and condenser water flow rate is constant at 2 LPM, in third mode condenser and evaporator water flow rate is varied from 2 to 10 LPM.

Following are the parameter that measured during the performance by varying the water flow rate through the rotameter
1) Temperature of refrigerant Condenser Inlet
2) Temperature of refrigerant Condenser Outlet
3) Temperature of water Condenser Inlet
4) Temperature of water Condenser Outlet
5) Temperature of refrigerant Evaporator Inlet
6) Temperature of refrigerant Evaporator Outlet
7) Temperature of water Evaporator Inlet
8) Temperature of water Evaporator Outlet
9) Pressure in condenser
10) Pressure in evaporator.
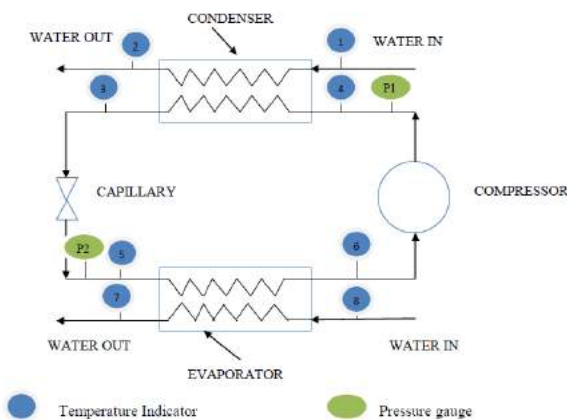
Fig.1 Schematic diagram of test rig.

After it in existing system R22 is replaced by R134a. And same performance is done as explain with R22.

3. Theoretical analysis

The thermodynamic properties of both R22 and R134a are evaluated using COOL PACK [5].The overall performance of the plant is determined by evaluating its COP, calculated as the ratio between refrigerating capacity and electrical power supplied to the compressor:

The rate of heat absorbed by evaporator is given by

$$Q_k = \dot{m}(h_1 - h_4) \tag{1}$$

The rate of heat rejected by condenser is given by

$$Q_0 = \dot{m}(h_2 - h_3) \tag{2}$$

Compressor power consumption is given by

$$\dot{W} = \dot{m}(h_2 - h_1) \tag{3}$$

Coefficient of performance for cooling

$$COP_{cooling} = \frac{Q_k}{\dot{W}} \tag{4}$$

$$COP_{cooling} = \frac{h_1 - h_4}{h_2 - h_3}$$

Coefficient of performance for heating

$$COP_{heating} = \frac{Q_o}{\dot{W}} \tag{5}$$

$$COP_{heating} = \frac{h_2 - h_3}{h_2 - h_1} \tag{6}$$

$$COP_{carnot} = \frac{T_o}{T_k - T_o} \tag{7}$$

Second law efficiency (η_{II})of vapour compression cycle,

$$\eta_{II} = \frac{\text{Minimum available energy required for the cycle}}{\text{Actual available energy consumed in the cycle}} \tag{8}$$

$$\eta_{II} = \frac{COP}{COP_{Carnot}} \tag{9}$$

Where,
  Q_k = heat absorbed
  Q_o = heat rejected
  $\dot{m}$ = mass flow rate
  h = enthalpy
  COP = co-efficient of performance
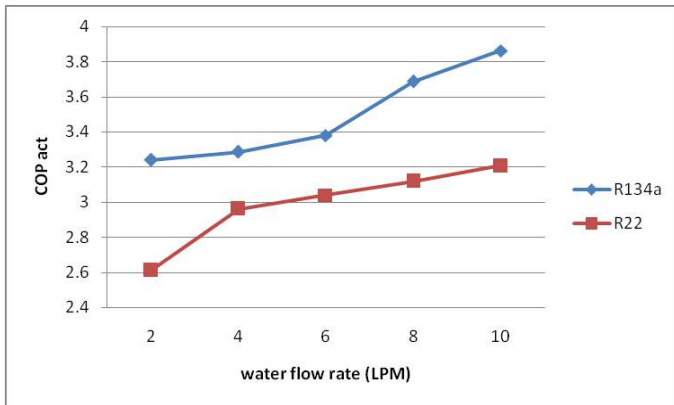 η_{II} = second law efficiency

4. Results and discussion

Fig.2 COPact vs water flow rate through condenser
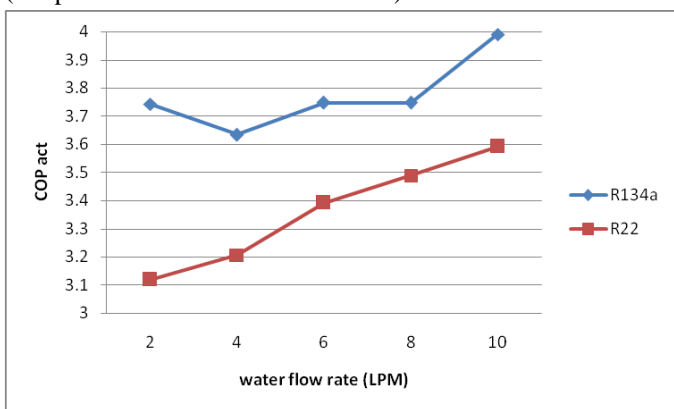(Evaporator water flow rate constant)

Fig.3 COPact vs water flow rate through evaporator
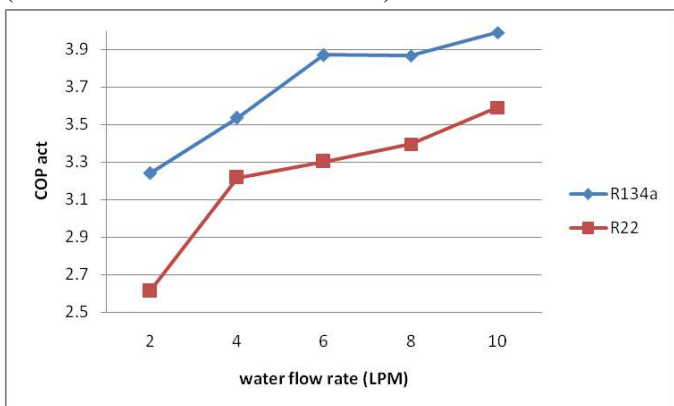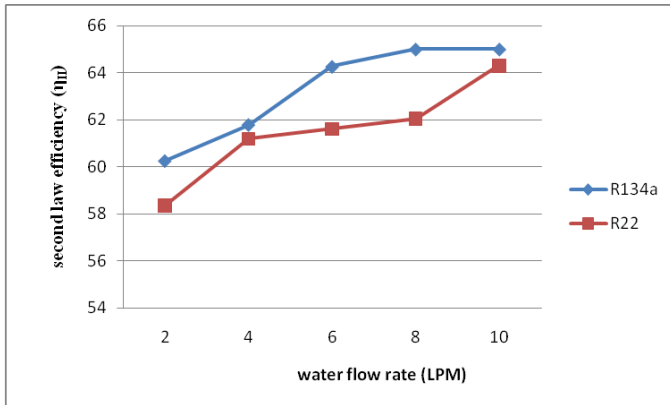(condenser water flow rate constant)

Fig.4 COPact vs water flow rate through evaporator and
condenser

The variation of the actual coefficient of performance with the condenser water flow rate changing from 2 LPM to 10 LPM and evaporator water flow rate is constant at 2 LPM (Fig.2) . As water flow rate is increase the COP of the heat pump system is increase. At 10 LPM condenser water flow rate system performance is maximum. This is due to an increase of the heat exchanger overall heat transfer coefficient that

resulting too high for the evaporation power fixed, determines an increase of the evaporation pressure, a decrease of the compression ratio and of the compression work and so an increase of the COP.

While the effect on COP by keeping the condenser water flow rate constant and by varying evaporator water flow rate (Fig.3). As the water flow rate change from 2 LPM to 10 LPM, COP of system is increase. The performance of heat pump system varies considerably with both vaporizing and condensing temperature. As the condenser water flow rate is increase, the condensing temperature decrease and COP of the system is improved (Fig.4).

The heat pump system involves internal irreversibilities due to the throttling process and also due to the superheat horn. Hence the value of second law efficiency of heat pump system is less then 1. The Second law efficiency is good indication of the deviation of standard vapour compression refrigeration (VCR) cycle from the Carnot cycle [20].
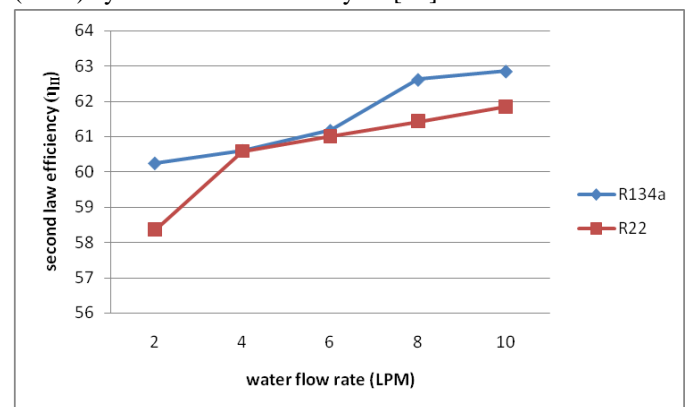
Fig.5 second law efficiency vs water flow rate through condenser (evaporator water flow rate constant)
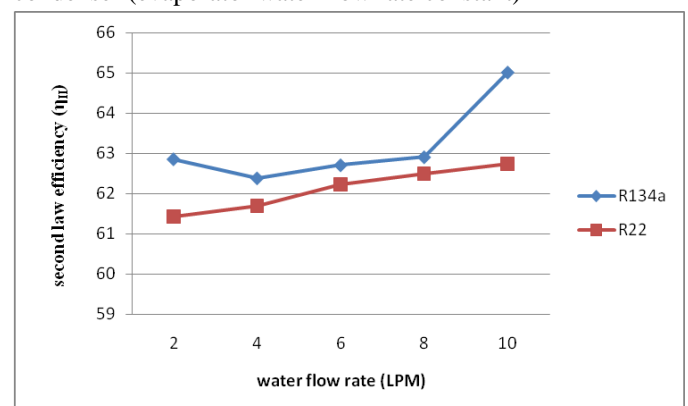
Fig.6 second law efficiency vs water flow rate through evaporator (condensr water flow rate constant)
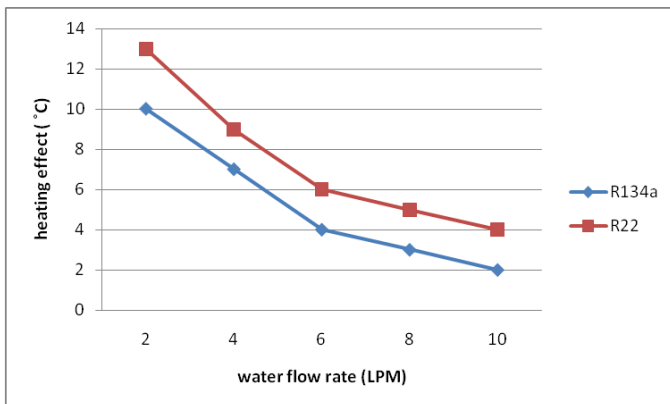
Fig.7 second law efficiency vs water flow rate through evaporator and condenser

At constant evaporator water flow rate constant (Fig.5) and condenser water flow rate varying from 2 to 10 LPM. As the water flow rate increase, the second law efficiency also increased as described in (Fig.6) condenser water flow rate constant and evaporator water flow rate varied from 2 to 10 LPM, at 2 LPM second law efficiency of heat pump system is low but as flow rate increase the second law efficiency start increasing. While by changing both water flow rate of condenser and evaporator from 2 to 10 LPM its effect on second law efficiency is as depicted in Fig.7.

Fig.8 heating effect (˚C) vs water flow rate through condenser (evaporator water flow rate constant)
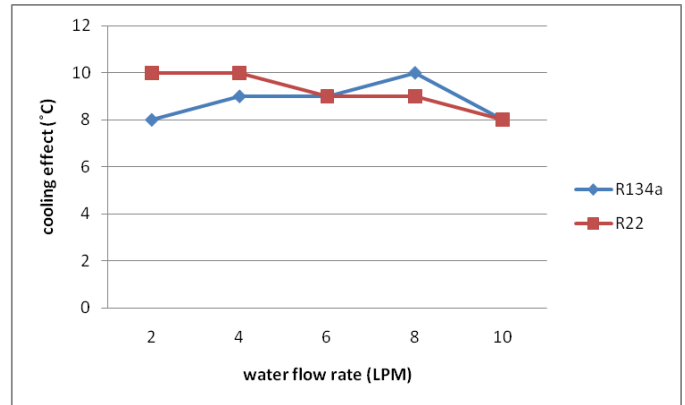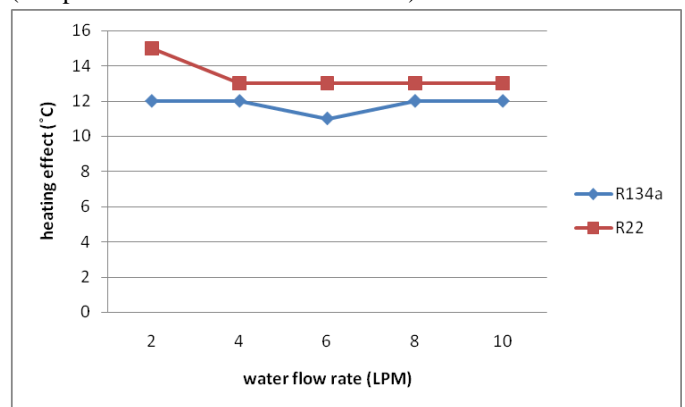
Fig.9 cooling effect (˚C) vs water flow rate through condenser (evaporator water flow rate constant)

Fig. 10 heating effect (˚C)vs water flow rate through evaporator　　(condensr water flow rate constant)

In experimental setup tube to tube heat exchanger is used in evaporator and condenser. Mainly three tube are there in which middle tube is carried the refrigerant and remaining two tube carried water. Heat transferred to the water in condenser and evaporator is, (Fig. 8, 9, 10, 11, 12, 13) When evaporator water flow rate (2 LPM) is keep constant and condenser water flow rate is changed from 2 to 10 LPM or vice-versa and by varying both water flow rate it is observed that at lowest water flow rate maximum heat is transferred to the water as compare to highest water flow rate for both cooling as well as heating effect.
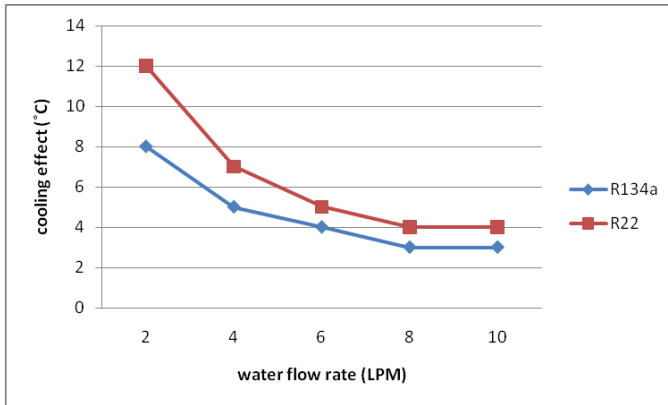
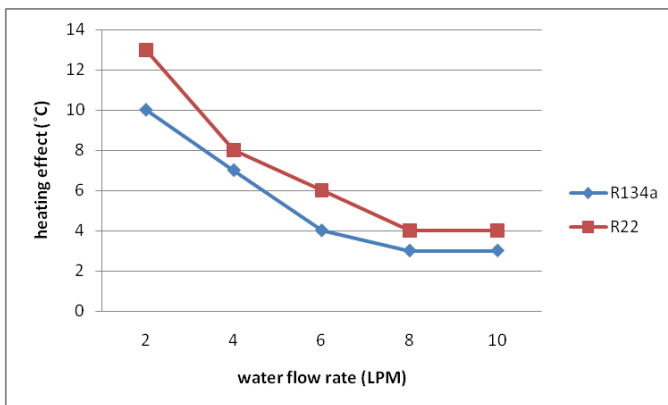Fig.11 cooling effect (˚C) vs water flow rate through evaporator (condenser water flow rate constant)

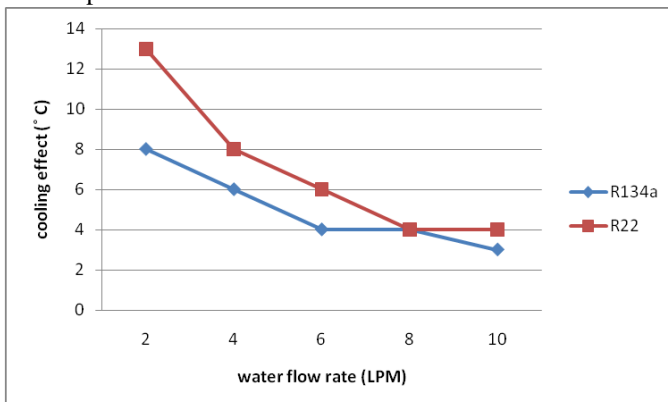Fig.12 heating effect (˚C) vs water flow rate through condenser and evaporator

Fig.13 cooling effect (˚C) vs water flow rate through condenser and evaporator

R22 has a higher discharge temperature than R134a, and lower boiling point then R134a. So R22 has a more refrigerating effect then R134a. At a same time critical temperature of R22 is low as compare to the R134a, while critical pressure of R134a is low as compare to R22 so R134a has a higher COP as compare to the R22 during the test.

5 Conclusions

In this work water cooled tube-tube heat exchanger is used for evaporator and condenser and the influence of the water flow rate through evaporator and condenser on performance of heat pump has been studied by using R22 and R134a. It is observed that R22 has a higher refrigerating effect then R134a due to the higher discharge temperature and lower normal boiling point then R134a and R22 has a lower COP then R134a because of the R22 is high pressure refrigerant and requiring more power to run the compressor.

REFERENCES

[1] S D White, D J Cleland, S D Cotter, R A Stephenson, R D S Kallu, A K Fleming, " A heat pump for simultaneous refrigeration and water heating" IPENZ Transactions,1997; 24:36-43.

[2] Hoon Kang, Youngju Joo, Hyunjoon Chung, Yongchan Kim, Jongmin Choi "Experimental study on the performance of a simultaneous heating and cooling multi-heat pump with the variation of operation mode" international journal of refrigeration, 2009; article in press:1-8.

[3] Youngju Joo, Hoon Kang, Jae Hwan Ahn, Mooyeon Lee, Yongchan Kim, "Performance characteristics of a simultaneous cooling and heating multi-heat pump at partial load conditions" international journal of refrigeration, 2011; 34: 893-901.

[4] J. Sarkar, Souvik Bhattacharyya, M. Ram Gopal, "Optimization of a transcritical CO2 heat pump cycle for simultaneous cooling and heating applications" International Journal of Refrigeration, 2004; 27: 830–838.

[5] A.M. Foster , T. Brown , A.J. Gigiel , A. Alford , J.A. Evans, "Air cycle combined heating and cooling for the food industry" International Journal of Refrigeration, 2011; 34: 1296-1304.

[6] Paul Byrne, Jacques Miriel, Yves Lenat, "Design and simulation of a heat pump for simultaneous heating and cooling using HFC or CO2 as a working fluid" International Journal of Refrigeration, 2009; 32: 1711-1723.

[7] W. Chen, "A comparative study on the performance and environmental characteristics of R410A and R22 residential air conditioners" Applied Thermal Engineering, 2008; 28: 17.

[8] M.Ashok Chakravarthy, M.L.S.Deva Kumar, " Experimental investigation of an alternate refrigeration for R22 in window air conditioning system" international journal of scientific and research publication, 2012; 2: 2250-3153.

[9] Mark W. Spatz, Samuel F. Yana Motta, "An evaluation of options for replacing HCFC-22 in medium temperature

refrigeration systems" International Journal of Refrigeration, 2004; 27: 475–483.

[10] R.Cabello , E.Torrella , J.Navarro-Esbr, "Experimental evaluation of a vapour compression plant performance using R134a, R407C and R22 as working fluids" Applied Thermal Engineering, 2004; 24 : 1905–1917.

[11] Vincenzo La Rocca , Giuseppe Panno, "Experimental performance evaluation of a vapour compression refrigerating plant when replacing R22 with alternative refrigerants" Applied Energy, 2011; 88: 2809–2815.

[12] M. Fatouh , Talaat A. Ibrahim , A. Mostafa, "Performance assessment of a direct expansion air conditioner working with R407C as an R22 alternative" Applied Thermal Engineering, 2010; 30: 127–133.

[13] Jianyong Chen, Jianlin Yu, "Performance of a new refrigeration cycle using refrigerant mixture R32/R134a for residential air-conditioner applications" Energy and Buildings 2008; 40: 2022–2027.

[14] S. Karagoz, M. Yilmaz , O. Comakli, O. Ozyurt, "R134a and various mixtures of R22/R134a as an alternative to R22 in vapour compression heat pumps" Energy Conversion and Management, 2004; 45: 181–196.

[15] Tun-Ping Teng, Huai-En Mo, Hung Lin, Yuan-Hong Tseng, Ren-Hao Liu, Yu-Fan Long, "Retrofit assessment of window air conditioner" Applied Thermal Engineering 2012; 32: 100-107.

[16] Anderson johansson "Replacement of R22 in existing system" International Journal of Refrigeration, 2011; 34: 1296-1304.

[17] B. Hadya, P. Usha Sri and Suresh Akella, "Comparative Study of Eco-friendly Refrigerants in a Lower Capacity Air-Conditioning System" International Conference on Mechanical and Automotive Engineering, 2012: 48-51.

[18] Milind V. Rane , Madhukar S. Tandale, "Water-to-water heat transfer in tube–tube heat exchanger: Experimental and analytical study" Applied Thermal Engineering, 2005; 25: 2715–2729.

[19] Ozone cell,ministry of environment and forests, "Roadmap for phase out of HCFCs in india", Government of india.

[20] A text book on "Refrigeration and air conditioning" by C P Arora.

[21] A text book on "Refrigeration and air conditioning" by R K Rajput.

Design and Analysis of a High Pressure vessel using ASME code

M J Mungla, K N Srinivasan, Prof. V R Iyer

(mitesh.mungla@git.org.in)

Abstract—**This paper contains design and analysis of various components of pressure vessels like shell, heads, flanges, nozzle and support structures along using ASME code.**

Index Terms—**wind loads, seismic loads, membrane stress, peak stress**

I. INTRODUCTION

Process and Chemical engineering involves the application of the science to the industries such as chemical, petrochemical, gas fertilizer, dairy products etc. But, as and when process industries come into the existence, growth and use of pressure vessel becomes extensive and inevitable.

Pressure vessels are mainly used for storing, handling and processing of various chemicals and/or it's compositions in process industries

Regardless of application of the vessel, a number of factors usually must be considered in designing of the unit. The most important factors are selection of materials for various components, manufacturing & transportation aspects, service life etc.

Generally, main components of the pressure vessel are shell, support structure, heads, openings (Nozzles) and joints of openings. For vessels, function and location, the nature of fluid contained, operating temperature and pressure, volume of storage etc are significant parameters, playing important roles for selection of type of shell (vessel).

II. DESIGN CRITERION FOR PRESSURE VESSEL COMPONENTS

Shell and heads:

The chief function of process equipment is to contain a media under desired pressure and temperature. Therefore, the shape (cylindrical or spherical) of vessels is mainly designed by internal pressure consideration. In doing so, it is also subjected to the action of steady (dead or operating weight) and dynamic (wind and seismic) support loads, piping reactions and thermal shocks. It requires an overall knowledge of stresses imposed at these conditions. The final thickness of a process vessel should, therefore, be so chosen that it is not only adequate against the induced stresses caused by internal pressure but also ensures safety against stresses caused by other loads as mentioned above.

Many of the chemical process equipments are required to be operated under such condition, when the inside pressure is lower than the outside pressure. This may be due to inside vacuum or outside higher pressure or combination of both.

Because of external pressure effects, the cylindrical vessel experiences induced circumferential and longitudinal compressive stress. As a result the vessel is apt to fail because of elastic instability caused by the circumferential compressive stress. Uniformly spaced internal or external circumferential stiffening rings can increase the rigidity of the vessels under such condition. This helps to withstand against Elastic instability or buckling load.

Support structure:

Support structures have to be designed on the criteria of combined load considerations. Several loads such as Wind/Seismic loads, External loads on nozzles due to piping joints, Operating weight of vessel etc. are acting on support structures simultaneously. With these combinations of loads, stresses are analyzed in structures.

If we assume that various load combinations are acting on support structures like skirt, base ring etc. Various possibilities of failure for them (support structures) must be considered, which are listed as per followings.

A.   Skirt may fail in following conditions,

   a   Induced tensile stress due to uneven expansion of different materials at skirt to shell junction where temperature gradient along skirt length is very high,

   b   Induced compressive stress due to operating weight of entire vessel along with Wind/Seismic bending moments,

   c   If the length of skirt is considerably long, it may lose it's elastic stability, and buckle under (self-weight)load of the vessel and/or external loads (if in considerable amount) at nozzles.

To design skirt is an iterative method. In which, first assume thickness of skirt, with this thickness analyze stresses corresponding to above load combinations. If stresses, induced

due to above combined loads are not within the allowable limits, increase the thickness and repeat it till satisfy the condition.

While, for safe side of design, thickness of skirt sections are chosen such that, with all above acted loads, induced stresses (both tensile and compressive) must be lesser than corresponding permissible values at given condition for skirt and other related sections.

B. Main function of **basering** is to distribute the vertical, concentrated load over the sufficient area of foundation of the vessel.

Here an assumption, load of entire vessel is equally distributed to width of basering, has been made.

Base ring failure may occur due to,

a   Compression and tensile stresses induced on basering due to bending moments, operating weight of various components of vessel, external loads due to nozzle etc.,

b   Overturning of vessel due to bending moments induced by Wind/Seismic and/or cumulative external forces/moments at piping junction, overturning may occur due to weaker reinforcement of bolt to foundation of vessel,

c   Weaker foundation of the vessel, it is because whatever loads (compressive or tensile) acting on basering are assumed to transferred at the foundation of the vessel.

Design of base ring is again an iterative method. In which, maximum induced tensile and compressive stresses of base ring and foundation material are calculated by considering all above acted loads. With these induced stresses, thickness required for basering section at compression and tensile side has to be calculated. Total thickness of basering is summation of both above thicknesses. By providing gussets and compression ring, the thickness required for base ring can be reduced.

The maximum load on the compression ring and gussets occurs due to wind/seismic bending moment on vertical side of vessel where reaction of the bolts produces compression load.

Flange
Criterion, adopted for flange design and stress analysis, is carried out according to ASME code, in which following assumptions have been adopted.
1.   For hub and shell sections of the flange, local pressure acting on their surfaces is neglected.
2.   The effect of the external moment applied to the flange, equal to the product of the bolt load and the lever arm, is independent of the location of the bolt-loading circle and of the forces balancing the bolt load.
3.   Creep and plastic yield do not occur.

For understanding of design and stress analysis of flange, integral weld neck flange has been taken in to consideration. In which, flange is divided into three sections. All three sections are separate entities and analyzed individually. Various loads & moments, act on each section are discussed as follows,
1.   **Annular ring section**: For the analysis of this section loads, acting on it, are
   (a).   Overturning moment, acting on the ring, due to non-concentricity of bolt load and gasket reaction load is replaced by two equal and opposite forces (W_{eq}) at the inner and outer circumference of the ring such that overall moment is unchanged.
   (b)   Internal hydrostatic pressure acting radially on the base of the flange.

2.   **Tapered hub section**: In the analysis of the hub section, the assumption is made that the stresses and deformations are the same as those for a beam with a varying section. In this case a longitudinal strip of unit represents the beam. Loads acting on this section, shear force (P_1) and bending moment (M_{h1}) at the hub/ring interface due to imposed loads on the ring and internal hydrostatic pressure acting radially on entire inside periphery of hub.
3.   **Shell ring section**: This portion is designed with same assumption, made for hub, as beam with the same loading condition, for stress analysis, except discontinuity shear force (P_0) and bending moment (M_{h0}) are at shell/hub interface. In the design, length of shell must be sufficiently long such that the effect of edge loads P_0 and M_{h0} are not felt at the other extremity of the shell.

Exploration of three sections will give longitudinal, tangential and radial stresses at corresponding design & gasket seating condition. Once various stresses are calculated, Check whether these induced stresses are with in given permissible stresses, as per ASME section VIII div 2, Mandatory Appendix 3, if not change design variables, within its constraints, and repeat it till satisfy the given condition.

Nozzle
Design of nozzle has to be done based on "area compensation" criterion. In this criterion, nozzle is designed such that area available for reinforcement with in 'certain' limits at the junction must be compensated to area removed from shell/head to make that opening. For taking care of external loads on nozzle at the piping joints, extra area must be given as cushion. These external loads on nozzles can be analyzed with FEA or WRC (Welding Research Council) Bulletin–107/297. Also, Stresses are more at this junction due to stress concentration, which has to analyze in FEA.
In the design of nozzle, according to ASME, strength of nozzle material must not be given additional importance compared to corresponding counter-joint (with whom nozzle is joined, shell or head) material strength. Because as per ASME, a ratio of S_n/S_s (allowable intensity of nozzle material to stress intensity of counter-joint material) must not be greater than 1.0. A

factor, which is ratio of S_n/S_s, is used as multiplier for area calculations of nozzle. So additional strength to nozzle material is not productive for area calculations.

III. SPECIFICATION OF PV COMPONENT DESIGN

For the design of various components of pressure vessel, one must have specific required data like code of design, material data of various components, external Forces and Moments on nozzles due to piping joints, constrained values of design data for various components, design and operating conditions etc. The specification contains all these required fundamental data & dimensions for all components. These data contain code-related information, material specification, design data, external loading on various nozzle etc. For easy to understand design principles of various components, all components are designed here with same design and operating condition.

The design principles can be best understood with an illustration. For this purpose, data for a typical pressure vessel is reproduced here.

REQUIRED DATA		VALUE	UNIT
Design Pressure	Internal	1260(8.69)	PSI(N/mm^2)
	External	15(0.10)	PSI(N/mm^2)
Design Temperatures	Internal	830(443.33)	° F(° C)
	Atmospheric	30(-1.11)	° F(° C)
Corrosion Allowance Shell		0.375(9.525)	Inch(mm)
Heads		0.375(9.525)	Inch(mm)
Skirt		0.125(3.175)	Inch(mm)
Basering		0.125(3.175)	Inch(mm)
Gussets		0.125(3.175)	Inch(mm)
Compression ring		0.125(3.175)	Inch(mm)
Operating condition	Pressure	1130(7.79)	PSI(N/mm^2)
	Temperature	760(404.44)	° F(° C)
Shell I D Shell height		162.59(4130) 602(15291)	Inch(mm) Inch(mm)
Overlay Thickness		0.3(7.62)	Inch(mm)
Head Inside Radius (Bottom and top)		81.89(2080)	Inch(mm)
Insulation thickness for Reactor		4.0000(101.6)	Inch(mm)
Inside	C. S. Skirt	169.84(4314)	Inch(mm)
diameter	A.S. Skirt	169.84(4314)	Inch(mm)
Height	C. S. Skirt	48(1219.2)	Inch(mm)
	A.S. Skirt	240(6096)	Inch(mm)
Basering inside diameter		162.00(4115)	Inch(mm)
Basering, Gusset & Comp. Ring corrosion allowance.		0.125(3.175)	Inch(mm)

Component	Material specification
Shell	SA387 Gr22 CL2
Dished End	SA387 Gr22 CL2
Nozzle	SA182 F22
Flange	SA182 F22
Skirt(LAS)	SA387 Gr22 CL2
Skirt(CS) at 450˚F	SA516 Gr70
Basering	SA516 Gr60
Compression Ring	SA 516 Gr60
Gussets	SA 516 Gr60
Bolt Material	Basering	SA 193 B16
	Flange	SA 193 B7

NOZZLE LOAD AT FLANGE FACE		
FORCES/MOMENTS	TOP HEAD	BOTTOM HEAD
$F_{XF,}$ lbf (N)	10000(44482.22)	10000(44482.22)
$F_{YF,}$ lbf (N)	12000(53378.66)	12000(53378.66)
$F_{ZF,}$ lbf (N)	10000(44482.22)	10000(44482.22)
$M_{XF,}$ lbf-ft (N.mm)	2.50E+04(33895436.4)	2.50E+04(33895436.4)
$M_{YF,}$ lbf-ft (N.mm)	2.50E+04(33895436.4)	2.50E+04(33895436.4)
$M_{ZF,}$ lbf-ft (N.mm)	2.50E+04(33895436.4)	2.50E+04(33895436.4)

IV. Maths and Calculation

A. Using Wind loads

In the Wind design consideration, calculation of Shear Forces and Bending Moments at different elevations can be calculated as per following steps as according to UBC-1997 Code system.

1. First of all, one has to find out pressure induced due to wind velocity and exposure of nearby site of vessel installation. Moreover, Pressure induced due to wind varies with height so pressure differs at various sections (skirt, shell, dished end etc.) of vessel.

2. Once, wind pressure is calculated, area of exposure of each section on which this wind induced pressure acts, needs to determine. For wind effective area for each section, insulation corresponding to that section should also be added with shape factor multiplication as a conservative consideration of additional area for wind.

3. Multiplication of wind induced pressure and corresponding wind effective area of each section will yield Shear Force for that section, subsequently cumulative Shear Force and Bending Moment for that section can be calculated.

Herein, as per above steps, one section (C. S. Skirt) has been explored and its Shear Force and Bending Moment have been calculated for easier understanding of above steps. While other sections can be explored and subsequent required calculations can be determined by same methodology.

As per required data for wind calculation as per given specification,

Code   : **UBC-1997**
Basic wind speed   : 70 miles per hour (31.293 m/s)
Importance factor I_w : 1.15
Exposure for wind   : D

Using combined load as Internal Pressure + Operating Weight + Wind Load:

Induced stress for combined loads,

$$S_{css} = \frac{pD_{css}}{4t_{css}} \pm \frac{4M_{wind}}{\Pi D_{mcss}^{2} t_{css}} - \frac{(W_{ope})_{css}}{\Pi D_{mcss} t_{css}}$$

Table no 1 displays stresses induced at different locations of vessel.

B Using Seismic loads

In this Seismic Design consideration, calculation of Shear Forces and Bending Moments at different elevations can be calculated as per following steps as according to UBC-1997 Code system.

1 Seismic consideration is purely related to intensity of vibration. Vibrational intensity is directly proportional to time interval (no. of cycles per second). At first, time period of vibration due to possible earthquake intensity or according to seismic zone as per given specification, has to be calculated. Design Base Shear is inversely proportional to time period, subsequently it can be calculated. Time period varies with height and weight of section. So time period at primarily and design base shear secondarily are different for various sections (skirt, shell, dished end etc.) of vessel.

2 There are Maximum and Minimum limits for Design base shear, which have been proposed in UBC-1997. These both limits are universal for all sections. Once these limits are calculated, check whether induced values of design base shear, calculated by step 1., of various sections are within proposed limits.

3 Shear Force of section depends upon above calculated Design base shear, weight and height of that section. Simple empirical formulae will yield the calculation of Shear Force. Subsequently, Cumulative Shear Force and Bending Moment for that section can be obtained as same way as corresponding wind calculations.

Herein, as per all above steps, one example of a section (C. S. Skirt) will make simple and easier understanding of above steps. Other sections can be explored and subsequent calculations can be carried out by same methodology whose values are tabulated in table 4.7.

As per required data for wind calculation given in specification:

Code   : **UBC-1997**

Importance factors   : I = 1.25   & I_P= 1.50

Near source factors   : N_v = 1.2 & N_a = 1.0

Seismic zone factor   : 4.0

Exposure for seismic   : D

Using combined load as Internal Pressure + Operating Weight + Seismic Load:

Induced stress for combined loads,

$$S_{css} = \frac{pD_{css}}{4t_{css}} \pm \frac{4M_{seismic}}{\Pi D_{mcss}^{2} t_{css}} - \frac{(W_{ope})_{css}}{\Pi D_{mcss} t_{css}}$$

Table no 2 displays stresses induced at different locations of vessel.

Table No 1.										
INTERNAL DESIGN + OPERATING WEIGHT + WIND LOAD										
INT. DESIGN PRESSURE=		**1260**	**PSI**							
Section	**Dia.of each section. Inch**	**Operating Weight per section lb**	**Wind Bending Moment lb-ft**	**Thickness Inch**	**Induced Tensile Stress PSI**	**Induced Compressive Stress PSI**	**Allow. Tensile Stress PSI**	**Tensile Stress Ratio**	**Allow. Compressive Stress PSI**	**Comp. Stress Ratio**
SKIRT (C.S.)	169.84	88000	2770468	1.496	**854.58079**	**-1073.147**	12936	**0.07**	-11177.09	**0.10**
SKIRT (A.S.)	169.84	13450	1728135	1.2598	**696.06455**	**-735.7884**	18547	**0.04**	-9212.09	**0.08**
BT HEAD	164.53	65000	1533157	2.4016	**21878.593**	**21178.541**	26496	**0.83**	-10751.5	**1.97**
SHELL	163.35	873660	1466667	4.825	**10485.796**	**10157.374**	26496	**0.40**	-12015.84	**0.85**
TOP HEAD	164.53	33570	198610.1	2.4016	**21598.865**	**21508.178**	26496	**0.82**	-10751.5	**2.00**
	W$_{total}$ =	**1073680**	**lb**							

|										
Table No 2.										
INTERNAL DESIGN + OPERATING WEIGHT + SEISMIC LOAD										
INT. DESIGN PRESSURE=		**1260**	**PSI**							
Section	**Dia.of each section. Inch**	**Operating Weight of section lb**	**Seismic Bending Moment lb-ft**	**Thickness Inch**	**Induced Tensile Stress PSI**	**Induced Compressive Stress PSI**	**Allow. Tensile Stress PSI**	**Tensile Stress Ratio**	**Allow. Compressive Stress PSI**	**Comp. Stress Ratio**
SKIRT (C.S.)	169.84	88000	1.94E+07	1.496	**6643.1**	**-6861.6**	14337.4	**0.46**	-12387.94	**0.55**
SKIRT (A.S.)	169.84	13450	1.16E+07	1.2598	**4801.0**	**-4840.8**	20556.48	**0.23**	-10210.07	**0.47**
BT HEAD	164.53	65000	1.01E+07	2.4016	**22130.9**	**19222.6**	26496	**0.84**	-10751.5	**-1.79**
SHELL	163.35	873660	1.00E+07	4.825	**10773.8**	**9198.2**	26496	**0.41**	-12015.84	**-0.77**
TOP HEAD	164.53	33570	250112.5	2.4016	**21581.1**	**21496.4**	26496	**0.81**	-10751.5	**-2.00**
	W$_{total}$	**1073680**	**lb.**							

C. Nozzle calculation

As per the brief introduction to the criterion for design of self-reinforced nozzle by ASME code, which is designed here, where area available for reinforcement has to be greater than area required. For the dimensions of area due to hub section, hub height and length (of hub) unto beveled transition have to be initially assumed. With this dimensions of hub, area required and area available for reinforcement have to be calculated. If area available is not more than area required, change either hub height or hub length, with in its 'certain' limits specified in ASME, and proceed till area available with given cushion, for external loads on nozzle, predominates to area required.

AREA	Symbol	Magnitude Inch^2 (mm^2)
Area required for reinforcement	A_{req}	**35.06 (22620)**
Area available in shell	A_{shell}	0.3 (194)
Area available in nozzle	A_{nozzle}	0.0 (0)
Area available in weld	A_{weld}	0.5625 (363)
Area available in hub straight section	A_{hub}	40.66 (26235)
Area available in bevel transition	A_{trans}	0.00 (0)
Total Area available	A_{total}	**41.53 (26793)**

D. Flange Calculation

Design and stress analysis general procedure is already explained earlier in this paper. Following equations are used to calculate stresses induced in flange.

Longitudinal hub stress,
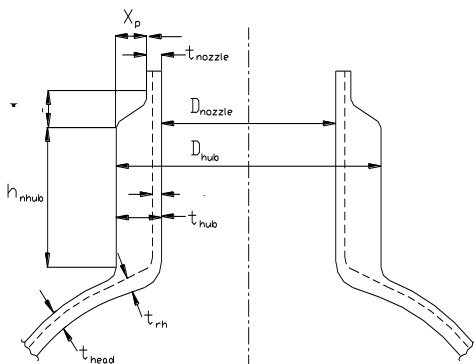
For operating,

$$S_{HO} = \quad = \frac{fM_o}{L_{factor}G_l^2 B}$$

Radial flange stress,

For operating,

$$S_{RO} = \frac{(1.33t_{flange}e + 1)M_o}{L_{factor}t^2 B}$$

Tangential flange stress,

For operating,

$$S_{TO} = \frac{yM_o}{t_{flange}^2 B} - ZS_{RO}$$

Type of stress	Stress in PSI (N/mm^2)			
	Operating condition		Seating condition	
	Actual	Allowable	Actual	Allowable
Longitudinal hub stress	13900 (95.84)	33120 (228.36)	14842.11 (102.34)	37500 (258.56)
Radial flange stress	14767.18 (101.82)	22080 (152.24)	15768.76 (108.73)	25000 (172.38)
Tangential flange stress	9963.87 (64.59)	22080 (152.24)	21423.15 (147.72)	25000 (172.38)
Maximum average stress	14333.06 (98.83)	22080 (152.24)	18132.63 (125.03)	25000 (172.38)
Bolt stress	17640.65 (121.64)	21400 (152.24)	5870 (40.47)	22000 (172.38)

V CONCLUSION

Pressure vessel components like shell, head, flange and nozzle are designed as per ASME Section VIII Div-2, Edition 2001. Shell, head and skirt support dimensions are derived based on various design conditions, viz., internal pressure, external pressure along with wind / seismic effects. With the

dimensions arrived at, the stresses have been verified to be within allowable limits. Stress analysis of flange has been carried out as per appendix 3 of ASME Section VIII Div.2, it has been determined that induced stresses (longitudinal, tangential and radial) are within the corresponding given allowable limits.

Design of basering and skirt sections has not been covered under ASME code and their dimensions are calculated with general design principles. Stress analysis of these components has been carried out with combined load cases, it has been found that stresses, produced due to combined loads, are within its allowable limits.

REFERENCES

1. ASME Boiler and Pressure Vessel Code – Section II Part-D, Edition-2001.
2. ASME Boiler and Pressure Vessel Code – Section VIII Division 2, Edition-2001.
3. ASME B-16.5, Edition-1996.
4. ASME B-16.47, Edition-1996.
5. ASME B-16.20, Edition-1993.
6. ASME B-16.1, Edition-1989.
7. American Institute for Steel Construction.
8. Uniform Building Code, Edition-1997.
9. Process Equipment Design By   L. E. Brownell & E. H. Young
10. Pressure vessel design handbook By   Henry H. Bednar

Studies on effect of process parameters on tensile properties and failure behavior of friction stir welding of Al alloy

B.R.Rana[$],L.V.Kamble*,S.N.Soman[#]V.V.Mathane[#]

[$]*Metallurgical and materials Engineering Department, Indus University, Rancharda, via Thaltej, Ahemedabad-382 115*

[#]*Metallurgical and Materials Engineering Department, The M. S. University of Baroda,Vadodara 390 001 Address*,

[$] bhaveshrana.mt@iite.edu.in
[#] somansn@yahoo.com
[#]mathne2v@gmail.com

[*]*L.V.Kamble*

Mechanical Engineering Department,The M. S. University of Baroda,Vadodara 390 001
[*]lvkamble@yahoo.co.in

Abstract: **The friction stir welding is recently developed solid state welding process which overcome the problem associated with fusion welding technology. The properties achieved by friction stir welding is better than that achieve by fusion welding technique. The aim of present study is to determine the effect of process parameters on tensile properties and failure mechanisms of friction stir welding of Al alloy. AA 6101 T6 alloy was selected as base material and friction stir welding was carried out with hexagonal pin with concave shoulder. The thickness of the pin was 6mm having length of 5.7mm with 20mm shoulder diameter. The friction stir welding was carried out at three different rotating speed i.e 545, 765, 1070 rpm and tool traverse speed i.e 50, 78,and 120 mm/min. The characterization was carried out in view to understanding of microstructure, tensile properties and the failure behavior of weldments. The result indicated the better contrast in each zone developed after friction stir welding. The weld samples which was prepared at 765 rpm tool rotation speed and 120 mm/min welding speed posses the pure ductile failure of weldment and fracture occurred at the base metal region at advancing side of weld.**

Keywords: **FSW,** Microstructure analysis,Tensile test ,Fractrography.

I.INTRODUCTION

The development of new materials and their practical application constitute a great challenge for manufacturing sector in many branches of industry. Numerous efforts concentrate on considerable reduction of manufacturing costs of various components and their assemblies. For this reason the noble concept are under continuous development.

invented in 1991 by The welding Institute, friction stir welding is novel solid state joining process that is gaining the popularity in the manufacturing sector [1,2]. FSW utilizes a rotating tool design to induce plastic flow in the base metals and to essentially "stir" them together. During the Friction stir welding ,the tool pin attached with shoulder ,is inserted between the abutting edges of plates to be joined. As the tool traversed along the joint line, the rotation of shoulder under the influence of an applied, fixed load heats the metal surrounding the joint and with the rotating action of the pin induces the metal from each work piece to flow together and form weld. The schematic figure representing the principle of friction stir welding is shown in the following fig 1.
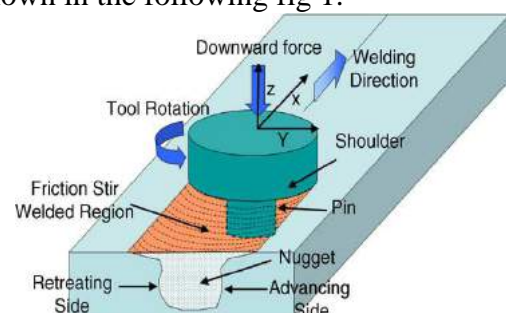

Figure 1 Schematic illustration of principle of friction stir welding[10]

The microstructure resulting from the influence of plastic deformation and elevated

temperature is generally a complex array of fine, recrystalized grains. The friction stir welding gives the best joining efficiency and mechanical properties with less negligible defect or defect free weld. Over the last fifteen years, numerous investigation have sought to characterize the principles of FSW and to model the microstructural development. The majority of these investigations pertains to heat treatable aluminum (2xxx,6xxx and 7xxx series) [3-6] and were simulated by the complex evolution of microstructure and thus properties in these alloys during FSW process. The current status of FSW research has been well summarized by Mishra and Ma [7]. Since no melting occurs during FSW, the process is performed at much lower temperatures than conventional welding techniques and circumvents many of the environmental and safety issues associated with these methods.

FSW is considered to be the most significant development in metal joining in a decade and is a 'green technology' due to its energy efficiency, environment friendliness, and versatility.

Aluminum & Aluminum alloy are difficult to weld, requiring weld pool shielding gas & specialized heat sources, require the oxide layer to be stripped prior to or during the welding process. In addition, aluminum and its alloy are subject to voids & solidification cracking defects when they cool from a liquid state. Consequently, in order to manufacture large panels of aluminum & aluminum alloys extrusion has become choice of manufacturing. However, even extrusion has size limitations.

As compared to the conventional welding methods, FSW consumes considerably less energy. No cover gas or flux is used, thereby making the process environmentally friendly. The joining does not involve any use of filler metal and therefore any aluminum alloy can be joined without concern for the compatibility of composition, which is an issue in fusion welding. When desirable, dissimilar aluminum alloys and composites can also be joined with equal ease.

In contrast to the traditional friction welding, which is usually performed on small asymmetric parts that can be rotated and pushed against each other to form a joint, friction stir welding can be applied to various types of joints like butt joints, lap joints, T butt joints, and fillet joints. that the microstructure and resulting properties produced during FSW of aluminum alloys are dependent on several factors. The contributing factors include alloy composition, alloy temper, welding parameters, thickness of the welded plates as well as the shape and geometry of applied tools. These changes are exceptionally evident in age-hardenable alloys where severe plastic deformation accompanied by mixing of material as well as heating and cooling cycles alters the microstructure (and thus properties) in a significant manner.

The quality of friction stir welding depending on the geometry of tool pin & shoulder of tool the process parameters also affect the quality of weld i.e. tool rotation speed, traverse speed, tool tilt angle, D/d ratio where D indicates diameter of shoulder & d indicates diameter of tool pin, etc.

The aim of this present study is to determine the effect of tool design and process parameters on failure behavior of Friction stir welding of Al alloy. For the present study AA6101 T6 age hardenable alloy was selected as basemetal. The friction stir welding was carried out with two different tool geometry. i.e hexagonal pin with concave shoulder and square pin with flat shoulder. The tool pin having 6 mm thickness and 5.7 mm pin length with 20 mm shoulder diameter. The friction stir welding was carried out at three different tool rotation speed i.e 545, 765, 1070 rpm and welding speed i.e 50, 78, 120 mm/min. The characterization was carried out to understand the various zones created after the welding through microstructure analysis. The tensile test was carried out to study the effect of tool geometry on tensile

strength and the fracture behavior of the weld samples.

II. EXPERIMENTAL PROCEDURE

In this present research work the attempt was made to study the effect of process parameters on quality of friction stir welding of Al alloy. For this purpose the extrusion product of AA6101 T6 was utilized for the joining by friction stir welding. The T6 is the temper designation of the alloy indicating that the alloy was solution heat treated and artificially aged. The thickness of the plate utilized for FSW was 6mm. The FSW of AA 6101 T6 was carried out at metallurgical and materials Engineering Department of the Maharaja sayajirao university of Baroda, vadodara. The vertical milling machine was used for friction stir welding with tool tilt angle of 2 degree and 8 -10 KN load applied downward during tool traverse. The tool was made up of EN24 steel. The chemical composition of the AA 6101 T6 is indicated in the following table [1]

Table 1 The chemical composition of AA 6101 T6 alloy

Elements	%
Al	Balance
Mg	0.6
Si	0.5
Zn	0.021
Cu	0.074
Cr	0.015
Zr	-

The chemical composition of the AA 6101 T6 was confirmed by the EDS (Energy Dispersive Spectroscopy).

The two plates of AA 6101 T6 having dimensions of 100mm x 100mm x 6mm were butt welded by friction stir welding. The following fig 2 indicates the dimension of the weld sample.
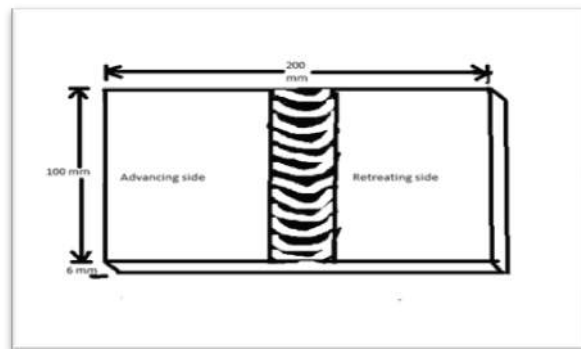

Figure 2 dimension of weld sample

For the present research work the following process parameters were selected . The friction stir welding was carried out with hexagonal pin with concave shoulder. The diameter of the shoulder and pin length was 20mm and 5.7mm respectively. The samples were welded with three different tool rotation speed and tool traverse speed. i.e 545, 765,1070 rpm and 50,78 and 120 mm/min.

After welding the microstructure analysis was carried out with help of Neophot 2 and SEM (scanning Electron Microscope) at 250X magnification. The etchant use for the development of microstructure was 4M keller. It was prepared by mixing of Hydrofluoric acid 6ml (HF), Hydrochloric acid 12ml(HCl), Nitric acid 22ml (HNO_3) and 60 ml distilled water. The immersion time for the eatching was 1 to 3min[8]

The tensile test was carried out as per ASTM E8 standard. The following fig. 3 indicating the dimension of the tensile specimen as per ASTM E8 standard[9]
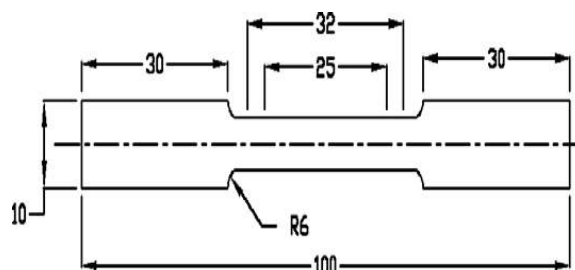

Figure3 dimension of tensile test specimen as per the ASTM E8 standard

The fractrography of failed tensile sample was carried out at metallurgical and Materials Engineering department, The M.S.University of Baroda. The fractrography was conducted with help of Scanning Electron Microscope at different magnifications i.e 50x,100x 250x 500x and 1000x

III. RESULT AND DISCUSSION

The typical microstructure of as received conditions (base material) is shown in fig.4 The microstructure comprises of the coarse grains of aluminum with the hardening precipitates of Mg_2Si. From the microstructure analysis, there were different zones observed in the weld samples.
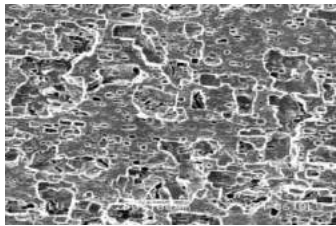

Figure 4 Microstructure of AA 6101 T6 alloy

The different zone observed are weld centre, Nugget zone, thermo mechanically affected zone, heat affected zone, and unaffected or base metal region as shown in following fig ( ).
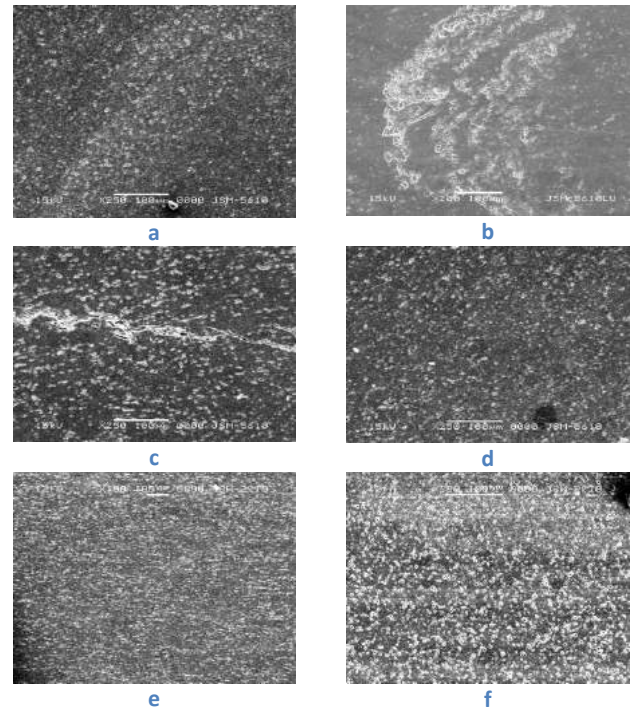

Figure 5 SEM micrographs of fsw sample at 250x magnification a.weld centre, bNuggaet c.TMAZ at RS, d.TMAZ at AS, e. HAZ at AS, f. HAZ at RS

The formation of nugget region in the centre of the weld region is still unknown why it forms? But the lots of research work is going on to find out the origin of nugget region. The weld centre consist of extremely fine recrystalized grains of Al with the breaking of the coherent precipitates of Mg_2Si.The size of the precipitates are extremely finer compare to the other zone of the weld. The distribution of the precipitates is uniform throughout the weld centre region. There was sever plastic deformation was observed and the precipitates get destroyed and also some reprecipitation observed. There was also formation of some oxide layer form at either at the advancing side or at the retreating side of the weld sample forming some uneven boundary between the weld centre and the TMAZ and thus make some differentiation between them.

In the TMAZ, the microstructure consists of extremely fine grains of the Al with fine size of the precipitates of Mg_2Si. There are presences of more precipitates free zones compare to weld

centre. At boundary near the TMAZ and weld centre, there is formation of an oxide layer. The formation of this oxide layer is also became the interesting part of the research why it was form? But from findings, it may be generated during the rotation of tool, metal gets oxidized.

The nugget region was observed near the bottom root portion of the weld centre region. The nugget region comprising of banded structure. It is also called as onion ring structure. The bands are distributed in such a way that there was formation of alternate bands of light and dark bands with different coherency and density difference of precipitates.

The HAZ forms on the both the side of the weld.i.e.advancing and retreating side of weld. The reason behind formation of the heat affected zone is temperature difference across the weld. Because before the welding, the alloy plate was at room temperature. When the welding done by the rotation of tool there was substantial increase in temperature due to the friction generated between the tool and work piece and due to the plastic deformation of work piece. So, the grain growth was observed in the HAZ. The microstructure comprising of the coarse grains of aluminum with ripen precipitates of the Mg_2Si

From the tensile test result it was observed that the weld sample prepared at 765 rpm tool rotation speed and 120 mm/min welding speed with hexagonal pin profile that posses the highest ultimate tensile strength of value 144 Mpa with elongation of 21.88%. and fracture occurred at the base metal region. In case of weld prepared by square pin profile with 765, and 1070 rpm at 78 mm/min welding speed posses the ultimate tensile strength of value 125 and 128 and elongation of 25.56% and 20.84% respectively. The fracture occurred at the base metal region at the advancing side of weld.

The failure analysis of the failed tensile test specimen was carried out which posses the highest tensile strength and lowest tensile strength.

From the tensile test result it was confirm that the weld which was prepared at 765 rpm and 120 mm/min welding speed with hexagonal tool pin profile posses the maximum tensile strength of 144 mpa and elongation of 21.88%. The failure analysis indicated the pure ductile failure of the weld sample. The fracture surface comprised of the pure dimple structure in the elongated form as shown in fig (6)

Figure 6 Fractrodraph of weld sample prepared at 765 rpm tool rotation speed and 120 mm/min welding speed a. 50x b.100x c,250x, d. 500x, e. 1000x magnification

The weld which was prepared at 1070 rpm tool rotation speed and 120 mm/min welding speed that posses the tensile strength value of 123 mpa with 13.6 % elongation the fracture surface reveals the mixed mode failure of ductile and brittle behavior as shown in fig (7), there is presence of elongated and equiaxed dimple in the fracture surface. There were also the micro cracks and voids presence which reveals the no time for proper agglomeration of weld metal.
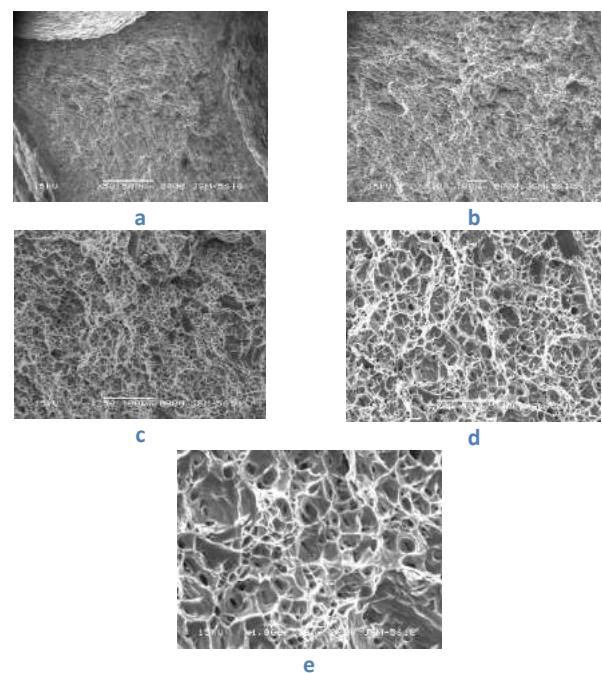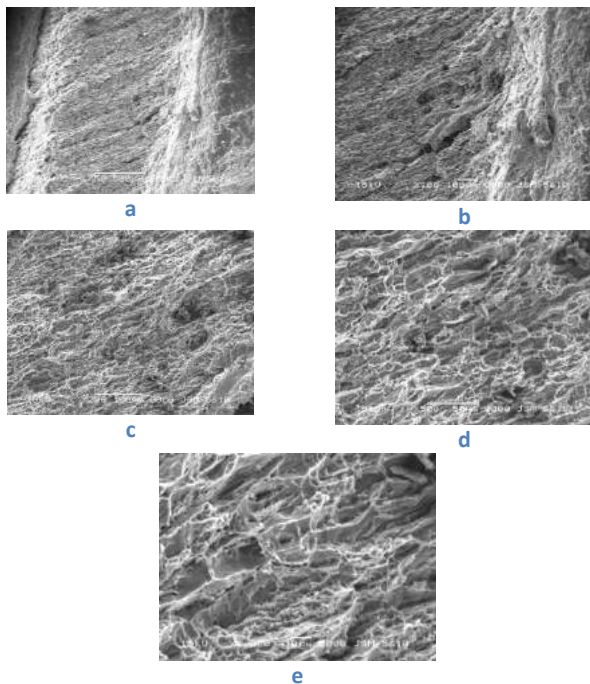
Figure 7 Fractrodraph of weld sample prepared at 1070 rpm tool rotation speed and 120 mm/min welding speed a. 50x b.100x c,250x, d. 500x, e. 1000x magnification
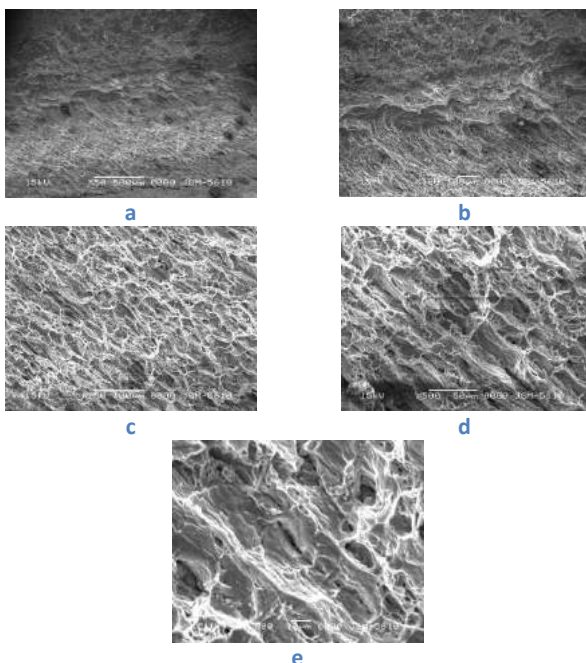

Figure 8 Fractrodraph of weld sample prepared at 1070 rpm tool rotation speed and 78 mm/min welding speed a. 50x b.100x c,250x, d. 500x, e. 1000x magnification

When the welding was carried out at 1070 rpm and 78 mm/min welding speed, the tensile strength obtained was 108 mpa with 11.32% elongation. The fracture surface indicated the mixed mode fracture of ductile and brittle behavior. The fracture surface comprised of some cleavage and step structure there was also presence of wide long micro cracks as show in fig (8)

IV. CONCLUSION

1) With increase in the tool rotation speed, in the weld centre region, the plastic deformation of the material increases, which lead to the deformation of the grain structure.

2) The microstructure of weld comprise of the different zones namely, weld centre,TMAZ,HAZ on both side of the weld centre,i.e Advancing side and Retreating side.the each zone is having its own characteristics in terms of the grain structure and distribution of Mg_2Si precipitates. There was good transition observed from one zone to other.

3) From the tensile test result it was confirm that the weld which was prepared at 765 rpm and 120 mm/min welding speed with hexagonal tool pin profile posses the maximum tensile strength of 144 mpa and elongation of 21.88% the fracture surface indicated the pure ductile failure having elongated dimples in the fracture surface

4) From the experimental work it was confirm that with increase in tool rotation speed the tensile strength is decreases and fracture behavior showing mixed mode failure of ductile and brittle behavior

REFERANCES

[1]W.M.Thomas,E.D.Nicholas,J.C.Needham,M.G.Murch,P.Templesmith, C.J.Dawes,G.B.Patent application no 9125978.8(December 1991)

[2] C.Daws, W.Thomas, TWIBulletin 6,124,November/December 1995

[3] R. Braun,L.Litynska-dobrzynska,materials science fourm 362-402, 1531, (2002)

[4]L.Litynska,R.Braun,G.satniek,C.dalle,Donne,J.Dutkiewicz,mat.Chem.P hys.81,293(2003)

[5]I.shigematsu,K.Suzuki,T.Imai,Y,Jkwon,N.saito,J.Mat.Sci.40,2971(2005)

[6] M.Dumont,A.Steuwer,A.Deschamps,M Peel,J.Withers,Acta Met.54,4793 (2006)

[7] R.S.Mishra, Z.Y.Ma,Mat.Sci.Eng.R.50,I(2005)

[8] ASM handbook for Metallography and microstructure,vol 9, page no 1720.

[9] 1983,Annual Book of ASTM standards, section 3,vol 3.01 metals – mechanical testing ,elevated and low temperature tests, ASTM E8

[10]http://www.twi.co.uk/j32k/unprotected/band_1/fswintro.Html

Review on The Energy Savings And Economic Viability Of Heat Pump Water Heaters In The Residential Sectors – A Comparison With Solar Water Heating Systems

Vinod P. Rajput, Ankit K. Patel, Nimesh Gajjar

(rajputvinodp@gmail.com.patel.ankit27789@gmail.com)

Abstract— **The paper presents the comparison of heat pump water heater with solar water heater. This comparison also compares the energy consumption, installation cost, and payback period of both the units for residential sector. This research paper also justifies the economic viability of heat pump water heaters to residential sectors.**

Index Terms—**heat pump water heaters, solar water heater, residential sector, viability.**

I. Introduction

Due to recent and on-going power supply problems experienced This will result in the different markets sectors required to reduce energy consumption by a predetermined percentage, for instance 10% for the residential sector and 20% for the hospitality industry. This will be done in the hope of improving the stability of the electricity supply. While this is being put forward as a short term solution of a couple of months, it is evident that long term solutions should be implemented to ensure a reliable electricity supply for the next few years.

The main challenge confronting us is how to reduce the energy consumption with a sustainable demand side management effort. The only way to achieve a sustainable energy consumption reduction will involve the implementation of energy efficient programs in all sectors.

In the field of sanitary water heating ESKOM identified solar water heaters as the energy efficient technology it wants to support and thus implemented a subsidy scheme to promote a full scale country wide implementation thereof. However, solar energy is not always the optimum solution. In this paper solar water heaters will be compared to another energy efficient technology called heat pump water heaters by doing an economic comparison.

II. Heat Pump Water Heaters

There is another energy-efficient water heating concept that has proven itself highly successful; known as a heat pump. Until now this success was mainly achieved in the commercial building market (hotels, hospitals, university residences, etc.)[3].

This cycle typically consumes 1 unit of electrical energy for every 3 units of heating produced; i.e. only $33kWh_{electrical}$ is used to produce $100kWht_{hermal}$. Therefore on average two thirds (67%) of the electrical energy consumption can be saved compared to conventional electrical resistance heating.

A. Several benefits and disadvantages:

Heat pumps can, as mentioned already, save up to 67% of the energy required to heat water. With water heating by conventional geysers contributing 30-50% of a typical household electricity cost, it means that a heat pump can save 20-33% of the cost. This is more than what is currently required from the power ration scheme for the residential sector (10%) or the hospitality industry (20%).

- Heat pumps are relatively easy to install. All that a heat pump requires is a free air arrangement resulting in it usually being an outside installation. Heat pumps are built to be weather proof and comply with the SANS IP ratings for outdoor electrical installations.
- At large centralized water heating installations typically found at commercial buildings such as hotels and hospitals, heat pumps are relatively easy to install. For example, to provide 25000 liters of sanitary hot water at 60ºC per day a heating capacity of typically 100kW would be required. This can be achieved by installing 2 x $50kW_{thermal}$ heat pumps. These heat pumps can be installed on a hotel premises near the current water heating plant, taking up a space of approximately 10m². This is opposed to

a solar heating installation where 25000 liters of hot water at 60ºC per day would require solar panels covering approximately 267m² based on an average solar radiation value of 4.8kWh/m² per day.

- Heat pump installations, whilst more expensive than a conventional electrical resistance heater, are much less expensive than solar water heating installations. This will be shown in this article. In addition, ESKOM has launched a subsidy program for heat pumps, with this subsidy typically representing a 40-50% reduction in project cost. The economic returns on a large centralized heat pump installation, aided by the ESKOM subsidy; result in competitive payback periods of between 2 and 3.5 years. Payback periods in the residential sector vary between 2 and 4 years. The variance in payback periods is a function of several factors including levels of usage and the ease of installation.
- The only disadvantage of heat pumps is that it is still dependant on an electricity supply if compared to some solar water heaters that can be operated completely independent.

III. CASE STUDY

Several arguments for and against the use of either heat pumps or solar water heaters have been made in the previous section. This section provides simulated case studies for both residential and commercial building sanitary hot water facilities. Comparisons are made between conventional electrical resistance heaters, heat pumps and solar water heaters in the residential sector and between ASHRAE standard electrical systems and heat pumps in the commercial building sector. Data for solar water heating was obtained from the comprehensive website created by ESKOM DSM [2]. Data for heat pump systems and conventional electrical heating systems is obtained from previous studies ([3], [4], [6], [7], [8], [10]). Detailed comparisons will be made for the Johannesburg region in Gauteng.

Assumptions to allow the three concepts to be evaluated on equal terms

- Average inlet water temperature for Johannesburg is 14˚C.
- Average solar radiation values are: 1750kWh/m² annually for Johannesburg.
- Hot water is stored at 60ºC in an insulated vessel with heat loss characteristics as typically found in the industry:

$$Q_{loss,daily} = 0.125 \times Q_{max.vessel} \quad (1)$$

Where $Q_{max.vessel}$ represents hot water stored at 60°C.

- For the residential sector the vessel configuration found in most homes will be used as is to store hot water generated by the heat pump. Solar water heaters will however have their own storage vessels installed.

- In commercial buildings the existing hot water storage vessels will be used together with heat pumps.

A. Residential sector

In this specific case study the three heating methods will be evaluated on residential level. The results will be shown for houses having 2, 3, 4 and 5 persons using the sanitary hot water facilities. Typical hot water consumption patterns and figures have been obtained from a study by Meyer [6]. Consumption varies between 75 liter at 60°C per person in summer and 110 liter at 60°C per person in winter. Several other studies have used these figures in hot water system design and evaluation ([6], [8], [9]).

The conventional geyser found in most homes is usually a 3kW, 150 liter unit (2-3 people) or a 4kW, 200 liter unit (4-5 people).

The proposed heat pump unit for both vessel sizes is 2.4kWthermal, using 0.8kWelectrical.

The solar heating system varies as follows

1. 150 liter, 1.89m² collector span (2 people)
2. 200 liter, 2.45m² collector span (3-4 people)
3. 300 liter, 4.52m² collector span (5 people)

The systems as specified are provided as inputs to a simulation program [7]. The simulation program performs a first law conservation of energy analysis, and takes into account the annual distribution of hot water consumption and daily consumption profile as proposed by Meyer [5].
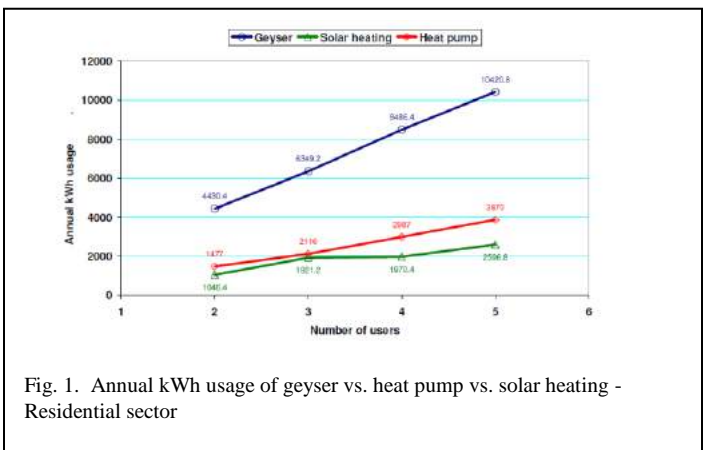

Fig. 1. Annual kWh usage of geyser vs. heat pump vs. solar heating - Residential sector

The above figure shows the annual electricity consumption per heating method. It can be seen that both the heat pump and solar water heater provide significant savings over the conventional electrical resistance geyser heater. Furthermore solar water heating saves a higher fraction of energy compared to a heat pump. This is due to the heat pump still consuming electricity to drive the cycle, amounting to about 33% of the electricity consumed by an electrical resistance heater. However, the solar water heater system also uses electricity in the form of backup electrical heating to assist i) during the night time when solar energy is not available, and ii) during

winter when daily hot water demand exceeds the daily delivery capacity of the solar panel.

The following installation cost estimates is provided. Please note that the ESKOM subsidies has already been subtracted for both solar and heat pump systems.

TABLE I
INSTALLATION COST ESTIMATION FOR SOLAR WATER HEATER SYSTEM AND HEAT PUMP WATER HEATER SYSTEM

	Solar type	Solar cost	Heat pump type	Heat pump cost
2 users	200l, 2.45m²	Rs.13200	2.4kW	Rs.7000
3 users	200l, 2.45m²	Rs.13200	2.4kW	Rs.7000
4 users	300l, 4.52m²	Rs.17700	2.4kW	Rs.7000
5 users	300l, 4.52m²	Rs.17700	2.4kW	Rs.7000

The following graph indicates the payback period calculated using the above installation cost estimates and the calculated energy savings (kWh), using an average energy cost of 0.45c/kWh.
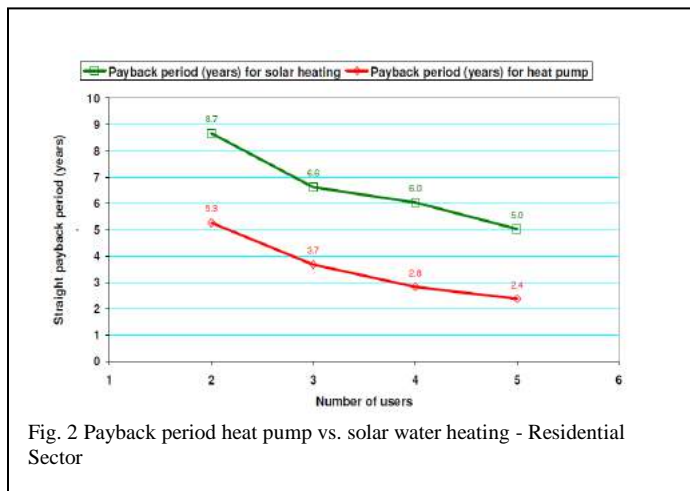

Fig. 2 Payback period heat pump vs. solar water heating - Residential Sector

From the graph it is clear that heat pumps provide a significantly better payback period when compared to solar water heating. The main reason for this is the much lower installation cost of heat pumps, whilst still achieving at least 80% of the savings that solar water heating can provide.

IV. CONCLUSION

This article showed that heat pumps can provide a very feasible alternative to solar water heating in the residential market. Heat pumps achieve more than 80% of the savings that are possible with a comparable solar water heating system, but at a much lower installation cost, thus leading to a significantly improved payback period. Typical payback periods for heat pumps vary be between 2.3 – 3.7 years for homes with 3 to 5 residents. These payback period estimates are typically 40-

55% lower than for solar water heating.

It is shown that there is good potential for heat pump installations in the commercial building sector. Typical payback periods for these installations vary between 2.3 and 3.2 years, depending on factors such as occupancy and climatic region. These results also provide a good estimate of savings and payback periods that can be achieved for any centralized water heating system, including those at hospitals, university residences, mine shaft change houses.

V. NOMENCLATURE

Q   Heat

Subscripts
Max   Maximum

REFERENCES

[1] ESKOM DSM website for solar heating http://www.eskomdsm.co.za/swh_5_savings_calc.htm
[2] Greyvenstein, G.P. (1995). A life-cycle cost comparison between heat pumps and solar water heaters for the heating of domestic water in South Africa, Household Energy for Developing Communities Conference, South African Institute of Energy, Johannesburg, South Africa.
[3] Greyvenstein, G.P. & Rousseau, P.G. (1997). Improving the cost effectiveness of heat pumps for hot water installations. Proceedings of the 5th international energy agency conference on heat pumping technologies. Toronto. Canada.
[4] Greyvenstein, G.P. & Rousseau, P.G. (1999). Application of heat pumps in the South African commercial sector. Energy and the Environment. Vol 15, p247-260.
[5] Meyer, J.P. (2000). A review of domestic hot water consumption in South Africa. R&D Journal. Vol 16, p55-61.
[6] Rankin, R., Rousseau, P.G & Van Eldik, M. (2004). Demand Side Management for Commercial Buildings using an In-line Heat Pump Water Heating Concept. Energy Conversion & Management. Vol 45(9-10), p1553-1563.
[7] Rankin, R. (2006) Optimization of the in-line sanitary water heating system for Demand Side Management in the South African commercial and industrial sectors. PhD Thesis in Engineering. Northwest University
[8] Rankin, R & Rousseau, P.G. (2006). Sanitary hot water consumption patterns in commercial and industrial sectors in South Africa: Impact on heating system design. Energy Conversion and Management. Vol 47 p687-701.
[9] Rousseau, P.G., Greyvenstein, G.P. & Strauss, J.P. (2000). Demand side management in the commercial sector using an improved in-line heating methodology, International Journal of energy research. Vol 25(4).
[10] Van Eldik, M. (1999). Simulation of a micro heat pump cycle. Masters Degree in Engineering. School of Mechanical and Materials Engineering. Potchefstroom University for Christian Higher Education. South Africa.

EFFECT OF PWHT SOAKING TIME ON MECHANICAL AND METALLURGICAL PROPERTIES OF 9 Cr- 1Mo- V STEEL

N. P. Patel[1], P. Maniar[2], M.N. Patel[3]

naishadh.patel27@gmail.com[1], pavan.maniar@lntpower.com[2], mnp_31554@yahoo.com[3]

Abstract

Modified 9Cr–1Mo-V is generally used in petroleum industries, chemical processing and thermal power plants in steam piping, headers and superheater piping. Compared to conventional Cr-Mo steels, it is having advantages of thickness reduction and reduction in thermal stresses and thus improves service life at elevated temperature. Modified 9Cr–1Mo-V steel has excellent mechanical properties and corrosion resistance combined with low creep rate and low thermal expansion makes it a wonderful material for high temperature applications. In present investigation, study was carried out on 9Cr-1Mo-V steel involving combination of different soaking time in Post weld heat treatment. SA 335 Gr. P91 base metal was used for welding with two different welding processes i.e. GTAW and SMAW. In this experiment, three trials were carried out at same welding parameters with different PWHT soaking time. The effect of different PWHT soaking time on mechanical and metallurgical properties of weld metal investigated.

Index Terms— Modified 9Cr-1 Mo- V steel, Post Weld Heat Treatment, Welding Cycle

I. INTRODUCTION

The development of power plant technology towards larger units and higher efficiencies can be linked to the development of creep resistant ferritic steels. Starting with simple C-Mn steels, creep strength has improved successively by introducing new alloying elements and new microstructures. 9-12 %Cr ferritic creep resisting steels have been developed worldwide over the last two decades for elevated temperature service for nuclear and fossil energy applications. P91 is a martensitic chromium-molybdenum steel, microalloyed with vanadium and niobium, and with controlled nitrogen content. Modified 9Cr-1Mo-V, commonly referred to as P91, and is widely used in the power industry because of its superior properties at elevated temperatures. The advantages over conventional CrMo steels can be used either for weight reductions or to permit an increase in operating temperature. Comparison of the pipe wall thickness required for different creep-resistant materials in certain operating conditions and demonstrated that the wall thickness can be reduced by quarter if P91 is chosen instead of 2.25Cr-1Mo steel is shown in fiure 1 (a). In order to achieve steam temperatures higher than 600°C while maintaining reliability, improved high strength of advanced CrMo steel over conventional CrMo steel for higher temperature use is shown in Figure 1(b).
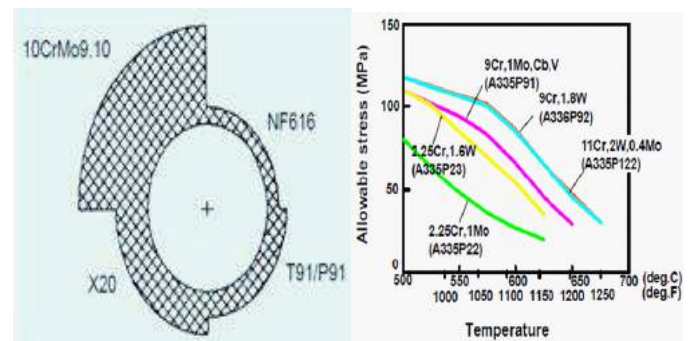

Fig. 1: (a) Comparison of the pipe wall thickness for different creep-resistant materials. (b) Comparison of allowable stress of advanced and conventional Cr-Mo steel.

Welding is one of the most essential fabrication processes for component manufacturer. P91 being air hardenable material (fully martensitic structure), Weldability is very good but much precaution needs to be taken while welding and post weld heat treatment of this steel. Higher preheat & interpass temperatures are required to weld this material which makes uncomfortable condition for a welder to weld. From fabrication point of view, it is not economical and increases the overall cycle time of manufacturing.

In the present study, an effort was made through different sets of experiment to study the effect of PWHT soaking time on P91.

II. EXPERIMENTAL WORK

9Cr-1Mo-V type of steel, SA 335 GR P91 was used as a base material for experiments. Chemical composition of 9Cr-1Mo-V steel is given in table 1. Groove design for the experiments is shown in figure 2.

Table 1: Chemical Composition of SA 335 Gr.P91

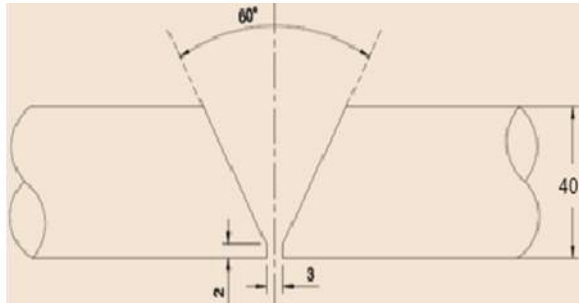| C	Si	Mn	P	S	Cr
0.08-0.12	0.2-0.5	0.3-0.6	0.02	0.01	8.0-9.5
Ni	Mo	V	Al	Nb/Cb	N2
0.4	0.85-1.050	0.18-0.25	0.04	0.06-0.1	0.03-0.07

Figure 2: Groove design for experiments.

P91 base metal was welded using two different welding processes i.e. Gas Tungsten Arc Welding (GTAW) and Shielded Metal Arc Welding (SMAW). Also a study was carried out to see the effect of simulated heat treatment cycle on the mechanical properties and microstructure evaluation of the material.

In the current practice for welding of P91 steel, preheating- interpass temperature is maintained in the range of 200 °C – 350 °C. After completion of welding, preheating temperature is maintain and then post heating is given to the weld at temperature of 400 °C for 4 Hr. After completion of Post heating, weld is cooled to room temperature. NDT is carried out after the completion of post heating. PWHT is carried out at the temperature of 760 °C ± 10 °C for required time depending upon the thickness of the material.

Welding processes and parameters were same during both the sets of experiments. Preheating temperature were 200 °C - 350 °C for these experiments. Radiography was carried out after and before the PWHT of P91 steel. Post heating temperature and holding time for these experiments were 400 °C for 4 hour.

These Experiments covers the effect of PWHT soaking time 2.5 hr, 7.5 hr and 15 hr as experiment no. 1, experiment no.2 and experiment no.3 respectively on mechanical and metallurgical properties of 9Cr-1M0-V steel.

After completion of PWHT, various mechanical & metallurgical testing was carried out as per the ASME code.

III.   RESULTS AND DISCUSSION

As PWHT soaking time increases from 2.5 hr to 15 hr, UTS value decreases significantly go around 80 MPa, but there is not much difference in UTS value from 2.5 hr to 7.5 hr soaking time. When hot tensile testing carried out then it was observed that values of UTS at higher temperature is directly correlated with the Values of UTS at room temperature. At higher temperature material strength is reduced. Generally PWHT reduces the strength and improves the ductility of the material. It was observed that these effects become more significant as the tempering time and temperature are increases.

As PWHT soaking time increases from 2.5 hr to 15 hr, a marginal decrease in hardness of 20 Hv is found. In the as-welded condition, P91 exhibits very high hardness due to its martensitic structure. After PWHT the hardness of P91 weld metal is lowered as a result of tempering reaction in weld metal and HAZ zone which includes a reduction in dislocation density, lath break up and development of polygonized structure, reduction in solid solution strengthening due to precipitations and coarsening of precipitates.

As PWHT soaking time increases from 2.5 hr to 15 hr, there was no significant change in toughness of the material. These was marginal increase of the toughness value in the material can be attributed to softening behavior of the material during PWHT. The toughness of the material increases on increasing the tempering duration of the material.

As PWHT soaking time increases from 2.5 hr to 15 hr, changes were observed distinctly in the microstructure of the weld metal. It was observed that on increasing the soaking time, the lath type martensitic structure changes from coarse to fine martensitic structure. Evidence of precipitation can be noticed through optical micrographs. However, the distribution of carbide precipitates in the microstructure can be viewed more clearly in the micrograph taken at higher magnification using scanning electron microscope. Figure 3 reveals fine martensitic laths and fine carbides particles distributed not only along the previous austenite grain boundaries but also throughout the matrix.

(a) Experiment no. 1   (b) Experiment no. 2
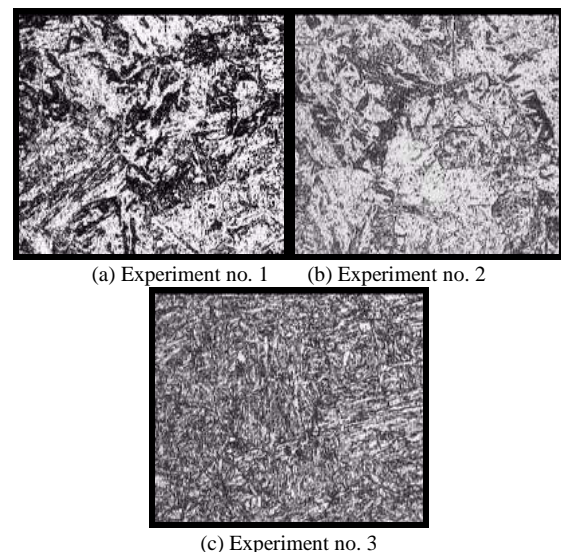

(c) Experiment no. 3

Fig.3: Weld metal Microstructure at 500X Magnification

IV. CONCLUSION

As the PWHT soaking time increase at the given temperature of P91 weldments, significant reduction in ultimate tensile strength of material and conversely improve the ductility of the material as the strength reduces.

As the PWHT soaking time increase at the given temperature of P91 weldments, hardness of material is decreases.

As the PWHT soaking time increase at the given temperature of P91 weldments, there is marginal increase in the toughness of material.

As the PWHT soaking time increase at the given temperature of P91 steel, coarse to fine tempered martensite structure is observed.

REFERENCES

[1] Samsiah SULAIMAN, Structure of Properties of Heat affected Zone of P91 creep resisting steel, university of Wollongong year 2007.

[2] Use of 9Cr-1Mo-V (Grade 91) Steel in the Oil Refining Industry, API TECHNICAL REPORT 938-B, FIRST EDITION, JUNE 2008.

[3] Masataka Yoshino1), Yoshinao Mishima1), Yoshiaki Toda2), Hideaki Kushima2), Kota Sawada2) and Kazuhiro Kimura2 Influence of Normalizing Heat Treatment on Precipitation Behavior in Modified 9Cr-1Mo Steel ECCC Creep Conference, 12–14 September 2005, London.

[4] An introduction to the 9Cr-1Mo-V alloys, Valve Magazine, Volume 13, No.1 Winter 2011.

[5] G.Guntz-M Julien-G Kottmann-F. Pellicani- A.pouilly-J.C.Vaillant ; The T91 Book'1990 Vallourec Industies France.

[6] Effect of Normalization and Temper Heat Treatment on P91 Weldment Properties EPRI technical report December 2003.

[7] Recommended Practices for Welding of Chromium-Molybdenum Steel Piping and Tubing Supersedes AWS D10.8-86 American welding society.

[8] Guideline for Welding Creep Strength-Enhanced Ferritic Alloys, EPRI December 2006.

[9] Fossil Plant High-Energy Piping Damage: Theory and Practice EPRI technical report Volume 1: Piping Fundamentals June 2007.

[10] J. Siefert, J. Sanders, J. Tanzosh Babcock and Wilcox Research Cen ,B. Alexandrov, J. Lippold The Ohio State University Welding Engineering Group, Columbus, OH, USA An Update of Phase Transformations During PWHT of Grade 91.

[11] Peter Mayr Evolution of microstructure and mechanical properties of the heat affected zone in B-containing 9% chromium steels Faculty of Mechanical Engineering Graz University of Technology, Austria July 2007.

[12] D Abson and J S Rothwell, Review of type IV cracking in 9-12 % Cr Creep Strength Enhanced ferritic steel, TWI, june 2010.

[13] WILLIAM F. NEWELL JR Welding and Post weld Heat Treatment of P91 Steels.

[14] A M Barnes Effect on composition on creep properties of 9%Cr-1%Mo weld metal for grade 91 steel TWI November 1998.

[15] LI Yongkui 'Study on Creep Damage in Thick Welded Joint of Mod.9Cr-1Mo Steel Plates' Kochi University of Technology Graduate School of Engineering Course 2009

[16] J.A. Francis, W. Mazur H.K.D.H. Bhadeshia Welding Procedures and Type IV Phenomena.

[17] Kulvir Singh, G Jaipal Reddy, D V Vidyasagar and V Thyagarajan * Creep and Creep Damage Assessment in P91 Weld Joints ECCC Creep Conference, 12–14 September 2005, London. Metallurgy Department, Corporate R&D, BHEL, Hyderabad.

[18] ASME Boiler and Pressure vessel Code, Section II part A, New York Edition 2010.

[19] ASME Boiler and Pressure vessel Code, Section II part C, New York Edition 2010.

[20] ASME Boiler and Pressure vessel Code, Section IX, New York Edition 2010.

[21] ASME B 31.1 Power Piping Code

[22] Volume 6- Welding, Brazing and Soldering, Metals handbook, ASM international, 1993

[23] Spector, A. Z. 1989. Achieving application requirements. In Distributed Systems, S. Mullende

Heat Transfer Coefficient and Pressure Drop over Staggered Pitch Variation Using CFD

Nirav R. Bhavsar, Rupen R. Bhavsar

E-mail: er_niravbhavsar@yahoo.co.in

*Abstract-***Cross-flow over tube banks is generally encountered in heat exchangers. Steady state Navier-Stokes and the energy equations are applied for "staggered" cylinders having pitch to diameter ratios of 1.25, 1.5, 1.75, 2.0 and 2.5 to obtain the numerical solutions of governing equations using Euler's explicit algorithm. Analyses have been done for mass flow rates ranging from 0.01 kg/s to 0.09 kg/s. The effect of change of horizontal pitch on heat transfer rate and pressure has been analyzed using CFD tool. The contours of streamlines, pressure, velocity and temperature are generated to study the effect of mass flow rate and longitudinal pitch variation. Also the local and average Nusselt numbers, pressure distributions around the cylinders are presented. Results obtained are for forced convection which suggests that with increase in the longitudinal tube distance, the range of pressure drop increases, the operating temperature range increases also the drop in the heat transfer coefficient increases. This result is helpful in predicting the performance of heat exchangers.**

Index Terms- Staggered tube, Pitch distance, pressure drop

I. INTRODUCTION

Cross-flow over tube banks is generally encountered in heat transfer equipments like the evaporators and condensers of power plants, air conditioners where one fluid moves through the tubes while the other moves over the tubes in a perpendicular direction.

Number of experimental and numerical investigations has been conducted on the flow and heat transfer over a single tube or tube banks (bundles). Many previous works are found which are concerned with overall heat transfer through the banks Pierson, (1937); Huge, (1937); Grimison, 1937). Žukauskas (1972) reviewed characteristics of flow and heat transfer for a single cylinder and tube banks. Later Achenbach (1989) measured local heat transfer from one staggered tube bank at high Reynolds numbers (Re≥10^5), and found boundary layer separation and transition to turbulence. Aiba et al. (1982) used Reynolds number of 1 x 10^4 to 6 x 10^4, and found the effect on the heat transfer around cylinder in the staggered tube banks. Park et al (1998), Buyruk et al. (1998) simulated the flow past a circular cylinder at low Reynolds numbers, and compared their results with the

previous experimental and numerical results. Buyruk (2002) predicted the heat transfer characteristics in tube banks with tube arrangement and flow condition below 4 x 10^2 Reynolds numbers.

When fluid passes through tube banks, different flow phenomenon are observed such as stagnation, separation, reattachment, vortex formation or recirculation which affect the local heat transfer characteristics. In such flow situations, it is difficult to measure local heat transfer coefficients by conventional heat transfer measurements. In this study, the fluid considered is water to measure the local heat transfer coefficients. The purpose of this study is to investigate the average heat transfer and pressure characteristics at various longitudinal tube distances for different mass flow rates for staggered tube bank in cross-flow.

II. METHODOLOGY

A. FUNDAMENTAL EQUATIONS [1,2]

For Staggered Tube Layout correlations, byA. A. Zhukauskas and R. V. Ulinskas)

$$\text{Nu} = 0.35(\frac{\sigma 1}{\sigma 2})\, Re^{0.6}\ Pr^{0.33} \ , \ \frac{\sigma 1}{\sigma 2} < 2 \qquad (1)$$

$$\text{Nu} = 0.4\ Re^{0.6}Pr^{0.33}, \ \frac{\sigma 1}{\sigma 2} > 2 \qquad (2)$$

Correlations given by V. K. Migai and E. V. Firsova,

$$\text{Nu} = 0.312\ \sigma_1^{0.23}\ \sigma_2^{-1.048}\ Re^{0.6}\ Pr^{0.33}, \text{For } \sigma_2 > 1.13 \text{ and } \sigma_1 < 3 \qquad (3)$$

$$\text{Nu} = 0.343\ \sigma_1^{0.23}\ \sigma_2^{-0.864}\ Re^{0.6}\ Pr^{0.33}, \text{For } \sigma_2 > 1.13 \text{ and } \sigma_1 < 3 \qquad (4)$$

$$\text{Nu} = 0.386\ \sigma_1^{0.00}\ \sigma_2^{-0.148}\ Re^{0.6}\ Pr^{0.33}, \text{For } \sigma_1 > 3 \qquad (5)$$

Where,
Nu = Nusselt Number,
σ_1= Transverse tube distance
Re = Reynold's Number ,
σ_2= Longitudinal tube distance
Pr = Prandtl Number,
σ_3= Diagonal tube distance

B. PROBLEM DEFINITION

This problem considers a two dimensional section of a tube bank. A schematic of the problem is shown in Fig.1. The bank consists of uniformly spaced tubes with a diameter of 0.01 m; they are staggered in the direction of cross fluid flow. Their centers are separated by a distance of 0.02 m in the X direction, and 0.02 m in the y direction. The bank has a depth of 1 m. Because of the symmetry of the tube bank geometry, only a portion of the domain needs to be modeled. A mass flow rate of 0.05 kg/s is applied to the inflow boundary of the periodic module. The temperature of the tube wall (T_{wall}) is 400 K and the bulk temperature of the cross-flow water (T_b) is 300 K. The properties of water that are used in the model are shown in Figure. $\rho = 998.2$ kg/m^3, $\mu= 0.001003$ kg/ms, $c_p = 4182$ J/kgK, k = 0.6 W/mK. [6]
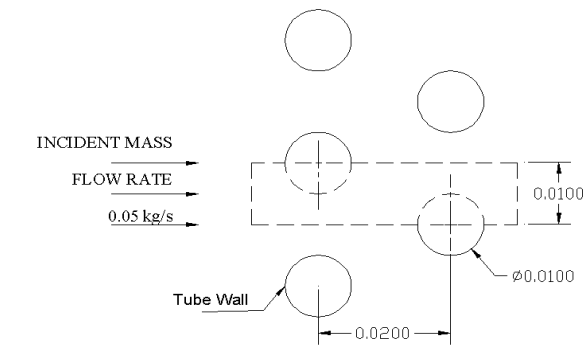
C. CONTROL VOLUME

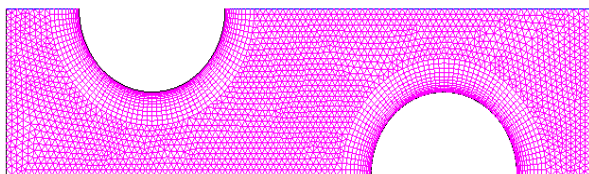

Figure 1. Computational Domain Geometry

Figure 2. Meshing [6]

The analysis has been done for following Inline tube layout geometries,

TABLE.1 Inline Tube Layout Geometries; (Transverse pitch (PT): 0.02m) [4,5]

Sr. No.	1	2	3	4	5
Longitudinal Pitch P_L (m)	0.0125	0.015	0.0175	0.02	0.025

III. RESULT & DISCUSSION

A. FOR 0.02M HORIZONTAL X 0.02 VERTICAL STAGGERED TUBE LAYOUT
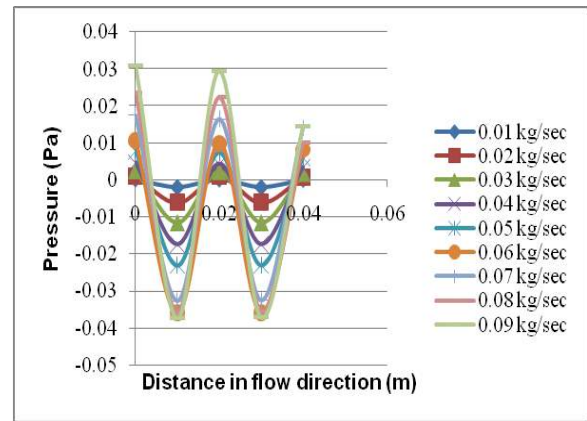

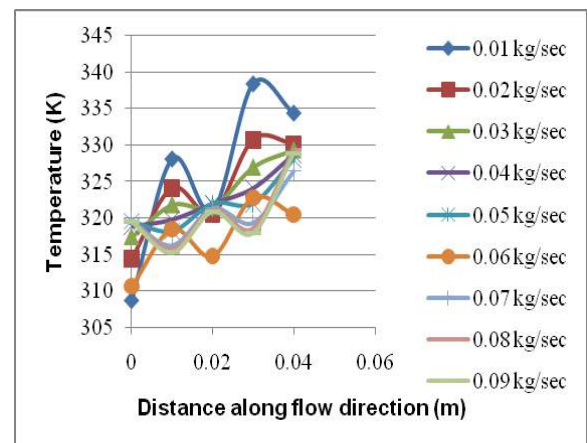Figure 3. Pressure plot in flow direction for different mass flow rates

Figure 4. Temperature in flow direction for different mass flow rates
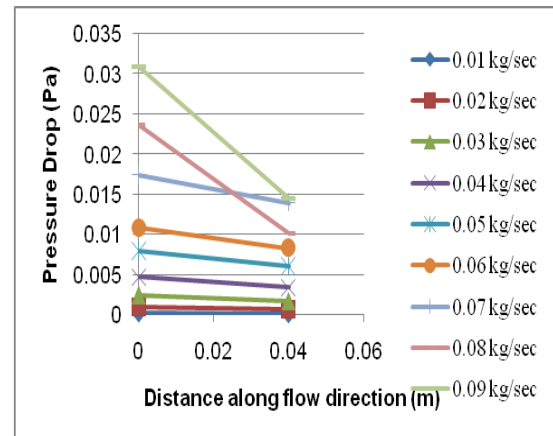

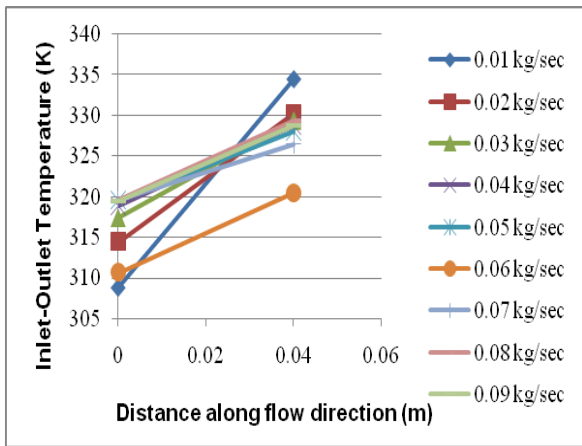Figure 5. Pressure drop range (from Inlet to Outlet) for different mass flow rates

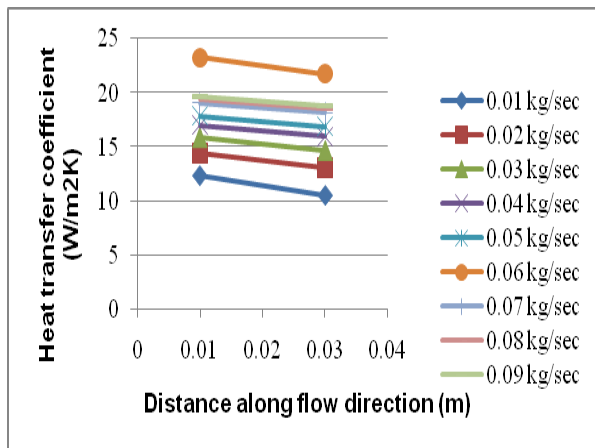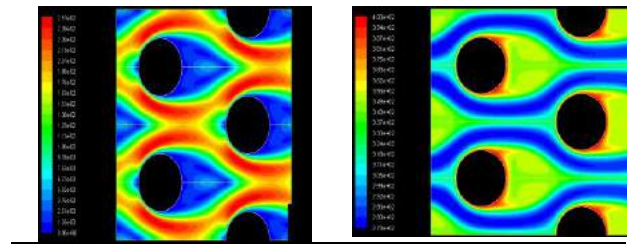Figure 6. Temperature range from Inlet to Outlet for different mass flow rates

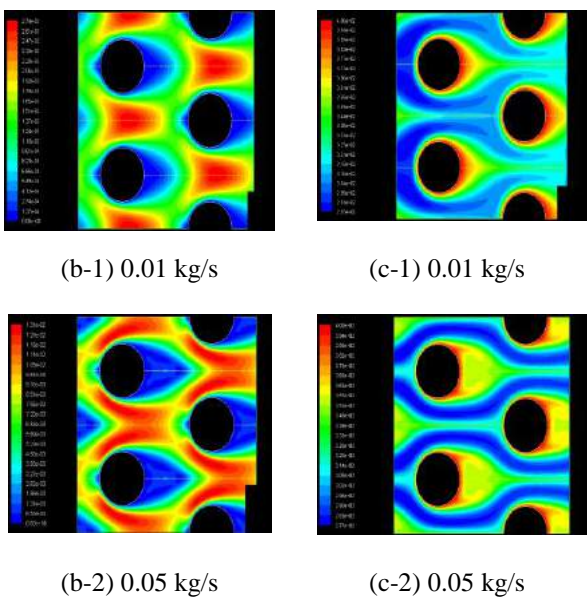
Figure 7. Heat transfer coefficient over each tube for different mass flow rates

B. CONTOURS OF PRESSURE, VELOCITY AND TEMPERATURE IN CONTROL DOMAIN 0.02M HORIZONTAL X 0.02M VERTICAL STAGGERED TUBE LAYOUT.

(b-1) 0.01 kg/s   (c-1) 0.01 kg/s

(b-2) 0.05 kg/s   (c-2) 0.05 kg/s

(b-3) 0.05 kg/s   (c-3) 0.05 kg/s

Figure 9 Velocity Contour   Figure 10. Temperature Cont.

C. COMPARISON FOR DIFFERENT STAGGERED LONGITUDINAL PITCH (0.01 KG/S)
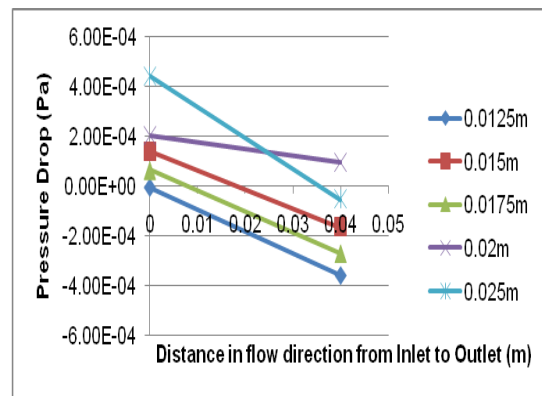

Figure 11. Comparison of Pressure drop for various
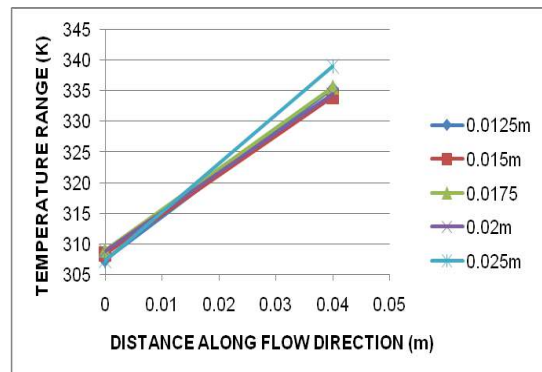

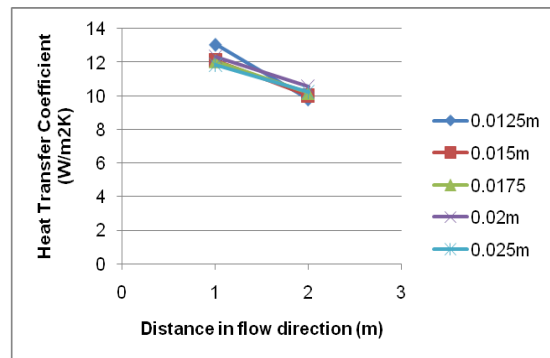Figure 12. Comparison of Temperature Range

Figure 13. Comparison of Heat Transfer Coefficient

The figure 11 shows that for mass flow rate of 0.01 kg/sec the maximum pressure drop is found for 0.025m (Horizontal) X 0.02m (Vertical) staggered tube

layout and the minimum pressure drop is found for 0.015m (Horizontal) X 0.02m (Vertical) Staggered layout. The graph also explains that for different layouts the working fluid Water works in different pressure range and as the longitudinal tube direction increases the range of operating pressure drop increases.

The figure 12 shows that for a same mass flow rate of 0.01 kg/sec the staggered tube layout of 0.025m (Horizontal) X 0.02m (Vertical) gives maximum temperature rise of water that is of the order of 10.36%. It is also explainable that as the tubes distance for staggered tubes in horizontal direction for 0.0125m and 0.025m which are our minimum and maximum model conditions that gives maximum temperature range. This can be useful to decide number of stages to achieve the required cooling effect of the fluid inside the tube.

The figure 13 shows that there is maximum drop of Heat transfer coefficient for the staggered layout of 0.0125m (Horizontal) X 0.02m (Vertical). It also shows that as the horizontal distance between tubes in staggered layout increases the drop in Heat transfer coefficient decreases. This plot can be helpful to go for alteration of working fluid over tube and substitution of tube material.

IV. CONCLUSION

The analysis performed indicates that as the longitudinal tube distance increases the range of pressure drop from inlet of control volume to outlet increases which is useful to decide the number of baffles and end supports in heat exchangers. As the longitudinal tube distance increases the operating temperature range increases which can be useful to identify the number of tubes, number of passes. As the longitudinal tube distance in staggered tube pitch increases the heat transfer coefficient drop increases.

REFERENCES

[1] Fluid flow and heat transfer around two circular cylinders in side-by-side arrangement, Minter Cheng, Proceedings of HT-FED04 2004 ASME Heat Transfer/Fluids Engineering Summer Conference July 11-15, 2004, Charlotte, North Carolina USA, pp. 1-3.

[2] E. N. Pis'mennyi, Universal Relation for Calculating Convective Heat Transfer in Transversely Streamlined Bundles of Smooth Tubes, (2010), pp. 1-5

[3] V. Yu. Semenov, A. I. Smorodin, and V. K. Orlov, Heat Exchange of a Bank of Tubes in the Transverse Flow.

[4] Modeling Periodic Flow and Heat Transfer, Ansys Tutorial, Case-2

[5] Haitham M. S. Bahaidarah and N. K. Anand, A Numerical Study of Fluid flow and Heat Transfer Over a Bank of Flat Tubes, Numerical Heat Transfer, Part A, 48: 359–385, 2005, ISSN: 1040-7782

[6] Anderson, J.D., \Fundamentals of Aerodynamics", 2nd Edition

[7] S. Jayavel and Shaligram Tiwari, Numerical Investigation of Incompressible Flow Past Circular Tubes in Confined Channel, Indian Institute of Technology Madras, INDIA, pp. 1-5

Application of Porous Medium Technology to Internal Combustion Engine for Homogeneous Combustion- A Review

Ratnesh Parmar*, Vimal Patel**

*(PG Student, Mechanical Engineering Department, L.D. College of Engineering, Ahmedabad
Email: parmar.ratnesh93@gmail.com)
** (Assistant Professor, Mechanical Engineering Department, L.D. College of Engineering, Ahmedabad
Email: vimalpatel@live.com)

ABSTRACT

The advantages of homogeneous combustion in internal combustion (I.C.) engines are well known and many research groups all over the world are working on its practical realization. Dr. Franz Drust has proposed a new combustion concept that fulfils all requirements to perform homogeneous combustion in I.C. engines using the Porous Medium Combustion Engine, called "PM -engine". The porous member is heated to high temperatures during the exhaust cycle of the engine and preheats a fresh charge of air during the compression takes place with a fuel charge, thereby decreasing heat loss to the engine, the engine's efficiency will be increased and the engine may operate at lower compression ratio also. This review paper presents the recent advancement and capabilities of porous medium combustion technology for energy efficient and environmentally safe operations in IC engine. Homogenization, 3-D thermal self-ignition, wide and dynamic power regulation, extremely low pollutant emissions, incorporation of porous medium in open type- and closed type- PM engines & their working. It has not only been studied theoretically but has been technically realized. Practical results show an overall improvement in efficiency along with the drastic reduction in exhaust emissions and soot formation.

Index Terms – porous medium technology, internal combustion engine, homogeneous combustion, low emission, porous medium materials.

I. INTRODUCTION

An internal combustion engine (especially for road vehicle application) has to operate in a wide range of loads and speeds. From the point of view of reduction of combustion emissions and fuel consumption, especially attractive would be application of lean homogeneous charges for operation at engine part loads. An efficient IC engine will be characterized by a (nearly) zero emissions level (for both gaseous and particulate matter components) under possible lowest fuel consumption at all operational conditions These parameters strongly depend on the mixture formation and combustion process which are difficult to be controlled in a conventional engine combustion system. Especially important are air flow structure, fuel injection conditions, and turbulence as well as ignition conditions. The art of mixture formation, art of ignition and combustion realized in conventional direct injection (DI) engines indicate a lack of mechanisms for homogenization of the combustion process.

The homogenization of combustion process, however, is necessary for radical reduction of engine emissions directly

in a primary combustion process keeping very low specific fuelconsumption.

II. HOMOGENEOUS COMBUSTION PROCESS

The homogeneous combustion is here defined as a process in which a 3D-ignition (volumetric) of the homogeneous (premixed) charge is followed by simultaneous (no flame front) heat release in the whole combustion chamber volume characterized by a homogenous temperature field. (See Fig.1)
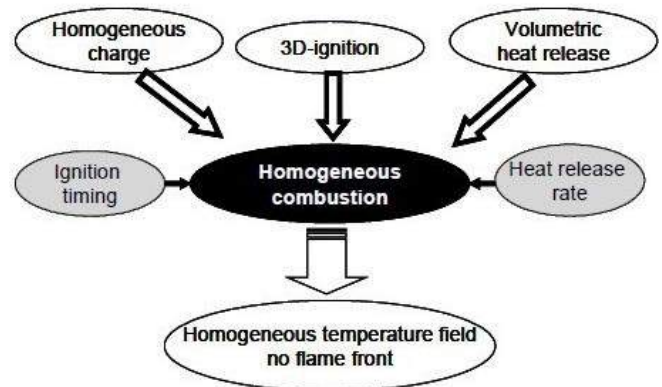

Figure 1: Possible Model of homogeneous combustion in an engine.

According to this definition a three steps of the mixture formation and combustion may be selected that define the ability of a given realistic engine to operate as a homogeneous combustion system:

- degree of charge homogenization (with a goal to get a homogeneous, premixed, gaseous charge);
- art of ignition (goal is to realize a volumetric ignition);
- homogeneity of combustion process and its temperature field (represented by simultaneous heat release in combustion chamber volume).

There are two principal requirements given to the combustion system that are necessary for satisfying the homogeneous combustion conditions:

- Controlling of the ignition timing under variable engine operational conditions,
- Controlling of the heat release rate for different mixture compositions.

There are four basic arts of ignition that may be realized in I.C. engine (Fig.2):

- Local ignition (e.g. spark plug)
- Compression ignition (thermal self-ignition)
- Controlled-auto-ignition (low temp. chemical ignition)
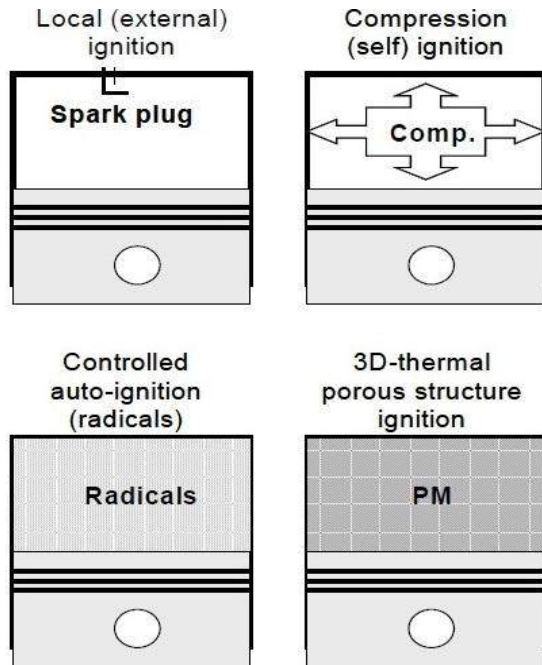- 3D-thermal-PM-ignition (thermal ignition in a porous medium volume) [1-2]

Figure 2: Arts of ignition in I.C. Engine

In the case of local ignition, even if homogeneous and premixed charge is applied, we cannot satisfy the requirements of the ignition defined for a homogenous combustion. In this case a flame kernel will be followed by the flame front propagating throughout the combustion chamber. The resulting combustion process is not homogeneous.

In the case of compression ignition applied to a strongly non-homogeneous and heterogeneous charge, a multi-point ignition can be achieved. The resulting combustion process is highly non-homogeneous and diffusion (mixing) controlled. If in the same system a homogeneous charge is applied, a nearly volumetric ignition would be possible (HCCI system). Such a process (if volumetric) would lead to very high pressure gradients in the cylinder depending on the mixture composition and thermodynamic parameters of the cylinder charge. Control of the ignition timing and following heat release rate are the most critical factors limiting practicability of the conventional concepts of HCCI systems.

The last considered ignition system has been recently proposed by Durst and Welcas and uses a 3D-structured porous medium (PM) for the volumetric ignition of homogeneous charge. The PM has homogeneous surface temperature over the most of the PM-volume, higher than the ignition temperature. In this case the PM-volume defines the combustion chamber volume. As a model, we could consider the 3D-structure of the porous medium as a large number of "hot spots" homogeneously distributed throughout the combustion chamber volume. Because of this

feature a thermally controlled 3D-ignition can be achieved. Additionally, the porous medium controls the temperature level of the combustion chamber permitting the NOx level control almost independently of the engine load or of the (A/F) ratio.

III. HOMOGENEOUT COMBUSTION IN THE IC ENGINE USING PM TECHNOLOGY

Combustion is a basic phenomenon from which we derive out the energy in the form of heat and use it for different purposes. Unlike conventional premixed combustion process, the porous medium technology does not operate with a free flame. Rather the combustion takes place in a three dimensionally arranged cavities of a porous and inert media, resulting in a totally different flame itself compared to conventional combustion process.

There are two new concepts that utilize a porous medium technology for permitting the homogenous combustion under variable engine operational conditions:

Multi-mode Combustion: Mixture preparation system that may change its combustion mode according to actual engine operational conditions to keep homogenous combustion conditions, so-called intelligent (multi-mode) combustion. (See Fig.3)
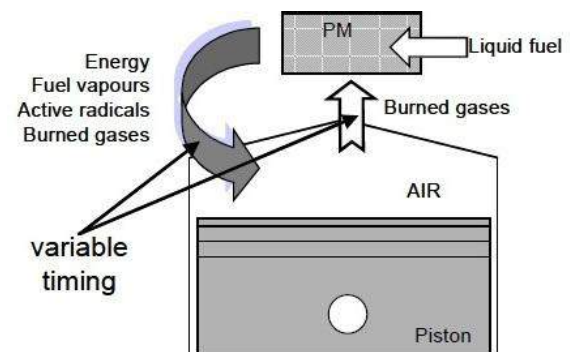

Figure 3: Concept of Multi-mode combustion system

Mono-mode Combustion: System that may operate independently of the engine operational conditions permitting homogeneous combustion conditions from very light to full loads, so-called mono-mode combustion system. (See Fig.4) [1, 2]
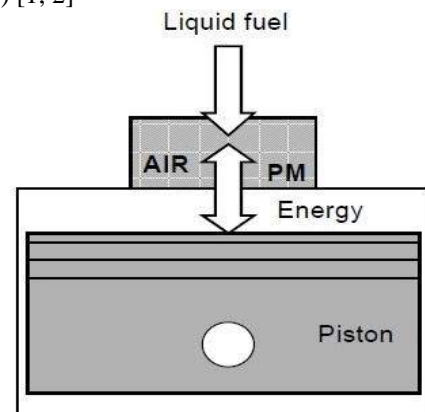

Figure 4: Concept of Mono-mode combustion system

Porous medium (PM) technology is here defined as a utilization of specific and unique features of a highly porous medium as applied to individual processes of mixture formation, ignition and combustion realized in engine. [3, 4] The most important features of a highly porous media are: large specific surface area, high porosity, high heat capacity, excellent heat transfer properties (especially heat radiation), variability of structure, pore density and pore geometry, high thermal and mechanical stability.

The following engine processes may be supported by the porous medium (see Fig.5):
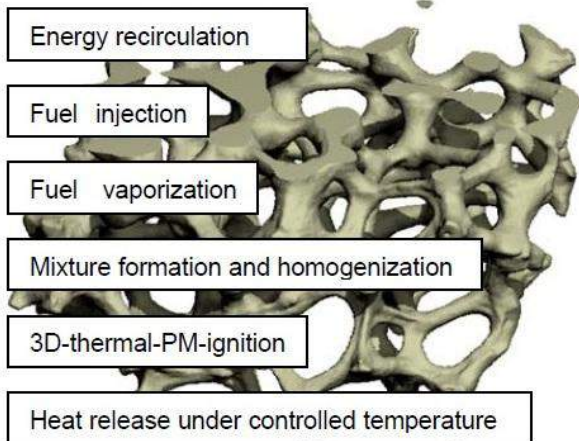

Figure 5: The important engine processes that may be supported by the PM technology

Energy recirculation in engine cycle in the form of hot burned gases recirculation or combustion energy: This may significantly influence thermodynamic properties of the charge in the cylinder and may control its ignitability (activity). This energy recirculation may be performed under different pressures and temperatures during the engine cycle. Additionally, this heat recuperation may be used for controlling the combustion temperature level (Fig.6).
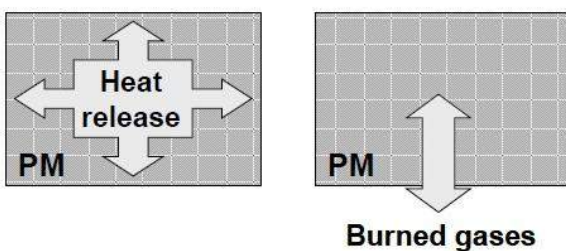

Figure 6: Heat accumulation and recirculation in porous medium

Fuel injection in PM-volume: especially unique features of liquid jet distribution and homogenization throughout the PM-volume (effect of self homogenization) is very attractive for fast mixture formation and its homogenization in the PM volume (Fig.7). [5]
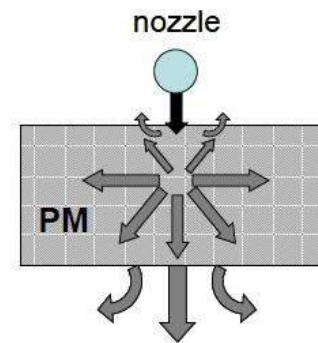

Figure 7: Fuel distribution in PM volume

Fuel vaporization in PM-volume: combination of large heat capacity of the PM-material, large specific surface area with excellent heat transfer in PM volume make the liquid fuel vaporization very fast and complete. Here two different conditions of the process have to be considered: vaporization with presence and without presence of combustion air (e.g. also "cool-flame" and "blue-flame" reactions).

Mixing and homogenization in PM-volume: unique features of the flow properties inside 3D-structures allow very effective mixing and homogenization in PM-volume.

3D-thermal-PM-ignition (if PM temperature is at least equal to ignition temperature under certain thermodynamic properties and mixture composition): There is a new kind of ignition, especially effective if the PM-volume creates the combustion chamber volume. [1]

Heat release in PM-volume under controlled combustion temperature (properties of homogeneous combustion): this is only one known to the author kind of combustion, which permits homogeneous combustion conditions almost independently of the engine load with possibility of controlling the combustion temperature level. [1, 2]

IV. PRINCIPLE OF PM ENGINE

The PM-engine is here defined as an internal combustion engine with the following processes realized in a porous medium: internal heat recuperation, fuel injection, fuel vaporization, mixing with air, homogenization of charge, 3D-thermal self-ignition followed by a homogeneous combustion. PM-Engine may be classified with respect to the heat recuperation as:

- Engine with periodic contact between PM and working gas in cylinder (closed chamber).
- Engine with permanent contact between PM and working gas in cylinder (open chamber).

On the other hand, possible positioning of the PM-combustion chamber in engine can be used to design different engines:

- Cylinder head (PM is stationary).
- Cylinder (PM is stationary).
- Piston (PM moves with piston).

During intake and early compression stroke, there is not remarkable influence of PM thermal capacitor on thermodynamic condition inside the cylinder. The heat

exchange process (between PM material and compressed air) increases with upward motion of piston. At the TDC, almost all the air is compressed and closed to PM volume.

Near the TDC of compression stroke, fuel is injected into PM volume and is spreaded widely by interaction with a large number of PM pore junctions ("self – homogenization"). A strong heat transferred from hot PM surface to liquid fuel makes fast and complete fuel vaporization. Very fast mixing with gaseous charge occurs and the combustible mixture is ignited in the whole PM volume. Amount of burned gases that trapped in PM volume defines accumulated energy for next cycle. The three fundamental conditions for a homogeneous combustion are satisfied: homogenization of charge in PM volume, 3D thermal self ignition and volumetric combustion with a homogeneous temperature.

One of the most interesting features of PM-engine is its multi-fuel performance. Independently of the fuel used, this engine is a self-ignition engine characterized by its 3D-thermal ignition in porous medium. Finally, the PM-engine concept may be applied to both two- and four-stroke cycles. [6]

V. PM MATERIAL

There are number of important parameters that have to be considered in selection of PM materials for application to combustion processes realized in porous media. The main features of the porous structures, that are been used to support the different engine processes are as shown in fig.8.
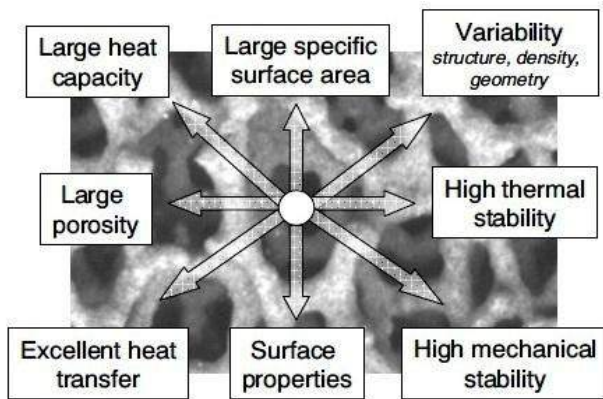

Figure 8: The main features of porous structures to be utilized to support engine processes

The volume of a highly porous structure may be divided in to pore volume (free volume for gas), material volume, hollow tube junctions and micro porosity. (Fig. 9)
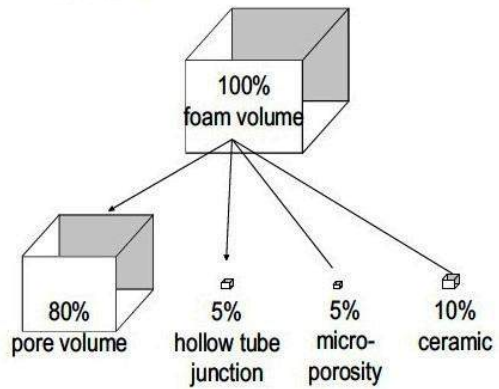

Figure 9: Volume sharing of highly porous structure

Generally, the most important parameters of PM for application to combustion technology in can be selected as follows:
- Specific surface area
- Heat transport properties
- Heat capacity
- Transparency for fluid flow and flame
- Pores size, pores density
- Mechanical resistance and mechanical properties under heating cooling conditions
- Thermal resistance
- PM material surface properties
- Electrical properties

Typical ceramic materials being of interest in application to PM-combustion technology are (see Fig.10): Oxidides (e.g. Al2O3, ZrO2), and Non-oxides (e.g. SiC). The cells of ceramic foam can be idealized as a pentagonal dodecahedron.
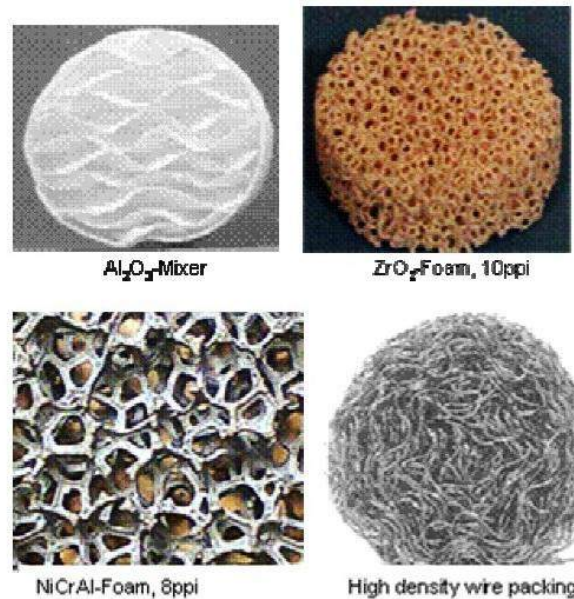

Figure 10: Examples of different porous structures

In some application chromium iron alloys and nickel base alloys are also used. The edges of the dodecahedron are the struts of the ceramic foam. In the case of flowing gas

through the foams, the flow is forced to separate and reattach at the struts, resulting in a good mixing and strong interaction between flowing gas and the PM material.

VI. PM COMBUSTION TECHNOLOGY APPLIED TO AN IC ENGINE

Homogeneous combustion in IC engines can be achieved by a system proposed recently by the technique termed as 3D-thermal PM-self-ignition (3D-grid structure of a high temperature) and it uses a 3Dstructured PM for volumetric ignition of homogeneous charge. The PM has homogeneous surface temperature over the most of the PM volume, higher than the ignition temperature. In this case the PM-volume defines the combustion chamber's volume. We could consider the PM volume as a large number of "hot spots"

Figure 11: Principle of PM engine operation with a closed chamber; 1-intake valve, 2-exhaust valve, 3-PM chamber valve, 4-fuel injector, 5-piston


homogeneously distributed throughout the combustion chamber volume. This feature provides a thermally controlled 3D-ignition system. More over the PM controls the temperature level of the combustion chamber permitting the NOx level almost independent of the engine load or the A/F ratio.

PM-engine may be classified with respect to the timing of heat recuperation in engine as:

- Engine with periodic contact between PM and cylinder (so-called closed PM-chamber).
- Engine with permanent contact between PM and cylinder (so-called open PM-chamber).

A. *PM ENGINE WITH COLSED CHAMBER*

Let us start an analysis of the PM-engine cycle with a case of closed PM chamber, i.e., engine with a periodic contact between working gas and PM-heat recuperator. (See Fig.11)
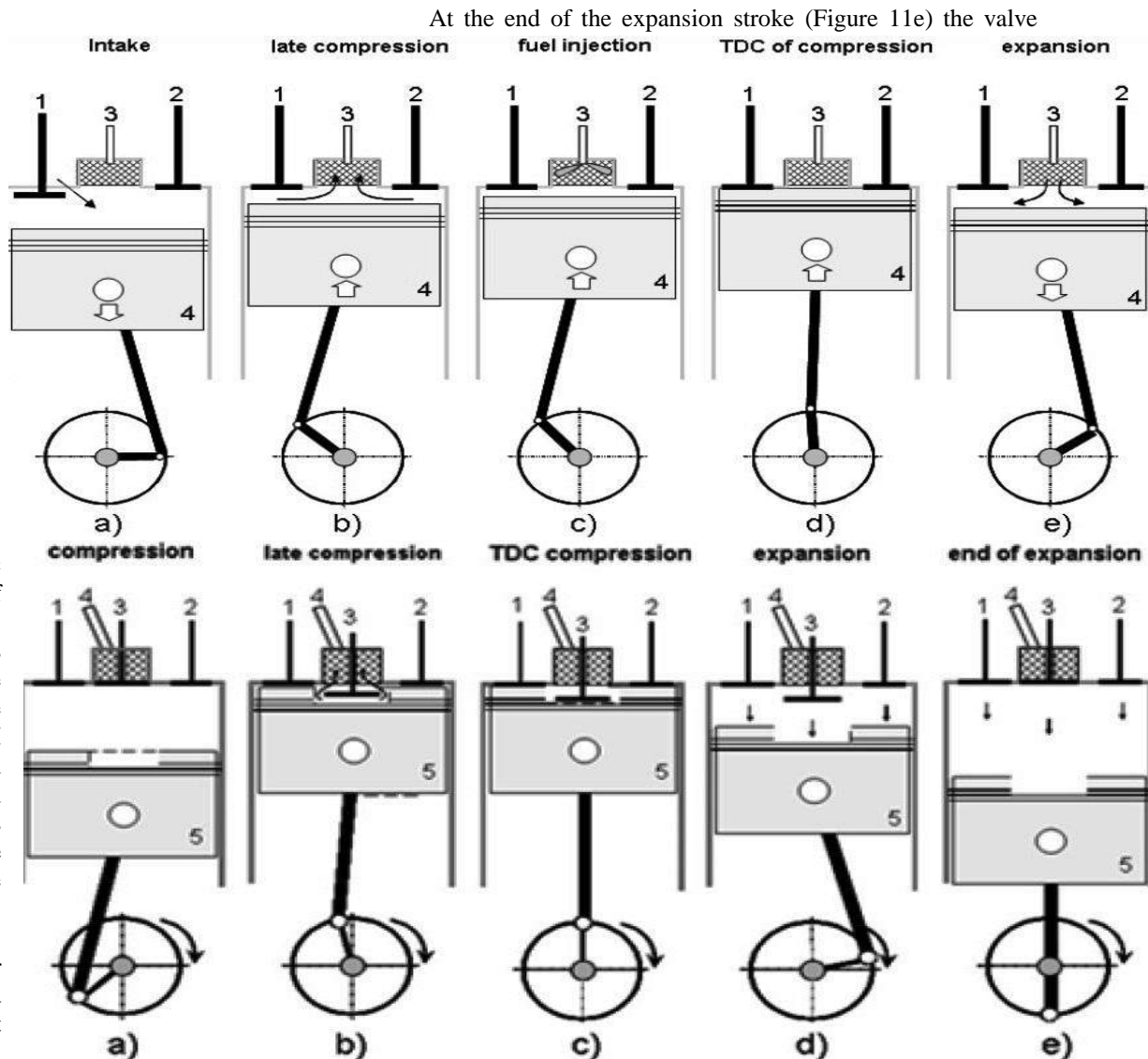
At the end of the expansion stroke (Figure 11e) the valve controlling timing of the PM-chamber closes and fuel is injected in the PM-volume. This volume represents in thermodynamic sense a low-pressure chamber and a long time is available for fuel injection and its vaporization in the PM. These processes may continue through exhaust, intake and compression strokes (Figure 11a).

Near the TDC of compression (Figure 11b) the valve in PM-chamber opens and the compressed air opens and the compressed air flows from the cylinder into the hot PM volume containing fuel vapors. Very fast mixing of the gaseous charge occurs and the resulting mixture is ignited in the whole PM volume (Figure 11c). The resulting heat released process performs simultaneously in whole PM volume the three essential conditions for homogeneous combustion is here fulfilled: Homogenization of charge in PM volume, 3D-thermal self-ignition in PM and volumetric combustion with a homogeneous temperature field in PM volume. Additionally, the PM material deals as a heat capacitor and, hence, controls the combustion temperature.

B. PM ENGINE WITH OPEN CHAMBER

Another possible realization of the PM engine is the combustion system characterized by a permanent contact between working gas and PM volume as schematically shown in figure 12.

Figure 12: Principle of the PM engine operation with an open chamber; 1- intake valve, 2-exhaust valve, 3- fuel injector, 4-piston

Here, it is assumed that the PM combustion chamber is mounted in the engine head. During the intake stroke there is a weak influence of the PM–heat capacitor on the in cylinder air thermodynamic conditions. Also during the early compression stroke only a small amount of air is in contact with hot PM. The heat exchange process (non-isentropic compression) increases with continuing compression, and at the TDC the combustion air is closed in the PM volume.

Near the TDC of compression the fuel is injected into the PM volume and very fast fuel vaporization and mixing with air occur in 3D-structure of the PM volume. Again, the requested 3D-thermal self-ignition of the resulting mixture follows in PM volume together with the volumetric combustion characterized by a homogeneous temperature distribution in PM-combustion volume. Again, all necessary conditions for the homogeneous combustion are fulfilled in the PM-combustion chamber.

VII. ADVANTAGES OF PM ENGINE

- Theoretically higher cycle efficiency due to similarity to the Carnot cycle.
- Lower compression ratio may be used.
- Very low combustion noise due to significantly reduced pressure peaks.
- Nearly constant and homogeneous combustion temperature field.
- Very fast combustion yielding good engine performance.
- Multi-fuel combustion system.
- May operate with homogeneous charge: from stoichiometric to very lean mixture compositions.
- Mixture formation and combustion processes are almost independent of in-cylinder flow structure, of turbulence or of spray atomization.

VIII. LIMITATIONS OF PM ENGINE

However amount of work done by permanent contact cycle
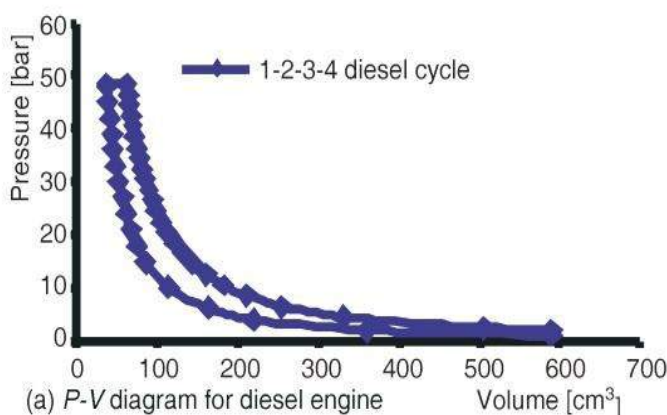
is very less though it claims very high efficiency (same as Carnot cycle). Hence is suitable only for low power requirement systems. Heat transfer and thermal stress problems may occur in engine parts neighboring with a combustion chamber. The strength may not be sufficient in the case of heavy engines.

IX. RESULT ANALYSIS

Using porous medium in the engine cylinder helps in regeneration of energy and improves the overall performance of the engine. For the same compression ration efficiency of PM cycle is greater that of Otto and Diesel. Thermodynamically it is shown that at a maximum pressure of 3000 kPa, with cutoff ration 1.1 permanent contact cycle has got an efficiency of 65%, which is closer to the Carnot cycle. The permanent contact cycle operates at lower compression ratios compared to other cycles to develop the same efficiency. Hence specific weight required of this cycle is very less and leads to the development of compact engine.

In addition, due to low compression ratios peak pressures induced inside the combustion chamber are less thus reducing the level of vibrations and noise and hence relatively low cost materials can be used due to low peak pressured and temperatures inside the combustion chamber. Due to presence of porous medium, the combustion is homogeneous and uniform leading to low emissions. Here, Very fast combustion yielding good engine performance. The engine may operate with homogeneous charge from stoichiometric to very lean mixture compositions. The mixture formation and combustion processes are almost independent of in-cylinder flow structure, of turbulence or of spray atomization. The PM concepts offers the realization of IC engines with emissions level of the primary combustion process being close to the long time requested zero –emission. Thus, PM – engine concept has the potential to realize a near zero emission engines under both part and full load operational conditions.

The results of the experiment carried out on the engine with the PM is compared with the normal engine and it is found that the efficiency of the engine has improved, exhaust emissions like NOx, CO, and UHC are reduced drastically, and also it has been recorded that the soot formation is almost negligible, Fig. 13(a)-(d) and Fig. 14 (a) - (b).

(a) *P-V* diagram for diesel engine

(b) *P-V* diagram for PM engine
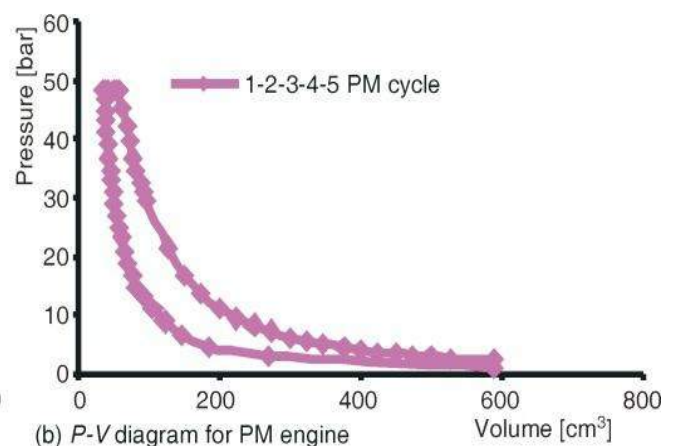
and combustion) can be controlled or positively influenced with the help of PM/ceramic foams or other structures. If composites are employed they will definitely better in
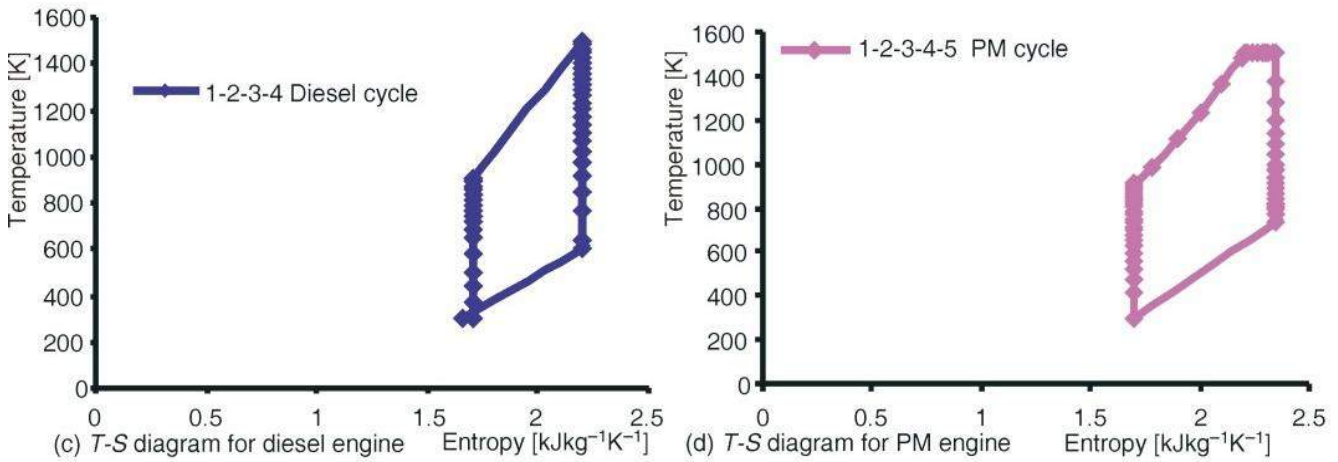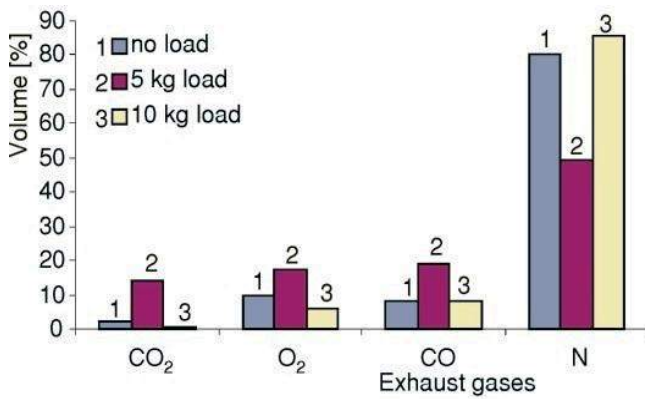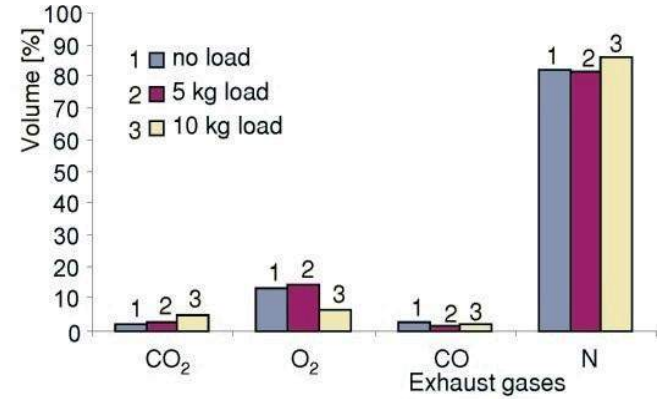

(c) T-S diagram for diesel engine   (d) T-S diagram for PM engine

Figure 13: Comparison of engine cycles characteristics

future.

(a) Diesel engine exhaust emissions by % volume   (b) PM engine exhaust emission by % volume

Figure 14: Comparison of exhaust emissions

X. CONCLUSIONS

A porous medium technology has been defined as a utilization of large specific surface area, large heat capacity, high porosity, etc. of open cell structures for supporting different processes realized in engine. Especially important is the application of this material for homogenous mixture formation and complete combustion in engines.

In this paper novel concepts for combustion engines based on the application of PM technology is presented and discussed. The main attention is focused on the engine concepts having potential for homogeneous combustion process under variable engine operational conditions: intelligent engine and engine with combustion in a PM. It was shown that PM could be used for a great variety of improvements in the combustion process, especially for elimination of soot emissions and significant reduction of NOx. Combustion process in porous reactor is homogeneous, and uses a new art of volumetric thermal ignition in the porous medium.

All these processes (e. g. gas flow, fuel injection and its spatial distribution, vaporization, homogenization, ignition,

All the findings are claimed after conducting trails and observations during the experimentation; it is unique research work being conducted and a good approach towards the development of a near zero emission engine and engine efficiency, which is the need of the current scenario in the field of Automobile. This technology can be further applied to reciprocating engine power systems for load matching and to make a higher dynamic power range, hence higher overall efficiency.

XI. REFERENCES

[1] Durst F., Weclas M., 2001, A new type of internal combustion engine based on the porous medium combustion technique, J. Automobile Engineering, Part D, No. D04999, 215

[2] Durst F., Weclas M., 2001, A new concept of I.C. engine with homogeneous combustion in porous medium (PM), 5th Int. Symposium COMOMIA-2001, Nagoya, Japan.

[3] Weclas M., 1999, New concepts for reduction of engine emissions by application of porous medium (PM) technology to mixture formation and combustion processes, Internal Report, Invent GmbH.

[4] Weclas, M. 2002, Anwendung von hochporösen Schäumen in stationären und nicht-stationären Verbrennungsprozessen, Seminar Industrietag Schaumkeramik, Fraunhofer IKTS, Dresden, April, 2002.

[5] Weclas, B. Ates, V. Vlachovic, 2003, Basic aspects of interaction between a high velocity Diesel jet and a highly porous medium (PM), 9th Int. Conference on Liquid Atomization and Spray Systems ICLASS 2003.

[6] Dr. Franz Durst, Dr. M. Weclas, Stefan: A new concept of porous medium combustion in IC engines. Recent trends in Heat and Mass Transfer, IIT Guwahati, pp316-332, Jan2002.

[7] Dhale A. A., Awari G. K., Singh M. P., 2010, Analysis of Internal Combustion Engine with a new concept of porous medium combustion for the future clean engine, Thermal Science, Vol. 14, No. 4. Pg. 943-956.

[8] Adil SMH, Hura V., Mehrotra A., Khaliq A., 2004, Recent Advancements of Porous Medium Combustion Technology in I.C. engine and a new concept of Cogeneration in PM engine, COGNIZANCE- IIT Roorkee.

[9] Durst F., Weclas M., 2002, A new concept of Porous Medium Combustion in I.C. engines, International Symposium on Recent Trends in Heat and Mass Transfer, Guwahati, India.

[10] Schäfer-Sindlinger, A., Vogt, C.D., Hashimoto, S. Hamanaka, T., Matsubara, R., New Materials for Particulate Filters in Passenger Cars, Auto Technology, 2003, No. 5.

[11] Brenn, G., Durst, F., Trimis, D., Weclas, M., Methods and tools for advanced fuel spray production and investigation, Atomization and Sprays, 1997, vol. 7, pp. 43-75.

[12] Miroslaw Weclas., "Potential of porous medium combustion technology as applied to internal combustion engines.", ISSN 1616-0762 Sonderdruck Schriftenreihe der Georg-Simon-Ohm-Fachhochschule Nurnberg Nr. 32..

Fabrication and Characterization of Cast Aluminium Fly Ash Composite

Dr. Vandana J. Rao, Hemant N. Panchal, Sonam M. Patel
Email: vandana11866@yahoo.co.in

Abstract - **Generally, the particulate reinforced composites contain the particles that strengthen the soft matrix by means of dispersion strengthening mechanism due to in-situ reactions. In the present study the idea is to prepare a cast particulate composite by adding different types of (Class C and Class F) fly ash into commercially pure aluminium. Synthesis of fly ash based composite is done by low cost, stir cast method. Magnesium (5 wt. pct.) is added into the melt in order to help the wetting of fly ash oxides. Mechanical and microstructural characterization is done by testing the composite under tensile test, hardness test, optical microscope (OM), Scanning Electron Microscope (SEM), Energy Dispersive X-ray Spectroscopy (EDS), Energy dispersive X-ray Florescence Spectroscopy (EDXRF), Spectrometer and X-ray diffraction (XRD). Uniform distribution of fly ash particles is observed under optical microscope in unetched and etched both conditions. SEM micrograph, under the back scattered mode indicate the distribution of different phases like network of Mg_2Si and heavy elements distribution that has been confirmed by EDS. X-ray diffraction of solid composite samples reveals the presence of mullite and silica into commercially pure aluminium matrix. Both types of fly ash gives almost equal mechanical properties, in fact Class-C fly ash composite (NFA) pursued better tensile strength and ductility than Class-F fly ash composite (WFA).**

Index Terms — **Class-C and Class-F fly ash, in-situ composite; Mg_2Si network; Mullite; Silica; Stir cast**

I. INTRODUCTION

It is quite well known that particle reinforced metal matrix composites (MMC's) has excellent mechanical properties due to the addition of high strength and high modulus particles such as TiC, SiC, Al_2O_3, TiB_2, TiO_2, etc.[1,2,3]. Metal matrix composites (MMCs) have high properties such as strength, stiffness, hardness; wear resistance and damping capacity [4]. However, there use is limited due to their high production cost. Among various types of discontinuous reinforcement used, fly ash is one of the most inexpensive and easily available sources. It has a low density, which makes it more attractive to the developed cost effective composites. Among the different classes of fly ash, Class-F fly ash is more suitable to make MMC because its low CaO content [5]. Each fly ash has different chemical composition due to different operational condition in thermal power plants and the type of coal used [5,6]. In the present work, MMC was produced by adding of 5

wt. pct. Class-C and Class-F fly ash along with 5 wt. pct. magnesium into commercially pure aluminium (LM 0). Mg is added into the melt to improve the wetting of fly ash oxides particles and generated in-situ reinforced particles. Presence of generated in-situ particles is due to reduction of various fly ash particles by molten aluminium. The fly ash was procured from two different places of Gujarat (INDIA) as Naroli and Wanakbori. Finally, the addition of fly ash and magnesium improves the mechanical properties of MMC. Aluminium fly ash composite have the numerous potential applications as covers, pans, casing, pulleys, manifolds, valve covers, rack rotor, engine blocks in automotive, small engines and in electromechanical sector [7,8].

II. EXPERIMENTAL

Commercially pure aluminium (LM 0) was used as metal matrix. Chemical composition of LM 0 is given in table 1. It was done on Spectro Maxx LMM 04 (Germany) spectrometer.

Table 1. Chemical composition of LM 0 in weight percentage.

%Si	%Fe	%Mg	%Cu	%Mn	%Al
0.355	0.474	0.59	0.031	0.057	98
to	to	to	to	to	
0.378	0.456	0.64	0.029	0.055	

The Fly ash particles used to synthesis the composite material, were received from two different locations of Gujarat (INDIA) like Naroli and Wanakbori. The composition of fly ash particles is given in table 2. It was done on EDXRF 800 instrument (Shimadzu) of oxide mode. Naroli fly ash is represented as NFA and Wanakbori fly ash can be as WFA.

Table 2. Typical chemical composition of fly ash in weight percentage
* LOI = Loss on Ignition

Type	$\%SiO_2$	$\%CaO$	$\%Al_2O_3$	$\%Fe_2O_3$	$\%TiO_2$	$\%V_2O_5$	$\%SrO_2$	$\%LOI^*$
NFA	11.87	49.58	5.38	20.68	2.62	0.18	0.14	9 to 10
WFA	53.50	1.66	26.66	8.33	3.91	0.17	0.08	6 to 10

The size analysis of fly ash particles was measured by sieve analysis techniques and result is shown in figure 1.
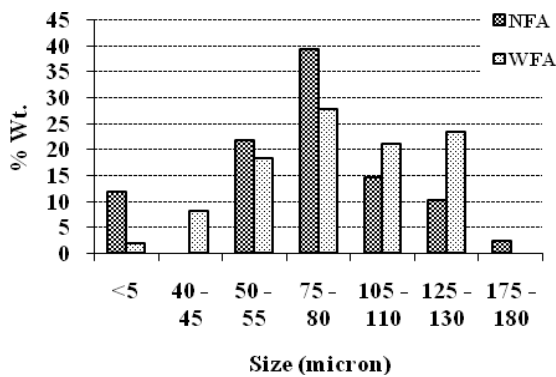

Fig.1. The size analysis of fly ash particles

The true density value of fly ash is 0.6987 gm/cc in case of NFA and 0.7720 gm/cc in case of WFA. The specific gravity value is 1.7581 and 1.7001 gm/cc for NFA and WFA respectively. For the measurements of true density of fly ash sample, a fixed volume of the sample was taken in a measuring cylinder and then the weight was measured. The specific gravity of fly ash sample was measured by using specific gravity bottle method. Commercially pure aluminium has been reinforced with 5 wt. pct. of NFA and WFA fly ash in different experiments to check their effect on the properties. The composite was fabricated by liquid metal stir casting technique [9]. Commercially pure aluminium was melted in clay graphite crucible using electric resistance furnace as indicated in figure 2. 5 wt. pct. Mg has been added in order to achieve strong bonding by change in surface energy (wetting angle) between molten matrix and reinforcement particles [10,11].The addition of pure magnesium also enhanced the fluidity of the molten metal [12,13,14]. The melt was mechanically stirred by using an impeller after the addition of preheated fly ash particles (100 - 200° C). The processing of the composite was carried out at a temperature range of 720-730° C with a stirring speed of 300 rpm [9]. The melt was poured into metallic die of 23 x 23 x 1.5 cm size. Specimen for metallography study was prepared by standard metallographic technique. Samples were microscopically analyzed under etching and without etching conditions. Metallurgical characterization of both types of samples has done by Neophot 02 optical microscope and SEM (JEOL-56 LV). XRD, EDS and Spectrometer were carried out for phase analysis and chemical analysis of synthesized composite. XRD had been done with Cu-K∝ radiation with scanning speed of 2° per minute in 10 - 90° range. Under mechanical test, hardness and tensile tests have been carried out. Hardness test had been performed with a load 31.625 kg for 10 seconds by a steel ball indenter of 2.5 mm diameter. The average of six values has been considered as the hardness. Monsanto 20 tensile testing machine with cross head speed of 0.5 mm per minutes was used to carry out the tensile test and the average of three values has been considered as the tensile strength value.
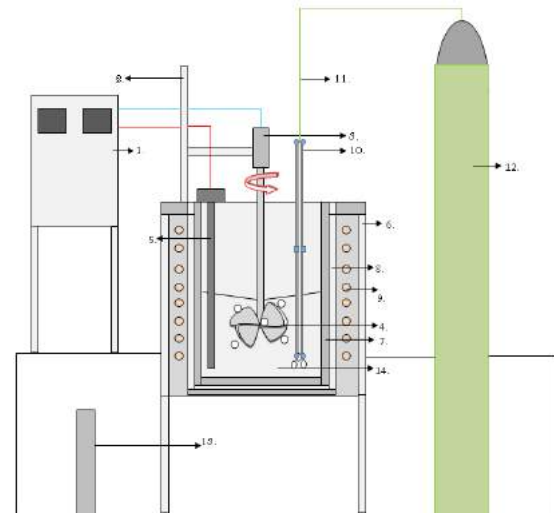
1. Temperature /display unit
2. Movable stirrer's stand
3. Motor for rotate stirrer
4. Turbine type stirrer
5. Chromel-Alumel thermocouple
6. Outer M.S. furnace wall
7. Inner furnace wall
8. Thermal insulation-Asbestos
9. Kanthal wire-wounded
10. Hollow Stainless Steel pipe (N2 inlet)
11. Rubber tube
12. N2 cylinder
13. Metallic die
14. Composite melt

Fig. 2. The experimental set up.

III. RESULT AND DISCUSSION

A. Chemical, Mineralogical and Size Analysis:

Table 2 indicates the variations in chemical compositions of both fly ashes. In case of NFA, CaO content is predominant hence it is to be considered as Class-C type fly ash. In WFA, SiO_2 content is predominant hence; it is to be considered as Class-F type fly ash. By considering its specific gravity value, it is of the precipitator type fly ash [15].

SEM photograph presented in figure 3(a) and (b) indicates the shape morphology of both types of fly ash. NFA has a flaky type shape whereas the WFA is a mixture of both spherical and flaky types. The Size of NFA is very small and uniform compared to WFA, and it can be confirmed by size distribution of it presented in figure 1.

(a)   (b)
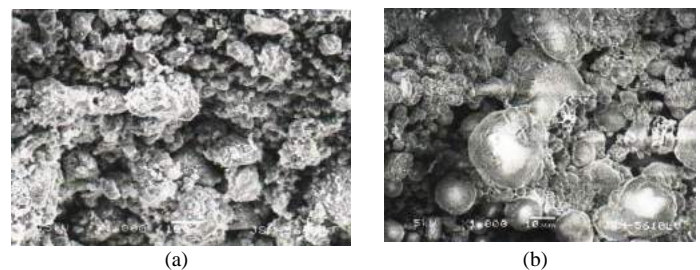
Fig. 3. (a) and (b), the SEM micrograph of NFA and WFA fly ash particles

The XRD pattern indicates the presence of different phases in both types of fly ash. It is indicated in fig 4(a) and (b).

(a)   (b)
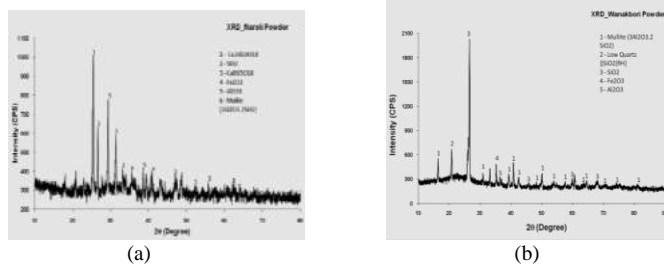
Fig. 4. (a) NFA and (b) WFA represent, the main mineral phases present into the two fly ashes by XRD

In the case of NFA, the presence of SiO_2, Al_2O_3, Mullite ($3Al_2O_3.2SiO_2$), Fe_2O_3 and a majority of complex calcium silicate phases were confirmed. It is because of the presence of major oxides phases like CaO, SiO_2 and Fe_2O_3 into the fly ash as per EDXRF results. In the case of WFA the presence of mullite, Al_2O_3, SiO_2 and Fe_2O_3 was confirmed. Here the amount of mullite was quite higher than the other phase The Sieve size analysis indicates that majority of the particles are in the range of 70-80 μm in size in both types of fly ashes. Chemicals analysis of commercially pure aluminium were done by Spectro Maxx LMM 04 (Germany) spectrometer indicate the presence of Fe (0.46), Mg(0.56) Si(0.36) along with major amount of aluminium around 90 pct

B. Microstructure of Al-FA/MMC:

Figure 5 (a) and (b) indicate the selected optical micrograph of unetched NFA and WFA composites. Micrograph 5 (a) indicates the fly ash particles appearing to segregate along the aluminium dendrite boundary. Rohatagi and co-workers [14-16] have explained this segregation like a lack of nucleation of α-aluminium dendrites during solidification [17].

(a)   (b)
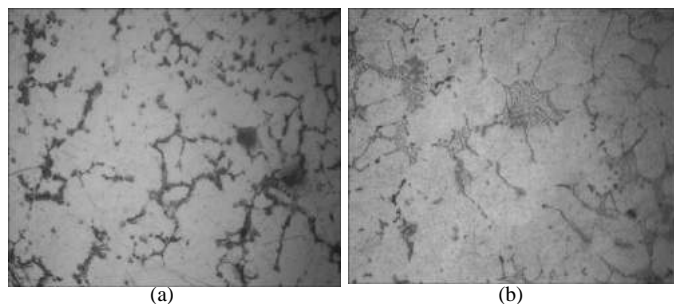
Fig. 5. (a) and (b), selected optical micrograph of unetched NFA and WFA composites

Figure 6(a) and (b) included selected etched optical micrograph of NFA and WFA composites. Both the micrographs compare to 5(a) and 5(b) is better to reveal the information like segregation of particles, Mg_2Si network and boundary of dendrites.

(a)   (b)
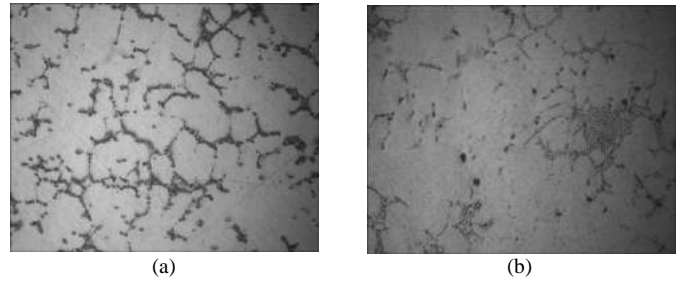
Fig. 6. (a) and (b), selected etched optical micrograph of NFA and WFA composites

Figure 7 (a) and (b) include SEM photo of the Al-NFA and Al-WFA MMCs. SEM Photograph of both fly ash clearly indicate the network of Mg_2Si [16] and heavy particles in white Chinese script and as a line shape at the end of the α aluminium dendrites. Back scattered micrograph of SEM easily indicate the difference in the distribution of heavy and light elements into the aluminium matrix. In case of NFA, heavy particles separation are in form of dots, clusters and Chinese script type, but in WFA it is mostly in the form of white needles or lines in shape which can control the mechanical properties of composite.

(a)   (b)
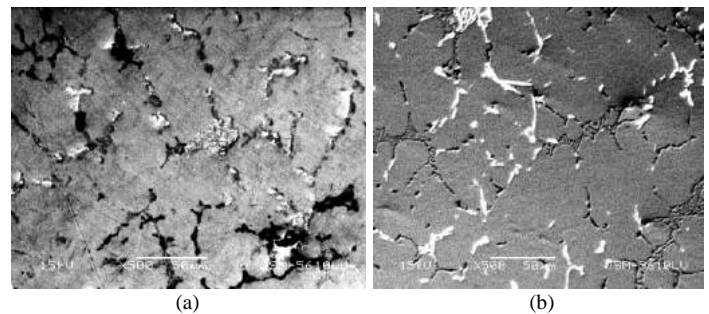
Fig. 7. (a) and (b), SEM photo (BSE mode) of the Al-NFA and Al-WFA MMCs.

The reason behind the network of Mg_2Si and heavy particles presence is discussed with the help of probable chemical reactions between molten aluminium, magnesium and fly ash particles The thermodynamic data's at 727 ˚C [18,19] for the possible reactions are like;

$$SiO_2 + Mg \rightarrow 2MgO + Si \qquad \Delta G° = -255.6 \text{ KJ} \quad (1)$$
$$3SiO_2 + 4Al \rightarrow 2Al_2O_3 + 3Si \qquad \Delta G° = -532.2 \text{ KJ} \quad (2)$$
$$Fe_2O_3 + 2Al \rightarrow Al_2O_3 + 2Fe \qquad \Delta G° = -799.6 \text{ KJ} \quad (3)$$
$$Fe_2O_3 + 3Mg \rightarrow MgO + 2Fe \qquad \Delta G° = -917.0 \text{ KJ} \quad (4)$$
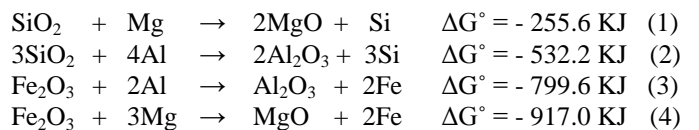
As per the above reactions, equation (1) and (4) have more chances because of the lower position of "Mg" in Ellingham diagram than "Al". Reactions 1 and 2, release the silicon, which react with externally added and available magnesium to form Mg_2Si network, which strengthens the composites.

In order to verify the above mention reaction and their effect on chemical composition was checked by spectrometer. Table 3 indicates the same.

Table 3. Indicate the chemical analysis of solid composite sample by Spectro Maxx LMM 04 (Germany) spectrometer of NFA and WFA

Type of composite	Wt. % of elements			
	Si	Mg	Fe	Al
NFA	1.824	4.94	0.438	Balance
WFA	3.61	4.92	0.60	Balance

In case of WFA type composites, more silica can be present and as per reaction (1) More silicon dioxide can reduce by magnesium and release free silicon. Free silicon reacts with available magnesium and forms the network of Mg_2Si and it is clearly observed in microphotograph of WFA composites. The extent of chemical reactions depends on temperature and time. However the X-ray analyses of solid fly ash composites are presented in figure 8(a) and 8(b).

8(a) and (b) represent for both types of fly ash solid composites samples without the presence of the Mg_2Si phase but it indicate the presence of phase like mullite and silica (SiO_2). The presence of mullite and silica (SiO_2) occurs due to the presences of mineralogical phases directly into the fly ash and the same reflected into solid composite samples. The stable phase would not involve in the chemical reaction and hence their presence is confirmed in X-ray analysis.
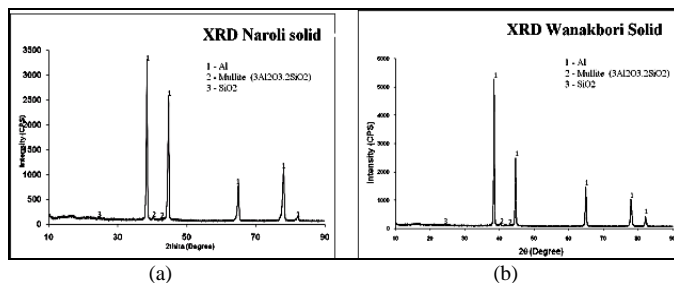
(a)   (b)
Fig. 8. (a) and (b), indicate X-ray diffraction pattern of the Al-NFA and Al-WFA solid MMCs

C. Mechanical properties of Al-FA/MMC:

Mechanical properties like hardness, ultimate tensile strength and percentage elongation are presented in table 4.

Table 4. Indicates the Mechanical properties of composite

Specimen	Hardness (BHN)	UTS (MPa)	%Elongation
LM 0	24	80	20
NFA	67	209.97	8
WFA	75	188.50	5

Both the composite have almost equal hardness value. The NFA composite presents better tensile property than WFA composite. In WFA the presence of needle or platelet shaped morphology of heavy metal element phase like β(FeSiAl$_5$) can be more detrimental than Chinese script phase like α(Fe$_2$SiAl$_8$) [20]. The phase β(FeSiAl$_5$) probably reduce the percentage of elongation of composite in WFA and turn around 5 %. in

WFA while in NFA it turn around about 8 %t which is higher than WFA. The tensile strength value of NFA composite is 210 MPa and which is around 10 pct. more than WFA composites.

IV CONCLUSION

The conclusions drawn from the research study are as follows:
1. Fly as Class-C (NFA) and Class-F (WFA), both the type gives almost equal hardness properties. Class-C (NFA) type fly ash gives better tensile and elongation properties than Class-F (WFA).
2. Presences of CaO (Major phase of Class-C), gives better tensile strength than SiO$_2$ (major phase of Class-F).
3. X-ray analyses of solid composite samples (both WFA and NFA) indicate presence of phase like mullite and silica into the structure.
4. SEM and OM both indicate the presence of a network of Mg_2Si into the matrix of LM 0.
5. In case of Class-F (WFA) the presence of high silicon and Mg (by Spectroscopy analysis) indicate the reduction of SiO_2 by Mg and the formation of Mg_2Si network into the matrix materials and it is seen clearly in case of WFA than NFA type fly ash.

REFERENCES

1) Zhang Z.F., Zhang I.C. and Mai Y.W., *J Mater Sci.* vol. 30 (1995), 1961.
2) Hamid A.A., Jain S.C., Ghosh P.K. and Ray S., *Met. & Mat. Trans B*, 37 B (2006), pp. 519-529.
3) Hamid A.A., Jain S.C., Ghosh P.K. and Ray S., *Met. & Mat. Trans B*, 37 A (2006), pp. 469-480.
4) Sudarshan S., Surappa M.K., *Mat. Sci. & Engg. A*, 480 (2008), pp. 117-124.
5) Gikunoo E., Omotoso O., Oguocha I.N.A., *Journal of Mater Sci.*, 39 (2004), pp. 6619-6622.
6) Gikunoo E., Omotoso O., Oghuocha I.N.A., *Mat. Sci. & Tech.,* 21 (2005), 143-152.
7) Rohatgi P.K., Guo R.P., Iksan H., Borchelt E.J., Asthana R., *Mat. Sci & Engg. A*, 244 (1998), pp. 22-30.
8) Moutsatsou A., Itskos, Koukouzas N. and Vounatsos P.P., *2009 World Coal Ash Conference (Wof A)*, May 4-7, 2009 in Lexington, KY, USA.
9) Balasivananda Prabhu S., Karunamoorthy L., Kathireson S. and Mohan B., *J of Mat. Proc. Tech.*, 171 (2006), pp. 268-273.
10) Sangghaleh A and Halali M, *Application of surface science*, vol. 255, issue 19, 15 july (2009) pp 8197-8308.
11) Jer-Horng Hsieh,Chun-Guang Chao, *Material Science and Engineering A*, 212(1996), pp. 102-107.
12) Behera R., Dutta A., Das S., Majumdar K., Chatterjee D. and Sutradhar J., *Indian Foundry Journal*, vol. 56, No. 5, pp. 43-50.
13) Hamid A.A., Jain S.C., Ghosh P.K. and Ray S., *Met. & Mat. Trans A*, 36 A (2005), pp. 2211-2223.
14) Maity P.C., Chakraborty P.N., Panigrahi S.C., *Mat. Laters*, 20 (1994), pp. 93-97.
15) Rohatgi P.K., Guo R.P., Huang and Ray S., *Met. & Mat. Trans A*, 28(A) (1997), pp. 245-251.
16) Rohatgi P.K. , JOM 46 (1994), 55-59
17) Rohatgi P.K., Guo R.P., Keshavram B.N., Golden D.M., *Trans American Foundry Society,CASF Transaction*, 103 (1995), pp. 575-579.
18) Bienias J., Walczak M., Surowska B., Sobczak J., *J of Optoelectronics and advanced materials*, vol. 5, No. 2 (2003), pp. 493-502.
19) R.C. Weast, *CRC Handbook of chemistry and physics*, 70th Ed (CRC Press, Boca Raton., Florida, USA 1990), D-33.
20) Sreeja kumara S.S., Pillai R.M. and Pai B.C., *Indian foundry journal*, Vol. 48, No. 1 January 2002.

Review on CO$_2$ Laser Cutting Process Parameter

Dhaval P. Patel, Asst. Prof., Mechanical Engineering Dept., Gandhinagar Institute of Technology
(dhaval.patel@git.org.in)

Abstract— **An experimental investigation is presented, which analyses the Co$_2$, laser cutting process for S.S and M.S sheet. It shows that by proper control of the cutting parameter, good quality cuts are possible at high cutting rates. Some kerf characteristics such as the width, heat affected zone (HAZ) and dross; in terms of the process parameters are also discussed. There are many research work done by researchers in the same field but still there is a scope to proper control of Assist gas (Oxygen) for M.S and (Nitrogen) for Aluminum material to achieve good finishing in cutting operation.**

Index Terms— **Laser Cutting, Process parameter, HAZ, Assist gas**

I. INTRODUCTION

A statistical analysis has arrived at the relationships between the cutting speed, laser power and work piece thickness, from which a recommendation is made for the selection of optimum cutting parameters for processing S.S and M.S material. The analysis of kerf width for constant cutting speed by varying power and assist gas pressure and for constant assist gas pressure by varying power and cutting speed. The author has explained the variation in cutting speed by changing plate thickness at constant power for both the materials of S.S. and M.S., by using experimental data. Some experiments also carried out for power by changing the thickness of plate at constant cutting speed for same materials.

The author has also carried out the comparison between M.S and S.S for various process parameters and microscopic examination results. Finally, here some general conclusions are concluded from various experiments carried out for different process parameters and also important of pressure of assist gas during cutting of material edge.

II. RELATION BETWEEN CUTTING SPEED AND LASER POWER

1. Experiement-1

Data for high power co$_2$ laser cutting process parameter (Material - M.S.)

Material Thickness (mm)	2	3	4	5	6	8
Assist gas (Oxygen) pressure (KPa)	10	10	10	8	7	7
Laser Power (Watt)	700	700	800	800	800	900
Cutting Speed (mm/min)	3000	2600	1800	1200	1000	800

General Conclusion:
If we have

Material Thickness (↑) (mm)	→	Laser Power (↑) (watt)	→ (but)	Cutting Speed (↓) (mm/min)

If we have increase material thickness of sheet metal then laser

power increase but cutting speed decrease.

2. Experiement-2

At constant thickness, to check other process parameter such

as Laser Power and Cutting Speed.

Material – Mild Steel

Assist gas pressure – 10 KPa

1. At 2 mm thickness:

(a) 2 mm thick sheet
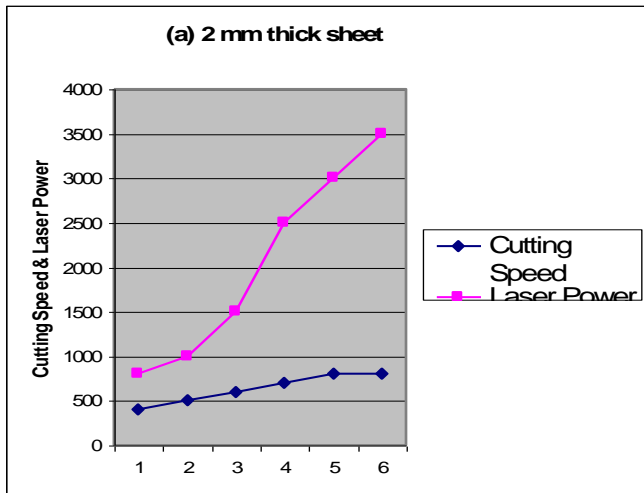
Laser Power (watt)	Cutting Speed (mm/min)
400	800
500	1000
600	1500
700	2500
800	3000 to 3500

2. At 3 mm thickness:

(b) 3 mm thick sheet
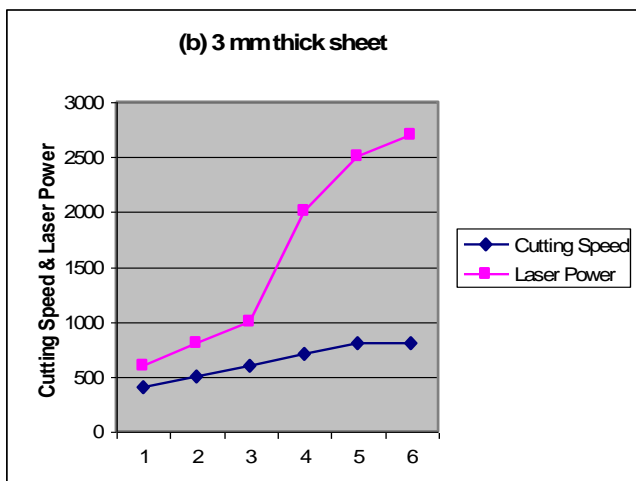
Laser Power (watt)	Cutting Speed (mm/min)
400	600
500	800
600	1000
700	2000
800	2500 to 2700

3. At 4 mm thickness:

(c) 4 mm thick sheet
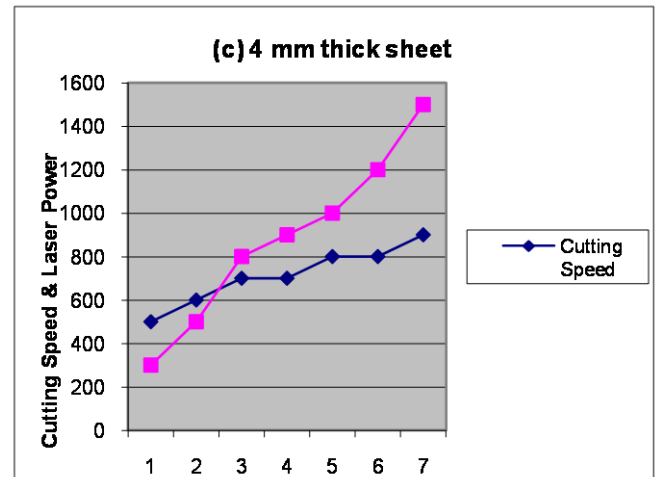
Laser Power (watt)	Cutting Speed (mm/min)
500	300
600	500
700	800 to 900
800	1000 to 1200
900	1500 (MAX.)

Conclusion:
If we have increased Laser Power then increase Cutting Speed at constant thickness.

3. Experiement-3

For stainless steel (S.S.) material:

(3.1) 400 Watt Power

Thickness (mm)	Cutting Speed (mm/min)
2	1500
3	1200
4	800 to 850

(3.2) 500 Watt Power

Thickness (mm)	Cutting Speed (mm/min)
2	2000
3	1500
4	1200

(3.3) 700 Watt Power

Thickness (mm)	Cutting Speed (mm/min)
2	3000
3	1800
4	1400

For mild steel (M.S.) material:

(3.4) 400 Watt Power

Thickness (mm)	Cutting Speed (mm/min)
2	800
3	600
4	300

(3.5) 500 Watt Power

Thickness (mm)	Cutting Speed (mm/min)
2	1000
3	800
4	300

(3.6) 700 Watt Power

Thickness (mm)	Cutting Speed (mm/min)
2	2500
3	2000
4	800 to 900

From above experimental data, we can see that the cutting speed decreases with increase in material thickness at constant power supply.

III. EXPERIEMENT FOR KERF CHARACTERISTIC

1. Experiment –1 (Kerf width in μm)

Material – Mild Steel; Thickness – 4 mm; Cutting Speed – 1350 mm/min

(1.1) Top surface of work-piece:
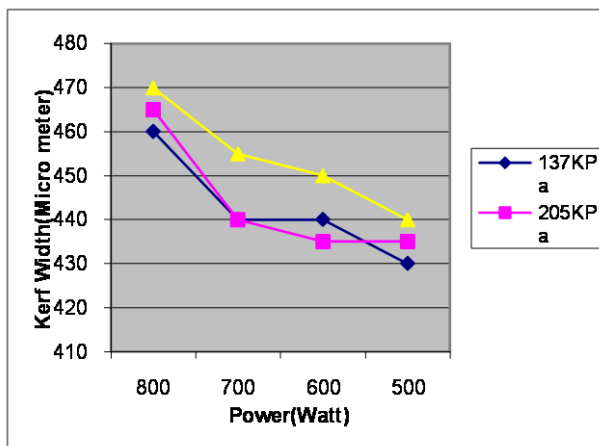
Laser Power (Watt)	Pressure (KPa)		
	137	205	274
800	460	465	470
700	440	440	455
600	440	435	450
500	450	435	440

(1.2) Bottom surface of work-piece:
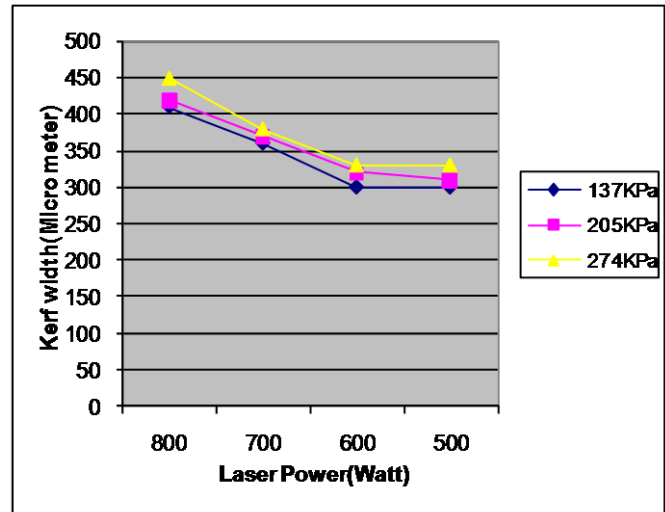
Laser Power (Watt)	Pressure (KPa)		
	137	205	274
800	410	420	450
700	360	370	380
600	300	320	330
500	300	310	330

2 Experiment – 2 (Kerf width in μm)

Material – Mild Steel; Thickness – 4 mm; Pressure – 102KPa

(2.1) Top surface of work-piece:
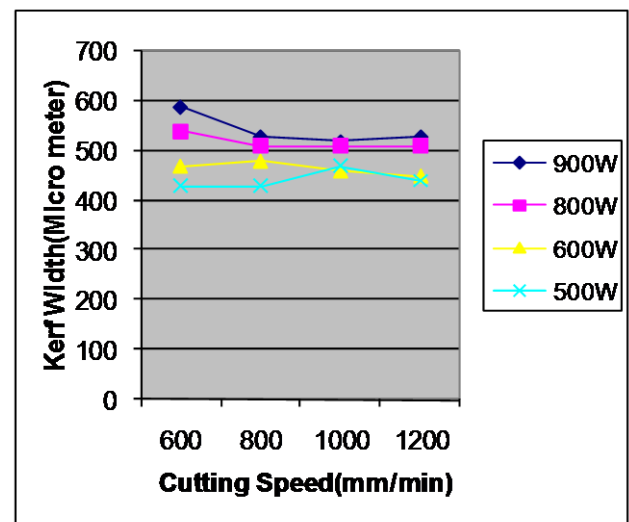
Laser Power (Watt)	Cutting Speed (mm/min)			
	600	**800**	**1000**	**1200**
900	590	530	520	530
800	540	510	510	510
600	470	480	460	450
500	430	430	470	440

Laser Power (Watt)	Pressure (KPa)		
	137	**205**	**274**
800	100	100	50
700	70	110	120
600	200	150	130
500	150	150	120

Material – Mild Steel; Thickness – 4 mm; Pressure – 102KPa

(2.2) Bottom surface of work-piece:
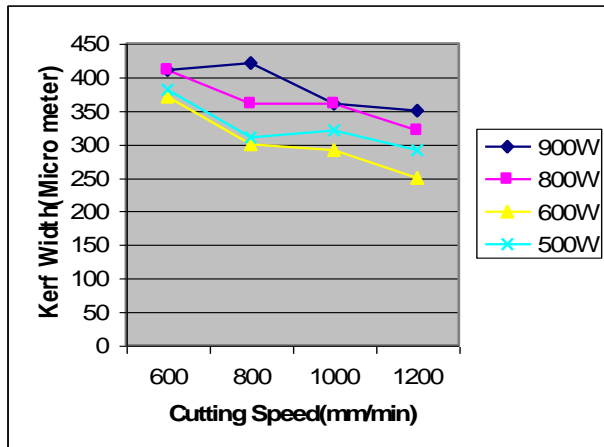
Laser Power (Watt)	Cutting Speed (mm/min)			
	600	**800**	**1000**	**1200**
900	410	420	360	350
800	410	360	360	320
600	370	300	290	250
500	380	310	320	290
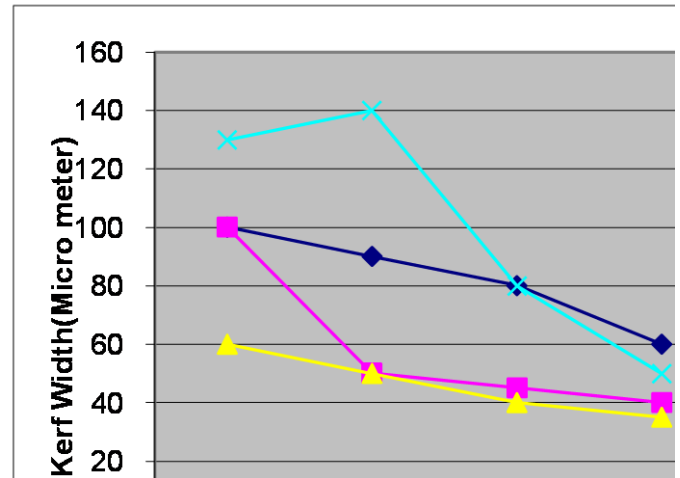
Laser Power (Watt)	Cutting Speed (mm/min)			
	600	**800**	**1000**	**1200**
900	100	90	80	60
800	100	50	45	40
600	60	50	40	35
500	130	140	80	50
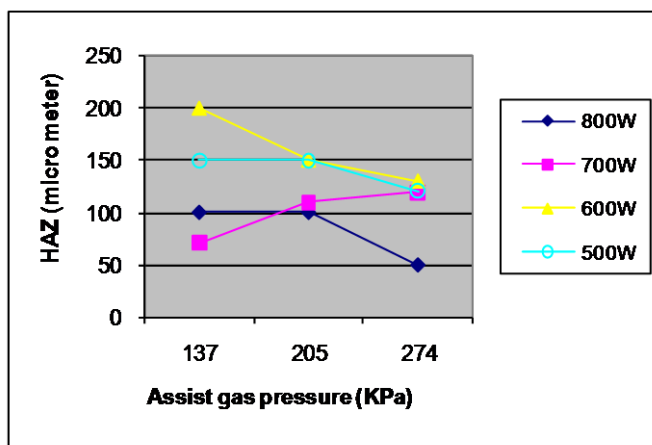
Conclusion:

The kerf width generally increases with increase in assist gas pressure and laser power and decrease in cutting speed.

By actual ready of M.S. material of thickness 4mm in which kerf width increase with increase in assist gas pressure and laser power and decrease in cutting speed.

Size of HAZ increases with an increase in laser power, but reduces with an increase in cutting speed.
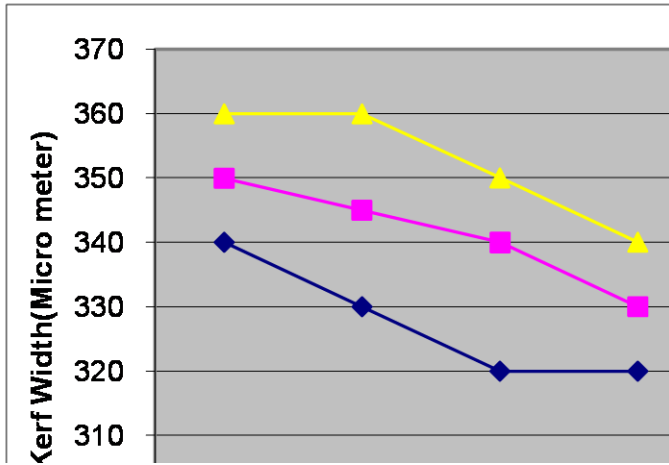
4. Experiment – 1 (Kerf width in μM)

Material – Stainless Steel; Thickness – 4 mm; Cutting Speed – 1350 mm/min
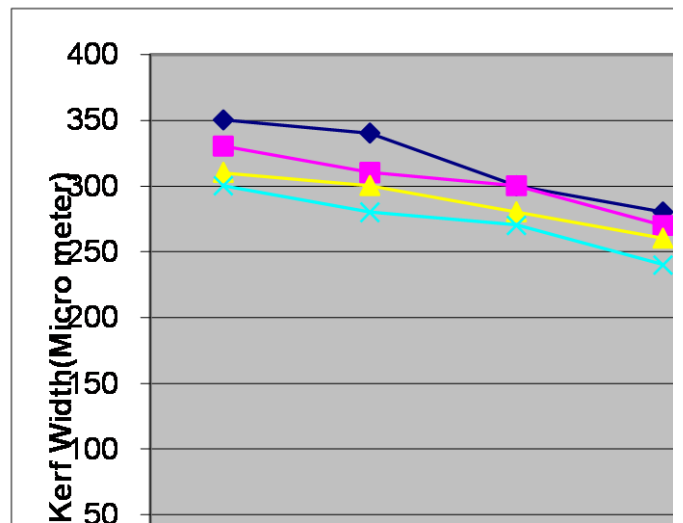
(4.1) Top surface of work-piece:

3. Experiment –3 (HAZ -Heat Affected Zone in μm)

Material – Mild Steel; Thickness – 4 mm; Cutting Speed – 1350 mm/min

Laser Power	Pressure (KPa)		
(Watt)	137	205	274
800	250	260	320
700	235	250	300
600	220	250	270
500	210	230	260

(4.2) Bottom surface of work-piece:

Laser Power	Pressure (KPa)		
(Watt)	137	205	274
800	340	350	360
700	330	345	360
600	320	340	350
500	320	330	340

5. Experiment –2 (Kerf width in μm)

Laser Power	Cutting Speed (mm/min)			
(Watt)	600	800	1000	1200
900	150	130	70	40
800	110	80	90	70
600	110	90	100	80
500	150	140	80	50

Material – Stainless Steel; Thickness – 4 mm;
Pressure – 102KPa

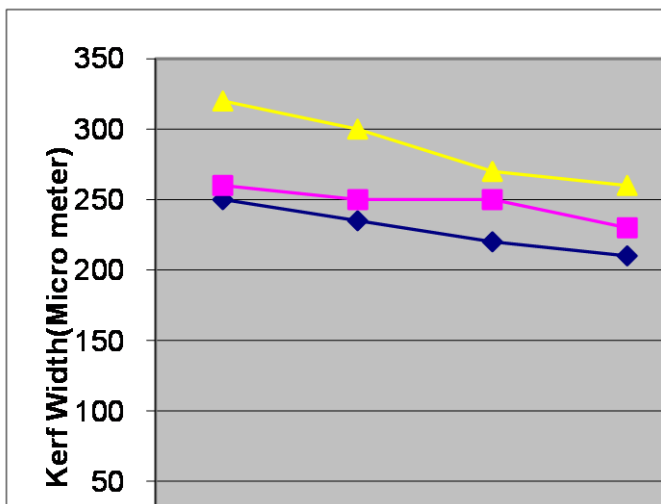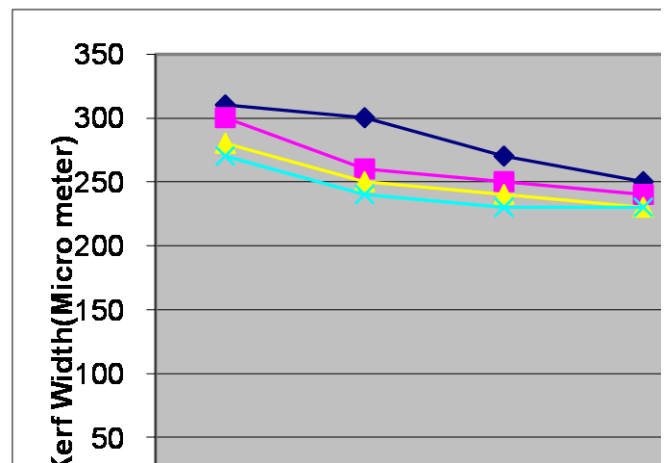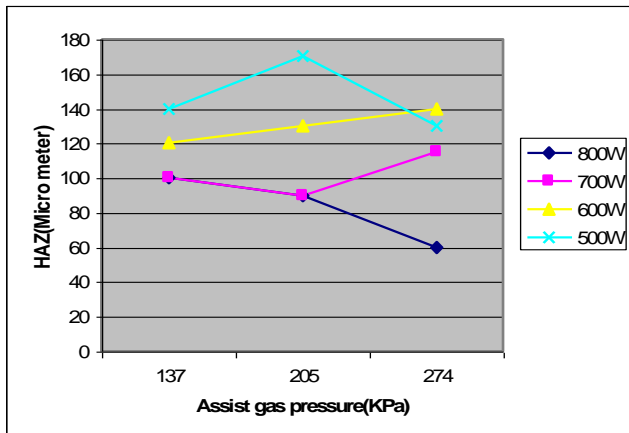| Laser Power	Cutting Speed (mm/min)			
(Watt)	600	800	1000	1200
900	350	340	300	280
800	330	310	300	270
600	310	300	280	260
500	300	280	270	240

(5.1) Top surface of work-piece:

(5.2) Bottom surface of work-piece:

6. Experiment –3 (HAZ -Heat Affected Zone in μm)

Material – Stainless Steel; Thickness – 4 mm;
Cutting Speed – 1350 mm/min

Material –Stainless Steel; Thickness – 4 mm;
Pressure – 102KPa

Laser Power	Pressure (KPa)		
(Watt)	**137**	**205**	**274**
800	100	90	60
700	100	90	115
600	120	130	140
500	140	170	130

Conclusion:

 The kerf width generally increases with increase in assist gas pressure and laser power and decrease in cutting speed.

By actual ready of S.S. material of thickness 4mm in which kerf width increase with increase in assist gas pressure and laser power and decrease in cutting speed.

Size of HAZ increases with an increase in laser power, but reduces with an increase in cutting speed.

IV. COMPARISON OF QUERRY'S MODEL AND MIYAZAKI'S MODELS FOR PROCESS PARAMETERS:

There are three classes of through cuts. In class I cut, the kerf width at bottom is greater than that of top surface and also cuts were obtained with massive dross attached at the bottom edges and surrounding area. In class II cuts also obtained with massive dross attached at the bottom edges and surrounding area. To achieve class III cuts are very difficult, because class III cuts are very accurate. For getting class III cuts with optimize   process parameters, here considering the comparison of two models given by Querry and Miyazaki. For this comparison all reading are taken from the previous experimental data.

Querry's model:

$$V = 7430 \ e^{-1.06} \ P^{\ 0.63}$$
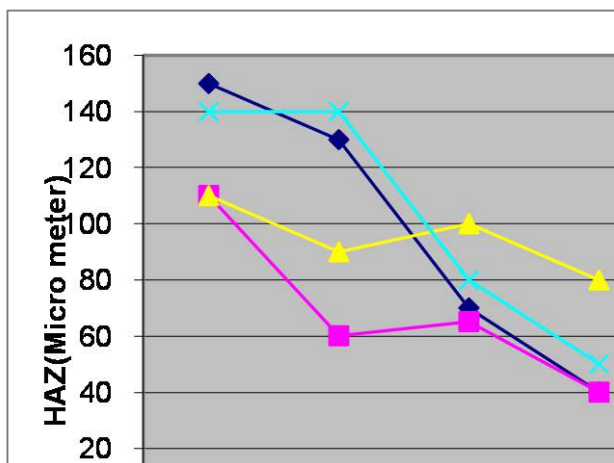
Miyazaki model:

$$V = 3500 \ e^{-0.56} \ P^{\ 0.5}$$

Where,
   V = Cutting speed
   e = Material thickness
   P = Laser power supply (kW)

Thick-ness (mm)	Assist oxygen pre. (kPa)	Laser Power (W)	Cutting Speed (mm/min)	Querry model	Miyazaki model
2	10	600	1500	2593	1839
3	10	700	2000	1857	1582
4	10	800	1200	1489	1440

Laser Power	Cutting Speed (mm/min)			
(Watt)	**600**	**800**	**1000**	**1200**
800	310	300	270	250
700	300	260	250	240
600	280	250	240	230
500	270	240	230	230

Table. (4.1)

For analysis, if cutting speed and energy consumption (laser energy input) are considered as economic measures, and cut quality is the technological performance measure, the

combinations of process parameters, which may be used for good quality cuts, are given in *Table (4.1)*. This recommendation is also consistent with that derived from the energy efficiency analysis presented above. The calculated cutting speeds for a given laser power and assist gas pressure from the two empirical models (curve fitted from experimental data) in the literature for sheet metals are also obtained for comparison. It is apparent that Querry's model can give cutting speeds to obtain class III cuts for the materials. But Miyazaki's model may be more applicable because all calculated cutting speeds are lower than that of Querry's model. Nevertheless, higher productivity can be achieved by using the recommendation from this study.

V. COMPARISON OF PROCESS PARAMETER FOR M.S. AND S.S

- From the observed results, we can conclude that, for the same Laser Power, Kerf Width in M.S. is greater than that of the S.S.

- At same Laser Power, Kerf width in M.S. for top surface is comparatively greater than that of the S.S. by varying the Assist gas pressure at constant Cutting Speed.

- At same Laser Power, Kerf width in M.S. for bottom surface is comparatively greater than that of the S.S. by varying the Assist gas pressure at constant Cutting Speed.

- At same Laser Power, Kerf width in M.S. for top surface is comparatively greater than that of the S.S. by varying the Cutting Speed at constant Assist gas pressure.

- At same Laser Power the HAZ in M.S. and S.S. is nearly same by varying Assist gas pressure at constant Cutting Speed.

- At same Laser Power the HAZ in S.S. is comparatively greater than that of M.S. by varying Cutting Speed at constant Assist gas pressure.

VI.   REVIEW OF RESEARCH ON CO_2 LASER CUTTING PARAMETER

Frank R. Wagner*a has worked on water-jet guided laser technology. Cutting of thin material, c.f. stencils, stents and thin wafers, is an important market for laser machining. Traditionally this task is performed using flash lamp pumped,

free-running Nd: YAG lasers. Using the water-jet guided laser technology, we experienced that the use of Q-switched lasers leads to superior results while cutting a variety of thin materials. In this technique, the laser is conducted to the work piece by total internal reflection in a thin stable water-jet, comparable to the core of an optical fiber. Utilizing this system, we obtain burr-free, slightly tapered cuts at the same speed as the classical laser cutting and without distinguishable heat affected zone.

Sang-Heon Lim1, Choon-Man Lee2 and Won Jee Chung2 has worked on optimization of process parameter by using Tacuchi method. Cutting by a high-speed laser-cutting machine is one of most effective technologies to improve productivity [3]. They have presented the cutting characteristics and optimal cutting conditions in a high speed feeding type laser cutting machine by using Tacuchi method in the design of experiment. An L9 (34) orthogonal array is adopted to study the effect of adjustment parameters. The adjustment parameters consist of cutting speed, laser power, laser output duty and assistant gas pressure. The surface roughness of sheet metal is regarded as a quality feature. Analysis of variance is performed in order to evaluate the effect of adjustment parameters on the quality feature of laser cutting process.

VII. CONCLUSION

- For the same Laser Power, Kerf width in M.S. is greater than that of S.S.

- At the same Laser Power. Kerf width in M.S. for top surface is comparatively greater to the tune of 23% than that of the S.S. when the Assist gas pressure is varying, keeping cutting speed constant.

- At the same Laser Power, Kerf width in M.S. for bottom surface is comparatively greater to the tune of 28% than that of the S.S. when the Assist gas pressure is varying, keeping cutting speed constant.

- At the same Laser Power, Kerf width in M.S. for top surface is comparatively greater to the tune of 47% than that of the

S.S. when the Cutting speed is varying, keeping Assist gas pressure constant.

- At the same Laser Power, Kerf width in M.S. for bottom surface is comparatively greater to the tune of 28% than that of the S.S. when the Cutting speed is varying, keeping Assist gas pressure constant.

- At same Laser Power the HAZ in M.S. and S.S. is nearly same when Assist gas pressure is varying, keeping Cutting speed constant.

- At same Laser Power the HAZ in S.S. is comparatively greater than that of M.S. when Cutting speed is varying, keeping Assist gas pressure constant.

The conclusion of this paper is to review of cutting parameter of laser cutting machine in which there is scope of change material property, assist gas pressure for different material cutting for fine cut for reducing scrape or more optimum use of material for fabrication work.

There are many method to use for analysis of cutting parameter from researcher was applying and also scope of unique method will apply for Laser cutting parameter which achieve good quality cutting edge.

REFERENCES

[1]   Charles L. Caristan "*Laser Cutting – Guide for manufacturing*", Society of Manufacturing Engineers, 2004, pp 1-13.

[2]   J. wang, " *An experimental analysis and optimization of CO_2 laser cutting process for metallic coated sheet steels*", the International Journal of Advance Manufacturing Technology, 200, pp 334-340.

[3]   Konig W., Meis F.U., Willerschied H., Schmitz-Justen C1, "*Process Monitoring of high power CO_2 lasers in manufacturing*", Proceedings of the second international Conference on Lasers in Manufacturing, IFS, 26-28 March, Birmingham, UK, 1985, pp 129-140.

[4]   M.Querry, *"Laser cutting*", in A. Niku-Lari and B. L. Mordike (ed.), High Power Lasers, Institute for Technology Transfer, Pergamon, 1989, pp 195-211.

[5]   Sang-Heon Lim, Choon-Man Lee and Won Jee Chung, "*A study on the optimal cutting condition of a high speed feeding type laser cutting machine by using Taguchi method",* the International Journal of Precision Engineering and Manufacturing, Vol.7, No.1.

[6]   O' Neil, W., Steen, W.M., "*Review of mathematical Model of laser cutting of steels*", Laser in Engineering, Vol. 3, 1994, pp 281-299.

[7]   www.sahajanandlaser.com

[8]   www.resonetics.com

[9]   www.trumpf.com

[10] www.lancerlaser.com

Effect of Silicon addition in LM25 Aluminium Alloy

Mr.Hitesh H. Patel

(email ID:hit2424@gmail.com)

Abstract—

  Aluminium alloys find wide application in all kind of industries. The major areas are Building and Construction, Container and Packaging, Transportation, Electrical conductor, Machinery and Equipments. These alloys have good casting properties, relatively high strength, high corrosion resistance and also it has good weldabilty etc. Typical alloying elements in Al alloys are copper, zinc, manganese, silicon, and magnesium.
Si is present as needle shape in cast condition. This needle shaped Si act as stress riser resulting in decreases in the ductility of alloy. The alloy was cast in to metal mould and was solution treated at 540o temperature for 4hrs, water quenched and precipitation hardened for 12 hrs at 1800C. Mechanical properties in terms of hardness and tensile test have been investigated inalloyed and unalloyed casting for both non-treated and heat treated condition. The fracture
surface of tensile specimens has been studied.

  Index Terms—LM25,SEM,UTM.

I. INTRODUCTION

Light weight and fuel efficiency in automobile industries are two important parameters due to more and more serious environmental problems nowadays. Aluminium alloys are desirable materials due to their high specific strength and stiffness for use in automobile industries as components of internal combustion engines, e.g., cylinder blocks, cylinder heads and pistons[1]. The properties of castability in an alloy depends on several factors as fluidity, volume shrinking, hot tearing, mould filling abilities and porosity forming, due to the chemical composition and mould design. Aluminum alloys are rejected in critical applications because of that porosity and shrink defects is common. By adding right content of alloying elements to the melt you will increase the mechanical properties. They are divided into two groups cast and wrought alloys[2].

  Aluminum-silicon alloys supplies a good combination of mechanical properties and castability and for those reasons, they are widely used in the automotive and aerospace industry [3]. Silicon increases the fluidity in aluminum casting alloys and reduces the solidification interval and hot tears tendencies.

Adding more than 13 % makes the alloy extremely difficult to machine but the volume shrinkage is reduced. Mechanical properties depend more on the way silicon are distributed then the amount of it in the alloy. In alloys where silicon particles are small, round and evenly distributed are usually displaying high ductility. Silicon are inexpensive and one of the few elements that can be added without increasing weight [4]. Porosity slightly decreases with increasing the silicon content [5].

II. EXPERIMENTAL TECHNIQUES

Fresh ingots of LM25 of about 600 gms weight were meltedin crucible type electrical resistance furnace. Melting was carried out under cover flux. Just prior to pouring N2 was used as degaser. Lime coated clean iron tools were used. The molten metal was stirred by graphite rods and was poured in metal mould to 200^0 C in order to overcome chilling effect. Finally metal mould casting was obtained. Then after Solution treatment was carried out at $540+5^0$C for 4 hours. Samples were quenched in water and ageing was carried out at 160^0C for 12 hrs. Samples for metallographic observation were prepared by grinding on emery paper using kerosene as lubricant. Those were then polished on sylvtan cloth with Al_2O_3 abrasive powder. Samples were then etched with 0.5%HF solution. Etched samples were then observed at 250X and 500 X magnifications on Neophot-2. The samples prepared for Metallography studies were also used for hardness testing. Hardness was measured on vicker hardness. Tensile test was measured on Universal tensile testing. UTS was found with the help of initial diameter of samples.
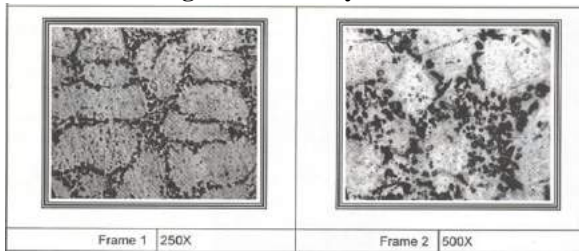
III. RESULTS

Samples	Ultimate Tensile strength Kg/mm2	%Elongation	Hardness VHN	Q index
A356 (Unalloyed)	165.4	2.30	72	219.65
A356 +T6	237.1	1.48	88.33	262.63

  Table.1Tensile Test &hardness of as cast and heat treated unalloyed A356
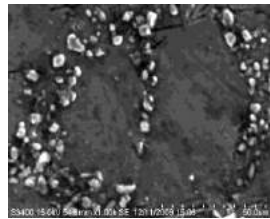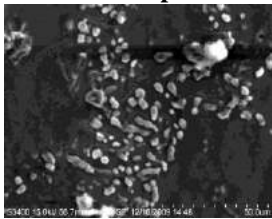
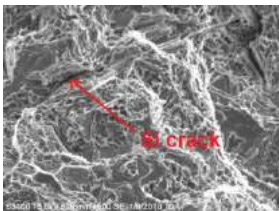- **Microstructure Observation:**
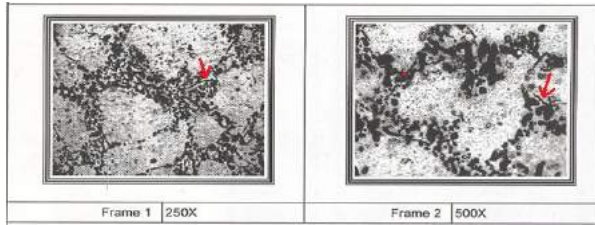
Figure 1: Unalloyed A-356

Figure 2.: A356 with 12 hrs Ageing

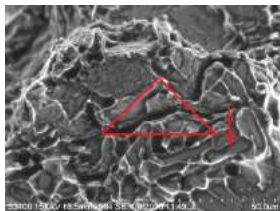- **Microstructural Observation By Scanning Electron Microscope:**

Fig 3:A356 as cast1.00k   **Fig 4:A356 12hrs ageing 1.00k**

- **Microstructure Of Tensile Fracture Samples Using Sem:**

Fig 6: A356 500x   **Fig 7: A356 after ageing 1.00k**

IV. RESULT DISCUSSION

The results of ultimate tensile, hardness and elongation measurement are shown in above table1. Here we can observe that after 4 hrs of solution treatment and 12 hrs of ageing process ultimate tensile strength and hardness increases. In A356 pure alloy the value of ultimate tensile strength (UTS) increases from 165.4 to 237.1 Kg/mm^2 and hardness increases from 72VHN to 88.33VHN as compared to as cast A356. In unalloyed 356 because of lower alloying elements that contributing to the formation of precipitates during aging process such as Mg, aging process did not high effect on the improvement of the mechanical properties clearly state the units for each quantity in an equation.

Fig. 1 consists of dendrite of primary α-Al phase together with interdendritic Al-Si irregular eutectic. Due to rapid rate of casting in metal mould, The majority of the eutectic silicon phase exhibits a modified morphology which is fibrous, and a small fraction of eutectic silicon phase has a coarse acicular shape. Intermetallic phase such as iron-rich phase may be observed at 500 X (indicated by arrowed in fig. 2). After a solution treatment at 540^0 C for 4 hrs all the fibrous silicon particles are transformed in to spherical shape as shown in fig.2.the dendrite arm spacing is to be reduced after ageing.

Fig.3 shows microstructure of A356 sample without heat treatment at different magnification alloy without addition of grain refiner/modifier inoculants. It is clear from the Fig.3 at 1000 X that the microstructure consists of coarse α-Al dendrites (∼50 μm in size) together with large plate like eutectic silicon needles in the interdendritic regions. It is well-known that this kind of microstructure is detrimental to the mechanical properties of the A356 alloy. After 12 hrs of ageing microstructure indicates uniform distribution rounded Si particles and its spherodisation (fig.4).

To better understand the failure mechanism of the castings under various loading conditions, the fracture surface of each specimen was examined with a scanning electronic microscope. The SEM of the tensile test specimen of the three cast alloy with and without heat treatmetn is shown in fig 6. Fracture surface are mainly composed to ductile fracture and cleavage fracture region are hardly observed in fig 6. There are some silicon cracks indicated by a mark in fig 6. in as cast unalloyed 356. Before heat treatment a number of small dimples, which is a typical characteristic of the ductile fracture, can be easily recognized. Studies have found that the fracture of cast aluminium alloys is often initiated by the cracking of silicon particles. [6]. Hence Si size, shape and distribution plays major role in the properties of Al-Si alloy.

V. CONCLUSION

Mechanical Properties improved after ageing process. The SDAS after solidification have an influence on when the aging peak is achieved. A small value of SDAS provides a faster time for the alloy to reach the aging peak.

REFERENCES

[1] Liu Yao-hui "High temperature friction and wear behaviour of Al2O3 and/or carbon short fibre reinforced Al–12Si alloy composites,2004,pp.275-285.

[2] U.S geological survey http://minerals.usgs.gov/ds/2005/140/aluminium.pdfH.

[3] On the uniform elongation of cast Al–7%Si–0.6%Mg (A357) alloys Nikolaos D. Alexopoulosa, Murat Tiryakio˘glubJ.

[4] Aluminium die casting alloys: alloy compostion and microstructure, and properties –preformence relationship. L. Wang, M. Makhlouf, and D. Apelian

[5] Microporosity formation in Al-Si-Cu-Mg casting alloy G.A Edwards, G.K Sigworth, C.H Caceres, D.H ST John, J Barresi

[6] M.N.Mazlee, Study of fracture of recycled aluminium alloys from automotive component,Feb 2007.

Numerical Investigation of Flow over cylinder for the study of different flow pattern

Prof. Hardik R Gohel[a], Prof. Absar M Lakdawala[b]

(hardik.gohel@git.org.in[a], absar.lakdawala@nirmauni.ac.in[b])

Abstract—**Numerical Investigation of a Flow Induced Vibration in Cross Flow around Triangular Array of Circular Cylinders was studied numerically, where the cylinder was allowed to vibrate in the transverse (cross-flow) and longitudinal directions. The computations were carried out at Reynolds number range of 500, 1000, 2000, 5000 and 10^4 with multi-cylinder with change in upstream cylinder positions at 20^0, 30^0, 45^0 and 60^0 and varying p/D ratio of 1.5 and 2, using FLUENT (version 6.3). The seven different flow patterns (Single Bluff Body (SBB), Base Bleed Flow (BBF), Shear Layer Re-attachment (SLR), Induced Separation (IS), Vortex Pairing and Enveloping (VPE), Vortex Pairing, Splitting and Enveloping (VPE), Periodic Gap Vortex Shedding (PGVS)) were identified from the present simulation.**

Index Terms—**Flow Induced Vibration, Cross Flow Over an Array of Cylinders, Vortex Shedding.**

I. INTRODUCTION

THE problem of vortex-induced vibration of structures is important in many fields of engineering. It is a cause for concern in the dynamics of riser tubes bringing oil from the seabed to the surface, in flow around heat exchanger tubes, in the dynamics of civil engineering structures such as bridges and chimneys, and also in many other situations of practical importance. The wide range of problems caused by vortex-induced vibration has led to a large number of fundamental studies.

For low sub-critical Reynolds number regime numerical simulations of the flow patterns around two staggered circular cylinders in cross-flow are presented in year 2005 by M.H.Akbari. The unsteady two-dimensional Navier-Stokes equations for this flow are solved using a numerical vortex method [1]. The characteristics of wake frequency, the switching phenomenon, and fluid forces acting on two circular cylinders in a side-by-side arrangement were investigated by Mahbub Alam in 2003 in detail [2]. Experimental setup prepared for cylinder in tandem arrangement by Mahbub Alam In 2003. The viability and accuracy of large-eddy simulation (LES) with wall modeling for high Reynolds number complex turbulent flows is investigated by Pietro Catalano (2003),

considering the flow around a circular cylinder in the super critical regime (Re $= 5 \times 10^5$ and 10^6) [3]. Numerical solutions have been obtained for steady viscous flow past a circular cylinder at Reynolds numbers up to 300 [4]. Z. Huang (2006) had performed a systematic study of flow around one cylinder, two side-by-side cylinders, one row of cylinders and two rows of cylinders [5]. The flow pattern through two rows of inline cylinders showed incomplete vortex shedding behind the first row at a separation distance. Karman vortices were not formed and a near-stagnant separated flow region appeared between the aligned cylinders. High Reynolds number flows (Re $= 1 \times 10^6$, 2×10^6 and 3.6×10^6, based on the free stream velocity and cylinder diameter) covering the super critical to upper-transition flow regimes around a two dimensional (2D) smooth circular cylinder, have been investigated by M.C.Ong (2009) numerically using 2D Unsteady Reynolds-Averaged Navier-Stokes (URANS) equations with a standard high Reynolds number $k - \varepsilon$ turbulence model [6]. Nine different flow patterns were identified, and processes of shear layer reattachment, induced separation, vortex pairing and synchronization, and vortex impingement, were observed by D.Sumner (2000). The flow around two circular cylinders of equal diameter, arranged in a staggered configuration, was investigated using flow visualization and particle image velocimetry for centre-to-centre pitch ratio p/D = 1.0 to 5.0 and angle of incidence $\theta = 0^0$ to 90^0[7]. In year 1996, C.H.K. Willamson had studied the three dimensional vortex behavior of flow past a bluff body [8]. Results predict that for a low Reynolds number flow (Re < 260) in wake region of the bluff-body the flow remains two dimensional behavior. Above Re > 260 the vortex generated due to flow past a bluff-body having a three dimensional nature of flow. A 2-D analysis is made for the dynamic interactions between viscous flow and one or more circular cylinders. The numerical procedure is based on the finite volume discretization of the Navier-Stokes equations on adaptive tri-tree grids which are unstructured and non-orthogonal [9]. Both a fully implicit scheme and a semi-implicit scheme in the time domain have been used for the momentum equations by G.X. Wu (2006), while the pressure correction method based on the SIMPLE (Semi Implicit Method for Pressure Linked Equation) technique is adopted to satisfy the continuity equation.

II. PROBLEM STATEMENT AND FORMULATION

Consider unsteady, two-dimensional, viscous, incompressible flow past triangular array of circular cylinder placed in a uniform stream, as shown schematically in fig 1. The flow is bounded by the plane at upper and lower side boundaries. These are treated as symmetry boundary condition, while vertical plane at left side and vertical plane right of the domain are considered as the flow inlet and outlet planes respectively. Three stationary cylinders are placed in triangular array, two upstream sides and one downstream side. Consider upper upstream side cylinder as cylinder-1, lower upstream side cylinder as cylinder-2 and downstream cylinder as cylinder-3 hereafter. All three stationary circular cylinders are of diameter D. It is observed from fig 1 that upstream cylinders were placed at $10D$ and $45D$ distance away from the inlet and outlet boundaries, respectively. The downstream cylinder-3 position is located with respect to upstream cylinders 1 and 2, by varying pitch p and orientation angle θ. Two different pitch (i.e. $1.5D$ and $2D$) and four different orientation angle θ (20^0, 30^0, 45^0 and 60^0) are considered in the present study.

A. Mathematical Modeling and Numerical Approach

Due to two-dimensional nature of flow, there is no flow in z-directions and no flow variables depend upon the z coordinate. Under these conditions, the equations of the continuity and momentum for an incompressible fluid reduce to:

Continuity equation:
$$\frac{\partial u}{\partial x} + \frac{\partial v}{\partial y} = 0 \tag{1}$$

X momentum equation:
$$\left[\frac{\partial u}{\partial t} + u\frac{\partial u}{\partial x} + v\frac{\partial u}{\partial y}\right] = -\frac{\partial p}{\partial x} + \frac{1}{Re}\left[\frac{\partial^2 u}{\partial x^2} + \frac{\partial^2 u}{\partial y^2}\right] \tag{2}$$

Y momentum equation:
$$\left[\frac{\partial v}{\partial t} + u\frac{\partial v}{\partial x} + v\frac{\partial v}{\partial y}\right] = -\frac{\partial p}{\partial y} + \frac{1}{Re}\left[\frac{\partial^2 v}{\partial x^2} + \frac{\partial^2 v}{\partial y^2}\right] \tag{3}$$

The variables for length, x and y velocity, time, pressure and temperature in governing equations were converted to dimensionless form as:

$$x = \frac{x^*}{D},\; u = \frac{u^*}{U_\infty},\; v = \frac{v^*}{U_\infty},\; t = \frac{U_\infty t^*}{D},\; P = \frac{P^*}{\rho U_\infty^2} \tag{4}$$

Vortex shedding from a smooth, circular cylinder in a steady flow is a function of Reynolds number. The Reynolds number is based on free stream velocity U and cylinder diameter D,

$$Re = \frac{\rho U_\infty D}{\mu} \tag{5}$$

The cylinder has been modeled as a two degree-of-freedom system with independent responses in x - the drag direction, and y - the lift direction. The initial conditions of the cylinder are zero displacement and velocity. As discussed in the introduction, the response is assumed to be two-dimensional with symmetry along the cylinder axis.

B. Boundary Conditions:

The appropriate boundary conditions for this flow are as follows:

1) *Inlet boundary at left vertical plane:* Uniform velocity inlet in x direction i.e.

$$u = 1,\; v = 0 \tag{6}$$

2) *Exit boundary at right vertical plane:* Constant pressure condition was applied. i.e.

$$P = 0,\; u = 1,\; v = 0 \tag{7}$$

3) *Side boundary at upper and lower plane:* Symmetry boundary was applied i.e.

$$\frac{\partial U_X}{\partial y} = 0, U_Y = 0 \tag{8}$$

4) *Cylinder wall:* No slip condition was applied i.e.

$$u = 0,\; v = 0 \tag{9}$$

C. Modeling in GAMBIT:

A bottom up modeling approach is followed for the present work. The flow domain is rectangular with multi-cylinder (fig 2). GAMBIT was used to generate a structured multi-block mesh around a cylinder of diameter $D = 1$.

D. Computational procedure in FLUENT:

A segregated, unsteady solver with 1st order implicit formulation, laminar viscous model was applied. Fluid properties were defined to adjust the Reynolds number. Operating pressure was selected as atmospheric pressure. Controls for solution were set to PISO second order central difference scheme with no skew-ness neighbor coupling. Model was initialized at inlet boundary. Animation for each time step was applied for vorticity contours. Total no of time step 34375 and time step size 0.016 was executed for analysis. Vorticity contour, pressure contour, xy plot of total pressure verses curve length is done as a part of post processing work.

III. RESULTS AND DISCUSSION

Computational domain, Grid, Time step was optimized by performing Domain independent study, Grid independent study, Time step independent study. Prior to presenting the new results obtained in this study, it is appropriate to establish the reliability and accuracy of present results.

A. Qualitative Results:

The computations were carried out at high Reynolds number range of 500, 1000, 2000, 5000 and 10^4 with multi-cylinder with change in upstream cylinders positions with respect to downstream cylinder at 20^0, 30^0, 45^0 and 60^0 with varying pitch ($1.5D$ and $2D$). Total 40 simulations on multi-cylinder array were performed for this study. Note that the total number of computations performed (40) on multi cylinder was arrived at by considering two different pitch (i.e. $1.5D$ and $2D$) × four different orientations (i.e. 20^0, 30^0, 45^0 and 60^0) × five different Reynolds number (i.e. 500, 1000, 2000, 5000 and 10^4).

Fig 3 describes the vorticity generation and Karman vortex street phenomenon for multi cylinder triangular array with $Re = 5000$, domain size $55D \times 30D$, total no of elements 33752 and time step size $\Delta t = 0.016$. Fig 3 shows the multi cylinder arrangement with triangular array with $p = 2$ and angle between downstream cylinder 30^0. Note that in these cases time step size is taken as $\Delta t = 0.016$, and Reynolds number taken as $Re = 5000$.

On cross flow over multi cylinder it was observed that the flow got supported from upstream cylinder and no wake formation was observed between upstream and downstream cylinder. However, the length of recirculation zone increases as pitch between upstream and downstream cylinder increase from $1.5D$ to $2D$. It was also observed that, for all configurations the cylinder array acted as a bluff body with recirculation zone between upstream and downstream cylinder. It was observed that the vortex of negative vorticity was started from the upper upstream cylinder and the vortex of positive vorticity was started from the lower upstream cylinder with a gap flow in between the upper and lower upstream cylinder. However, because of the influence of gap flow between upper and lower upstream cylinder, two separate vortex street generated, due to single centre downstream cylinder these vortex street get separated from each other and wake becomes wider (Fig 3). Similar trend were observed at different orientation of angle and different pitch. It was also observed that the onset of two different vortex street formations from upper upstream cylinder and lower upstream cylinder was affected by orientation angle and pitch.

B. Flow Pattern

Three different flow patterns were observed while cross flow takes place over array of triangular cylinder.

1. Single bluff-body pattern - For the triangular array of circular cylinder this phenomena is very critical. Array of circular cylinder act as a single body.
2. Flow patterns at small orientation angle θ.
3. Flow patterns at large orientation angle θ.

1. Single Bluff-Body Flow Pattern

When the cylinders are in contact, at p/D = 1.5 and $\theta = 20^0$ (figure 4), the flow pattern resembles that of a single bluff body. The near-wake region of the cylinder pair contains two free shear layers that alternately shed Karman vortices at the same frequency, much similar to single isolated circular cylinder. A single Karman vortex street, with two rows of vortices of opposite sign, is found downstream. A second single bluff-body flow pattern, with the added effect of gap flow, was also observed. The base-bleed flow pattern (BBF, figure 5), is seen at pitch ratios (p/D = 2) and very small angles of inclination ($\theta = 20^0$).

SBB

Single Bluff Body flow pattern (SBB, figure 4) was observed at small angles of incidence. For these configurations, the lengths of the two shear layers were considerably different, since the shear layer from the two upstream cylinders were significantly stretched in the stream-wise direction. This shear layer was prone to the development of instabilities. As the shear layer extends further from the upstream cylinders, the instabilities take on the appearance of small, Kelvin-Helmholtz vortices. Several of these instability vortices were then incorporated into the Karman vortex that rolls up in the near-wake region of the cylinders. In contrast, the small, instability vortices were absent in the shear layer formed behind the downstream cylinder. Regular Karman vortex shedding from the downstream cylinder was rarely interrupted, and, without the instabilities, the formation of Karman vortices occurred without the coalescence of smaller vertical structures.

BBF

Base Bleed Flow, a second single bluff-body flow pattern can be distinguished at angles of incidence, $\theta = 20^0$, and pitch ratio p/D = 2. The base-bleed flow pattern (BBF, figure 5) was essentially a modification to the SBB flow pattern, where the narrow gap permits a base-bleed flow to occur (hence it has been included with the single bluff-body flow patterns). Otherwise, this configuration of cylinders resembles a single bluff-body, with a single Karman vortex street in the combined wake (shown forming in figure 5). The main effect of the narrow gap was to permit fluid to enter the base region of the cylinder pair, which causes a stream-wise lengthening of the near wake region and the vortex formation length, compared with the previous case. Typically, a wider near wake region forms behind the downstream cylinder, since the base flow was deflected away from the mean flow direction.

2. Flow Pattern at Small Angle of Inclination

At small angles of incidence (θ) flow through the gap between the cylinders and vortex shedding from the upstream cylinder are mostly suppressed, except at large pitch ratios. Two flow patterns were identified within this range of incidence angle, as described in the following sections, and shown in figures 6 and 7. It is within this range of incidence that some of the more interesting lift and drag force changes have been observed by other researchers, in the upper sub-critical regime.

SLR

Shear Layer Re-attachment flow pattern (SLR) observed for small pitch ratio, p/D = 1:5 and small inclination angle, $\theta = 30^0$ (figure 6). The flow was not substantially different from the single bluff-body case, (the SBB pattern, specifically) see figure 6. Although there was now a gap between the two cylinders, flow through the gap was prevented by the formation of a separated shear layer from the inside surface of the upstream cylinder. Consequently, the structure of the combined wake remains essentially the same as the SBB flow pattern, with a single Karman vortex street (and Strouhal number) in the combined wake of the cylinder pair. As with the SBB flow pattern, the outer shear layer of the upstream cylinder remains highly stretched in the stream-wise direction, and was prone to the same waviness and instability vortices. Consequently, the periodic, alternate vortex shedding process was often interrupted, particularly from the stretched shear layer from the upstream cylinder. Through analysis of the vorticity contours at different time step, the shear layer reattachment process was observed to be a steady phenomenon. Synchronized, alternating shear layer reattachment was thus unique to this configuration. Within the interstitial region, bounded by the reattached shear layer on one side, and by the free shear layer from the upstream cylinder on the opposite side, the flow visualization images (figure 6) show mostly stagnant fluid in the gap between the cylinders.

IS

Induced Separation flow pattern observed at p/D = 2 and $\theta = 30^0$. Here, the downstream cylinder was now situated further away from the flow axis of the upstream cylinder, and it was now easier for the inner shear layer from the upstream cylinder to be deflected into the gap between the cylinders. In addition, some of the oncoming mean flow was now permitted to penetrate the gap between the cylinders. This gap flow effectively signals the end of the stretched shear layer from the outside of the upstream cylinder. In its place, a small near-wake region forms behind the upstream cylinder (figure 7), this small region was highly constrained within the gap between the cylinders, and was biased away from the downstream cylinder and the flow axis. Each of the shear layers bounding the near-wake region rolls up in an alternating, periodic fashion, into small diameter Karman vortices. The Karman vortices from the inner shear layer, however, form very close to the surface of the downstream cylinder, and induce a separation of the flow from this cylinder. Production of vorticity about the second cylinder accompanies the separated flow. The induced separation is periodic, at the same frequency as the Karman vortex shedding from the upstream cylinder. A pairing of vorticity of opposite sign was noticed across the gap, but the paired vorticity was enveloped by a vortex from the outer shear layer of the upstream cylinder, to form a single larger composite vortex (figure 7). Within the pair, the dominant vorticity was that induced on the surface of the downstream cylinder (figure 7). The induced separation and vorticity production on the inner surface of the downstream cylinder was distinct from Karman vortex formation, since it did not involve the formation and roll-up of a free shear layer. The induced vortex formation occurs at the same frequency as Karman shedding from upstream cylinders, and pairing of vorticity of opposite sign is seen just beyond the second row. The combined wake of the cylinder group remains similar to that for the type single bluff body and shear layer reattachment flow patterns, with two rows of Karman vortices. However, the frequencies of Karman vortex formation were different for each row, since those formed from the outer shear layer of the downstream cylinder are considerably lower. This difference in the rate of vortex formation, found in the combined wake of the cylinder pair, was an important flow feature of the staggered configuration for a wide range of p/D and θ.

3. Flow Pattern at Large Angle of Inclination

At larger angles of incidence $\theta > 30$, a portion of the oncoming mean flow was always permitted to enter the gap between the two cylinders (figure 8). Vortex shedding now occurs from each of the cylinders, for all the flow patterns at higher angles of incidence. The flow patterns at higher angles of incidence appear as evolutions of the induced separation flow pattern. Vortex shedding from each cylinder occurs for two reasons. First, the angle of incidence was now sufficiently high that the inner shear layer from the upstream cylinder no longer reattaches onto the downstream cylinder consequently, the shear layer reattachment flow pattern was not observed. Second, the potential for vortex impingement decreases at larger angles of incidence θ, since the downstream cylinder was situated further from the flow axis of the upstream cylinder.

VPE

Vortex Pairing and Enveloping flow patterns observed at p/D = 1.5 and 2. At smaller pitch ratios the gap flow for the higher incidence cylinder pairs was appreciably narrower, and the near-wake region behind the upstream cylinder was more constrained and distorted (figures 8). However, the pairing of vortices of opposite sign across the gap results in a counter rotating vortex pair structure at the gap exit, which was then enveloped by a Karman vortex from the outer shear layer of the upstream cylinder, see figure 8. The first pattern involves complete enveloping of the gap vortex pair, designated as the Vortex Pairing and Enveloping flow pattern (VPE, figures 8). This flow pattern was marked by two rows of vortices in the combined wake of the cylinders.

VPSE

A second pattern with incomplete enveloping, involving splitting of the vortex pair, was designated as the Vortex Pairing, Splitting and Enveloping flow pattern (VPSE, figures 8). The more prevalent of the two gap vortex pairing and enveloping flow patterns was the VPSE pattern, in which the enveloping process was incomplete. Because of the greater distance between the gap shear layers, and the Karman vortices formed from them, each inner gap vortex splits into two concentrations of vorticity during the enveloping process. The split vorticity typically forms a third row of smaller vortices in the combined wake of the cylinders. The combined wake of the cylinder pair then contains three rows of vortices, with two rows of like sign vortices behind the upstream cylinder, these two like sign vortex rows represent an unstable arrangement. In both the VPE and VPSE flow, as demonstrated by the vorticity contours, three of the four shear layers and their associated vortex formation and shedding process had the same high frequency of vortex shedding. These contrasts with the traditional understanding of the staggered configuration, which implies that high and low frequency vortex shedding, were associated with individual cylinders, rather than with individual shear layers. The two different frequencies of vortex shedding mean that the combined wake of the cylinders contains an irregular street of two rows of vortices. The low frequency shedding from the outer shear layer of the downstream cylinder was often modulated by the high frequency vortex shedding occurring elsewhere. When this modulation occurred, the low frequency shedding was interrupted this often meant that two subsequent Karman vortices combined to form a composite vortex. As the angle of incidence was increased within the VPE flow pattern, the gap flow becomes less deflected, and enveloping occurs further downstream. If the pitch ratio was reduced, meaning the cylinders were positioned closer together, Karman vortex formation was suppressed from the inner shear layer of the downstream cylinder.

PGVS

The periodic gap vortex shedding was observed at very high angle of incidence $\theta = 60^0$ and p/D = 1.5 and 2. This flow pattern was found similar to VPE and VPSE, however the vortices shed from the upstream cylinders were periodic in nature. The positive and negative vortices shed from top and bottom upstream cylinder periodically.

IV. CONCLUSIONS

Numerical Investigation of a Flow Induced Vibration in Cross Flow around Triangular Array of Circular Cylinders was carried out using available commercial CFD package FLUENT-6.3. The computations were carried out at high Reynolds number range with multi-cylinder with change in upstream cylinder positions and varying pitch. For the case of multi cylinder arrangement gap flow effect was observed, which was a new finding from present study. It was also observed that, because of influence of gap flow, vortex generated from upper downstream cylinders interacts with the vortex generated from downstream cylinder. Seven different flow patterns were observed, which are Single Bluff Body (SBB), Base Bleed Flow (BBF), Shear Layer Re-attachment (SLR), Induced Separation (IS), Vortex Pairing and Enveloping (VPE), Vortex Pairing, Splitting and Enveloping (VPSE), Periodic Gap Vortex Shedding (PGVS).

V. REFERENCES

[1] Akbari M.H., Price S.J., 2005, "Numerical investigation of flow patterns for staggered cylinder pairs in cross flow" Journal of Fluids and Structures 20, 533-554.

[2] Alam M.M., Moriya M., Sakamoto H., 2003, "Aerodynamic Characteristic of two side by side circular cylinders and application of wavelet analysis on the switching phenomenon". Journal of Fluids and Structures 18, 325-346.

[3] Catalano P., Wang M., Iaccarino G., Moin P., 2003, "Numerical Simulation of the flow around a circular cylinder at high Reynolds number". International Journal of Heat and Fluid Flow 24, 463-469.

[4] Fornberg B., 1980, "A numerical study of steady viscous flow past a circular cylinder". Journal of Fluid Mechanics, vol. 98, part 4, 819-855.

[5] Huang Z., Olson J.A., Kerekes R.J., Green S.I., 2006, "Numerical simulation of the flow around rows of cylinders". Computers and Fluids 35, 485-491.

[6] Ong M.C., Utnes T., Holmedal L.E., Myrhaug D., Pettersen B., 2009, "Numerical simulation of flow around a smooth circular cylinder at very high Reynolds number". Marine Structures 22, 142-153.

[7] Sumner D., Price S.J., Paidoussis M. P., 2000, "Flow pattern identification for two staggered circular cylinders in cross-flow". Journal of Fluid Mechanics, vol. 411, 263-303.

[8] Williamson C.H.K., 1996, "Three-dimensional vortex dynamics in bluff body wakes". Experimental Thermal and Fluid Science 12, 150-168.

[9] Wu G.X., Hu Z.Z., 2006, "Numerical simulation of viscous flow around unrestrained cylinders". Journal of Fluids and Structures 22, 371-390.
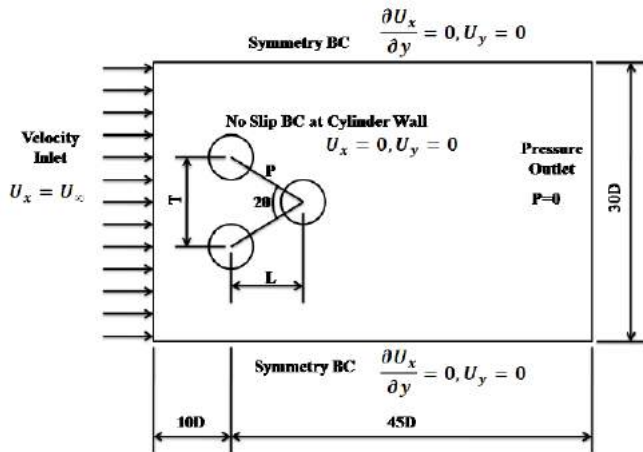
List of Figure

Figure 1 Computational configuration for multi cylinder triangular array

Figure 2 Triangular array multi-cylinder domain with meshing (a) Domain mesh in GAMBIT, (b) Zoomed view of quadrilateral mesh near cylinder wall in GAMBIT and (c) Boundary layer applied near cylinder wall in GAMBIT
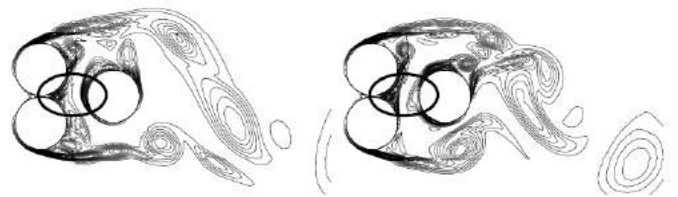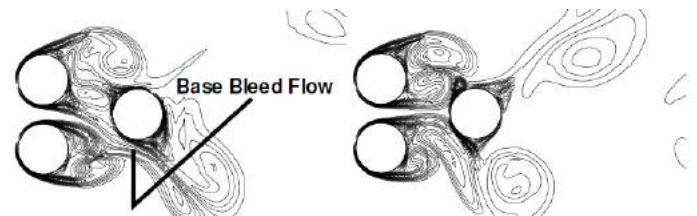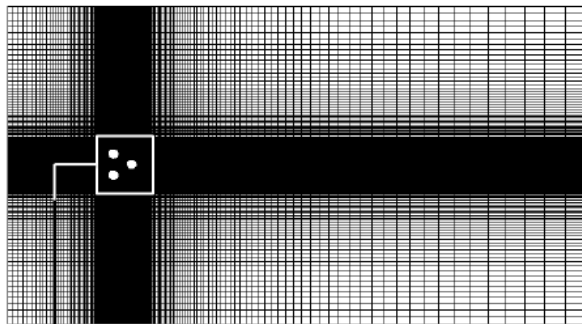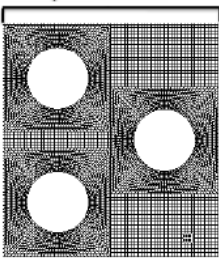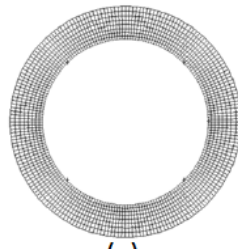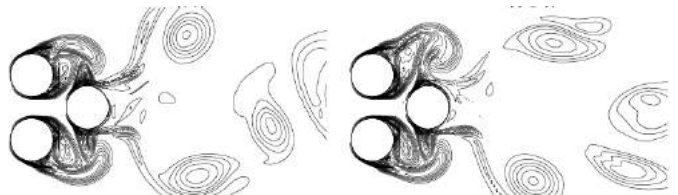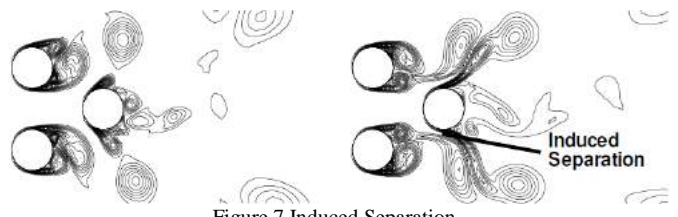

Figure 3 Evolution of vorticity contour

Figure 4 Single Bluff Body

Figure 5 Base Bleed Flow

Figure 6 Shear Layer Re-attachment

Figure 7 Induced Separation

Figure 8 Vortex Pairing and Enveloping; Vortex Pairing, Splitting and Enveloping

Development of Test Rig for Vibration Monitoring of Bearing

Amit R Patel

amit.er1984@gmail.com

Abstract — **Bearing failure is one of the foremost causes of breakdown in rotating machines, result in time and economical losses. In this paper Test rig for vibration monitoring of bearing have been designed. The design of test rig includes design of Shaft, Bearing selection, pedestal selection, motor selection, and base preparation. A 3-D model have been developed using Pro-engineer modelling software. The vibration signals generated by the healthy/faulty bearing can be captured by the accelerometer mounted on the test bearing. The analysis of the vibration signal is useful for the condition monitoring of rolling element bearings.**

Keywords - **Bearing defect, Defect detection, Vibration monitoring and analysis, Design and Analysis.**

I. INTRODUCTION

Bearings are among the most important and frequently used components in the majority of rotating machines. Breakdowns in rotating elements result in loss of time and cost. The study of vibrations generated by mechanical structures and electrical machines are very important. Till today a lot of study had been completed in various fields like, Expert systems (fixed plant, laboratory and industry testing), Gear box, Planetary Gear box, Railway freight cars, A Conveyor Drive unit, Lathe machine elements, Paper mills, Electrical equipments like Induction machines, Reactor coolant pumps, Nuclear power plants etc.
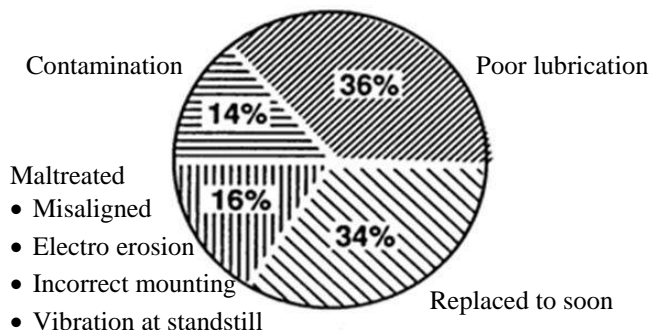

Figure 1: Classification & distribution of the causes of failure [1]

Ball bearings may contain manufacturing errors or mounting defects. Damage may also occur during working conditions. Such errors cause vibration, noise, and even failure of the whole system. The main problems are concentrated on the lubrication situation of the bearings. Figure 1 gives the classification and distribution of the reasons for which rolling element bearings did not reach their calculated lifetime.

A. Types of bearing

i) Plain bearing: Rubbing surfaces usually with lubricant.
ii) Rolling element bearing: ball or rollers are used to prevent or minimize rubbing. Deep groove ball bearing, angular contact ball bearing, cylindrical roller bearing, taper roller bearing, spherical roller bearing.

B. Possibilities of bearing failure

i) *Distributed defects:* Surface roughness, waviness, and misaligned races of bearing.
ii) *Localized Defects*: Cracks, Pits and spall caused by fracture on the rolling surface.

C. Methods for Bearing Fault Detection

The approaches used to study the effect of localized defects are,

i) Run the bearing until failure and monitor the changes in their vibration response.
ii) Intentionally introduce the defect in the bearing by techniques such as spark erosion, scratches and indentation and measure the vibration response. Compare the response with the defect and healthy bearing.

II. DIFFERENT CONDITION MONITORING TECHNIQUES

Many different techniques have been used for condition monitoring of bearing. Some of them are listed below.
- Vibration measurement in time and frequency domains
- Shock pulse method, Sound pressure and Sound intensity techniques.
- Acoustic emission method
- Temperature measurements
- Wear debris analysis
  - o Vibration, shock pulse, spike energy
  - o Ferrography and chip detection
  - o Spectrographic oil analysis

A. Time Domain Approach

Time domain refers to a display or analysis of the vibration data as a function of time. Time wave form analysis includes the visual inspection of the time history of the vibration signals, time wave form indices, probability density function, and probability density moments. The first and second moments are well known, being the mean value and the variance, respectively. The third moment normalized with respect to the cube of standard deviation is known as the coefficient of "skewness". The fourth moment, normalized with respect to the fourth power of standard deviation, is quite useful, is called "kurtosis"[2,7].

B. Frequency Domain Approach

The time domain vibration signal is typically processed into the frequency domain by the application of Fourier transform, usually in the form of fast Fourier transform FFT algorithm. The principal advantage of the method is that the repetitive nature of the vibration signals is clearly displaced as peaks in the frequency spectrum at the frequency where the repetition takes place [3]. The interaction of the defect in the rolling element bearings produces pulses of very short duration. Each bearing element has a characteristic rotational frequency.

With a defect on a particular bearing element, an increase in the vibration energy at this element rotational frequency may occur. The ability to diagnose a mechanical fault is enhanced if the monitoring signal can be pre processed to reduce the effect of unwanted noise. *Adaptive Noise Cancelling ANC*, is a method to improve the signal to noise ratio.

By using a method called *High Frequency Resonance Technique (HFRT)*, or envelope technique. The filtered signal is rectified and demodulated in order to extract the envelope of the modulated carrier frequency signal [4].

C. Proximity Transducer Technique

Non-contact type, the transducer senses the displacement of the outer race directly as the rolling elements pass under it. Thus the extraneous vibrations of the housing structure are reduced or eliminated and the signal-to-noise ratio is improved [2].

D. Acoustic Emission Technique

It is an important tool for condition monitoring through non-destructive testing. AE instrumentation consists of a transducer, mostly of the piezoelectric type, a preamplifier and a signal-processing unit. AE transducers are designed to detect the very high frequency stress waves that are generated when cracks extend under load. The bandwidth of the AE signal can also be controlled by using a suitable filter in the preamplifier. The advantage is that it can detect the growth of the subsurface cracks [2, 3].

E. Automated Diagnostic System:

The techniques discussed above need a human interpreter to analyse the results. An Artificial Neural Network (ANN) can be defined as a mathematical model of the human brain and has the ability to learn to solve a problem, rather than having to be pre-programmed with a precise algorithm. ANN emerges as a popular tool for signal processing and pattern classification task. Bearing vibration to be used by a pattern classifier to detect and diagnose the defect.

III. DESIGN PROCEDURE FOR DEVELOPMENT OF TEST RIG

A. Selection of Electric motor.

The main advantage of a DC motor over an AC motor is that it can operate directly from a battery. The speed of a DC motor can be controlled with armature voltage controlling. Here, ROTOMAG make, PMDC motor having model number M7-T of power rating 1hp, torque capacity 4.8 N.m have been selected.

B. Belt Pulley Design:

As the V belts are endless type and can have very small belt slip. These belts are available in various sections (A, B, C, D, E) depending upon power rating [9]. If the required power transmission falls in the overlapping zone, then one has to justify the selection from the economic view point.

As per the standard data available for 1 to 25 HP, V Belt having 'B' sections have been selected [6].

Design Horsepower = Transmission hp x Service Factor

By using Design horsepower and motor rotational speed one can calculate minimum pulley diameter.

Minimum Pulley dia $(D_{pm}) = 1.3 \times \sqrt{\dfrac{p}{N_{motor}}}$

Available pulley have been selected for component shaft side. Component Shaft side pulley Diameter (D_{ps}) and from that one can calculate,

Velocity ratio = $\left(\dfrac{D_{ps}}{D_{pm}}\right) \times (1 - s)$

Now, depending on available space the centre distance is selected. In the case of flat belts, there is virtually no limit to the center-to-center distance. Long center-to-center distances are not recommended for V belts because the excessive vibration of the slack side will shorten the belt life materially. In general, the center to center distance should be no greater than 3 times the sum of the sheave diameters and no less than the diameter of the larger sheave [9].

Center distance (C) = $D_{ps} < C < 3 \ (D_{ps} + D_{pm})$

Calculations involving the belt length and belt speed have been carried out based from the following equations.

$\text{length} = L = \left(D_{ps} + D_{pm}\right) \times \dfrac{\pi}{2} + 2C + \dfrac{(D_{ps} - D_{pm})^2}{4 \times C}$

Belt speed = $\dfrac{\pi D_{pm} N_{motor}}{60}$

If speed is higher, then centrifugal tension F_c can be calculated as,

$$F_c = m \ v^2$$

Arc of contact have been calculated from the following equation,

$$\theta = 180 - 2\sin^{-1} \dfrac{(D_{ps} - D_{pm})}{2C}$$

Now, Number of belt require to transmit the power have been calculated from the below equation,

$$\text{Number of belt} = \dfrac{\text{Design power}}{\text{power rating of belt(kw)} \times C_{vw} \times C_{vl}}$$

C. Maximum Stress Calculations for the Shaft

First, Minimum diameter of shaft have been selected. Further, provision of different steps of diameter on the shaft will increase the future research scope. The load application

and maximum bending moment have been calculated at each point on the component.

Figure 2: Shaft considering as load applied at each point

i) Load calculation at Belt – Pulley end point.
Here, due to belt pulley assembly, tight side and slack side tension have been calculated first.
From the below equation,

$$\left(\frac{T_1}{T_2}\right) = e^{\mu\theta} \qquad (1)$$

Torque at motor shaft output $T = (T_1 - T_2) \times R \qquad (2)$

T_2, T_1 value can be solved by equation (1) and (2). Adding the weight of pulley will give the maximum load at this end.

Bending moment at Pulley side and load side can be calculated from the following equation,

$$= \text{Total load on shaft end x overhung distance}$$

Now, from the plotting a shear force and bending moment diagram for each loading and supporting point, Calculation have been carried   one can have clear idea, about the maximum bending moment generated on each point of the shaft.

D. Selection of Shaft Material

First, calculation of torque at shaft component have been carried out from the equation, $N_1T_1 = N_2T_2$

When the shaft is subjected to combined twisting moment and bending moment, then the shaft must be designed on the basis of the two moments simultaneously. The following two theories have been considered while designing the shaft [5].
1. Maximum shear stress theory or Guest's theory.
   - It is used for ductile materials such as mild steel.
2. Maximum normal stress theory or Rankine's theory.
   - It is used for brittle materials such as cast iron

According to maximum shear stress theory, the maximum shear stress in the shaft,

$$\tau_{max} = \frac{1}{2}\sqrt{(\sigma_b)^2 + 4\tau^2} \qquad (3)$$

$$M = \frac{\pi}{32} \times \sigma_b \times d^3 \implies \sigma_b = \frac{32 \times M}{\pi \times d^3}$$

(4)

$$T = \frac{\pi}{16} \times \tau \times d^3 \implies \tau = \frac{16 \times T}{\pi \times d^3}$$

(5)

Putting the value of equation (4) and (5) in the equation (3),

$$\tau_{max} = \frac{1}{2}\sqrt{\left(\frac{32 \times M}{\pi \times d^3}\right)^2 + 4\left(\frac{16 \times T}{\pi \times d^3}\right)^2}$$

$$\frac{\pi}{16} \times \tau_{max} \times d^3 = \sqrt{M^2 + T^2}$$

$$\tau_{max} = \left(\frac{16}{\pi d^3}\right) \times T_e \qquad (6)$$

The expression $\sqrt{M^2 + T^2}$ is known as *equivalent twisting moment* and is denoted by *Te*.

Now according to maximum normal stress theory, the maximum normal stress in the shaft,

$$\sigma_{bmax} = \frac{1}{2}\sigma_b + \frac{1}{2}\sqrt{(\sigma_b)^2 + \tau^2}$$

(7)

using equation (4) & (5) in equation (7)

$$\sigma_{bmax} = \frac{1}{2}\left(\frac{32 \times M}{\pi \times d^3}\right) + \frac{1}{2}\sqrt{\left(\frac{32 \times M}{\pi \times d^3}\right)^2 + 4\left(\frac{16 \times T}{\pi \times d^3}\right)^2}$$

$$\sigma_{bmax} = \frac{32}{\pi d^3}\left[\frac{1}{2}\left(M + \sqrt{M^2 + T^2}\right)\right]$$

$$\frac{\pi}{32} \times \sigma_{bmax} \times d^3 = \frac{1}{2}\left(M + \sqrt{M^2 + T^2}\right)$$

The expression $\frac{1}{2}\left(M + \sqrt{M^2 + T^2}\right)$ is known as *equivalent bending moment* and is denoted by *Me*.

$$\sigma_{bmax} = \left(\frac{32}{\pi d^3}\right) \times Me$$

(8)

In actual practice, the shafts are subjected to fluctuating torque and bending moments. In order to design such shafts like line shafts and counter shafts, the combined shock and fatigue factors must be taken into account subjected to combined bending and torsion,

The equivalent twisting moment,

$$T_e = \sqrt{(k_m \times M_b)^2 + (k_t \times T)^2}$$

And equivalent bending moment,

$$Me = \frac{(k_m \times M_b) + \sqrt{(k_m \times M_b)^2 + (k_t \times T)^2}}{2}$$

The maximum shear stress induced have been calculated using above equation (6) and (8). By considering *Maximum shear stress τ_{max}* and *bending stress stress σ_{bmax}* material selection procedure have been carried out.
First the material is selected and calculation of its tensile strength have been carried out as per the below procedure.

Minimum tensile strength, S_{yt}, and Factor of Safety

$$\tau_{max} = \frac{Syt}{2 \times \text{Factor of safety}}$$

Material selected procedure is such that, it can withstand the above calculated stresses.

The equation to calculate the toque that is required for the motor to make the inertia load start rotating is as follows.

$$T = I \times \alpha$$

Where I = the moment of inertia of the selected component,
   and α = angular acceleration

Various *types of keys* used for transmitting torque : Square Key, Flat Key, Round Key, Kennedy key, wood ruf key.

General drawing of designed shaft can be drawn using computer modelling software. One of the example is given below.
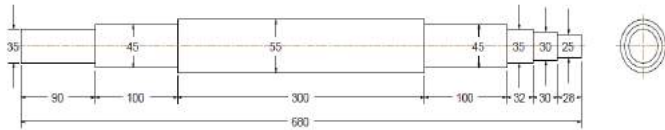

Figure 3: Wire frame model of shaft created by using Pro-e wildfire – 5 software [10]

Figure 4: Solid model of shaft created by using Pro-e wildfire – 5 software [10]

E. Bearing Selection and Pedestal Selection

Bearing selection should carried out by calculating the static and dynamic load carrying capacity.

i) *Static equivalent load for rolling contact bearings*
        The load carried by a non-rotating bearing is called a static load. The *basic static load rating* is defined
$$W_{0R} = X_0 \times W_R + Y_0 \times W_A$$

ii) *Basic dynamic load rating of rolling contact bearings*
        The dynamic equivalent radial load (W) for radial and angular contact bearings, under combined constant radial load (W_R) and constant axial or thrust load (W_A) is given by

$$W = X \times V \times W_R + Y \times$$

The value of Static and Dynamic load rating C and C_0 have been calculated for load applied at shaft end.

For life rating of bearing (L) in revolutions,

$$L = \left(\frac{C}{W}\right)^k \times 10^6 \text{ Revolutions}$$

$$C = W\left(\frac{L}{10^6}\right)^{1/k} \tag{9}$$

The approximate rating (or service) life of ball or roller bearings is based on the fundamental equation, The relationship between the life in revolutions (L) and the life in working hours (L_H) is given by

$$L = 60 \times N \times L_H$$

Dynamic rating C and static rating C_0 can be calculated first.

Then, from the standard catalogue [8] of bearing select the bearing which is suitable for calculated static and dynamic load carrying capacity. These bearings have been used to support the shaft.

If variable load is applied, then resultant load will be calculated from the below procedure.

We know that life of the bearing in revolutions,

$$L = L_1 = L_2 = L_3 = L_4 = 60 \times N \times L_H \text{ revolution.}$$

Then the resultant load can be calculated by,

$$W = \left[\frac{L_1(W_1^3) + L_2(W_2^3) + L_3(W_3^3) + L_4(W_4^3)}{L_1 + L_2 + L_3 + L_4}\right]^{\frac{1}{3}}$$

        According to bearing selected, Pedestal selection have been carried out from the standard catalogues of the company. Two major types are available for pedestal, Split type and Non-Split type.

        Suitable locating ring provided for preventing axial moment of the bearing and provision for seal ring to prevent bearing from the atmospheric conditions. Lubrication for the bearing have been provided through hole which is provided at the upper part of split pedestal.

        Loading plate and Base preparation have been carried out by considering size of shaft, Motor, bearing and pedestal.

F. 3-D Model Created using Computer Modeling Software

To create a wire frame model as solid model, here Pro-engineer wild fire version – 5 have been used. First, each individual component have been created by different module of software. Then assembly have been created as per their constrain provision.
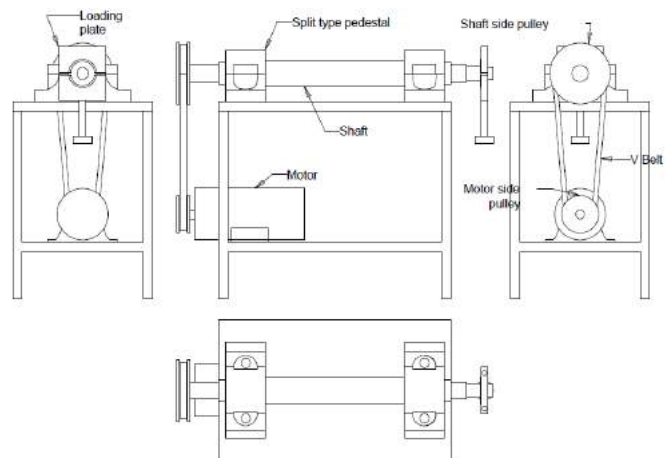

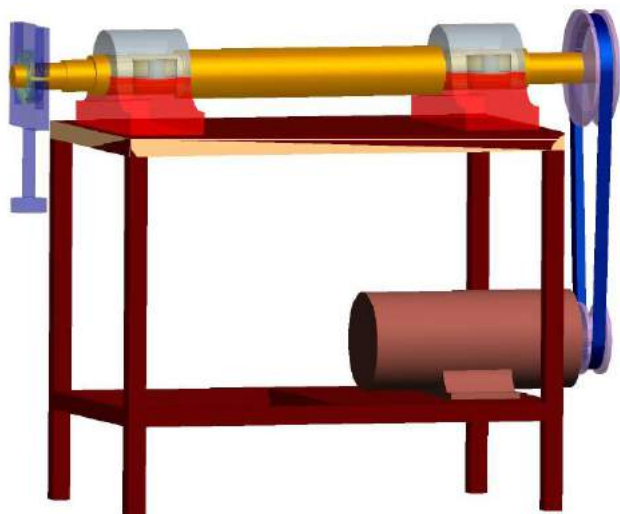Figure 5: Wireframe model of assembly drawing using Pro-E modeling software [10].

Figure 6: Solid model of assembly drawing using Pro-E modeling software(view 1)[10].

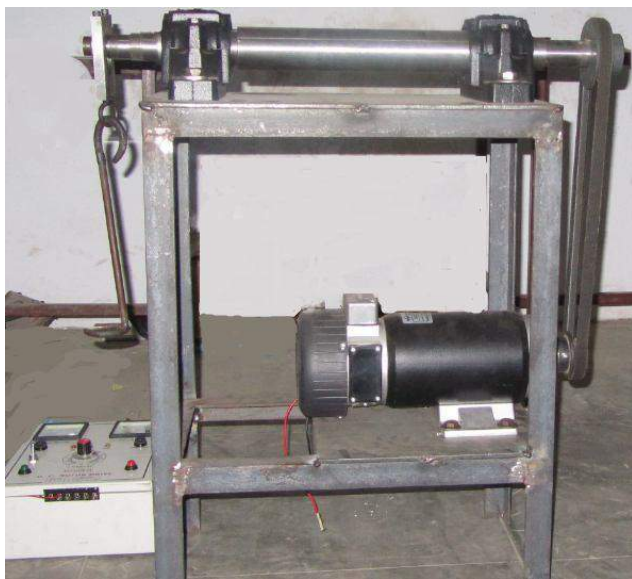Figure 7: Experimental set up [10]

IV. FUTURE SCOPE

The test rig designed in this paper is a versatile test rig. It can be used for health monitoring of all type of bearings. This test rig can be useful for vibration and noise monitoring of the bearing. The signal captured from the test bearing can be further analysed for the condition monitoring of the bearing. The data for the test bearing can be collected at different speed and different load using variable speed of DC motor.

V. REFERENCES

[1] Juha Miettinen,“ Condition monitoring of Grease Lubricated Rolling Bearing by Aoustic Emission Measurements ” Tempere University of Technology, Tempere 2000,Finland

[2] M S Patil, Jose Mathew, P K Rajendrakumar, “*Bearing Signature Analysis as a Medium for Fault Detection: A Review”* Journal of Tribology ,January 2008, Vol. 130 / 014001

[3] N Tandon, A Choudhury, “*A Review of Vibration And Acoustic Measurement Methods For The Detection Of Defects In Rolling Element Bearings*” Tribology International, October 1999, 32 (1999) 469–480

[4] P D McFadden and J D Smith, “ Vibration Monitoring Of Rolling Element Bearings By The High frequency Resonance Technique – A Review” Tribology International 0301-679X/84/010003-08, 1984

[5] A text book of Machine Design By R. S. Khurmi, & J. K. Gupta, 14th Edition.

[6] A text book of Mechanical Engineering Design, by J. E. Shigley, 8th Edition, McGraw hill publication.

[7] N. Tandon,“A Comparison of Some Vibration Parameters For The Condition Monitoring Of Rolling Element Bearing” , Elsevier Science *(1994) 285-289*

[8] www.skf.com

[9] www.rajendrapulley.com

[10] Amit Patel, 2012, “Test Rig Development for Vibration Monitoring of Rolling Element Bearing”, ME Thesis, BVM

Secondary Refrigerant System for Water Ice Candy Manufacturing Process with Calcium Chloride Brine

Prof. Keyur C. Patel[a], Dr. Vikas J. Lakhera[b]

([a]keyur.patel6786@gmail.com, [b]vikas.lakhera@nirmauni.ac.in)

Abstract—**Ozone depletion and Global warming are the recent problems concerned with the Environment. CFCs, HCFCs and HFCs refrigerants have forced designers to find other alternatives of refrigerant. In order to minimize the usage of the primary refrigerant, secondary refrigerant can be considered as one of the option available to overcome the global problem.**

The interest in application of secondary refrigerant systems in water ice candy manufacturing process shows the reduction in refrigerant losses and cost. Present work discusses about the viability of calcium chloride brine for a specific range of application in food processing industries.

Index Terms— **Secondary refrigeration, Calcium chloride brine.**

I. INTRODUCTION

REFRIGERATION system choice is a vital part of selecting an efficient freezing or chilling system for long-term use. The size of the refrigeration system will vary according to the amount heat that needs to be removed and ideally the heat load will be minimized. In cooling or freezing heat will be removed from the product whereas in storage, transport and retail the only heat loads ought to be from transmission across structures, infiltration through doors and openings and from lighting, defrosts and people and Machinery.

CFCs, HCFCs and HFCs refrigerants [1] are banned because of global environmental problem. Hence In many refrigeration applications, heat is transferred to a secondary fluid, which can be any liquid cooled by the primary refrigerant and then used to transfer heat without changing state. These fluids are also known as heat transfer fluids, brines or secondary refrigerants [2]. They are also found in many new applications and in low temperature refrigeration, enabling the use of environmentally friendly primary refrigerant such as ammonia and hydrocarbons.

Indirect refrigeration systems can have some significant potential advantages over direct refrigeration systems. in an indirect system.

An indirect system with a secondary refrigerant circuit means an extra cost for the pump and heat exchanger with an added temperature difference. If a secondary refrigeration system is not designed correctly, this may lead to higher total energy Consumption.

Therefore, it is vital to choose the right secondary refrigerant for the application in order to provide an economical and energy efficient system.

II. SECONDARY REFRIGERATION SYSTEM

The basic secondary refrigerant system uses brine or other one-phase liquid fluid. The secondary refrigerant is circulated by a pump and cooled by passing through the evaporator of a chiller. The temperature increases by absorption of thermal energy in the secondary heat exchanger but also due to dissipation of the pump energy and due to a certain amount of heat absorbed through the pipe insulation.

A. Secondary Refrigeration Option

Different concepts for secondary refrigerant systems include the basic secondary refrigerant system using brine or other single phase liquid fluid. Water is a perfect fluid for systems not needing to be cooler than the freezing point at any time. However, the main problem is the low temperature applications at -30°C to -40°C, which will be considered mainly in this paper.

There are a wide variety of secondary refrigerants on the market and the necessary thermo-physical property data are generally available.

The commercially available secondary refrigerants can be divided into two categories, namely aqueous (i.e. water based) and non-aqueous solutions [3]

Aqueous solutions are mixtures of various salts and water. The mixtures of such compounds as magnesium and calcium chloride have been used extensively since the early days of refrigeration.

More recently, mixtures of potassium acetate and potassium format have been introduced to the market to overcome some of the corrosion and physical property problems of the old mixtures, in particular for low temperature applications.

This includes fluids based on aqueous solutions such as different salt/water solutions, alcohol/water and ammonia/water. In addition, mineral oil based and synthetic fluids are also in use for low temperature secondary refrigerant systems.

B. Factors for Selecting Brine

Following factors [4] can be considered

- Cost: Generally aqueous solutions are cheaper than the pure liquids even allowing for mixing inhibitors and water treatment.

- Corrosion is controlled in salt based brines primarily by density regulation, with high density fluid having less air trapped between the more closely packed molecules. The result is limited by the extra pumping power required and where alkalinity is high. It is recommended that pH values of 7.5 to 8.5 should be maintained.

- Corrosion inhibitor in the form of Chromic Acid or Sodium Dichromate used to be added but due to the heavy metal content, disposal, handling and control of these substances makes them prohibitively difficult to use. Unfortunately, there is no simple method for determination of sodium dichromate concentration.

- The recommendation is to use only suitably corrosion resistant materials such as ABS plastic, copper, cupronickel and cast iron (grades of stainless steel lower than 316 are not suitable as the oxide layer is not adequate to stop the chloride leaching the iron out of the alloy and causing pin hole perforations).

- The glycol solutions are generally less corrosive, but may require inhibitors for specific applications.

- Pure 'brines' are not corrosive provided they are not contaminated with impurities such as moisture.

- Methylene chloride and trichloroethylene must not be used with aluminium or zinc and they will attack most rubber compounds and plastic.

- Toxicity is important if there is potential for exposure to food or people. Sodium chloride and propylene glycol have low toxicity and inhibited propylene glycol is being increasingly used in food plants. All other brines are toxic to some extent or produce odours, requiring closed circuits.

- The low flash points of acetone, methyl alcohol and ethyl alcohol mean extra precautions must be taken against fire and explosion.

- Specific heat of the brine determines the required mass flow rate at a given temperature rise for the cooling load in question. The low temperature brines have a specific heat value, about $\frac{1}{3}$ to $\frac{1}{4}$ of the water soluble brines.

- Density is not a significant factor other than from corrosion control and possible pumping costs.

- Stability is necessary at high temperatures where the brine may be heated. Methylene chloride may break down into acidic products at temperatures above 60 °C.

- Viscosity of brine affects pumping costs and the heat transfer coefficients.

- Freezing point is the low limit that the brines can be used. In practice, to avoid the risk of freezing, operating temperatures should be maintained 5 °C to 7 °C above the freezing point.

- Vapour pressure is important for brines used in an open system, especially if the brine warms to room temperature between usages. Possible risks are vapour losses, toxicity and flammability.

- Water solubility of brine in an open or semi open system can be important due to the risk of dilution of a salt based or glycol based brine, or the formation of water ice in a pure brine which will be pumped around the system and deposited on heat exchange surfaces.

- Foaming occurs if carbon dioxide in one of its phases has been immersed and bubbles through the brine for cooling or an agitation may introduce air into the brine with risk of corrosion.

III. CALCIUM CHLORIDE BRINE FOR WATER ICE CANDY MANUFACTURING

Calcium chloride brine is the most common secondary refrigerant used in food processing industries. Fig. 1 shows the schematic of the water ice candy manufacturing process. The system consists of primary refrigeration cycle followed by the secondary refrigeration cycle. Primary refrigeration cycle includes compressor, condenser expansion valve and the evaporator. Shell and tube heat exchanger acts as forced water cool type condenser and the other shell and tube heat exchanger acts as Direct Expansion evaporator.

Secondary refrigeration system carries the calcium chloride brine which flows through direct expansion evaporator, pump and candy tank. Candy mould cassettes are placed in candy tank and the flavored water is poured in to the mould of candy mould cassette. Circulation of brine takes place due to the brine pump. Care should be taken that brine will not come in direct contact with water ice candy. Candy tank and candy mould are made up of stainless steel just to take care of corrosion effect of brine.

IV. RESULT AND DISCUSSION

The majority of aqueous solutions are based on salt mixtures and they are relatively corrosive by nature. Therefore, it is vital to stabilize these solutions by means of corrosion inhibitor packages and chemical stabilizers for a long term use.

Table 1 shows the concentration of the most commonly used secondary refrigerant [5]. Ammonia works well as a refrigerant but for food processing equipment, Calcium chloride brine is the better option because of its non toxic nature.

As shown in Table 2 Calcium chloride Brine is highly corrosive but In the absence of air, it is not severely corrosive (steel brine pipes remain in good condition internally, but steel brine header and makeup tanks suffer severe corrosion at the brine/air interface). However, it is desirable to keep the brine slightly alkaline, with pH between 8·0 and 8·5. If found to be acid (e.g. litmus test papers), caustic soda should be added.

Density of the brine is not very significant factor from corrosion point of view but it should not be too high because it increases pumping power.

The cost is very low hence it is the most economical option for the water ice candy as the desired temperature of brine is -24 ˚C which is far away from the freezing temperature of the Calcium chloride brine.

V. CONCLUSION

No single secondary refrigerant is ideal for every type of application, and therefore designers must find the best solution for the particular application on basis of temperature range.

Aqueous solutions generally require less volume flow in comparison with non aqueous solutions.

Designers must compare the Corrosivity. Environmental pollution, toxicity and flammability, site handling and cost issues along with the thermo physical properties of the intended secondary refrigerants.

Calcium chloride brine is the most viable option for specific range of temperature required for candy manufacturing.

REFERENCES

[1] Heap R.D., "*European Developments Relating to Refrigerants*", Institute of Refrigeration Presentation, 2nd November 2000, London.
[2] 2003 ASHRAE Winter Meeting, Secondary Refrigeration European Experiences, Chicago, USA, 2003.
[3] Sassi Ubaldo, "*Caracteristiche dei fluidi secondari per basse temperature*" ZERO SETTO ZERO Magazine, October 1998, ITALY.
[4] Ure, Z. "*Benefits that flow from secondary systems*" RAC Journal, UK, July 2000 Issues, p. 32- 37.
[5] 2002 Malinker, Ake "*Thermophysical Properties of Liquid Secondary Refrigerants*", International Institute of Refrigeration, 1997, France.

Table 1 Aqueous Secondary refrigerant Solution

Description	Concentration		
	Freezing Temperature		
	-15°C	**-30°C**	**-40°C**
	5°F	**-22°F**	**-40°F**
Ethylene Glycol / Water	30.5	45.4	52.8
Propylene Glycol / Water	33.0	48.0	54.0
Ethyl Alcohol *I* Water	24.5	40.9	53.1
Methyl Alcohol / Water	20.0	33.6	41.0
Glycerol *I* Water	39.5	56.0	63.0
Ammonia/Water	10.8	17.7	21.1
Potassium Carbonate / Water	27.0	36.6	-
Calcium Chloride *I* Water	17.9	25.4	28.3
Magnesium Chloride / Water	14.0	20.5	-
Sodium Chloride *I* Water	18.8	-	-
Potassium Acetate *I* Water	24.0	34.0	39.0
Potassium Formate / Water	24.0	36.0	41.0

Table 2 Properties of water based secondary coolant

Description	In organic Sault	Glycols		Organic Sault	
	CaCl$_2$	EG	PG	K-Ac	K-F
Antifreeze	28.3%	50%	54%	39%	41%
Heat transfer	Exce-llent	Regular	Poor	Good	Exce-llent

Viscosity	Very Low	High	Very High	Low	Very Low
Corrosivity	Very High	Low	Low	Mode-rate	Mode-rate
Toxicity	Food safe	Toxic	Food safe	Food safe	Food safe
Costs	Very Low	Low	High	Low	Low

CaCl$_2$ – Calcium Chloride Brine
EG – Ethylene Glycol
PG – Propylene Glycol
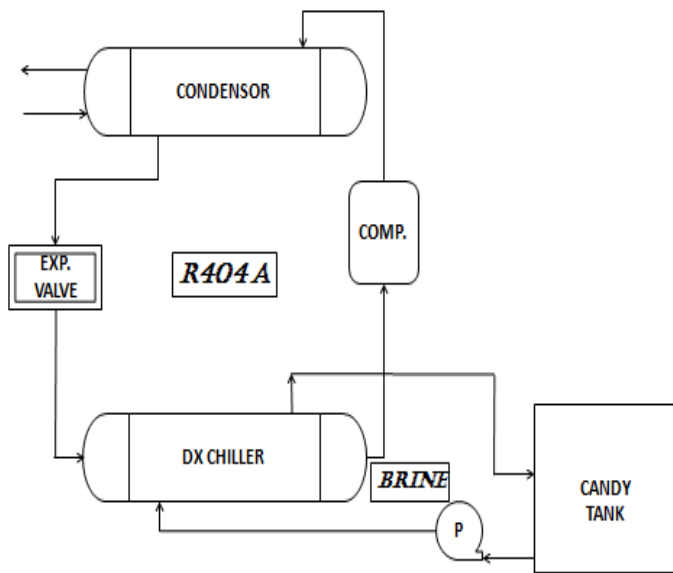K-Ac – Potassium Acetate
K-F – Potassium Formate

Fig. 1 Schematic of Water Ice Candy Making Machine

Development of Typical sample holder with Cryostat for the Measurement of Hall Effect and Magnetic Susceptibility at LN$_2$ Temperature.

Shaival R Parikh[1], Prof. Hardik A Shukla[2]

[1,] Student of (M.E. Cryogenics Engineering) L D College of Engineering
(shaival01@gmail.com)

[2] L D College of Engineering, Ahmedabad
(shuklahardik2@gmail.com)

Abstract— **A** cryostat is described for the measurement of Hall Effect and magnetic susceptibilities at temperatures from 77–300 K in one single experiment. The susceptibility is measured by the A.C. mutual inductance method. The sample, kept cold during the whole experiment, the small double walled cryostat directly immersed in a liquid nitrogen bath. The sample holder is prepared by teflon material Where primary and secondary winding is done for measurement of magnetic susceptibility and separate sample holder of SS304 using for measuring Hall Effect where the magnet is used. With the aid of an electrical heater and a temperature sensor of PT-100 and rare earth magnet is used to measure temperatures between 77 – 300 K can be produced and measured with an overall precision better than other .The sample is held so that its position can be adjusted inside the coils or removed completely at any temperature.

Index Terms— **Cryostat , Magnetic susceptibility Hall Effect**

I. Introduction

In a study of the magnetic properties and Hall Effect of some Cuprates material like YBCO and nickel salts and other sample made in our laboratory, it was convenient to have a cryostat capable of measuring magnetic susceptibilies at any temperature Between 77- 300 K without changing samples or the measuring system. It was also necessary to be able to move the sample at any temperature to compensate for the spurious variations of the mutual inductance due to the measuring coils (McKim and Wolf 1957). For measuring the Hall Effect provided the magnet whose magnetic filed is up to 0.3 T at outer vessel at a room temperature.

We then designed a cryostat in which a small Dewar Inside placed the susceptibility measuring coils, both immersed in a bath. Inside this Dewar, gases separately admitted for purging purpose, and liquefied in small quantities by means of the external bath to cool the sample. **A** heater and a PT 100 Sensor Were used for the measurements between 77-300 K

This apparatus was very convenient since it permitted precise measurements to be performed in the whole temperature range in a relatively short time, and also very rapid changes to samples without having to warm the cryostat.

Recently a lot of interest has been shown in the properties of amorphous magnetic materials (Handrich and Kobe 1970,Kaneyoshi 1973, Slechta 1975). Unfortunately it has been found that if amorphous films of the pure transition elements are required they can only be prepared in thin films of 200 **A** or less (Bennett and Wright 1972). The small bulk of these films and their method of preparation, normally the condensation from the vapour phase onto a cold (4K) glassy substrate, make conventional magnetic moment measurements difficult to perform. However it has been known for some time that the galvanomagnetic properties of ferromagnetic materials are directly related to their magnetic properties (Jan 1957). In an attempt, therefore, to obtain data,if indirectly, on the magnetic properties of these films it was decided to proceed with a series of measurements of their galvanomagnetic properties (Whyman 1974, Whyman and Aldridge 1975). This note describes the cryostat used in these measurements.

Hall Effect: A charge moving in the presence of a magnetic field experiences a Lorentz force given by q (v x B), where q is the charge, v is its velocity, and B is the field strength. When charge carriers are constrained to move in a conductor, the carriers tend to be deflected toward one of the boundaries of the conductor. These deflected carriers establish an electric field, which cancels the Lorentz force. The Hall voltage, which is this electric field times the width of the sample w, can be used as a measure of B.

Susceptibility: It is dimensionless proportionality constant that indicate degree of magnetization of material in response to applied the magnetic field.

II. DESCRIPTION OF THE APPARATUS

A simplified diagram of the cryostat is shown in figure 1. The Cryostat is a made double wall SS-304 tube with the space between the walls permanently evacuated.
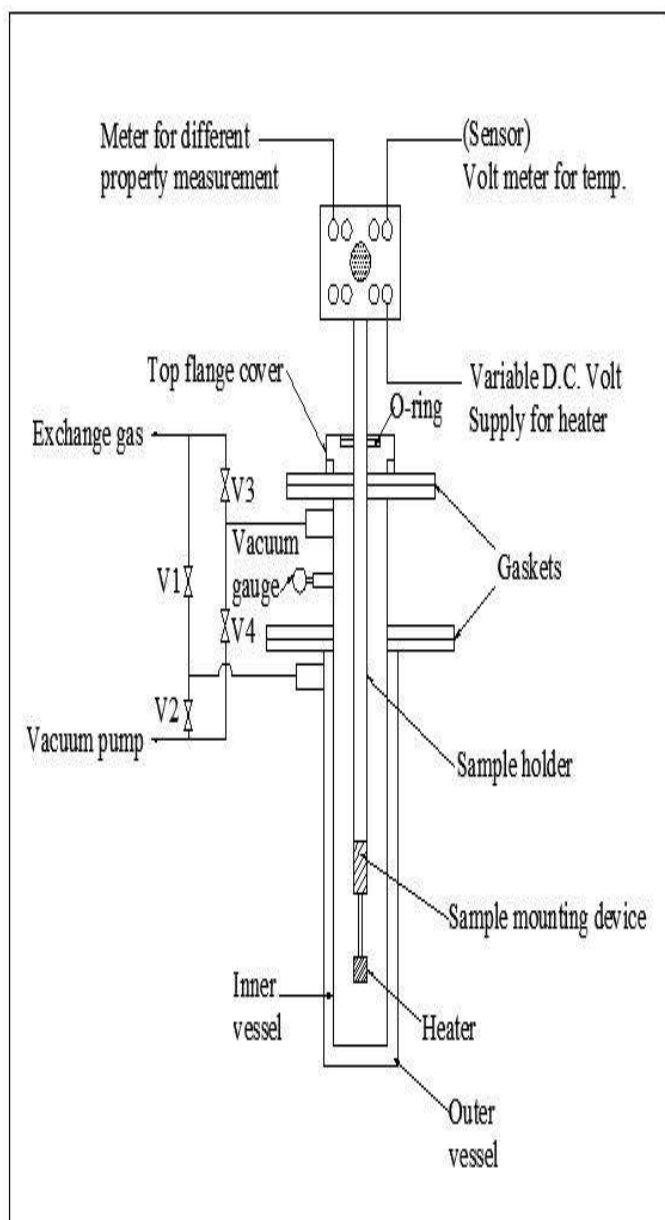
Fig–1 . **Cryostat for Different Property Measurement**

The internal wall is much longer than the external, thus providing an evacuated. During the whole experiment, is external a small glass Dewar immersed in a liquid nitrogen bath. The measuring coils placed inside the internal Dewar. In which the sample can be inserted into the sample holder. With the aid of an electrical heater and PT 100 Sensor, temperatures

between **77** and 300 K can be produced and measured with an overall precision. The sample is held so that its position can be adjusted inside the coils or removed completely at any temperature.
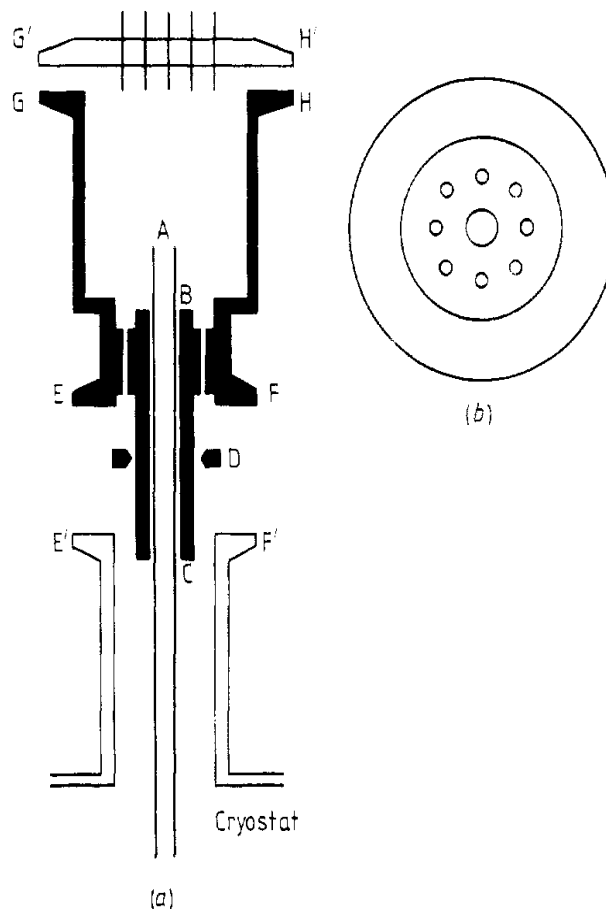
Fig 2.   Device for the supporting the sample bar in cryostat.

The upper end of the hollow alloy or S.S.bar **(A),** through which the electrical leads of the sample pass, is inserted in the tube (BC) and fastened in position by two series of three small Allen screws (D) placed at 120^0 to each other.

The base (EF) of the device allows a quick fitting to the flange (E'F') on top of the cryostat. The vacuum-tight connection between EF and E'F' is achieved by the interposition of a centring circlet with O-ring and is fastened by a clamping ring,. In a similar way, the top (GH) of the device is closed vacuum-tight by a current lead through flange (G'H').

If the standard components mentioned above are not available, or they do not have the proper dimensions, the two ends (EF) and (GH) of the device can be easily redesigned to fit vacuum-tight on the rest of the cryostat and to close at the top with a flange, by the use of O-rings and vertical screws going through the flanges. In the case of a home-made flange (G'H'). vacuum- tight seals for electrical leads through it can

be easily constructed in the way described by McKinnon (1968) and Rose-Innes (1973).

As shown in figure 2(b). Several holes are made around the tube BC connecting the interior of the device with the inner chamber of the cryostat.

The magnetic susceptibility is measured by an A.C. mutual inductance bridge similar to that described by Jastram et al. (1959). The secondary measuring coil is wound outside the primary and is made in three sections: the principal winding is at the centre; at each end there is a compensating section built in such a way that the mutual inductance of the empty coil system at liquid nitrogen temperature is below 10 **µH.** The details of the construction of the coils are described by Vargas and de Oliveira (1969). Copper wire (20 GAUGE) is wounded on the primary and the secondary (32 GAUGE) coils. For the 1st design, the number of turns in primary coil is 200 and in secondary coil it is 300 in which 150 turns is clockwise and another 150 turn is anticlockwise. The material chosen for the design is Teflon for its thermal conductivity. A Pt100 temperature sensor is put inside the secondary coil that touches to sample. This design was dipped in liquid nitrogen for achieving lower temp. But the dimension of the previous design is modified to fit in Closed Cycle Refrigerator to attain the liquid Helium temperature. Hence we modified the design. Lock-in amplifier is used to detect and measure very small A.C. signal. After that we performed our experiment. When measure the Hall Effect that time remove the primary and secondary windings and put magnet of the outside of outer vessel.

III. TEST PROCEDURE

A.C. susceptibility measurements were performed using inductance method consisting of primary and secondary coils. The primary coils (wounds in same direction) are coaxially wound on secondary coils (two sections connected in series but of opposite windings). The primary coil was connected to a Lock-In- Amplifier. A low frequency (10-300 Hz) sine wave current was generated using a signal generator and was fed to the primary coils as well as to the Lock-In-Amplifier as a reference signal. The alternating current produced an alternating magnetic field inside the primary coils, which induced voltage in the secondary coils. With no sample in the coil, the mutual inductance of the combined coils is zero. The signal from the secondary coil was fed back to the **Lock**-In-Amplifier for phase sensitive detection. Hence when a superconducting sample is placed in one of the sections of the secondary coils, any change in the magnetization of the sample (and hence the susceptibility) corresponds to a change in the e.m.f induced in the secondary coil which is measured by the Lock-In-Amplifier. AC susceptibility measurements have been employed to qualify the suitability of materials as superconductors.

AC susceptibility is one of the fundamental measurements used for characterizing magnetic samples. In particular, the temperature variation of the AC susceptibility is especially useful in identifying phase transitions. Most low-temperature measurements of AC susceptibility make use of liquid cryogens.

A set of mutual inductance coils Usually, there is a single primary outer coil to which an A.C. signal is applied, and two secondary coils in series opposition. In such an arrangement, the output voltage across the secondary coil combination should be zero when no sample is present, since the effect of direct coupling between the primary and secondary coils is to induce two opposing signals which should cancel in a balanced system. However, when a sample is placed at the center of one of the secondary coils, an AC signal, corresponding to the sample response, should be observed.

There are a number of problems associated with the use of cold finger cryostat as a cooling system for such a coil arrangement: (i) A physical thermal link between the cryostat cold finger and the sample is necessary to cool the sample. However, the presence of such a link may itself contribute to the measured susceptibility. This is due not only to the link's own magnetic response but also, if the link is metallic, to induced Eddy currents. (ii) Control and monitoring of the sample temperature may be adversely affected by thermal gradients. (iii) Thermal gradients may also cause differential expansion in the coil formers, changing the relative inductance of the coils. Thus, the background signals in the two secondary coils will no longer balance, and a spurious signal will be added to the measured response.

Data logging system for AC magnetic susceptibility measurements (77-300 K)**.**system suggested the semi-automated apparatus for the simultaneous measurement of various AC magnetic properties in low applied fields (1 kA $^{m-1}$) over the temperature range 77 -300 K is described. The system is based on a variable temperature cryostat and a high resolution data logger capable of measuring ten signals to 1 µV resolution. In these measurements the sample forms the core of a transformer with phase sensitive detection (PSD) of the secondary induced voltage being used to determine. The capability of the system is demonstrated by measurements obtained on the terbium crystal for which the secondary coil was wound directly on to the sample with the primary being wound around a nylon former in which the sample was a tight fit. Hold-times of 48 hr and 8-16 hr were obtained with liquid nitrogen and helium as the coolants respectively. A block diagram of the system, which consisted of a Keithley data logger and programmable calculating unit (PCU), a teletype, a Data ways Interface and a Hewlett-Packard 9830 desk-top calculator, is shown in figure 3.
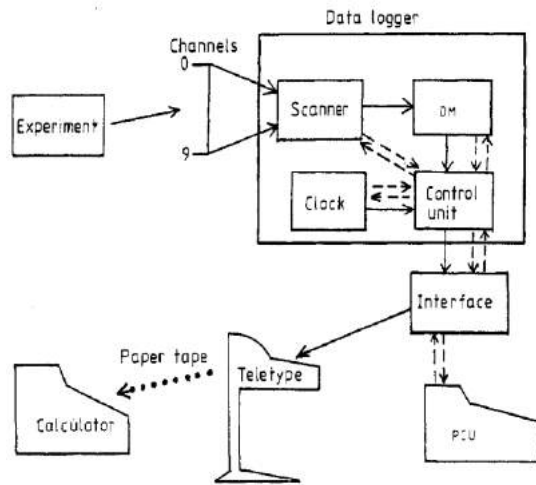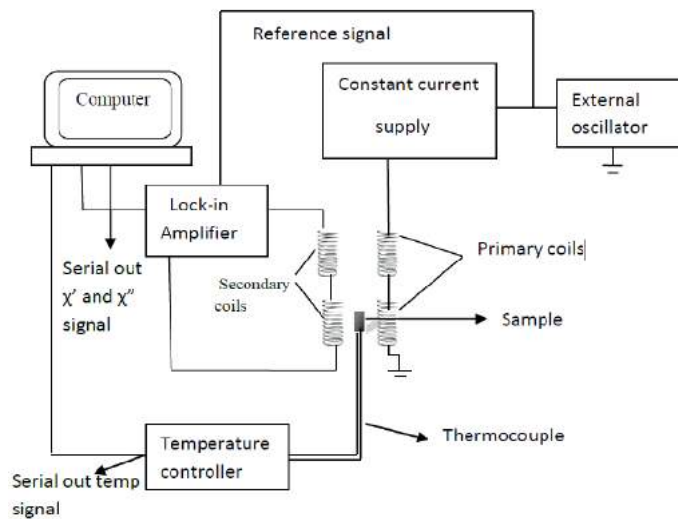
Fig. 3 - Block Diagram of Data Logging System

The system is based on a programmed measurement cycle which was activated every one to five minutes during an experiment lasting 20 h and has the capacity to measure signal voltages (1 µV-30 V) on ten channels. Data logger which consists of the following components: a low voltage scanner; a digital MultiMeter (DM); an interval time/clock and a control unit. Operation of the system was controlled by a program in the PCU which activated the measurement cycle at fixed time intervals. Although operating parameters such as the number of channels to be measured and the time delay between the measurement of each channel were set before the experiment commenced, the program could be interrupted and altered between measurement cycles. A method of assessing the effects of an average demagnetizing factor on x and S measurements on irregularly shaped samples is presented. Plot graph temperature Vs susceptibility.

The rectangle size of magnet is selected 50 mm length and 5 mm thickness and place around the sample holder so his field is passing perpendicular to sample for measuring the Hall Effect produced in the sample. Hall effect is used for finding

mobility, free electron present in to the sample, carrier concentration, material is p type or n type semiconductor that we have we to find at room temperature 300 K to liquid nitrogen temperature.

IV. DESIGN PROCEDURE

The main requirements of specification or design data available for cryostat are as under.

(1) The cooling media for producing cryogenic temperatures is liquid nitrogen.
(2) The capacity of cryocan for coolant LN_2 is 35 liters.
(3) The mouth piece hole of LN_2 container is 50 mm diameter.
(4) The sample lengths of aluminium wire and copper wire is minimum 10 meters for getting accurate and precise reading.
(5) There should be minimum heat leak to atmosphere through LN_2 vessel and cryostat.
(6) There should be minimum liquid nitrogen consumption as it is costly item.
(7) There should be sufficient space for sample mounting with insulation between other parts and whole length of sample.
(8) There should be provision for heating the space of cryostat with variable heat rate with low voltage.
(9) There should be provision of measurement of temperature of sample space.
(10) The experiment should be done with minimum time and cost.
(11) The cost of cryostat should be as low as possible.

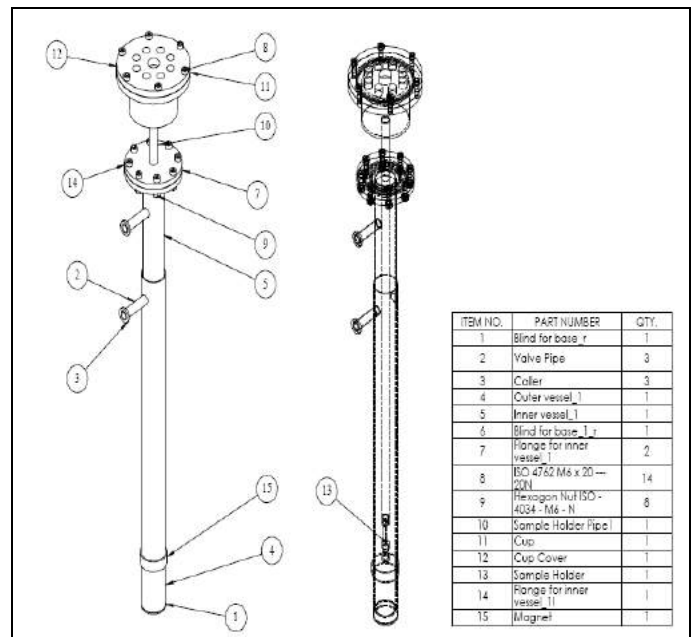| ITEM NO.	PART NUMBER	QTY.
1	Blind for base_r	1
2	Valve Pipe	3
3	Coller	3
4	Outer vessel_1	1
5	Inner vessel_1	1
6	Blind for base_1_r	1
7	Flange for inner vessel_1	2
8	ISO 4762 M6 x 20 — 20N	14
9	Hexagon Nut ISO - 4034 - M6 - N	6
10	Sample Holder Pipe1	1
11	Cup	1
12	Cup Cover	1
13	Sample Holder	1
14	Flange for inner vessel_11	1
15	Magnet	1

Fig. 4 - Assembly drawing of hall effect and magnetic susceptibility measurement cryostat

V. SAMPLE PREPARATION

The sample of YBCO created in this paper was created by combining yttrium oxide, barium carbonate, and copper (II) oxide. The chemical formula for the reaction is:

$$Y_2O_3 + 2\ BaCO_3 + 3\ CuO \rightarrow 2\ YBa_2Cu_3O_7$$

The ingredients were mixed together with a mortar and pestle to the ratio of the balanced equation above. After being ground together for thirty minutes, the powder was placed in an oven at 900o C for 24 hours. Once removed the sample was reground for 15 minutes and placed back in the oven. The next day it was removed, reground and then pressed into pellets. The resulting pellets were placed in the oven at 900o C once more for 24 hours. This was to harden the pellet and homogenize them. After verifying that the pellets stayed together, they were then placed back in at 450o C for 24 hours. The purpose of this step was to uptake as much oxygen into the sample as possible since the properties of the superconductive state are dependent on the oxygen concentration of the sample.

The method used creates random orientations of YBCO grains. Since the properties are dependent on the orientation of the copper planes, a random orientation of the grains does not have as low of a resistance. For this experiment this method was sufficient, but if one were to create a better sample the orientation of the grains would be important. Grain alignment could be achieved several different ways. First by applying pressure, the grains can be compressed into a particular orientation. Another way is to embed the grains in a composite material such as an epoxy resin. Once embedded, a strong magnetic field could be used to orient the grains. Third, an oriented sample can be produced by melting a granular powder sample then by using an oven where the temperature varies regularly across the sample for reforming of the material.

There are also different preparation methods for the creation of YBCO. One possibility is substituting barium carbonate with barium oxide. This substitution provides some advantages over barium carbonate. The decomposition temperature of barium oxide is lower and also acts as an internal oxygen source. This aids with the annealing process making it easier to get the YBa2Cu3O7 form. Also since there is no carbon in barium oxide, there is no formation of carbon 16 dioxides in the process. This is desirable since carbon dioxide can react with the YBCO to form non-superconducting phases at the grain boundaries. These slight differences result in a sharper transition into the superconducting state according to Rao et al. This method was not used due to the availability of materials in lab.

VI. SAMPLE HOLDER FOR MAGNETIC SUSCEPTIBILITY MEASUREMENT

The length of the S.S 304 cryostat is around 650 mm. The lower tail of the cryostat is a double-walled cylinder of inner diameter 32.44 mm and length 650 mm. It is dipped into liquid N2. The sample holder is a sapphire plate of length 70 mm and width 12 mm. It is attached to a hollow stainless steel rod through a non-metallic Teflon a fiber impregnated polymer extension of 150 mm length. The sample holder moves up and down through the Wilson seal inside the cryostat.

Primary and a set of secondary coils are wound on separate Teflon Rod. Teflon is chosen for its thermal and mechanical properties. First made two sets of the coil system. One major problem is that offset voltage, which cannot be changed by unwinding the few secondary turns, once the coil set is wound.. The uniformity and tension of the windings in the primary as well as secondary coils cannot be identical; hence the individual inductive and capacitive coupling of secondary with the primary is different.

Copper wire (20 GAUGE) is wounded on the primary and the secondary (32 GAUGE) coils. For the 1st design, the number of turns in primary coil is 200 and in secondary coil it is 300 in which 150 turns is clockwise and another 150 turn is anticlockwise. The material chosen for the design is Teflon for its thermal conductivity. A Pt100 temperature sensor is put inside the secondary coil that touches to sample.

VII. CONCLUSION

A simple sample-inverting cryostat for Hall resistance measurements and magnetic susceptibility has enabled us to measure the Hall resistance easily and precisely at temperatures from 77- 300 K in magnetic fields up to 0.3 T and magnetic susceptibility is measured by lock in amplifier in temperature range up to 77-300 K various cuprates materials for analysis superconductivity of material.

REFERENCES

[1] Jastram P S Pillinger W L and Dannt I G 1959 Reu. Sei. Instrum. 29 159-62.
[2] McKim F R and Wolf W P 1957 J. Sci. Instrum. 34 64-7
[3] Vargas H and de Oliveira N F An. Acad. Bras. Cinc. in the press
[4] M. Prasad, R.R. Rao, A.K.R. Chaudhuri, J. Phys. E 19 (1986) 1013.
[5] A.F. Deutz, R. Hulstman, F.J. Kranenburg, Rev. Sci. Instrum. 60 (1989) 113.
[6] A. Banerjee, A.K. Rastogi, M. Kamur, A. Das, A. Mitra, A.K. Majumdar, J. Phys. E 22 (1989) 230.
[7] McKinnon J B 1968 A particularly simple and inexpensive high vacuum lead-through J. Phys. E: Sci. Instrum. **1**969

[8] Rose-Innes A C 1973 Low Temperature Laboratory Techniques (Liverpool: The English University Press)

[9] G. O. Young, "Synthetic structure of industrial plastics (Book style with paper title and editor)," in Plastics, 2nd ed. vol. 3, J. Peters, Ed. New York: McGraw-Hill, 1964, pp. 15–64.

[10] SakikoMiyagawa, Satoru Noguchi, Takekazu Ishida, "A simple sample-inverting cryostat for Hall resistance measurement", Physica B 329–333, pp.1640–1641, 2003

[11] E Vitoratos and S Sakkopoulos, "A versatile device for supporting the sample holder in a cryostat", Journal of physics E, scientific instruments,vol.20, 1987.

[12] T J McKennat , S J Campbell and D H Chaplin, " A data logging system for AC magnetic measurements (4.2-300 K)", Journal of physics E, scientific instruments, vol. 15, pp. 227 -231, 1982.

A Review on Heat-pipe Oven for Plasma Wakefield Accelerator (PWFA) Experiment

First A. Milind A. Patel, Second B. Krunal Patel

Abstract—**Physicists use particle accelerators to answer some of the most profound questions about the nature of the universe. These machines accelerate charged particles to nearly the speed of light and then smash them together, re-creating the conditions that existed when our universe was cataclysmically born in the big bang. By analyzing the debris of the collisions, physicists hope to understand how the seemingly disparate forces and particles that exist in our universe are all connected and described by a unified theory. The most powerful particle accelerator presents at CERN, the European laboratory for particle physics on the French-Swiss border about 100m underground, is the 8.6-kilometer-diameter Large Hadron Collider (LHC). A new approach to particle acceleration, using the fourth state of matter (after solid, liquid and gas) called a plasma might dramatically reduce the size and cost of such an accelerator. In Plasma Wakefield Accelerator (PWFA) experiment plasma is created within Heat-Pipe Oven by photo-ionizing lithium vapor with the help of laser. Heat-pipe Oven has several features which make it very useful in large number of spectroscopic and other applications. It continuously generates homogeneous vapors of well defined temperature, pressure and optical path length.**

Index Terms—**Heat Pipe, Heat-pipe Oven, Plasma Wakefield Accelerator (PWFA)**

I. INTRODUCTION

A Plasma consists of fluid of positive & negative charged particles, generally created by heating or photo-ionizing a gas. Under normal conditions the plasma will be macroscopically neutral (or quasi-neutral), an equal mix of electrons and ions in equilibrium. However if a strong enough external electric or electromagnetic field is applied, the plasma electrons, which are very light in comparison to the background ions (at least by a factor of 1836), will separate specially from the massive ions created a charge imbalance in

F. A. Milind A. Patel (Author)
Department of Mechanical Engineering (ME Thermal)
Gandhinagar Institute of Technology
Gandhinagar, India
milindpatel@rocketmail.com

S. B. Asst. Prof. Krunal Patel (Guide)
Department of Mechanical Engineering (ME Thermal)
Gandhinagar Institute of Technology
Gandhinagar, India
krunal.patel@git.org.in

the perturbed region. A particle injected into such a plasma would be accelerated by the charge separation field.

Plasma Wakefield Acceleration is an acceleration technique to generate a "charged wave" in plasma. This can then be used to accelerate electrons over short distances up to a high energy. The goal is to shorten the required distance needed for acceleration and by doing this save costs for the construction of a future linear particle collider.

The heat-pipe oven consists of a tube the central portion of which is designed like a heat pipe with a capillary structure on inner surface made, for example, of several layers of woven mesh. Both ends are closed by a demountable unit which connects the tube to a vacuum system and holds the windows. The tube is heated in the middle by an induction heater which is surrounded by a vacuum chamber in order to prevent the outer surface of the pipe from oxidizing. The vacuum chamber is sealed against the tube by means of O-rings. The O-ring seals are cooled by the water in the cooling chamber and allow for any thermal expansion of the pipe. The whole arrangement is completely demountable so that the actual pipe can be easily replaced by another one without replacing any other part of the system.

In order to operate this device, the pipe is first of all filled with an inert gas at a suitable pressure. Heating up the central portion of the tube, the sample of metal will melt down and wet the wick. Depending upon the pressure of inert gas, which initially fills the whole tube, the metal then evaporates at a temperature given by the vapor pressure curve of the metal, for which the vapor pressure equals or just exceeds the inert gas pressure. This causes the vapor to diffuse towards both ends until it condenses again. The condensate returns through the wick back to the heated portion of the tube by capillary action. Finally equilibrium is reached, in which center part of the pipe is filled with a metal vapor at a pressure determined by confining inert gas at both ends of the pipe. Owing to pumping action of the flowing vapor the inert gas is completely separated from the vapor except of a short transition region whose thickness depends on the pressure and the type of vapor and inert gas used. The length of the metal vapor section depends almost entirely on the power input and the gas pressure, which determines the vapor temperature.

II. PLASMA PARTICLE ACCELERATORS [1]

Smashing charged particles together at nearly the speed of

light, high-energy accelerators have advanced understanding of the structure of matter, the fundamental forces of nature and origin of the universe. In 1930's Cyclotron accelerators generating energies of a million electron volts (MeV) simulated conditions in the cores of giant stars, providing a laboratory environment for studying nuclear reactions. More recently synchrotrons and linear accelerators, at billion electron volts (GeV), have explored the environment in the interior of neutron stars and proved the existence of antimatter. Today proton synchrotrons, at a trillion electron volts (TeV), are probing the conditions of the universe to within a billionth of a second of its birth. As plans are laid for the world's largest accelerator, the Superconducting Supercollider, accelerator technology is approaching practical limits. Fortunately a new technology, plasma particle acceleration, has emerged that could constitute a promising way to achieve still higher energies.

The $4.4-billion Superconducting Supercollider (ssc) will require an 87-kilometer accelerator ring to bust particles to 40 TeV. The ssc's tremendous size is due in part to the fact that its operating principle is the same one that has dominated accelerator design for 50 years: it guides particles by means of magnetic fields and propels them by strong electric field. If one were to build an equally powerful but smaller accelerator than the ssc, one need to increase the strength of guiding and propelling fields. Actually, however, the conventional technology may not be able to provide significant increase in field strength. There are two reasons. First, the forces from magnetic fields are becoming greater than the structural forces that hold a magnetic material together; the magnet that produce these fields would themselves be torn apart. Second, the energy from electric fields is reaching the energies that bind electrons to atoms; it would tear the electrons from nuclei in the accelerator's support structures.

It is the electric field problem that plasma particle accelerators can overcome. Plasma particle accelerators are based on principle that particles can be accelerated by the electric fields generated within a plasma: a state of matter heated to a temperature at which electrons are stripped from their atomic hosts. Because the plasma has already been ionized, plasma particle accelerators are not susceptible to electron dissociation. They can in theory sustain accelerating fields thousands of times stronger than conventional technologies. If accelerating fields of such magnitude could be produced over extended distances, a plasma particle accelerator a few hundred meters long could match the projected energy of 87-kilometer Superconducting Supercollider.

Electric fields that accelerate particles can be created in a plasma because of medium's remarkable properties. A plasma as a whole is electrically neutral, but because the electrons and positively charged ions are separated, a disturbance can create region of negative charge (high concentrations of electrons) and region of positive charge (high concentrations of positive ions). Such an uneven distribution of charge sets up an electric

field, which runs from positive to negative regions. The electric field pulls the electrons and ions together with equal force. Since electron's mass is much smaller than that of an ion, the electrons moves toward the positive regions, whereas the ions remain essentially stationary.

As the electrons from negative regions are drawn to positive regions, they steadily gain velocity and momentum. The momentum does more than carry the electrons to positive region: it causes them to overshoot it, whereupon the electric field reverses direction, first opposing the electrons' motion and slowing them down and then pulling them back again. The process repeats itself, establishing electron "pendulum". An array of such electron pendulums, created by disturbance in a plasma, can create electric field that accelerated charged particles. The combined motion of the electron pendulums forms a longitudinal wave of positive and negative regions travelling through the plasma – a plasma wave. In turn positive and negative regions establish an electric field that travels along with plasma wave. If a charged particle is injected into the plasma wave, it will stay in phase with the field, absorb energy from the field and accelerated steadily. This phenomenon is the basis for particle acceleration in the plasmas.

Since plasma waves promise stronger electric fields than conventional technologies, they are good prospects for accelerating particles to high energy. How, then, are plasma waves generated? So far two methods for creating plasma waves for accelerators have been proposed and tested: the wake field and the beat wave.

The wake-field method exploits a "bunch" of many electrons to generate waves in a plasma, thereby accelerating a group of a few electrons to higher energies. Just as a boat moving through the water pushes some of the water aside, making a wake, so a bunch of many electrons travelling through plasma generates a wake of plasma waves.

As an electron bunch enters a region, the plasma electrons move out of the way so that the combination of the plasma and the bunch remains electrically neutral. As the electron bunch exits, leaving a deficit of electrons in the region, the plasma electrons rush back to re-establish equilibrium. This movement of plasma electrons initiates the oscillation of electron pendulums and results in a plasma wave travelling at a velocity equal to that of electron bunch. The plasma wave establishes an electric field: the so-called wake field. A group of a few electrons, suitably placed in the wake field can then be accelerated to energies higher than those of driving bunch.

III. TABLETOP PLASMA ACCELERATORS [2]

Physicists use particle accelerators to answer some of the most profound questions about the nature of the universe. These gargantuan machines accelerate charged particles to nearly the speed of light and then smash them together, re-creating the conditions that existed when our universe was cataclysmically born in the big bang. By analyzing the debris
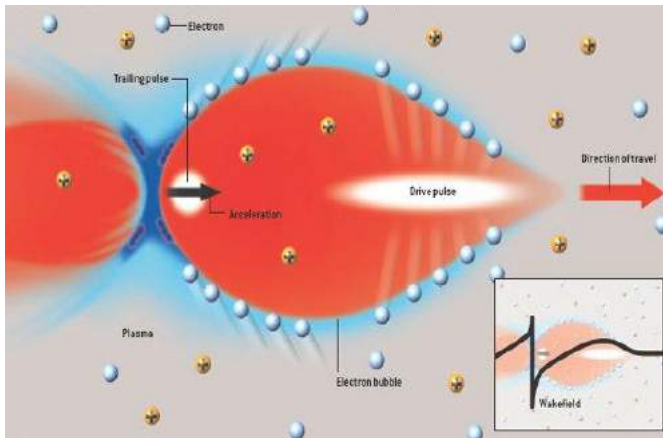
Fig. 1.   The Bubble Regime

of the collisions, physicists hope to understand how the seemingly disparate forces and particles that exist in our universe are all connected and described by a unified theory. Unfortunately, as they get closer and closer to solving this mystery of creation, physicists need particle accelerators of ever greater power (and expense).

The most powerful particle accelerator, now under construction at CERN, the European laboratory for particle physics on the French-Swiss border, is the 8.6-kilometer-diameter Large Hadron Collider (LHC). After the LHC is completed in 2007, the collisions of its two seven-trillion-volt proton beams should tell us what gives particles their mass [see "The Mysteries of Mass," by Gordon Kane; Scientific American, July 2005]. Other currently operating machines are attempting to explain why the universe contains more matter than antimatter and are giving us a peek into the primordial state of matter called a quark-gluon plasma. All these colliders are based on a bulky decades-old technology in which microwaves accelerate the particles.

Over the past 75 years these machines and their predecessors have produced remarkable discoveries about the nature of fundamental particles and the behavior of nuclear matter. Advances in the science and engineering of particle accelerators made that continual stream of revelations possible by allowing scientists to build machines whose energy was greater by roughly a factor of 10 every decade. Will such advances continue? The microwave-based machines may well be approaching the limits of what is technologically and economically feasible. In 1993 Congress cancelled the $8-billion Superconducting Super Collider project, a 28-kilometerdiameter accelerator that would have had more than twice the power of the LHC. Many particle physicists now hope to follow the LHC with a 30-kilometer- long linear collider, but no one can predict if that proposed multibillion-dollar project will fare better than the Super Collider.

Perhaps just in time, new approaches to particle acceleration, using the fourth state of matter (after solid, liquid and gas) called a plasma, are showing considerable promise for realizing an accelerator for physics at the highest energies (100 billion electron volts and up). This plasma-based approach might dramatically reduce the size and cost of such an accelerator.

A plasma as a whole is electrically neutral, containing equal amounts of negative charge (electrons) and positive charge (ions). A pulse from an intense laser or particle beam, however, creates a disturbance in the plasma. In essence, the beam pushes the lighter electrons away from the heavier positive ions, which in turn get left behind, creating a region of excess positive charge and a region of excess negative charge [see Fig. 1]. The disturbance forms a wave that travels through the plasma at nearly the speed of light. A powerful electric field points from the positive to the negative region and will accelerate any charged particles that come under its influence.

IV.   HEAT PIPE [3]

One of the main objectives of energy conversion systems is to transfer energy from a receiver to some other location where it can be used to heat a working fluid. The heat pipe is a novel device that can transfer large quantities of heat through small surface areas with small temperature differences. The method of operation of a heat pipe is shown schematically in Fig. 2. The device consists of a circular pipe with an annular layer of wicking material covering the inside. The core of the system is hollow in the center to permit the working fluid to pass freely from the heat addition end on the left to the heat rejection end on the right. The heat addition end is equivalent to an evaporator, and the heat rejection end corresponds to a condenser. The condenser and the evaporator are connected by an insulated section of length L. The liquid permeates the wicking material by capillary action, and when heat is added to the evaporator end of the heat pipe, liquid is vaporized in the wick and moves through the central core to the condenser end, where heat is removed. Then, the vapor condenses back into the wick and the cycle repeats.

- ▪ The three basic components of a heat pipe are as follows:
1. The working fluid
2. The wick or capillary structure
3. The container.

A large variety of fluid and pipe material combinations have been used for heat pipes. Some typical working fluid and material combinations, as well as the temperature ranges over which they can operate, are presented in Table 1. The fourth
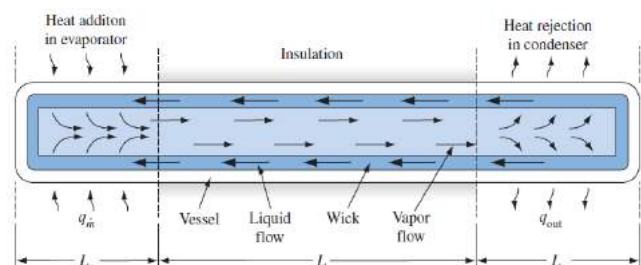
Fig. 2.   Schematic diagram of a heat pipe and the associated flow mechanisms

and fifth columns of the table list measured axial heat fluxes and measured surface heat fluxes, and it is apparent that very high heat fluxes can be obtained.

TABLE 1: SOME TYPICAL OPERATING CHARACTERISTICS OF HEAT PIPES

Temperature Range (K)	Working Fluid	Vessel Material	Measured Axial Heat Flux (W/cm²)	Measured Surface Heat Flux (W/cm²)
230–400	Methanol	Copper, nickel, stainless steel	0.45 at 373 K	75.5 at 373 K
280–500	Water	Copper, nickel	0.67 at 473 K	146 at 443 K
360–850	Mercury	Stainless steel	25.1 at 533 K	181 at 533 K
673–1073	Potassium	Nickel, stainless steel	5.6 at 1023 K	181 at 1023 K
773–1173	Sodium	Nickel, stainless steel	9.3 at 1123 K	224 at 1033 K

In order for a heat pipe to operate, the maximum capillary pumping head, $(\Delta p_c)_{max}$, must be able to overcome the total pressure drop in the heat pipe. This pressure drop consists of three parts:

1. The pressure drop required to return the liquid from the condenser to the evaporator, Δp_e
2. The pressure drop required to move the vapor from the evaporator to the condenser, Δp_v
3. The potential head due to the difference in elevation between the evaporator and the condenser, Δp_g.

The condition for pressure equilibrium can thus be expressed in the form

$$(\Delta p_c)_{max} \geq \Delta p_e + \Delta p_v + \Delta p_g$$

If this condition is not met, the wick will dry out in the evaporator region and the heat pipe will cease to operate.

V. HEAT-PIPE OVEN [4]

The heat-pipe oven, shown schematically in Fig. 3 consists of a stainless steel tube heated along its central part with water-cooled jackets at both ends and a stainless steel mesh "wick" encircling the inner wall of the tube. The cold oven is filled with a given pressure P_{buffer} of helium buffer gas (200 mT in this experiment) and contains a 30-g ingot of Li. When heated, the Li melts and its vapor pressure increases. The Li vapor transports away from this evaporation zone and eventually condenses onto the wick some distance away. Condensation heats the wick through release of the Li heat of evaporation (19 J/g), while the transport of the vapor away from the center of the oven expels the helium buffer gas through lithium–helium collisions. As the heating power is increased, the evaporation rate of the liquid Li on the wick
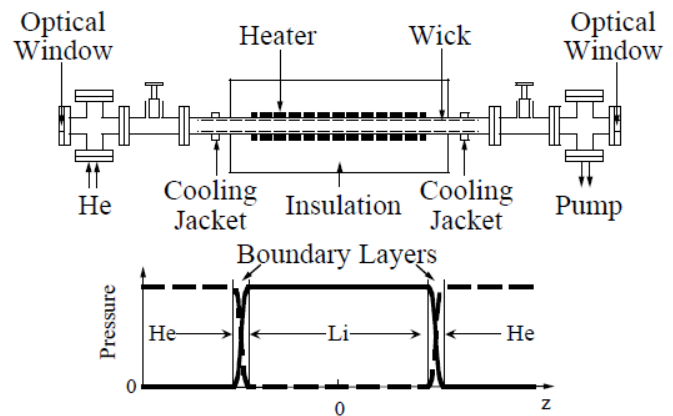
Fig. 3. Schematic of the heat-pipe oven (not to scale) and expected pressure profiles for the buffer gas (He) and the Li vapor (assuming no significant flow in the oven). The length of the Li column and width of the boundary layers are arbitrary on this figure.

increases, as do the temperature and pressure of the Li vapor. At some heating power, the oven reaches a temperature such that the vapor pressure of the liquid Li is equal to P_{buffer}. The evaporation zone of the oven now contains a column of pure Li with $P_{Lithium} = P_{buffer}$ (assuming the Li flow velocity from the evaporation to the condensation zone of the oven is substantially subsonic). Collisional diffusion of the Li vapor at the helium boundary ensures that the Li condenses onto the wick (where it returns to the evaporation zone through capillary action) and does not penetrate more than a few collisional mean-free paths into the helium, thus forming sharp boundaries. Further increasing the heating power increases the evaporation rate but not the Li temperature.

Instead, the column of Li vapor increases in length until the jackets cooling water temperature boundary condition imposed, ultimately limits the length of this column. The Li pressure and temperature (i.e., density) are fixed by the buffer pressure, while the Li column length is proportional to the heating power.

Temperature Profile Measurement

The length over which the Li vapor extends is estimated from temperature profiles measured with a thermocouple probe inserted along the axis of the heat-pipe oven. The profile without Li in the oven shows that the temperature is decreasing away from the oven center due to heat conduction along the oven. In contrast, the profiles measured with Li in the oven and with comparable heating power exhibit a relatively constant temperature in the center of the oven, followed by a rapid drop toward the end of the oven [see Fig. 4]. The constant temperature in the central section of the heat-pipe oven is the result of the combination of the heat transport by the Li vapor and of the relatively high heat conductivity of the liquid Li on the wick. In this oven, the length over which the vapor density drops to 80% of the center density is estimated from the temperature profiles and the Li vapor pressure curve. However, the temperature of the wick (and thus of the vapor) is expected to be more uniform than that measured by the thermocouple probe because of the heat conduction along the
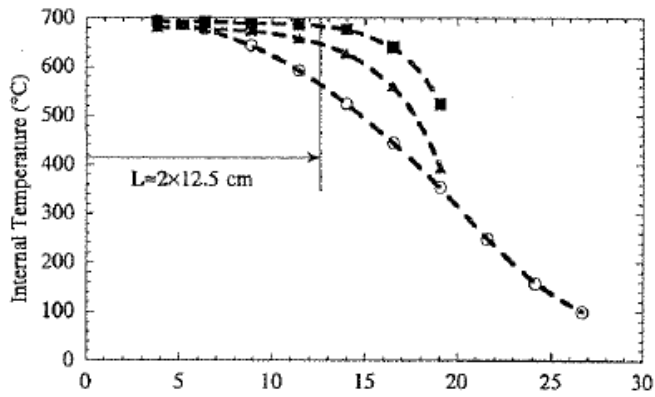
Fig. 4. Temperature profiles along the oven axis without Li in the oven and P_{heat} = 250 W (open circles) and with Li in the oven and P_{heat} = 265 W (filled triangles) and P_{heat} = 307 W (filled squares). The lines are drawn to guide the eye. The Li column length, defined as the length over which the density drops by 20% (according to the Li vapor pressure curve), is L = 25 cm with P_{heat} = 307 W and Text = 750 °C. P_{buffer} = 200 mT.

probe itself. Note that the temperature of the oven wall measured by a thermocouple placed outside of the oven, and referred to as Text hereafter, is about 60 °C higher than that measured inside the oven.

REFERENCES

[1]   John M. Dawson, "Plasma particle Accelerators", Scientific American, Vol. 260, March 1989, pp. 34-41.

[2]   Chandrashekhar Joshi, "Plasma Accelerators: A new method of particle acceleration in which the particles surf on a wave of plasma promises to unleash a wealth of application", Scientific American, Vol. 294, February 2006, pp. 24-29.

[3]   Frank Kreith, Raj M. Manglik, Mark S. Bohn, Principles of heat transfer, 7th Edn, Cengage Learning, 2011, pp. 672-673.

[4]   P. Muggli, K. A. Marsh, S. Wang, C. E. Clayton, S. Lee, T. C. Katsouleas, and C. Joshi, "Photo-Ionized Lithium Sources for Plasma Accelerator Applications", IEEE Transactions on Plasma Science, Vol. 27, No. 3, June 1999, pp. 791-799.

Cryostat for Measurement of Thermal Conductivity, Electrical Resistivity and Thermoelectric Power of $LaBa_2Cu_3O_{7-\delta}$

Ruchir Parikh[1], Prof. Dr. J M Patel[2]

[1,] Student of (M.E. Cryogenic Engineering) L D College of Engineering (ruchir.parikh@git.org.in)

[2] L D College of Engineering, Ahmedabad

(jmpatel2098@yahoo.co.in)

Abstract: **A universal double wall cryostat is design for simultaneous measuring thermal conductivity, electrical resistivity and thermoelectric power of superconducting material. The thermal conductivity, electrical resistivity and thermoelectric power measured in the temperature range from 77 K to 300 K for sample of a superconducting material is described. The intension behind to use a double wall cryostat to check out the evaporation rate and amount of cryogen required for the cryostat by total heat loss.**

I.   INTRODUCTION

The simultaneous study of transport phenomena in the presence of low temperature deformation of metals and alloys gives important information about the scattering of phonons and electrons at new scattering centers created on deformation. The seeback coefficient is an extremely sensitive property whose study as a function of temperature would give valuable information on the electronic structure of the system. Thermoelectric power (TEP) can be measured using the differential technique wherein we create a temperature gradient across the sample of High Temperature super conductor (HTS) and measured the voltage between hot and cold end of the sample connected to the positive of the measuring instrument the sign of the voltage developed give the sign of the thermopower difference between the sample and reference material. We describe in this paper a simple apparatus developed in our laboratory to measure the thermal conductivity, electrical resistivity and thermoelectric power of superconducting material in the temperature range of liquid Nitrogen. The technique that we have developed use very simple instrumentation and it is easier operationally than many of other reported techniques. The purpose of present work is to provide necessary experimental details which are generally absent in other papers. It has been developed mainly High Temperature Superconductor. Another expertise of this instrument is that it can give you the nature of material like conducting material, Smart material, die-electric material or insulator. A slight modification will also allow it to be used with other types of sample like metallic wire or metallic rod. There are several problems in the simultaneous measuring of thermal conductivity, electrical resistivity and thermoelectric power which one has to solve in order to be sure that the results obtained are correct: (i) the temperature of two ends of the sample has to be the same and should not vary during the experiment; (ii) the sample has to be part of an electrical chain for precision measuring of its resistivity; (iii) there should be high vacuum in the space around the sample; (iv) both ends of the sample have to be mechanically stabilized, so that the good thermal and electrical contacts remain unchanged during deformation (v) evaporation rate should be minimum. Section 2 discusses the description of experiment apparatus used for measurement of this three properties for the cuprates. Section 5 comprise of results and discussion based on quality analysis. Section 6 concludes the paper.

II.   DESCRIPTION OF EXPERIMENT APPARATUS

The schematic diagram of the cryostat is shown in figure. It essentially contains a high conductivity copper sample holder whose temperature can be controlled by an electronic controller. A 50 ohm manganin heater total length of 2.5 m wound on the bottom side of sample holder and attached by low temperature varnish is used for temperature variation. All the electrical leads are thermally anchored to the shield. This whole set-up is housed in a cryostat which is immersed in the liquid nitrogen. The sample whose properties are to be measured is held tightly in the sample holder using glass epoxy plate with brass screw as shown in figure. The investigation of the thermoelectric power, thermal conductivity, electrical resistivity of superconducting material can yield valuable information about their electronic and structural properties. Good thermoelectric can convert heat directly into electrical energy with a reasonable efficiency provided a substantial temperature gradient exists and the material has a high thermoelectric figure of merit (ZT). For efficient high temperature power generation, good thermoelectric materials with large ZT at high temperature are highly desirable. It is essential to evaluate and therefore measure the following key transport parameters: the Seeback coefficient, electrical resistivity, and thermal conductivity. In any case, the measurement should be done with high accuracy and over a wide range of temperatures. Techniques to measure transport properties at low temperature are described in the literature, [1 – 5]. On the contrary fewer papers are available dealing with high temperature transport property measurements. Almost two decades ago Wood *et al.* [6] developed an apparatus for the Seeback coefficient measurement. A brief mention of the experimental technique also appears only occasionally in research papers dealing with high temperature transport

studies [7 - 12]. In this paper we describe an apparatus that was setup in our laboratory to measure the Seeback coefficient at temperatures range from 77 K to 300 K.

III.   EXPERIMENTAL PROCEDURE

The schematic diagram is shown in figure-1. We have solved above stated problems in the following way: both ends of the sample are firmly attached and soldered to two massive copper blocks and having the temperature of the liquids in two Vessel (nitrogen or oxygen), in order to realize thermal, electrical and mechanical contacts. The liquids in the two Vessel are boiling under the same pressure since their vapors are simultaneously pumped out via the interconnected glass tubes. The distance between the levels of the liquids is kept constant using a bellows system for raising the outer Dewar, and a system for measuring the level of liquids. This distance must be equal to the length of the sample (superconducting material), which in our case was of the order of 7-8 cm. These precautions are necessary in order to ensure the same hydrostatic pressure for both ends of the sample. The flange is fixed and coupled to another flange with bolts passing through insulating rings and an insulating spacer ring made of the synthetic material whose mechanical properties are suitable, insulate the two parts of cryostat from each other. The thickness of the insulating spacer ring depends on the thickness of rubber packing. The dimensions of the stainless-steel tubes are determined by the requirement that their upper ends have to be at room temperature, and the external tube has to be subjected to the stress. The suitable thickness in our case was 1 mm for internal and 2 mm for external tubes. The connection of the sample to the electrical chain can be realized by flanges.

After putting cryostat in cryo vessel the valves are closed for pumping out its vapour. The variation of temperature is carried out by varying the speed of pumping out vapour from the common volume above the liquids in the Dewars. The female copper screw the cylindrical block and the bellows of the internal Dewar make thermal contact possible, and the variation of the length of the samples (of about & 7 mm). After the sample is fit the cover is tin soldered and the volume around the sample is evacuated through the tube. The temperature gradient from the middle to both ends of the sample can be created by electrical current through the sample (the magnitude of the current depends on the sample and is of the order of a few amps), or by a heater fixed in the middle of the sample. In our case the temperature difference between the middle and the ends was of the order of 0.5-2 K for different specimens and was measured using Pt thermometers or a differential constantan /copper-constantan thermocouple. The pumping out of vapour from the two refrigerant baths may be controlled by two valves on each of the tubes so that a suitable (better than if using of heaters into the baths) compensation of the superheating of the order of one tenth of a degree is possible (better than using heaters into the baths), by the creation of an almost negligible difference of the vapour pressure in two baths. Thermal changes of the

two ends of the specimen are also partly smoothed by thermal inertia of the copper blocks, and in this way the temperature difference between the ends of the sample was not larger than 0.01 K, which is convenient for performing the experiment.

IV.   METHOD FOR SAMPLE PREPARATION

There are many routes are available for the synthesis of High Temperature Super Conductor (HTSC). Mainly two methods are well known Solid state and Chemical method. We have selected Solid state routes for the sample preparation of HTSC system.

Synthesis of $LaBa_2Cu_3O_{7-\delta}$ By solid state method

The sample $LaBa_2Cu_3O_{7-\delta}$ were prepared using La_2O_3 , $BaCo_3$, Cuo, as precursors. The steps of preparing the sample of are explain below.

1. For small batch of 5 gms. The constituents oxides (or their precursors) were mixes in appropriate proportion. The proportion of precursors were decide with the help of molecular weight as follow.
2. After calculation of proportion, with help of digital weight m/c we had prepared stoichometric proportion of all precursors and mixed in pestle and mortar for 1 hrs. grinding. The 1 hr. grinding was divided in four parts and also add aceton in pestle after each 15 min. So we got finally the fine powder of oxides.
3. Collect the powder in ceramic boat and put in the furnace for heating at $800\,^\circ C$ for 12 hrs.
4. After heating the powder in furnace, grind the powder in pestle for 1 hr. and then palletized the powder with help of die in hydraulic press.
5. Put the pallet in the boat and then heat the pallet in the furnace at $930\,^\circ C$ for 24 hrs.
6. Break the pallet and regrind it. Then repalletized it and put in the furnace for heating at $950\,^\circ C$ for 24 hrs. Measure the resistivity with two probe multimeter.
7. Put the pallet for annealing in the stream of Oxygen at $950\,^\circ C$ for 24 hrs.

V.   METHOD OF DATA ACQUISITION

To begin with the base temperature is stabilized at the temperature of interest and small amount of power is applied to the top of copper disc using the heater attached to it (typically 20 mW to 200 mW depending on the temperature and the thermal conductance of the sample). The temperature oh the top copper disc increase steadily and consequently a small voltage will be developed across the hot and cold end. The temperature difference was typically 0.5 K to 5 K depending on the temperature. If the heater power is sufficient small so that the base temperature does not drift or $\Delta T/T$ is small the curve back in the reverse direction if the system is allowed to relax by switching off the heater power. The slope of the straight line thus traced is used to find out the seeback coefficient.

In many situations we find that an acceptable straight line is not obtained or the heating or cooling curve shows hysteresis. We found that such situation can come from the following reason.

1. Base temperature is not properly controlled ;
2. ΔT is to small (typically $\Delta T/T < 1\%$ gives problem).
3. Bed thermal contact between the sample and copper disc and also between thermocouple junctions and copper disc.Widely different equilibration times for the sample and the thermocouple gives rise to hysteresis behaviour if the heating rate is too fast compared to the larger of the time constants.

VI. FIGURE OF EXPERIMENTAL SET-UP
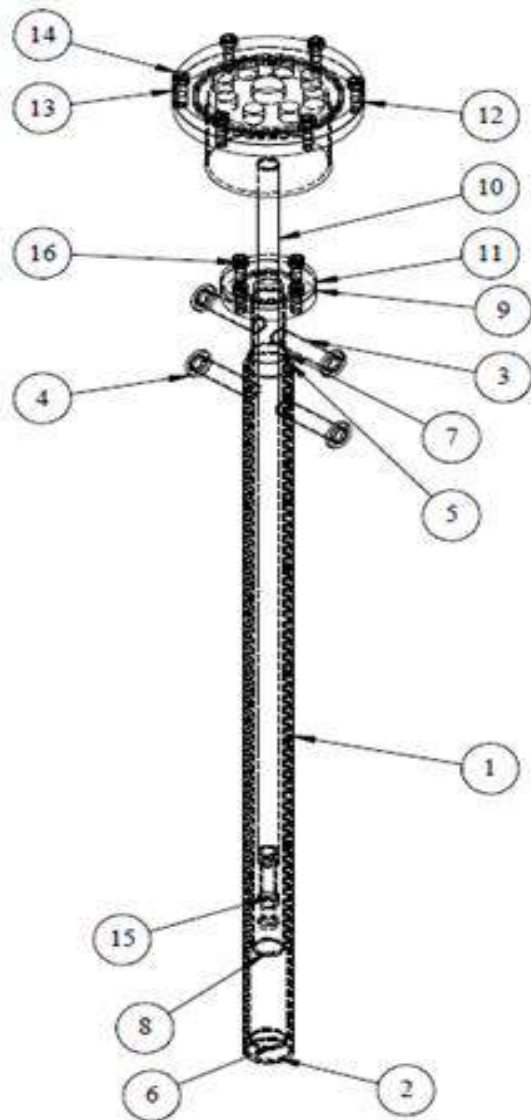
VII. CONCLUSION

We have described here a simple apparatus of moderate to good accuracy for measuring thermal conductivity, electrical resistivity and thermoelectric power of superconducting material in the range of 77 K to 300 K. The apparatus is simple to use and easily accessible to microprocessor data acquisition . The necessary detail have been given hare and or further detail the authors can be contacted.

REFRENCES

[1] T. M. Tritt, in: semiconductors & Semimetals, edited by T. M. Tritt, Academic, 2001, Vol.69,p. 25.
[2] C. Uher, Nav. Res. Rev. **48** (1996) 48.
[3] T. M. Tritt, Mater. Res. Soc. Symp. Proc. **478** (1997) 25.
[4] A. L. pope, R. T. Littleton IV, and T. M. Tritt, Tev. Dci. Instrum. **72** (2001) 3129
[5] G. R Caskey and D. J. Sellmyer, Rev. Sci. Instrum**. 40**, 1280 (1969).
[6] C. Wood, D. Zoltan, and G. Stapfer, Rev. Sci. Instrum. **56**, 719 (1985).
[7] B. A. Cook, J. L. Harringa, S. H. Han, and C. B. Vining, J. Appl. Phys. **78** (1995) 5474.
[8] R. T. Littleton IV, J. effries, M. A. Kaeser, M. Long, and T. M Tritt, Mater. Res. Soc. Symp. Proc. **545** (1998) 137.
[9] V. Ponnambalam, S. Lindsey, N. S. Hickman and T. M. Tritt, Rev. Sci. Inst. **77**(2006) 073904.
[10] O. Boffoue, A. Jacquot, A. Dauscher, B. Lenoir, Rev. Sci. Inst. **76**(2005) 053907.
[11] Y. Xin, D. Ford, Z. Z. Sheng, Rev. Sci. Inst. **63**(1991) 2263.
[12] S. R. sarath Kumar, S. Kasiviswanathan, Rev. Sci. Inst. **79**(2008) 024302

Enhancement in mapping capability of Feature Replace command in NX CAD software

Pankaj Sharma, Girish Deshmukh, Reena Trivedi

(11mmcc14@nirmauni.ac.in)

Abstract—**Replace Feature Command in Siemens NX needs to have better mapping capability without losing current Functionality such as maintaining associativity with downstream features and replacing non parameterized bodies with parametric features. Problems in automatic mapping can be solved only with efficient matching algorithms. There were various algorithms available but one has to judge its suitability by considering various factors such as consistency and efficiency. Some of the preliminary results show that automatic mapping has helped in improving replace feature workflow.**

Index Terms— **Matching, Replace Feature, Dumb body, Re-parent**

I. INTRODUCTION

ACAD software comprises of a very important position in product life cycle. Moreover there is a lot of competition in the market so if a CAD system wants to survive in the market it needs to developed and improved continuously without losing the robustness and consistency of the features. All stages of product development are supported, from conceptualization, to design (CAD), to analysis (CAE), to Manufacturing (CAM). NX is a parametric solid / surface feature based package based on Parasolid. NX is widely used throughout the engineering industry, especially in the automotive and aerospace sectors. NX can provide users with industry specific tools known as wizards to help streamline and automate complex processes, as well as improve product quality and user productivity. For example, the Mold Wizard module addresses the specific requirements of plastic injection applications while the Progressive Die Wizard addresses the specific requirements of die stamping applications.

Replace Feature Command needs to have better mapping capability without losing current Functionality such as maintaining associativity with downstream features and replacing non parameterized bodies with parametric features.

A geometric matching primitive under a variety of transformations is an important problem in computer vision, robotics, and many other applications. Over the last decade, a number of techniques have been proposed for finding globally optimal solutions to such matching problems. Such techniques work by recursively subdividing the space of transformation parameters and computing upper bounds on the possible quality of match within each sub-region, and they can guarantee returning globally optimal solutions to geometric matching problems.

Various types of matching algorithms are Branch and bound method[1], least square fitting method[2] and based on linear features, feature points, feature edges.

In replace feature command, geometric matching algorithm plays a very important role as we need to compare points, edges, faces and bodies of "Features to Replace" with "Replacement Feature". Here we have enhanced the performance by making use of smarter Algorithms.

Geometric matching is all about matching points, lines, edges, faces, bodies. It takes help of length of line (curve) and sample points. Faces are generally recognized as parametric faces. They are matched with the help of sample points. A parametric face is a face in the Euclidean space which is defined by a parametric equation with two parameters. Parametric representation is the most general way to specify a surface. Surfaces that occur in two of the main theorems of vector calculus, Stokes' theorem and the divergence theorem are frequently given in a parametric form. The curvature and arc length of curves on the surface, surface area, differential geometric invariants such as the first and second fundamental forms, Gaussian, mean, and principal curvatures can all be computed from a given parametrization.

Let the parametric surface be given by the equation

$$r = r(u, v)$$

where,

r is a vector-valued function of the parameters $r(u, v)$

and the parameters vary within a certain domain D in the parametric u-v plane. The first partial derivatives with respect to the parameters are usually denoted and similarly for the higher derivatives.

Matching between all entities of replace object and replacement object is carried out within matching tolerance. Sample points are distributed along u-v parameters.

II. METHODOLOGY

Study of NX Modeling Software, NX framework, geometric kernel Parasolid, OM, and CMOD and Feature code. Implementation of automatic matching capabilities and added diagnostic messages.

III. RESULTS AND DISCUSSION

We use Replace Feature command to make changes to the basic geometry of a design without having to edit or recreate all of the dependent features. You can replace bodies and datum and map the dependent features from the original feature to replace, to the new replacement feature.

It can replace a parent feature and its dependent features while maintaining associativity with downstream features. Replace old versions of bodies imported from other CAD applications with updated versions. Replace one freeform surface with another. Re-specify the selection intent of the downstream features. Reorient the input direction of a Replacement Feature, so that it can be used by downstream features. Re-parent child features in other parts.[3]

A replacement feature defines set of objects and geometry eligible for reference mapping. This means, if a feature is a member of the replacement feature set its object and geometry can be selected during reference mapping. Conversely, if a feature is not a member of the replacement feature set its object and geometry cannot be selected during mapping. One or more features are explicitly input.[4]
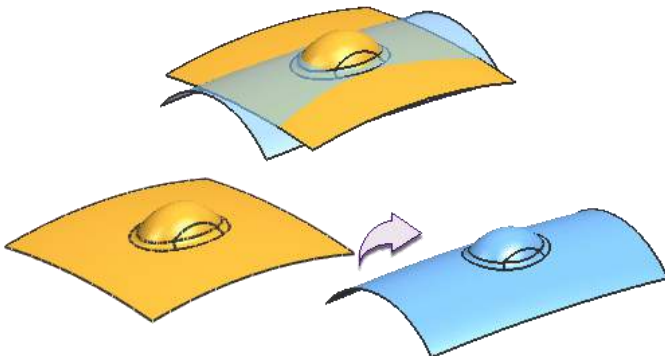
Fig. 1. Replace Feature does not replace the Copy Feature, Paste Feature or any other Edit Feature commands. It enables you to make edits to a body based on its parent geometry.
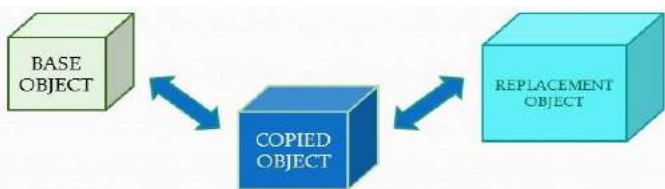
Fig. 2 . Working of Feature Replace Command.

It can replace a parent feature and its dependent features while maintaining associativity with downstream features. Replace old versions of bodies imported from other CAD applications with updated versions. There is a rollback of base

object up to parent object. Concept of matching and comparable state is used in between copied object and replacement object.

In Replace Feature, feature may fail to migrate because a comparable NX feature does not exist, or because of bugs, or the need for extra input. These features are migrated in various ways, one of which is to create a non-associative (dumb) body, a special feature called Data Access (which has information that can be used to rebuild the feature in NX), and a Patch feature that patches the dumb body surfaces into the part. Downstream features are then based on that body represented by the Patch.
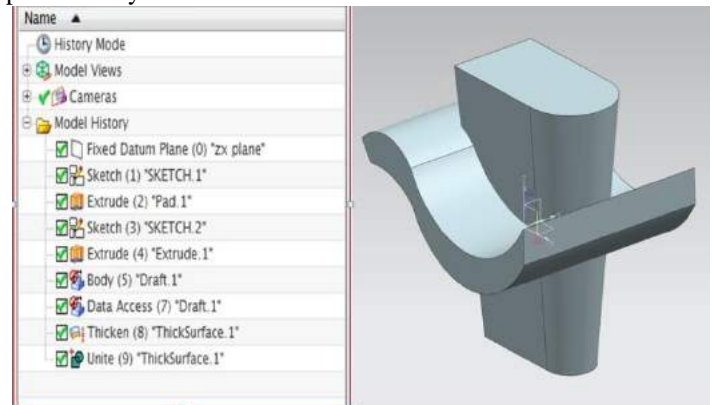
After migration is complete, the user wants to replace the dumb body and Patch with a corresponding NX feature that he creates. After the proper feature is created, Replace is used to replace the dumb body with it, if required. Above problem has been overcome.

A Part or an assembly is accompanied by:

1. Construction history: The procedure used to construct the shape model;
2. Parameters: Variables associated with dimensional or other values in the model, providing an indication of what it is permissible to change;
3. Constraints: Relationships between parameter values or between geometric or topological elements of the model, specifying invariant characteristics in the model under editing operations, usually in the interests of maintaining product functionality during modification;
4. Features: Local shape configurations in the model that have their own semantics.[5]

Matching of features in CAD software plays an important role. It facilitates user to increase performance while replacing a feature.

There are various types of matching available in CAD software:-

1. User defined matching: The user has defined this match through a screen pick or otherwise
2. Geometric matching: The match was inferred by the geometric matching algorithm.
3. Inferred matching: The match was inferred from previously accepted matches.
4. Mixed type matching: The match was created by a combination of multiple methods.[3]

This paper mainly focuses on how "Geometry Matching" would help in typical replace workflow and what productivity

NX users will get with this. It can be well understood with an example.

BLOCK 2(INDEPENDENT BODY WITH NO CHILD)

BLOCK 1 WITH BLEND AS CHILD
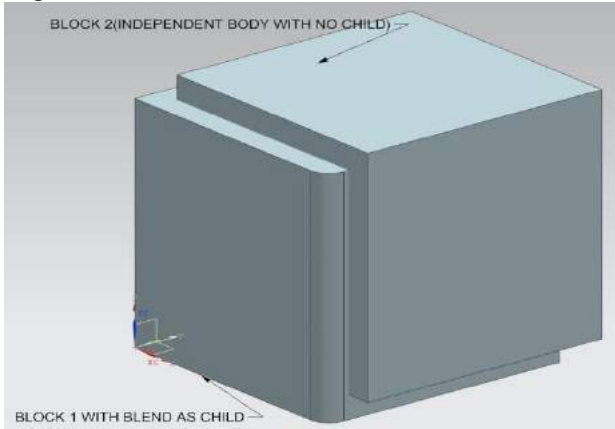
Concept of Geometric Matching is mainly facilitated by Geometric Matching Allowance. In Present example, there are two blocks one as independent body (Block 2) with no child and another block with edge blend (Block 1). Here Block 1 and Block 2 are overlapping. In Feature Replace we want to replace Block 1 with Block 2 or in other words ,blend on block1 will be placed on block 2.In next figure UI of feature replace is shown, where in Feature to replace(Block 1) ,Replacement Feature(Block 2) and Edge Blend are the concern.

BLOCK 2 WITH BLEND AS CHILD(AFTER FEATURE REPLACE)

BLOCK 1 WITH NO BLEND AFTER FEATURE REPLACE
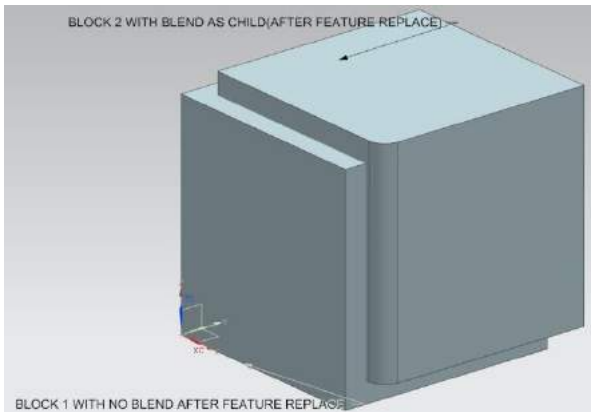
Here, the requirement is to transfer blend from block 1 to block 2 without manual selection. Here geometric matching allowance shown in next figure is set to 1 mm. Size of the two blocks are similar. Internal geometric matching algorithm iterates over all the edges of the replacement feature and matches with the best possible edge. Even it is possible to get more than one possible matches, in such cases it picks first best match. Such behavior helps in the area where there is large number of dependents on body.

IV. CONCLUSION

It has been found that there has been improved replace feature workflow after implementing automatic geometric concept. Enhancement in usability in terms of mouse clicks. There has been elimination of Migration Problem.

REFERENCES

[1] Breuel T.M., "Implementation techniques for geometric branch-and-bound matching methods" , Computer Vision and Image Understanding ,258 294,2003
[2] Borkowski J., Matuszewski B.J. , Mroczka J., Shark L.K. "Matching of circular features by least squares fitting", Pattern Recognition Letters, 23:885-894,2002
[3] Siemens NX internal documentation.
[4] NX CAST Documentation

[5] K. Jha, B. Gurumoorthy, "Automatic propagation of feature modification across domains", Computer-Aided Design , 32nd ed. vol., pp. 691-706, May 2000.

[6] V.B. Sunil, S.S. Pande, "Automatic recognition of features from freeform surface CAD models, 40th ed. vol., Computer-Aided Design, , pp. 502-517, 2008.

[7] Qiang Ji and Michael M Marefat, "Bayesian approach for extracting and indentifying features ", Vol. 27. No. 6, Computer-Aided Design, ch. 4. pp. 435-454, 1995.

[8] Wenfeng Li,Feature, "Modeling From 2D Drawings and Product Information Description", Chapter Computers ind. Engng, Vol 31:681 – 684,1996

[9] Atalay Volkan, Yilmaz M. Ugur, "A matching algorithm based on linear features", Pattern Recognition Letters,19:857 867,1998

Waste Heat Recovery from VCR Systems – A Review

Ankit K Patel, N M Bhatt, N M Gajjar

(patel.ankit27789@gmail.com, director@git.org.in, nimesh.gajjar@git.org.in)

Abstract— **Energy saving is one of the key issues, not only from the view point of fuel consumption but also for the protection of global environment. So, it is imperative that a significant and concrete effort should be made for conserving energy through waste heat recovery. The main objective of this paper is to study and analyse the feasibility of different methods for waste heat recovery from condenser of VCR cycle. This paper includes different methods to extract heat from condenser are water cooled condenser connected with air cool condenser in parallel in conventional air conditioning thermodynamic cycle, Gas side heat recovery by connecting the auxiliary condenser(Canopus Heat Exchanger) in series with main condenser**

Index Terms—**Waste heat recovery, Canopus Heat Exchanger, Vapour Compression Refrigeration, Refrigeration and Air Conditioning**

I. INTRODUCTION

Waste heat is the heat, which is generated in a process by way of fuel combustion or chemical reaction, and then "dumped" into the environment even though it could still be utilized for some useful and economic purposes. Waste heat, in most general sense, is the energy associated with the waste streams of air, gases, and liquids that leave the system and enter into the environment. Waste heat which is rejected from a process at a temperature sufficiently above the ambient temperature permits the recovery of heat for some useful purposes in an economic manner. The essential quality of heat is not the amount but its "value". The strategy of how to recover this heat depends not only on the temperature of the waste heat sources but also on the economics involves behind the technology incorporated.

Refrigeration and air conditioning (RAC) plants remove heat from the space to be conditioned and pumping it to the higher temperature sink. Added to this heat which is taken from the space, there is work added by the compressor in a vapour compression system and the total heat is rejected to the environment. Heat rejected from the air conditioning system is the superheat and latent heat of the refrigerant.

Heat rejected from air conditioning systems is of low grade quality. Due to the high costs associated with the recovery of such heat and the availability of alternate means for meeting low grade heat requirements, low grade waste heat is generally rejected to the atmosphere.

A rough estimate of waste heat available from an RAC system indicates that about 3 -5 kW of waste energy is rejected to the environment for every kilowatt of energy consumed by the compressor. Recovery of this energy will contribute to the saving of overall energy costs [1] – [2].

Some of the issues which are involved are matching of the cooling demand in RAC system and availability of low grade heat. Unlike industrial heat rejection, which is available in larger quantities and at higher temperatures, the heat rejection from RAC systems has a fluctuating availability. While the availability of heat rejection from industry is dependent on fixed operating parameters, the heat rejection from RAC systems is dependent on ambient weather conditions. Against industrial applications, apart from internal cascading of low grade heat sources to low temperature processes within the plant, there are low temperature heat requirements in grain drying and food processing. The scope of this paper is limited to the collection of waste heat from RAC plants considering the simultaneous generation of both cooling and heating.

The utilization of waste heat is profitable wherever heating and refrigeration are required at the same time, or where waste heat can be stored:

- In air conditioning systems to reheat dehumidified air
- In butcheries, dairies, hotels, etc., where, on the one hand, cold storage rooms/air conditioning rooms are operated and where, on the other, there is always a great demand for domestic hot water
- In shops, where in addition to cooling foodstuff, heat demand also occurs, e.g. mall heating
- In cold storage facilities, for heating and domestic hot water
- In industrial processes (e.g. drying processes)
- In cold storages where vegetables may be cleaned/dried prior to the storage

II. HEAT RECOVERY METHODS

A. Gas side heat recovery

The condenser heat can be utilized in several ways. Gas-side heat recovery methods are discussed here. They have several major advantages over other solutions. Direct use of the condensation heat usually provides a higher temperature and heat yield than conventional, indirect heat exchange methods.

Additionally, the three-port valve for gas-side control permits a simplification of the water circuit on the demand side, especially in the case of reheating of the heating medium above the condensation temperature (e.g. hot water heating systems with electric water heaters). Three-port valves prevent the occurrence of undesirably high pressures in the condenser at high return temperatures, thus increasing operational safety at little expense.

Gas-side heat recovery takes place in auxiliary condensers. They can be connected to the main condenser by various circuits. Two basic configurations are explained here.

1) Condensers connected in series

If an additional condenser is connected upstream of the main condenser for the purpose of heat recovery, the term series-connected condensers is used.
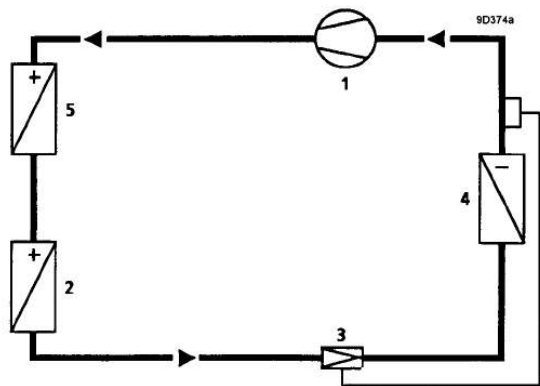
1. Compressor
2. Main condenser
3. Expansion valve
4. Evaporator
5. Additional condenser

Fig.2.1 Refrigeration system with condensers connected in series

This configuration is selected for following cases if the additional condenser is used for heating domestic hot water whose temperature is higher than the condenser temperature. This is achieved by using the extracted heat. The achievable water temperature depends on the size of the auxiliary condenser and on the pressure prevailing in the condenser downstream from it:

- If the additional condenser is used for reheating the air in an air conditioning system with dehumidification
- If the heat recovery condenser needs higher

condensation temperature than the main condenser with the aid of additional pressure control

In the case of series connection, the pressure losses in the condensers and refrigerant pipes manifold. Therefore, the pressure loss between the compressor and the refrigerant receiver must not be too large; otherwise the efficiency of the system decreases.

2) Condensers connected in parallel

If the additional condenser is placed alongside the main condenser and supplied simultaneously with the same gas, this is a parallel connection of condensers. This is used where:

- Both condensers have a relatively large pressure drop, be it due to long pipe runs or due to a great pressure loss in the condenser itself
- Multiple condensers are used for heat recovery, e.g. for domestic hot water heating and air heating in the retail area and butchery
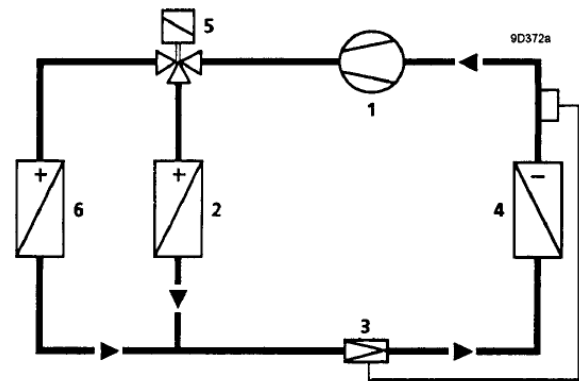
1. Compressor
2. Main condenser
3. Expansion valve
4. Evaporator
5. Hot gas diverting valve M3FB
6. Auxiliary condenser

Fig.2.2 Refrigeration system with condensers connected in parallel

In the case of parallel connection, the pressure losses are divided among the condensers. Therefore, such systems are especially efficient.

In both series and parallel connection the condenser that is shut down is partially or fully flooded with refrigerant, regardless of its supply control. This occurs until the condenser at the lower ambient temperature is flooded to such an extent that the pressure is equalized between the condensers.

III. APPLICATION OF HEAT RECOVERY METHODS

A. Condensers connected in series

A vapour compression refrigeration system with a Canopus Heat Exchanger[8] shown in figure Fig.3.1 is a work absorbing thermodynamic system based on the reversed heat engine principle. It consists of a mechanical

compressor, a condenser, an expansion device for throttling and an evaporator. Working fluids with desirable thermodynamic characteristics, such as Freons and Ammonia are used as refrigerants [3]-[5]. In a simple saturated thermodynamic cycle, the saturated vapour of the refrigerant coming from the evaporator is drawn by the compressor and compressed isentropically at the expense of input work W (process 1- 2). The compressed vapour is taken into the condenser where it condenses (process 2-3) at constant pressure (p_c) as a result of the removal of latent heat of condensation (Q_c), with an external cooling fluid (air or water). The liquid refrigerant coming from the condenser undergoes adiabatic expansion through the expansion valve, accompanied by a drop in pressure at constant enthalpy (process 3-4). This arrangement of isenthalpic expansion, rather than isentropic expansion is good from the point of view of practical convenience and economic constraints. However, this may be a cause of energy loss during throttling. The liquid refrigerant under pressure (p_e) evaporates in the evaporator, thereby absorbing heat (Q_e) from the space to be cooled. The low pressure vapour from the evaporator at state 1 is compressed by the compressor and the cycle is repeated. In
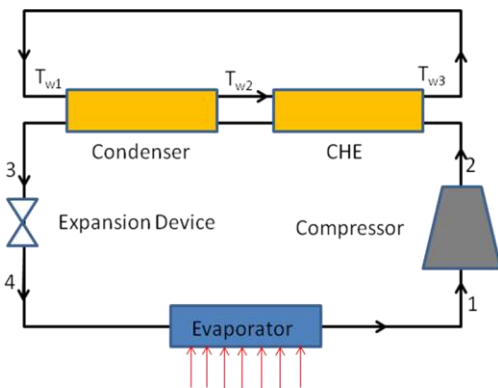
Fig.3.1 Heat Recovery by Canopus Heat Exchanger

order to recover heat from the condenser, an additional Canopus heat exchanger between the compressor and the condenser is incorporated, as shown in the same figure. Water is used to remove heat from the condenser and the Canopus heat exchanger. The water temperature rise in the condenser is below the temperature of condensation of the refrigerant vapour. After compression, the superheated refrigerant vapour transfers a large amount of heat to the water stream through the Canopus heat exchanger. A counter-flow arrangement is used in which the incoming water stream first comes in contact with the condensing refrigerant vapour and attains a temperature near to the condensation temperature. After leaving the condenser, the water comes in contact with the higher temperature superheated refrigerant vapour leaving the compressor and attains a temperature higher than the condensing temperature of water.

B. Condensers connected in parallel

Air-cooled air-conditioner is widely used in residential and commercial buildings. With the development of civil

engineering, building service equipment such as air conditioning system needs higher energy efficiency. Then the heat dissipated from air-cooled condenser of conventional air-conditioner has been considered to be reused and air-conditioner combined with hot water production is proposed to improve operational performance [6]-[7].

An air-water heat pump scheme proposed in this paper is shown in Fig.3.2 of Water cool condenser parallel to Air cool condenser of conventional air conditioning thermodynamic cycle [10]. In summer, this equipment draws heat from cooling room and releases the heat to water tank and atmosphere. Pump1 transports heated water from water-cooled condenser to water tank continuously. Pump 2 transports cooled water in evaporator to terminal equipments such as fan-coil for residential room cooling.
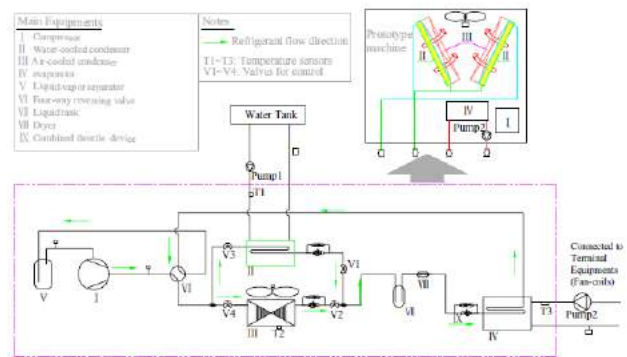
Fig. 3.2 Schematic diagram and prototype machine configuration of air-water heat pump

Water temperature in water tank affects operational performance of the equipment. With the increase of water temperature in water tank, heat-transfer performance of water-cooled condenser gets weakened. Then a control strategy is considered to maintain the equipment operating efficiently. The operating states of air water heat pump are shown in Table 1 below.

TABLE I
OPERATION STATE OF AIR-WATER HEAT PUMP

Devices	Air conditioning & hot water making		
	STATE A	STATE B	STATE C
	T1<35°C	35°C<T1<40°C	T1≥40°C
V1	ON	ON	OFF
V2	OFF	ON	ON
V3	ON	ON	OFF
V4	OFF	ON	ON
PUMP1	ON	ON	OFF

IV. CONCLUSION

Proper technique is essential for efficient waste heat recovery. So, paper covered various waste heat recovery techniques for different VCR system. Auxiliary condenser in

series method is useful for domestic water heating system and auxiliary condenser in parallel is useful for pressure drop reduction. Application of various method is also referred which is useful for efficient method selection.

V.   NOMENCLATURE

p_c	condenser pressure
p_e	evaporator pressure
Q_e	refrigeration effect (kJ/kg)
Q_c	total heat rejected by the condenser (kJ/kg)
T	absolute temperature (K)
W	compressor power

VI.   REFERENCES

[1] C. J. Andereen (Editor), Recovering Energy From Refrigeration, Energy Technology, pp. 12- 13 (1988).

[2] G. E. Stinson, Design principles of refrigeration waste energy recovery. Australian Refrigeration, Airconditioning & Heating, May, 25-30, (1985).

[3] Filippo de'Rossi, Rita Mastrullo and Pietro Mazzei, Working fluids thermodynamic behaviour for vapour compression cycles. Appl. Energy 38, 163-180 (1991).

[4] S. Devotta and S. Gopichand, Comparative assessment of HFC 134a and some refrigerants as alternatives to CFC(R-12). Int. J. Refrig. 15(2), 112-118 (1992).

[5] M. O. Mclinden and R. Radermacher, Methods of comparing the performance of pure and mixed refrigerants in the vapour compression cycle. Int. J. Refrig. 10, 318-325 (1987).

[6] Praitoon Chaiwongsa,Weerapun Duangthongsuk. Hot water making potential using of a conventional air-conditioner as an air-water heat pump, Procedia Engineering, vol.8, pp.165-170,2011.

[7] J.Zhang, R.Z. Wang, J.Y. Wu. System optimization and experimental research on air source heat pump water heater, Applied Thermal Engineering, vol.27,pp.1029-1035,2007.

[8] S. C. Kaushik, M. Singh. Feasibility and Design Studies for Heat Recovery from a Refrigeration System with a Canopus Heat Exchanger, Received in revised form 5 March 1994.

[9] Siemens, Heat Recovery in the refrigeration Cycle.

[10] Yu Wang, Yuwen You, Zhigang Zhang. Experimental Investigations on a Conventional Air conditioner Working as Air Water Heat Pump. Procedia Engineering 23 493 – 497, (2011).

Brand Awareness, Preferences and Media Choices for Branded Toys among Schoolers in Ahmedabad City

A. Prof. Nehal A. Shah   , B. Dr. Ritesh K. Patel

Abstract - The Rs 1000 crores Indian toy industry offers a host of products that include fun games, electronic toys, stuffed toys, educational games, toy cars etc. India faces big challenges from the unorganized sector which contributes about 70 percent of the total toys demand. Out of this, stuffed toys contribute about 15 percent. Indian Toy industry is large and growing which needs more organized approach to face the challenges of factor distribution & marketing. Many of these toys are usually imported through Dubai, Malaysia and China, but Indian markets still have design or modification to some games that reflect Indian taste in them which is absolutely true. Social relevance is majorly used as a factor that is being used. The current study focuses on Children in the age group of 06 to 13 years (popularly known as schoolers) and their preferences for branded toys were collected along with their exposure to various media like television, internet, newspaper, magazine and billboards. At the end of research, vital suggestions were made to help marketers to better understand their marketing patterns for schoolers.

Index Terms - Brand Awareness, Brand Preferences, Marketing to Schoolers, Media Choices, Toys Marketing.

I. OVERVIEW OF WORLD TOY MARKET

Port Washington, New York, June 20, 2011 – According to Global Toy Market Estimates: 2011 Edition, the most recent report from leading market research company, The NPD Group, global toy sales grew by nearly 5% (4.7%) in 2010 to $83.3 billion USD.

While the growth was driven by strong performance in the Asia region, which increased at a rate nearly double the average (9.2%), the U.S. market remains the largest market with sales of nearly $22 billion, followed by Japan, China, United Kingdom and France. The toy market remains very concentrated within these top five countries, which captured just over 50 percent of global sales.

The NPD Group continues to see strong growth in emerging markets, with the BRIC countries (Brazil, Russia, India, China) showing growth of 13 percent. Conversely,

A. Working with Gandhinagar Institute of Technology (A Center for Management Studies), Gandhinagar, 382721, Gujarat, INDIA (e-mail: nehalshahmba@gmail.com).

B. Working as an Academic Associate, Marketing Area, Indian Institute of Management, Ahmedabad, Gujarat, INDIA   (e-mail: drriteshkpatel@yahoo.com).

due in part to exchange rate fluctuations, 2010 sales in Europe was down slightly. In 2007, sales in Europe accounted for 32 percent of the global market; in 2010, they accounted for 28 percent. Looking at Asia, which was less than 25 percent of the market in 2007, it was on par with 2010 European and North American sales.

The toy Industry across the world is highly fragmented. The present size of the toy market can be estimated to be about Rs.4.5 billion. The biggest problem in estimating the size of the industries is the presence of large number of very small players. Besides there is no excise imposed so even the figure of production are not available. Four very large players have global operations namely Mattel, Lego, Hasbro, and Bandai. Mattel Toys are the largest toy manufacturer in the world. Bandai of Japan & Mattel has a strategy alliance worldwide for marketing each other's product. Mattel has been in India since 1985. The company sells toys under the brand name of Barbie, Hot Wheels, and Star Beans etc. The Mattel Company is a $6 Billion company out of which their market share in India is around 20 percent[1].

Apart from that the Indian Toy Industry is very fragmented and very region based. The Indian market is largely unorganized and the market is very small compared to the population and per capita income. Small Scale nature of business has resulted into low product innovation and low investments in new equipment and technology, which has over all resulted into small market size. The toy business is based on constant innovation and you need to be on your toes and produce new innovative toys if you want to survive in the market. Another reason of small size market may be because of large number of small players and low advertising and marketing money spent. But since the last four or five years the market has shown a healthy growth rate. The market is said to grow at 15% to 20% per annum, which is said to be a sound situation and it is further said to grow for least five or six years.

However, the Indian market is highly price sensitive. Reduction in prices of our products has been a contributor to increase in the sales. There are reservations in the Small Sector Industries (SSI), which the government is thinking to de-reserve which will allow the companies to take up capital investments over Rs.100 million and also they would be allowed to collaborate with foreign companies. In addition, the formation of task force by the department of SSI has proved to be a positive development. Many toy associations of India in association with others has started funding programs for providing good infrastructure which at present is very poor compared to China who has developed strong

manufacturing facilities and infrastructure. Funding is also required for improving technology and quality standards. In addition, sufficient amount is required for brand building, which is a challenging task for Indian manufactures in view of the size of the industry. Brand building is an expensive option and requires deep pockets. Returns on investment have to be spread at least over 5 years. One even requires being financially strong in order to face international competition, so these funding programs with the help of associations will definitely prove to be a growing point for the industry. In addition to this, with the advent of multi-format retailing and mall concepts taking place in the country the reach of toys is increasing. Also Free exports were there from first, which has helped in boosting the industry further.

II. INDIAN TOY INDUSTRY

Brief Introduction[2]

Indian Toy industry is large and growing which needs more organized approach to face the challenges of factor distribution & marketing. Many of these toys are usually imported through Dubai & Malaysia. The Chinese toy market is also flooding the domestic market but Indian markets still have design or modification to some games that reflect Indian taste in them which is absolutely true. Social relevance is majorly used as a factor that is being used.

Indian Toy Industry is fragmented and region based but even is largely unorganized as the market is very small compared to the population and per capita income. The Toy business is generally based on constant innovation and one need to always be abreast with the changing tastes of the customers to produce new innovative toys for survival in the market. Since the last four or five years the Indian Toy Industry has shown a healthy growth rate. The market is growing at 15% to 20% per annum, which is a sound situation and it is further is estimated to grow for least five or six years. As Indian market is highly price sensitive, the reduction in prices of the products would contribute to increase in the sales.

Across the world the toy Industry is highly fragmented. The size of the toy market can be estimated to be about Rs.4.5 billion. There is no excise imposed so the figure of production would not be available. The four large players who have global operations are Mattel, Lego, Hasbro, and Bandai. Mattel Toys are the largest toy manufacturers in the world. Bandai of Japan even is famous. Mattel has been in India since 1985; it sells toys under the brand name of Barbie, Hot Wheels, and Star Beans, etc. The Mattel Company is a $6 Billion company out of which their market share in India is around 20%. Today India has over 800 Indian toys and games manufacturers, exporters and suppliers. Indian Toys and games can be classified as fun or educational toys. Toys and games which are available in India include soft toys, computer games, dolls, electronic games, etc.

Market capitalization

The Indian Toy Industry is of Rs 150-crore and is set to grow at 25 % due to rising demand from India and abroad. India is producing the incomparable quality of toys, which is

unmatched elsewhere and therefore, the demand for Indian-made toys is rising by leaps and bounds. More emphasis on quality and innovation along with Indian taste has helped both children and profit margins. According to analysts at Maya Organic, such toys easily account for approximately Rs 200,000 to Rs 250,000 (US$1=Rs. 42) of their business each month.

Size of the industry

Indian Toy Industry's market size is about Rs.250 Crores where 10% constitutes of organized sectors and 90% constitutes of unorganized sector. India has been ranked 8th and UK is ranked 1st for the Toy Industry in the world. An average Indian kid today spends Rs 250 on a toy, UK kid spends Rs 281$(14000 Rs). Funskool has a market in India of 30%. The Toy Association of India estimates that about 90 % of the Indian toy industry belongs to the non-organized sector.

Total contribution to the economy/sales

Indian Toy Industry is estimated at Rs.800-Rs.1200 billion which is dominated by approximately 1250 small and very small producers scattered across the country. The producers are mostly based in the Delhi, Mumbai, Northern State of Punjab, Uttar Pradesh and Haryana, also some in the Southern State of Tamilnadu and in other clusters across India's central states. India has 35 - 40 crores manufacturing base out of which Delhi especially Noida rules 30 crore of markets and Mumbai rules the other 10 crore market.

Employment opportunities

Indian Toy Industry has tremendous potential to raise its productivity, create employment and for all-round development of the economy. Today Indian entrepreneurs have great opportunities to produce toys for the children in the country as they are molded with tradition and culture.

Structure of Indian Toy Industry

Toys are made from a wide range of materials such as plastic, metal, clay, glass, cloth, woods etc. use of new materials and technologies have added value to a variety of toys. Selling a toy often involves selling to three individuals simultaneously, namely the child, who will use the toy, the mother, who is concerned about safety, space to play, etc., and the father who controls the purse strings. The target market for the toy selling firms is middle class and upper income group. According to a study conducted by Funskool, most of the toys are for kids in the age group of 2-5 years (31% of sales) with a particular skew towards the male child (60%).

According to (Dale Hoiberg and Indu Ramchandani, 2000) Indian toys can be categorized into four groups:

- ➢ Toys developed and produced by craftspeople.
- ➢ Mela toys, dynamic folk toys developed and produced by the artisans (skilled and semi skilled person).
- ➢ Toys developed by the layperson or invented by children themselves for their own unique purposes.
- ➢ Factory made toys.

A brief discussion on various toys made from a variety of materials is given below.

Metal Toys: Copper and bronze were the earliest non-ferrous metals which man shaped into tools. References to the casting of bronze images were found in ancient texts like the *Matsya Purana*. Gujarat and Uttar Pradesh in the north and Tamil Nadu and Andhra Pradesh in south India are known for their bronze and copper items.

Wooden Toys: Workmanship on wood has flourished in India over the centuries. Dolls made from wood are very popular. Sikkim is known for its carved objects and dolls. Traditional designs are carved on wood and then painted over giving the whole object a rich effect.

Clay Toys: Terracotta is the most ancient and original form of expression of clay-art. Terracotta figurines in India, ranging over a period of 3,000 years, belong to times both before and after the use of stone in sculpture. Though it is fragile and disintegrates quickly, a continuous stream of art throughout different stages of civilization can still be found. Pottery in India has deep religious significance. Figurines of Gods and Goddesses are made of clay during festivals like *Durga Puja* in Bengal and *Ganesh Chaturthi* in Maharashtra. Also popular are the *gram devtas* (village deities) regularly created by local craftsmen. Delhi is known for its blue pottery which is almost translucent. The Jaipur Blue pottery is even more unique with its arabesque.

Toys made of Stone: Orissa was traditionally known as "*Utkal*", land of excellence of art, because of the vast communities of painters, potters, weavers and other artists who were attached to the major temple complexes. In fact the art of stone carving in Orissa dates back to *Kalinga*(previous name of Orissa) period. Stone carving is carried out on sandstone, Nilgiri stone, soft stone (*Kochilla*) and serpentine stone. Popular themes include the images of Hindu gods and goddesses and dancers. Makrana in Rajastan produces fabulous marble dolls and figurines.

Glass Toys: It was the Mughals who discovered the decorative potential of glass - the fact that when it is cut, it has the opalescence and the glitter of a myriad diamond. Glass engravings from India, exported to Europe till the 16th century, are said to have influenced the Venetians. Today this art has declined but glass items are still part of everyday life. Saharanpur of Uttar Pradesh makes glass dolls and toys filled with colored liquid called *panchkora.*

Paper Mache Toys: Paper Mache is a comparatively new craft in India, which has caught on very well in many parts of the country, since the raw material is easily available and inexpensive. Kashmir is famous for paper mache craft. Kashmir produces some of the most beautifully handcrafted paper mache items. Gwalior in Madhya Pradesh makes paper mache toys, while in Ujjain figures of popular deities are made of this material. Jaipur (Rajasthan) and Chennai are also famous for their paper mache crafts.

Growth of Indian Toy Industry[3]

The Rs 150-crore Indian stuffed toy industry is set to grow at 25 percent due to rising demand from India and abroad. The incomparable quality of toys, India is producing, is unmatched elsewhere and therefore, the demand for Indian-made toys is rising by leaps and bounds. The retail value of the global toy industry is estimated at around $150 billion for 2005.

Toys can be classified into radio-controlled electronic/mechanical toys, regular soft plush toys, DIY (do-it-yourself) toys and educational games/toys, dolls, computer games, collectibles and so on. The export (ex-country) market size of regular soft plush toys is estimated at US$ 2.2 billion, of which roughly 70 percent is controlled by China. Stuffed plus toys exports from China were estimated at US $ 1.75 billion in 2005. There are about 5,000 different designs available in India and about 50 new designs are introduced every month to meet consumers' taste. The leading producer, Hanung Toys and Textiles Limited, alone produces toys with 4000 designs and exports most of its products to the US and European countries. Other producers are mainly from the unorganised sector which Hanung feels cannot match when the matter of quality and designs come.

The overall demand for toys and cotton made-ups is growing at 6 percent in the US and Europe. Despite 10 percent decline in the demand from India in the recent past, toys and made-ups manufacturers are hopeful of a speedy recovery from losses.

The Rs 1000-crore Indian toy industry offers a host of products that include fun games, electronic toys, stuffed toys, educational games, toy cars etc. India faces big challenges from the unorganised sector which contributes about 70 percent of the total toys demand. Out of this, stuffed toys contribute about 15 percent.

III. LITERATURE REVIEW

Sandra L. Calvert (2008)[4], said that marketing to children and adolescents is a way of life in the United States. Children have both their own disposable income and influence over what their parents buy, and marketers attempt to determine how those dollars are spent. Television now reaps most of the advertising dollars, but newer technologies are providing new ways for marketers to reach children. Marketing practices such as repetition, branded environments, and free prizes are effective in attracting children's attention, making products stay in their memory, and influencing their purchasing choices. Immature cognitive development, however, limits the ability of children younger than eight to understand the persuasive intent of commercials. Thus, public policy regulates how advertisers can interact with children via television. Online environments are now and probably always will be less heavily regulated than more traditional media. Although marketing and advertising fuel the U.S. economy, the cost of that economic success requires considerable scrutiny.

Studies of Consumers Association of India (2003)[5], show the spending patterns of children reflect the raging advertisement battle now taking place within the snack and toy industries. Most children use their money to purchase candy (58%) or toys (30%).

Ward et al., (1977)[6], the data provide some support for the three alternative roles of the family in the development of consumer information-processing skills:

- The family has a direct impact on the development of general cognitive abilities and, therefore, an indirect impact on the development of consumer skills.

- The family has an impact on motivating children to apply general cognitive abilities in areas of consumer behavior.
- The family has an impact by directly teaching consumer skills which are not highly integrated with cognitive abilities.

Adya Sharma (2011)[7], said that Children have been identified as an important and different consumer segment. They are three markets in one- the present market for their current product requirements, future market for all goods and influential market which influences their parents to spend on different products. From an Indian perspective this segment specially becomes important as 30% of our population is below the age of 15 years (Census 2011) Also the age pyramid of Indian population shows that we will continue to be a young nation for some time. Understanding the consume socialization of Indian child is important for the marketer who wants to reach out to this segment, forth researcher to understand the unique features of this segment and for policy makers to ensure that consumer socialization of children happens in correct and ethical manner.

Pike, D., & Jackson, N. (2006)[8], said that the child-centered focus group data suggests that the age group most influenced by marketing public relations messages is children aged 6–8, probably due to their limited cognitive ability and consumer knowledge. In contrast to the expected age association outlined by Piaget (1975)[9], Selmen (1980)[10], and Barenboim (1981)[11], however, the influence of consumer communication messages does not necessarily decrease with age. Of course, the complexities of influence do not provide a determining level of impact and thus the specific effect of public relations activities cannot be easily isolated and defined. Industry interviews suggest that in the pursuit of profit maximization. The actions of the toy industry are justified as ethical. In contrast, the survey of wider public opinion identified that such promotional activities were perceived to be unethical. In order to increase ethical perceptions, industry experts must recognize the gap between these two sets of ethical expectations and act, or at least be perceived to act, in a more socially desirable way.

Rhonda P. Ross et. al. (2002)[12], said that when celebrities talk, children listen: An experimental analysis of children's responses to TV ads with celebrity endorsement. Two studies tested the effects of TV ads with celebrity endorsement on the product preference and understanding of 8- to 14-year-old boys. Study 1 compared two ads for a model racer. One had celebrity endorsement (by a famous race driver) and footage of real automobile racing featuring the celebrity (live action); the second had neither feature. Study 2 employed one ad for a different brand of model racer edited to generate a 2 (endorser presence) by 2 (inclusion of live racetrack action) factorial design. A total of 415 boys were exposed to one of the experimental ads or a control ad, embedded in a new animated children's adventure program. Preference for the advertised brand of model racer (pre- and post-viewing) and a number of cognitive variables were assessed. Exposure to endorsement led to increased preference for the toy and belief that the celebrity was expert about the toy. Live action led to

exaggerated estimates of the physical properties of the toy and the belief that the ad was *not* staged. The 8- to 10-year-olds associated the glamour of the endorser with the toy and were more reliant on his advice than were 11 to 14 years old. However, the two age groups were not differentially affected by the ads. Contrary to the speculation of many researchers, understanding about advertising intent and techniques and cynicism about ads had almost no influence on product preference after viewing.

Seth et al. (2009)[13], product recalls, imperfect information, and spillover effects: Lessons from the consumer response to the 2007 toy recalls. In 2007, the Consumer Product Safety Commission (CPSC) issued 276 recalls of toys and other children's products, a sizeable increase from previous years. The overwhelming majority of the 2007 toy recalls were due to high levels of lead content and almost all of these toys were manufactured in China. This period of recalls was characterized by substantial media attention to the issue of consumer product safety and eventually led to the passage of the Consumer Product Safety Improvement Act of 2008.

This paper examines consumer demand for toys following this wave of dangerous toy recalls. The data reveal four key findings. First, the types of toys that were involved in recalls in 2007 experienced above average losses in Christmas season sales. Second, Christmas sales of infant/preschool toys produced by manufacturers who did not experience any recalls were about 25 percent lower in 2007 as compared to earlier years, suggesting industry-wide spillovers. Third, a manufacturer's recall of one type of toy did not lead to a disproportionate loss in sales of their other types of toys. And, finally, recalls of toys that are part of a brand had either positive or negative effects on the demand for other toys in the property, depending on the nature of the toys involved. Our examination of the stock market performance of toy firms over this period also reveals industry wide spillovers. The finding of sizable spillover effects of product recalls to non-recalled products and non-recalled manufacturers has important implications for regulation policy.

Pike, D., & Jackson, N. (2006)[14], Child psychology: Age-related cognitive developments from birth to adolescence contribute to the development of decision making, consumer knowledge and understanding (Hansen et al., 2002)[15]. The ability of children to make mature 'adult' consumer decisions increases with age (Solomon et al., 2002)[16]. Piaget's (1975)[17] theory of cognitive development identifies three stages of cognitive ability: pre-operational (3–7 years); concrete-operational (7-11 years); and formal operational (after age 11). The last stage develops abstract reasoning, which aligns with the information processing abilities known as limited, cued and strategic (Solomon et al., 2002) and with Selman's (1980)[18] stages of consumer socialization (perceptual, analytical and reflective). These stages indicate that the under-developed cognitive defenses of younger children are more vulnerable to persuasive appeals. Younger children (aged 6–8) exist in a pre-operational stage of cognitive development (Hansen et al., 2002) in which pre-logical thought is driven by emotional stimuli (Acuff, 1997)[19]. An egocentric focus enables

information to be infiltrated in a linear fashion in which the dual consideration of both perspectives is replaced by a perceptually bound audience with limited reasoning power (Selman, 1980).

Indeed, Christenson (1982)[20], believes children's cognitive defenses create little or no evaluation preferences for promoted products. While many issues in the theoretical debate are still being debated, there is certainly widespread awareness in the literature that a child's age has some effect on their susceptibility to marketing communication messages, including marketing public relations.

IV. OBJECTIVES OF THE STUDY

- Analyzing how branding affects preference of children towards purchasing of toys.

- Identifying the factors those can affect the purchase decision of children.

- To identify the media preferences for targeting schoolers market.

- To identify appropriate media vehicles for presenting an advertisement for toys.

V. RESEARCH METHODOLOGY

Research type	Quantitative research
Research design	Descriptive research design
Primary data sources:	Children (age 06 to 13 years): 150 respondents
Secondary data sources:	Reference materials, books, encyclopedia, magazines & newspapers, government published reports, Ebsco, J-gate, census, etc.
Data collection method	Survey method
Population	Children (age 06 to 13 years) of Ahmedabad city
Sampling method	Judgmental/Selective/Purposive sampling
Date collection instrument	Structured Questionnaire

Table 1: Details of Research Methodology
VI. DATA ANALYSIS & INTERPRETATIONS

(A) Respondents awareness towards various brands of toys:

Brand Awareness	Respondents	Percentage
Fisher Price	46	30.67
Barbie	86	57.33
Funskool	50	33.33
Hot Wheels	79	52.67
Lego	29	19.33
Local	81	54.00
Other	24	16.00

Table 2: Respondents awareness towards various brands of toys
(See Graph 1 from Annexure)

Table 2 shows that out of 150 children respondents we have surveyed, 57.33% were aware about Barbie and 54% were aware about Local brands. Awareness for Hot Wheels is 52.67%. Awareness about Fisher price, Funskool, Lego is comparatively lower.

This shows that children are more aware about Barbie and Hot Wheels.

(B) Sources to know about various toy brands:

From below given table 3, we can say that for branded toys Television and Internet are the important advertising mediums. For local brands and other toys Newspaper and Pamphlet are important advertising medium.

So the marketers should place their advertising in Television and Internet.

(% out of 150 children)	Television	Newspaper	Magazine	Internet	Billboard	Pamphlet	Promotional Offers
Fisher Price	29.33	5.33	9.33	22.00	1.33	1.33	8.67
Barbie	52.00	12.00	22.00	42.67	0.00	0.67	22.00
Funskool	26.00	4.00	4.67	24.67	1.33	1.33	4.67
Hot Wheels	50.00	8.00	23.33	32.00	1.33	4.00	11.33

Lego	12.00	2.67	4.67	16.67	1.33	2.00	4.00
Local	28.00	37.33	10.00	9.33	0.67	49.33	17.33
Other	1.33	8.00	0.00	1.33	0.00	13.33	2.67

Table 3: Sources to know about various toy brands

(C) Exposure to various TV channels by schoolers:

Channel	Respondents	Percentage
Pogo	120	80.00
Cartoon Network	121	80.67
Cbeebies	24	16.00
Hungama	111	74.00
Nickelodeon	72	48.00
DisneyXD	41	27.33
Playhouse Disney	52	34.67

Table 4: Exposure of various TV channels
(See Graph 2 from Annexure)

From table 4, we can say that out of 150 children respondents we have surveyed 80.67% watch Cartoon network. 80% of them watch Pogo, 74% Hungma, 48% Nickelodean. Children watching Playhouse Disney, Disney XD, and Cbeebies are less, 34.67%, 27.33% and 16% for Playhouse Disney, Disney XD, and Cbeebies respectively.

So the marketers can place their advertisements in Cartoon Network and Pogo for maximum coverage.

(D) Preferences of TV programmes by schoolers:

Programmes	Respondents	Percentage
Tom & Jerry	101	67.33
Doraemon	77	51.33
Chota Bhim	77	51.33
Scooby Doo	30	20.00
Popeye	30	20.00
Richie Rich	77	51.33
Bob the Builder	59	39.33
Other	105	70.00

Table 5: Preferences of TV programmes by schoolers
(See Graph 3 from Annexure)

As shown in table 5, 70% of 150 children see other programmes on television. Second highest is 67.33% which is of Tom and Jerry. 51.33% is for Chota Bhim, Doraemon and Richie Rich.

So the Marketers can place there advertisement during Tom and Jerry, Chota Bhim, Doraemon and Richie Rich.

(E) Influencing factors those can affect purchasing of toy brand:

Influencing Factor	Respondents	Percentage
Package	95	63.33
Friends	111	74.00
Demonstration	54	36.00
Free Gifts	83	55.33
Colour	119	79.33
Lights	97	64.67
Sound	84	56.00
Other	32	21.33

Table 6: Influencing factors those can affect purchasing of toy brand
(See Graph 4 from Annexure)

From the above table 6, we can interpret that the most Influencing Factor is Colour of the toy. Second most Influencing Factor is Recommendation by Friends. Lights, Package, Sound, Free Gifts, Demonstration and Other factors account for 64.67%, 63.33%, 56%, 55.33%, 36% and 21.33% respectively.

From this we can recommend to marketers to focus on the Colour, Word of mouth, Lights, Sound and Packaging of the toys.

(F) Purchase history of schoolers:

From the below table 7, we can see that Brand Usage is more for Local brands that is 51.33%. Brand Usage for Barbie and Hot Wheels is 48% and 39.33% respectively. Usage of Funskool, Fisher Price and Lego is comparatively low.

So these brands need to promote their brands more and should increase the usage of their brands by children by implementing various promotional schemes.

Brands Ever Used	Respondents	Percentage
Fisher Price	30	20.00
Barbie	72	48.00
Funskool	34	22.67
Hot Wheels	59	39.33
Lego	18	12.00
Local	77	51.33
Other	18	12.00

Table 7: Purchase history of schoolers
(See Graph 5 from Annexure)

(G) Rating of satisfaction level towards purchased brand by schoolers:

Experience	Respondents	Percentage
Highly Happy	43	28.67
Happy	59	39.33
Neutral	27	18.00
Unhappy	16	10.67
Highly Unhappy	5	3.33
Total	150	100.00

Table 8: Rating of satisfaction level towards purchased brand by schoolers

The above table 8 shows that out of 150 children we have surveyed 39.33% are Happy with the Brands they have used. 28.67% of them are Highly Happy, 18% are Neutral, 10.67% are Unhappy and 3.33% are Highly Unhappy.

VII. HYPOTHESIS TESTING

HYPOTHESIS NO: 1

H_0: Age and Influence of Friends are independent
H_1: Age and Influence of Friends are dependent

Age*Friends Cross tabulation

		Friends		Total
		No	Yes	
Age	7-11	21	41	62
	11 above	18	70	88
	Total	39	111	150

Count

Chi-Square Test

	Value	df	Asymp. Sig. (2-sided)	Exact Sig. (2-sided)	Exact Sig. (1-sided)
Pearson Chi-Square	3.403[a]	1	.065		
Continuity Correction[b]	2.741	1	.098		
Likelihood Ratio	3.367	1	.067		
Fisher's Exact Test				.088	.049
Linear-by-Linear Association	3.380	1	.066		
N of Valid Cases	150				

a. 0 cells (.0%) have expected count less than 5. The minimum expected count is 16.12.
b. Computed only for a 2x2 table

Table 9: Data table for Hypothesis No. 1

Interpretation:

Here the calculated Chi-square value is 3.403 and tabulated Chi-square value (At dof=1 and Significance level= 0.05) is 3.841. So we do not reject H_0.

This shows that Age and Influence of Friends are independent.

HYPOTHESIS NO: 2

H_0: Education Medium and Brand Awareness are independent
H_1: Education Medium and Brand Awareness are dependent

Brand Awareness*Education Medium Cross tabulation

			Medium			Total
			English	Gujarati	Hindi	
Brand Awareness	Fisher Price	Count	37	2	7	46
	Barbie	Count	48	24	14	86
	Funskool	Count	38	5	7	50
	Hot wheels	Count	52	16	11	79
	Lego	Count	22	4	3	29
Total		Count	75	32	26	133

Table 10: Data table for Hypothesis No. 2

Calculation:
Degree of freedom= (Rows-1) (Columns-1)
   = (5-1) (3-1)
   = 8
Significance level= 0.05
Table value of Chi-square (χ^2) [At dof=8 and α=0.05] = 15.507
Calculated value of Chi-square [$\chi^2 = \Sigma$ (fo-fe) ^{2}/fe] = 29.373438

Interpretation:

The table value of χ^2 for 8 degree of freedom at 5 percent level of significance is 15.507. The calculated value of χ^2 is higher than this table value and hence the result of this test does not support the null hypothesis so we reject H_0.

We can, thus, conclude that **Medium of study and Brand Awareness are dependent.**

HYPOTHESIS NO: 3

H_0: Education Medium and Internet Usage are independent
H_1: Education Medium and Internet Usage are dependent

Internet Usage*Education Medium Cross tabulation

			Medium			Total
			English	Gujarati	Hindi	
Internet Usage	Fisher price Internet	Count	27	2	4	33

Barbie Internet	Count	42	14	8	64
Hot wheels Internet	Count	32	11	5	48
Funskool Internet	Count	27	4	6	37
Lego Internet	Count	20	4	1	25
Local Internet	Count	5	3	6	14
Other Internet	Count	2	0	0	2
Total	Count	61	19	15	95

Table 11: Data table for Hypothesis No. 3

Calculation:
Degree of freedom= (Rows-1) (Columns-1)

= (7-1) (3-1)

= 12

Significance level= 0.05

Table value of Chi-square (χ^2) [At dof=12 and α=0.05] = 21.026

Calculated value of Chi-square [$\chi^2 = \Sigma$ (fo-fe) ^{2}/fe] = 21.554514

Interpretation:

The table value of χ^2 for 12 degree of freedom at 5 percent level of significance is 21.026. The calculated value of χ^2 is higher than this table value and hence the result of this test does not support the null hypothesis so we reject H_0.

We can, thus, conclude that **Medium of study and Internet Usage are dependent.**

HYPOTHESIS NO: 4

H_0: Brand Awareness and Brand Usage are independent
H_1: Brand Awareness and Brand Usage are dependent

Brand Awareness*Brand Usage Cross tabulation							
			Brand Usage				
			Fisher Price	Barbie	Hot Wheels	Funsko ol	Lego	Tota l
Brand awareness	Fisher Price	Count	29	26	24	18	8	44
	Barbie	Count	17	72	19	24	12	79
	Funskool	Count	16	30	27	34	9	49
	Hot wheels	Count	20	26	59	21	12	75
	Lego	Count	8	17	16	11	18	29
Total		Count	30	72	59	34	18	121

Table 12: Data table for Hypothesis No. 4

Calculation:
Degree of freedom= (Rows-1) (Columns-1)

= (5-1) (5-1)

= 16

Significance level= 0.05

Table value of Chi-square (χ^2) [At dof=16 and α=0.05] = 26.296
Calculated value of Chi-square [$\chi^2 = \Sigma$ (fo-fe) ^{2}/fe] = 155.1047648

Interpretation:

The table value of χ^2 for 16 degree of freedom at 5 percent level of significance is 26.296. The calculated value of χ^2 is much higher than this table value and hence the result of this test does not support the null hypothesis so we reject H_0.

We can, thus, conclude that **Brand Awareness and Brand Usage are dependent.**

HYPOTHESIS NO: 5

H_0: Brand Usage and Experience are independent
H_1: Brand Usage and Experience are dependent

Brand Usage*Experience Cross tabulation								
			Experience					
			Very Happy	Happy	Neutral	Unhappy	Highly Unhappy	Total
Brand Usage	Fisher Price	Count	9	16	4	0	1	30
	Barbie	Count	25	32	12	2	1	72
	Hot Wheels	Count	25	28	6	0	0	59
	Funskool	Count	15	18	1	0	0	34
	Lego	Count	8	8	2	0	0	18
Total		Count	43	57	17	2	2	121

Table 13: Data table for Hypothesis No. 5

Calculation:
Degree of freedom= (Rows-1) (Columns-1)

= (5-1) (5-1)

= 16

Significance level= 0.05

Table value of Chi-square (χ^2) [At dof=16 and α=0.05] = 26.296

Calculated value of Chi-square [$\chi^2 = \Sigma$ (fo-fe) ^{2}/fe] = 12.134204

Interpretation:

The table value of χ^2 for 16 degree of freedom at 5 percent level of significance is 26.296. The calculated value of χ^2 is less than this table value and hence the result of this test does support the null hypothesis so we reject H_0.

We can, thus, conclude that **Brand Usage and Experience are dependent.**

VIII. FINDINGS

Out of 150 children respondents we have surveyed, 57.33% were aware about Barbie and 54% were aware about

Local brands. Awareness for Hot Wheels is 52.67%. Awareness about Fisher price, Funskool, Lego is comparatively lower. This shows that children are more aware about Barbie and Hot Wheels.

For branded toys Television and Internet are the important advertising mediums. For local brands and other toys Newspaper and Pamphlet are important advertising medium.

Out of 150 children respondents we have surveyed, 80.67% watching Cartoon network. 80% of them are watching Pogo, 74% Hungama, 48% Nickelodeon. Children watching Playhouse Disney, Disney XD, and Cbeebies are less, 34.67%, 27.33% and 16% for Playhouse Disney, Disney XD, and Cbeebies respectively.

70% of 150 children see other programmes on television. Second highest is 67.33% which is of Tom and Jerry. 51.33% is for Chota Bhim, Doraemon and Richie Rich.

The most Influencing Factor for purchase of toy is Colour of the toy. Second most Influencing Factor is Recommendation by Friends. Lights, Package, Sound, Free Gifts, Demonstration and Other factors account for 64.67%, 63.33%, 56%, 55.33%, 36% and 21.33% respectively.

Brand Usage is more for Local brands that is 51.33%. Brand Usage for Barbie and Hot Wheels is 48% and 39.33% respectively. Usage of Funskool, Fisher Price and Lego is comparatively low.

Out of 150 children we have surveyed, 39.33% are Happy with the Brands those they have used. 28.67% of them are Highly Happy, 18% are Neutral, 10.67% are Unhappy and 3.33% are Highly Unhappy.

The Age and Influence of Friends are independent, the Medium of study and Brand Awareness are dependent and the Medium of study and Internet Usage are dependent. Also the Brand Awareness and Brand Usage are dependent. Brand Usage and Experience are again found to be dependent.

IX. SUGGESTIONS

The result of our analysis shows that Television and Internet are most important advertising mediums so marketers should place most of their advertising in Television and Internet. Most seen television channels are Cartoon Network and Pogo, so marketers can place their advertisements in Cartoon Network and Pogo for maximum coverage. Marketers can place there advertisement during Tom and Jerry, Chota Bhim, Doraemon and Richie Rich because these are the most seen television programmes. Marketers should focus on the Colour, Word of mouth, Lights, Sound and Packaging of the toys because these are the most influencing factors in the purchase of toys. So we can say that "Visual merchandising" is an important factor for branding and selling of toys. Usage of Funskool, Fisher Price and Lego is comparatively low. So these brands need to promote their brands more and should increase the usage

of their brands by generating awareness campaign for children through various promotional schemes.

X. CONCLUSION

450 million kids (below the age of 18) and another 8 million being added each year! What do you know about them? It's not only about their rising numbers. It's about their mindsets. It's about their approach. It's about their thinking, their preferences, likes, dislikes and everything else that make a kid a kid.

Children are also the main focus of Indian families, and their aspirations in terms of education and career choices are quite high today. The average family size in India has been on a decline, coming in now at almost 4.3 as compared to earlier years when it was more than 5. With the reduction in their average size and the increase in their incomes, Indian families have more money to spend. And children being the main focus, parents try their best to fulfil their aspirations. Net result, they get more attention and participate a lot in the decision making process. Our study shows that most Parents' purchase decision is influenced by their children. These recent trends are very important for toy industry.

With consumers today exposed to choices in terms of new categories, new brands and new shopping options enabling them to seek more information in the crowded retail environment, it is a major challenge for Toy manufacturing companies. Also the price sensitivity is waxing and brand loyalty is waning. And the consumers, who once stuck to favorite local toy brands, are now, willing to try any quality & branded products at an affordable price.

The Indian consumer is extremely price conscious and won't pay for something in which he does not see incremental value. So in effect, companies are not matching the premium, they are charging for their products with adequate increase in product attributes and usage.

This requires use of promotional schemes which are the most essential in today's market. Though this could not guarantee brand loyalty by the customers but at-least the customers will try the products and generate sales for the companies. Usage of Funskool, Fisher Price and Lego is comparatively low. So these brands need to promote their brands more and should increase the usage of their brands by generating awareness campaign for children through various promotional schemes.

Marketers should focus on the Colour, Word of mouth, Lights, Sound and Packaging of the toys because these are the most influencing factors in the purchase of toys. So we can say that "Visual merchandising" is an important factor for branding and selling of toys. Marketers should focus more on their pricing policy and toxicity content of their toys. They should also focus on Quality and Branding of their toys. Because these factors mostly influence the purchase of toys.

We believe that toy industry is still an industry to be researched much. And ideas and findings of this project could stimulate further research and might help to explore new insights into this emerging industry.

XI. ANNEXURE
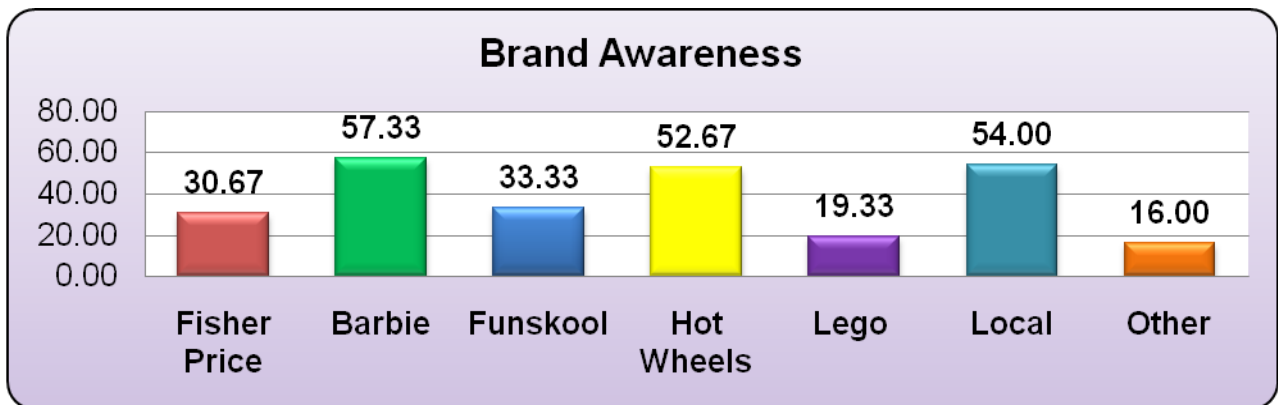
Graph 1: Respondents awareness towards various brands of toys
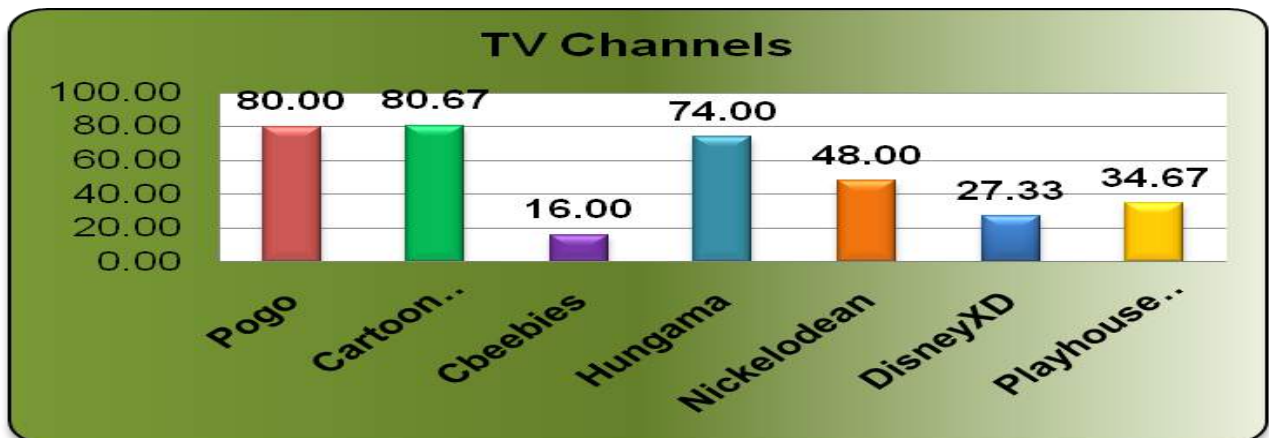
Graph 2: Exposure of various TV channels
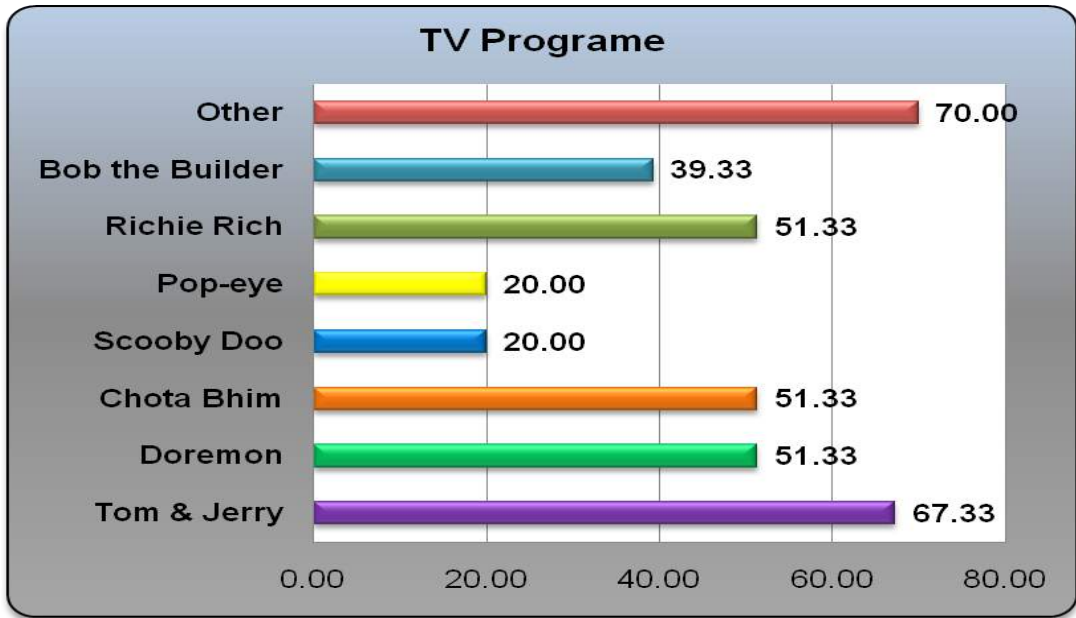
Graph 3: Preferences of TV programmes by schoolers
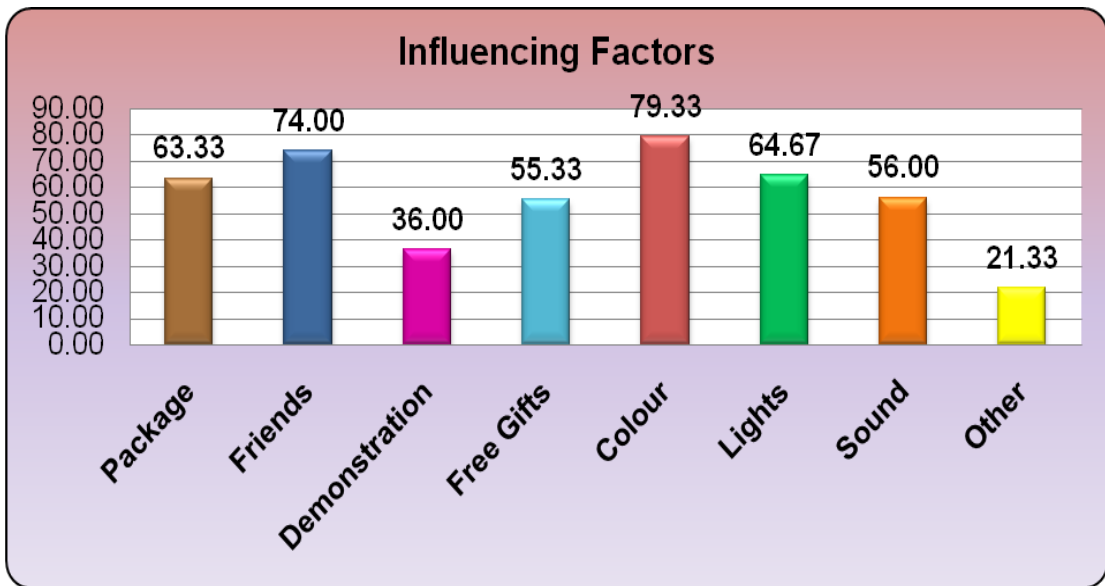
Graph 4: Influencing factors those can affect purchasing of toy brand

Graph 5: Purchase history of schoolers

XII. ACKNOWLEDGMENTS

The researchers are highly indebted to Mr. Prashant Jain and Ms. Shefali Tailor for their sincere effort during the current study.

XIII. REFERENCES

[1] https://www.npd.com/wps/portal/npd/us/news/pressreleases/pr_110702, accessed on 15th December 2012.

[2] http://www.indianmirror.com/indian-industries/toy.html, accessed on 27th Nov 2012.

[3] http://www.business-standard.com/india/news/indian-toy-industry-set-to-grow-at-25/259652/: Accessed on 22nd Dec 2011.

[4] Sandra L. Calvert (2008), Children as Consumers: Advertising and Marketing, Literacy Challenges for the Twenty-First Century, Vol. 18, No.1, spring, p. 205-234, ISSN: 1054-8289.

[5] http://www.caiindia.org/caiindia/PDFs/consumer%20law/children_consumers2.pdf, accessed on 2nd August 2012.

[6] Scott Ward, Daniel Wackman, and Ellen Wartella (1977),"The Development of Consumer Information-Processing Skills: Integrating Cognitive Development and Family Interaction Theories", in Advances in Consumer Research Volume 04, eds. William D. Perreault, Jr., Advances in Consumer Research Volume 04: Association for Consumer Research, Pages: 166-171.

[7] Sharma Adya (2011), Role Of Family In Consumer Socialization Of Children: Literature Review, Researchers World – Journal of Arts, Science & Commerce, Vol. II, Issue- 3, July, p. 161- 167 E-ISSN, 2229-4686.

[8] Pike, D., & Jackson, N. (2006), Ethics and the promotion of consumer brands to children: Marketing public relations in the UK toy industry. Prism 4(1): http://praxis.massey.ac.nz/prism_on-line_journ.html, accessed on 20th Dec. 2011.

[9] Piaget, J. (1975). The moral judgement of the child, London: Routledge.

[10] Selman, R. L. (1980), The growth of interpersonal understanding. New York: Academic Press.

[11] Barenboim, C. (1981, March). The development of person perception in childhood adolescence: From behavioral comparisons to psychological constructs to psychological comparisons. Child Development, 52,129–144.

[12] Rhonda P. Ross, Toni Campbell, John C. Wright, Aletha C. Huston, Mabel L. Rice, & Peter Turk (1984), "When celebrities talk, children listen: An experimental analysis of children's responses to TV ads with celebrity endorsement", Journal of Applied Developmental Psychology, Volume 5, Issue 3, July–September 1984, Pages 185–202.

[13] Seth M. Freedman & Melissa Schettini Kearney & Mara Lederman (2009), "Product Recalls, Imperfect Information, and Spill over Effects: Lessons from the Consumer Response to the 2007 Toy Recalls," NBER Working Papers 15183, National Bureau of Economic Research, Inc.

[14] Pike, D., & Jackson, N. (2006), Ethics and the promotion of consumer brands to children: Marketing public relations in the UK toy industry. Prism 4(1): http://praxis.massey.ac.nz/prism_on-line_journ.html, accessed on 17th Sept. 2011.

[15] Hansen, F., Rasmussen, J., Martensen, A., & Tufte, B. (2002). Children: Consumption, advertising and media. Copenhagen: Samfundslitteratur.

[16] Soloman, M., Bambossy, G., & Askegaard, S. (2002). Consumer behavior: A European perspective. London: Prentice Hall.

[17] Piaget, J. (1975). The moral judgement of the child. London: Routledge.

[18] Selman, R. L. (1980), The growth of interpersonal understanding. New York: Academic Press.

[19] Acuff, D. S. (1997), What kids buy and why: The psychology of marketing to kids. New York: The Free Press.

[20] Christenson, P. G. (1982, October). Children's perceptions of TV commercials and products: The effects of PSA. Communication Research, 9, 491–524.

To Study Online Purchase Behaviour of Customers & their Future Expectations

A.   Prof. Nehal A. Shah   ,   B.   Prof. Jaideepsingh H. Jetawat

Abstract - The growth of e-tailing over the past decade has created an entirely new set of expectations on the part of consumers around the level of personalization in their shopping experience. This has in turn created challenges for merchants to adopt the right technology and business strategies to meet those consumer demands and drive incremental sales. In India where the internet users are growing at an alarming rate it will be helpful for the consumer as well as for the companies, to discuss on e-retailing models, payment methods, security features, future trends and benefits etc. This research study reveals the behavior shown by respondents towards various parameters of e-tailing (On-Line Shopping) industry. At last researchers have collected future expectations of respondents which can give an insight to retailers about how to serve their on line customer better.

Index Terms: Convenience, e-commerce, E-tailing, Internet, Retailing.

I. INTRODUCTION

Fig 1: Major Players of Indian e-tailing industry

A. Works with Gandhinagar Institute of Technology (A Center for Management Studies), Gandhinagar, 382721, Gujarat, INDIA (e-mail: nehalshahmba@gmail.com).

B.   Works with Gandhinagar Institute of Technology (A Center for Management Studies), Gandhinagar, 382721, Gujarat, INDIA (e-mail: jaideepjetawatmba@git.org.in).

Growth of e-Tailing

The growth in the E-tailing market is driven by the need to save time by urban India. Besides with over 5.3% of Indian population are the internet users (Source: World Bank, World Development Indicators), access to internet has also played an important role in growing the markets. Changing demographics (youthful India), changing lifestyles and exposure to the developed markets sure give a fillip to this fledgling industry. The soaring real estate costs in India have certainly inspired many an online venture. Also E-tailers have developed many innovative promotions to lure customers and there by growing the market.

The growth of e-commerce in India can be associated with a number of factors. Prominent among them are the increasing Internet user base, accessibility to computer, growing affluence of the middle class, awareness among customers, payment gateways etc.

The option of purchasing tickets (rail, air, bus, and movie) without waiting in queues has also played its part in growth of e-commerce in India to an extent. E-tailing – which comprises buying consumer items including electronic products, home appliances, personal products such as apparels and jewellery and other accessories – is currently worth around Rs. 2700 crore.

Fig 2: E-tailing Growth from Dec 2007 to Dec 2011[1]
Evolution of Retailing: Impact of Technology

Impact of Technology on these developments requires both brick-&- mortar and online retailers to re-assess their value proposition to the end-customer. For many, the road to success might lie in a creative blending of the possibilities offered across different areas. New types business models that will transform business of retailing. The stage is set for the emergence of hybrid retailers that successfully tap into the opportunities offered by the convergence of these domains.

Fig 3: Evolution of Retailing Industry

Challenges of e-Tailing

Internet based e-commerce has besides, great advantages, posed many threats because of its being what is popularly called faceless and borderless.

Security issues - Security issues hold the center stage when it comes to consumer concerns while shopping through the online media. A lack of trust and privacy concerns prevents a lot of consumers from making online purchases. Consumers are also concerned with the use of their personal data provided during the online transactions.

Customer retention - In e-tailing, an increase in the customer retention by 5% leads to a corresponding increase in profits by 25%. Most of the people buying on the Internet do so out of curiosity and this makes a repeat purchase highly unlikely.

Unsuitable for certain product categories – In case of product categories that require relatively higher customer involvement, the e-tailing route is found to be grossly inadequate in providing sufficient information to the customers. Examples include retailing of products like clothes, cosmetics etc. Most customers are comfortable buying books and music on the Internet because the information required for making a purchase and the customer involvement is low.

Shopping is still a touch-feel-hear experience - some do not suffer from 'time-poverty' and shopping is still considered to be a family outing. Hence this type of an environment creates a problem of customer retention.

Complicated medium - Ease of use is a problem, as the web design may suffer from high complexity bordering on total chaos in some cases.

Navigation issues - E-tail stores do not have standardized designs in comparison to the physical retail stores and product catalogs. Therefore different user behaviors (navigation schemes) need to be learned for each e-tail store. This is a temporary issue as the evolution of the web continues.

Website design flaws - Graphic presentation and aesthetics may not be as compelling for a web site as in case of a physical retail store or a product catalog. This is a temporary issue that may resolve with the evolution of the web design.

Limited access to the Internet - Not all customers have access to the web, as they do to the postal system. This is a temporary issue as the evolution of the web continues.

Major Global e-Tailing Companies[2]

RANK	COMPANIES	SALES AND GROWTH
1st	Amazon.com Inc.	Sales: $34,200,000,000 2010 Growth: 39.5%
2nd	Staples Inc.	Sales: $10,200,000,000 2010 Growth: 4.1%
3rd	Apple Inc.	Sales: $5,227,500,000 2010 Growth: 23.0%
4th	Dell Inc.	Sales: $4,801,800,000 2010 Growth: 6.0%
5th	Office Depot Inc.	Sales: $4,100,000,000 2010 Growth: 0.0%
6th	Walmart.com	Sales: $4,095,000,000 2010 Growth: 17.0%
7th	Sears Holdings Corp.	Sales: $3,107,145,001 2010 Growth: 12.0%

Table 1: Top Seven Global e-tailing Companies

Fig 4: Top 10 Products in e-tailing by Survey of eBay Census report 2011[3]

According to survey conducted by eBay in 2011 around 50% of electronic product are traded which include cell phone, DVDs, Pen drives, headphone, video games. Out 100 %, 36% of products are lifestyle related like Pendants etc. 12% are Collectibles and 02% are media traded. So from the survey it is concluded that in e-tailing mostly electronic product have strong demand compare to other product.

II. LITERATURE REVIEW

Sriram A. (2011)[4], study gives an in-depth analysis of e-retailing in India and gives a clear picture, where India stands in e-retailing. The study depicts that India has got lot of potential to grab in this area. But we are still in the infancy stage due to infrastructure shortage and security threats. This area has to be tapped properly for more foreign exchange.

Ghosh D. (2011),[5] study revealed that with increasing internet penetration and flexible payment modes such as cash-on-delivery being used widely nowadays, Along with Bata many bigwigs like Reliance Retail, Aditya Birla Retail and Tata's Croma are looking at entering the Rs. 2,050 crore e-retailing markets, growing at over 30% annually. Industry experts point out that besides popular categories like electronics, mobile phones and books, fashion items like apparel, footwear, jewellery and accessories has a large share worldwide in e-commerce sales and the trend is catching fast in India too. The reason being the brand preference, ease of selection and shipping make this category a preferred good choice for online transactions

Ghosh D. (2011),[6] in second study said that with internet penetration gradually increasing and new modes of payment such as cash-on-delivery coming into vogue, rural India, alongside tier II and tier III towns, are breathing life into the country's Rs. 2,050-crore e-retailing market.

Online retailing portals such as e-Bay. in, Snapdeal.com, and Naaptol.com are registering anywhere between 40 and 60% of their sales from rural areas such as Sajiyavadar and Adala in Gujarat, apart from the tier II and III cities like Jaipur, Visakhapatnam, Kanpur, Lucknow, Vadodara, and Faridabad. That with people becoming more used to the convenience of the internet, online shopping is seeing higher growth in these places. Also there are very few avenues of spending money in these towns, so there is a significant amount of disposable income with the people. The benefits of variety, offers, discounted deals and convenience is driving the online shopping trend. Popular categories include mobile phones, cameras, DVD players, videogames and MP3 players, computer accessories like hard drives and pen drives, kitchenware, diamonds and jewellery, gift items, home decor and health accessories. According to some e-tailing companies, there is a surprising parity in the spending trends between tier II/III markets and urban centers. "The average size of transactions from tier II and III markets is R3,000, which is the same as urban areas However, the tier II & III and rural markets are yet to open up to the services offered on websites and are far from moving on from purchasing products. "The share of revenues from such markets will continue to grow, but growth will majorly be in the products business. Urban markets continue to dominate in the lifestyle and services segment

Sharma S. & Kurian B. (2011),[7] found that Global investors have placed a billion dollar bet on India's internet and mobile start-ups during 2011, reposing confidence in the fast-growing base of digital consumers in the country. These global investors are bullish on India's internet economy even as there's a waning appetite for the core sector investments stymied by high interest rates and lack of policy reforms. The belief in the Indian digital consumer story has been so robust

that start-up e-commerce firms managed to raise follow-on investments within six months, at significantly higher valuations. Online retail will lead the internet consumer with online travel, classifieds and advertising which dominate the digital consumer industry in India right now. E-tailing will develop into a $12 billion-strong business, accounting for half of the total e-commerce market in the next four years. The top e-commerce firms emerged as big advertisers and employed hundreds of courier boys in the most tech savvy neighborhoods to grow their businesses.

Silicon India (2011),[8] depicts that Indian E-commerce sector provides more job opportunities as they double the employee strength. ET Bureau reports that online retailers had already doubled the number of staff during this year and is looking forward to increase another half by next year. Reportedly India has 11 million people who do online purchasing. It is not amazing as Internet gifts a virtual world to engage. From food to household items are available online today. Who cares to queue for getting tickets? E-tickets are there. As the number of e-consumers increase, there should be the back support for e-business. The number of e-buyers will be rising to 38 million by 2015, Avendus Capital, a financial services firm reported. An increase of 35 percent will be happening by 2015 to 11.8 billion. **Motukuri K. (2011)** told that e-tail sector is witnessing a battle for brains. We are looking out for innovative software engineers, creative designers and product managers who understand consumer behavior so that e-shopping is delightful. Comparing the conventional trade growth, e-business is in a rapid growth of three times higher. There are so many e-tailing ventures such as Allschoolstuff.com, Infibeam.com, tradekeyindia.com, ebay.com and Indiamart.com

D. Muthamizh Vendan Murugavel (2010),[9] depicted that e-tailing has not picked up much business in India. The Indian market is totally different than all western countries. This will gather momentum, may be in 2015, to its full swing if there is proper planning right now on a small scale & build up goodwill. Indian looks for cheap, better products, branded

& door delivered. Although e-tailing has lagged in India, but hopefully in future, it would see a lot more action as internet habit of Indian online users is on a rise & many factors are in favour of its growth.

Ralitza Nikolaeva (2006),[10] showed that Organizational readiness and external influences were the main driving factors of the adoption decision. There is no strong support for the perceived benefits construct. This suggests that e-commerce adoption was to a great extent responsive to external pressures.

III. OBJECTIVES OF THE STUDY

- To study the penetration of on line shopping among customers.
- To study factors affecting on line purchase behavior of customers
- To find out what are the problems and challenges faced by consumer in e-tailing environment.
- To find out consumer's future expectations regarding e-tailing and ways to fulfill those expectations.

IV. SIGNIFICANCE OF THE STUDY

e-tailing is a new way of conducting and managing the business using computer and telecommunication networks. Now a day many businesses transaction are done online and day by day internet network connection and internet users are increasing resulting into e-tailing development which will creates many jobs and business opportunities in future. Marketers can't only rely on the traditional ways of doing business and need to know about e-tailing i.e. online customer buying behavior and their future expectation in order to successfully implement the e-tailing methods. This study can derive many suggestions to improve the online retailing and designing online sales program and strategies.

V. RESEARCH METHODOLOGY

The study is descriptive in nature. The researcher adopted this type of research design to gather information from the respondents to assess consumer behavior towards e-tailing

environment. The study was conducted with 150 samples from Ahmedabad city of Gujarat state. The sampling method adopted for the study was non-probability convenient sampling considered ideal for consumer behavior studies in which the researcher can select the sample elements based on the ease of access. Structured questionnaire was prepared to collect the feedback of the respondents. The primary data has been collected through a structured questionnaire from the respondents. The secondary data has been collected from the books, journals, magazines, Ebsco and websites. The data relating to the company were collected from the personal manual and past records of the company. The data was collected by contacting individual consumer directly.

VI. RESULT ANALYSIS & INTERPRETATIONS
DEMOGRAPHIC DETAILS

From 150 total samples around 73% that is 109 numbers of the respondents were male and remaining were female. About 6% of samples are below the age of 20 years, 16% of samples are 30-40 years age area and almost 78% of samples are in 20-30 age group. Most of the respondents that are 67.00 % are having graduate qualification. Out of 150 samples 31% of samples having 1 lac to 3 lac family income per annum, 45% of samples having 3Lac to 5Lac family income per annum, 15 % of samples having 5 Lac to 7 Lac family income per annum, and 9% of samples having more than 7Lac family income per annum. This study includes around 56% of students, 19% is salaried people and 22% are business people, and 3% are professionals.

RESEARCH DATA

(A) Penetration of online Purchase

PARTICULAR	NO. OF RESPONDENTS	PERCENTAGE
Yes	121	81%

No	29	19%
Total	150	100%

Table 2: Penetration of Online Purchase

From table 2, we can see that 81% of respondent have bought product/service online and 19% of respondents do not buy product or service through internet.

(B) Reason for Purchasing Online

PARTICULARS	NO. OF RESPONDENTS	PERCENTAGE
Convenient	63	52 %
Cost Saving	73	60 %
Wider Selection of varieties	41	34 %
Time Saving	67	55 %
Total Respondents =121 (multiple choice question)		

Table 3: Reason for Purchasing Online

Table 3 shows reasons as given by respondent for online purchase which are (in most to least order):

- shop at a time that is convenient to Consumer
- Easy payment method like COD
- Cheaper rate compare to traditional market
- Compare as many products and prices

(C) Challenges /Problem faced by E-Retailers

PARTICULAR	NO. OF RESPONDENTS	PERCENTAGE
Don't know how to purchase	9	29 %
Unaware about mode of Payment	1	3 %
Safety and Privacy issue	6	19 %
Fear while purchasing online first time	15	48 %
Total Respondents =29 (multiple choice question)		

Table 4.1: Challenges /Problem faced by E-Retailers

PARTICULAR	NO. OF RESPONDENTS	PERCENTAGE
High Shopping Price	2	6 %

Shipping and Handling issues	20	56 %
Took too long time	21	58%
Website was confusing	16	44 %
Product not as per description or Defective Product	16	44 %
Quality Issues	17	47%
Total Respondents =29 (multiple choice question)		

Table 4.2: Challenges /Problem faced by E-Retailers

Table 4.1 shows that out of 29 non online shoppers, 9 samples don't know how to purchase online, only 1 sample don't know about payment method, 6 samples having a problem of safety and privacy issue on online shopping, and major and most reason for non e-tailing is fear while purchasing online for first time almost 15, i.e. 48% of people are facing this problem. Table 4.2 revels that more over 2 respondents think that online shopping is very costly, almost 20 samples having problem of shipping and handling issues, 21 samples said online shopping take too many time to deliver product/service, 16 samples said website is too much confusion and product is not as per description, 17 samples having quality issues.

(D) Purpose of Purchasing Online

PARTICULAR	NO. OF RESPONDENTS	PERCENTAGE
Self-Consumption	110	91 %
For Gifting	11	9 %
Total	121	100%

Table 5: Purpose of purchasing online

From table 5, we can conclude that about 91% of samples use e-tailing services for their self-consumption and 9% of samples use e-tailing services for gifting other.

(E) Frequency of online purchase behavior

PARTICULAR	NO. OF RESPONDENTS	PERCENTAGE
Regularly	34	28 %

Frequently	25	21 %
Occasionally	62	51 %
Total	121	100%

Table 6: Frequency of online purchase behavior

Table 6 shows that out of 121 samples 34 samples i.e. 28% of respondent are regularly user, 25 are frequent user, and 62 respondent purchases occasionally.

(F) Types of Products generally purchased online

PARTICULAR	NO. OF RESPONDENTS	PERCENTAGE
Electronic	69	57 %
Life Style	29	24 %
Grocery	2	1.5 %
Coupons	2	1.5 %
Services	19	16 %
Total	121	100

Table 7: Types of Products generally purchased online

Table 7 depicts that out of 121 samples 1.5% of samples purchase Coupons and grocery items 19 samples that is 16% buy online services like office services, Indian railway ticket booking etc, and around 29 samples purchase lifestyle product like shoes. Most of the samples, i.e. 69 samples purchases electronic item.

(G) Amount spends on online shopping in the past 6 months:
(in INR)

PARTICULAR	NO. OF RESPONDENTS	PERCENTAGE
Less than Rs. 5,000	70	58 %
Rs. 5,000 to 10,000	35	29 %
Rs. 10,000 to 20,000	12	10 %
Above Rs. 20,000	4	3 %
Total	121	100%

Table 8: Amount spend on e-shopping in the past 6 months

Table 8 state that out of 121 samples, 3% samples spend more than 20,000 Rs, 10% spends 10, 000 to 20,000 Rs, almost 29% respondent spends 5000 to 10,000 Rs. and around 58%, i.e. 70 samples spend less than 5000 in last 6 months. 72

% of respondents said that online shopping is value for money and are highly satisfy with online transaction.

(H) Mode of payment used while shopping online:

PARTICULAR	NO. OF RESPONDENTS	PERCENTAGE
Cash on delivery (COD)	46	38 %
Net banking	48	40 %
Debit Card	31	26 %
Credit Card	40	33 %
Mobile payment	1	1 %
Total Respondents =121 (multiple choice question)		

Table 9: Mode of payment used while shopping online

From table 9, we can see that 1% of respondents use mobile payment, 33% uses credit card, 26% use debit card while most of respondents i.e. 40% use net banking and online bank transfer as mode of payment on online shopping which are expected to increase in future. Cash on delivery as payment mode is preferred by 38% of respondents.

(I) Factors that Influence Preference of the online shoppers:

a. Online shopping is Easy

RANK	1	2	3	4	5
No. of Respondents	52	41	33	9	15
Percentage	35 %	27 %	22 %	6 %	10 %
1-Strongly Agree , 2-Agree, 3-Neutral, 4-Disagree, 5-Strongly Disagree					

Table 10.1: Preference for: Online shopping is Easy

b. Online shopping is Convenient

RANK	1	2	3	4	5
No. of Respondents	22	71	37	19	1
Percentage	14%	47%	25%	33%	1%
1-Strongly Agree , 2-Agree,3-Neutral, 4-Disagree, 5-Strongly Disagree					

Table 10.2: Preference for: Online shopping is Convenient

c. Online shopping is Cost Saving

RANK	1	2	3	4	5
No. of	32	38	58	18	4

Respondents					
Percentage	21%	25%	39%	12%	3%
1-Strongly Agree , 2-Agree,3-Neutral, 4-Disagree, 5-Strongly Disagree					

Table 10.3: Preference for: Online shopping is Cost Saving

d. Online shopping is time saving

RANK	1	2	3	4	5
No. of Respondents	29	56	40	17	8
Percentage	19%	38%	27%	11%	5%
1-Strongly Agree , 2-Agree,3-Neutral, 4-Disagree, 5-Strongly Disagree					

Table 10.4: Preference for: Online shopping is time saving

e. Wider Selection of varieties in online shopping

RANK	1	2	3	4	5
No. of Respondents	24	23	69	21	13
Percentage	16%	15%	46%	14%	9%
1-Strongly Agree , 2-Agree,3-Neutral, 4-Disagree, 5-Strongly Disagree					

Table 10.5: Preference for: Online shopping gives wider selection of goods

f. Online shopping is Secure

RANK	1	2	3	4	5
No. of Respondents	6	39	31	68	6
Percentage	4%	26%	21%	45%	4%
1-Strongly Agree , 2-Agree, 3-Neutral, 4-Disagree, 5-Strongly Disagree					

Table 10.6: Preference for: Online shopping is Secure

g. Price comparison is easy through online shopping

RANK	1	2	3	4	5
No. of Respondents	18	90	22	17	3
Percentage	12%	60%	15%	11%	2%
1-Strongly Agree , 2-Agree, 3-Neutral, 4-Disagree, 5-Strongly Disagree					

Table 10.7: Preference for: Price comparison is easy through on line

h. More product information is getting through online shopping

RANK	1	2	3	4	5

No. of Respondents	46	44	40	18	2
Percentage	31%	29%	27%	12%	1%
1-Strongly Agree , 2-Agree, 3-Neutral, 4-Disagree, 5-Strongly Disagree					

Table 10.8: Preference for: Richer product information through on line

Above tables 10.1 to 10.8 shows that, about 62 % of respondent agreed that online shopping is easy, in the same way almost 61% of respondent agreed that online shopping convenient. From total respondent 46% and 47% believe that online shopping is cost and time saving respectively. Around 72% and 60% of respondent agreed that we can do better price comparison and gain more product information through online shopping. At the same time most of the respondent feels that online shopping is not secure 69% and wider selection is not available during online shopping i.e. 31%.

(J) Consumer future expectations regarding e-tailing or internet retailing:

PARTICULARS	NO. OF RESPONDENTS	PERCENTAGE (%)
More Price Reduction	123	82%
Improved Connectivity of Internet	63	42%
Reduce response time from E-tailer	45	30%
Speed of Internet	49	33%
Transaction Complete feedback	50	33%
Reduce goods delivery time	40	27%
Effective customer service through E-mail, Call Center	33	22%
Improved Security and Privacy over Internet	53	35%
Better / Understandable Product/Service Return Policy	51	34%
Latest Price and Product information update on website	57	38%
Proper Maintenance and updating of websites	48	32%

Table 11: Consumer future expectation regarding e-tailing

Table 11 shows that almost 82% of samples are expecting more price reduction in online retailing in future due to increase in competition. And 63 samples are expecting

improve in connectivity of online retailing services, customer care services and speed and reduction in transaction completion time and reduction in retailers response time i.e. Moreover respondent are expecting improve privacy and security over internet, i.e. 31% .In e-tailing companies main reason of failure is updating of site, updating of price and product and around 57 samples are expecting latest price updating and 48 samples are expecting for proper maintenance and updating of sites in future.

VII. FINDINGS

About 62 % of respondent rate that online shopping is easy, in the same way almost 61% of respondent agreed that online shopping convenient. From total respondent 46% and 47% believe that online shopping is cost and time saving respectively. Around 72% and 60% of respondent agreed that we can do better price comparison and gain more product information through online shopping. During survey it was founded that still there are 29 of sample who never shop online and the main reason behind it are 30% of them don't know how to buy online as well as sample also have complains like poor shipping, product handling , product and service quality issue ,fear of security and privacy etc. According to study 60% of responded Spends less than Rs. 5000 in last six months which is very poor compare to family income. Almost 82% of samples are expecting more price reduction in online retailing in future due to increase in competition. And 63 samples are expecting improve in connectivity of online retailing services, customer care services and speed and reduction in transaction completion time and reduction in retailers response time i.e. Moreover respondent are expecting improvement in privacy and security over internet, i.e. 31%.

VIII. LIMITATIONS OF THE STUDY

The major findings of the study is based on the information provided by respondents and hence may not be exactly true and finding of the study based on assumption that the respondents has given correct information. Most of those data are collected from on line questionnaire, so collected responses were more from younger age rather than old age respondents. Also mood & preference of the consumer may affect the validity & reliability of collected data.

IX. CONCLUSION

In India internet users are growing faster and this is strongly supporting e-tailing also. So we can say that e-tailing is the future virtual platform to meet buyer and seller, there is no boundary of information same as there is no boundary of e-tailing. This research shows that out of 150 internet users, around 80% of users have shopped once from online store. This shows that around 80% of respondents are aware about e-tailing, and majority of respondent found this concept as cost saving because they got lot of discounts from e-tailer compare to traditional "Mom & Pop" store. So ultimately consumer gets cheaper product compare to Physical buying. And this is the major reason why most of the audience is interested to purchase product/service from online store. Researchers had also collected future expectations of respondents. In which majority of respondents that is around 80% are expecting for more price reduction, almost 30% of samples are expecting for faster delivery of products. It indicates that e-tailing industry requires effective customer support; improvement in security and privacy over the internet.

X. FUTURE SCOPE OF THE STUDY

At the end researchers believe that e-tailing industry is still an industry to be researched more. Presented ideas and findings of this project could stimulate further research and might help to explore new insights into this emerging industry.

XI. REFERENCES

[1] trak.in/tags/business/2011/03/17/indian-e-commerce-market-2011-*online-travel-bookings-dominate, accessed on 20 December, 2011.*

[2] internetretailer.com, 2011.

[3] eBay census report 2011.

[4] E-retailing business models for Indian retail chains by Anand Sriram, Director - Retail Category Management Windows & Office at Microsoft.

[5] http://www.financialexpress.com/news/etailing-india/815627/2, accessed on 22nd December 2011.

[6] http://www.financialexpress.com/news/rural-india-fuels-growth-of-etailing/795840/4.

[7] http://timesofindia.indiatimes.com/tech/enterprise-it/strategy/Global-investors-bets-big-on-Indias-internet-mobile-start-ups/articleshow/11097317.cms, accessed on 23 December 2011.

[8] http://www.siliconindia.com/shownews/Etailers_to_Hire_More_IITians_and_IIMites_-nid-101170-cid-30.html?utm_source=feedburner&utm_medium=feed&utm_campaign=Feed%3A+siliconindianews+%28siliconindia-allnews%29, accessed on 23 December 2011.

[9] Murugavel, D. M. (2010), "e-Tailing Market scenario in India- A bird's eye view", *Indian Journal of Marketing*, August, pp. 31-37 & 61.

[10] Nikolaeva, R. (2006), "E-commerce Adoption in the Retail Sector: Empirical Insights", *International Journal of Retail & Distribution Management*, pp: 1-33.

[11] Khadilkar, S.M. (2012), "Does organized retailing is Really Growing in India?", *Indian Streams Research Journal*,Vol.1,Issue.V, June, pp.1-4.

[12] Mishra, S. (2008), "New Retail Models in India: Strategic Perspective Analysis*", Journal of Marketing & Communication*, September -December, Vol. 4, Issue 2, pp: 39-47.

[13] Copeland, A.; and Shapiro, A.H. (2010), "The Impact of Competition on Technology Adoption: An Apples-to-PCs Analysis", *Federal Reserve Bank of New York Staff Reports*, no. 462, July.

[14] Ferguson, S. (2010), "Intel, Dell Offer IT for Retail Stores", Retrieved from, http://www.eweek.com/c/a/IT-Infrastructure/Intel-Dell-Offer-Information-Technology-for-Retail-Stores-433039/, Accessed on March. 12, 2011.

[15] Rigby, D. (2011), "The Future of Retailing", *Harvard Business Review*, December, pp: 65-76.

[16] Satish, D.; and Venkatrama, R.D. (2010), "The Growth of Indian Retail Industry", *Advances In Management*, Vol. 3, July 2010.

Lower Limb Musculoskeletal Modeling By Using Musculoskeletal Modeling Software

Rahulsinh Chauhan[#1], Jignesh Vyas[*2]

[#*]*Department of Biomedical Engineering,Govt. Engineering College, Sec-28, Gandhinagar, India*

[1]rahul_07bm06@yahoo.in

[2]vyas.jb@gecg28.ac.in

Abstract— **This paper shows how the musculoskeletal modelling of the lower limb of humans is possible using MSMS (Musculoskeletal Modeling Software). Concept, significance and factors of musculoskeletal modeling of lower limb have been detailed. It presents how the complexity of biomechanics related to lower limb can modelled with MSMS and also represents how such model can be useful in generating MATLAB/SIMULINK® model that can be further used in the development of prototype neuroprosthesis model for paraplegic patients having lower extremity disorders. Proposed modeling includes 36 leg virtual muscles which shows its accuracy for event such as walking, jumping, sitting, standing and cycling with due consideration of the coordinating position, Mass, Inertia used for rigid body segment, and Joint Type, Translational Axes, Rotational Axes used for lower limb joints. The result generated by MSMS for proposed modeling has been presented. Merits and demerits of proposed modeling have also been discussed.**

Index Terms— **Biomechanics, Inverse dynamics, Inverse kinematics, Virtual muscles.**

I. INTRODUCTION

Models are used widely in all types of engineering, and especially in Biomechanics. The term model has many uses, but in the engineering context, it usually involves a representation of a physical system, a prototype, that may be used to predict the behavior of the system in some desired respect. These models can include physical models that appear physically similar to the prototype or mathematical models, which help to predict the behavior of the system, but do not have a similar physical embodiment. Many software develops procedures for designing models in a way to ensure that the model and prototype will behave similarly. A model is a representation of a physical system that may be used to predict the behavior of the system in some desired respect. Models of the lower extremity musculoskeletal system [1], [3] have made achievable a wide range of biomechanical investigation especially for paraplegic patients with lower extremity

disorders after spinal cord injury (SCI) or multiple sclerosis (MS). For example, Models of the musculoskeletal system facilitate individual to study neuroprosthersis, neuromuscular coordination, evaluate athletic performance, estimate musculoskeletal loads, simulate the effects of musculoskeletal surgeries such as joint replacements, investigate a possible cause of crouch gait and to study muscular coordination of walking, jumping, sitting [4], standing [5] and cycling [6]. MSMS (Musculoskeletal Modeling Software) [7] is open-source software that allows users to develop, analyze, and visualize models of the musculoskeletal system, and to create dynamic simulations of movement. In MSMS, a musculoskeletal model consists of rigid body segments connected by joints. Muscles span these joints and generate forces and movement. Once a musculoskeletal model is created, MSMS facilitates users to study the effects of musculoskeletal geometry, joint kinematics, and muscle-tendon properties of the forces and joint moments that the muscles can generate. In additions MSMS solves an inverse kinematics problem and an inverse dynamics problem using experimental data [2].

II. METHODS FOR LOWER LIMB MUSCULOSKELETAL MODELING IN MSMS

MSMS is used to build a standard model of a lower limb musculoskeletal modeling. Skeletal geometry integrates rigid models of the pelvis, femur, tibia, fibula, patella, talus, calcaneus, metatarsals, and phalanges that were shaped by digitizing a set of bones from a male adult subject with an approximate height of 1.8 m and an approximate mass of 75 kg. The model consists of 7 rigid body segments and includes the lines of action of 36 virtual muscles. For slanting the coordinate systems of each bone segment so that in the anatomical position the X-axis points anteriorly, the Y-axis points superiorly, and the Z-axis points to the right. Figure 1 illustrates different views of the proposed model with a proposed leg model in MSMS window. Left side of the window shows rigid segments and joints used in the model and right side of the window shows complete right leg model with the coordinate system of each joint.

1	Pelvis	10.7537	X= -0.0739512, Y= 0.0, Z= 0.0	$I_{XX} = 0.1027003$, $I_{YY} = 0.08701554$, $I_{ZZ} = 0.05784385$, $I_{XY}, I_{XZ}, I_{YX} = 0$ $I_{YZ}, I_{ZX}, I_{ZY} = 0$
2	Femur_r	8.5492	X= 0.0, Y= -0.199543, Z= 0.0	$I_{XX} = 0.16956431$, $I_{YY} = 0.0444489$, $I_{ZZ} = 0.17880867$, $I_{XY}, I_{XZ}, I_{YX} = 0$ $I_{YZ}, I_{ZX}, I_{ZY} = 0$
3	Tibia_r	4.6740	X= 0.0, Y= -0.2098, Z= 0.0	$I_{XX} = 0.08023514$, $I_{YY} = 0.00811903$, $I_{ZZ} = 0.08134951$, $I_{XY}, I_{XZ}, I_{YX} = 0$ $I_{YZ}, I_{ZX}, I_{ZY} = 0$
4	Talus_r	0.1260	X,Y,Z=0.0	$I_{XX} = 0.00202166$, $I_{YY} = 0.00202166$, $I_{ZZ} = 0.00202166$, $I_{XY}, I_{XZ}, I_{YX} = 0$ $I_{YZ}, I_{ZX}, I_{ZY} = 0$
5	Patella_r	0.0919	X,Y,Z=0.0	$I_{XX} = 0.00110296$, $I_{YY} = 0.00110296$, $I_{ZZ} = 0.00110296$, $I_{XY}, I_{XZ}, I_{YX} = 0$ $I_{YZ}, I_{ZX}, I_{ZY} = 0$
6	Calcn_r	1.0722	X= 0.102693, Y= 0.0308079, Z= 0.0	$I_{XX} = 9.0462E-4$, $I_{YY} = 0.00361848$, $I_{ZZ} = 0.00361848$, $I_{XY}, I_{XZ}, I_{YX} = 0$ $I_{YZ}, I_{ZX}, I_{ZY} = 0$
7	Toes_r	0.1861	X= 0.0359425, Y= 0.00616157, Z= -0.0184847	$I_{ZZ} = 9.0462E-4$, $I_{XX}, I_{XY}, I_{XZ} = 0$ $I_{YY}, I_{YX}, I_{YZ} = 0$ $I_{ZX}, I_{ZY} = 0$

In addition to this our proposed leg model has six joints with respect to ground pelvis. This can be explored below the "joint" block in the "model explorer" (Figure 1 (E)). Out of these six joints, three joints are movable joints (namely hip_r, knee_r, ankle_r) and residual are fixed joints (namely mtp_r, subtalar_r, tib_pat_r). Our proposed leg model contains the same joint type as the natural leg, e.g. hip joint in this model has a ball and socket joint with three degrees of freedom such as flexion/extension, adduction/abduction, and internal/external rotation which is same as the natural leg. Table (b) shows the data for the model of joints such as its type, proximal and distal segment, its translational and rotational axes.

Figure 1: Proposed right leg model in MSMS; (A) front view, (B) back view, (C) right view, (D) left view and (E) with the coordinate system of each joint.

In this model seven rigid body segments are used and coordinated that can be explored under "segments" block in "model explorer" (Figure 1 (E)). To model this rigid body segment we have considered the mass, Interia etc. as shown in table (a). Where, we have considered pelvis as a ground segment. Subsequently we have constructed femur_r under pelvis by taking into consideration pelvis as a parent segment. Similarly by putting together a new rigid body segment (namely tibia_r, talus_r, patella_r, calcn_r, toes_r) as a child segment just before it's respective parent segment.

Table (a): Data used while coordinating rigid body segment.				
Sr. No.	Rigid Body Segment	Mass (in kg)	Center of Mass (in m)	Inertia(in kg*m²)= $\begin{bmatrix} I_{xx} & I_{xy} & I_{xz} \\ I_{yx} & I_{yy} & I_{yz} \\ I_{zx} & I_{zy} & I_{zz} \end{bmatrix}$

Table (b): Data used in a proposed model for joints.					
Sr.No.	Joint Name	Joint Type	Proximal Segment	Distal Segment	Translational Axes (X,Y,Z)	Rotational Axes (X,Y,Z)
1	Ground _Pelvis	Planar	Ground	Pelvis	Pelvis_T_x = (1,0,0) Pelvis_T_y = (0,1,0)	Pelvis_R = (0,0,1)
2	Hip_r	Pin/ Revolute	Pelvis	Femur_r	None	Hip_R_z= (0,0,1)
3	Knee_r	Planar	Femur_r	Tibia_r	Knee_T_x = (1,0,0) Knee_T_y = (0,1,0)	Knee_R_z= (0,0,1)

4	Tib_Pat_r	Planar	Tibia_r	Patella_r	Tib_Pat_T$_x$= (1,0,0) Tib_Pat_T$_y$= (0,1,0)	Tib_Pat_R$_z$= (0,0,1)
5	Ankle_r	Pin/Revolute	Tibia_r	Talus_r	None	Ankle = (-0.105, -0.174, 0.979)
6	Mtp_r	Weld	Calcn_r	Toes_r	None	None
7	Subtalar_r	Weld	Talus_r	Calcn_r	None	None

Proposed right leg model contains 36 leg virtual muscles [8] which will help to achieve an equivalent response to natural leg response such as walking, sitting etc. Proposed leg virtual muscles are based on hill muscle model [9]. It can be explored below the "Actuators" block in the "model explorer". Data used in a proposed model for virtual muscle is given in the Table (c).

Table(c): Virtual muscle data used in a lower limb modeling. [From reference [3]]				
Sr. No.	Muscle Name	Optimal Fiber Length (in cm)	Optimal Tendon Length(in cm)	Physiological Cross-Sectional Areas (PCSA) (in cm)
1	Adductor Brevis	10.30	03.60	05.00
2	Adductor Longus	10.80	13.00	06.50
3	Adductor Magnus Distal	17.70	09.00	21.30
4	Adductor Magnus Ischial	15.60	22.10	21.30
5	Adductor Magnus Middle	13.80	04.80	21.30
6	Adductor Magnus Proximal	10.60	04.30	21.30
7	Biceps Femoris	09.80	32.20	11.60
8	Gastrocnemius Lateral Head	05.90	38.20	09.90
9	Gastrocnemius Medial Head	05.10	40.10	21.40
10	Gluteus Maximus Inferior	16.70	07.00	30.40
11	Gluteus Maximus Middle	15.70	07.30	30.40
12	Gluteus Maximus Superior	14.70	05.00	30.40
13	Gluteus Medius Anterior	07.30	05.70	36.10
14	Gluteus Medius Middle	07.30	06.60	36.10
15	Gluteus Medius Posterior	07.30	04.60	36.10
16	Gluteus Minimus Anterior	06.80	01.60	36.10
17	Gluteus Minimus Middle	05.60	02.60	36.10
18	Gluteus Minimus Posterior	03.80	05.10	36.10
19	Gracilis	22.80	16.90	02.30
20	Iliacus	10.70	09.40	10.20
21	Pectineus	13.30	00.10	07.09
22	Peroneus Brevis	04.50	14.80	05.00
23	Peroneus Longus	05.10	33.30	10.70
24	Peroneus Tertius	07.90	10.00	10.70
25	Psoas	11.70	09.70	07.90
26	Rectus Femoris	07.60	34.60	13.90
27	Sartorius	40.30	11.00	01.90
28	Semimembranosus	06.90	37.80	19.10
29	Semitendinosus	19.30	24.50	04.90
30	Soleus	04.40	28.20	58.80
31	Tensor Fascia Latae	09.50	45.00	09.93
32	Tibialis Posterior	03.80	28.29	14.80
33	Tibials Anterior	06.80	24.10	11.00
34	Vastus Intermedius	09.90	10.60	16.80
35	Vastus Lateralis	09.90	13.00	37.00
36	Vastus Medialis	09.70	11.20	23.70

III. MATLAB/SIMULINK® MODEL OF LOWER LIMB

One of the major advantages of MSMS is that, it can generate a simulink model (.mdl) by using command "Save Simulation". This simulink model represents the algorithms that can simulate the movement of the MSMS model in response to control excitations and external forces, This Simulink model can be opened and run in Matlab's Simulink environment which helps for further Biomechanics investigation. Here Figure 1 (F) shows a simulation model of a proposed leg model of MSMS. This simulink model can be used in generating and simulating the complete lower extremity model having external electrical stimulus such as the one used in neuroprosthesis models. Such neuroproshtesis model can be helpful for designing the prototype programmable functional electrical stimulator (FES) that can be helpful to the paraplegic patients with lower extremity disorders.
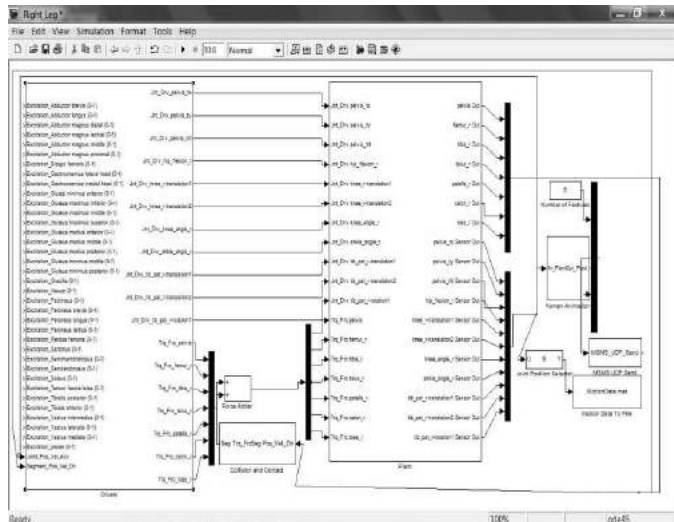
Figure 1(F): Simulink model of proposed leg model in MATLAB®

VI. RESULTS AND CONCLUSION

In this study, we formed a model that calculates the fiber lengths and forces of the muscles based on a vigorous data set of experimentally considered structural design. The model can be used to study the relationship between moments at different joint with respect to muscles responsible to produce respective joint movement. Figure 1 (G) shows the result of movement at the hip joint versus muscle at hip joint and Figure 1 (H) shows the result of movement of the knee joint versus muscle at the knee joint. The accuracy of the muscle paths was tested by qualitative evaluation of model expected to experimentally measured moment. Using this model further response of electrical stimulus to the lower limb model can be tested and if the open loop test results can be validated with the experimental setup data then closed loop control can also be implemented in future.
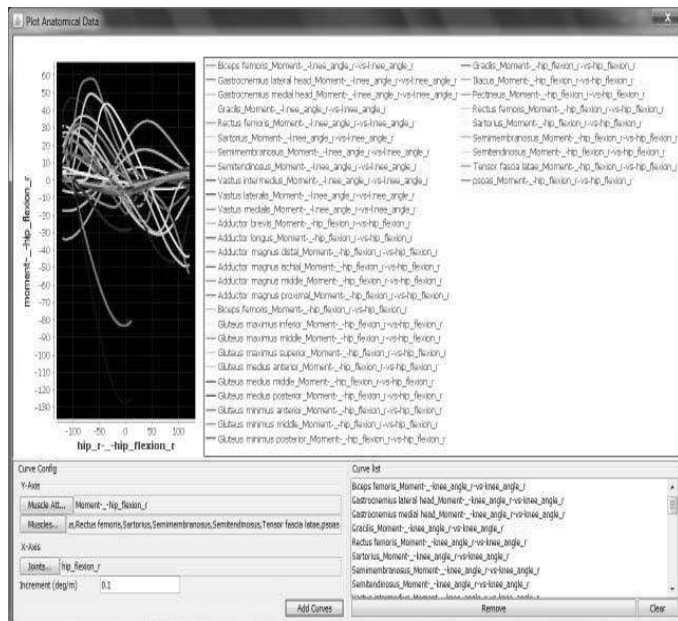
Figure 1(G) shows the result of movement at the hip joint versus muscle at hip joint.
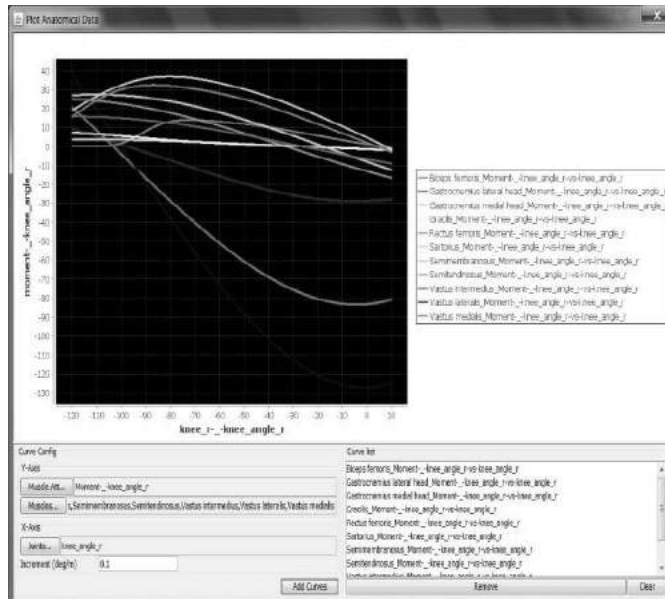
Figure 1(H) shows the result of movement at the knee joint versus muscle at the knee joint.

There are some limitations of this model that should be considered. There are several quite small muscles that were ignored. However, these muscles make small contributions to the overall joint moment and are not likely to alter simulation results of joint function.

REFERENCES

[1.] Scott Delp, Allison Arnold, Samuel Hamner," Introduction to Musculoskeletal Modeling", Neuromuscular Biomechanics Laboratory ,Stanford University.

[2.] Samuel Hamner, Clay Anderson, Eran Guendelman, Chand John, Jeff Reinbolt, Scott Delp,"Scaling, Inverse Kinematics, and Inverse Dynamics", Neuromuscular Biomechanics Laboratory ,Stanford University.

[3.] Edith M. Arnold, Samuel R. Ward, Richard L. Lieber, And Scott L. Delp," A Model Of The Lower Limb For Analysis Of Human Movement", Biomedical Engineering Society, November 2009.

[4.] Colleen Louise Mchenry,"A Biomechanical Model Of Femoral Forces During Functional Electrical Stimulation After Spinal Cord Injury In Supine And Seated Positions", University Of Iowa,2010.

[5.] Gustavo P. Braz, Michael Russold, Glen M. Davis, Facsm," Functional Electrical Stimulation Control Of Standing And Stepping After Spinal Cord Injury: A Review Of Technical Characteristics", Neuromodulation: Technology At The Neural Interface,2009.

[6.] Margit Gföhler, Thomas Angeli, And Peter Lugner," Modeling Of Artificially Activated Muscle And Application To Fes Cycling", 12th International Conference On Mechanics In Medicine And Biology, September, 2002.

[7.] R. Davoodi, I.E. Brown, G.E. Loeb," Advanced Modeling Environment For Developing And Testing FES Control Systems", Medical Engineering & Physics 25 (2003) 3–9, Elsevier, April 2002.

[8.] Ernest J. Cheng , Ian E. Brown, Gerald E. Loeb," Virtual Muscle: A Computational Approach To Understanding The Effects Of Muscle Properties On Motor Control", Journal Of Neuroscience Methods 101 (2000) 117–130, June 2000.

[9.] Jeffrey W. Holmes," Teaching From Classic Papers: Hill's Model Of Muscle Contraction", Advances In Physiology Education, August , 2012.

Displacement based Seismic Assessment of Elevated Water Tank over Alternate Column Proportionality

Chirag N. Patel[1], Shashi N. Vaghela[2], H. S. Patel[3]

[1]*Ph.D. Candidate, Faculty of Engineering Pacific Academy of Higher Education and Research University,*
Udaipur, Rajasthan, India.

[2]*P.G. Student, Applied Mechanics Department, L. D. College of Engineering, Ahmedabad, Gujarat, India.*

[3]*Associate Professor, Applied Mechanics Department, L. D. College of Engineering Ahmedabad,*
Gujarat, India

[1]cnpatel.693@gmail.com
[2]shashi_vghl@yahoo.com
[3]dr.hspatel@yahoo.com

Abstract—**Elevated water tanks are commonly used for storing water in public water distribution system and it should be competent of keeping the expected performance during and after earthquake. It has large mass concentrated at the top of slender supporting structure and hence extremely vulnerable against horizontal forces due to earthquake. They must be functional even after earthquakes to ensure water supply is available in earthquake-affected regions. A dynamic analysis of such tanks must take into account the motion of the water relative to the tank as well as the motion of the tank relative to the ground. Therefore, an understanding of the earthquake damage, or survival, of elevated water tanks requires an understanding of the effect of dynamic forces at each level from bottom to top. For certain proportions of the tank and the structure the displacement of the tank may be the dominant factor, whereas for other proportions the displacement of tank may have small effect. The main aim of this study is to understand the seismic behaviour of the elevated water tank under alternate column proportionality under different time history records using finite element software SAP 2000. The present work aims at checking the adequacy of water tank for the seismic excitations. The result shows that the structure responses are exceedingly influenced by different column proportionality and earthquake characteristics. The responses include displacement of elevated water tank at each level from bottom to top under the four different time history have been compared and contrasted.**

Index Terms —**Displacement; Seismic Analysis; Staging; Water tank.**

I. INTRODUCTION

WATER is essential to humans and other life forms. Supply of drinking water is essential immediately after destructive earthquakes. Without assured water supply, the uncontrolled fires subsequent to major earthquakes may cause more damage than the earthquakes themselves. So the water supply system should be designed as seismic resistant and seismic performance of water tanks draws special significance in the design. Generally, to store the water different types of structures are used like; underground, ground supported and elevated water tanks. Elevated water tank is a structure which is constructed at a sufficient height to cover a large area for the supply of water. The performance of elevated water tanks during earthquakes is of much interest to engineers, not only because of the importance of these tanks in controlling fires, but also because the simple structure of an elevated tank is relatively easy to analyse and, hence, the study of tanks can be informative as to the behaviour of structures during earthquakes. In the past earthquakes including Bhuj earthquake of 26 January 2001, damages had been observed widely in the support structures, which is typical of the damage sustained to a large number of water tanks of capacities ranging from 80 m^3 to 1,000 m^3 and as far away as 125 km from the epicentre (Rai, 2001). During the Chilean earthquakes of May, 1960 a number of elevated water tanks were badly damaged (K. V. Steinbrugge and R. Flores). Other elevated water tanks survived without damage (W. K. Cloud).

Most of the previous studies were focused on the tank containing liquid considering only one mass and it does not cover important aspect for analysis and design of water tanks related to the effect of hydrodynamic pressure of the water, which produce due to vibration of tank when earthquake strikes. But after the Bhuj earthquake, revision of current Indian code became inevitable. Hence, it was decided to develop guidelines under the project "Review of Building codes and preparation of Commentary and Handbooks" assigned by the Gujarat State Disaster Management Authority (GSDMA), Gandhinagar to the Indian Institute of Technology

Kanpur in 2003 [1]. The stimulus of the present study is to understand the behaviour of different supporting system of elevated water tank, under alternate column proportionality and acceleration time history records of different characteristics. Also, impulsive and convective water masses inside the container are taking in to consideration and modelled with FE software SAP2000 [3].

I. MODAL PROVISIONS

A satisfactory spring mass analogue to characterize basic dynamics for two mass model of elevated tank was proposed by Housner (1963) after the Chilean earthquake of 1960, which is more appropriate and is being commonly used in most of the international codes including GSDMA guideline. During lateral mode of shaking of the water tank, a upper part of the water moves in a long period sloshing motion, while the rest part moves rigidly with the tank wall. The former one is recognized as convective mass of water which exerts convective hydrodynamic pressure on tank wall and base, while the latter part is known as impulsive mass of water which accelerates along with the wall and induces impulsive hydrodynamic pressure on tank wall. The impulsive mass of water experiences the same acceleration as the tank container and contributes predominantly to the base shear and overturning moment. In spring mass model convective mass (mc) is attached to the tank wall by the spring having stiffness (Kc), whereas impulsive mass (mi) is rigidly attached to tank wall. For elevated tanks two-mass model is considered, which consists of two degrees of freedom system. Spring mass model can also be applied on elevated tanks, but two-mass model idealization is closer to reality. The two- mass model is shown in Figure 1.
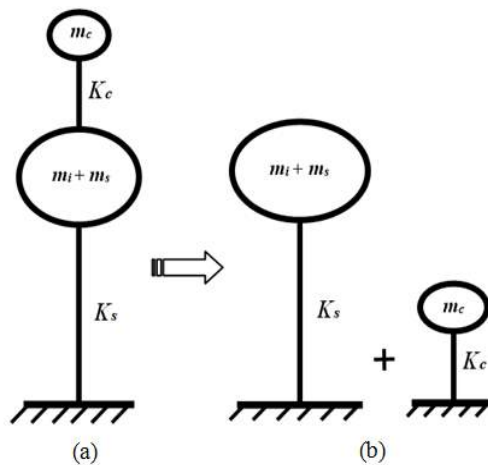
Fig.1 Two mass model

The two-mass model was first proposed by G. M. Housner (1963) and is being commonly used in most of the international codes. However, for most of elevated tanks it is observed that both the time periods are well separated. Hence, the two-mass idealization can be treated as two uncoupled single degree of freedom system as shown in Figure 1 (b). The stiffness (Ks) is lateral stiffness of staging. The mass (ms) is

the structural mass and shall comprise of mass of tank container and one-third mass of staging as staging will acts like a lateral spring. Staging part of elevated water tanks follows the provisions given by Criteria for design of RCC staging for overhead water tanks (First revision of IS 11682): Draft Code [2].

II. FLUID-STRUCTURE INTERACTION

During lateral base excitation seismic ground acceleration causes hydrodynamic pressure on the tank wall which depends on the geometry of tank, height of liquid, properties of liquid and fluid-tank interaction. Proper estimation of hydrodynamic pressure requires a rigorous fluid-structure interaction analysis. In the mechanical analogue of tank-liquid system, the liquid is divided in two parts as, impulsive liquid and convective liquid. The impulsive liquid moves along with the tank wall, as it is rigidly connected and the convective and sloshing liquid moves relative to tank wall as it under goes sloshing motion. This mechanical model is quantified in terms of impulsive mass, convective mass, and flexibility of convective liquid. Housner (1963) developed the expressions for these parameters of mechanical analogue for circular and rectangular tanks. Some researchers have attempted numerical study for tanks of other shapes (Joshi, 2000 and Damatty, 2000). There are some experimental studies on the effect of obstructions on the sloshing frequency (Kimura et al. 1995, Armenio 1996, and Reed et al. 1998). Fluid–structure interaction problems can be investigated by various approaches such as added mass approach (Westergaard, 1931), Barton and Parker, 1987), the Eulerian approach (Zienkiewicz and Bettes, 1978), the Lagrangian approach (Wilson and Khalvati, 1983; Olson and Bathe, 1983) or the Eulerian–Lagrangian approach (Donea et al., 1982). The simplest method of these is the added mass approach as shown in Figure 2, can be investigated using some of conventional FEM software such as SAP2000, STAAD Pro and LUSAS. The general equation of motion for a system subjected to an earthquake excitation can be written as,

$$M\ddot{u} + C\dot{u} + Ku = -M\ddot{u}_g \tag{1}$$

In which M, C and K are mass, damping and stiffness matrices with $\ddot{u}$, $\dot{u}$ and u are the acceleration, velocity and displacement respectively, and is the ground acceleration. In the case of added mass approach the form of equation (1) become as above.

$$M^*\ddot{u} + C\dot{u} + Ku = -M^*\ddot{u}_g \tag{2}$$

In which M* is the new mass matrix after adding hydrodynamic mass to the structural mass, while the damping and stiffness matrices are same as in equation (1).

Westergaard Model's method was originally developed for the dams but it can be applied to other hydraulic structure, under earthquake loads i.e. tank. In this paper the impulsive mass has been obtained according to GSDMA guideline

equations and is added to the tanks walls according to Westergaard Approach as shown in Figure 3 using equation 3. Where, ρ is the mass density, h is the depth of water and A_i is the area of curvilinear surface.
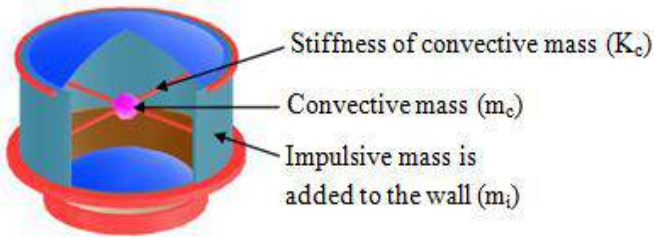

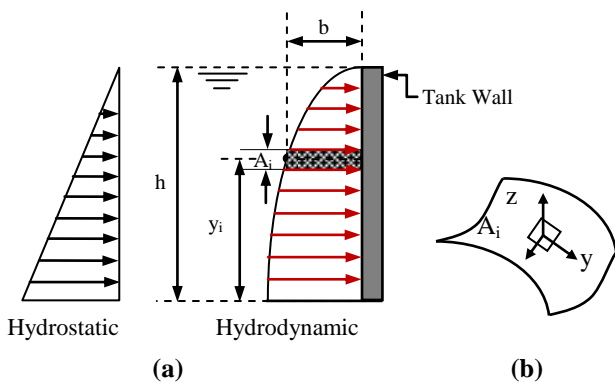Fig 2. FEM model for fluid-strucutre-interaction added mass approach

Fig 3. (a) Westergaard added mass concept (b) normal and cartesian directions.

$$m_{ai} = \left[\frac{7}{8}\rho\sqrt{h\left(h - y_i\right)}\right]A_i \qquad (3)$$

In the case of Intze tank where the walls having sloped and curved contact surface, the equation (3) should be compatible with the tank shape by assuming the pressure is still expressed by Westergaard's original parabolic shape. But the fact that the orientation of the pressure is normal to the face of the structure and its magnitude is proportional to the total normal acceleration at the recognized point. In general, the orientation of pressures in a 3-D surface varies from point to point; and if it is expressed in Cartesian coordinate components, it would produce added-mass terms associated with all three orthogonal axes. Following this description the generalized Westergaard added mass at any point i on the face of a 3-D structure is expressed by equation (4) (Kuo 1982 [7]).

$$m_{ai} = a_i A_i \lambda_i^t \lambda_i = a_i A_i \begin{bmatrix} \lambda_x^2 & \lambda_y\lambda_x & \lambda_z\lambda_x \\ \lambda_y\lambda_x & \lambda_y^2 & \lambda_z\lambda_y \\ \lambda_z\lambda_x & \lambda_z\lambda_y & \lambda_z^2 \end{bmatrix}$$

$$(4)$$

Where; A_i is the tributary area associated with node i; λ_i is the normal direction cosine $\left(\lambda_y, \lambda_x, \lambda_z\right)$ and a_i is Westergaard pressure coefficient.

(a)

(b)

Fig 4. (a) FE model of elevated water tank using SAP 2000 (b) Arrangement of different type of column on outer periphery of staging

III. PROBLEM DESCRIPTION

The frame type is the most commonly used staging in practice. The main components of frame type of staging are columns and braces. In frame staging, columns are arranged on the periphery and it is connected internally by bracing at

various levels. The staging is acting like a bridge between container and foundation for the transfer of loads acting on the tank. In elevated water tanks, head requirement for distribution of water is satisfied by adjusting the height of the staging portion. Different types of column pattern are used for water tank. The geometry of column is also the

important part to understand the behaviour of tank. A reinforced elevated water tank with different types of column system with full water level in the container has been considered for the present study. A reinforced elevated water tank with fixed base frame type staging system for different column configuration and no of panel 3, 4, and 5 with 12 m, 16 m and 20 m has been considered for the present study respectively. The storage capacity of water tank is 1000 m^3. A finite element model (FEM) is used to model the elevated tank system using SAP 2000 [3] structural software as shown in Figure 4.

Columns and bracings in the frame type support system are modelled as frame elements (with six degrees of freedom per node). Conical part, bottom and top domes and container walls are modelled with thin shell elements (with four nodes and six degrees of freedom per node). Other dimensions of the elevated tanks are illustrated in Table I.

The configuration of staging is nothing but the arrangements of columns and bracings in particular pattern. The orientation and section of column is also important in deciding the configuration for staging [4]. Several types of configuration can generate by changing the arrangement and pattern of columns.

In the present study three types of shapes have been considered like circular, square and rectangle. In rectangular type of column different two type of arrangement are considered in line of outer periphery and perpendicular to outer periphery named as rect_wide and rect_deep respectively. The arrangement of column on outer periphery of staging is as shown in Figure 5. The dimension of the different type of column on outer periphery of staging with variation in panel is shown in Table II.
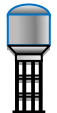
Total four numbers of earthquake records were used; the maximum PGA on the basis of acceleration gravity for

Imperial Valley (El Centro) (1979), Northridge (1994), Kobe (1995) and Loma Prieta (1989) are 0.314, 0.410, 0.509 and 0.644 respectively. Properties of recorded earthquakes are as shown in Table 2, with acceleration transverse component of four earthquakes as shown in Figure 5.

TABLE I
STRUCTURAL DATA FOR FRAME TYPE STAGING

Description	Data
Capacity of the tank (m^3)	1000
Unit weight of concrete (kN/m^3)	25
Thickness of Top Dome(m)	0.15
Rise of Top Dome (m)	2.2
Size of Top Ring Beam (m)	0.35×0.35
Diameter of tank (m)	13.6
Height of Cylindrical wall (m)	6.8
Thickness of Cylindrical wall (m)	0.33
Size of Middle Ring Beam (m)	1.2×0.6
Rise of Conical dome (m)	2.35
Thickness of Conical shell (m)	0.5
Rise of Bottom dome (m)	1.6
Thickness of Bottom dome shell (m)	0.2
Number of Columns (circular)	8
Number of Bracings Level	4
Size of Bottom Ring Beam (m)	1.0×1.2
Distance between intermidiate bracing (m)	4
Height of Staging above Foundation (m)	16
Size of Bracing (m)	0.5×0.5

TABLE II
Column dimension considering different panel and pattern

Number of panel	Column pattern	Column size			Height of Staging	Model No.
		Diameter (m)	Depth (m)	Width (m)		
3-panel	Circular	0.75	-	-	12	1
	Square	-	0.665	0.665	12	2
	Rect_deep	-	0.5	0.8	12	3
	Rect_wide	-	0.5	0.8	12	4
4-panel	Circular	0.75	-	-	16	5
	Square	-	0.665	0.665	16	6
	Rect_deep	-	0.5	0.8	16	7
	Rect_wide	-	0.5	0.8	16	8
5-panel	Circular	0.75	-	-	20	9
	Square	-	0.665	0.665	20	10
	Rect_deep	-	0.5	0.8	20	11

| Rect_wide | - | 0.5 | 0.8 | 20 | 12 |

TABLE III
Properties of Earthquake records

Record	Imperial Valley (El Centro), (1979)	North Ridge, (1994)	Kobe, (1995)	Loma Prieta, (1989)
Station	EC Meloland overpass	Canyon country -w cost cany	Nishi-Akashi	Corralitos
Component	IMPVALL /H-EMO000	NORTHR /LOS000	KOBE /NIS000	LOMAP /CLS000
PGA(g)	0.314	0.410	0.509	0.644
PGV(cm/s)	71.7	43.0	37.2	55.2
PGD(cm)	25.53	11.75	9.52	10.88
Magnitude	6.5	6.7	6.9	6.9

Fig 5. Acceleration transverse component of earthquake
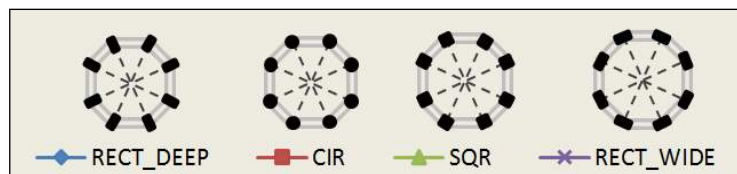
Fig.6 shows the graphical notification for different column patterns

IV. RESULT AND CONCLUSIONS

In this study, a reinforced elevated water tank with 1000 m^3 capacity and supported by fixed base frame type staging system with different column proportionality has been considered. With considering two-mass water model, seismic responses including displacement of tank at various locations from bottom to top were assessed under four earthquake records. The seismic responses of tank have been determined using time history analysis in three cases, i.e. 3-panel, 4-panel, 5-panel. Figure 6 shows the graphical notification for different column patterns. Displacement

variation of 3, 4 and 5 –panel tank for different column proportionality and time history records are shown in figure 7, 8 and 9 respectively. The obtained results are summarized as follows:

• The critical response depends on the earthquake characteristics and particularly frequency content of earthquake records.

• Top roof displacement is increased with the increase in the panel number and increase against high frequency earthquake.

• Roof top displacement has been increase towards higher number of panels, and it is in majority cases higher in rect_deep type of staging pattern.

• Amongst all type of column proportionality, rect_deep has been prove highly competitive to with stand against structural responses like base shear, Overturning moment and roof top displacement under different earthquake characteristics.
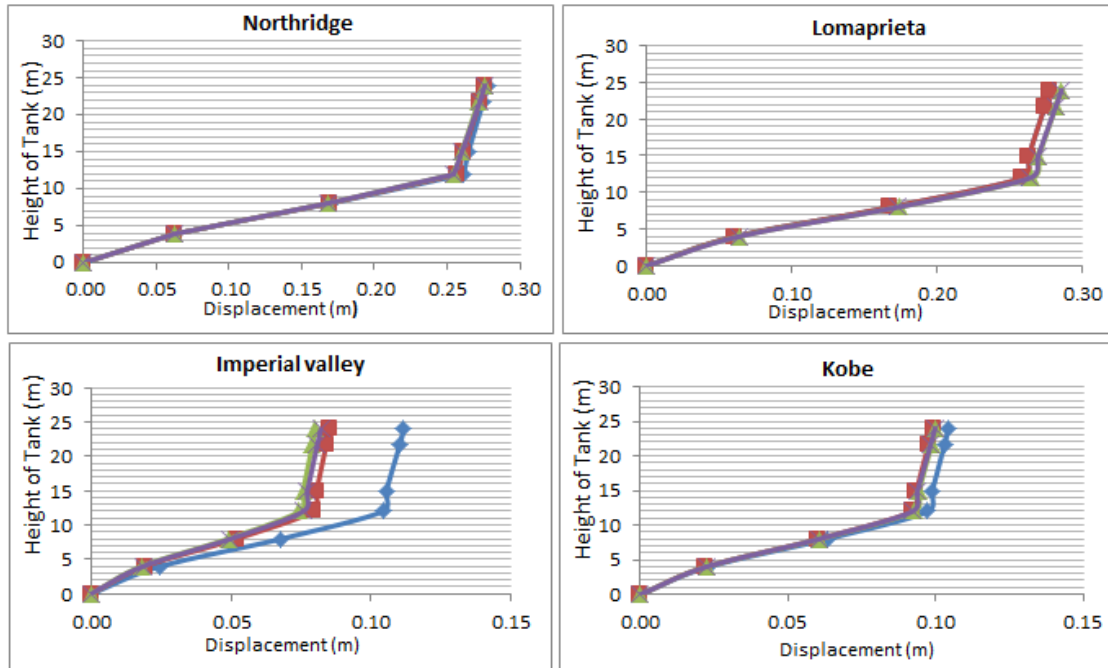
Fig.7 Displacement variation of 3-panel tank under four time history records
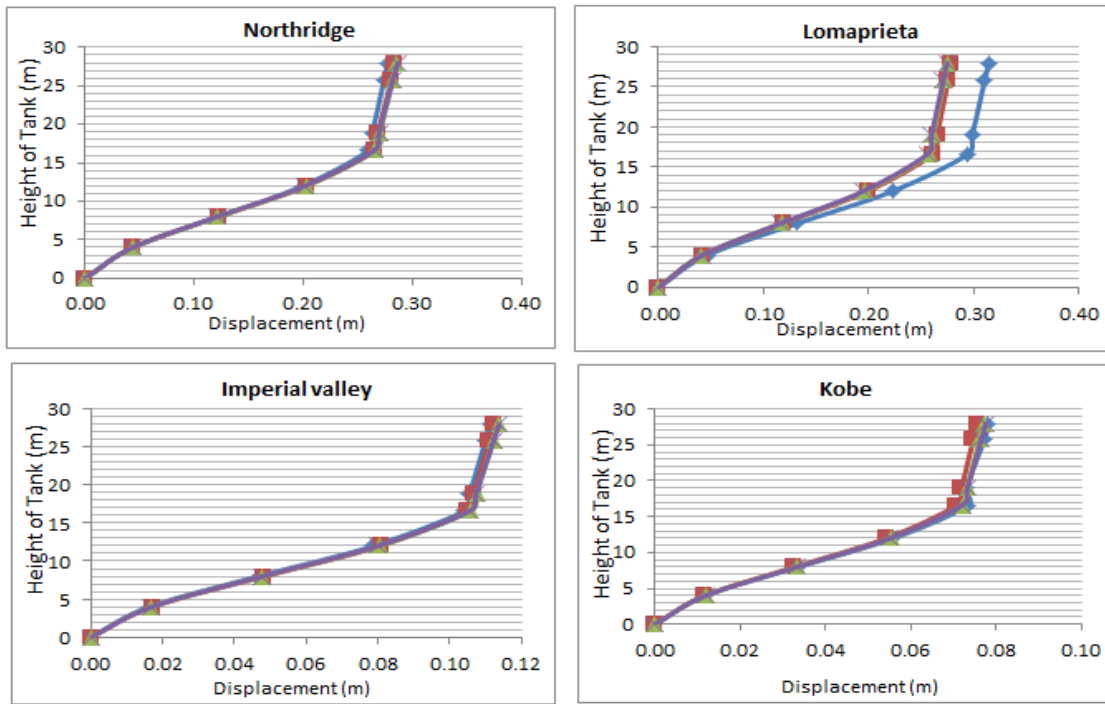
Fig.8 Displacement variation of 4-panel tank under four time history records
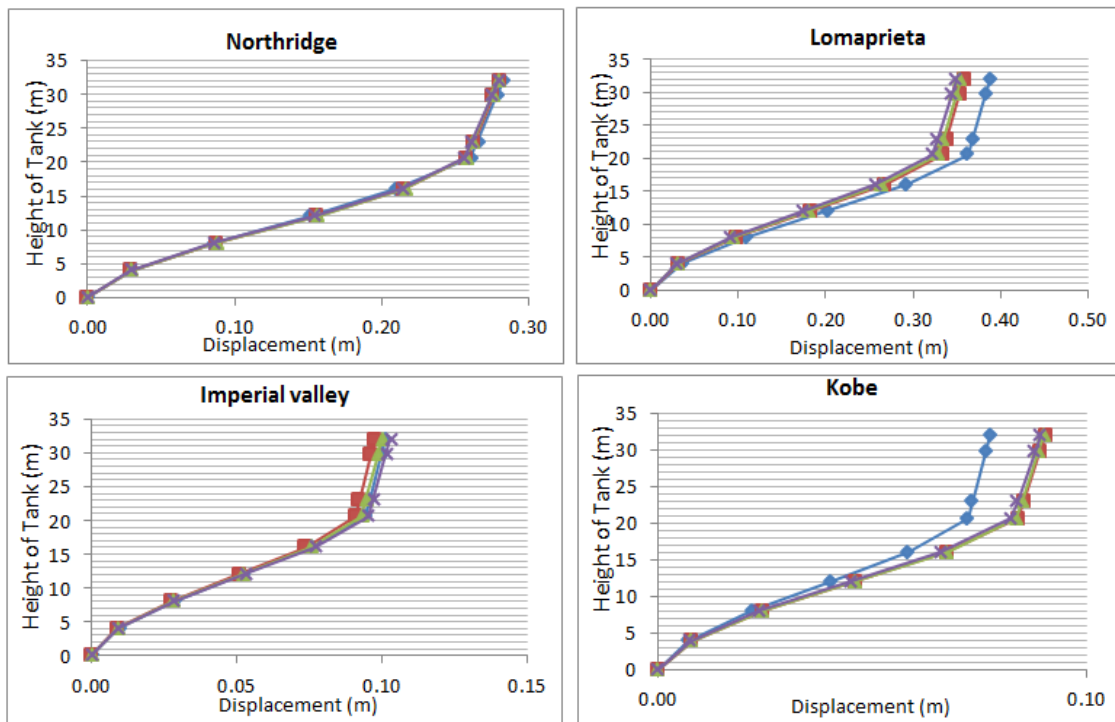
Fig.9 Displacement variation of 5-panel tank under four time history records

REFERENCES

[1]   IITK-GSDMA Guidelines for Seismic Design of Liquid Storage Tanks Provisions with commentary and explanatory examples, 2003.

[2]   Preliminary Draft code IS 11682:1985, "Criteria for Design of RCC Staging for Overhead Water Tanks", Bureau of Indian Standards, New Delhi, June 2011.

[3]   "Structural Analysis Program SAP2000. " User's manual, Computers and Structures, Inc., Berkeley, Calif.

[4]   R.K.Ingle," Proportioning of columns for water tank supported structures", The Indian Concrete Journal, April 1999, pg. 255-257.

[5] Gareane A. I. Algreane et al., "Behaviour of Elevated Concrete Water Tank Subjected to Artificial Ground Motion", EJGE, Vol. 16, 2011.

[6] Maunak Modi, "Analysis and Design of Elevated Water Tank with Frame and Shaft Type Tapered Staging", M. Tech. Major Project, Nirma University, Ahmedabad.

[7] Kuo, J.S.H., Fluid-structure interactions: Added mass computation for incompressible fluid, UCB/EERC-82/09 Report, University of California, Berkeley, 1982.

Influence of Frame Type Tapered Staging on Displacement of Elevated Water Tank

Chirag N. Patel[1], Burhan k. kanjetawala[2], H. S. Patel[3]

[1]*Ph.D. Candidate, Faculty of Engineering Pacific Academy of Higher Education and Research University, Udaipur, Rajasthan, India.*

[2]*P.G. Student, Applied Mechanics Department, L. D. College of Engineering, Ahmedabad, Gujarat, India.*

[3]*Associate Professor, Applied Mechanics Department, L. D. College of Engineering Ahmedabad, Gujarat, India*

[1]cnpatel.693@gmail.com
[2]burhan_kanjeta2000@yahoo.com
[3]dr.hspatel@yahoo.com

Abstract—As know from very upsetting past experiences, elevated water tanks were collapsed or heavily damaged during the earthquakes all over the world. These unusual events showed that the supporting system of the elevated tanks has more critical importance than the other structural types of tanks. So most of damages observed during the earthquakes arise from the causes like unsuitable design of supporting system, mistakes on selecting supporting system. Liquid storage tanks supported on staging are used extensively for storing water, inflammable liquids and other chemicals. Staging is formed by a group of columns and horizontal braces provided at intermediate levels to reduce the effective length of the column. The frame staging with a single row of columns placed straight (vertical) along the periphery of circle, are generally adopted for elevated water tanks to support the tank container. Apart from vertical column, tapered (inclined) columns are also used to support the tank container. The aim of this paper is to study the bottom to top displacement of elevated tank with frame type tapered staging under different time history records using software SAP2000. Analysis follows the guideline for "Seismic Design of Liquid Storage Tanks" provided by the Gujarat State Disaster Management Authority and Preliminary Draft of IS: 11682 "Criteria for Design of RCC Staging for Overhead Water Tanks".

Index Terms— Displacement; Seismic Analysis; Staging; Water tank;SAP2000

I. INTRODUCTION

THE water supply is essential for controlling fires that usually occur during an earthquake and which causes more damage and loss of life than the event itself. Therefore, the elevated tanks have to remain functional in the post-earthquake period to ensure water supply to earthquake affected regions. But, several elevated tanks damaged or collapsed during the past earthquakes. This type of upsetting experiences was shown by the damage to the staging of elevated tank in the some earthquakes occurred different regions of the World (Haroun and Ellaithy 1985). The extensive loss of life and damage caused by the recent earthquakes (Uttarkashi 1991 M.7.0, Jabalpur 1997, M.5.8, Chamoli 1999, M.6.5, and Bhuj 2001, M.7.7) has demonstrated the seismic hazard face by India. Since the elevated tanks are frequently used in seismically active regions. The bottom to top displacement is of important concern in the design of liquid storage structures. The clear understanding of displacement characteristics is essential for the elevated water tank. That is why, the Sloshing behavior of elevated tanks should be well known and they are designed earthquake resistant. The dynamic Response of liquid storage tanks subjected to earthquakes has subject of numerous studies in the past 30 years. In current Indian code for seismic design, limited provision on seismic design of elevated water tanks are given. Those provisions are highly inadequate compared to present international practice. Most of the previous studies were focused on the tank containing liquid considering only one mass and it does not cover important aspect for analysis and design of water tanks related to the effect of hydrodynamic pressure of the water, which produce due to vibration tank when earthquake strikes. But after the Bhuj earthquake, revision of current Indian code became inevitable. Hence it was decided to develop guidelines under the project "Review of Building codes and preparation of Commentary and Handbooks" assigned by the Gujarat State Disaster Management Authority (GSDMA), Gandhinagar to the Indian Institute of Technology Kanpur in 2003. The draft code for liquid retaining structure is one the outcomes of the project. The present study based on this draft code.The reinforced

concrete frame type staging of elevated water tanks generally has vertical columns resting on the perimeter of a circle. The columns are connected by circumferential beams at regular intervals. These circumferential beams divided staging configuration into a numbers of panels. This type of staging configuration more frequently used in practice has been referred as basic configuration. Apart from vertical column of elevated water tanks inclined or tapered column are also used to support the tank container.

I. MODAL PROVISIONS

A satisfactory spring mass analogue to characterize basic dynamics for two mass model of elevated tank was proposed by Housner (1963) after the chileane earthquake of 1960, which is more appropriate and is being commonly used in most of the international codes including GSDMA guideline. The pressure generated within the fluid due to the dynamic motion of the tank can be separated into impulsive and convective parts. When a tank containing liquid with a free surface is subjected to horizontal earthquake ground motion, tank wall and liquid are subjected to horizontal acceleration. The liquid in the lower region of tank behaves like a mass that is rigidly connected to tank wall, termed as impulsive liquid mass. Liquid mass in the upper region of tank undergoes sloshing motion, termed as convective liquid mass. For representing these two masses and in order to include the effect of their hydrodynamic pressure in analysis, two-mass model is adopted for elevated tanks. In spring mass model convective mass (mc) is attached to the tank wall by the spring having stiffness (Kc), whereas impulsive mass (mi) is rigidly attached to tank wall. For elevated tanks two-mass model is considered, which consists of two degrees of freedom system. Spring mass model can also be applied on elevated tanks, but two-mass model idealization is closer to reality. The two-mass model is shown in Fig. 1. where, mi, mc, Kc, hi, hc, hs, etc. are the parameters of spring mass model and charts as well as empirical formulae are given for finding their values. The parameters of this model depend on geometry of the tank and its flexibility. The two-mass model was first proposed by G. M. Housner (1963) and is being commonly used in most of the international codes. The response of the two-degree of freedom system can be obtained by elementary structural dynamics.

However, for most of elevated tanks it is observed that both the time periods are well separated. Hence, the two-mass idealization can be treated as two uncoupled single degree of freedom system as shown in Fig. 1 (b). The stiffness (Ks) is lateral stiffness of staging. The mass (ms) is the structural mass and shall comprise of mass of tank container and one-third mass of staging as staging will acts like a lateral spring. Mass of container comprises of roof slab, container wall, gallery if any, floor slab, floor beams, ring beam, circular girder, and domes if provided. Staging part of elevated water tanks follows the provisions given by Criteria for design of RCC staging for overhead water tanks (First revision of IS 11682): Draft Code [2]. This draft standard lays down criteria

for analysis, design and construction of reinforced cement concrete staging of framed type with columns.
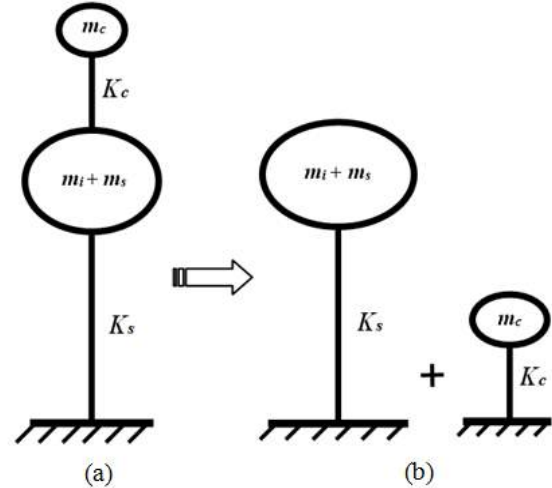

Fig.1. Two mass model for elevated tank

II. FLUID-STRUCTURE INTERACTION

During lateral base excitation seismic ground acceleration causes hydrodynamic pressure on the tank wall which depends on the geometry of tank, height of liquid, properties of liquid and fluid-tank interaction. Proper estimation of hydrodynamic pressure requires a rigorous fluid-structure interaction analysis. In the mechanical analogue of tank-liquid system, the liquid is divided in two parts as, impulsive liquid and convective liquid. The impulsive liquid moves along with the tank wall, as it is rigidly connected and the convective and sloshing liquid moves relative to tank wall as it under goes sloshing motion. This mechanical model is quantified in terms of impulsive mass, convective mass, and flexibility of convective liquid. Housner (1963) developed the expressions for these parameters of mechanical analogue for circular and rectangular tanks. Some researchers have attempted numerical study for tanks of other shapes (Joshi, 2000 and Damatty, 2000). There are some experimental studies on the effect of obstructions on the sloshing frequency (Kimura et al. 1995, Armenio 1996, and Reed et al. 1998). Fluid–structure interaction problems can be investigated by various approaches such as added mass approach (Westergaard, 1931), Barton and Parker, 1987), the Eulerian approach (Zienkiewicz and Bettes, 1978), the Lagrangian approach (Wilson and Khalvati, 1983; Olson and Bathe, 1983) or the Eulerian–Lagrangian approach (Donea et al., 1982). The simplest method of these is the added mass approach as shown in Figure 2, can be investigated using some of conventional FEM software such as SAP2000, STAAD Pro and LUSAS. The general equation of motion for a system subjected to an earthquake excitation can be written as,

$$M\ddot{u} + C\dot{u} + Ku = -M\ddot{u}_g \qquad (1)$$

In which M, C and K are mass, damping and stiffness matrices with $\ddot{u}$, $\dot{u}$ and u are the acceleration, velocity and displacement respectively, and is the ground acceleration. In

the case of added mass approach the form of equation (1) become as above.

$$M^*\ddot{u} + C\dot{u} + Ku = -M^*\ddot{u}_g \qquad (2)$$

In which M* is the new mass matrix after adding hydrodynamic mass to the structural mass, while the damping and stiffness matrices are same as in equation (1).
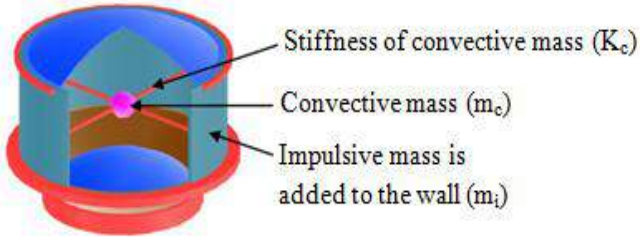

Fig 2. FEM model for fluid-strucutre-interaction added mass approach

Westergaard Model's method was originally developed for the dams but it can be applied to other hydraulic structure, under earthquake loads i.e. tank. In this paper the impulsive mass has been obtained according to GSDMA guideline equations and is added to the tanks walls according to Westergaard Approach as shown in Figure 3 using equation 3. Where, ρ is the mass density, h is the depth of water and A_i is the area of curvilinear surface.

Fig 3. (a) Westergaard added mass concept (b) normal and cartesian directions.

$$m_{ai} = \left[\frac{7}{8}\rho\sqrt{h(h-y_i)}\right]A_i \qquad (3)$$

In the case of Intze tank where the walls having sloped and curved contact surface, the equation (3) should be compatible with the tank shape by assuming the pressure is still expressed by Westergaard's original parabolic shape. But the fact that the orientation of the pressure is normal to the face of the structure and its magnitude is proportional to the total normal acceleration at the recognized point. In general, the orientation of pressures in a 3-D surface varies from point to point; and if it is expressed in Cartesian coordinate components, it would produce added-mass terms associated with all three orthogonal

axes. Following this description the generalized Westergaard added mass at any point i on the face of a 3-D structure is expressed by equation (4) (Kuo 1982 [7]).

$$m_{ai} = a_i A_i \lambda_i^t \lambda_i = a_i A_i \begin{bmatrix} \lambda_x^2 & \lambda_y\lambda_x & \lambda_z\lambda_x \\ \lambda_y\lambda_x & \lambda_y^2 & \lambda_z\lambda_y \\ \lambda_z\lambda_x & \lambda_z\lambda_y & \lambda_z^2 \end{bmatrix}$$

$$(4)$$

Where; A_i is the tributary area associated with node i; λ_i is the normal direction cosine $(\lambda_y, \lambda_x, \lambda_z)$ and a_i is Westergaard pressure coefficient.

III. PROBLEM DESCRIPTION

A reinforced elevated water tank with fixed base frame type staging system for tapering of 0°, 3°, 6° and 9° has been considered for the present study. The storage capacity of water tank is 1000 m³. A finite element model (FEM) is used to model the elevated tank system using SAP 2000 [3] structural software as shown in Figure 4.
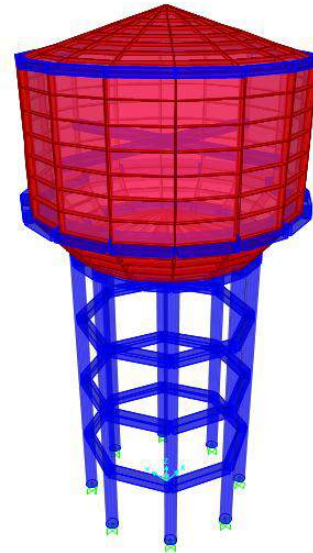
Fig 4. FE model of elevated water tank using SAP 2000.

Columns and beams in the frame type support system are modeled as frame elements (with six degrees of freedom per node). Conical part, bottom and top domes and container walls are modeled with thin shell elements (with four nodes and six degrees of freedom per node).

Other dimensions of the elevated tanks for various degrees of tapering are illustrated in Table 1. Mass and location of mass from ground level is 435.29 Kg and 21.86 m respectively under full condition, whereas for half condition 210.76 Kg and 20.89 m respectively under all types of tapering of water tank. Total four numbers of earthquake records were used; the maximum PGA on the basis of acceleration gravity for Imperial Valley (El Centro) (1979), Northridge (1994), Kobe

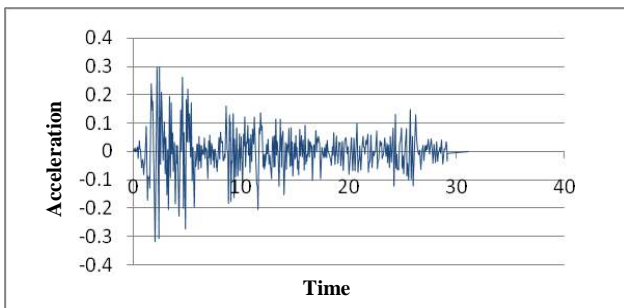(1995) and Loma Prieta (1989) are 0.314, 0.410, 0.509 and 0.644 respectively. Properties of recorded earthquakes are as shown in Table 2, with acceleration transverse component of four earthquakes as shown in Figure 5.
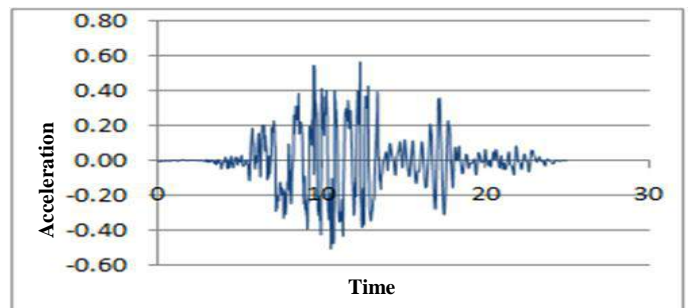
TABLE I
STRUCTURAL DATA FOR FRAME TYPE STAGING

Description	Data	Description	Data
Capacity of the tank (m^3)	1000	Thickness of Conical shell (m)	0.5
Unit weight of concrete (kN/m^3)	25	Rise of Bottom dome (m)	1.6
Thickness of Top Dome(m)	0.15	Thickness of Bottom dome shell (m)	0.2
Rise of Top Dome (m)	2.2	Number of Columns (circular)	8
Size of Top Ring Beam (m)	0.35×0.35	Number of Bracings Level	4
Diameter of tank (m)	13.6	Size of Bottom Ring Beam (m)	0.75×1.2
Height of Cylindrical wall (m)	6.8	Distance between intermidiate bracing (m)	4
Thickness of Cylindrical wall (m)	0.33	Height of Staging above Foundation (m)	16
Size of Middle Ring Beam (m)	1.2×0.6	Diameter of Columns (m)	0.75
Rise of Conical dome (m)	2.35	Size of Bracing (m)	0.5×0.5

TABLE II
PROPERTIES OF EARTHQUAKE RECORDS

| Record	Imperial Valley (El Centro), (1979)	North Ridge, (1994)	Kobe, (1995)	Loma Prieta, (1989)
Station	EC Meloland overpass	Canyon country -w cost cany	Nishi-Akashi	Corralitos
Component	IMPVALL /H-EMO000	NORTHR /LOS000	KOBE /NIS000	LOMAP /CLS000
PGA(g)	0.314	0.410	0.509	0.644
PGV(cm/s)	71.7	43.0	37.2	55.2
PGD(cm)	25.53	11.75	9.52	10.88
Magnitude	6.5	6.7	6.9	6.9

Imperial Valley (El Centro) (1979)

Lomaprieta (1989)
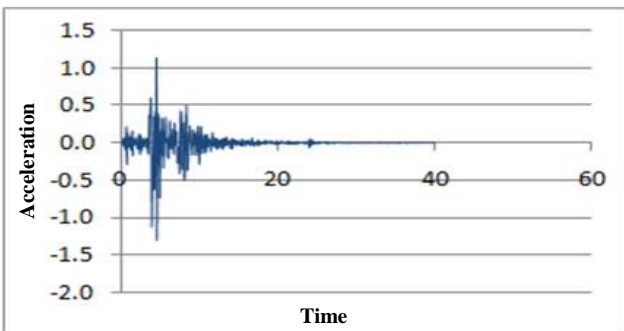
Northridge (1994)
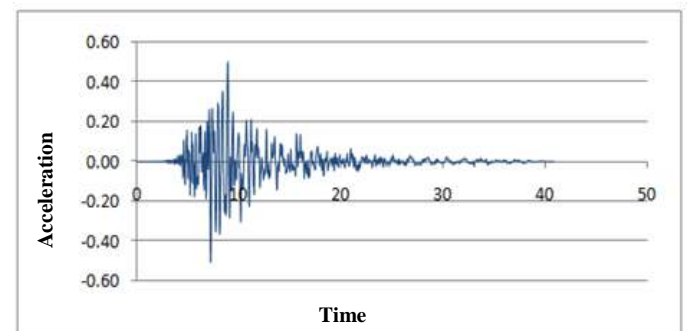
Kobe (1995)

Fig 5. Acceleration transverse component of earthquake

IV. RESULTS AND CONCLUSIONS

TABLE III
Displacement of tank at various heights and degree of tapering under tank full condition with different time history records

Level height (m)	Northridge (1994)				Lomaprieta (1989)				Imperial valley (1979)				Kobe (1995)			
	0°	3°	6°	9°	0°	3°	6°	9°	0°	3°	6°	9°	0°	3°	6°	9°
0	0.00	0.00	0.00	0.00	0.00	0.00	0.00	0.00	0.00	0.00	0.00	0.00	0.00	0.00	0.00	0.00
4	0.08	0.05	0.05	0.05	0.07	0.05	0.06	0.07	0.03	0.02	0.02	0.01	0.02	0.02	0.02	0.02
8	0.17	0.15	0.15	0.15	0.16	0.14	0.15	0.19	0.06	0.07	0.06	0.04	0.04	0.06	0.05	0.06
12	0.27	0.24	0.24	0.25	0.25	0.23	0.26	0.31	0.10	0.11	0.09	0.06	0.07	0.10	0.09	0.10
16.6	0.34	0.30	0.30	0.30	0.32	0.29	0.31	0.37	0.12	0.14	0.11	0.07	0.08	0.12	0.11	0.12
18.95	0.34	0.30	0.29	0.28	0.32	0.28	0.30	0.35	0.12	0.14	0.11	0.07	0.08	0.12	0.10	0.11
25.75	0.36	0.29	0.26	0.23	0.34	0.28	0.27	0.28	0.13	0.13	0.10	0.06	0.09	0.12	0.09	0.09
27.95	0.36	0.29	0.25	0.21	0.34	0.27	0.26	0.26	0.13	0.13	0.09	0.05	0.09	0.12	0.09	0.08

TABLE IV
Displacement of tank at various heights and degree of tapering under tank half full condition with different time history records

Level height (m)	Northridge (1994)				Lomaprieta (1989)				Imperial valley (1979)				Kobe (1995)			
	0°	3°	6°	9°	0°	3°	6°	9°	0°	3°	6°	9°	0°	3°	6°	9°
0	0.00	0.00	0.00	0.00	0.00	0.00	0.00	0.00	0.00	0.00	0.00	0.00	0.00	0.00	0.00	0.00
4	0.01	0.05	0.05	0.05	0.06	0.05	0.06	0.07	0.01	0.02	0.02	0.01	0.02	0.02	0.02	0.02
8	0.03	0.14	0.15	0.15	0.16	0.15	0.18	0.19	0.04	0.06	0.05	0.04	0.05	0.06	0.05	0.06
12	0.04	0.24	0.24	0.24	0.27	0.24	0.29	0.30	0.07	0.10	0.08	0.06	0.09	0.09	0.09	0.10
16.6	0.06	0.30	0.29	0.29	0.36	0.31	0.36	0.36	0.09	0.13	0.10	0.07	0.11	0.12	0.11	0.12
18.95	0.06	0.30	0.28	0.27	0.36	0.30	0.35	0.34	0.09	0.13	0.10	0.07	0.11	0.12	0.10	0.11
25.75	0.06	0.29	0.25	0.22	0.38	0.29	0.32	0.28	0.10	0.13	0.09	0.05	0.12	0.11	0.09	0.09
27.95	0.06	0.28	0.24	0.20	0.38	0.29	0.30	0.26	0.10	0.13	0.08	0.05	0.12	0.11	0.09	0.08

TABLE V
Displacement of tank at various heights and degree of tapering under tank empty condition with different time history records

| Level height (m)	Northridge (1994)				Lomaprieta (1989)				Imperial valley (1979)				Kobe (1995)			
	0°	3°	6°	9°	0°	3°	6°	9°	0°	3°	6°	9°	0°	3°	6°	9°
0	0.00	0.00	0.00	0.00	0.00	0.00	0.00	0.00	0.00	0.00	0.00	0.00	0.00	0.00	0.00	0.00
4	0.05	0.05	0.05	0.05	0.04	0.05	0.06	0.07	0.03	0.02	0.02	0.01	0.02	0.02	0.02	0.02
8	0.14	0.14	0.15	0.15	0.12	0.13	0.17	0.19	0.06	0.07	0.05	0.04	0.04	0.06	0.06	0.06
12	0.23	0.24	0.24	0.24	0.21	0.22	0.29	0.31	0.11	0.11	0.09	0.06	0.07	0.10	0.09	0.10
16.6	0.31	0.30	0.29	0.29	0.27	0.28	0.35	0.36	0.14	0.14	0.11	0.07	0.09	0.13	0.11	0.11
18.95	0.31	0.30	0.28	0.27	0.27	0.28	0.34	0.34	0.14	0.14	0.10	0.07	0.09	0.13	0.11	0.11
25.75	0.33	0.29	0.25	0.22	0.28	0.27	0.30	0.28	0.15	0.13	0.09	0.05	0.10	0.12	0.10	0.09
27.95	0.33	0.28	0.24	0.20	0.29	0.26	0.29	0.26	0.15	0.13	0.09	0.05	0.10	0.12	0.09	0.08
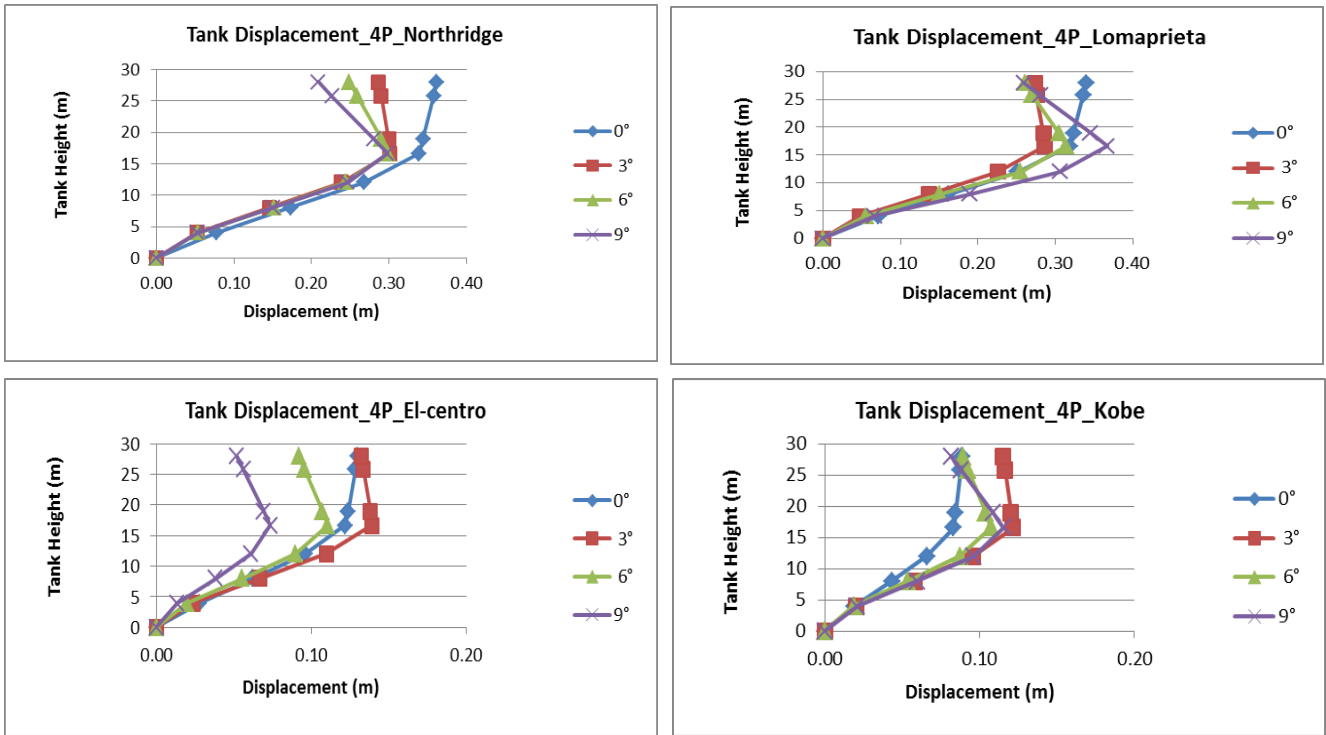
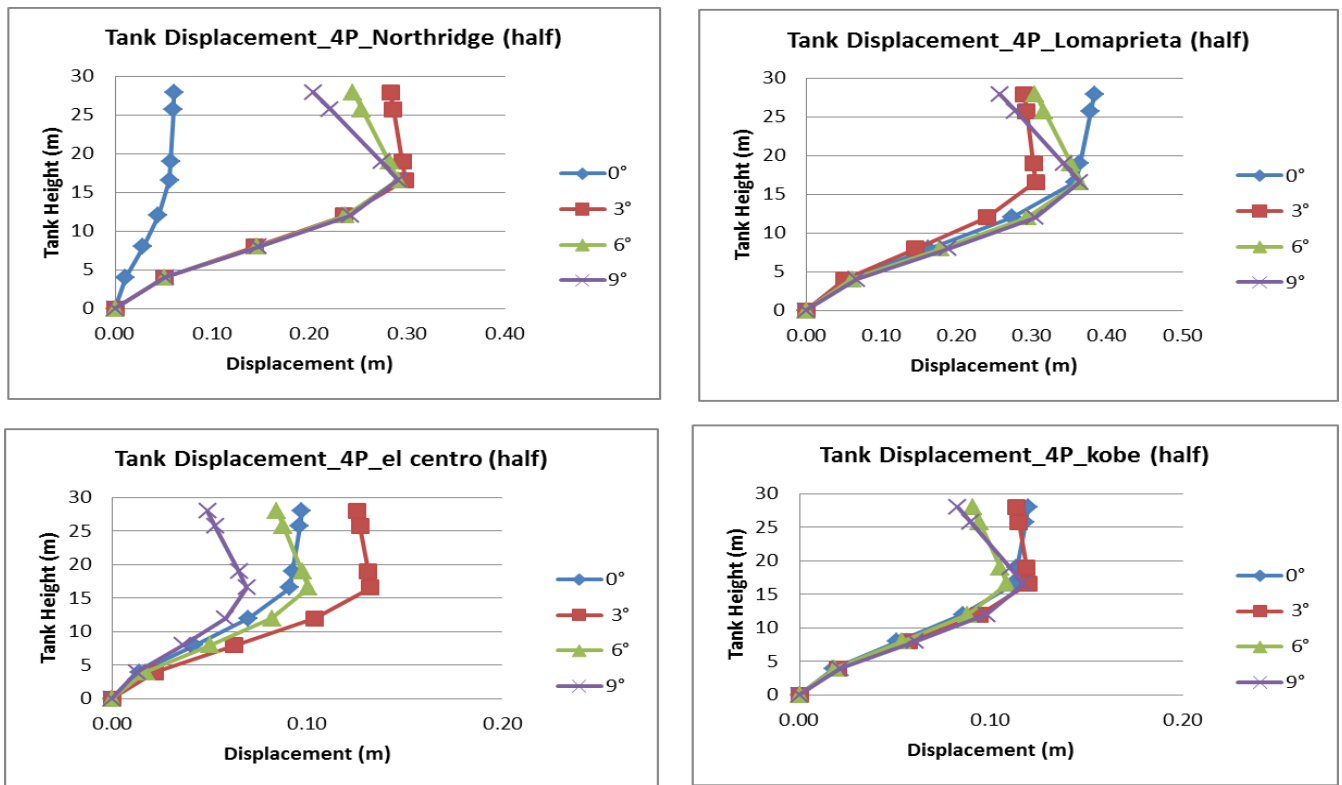Fig.5 Displacement variation of 4-panel tank for full condition under four time history records

Fig.6 Displacement variation of 4-panel tank for half full condition under four time history records
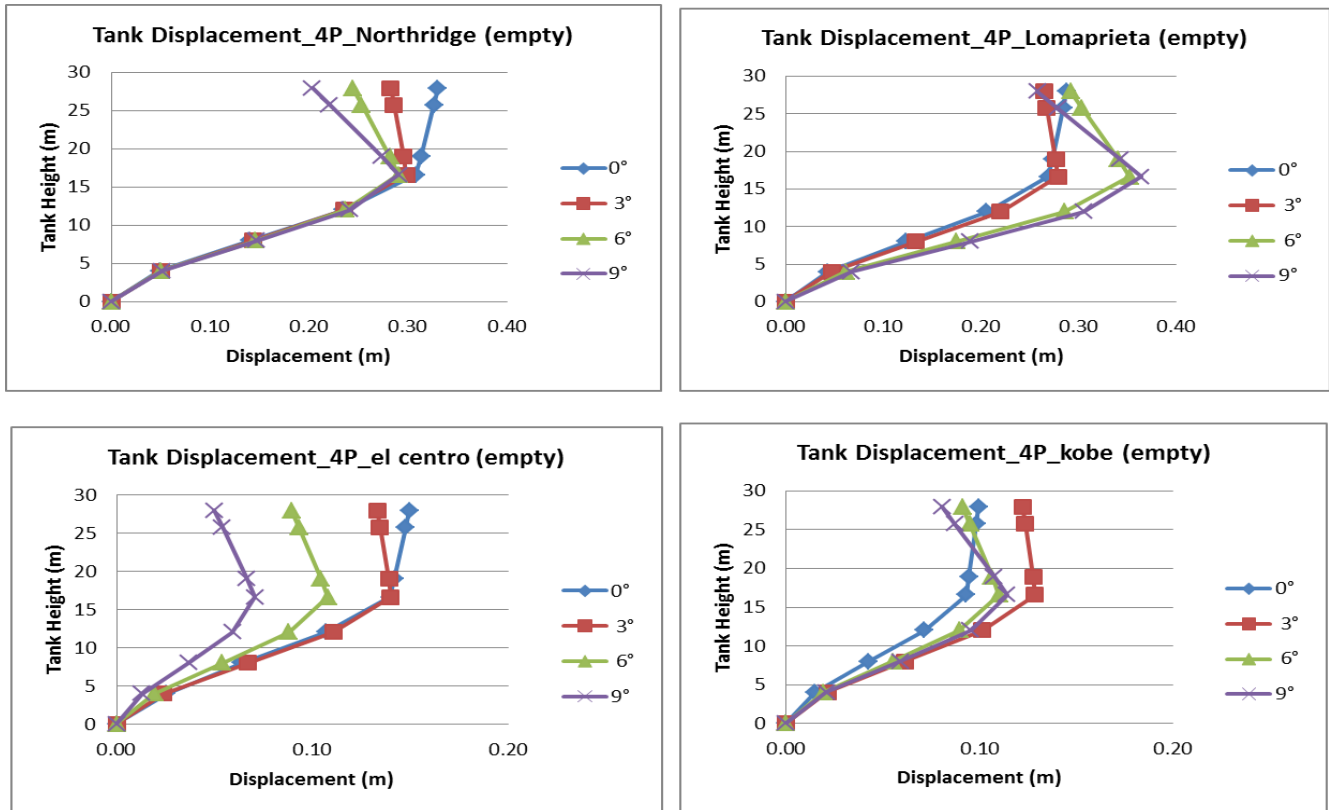
Fig.7 Displacement variation of 4-panel tank for empty condition under four time history records

In this study, a reinforced elevated water tank with 1000 m^3 capacity and supported by fixed base frame type staging system with tapering of 0°, 3°, 6° and 9° has been considered. With considering two-mass water model, bottom to top displacement were assessed under four earthquake records. The responses of tank have been determined using time history analysis in three cases, i.e. full, half and empty. The obtained results are summarized as follows:-

- The critical response of elevated tanks does not always occur in full condition, it may also occur under half condition. The critical response depends on the earthquake characteristics and particularly frequency content of earthquake records.
- The critical response of the elevated tank due to fact that the hydrodynamic pressures of container in half condition as compared with the full condition are higher. In addition to the critical response, depends on the earthquake characteristics and particularly frequency content of earthquake records.
- Thus, Structure response to each record in addition to the dynamic properties of the structure also depends on the above mentioned properties.

- Bottom to top displacement is constantly decreased with the increase in the tapering of staging during high frequency earthquake and produce different variation during low frequency earthquake with respect to different filled up conditions as per Fig. 5, 6 and 7.
- Displacement increases with increase in height up to the point of bottom circular girder and then decrease in all degree of tapering and three filled up conditions as per Fig. 5, 6 and 7.

REFERENCES

[1] IITK-GSDMA Guidelines for Seismic Design of Liquid Storage Tanks Provisions with commentary and explanatory examples, 2003.
[2] Preliminary Draft code IS 11682:1985, "Criteria for Design of RCC Staging for Overhead Water Tanks", Bureau of Indian Standards, New Delhi, June 2011.
[3] "Structural Analysis Program SAP2000. " User's manual, Computers and Structures, Inc., Berkeley, Calif.
[4] M. Kalani and S. A. Salpekar, A Comparative Study of Different Method of Analysis For staging of Elevated Water Tank, Indian Concrete Journal, July-Aug 1978.
[5] Maunak Modi, "Analysis and Design of Elevated Water Tank with Frame and Shaft Type Tapered Staging", M. Tech. Major Project, Nirma University, Ahmedabad.
[6] Gareane A. I. Algreane et al., "Behaviour of Elevated Concrete Water Tank Subjected to Artificial Ground Motion", EJGE, Vol. 16, 2011.

[7]   Kuo, J.S.H., Fluid-structure interactions: Added mass computation for incompressible fluid, UCB/EERC-82/09 Report, University of California, Berkeley, 1982.

Electron impact ionization of CO_2 – a molecule with pure and applied interest

Umang R. Patel[1,2] and K. N. Joshipura[2]

[1]Gandhinagar Institute of Technology, Gandhinagar - 382721

[2]Department of Physics, Sardar Patel University, Vallabh Vidyanagar - 388120

(umang.patel@git.org.in)

Abstract- **The advancement of knowledge of electron-atom/molecule collisions depends on an iterative interaction of experiment and theory. In this paper we have discussed measurements of total ionization cross sections of CO_2 at a fixed energy 1300 eV using time of flight mass spectrometry [5]. Continuing the investigation we have also calculated total ionization cross sections for electron impact on CO_2 molecules from threshold to 2000 eV using our theoretical approach [3, 4]. Our results are compared mutually as also with other available data.**

Index Terms—Time of flight mass spectrometer, Micro channel plate detector, Spherical complex potential and ionization cross section

I. INTRODUCTION

Electron impact ionization of molecules is fundamentally important in atmospheric science, plasma processes and mass spectrometry etc. Electron interactions with molecular species in various environments play a key role in creating the energetic ions that drives the chemistry in the atmospheres of planets and some of their satellites. To understand the electron impact ionization processes in space and in the laboratory, various accurately measured cross sections for the multiple ionization as well as dissociative ionization are needed. The above reasons make the study of ionization of atoms and molecules by electron impact both theoretically and experimentally challenging and important, and hence the present study.

II. EXPERIMENTAL METHODOLOGY

The mass spectrometer used for investigation is a *Time of Flight Mass Spectrometer.* Time of flight mass spectroscopy is a suitable technique for detecting and mass analyzing charged molecular fragments. The technique is based on the measurement of flight time of ions which arrived at detector while travelling over a known distance in an applied electric field. As seen in figure 1 the spectrometer is based on the well specified reaction zone (orange dot in figure 1) and the electric field guides all the ions and electrons towards the ion MCP detector and electron MCP detector respectively.

The detection of ejected electrons from the target molecule is treated as a trigger to start the clock for ion flight time measurement and it will stop when ions will be detected in ion micro channel plate (MCP) detector. The timing signal is converted into digital form using a TDC (time to digital converter) and accordingly we will have time of flight spectrum. The detailed description of the setup is given in [1, 6].
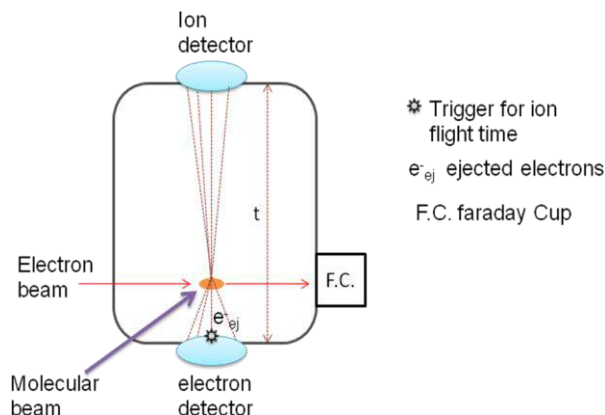

Fig. 1 Schematic of TOF spectrometer

In the present work we have used this time of flight data to evaluate the ionization cross sections of different ionic species and the details are described in [1].

The present experiment was performed for CO_2 molecule with fixed energy 1300 eV electrons.

III. THEORETICAL METHODOLOGY

Basically our theoretical method starts with simultaneous elastic and inelastic electron scattering treated in a spherical complex potential $V(r, E_i) = V_R(r, E_i) + iV_I(r, E_i)$. The incident energy is denoted by E_i and r is the radial distance of projectile from the centre mass of the target. Further $V_R(r, E_i)$ is the real part and $V_I(r, E_i)$ is imaginary part of the total potential. The real part consists of static, exchange and polarization terms, and the imaginary term is the absorption potential $V_{abs.}$ The basic input required in constructing all these model potentials is the single-centre molecular charge density which we calculate from the atomic wave functions.

The TCS Q_T obtained from the spherical complex potential is such that

$$Q_T(E_i) = Q_{el}(E_i) + Q_{inel}(E_i) \quad (1)$$

Where, Q_{el} is total elastic cross section and Q_{inel} is the total inelastic cross section at a given incident energy E_i. Further

$$Q_{inel}(E_i) = \sum Q_{exc}(E_i) + Q_{ion}(E_i) \qquad (2)$$

The first term on right hand side of equation (2) is the sum over total discrete-excitation cross sections for all accessible electronic transitions in the atom/molecule, while the second term indicates the sum of the total cross sections of all allowed (single, double etc.) ionization processes. The first term in equation (2) arises mainly from the electronic excitations having thresholds below the Ionization threshold I. The present energy range is from ionization potential to ~2 keV. The *CSP-ic* method, discussed in our recent publications, rests on bifurcating the Q_{inel} into discrete and continuum contributions, at incident energies above I. Specifically we have introduce a break-up ratio function,

$$R(E_i) = \frac{Q_{ion}(E_i)}{Q_{inel}(E_i)} \qquad (3)$$

Once this ratio, $R(E_i)$ is obtained, we can determine the Q_{ion} from Q_{inel}. This is the outline of *CSP-ic* method. Now, for the actual calculation of Q_{ion} from our Q_{inel} we need $R(E_i)$ as a continuous function of energy E_i. Therefore

$$R(E_i) = 1 - f(U) = 1 - C_1\left[\frac{C_2}{(U+a)} + \frac{\ln U}{U}\right] \qquad (4)$$

Here we have introduced the following dimensionless variable specific to the incident energy and the target.

$$U = \frac{E_i}{I} \qquad (5)$$

Equation (4) involves dimensionless parameters C_1, C_2, and a, which can be determined iteratively from semi-empirical physical arguments. Details of the method are given in [3, 4].

IV. RESULTS AND DISCUSSION

As listed in table 1 our ionization cross sections of dissociative species (O^+, C^+, CO^+) are in agreement with Straub *et al* [2] but our total ionization cross section and parent ionization cross section does not agreed well with Straub *et al* [2] and Hwang *et al* [7]. This disagreement can be due to the uncertainties come from ion counting statistics and electron current measurement. The dominant channel is the formation of stable CO_2^+ . The cross section of three dissociative channels are relatively small. The channel $CO_2 \longrightarrow O + CO$ has the highest cross section among the three dissociative channels. The total Cross section of measured channels is two order of magnitude higher than the double ionization and one order magnitude higher than the

TABLE I		
PRESENT Q_{ION} FOR CO_2 (EXPERIMENTAL)		
Ions	Cross sections (cm^2)	Cross sections (cm^2)
	Present	**Straub *et al* [2]**
CO_2^+	0.520×10^{-16}	0.686×10^{-16}
CO^+	0.740×10^{-17}	0.690×10^{-17}
CO_2^{++}	0.648×10^{-18}	0.627×10^{-18}
O^+	1.332×10^{-17}	1.28×10^{-17}
C^+	0.624×10^{-17}	0.733×10^{-17}
Total	0.803×10^{-16}	0.968×10^{-16}

dissociative ionization. This shows that single or parent ionization is dominant at such high energy.

As shown in figure 2 present total ionization cross sections are compared with Straub *et al* [2] and Kim and Rudd [7]. We have a very good agreement at low and high energies. Near peak region present results are slightly lower than Straub *et al* [2] and Kim and Rudd [8]. We have also indicated the ionization cross section which we have measured at 1300 eV using time of flight mass spectrometry.
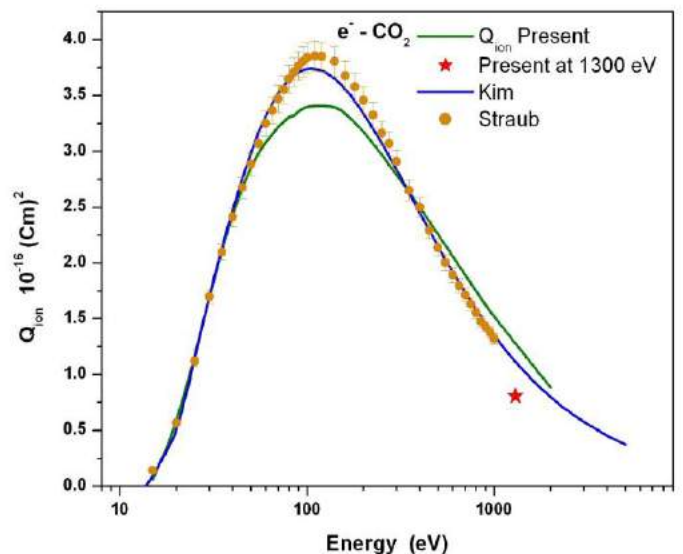
Fig. 2 Electron scattering cross sections with CO_2. Green solid line-present Q_{ion}, Star - present Q_{ion}, violet solid line - Kim and Rudd [8], orange dot – Straub *et al* [2]

We have compared our measured total ionization cross section

TABLE II	
COMPARISON OF PRESENT Q_{ION} (1300 EV)	
Theoretical	1.27×10^{-16} cm^2
Experimental	0.80×10^{-16} CM^2

(at energy i.e. 1300 eV) with the total ionization cross sections (see figure 2) calculated through the theoretical method developed by our group Joshipura *et al* [3, 4]. Our theoretical results are higher than that of the experimental results as shown in table 2. But theoretical results are in accord with the other available data. The discrepancy in experimental result may be due to variable detection efficiency which varies with detection method.

V. CONCLUSIONS

We have successfully measured the ionization cross sections of CO_2 for various ionized species, through experiment (at energy 1300 eV) which may be revised more carefully. In this paper our interest is on the calculation of electron impact ionization by theoretical method developed in our research group Joshipura *et al* [3, 4]. Our results of theoretical calculations have a good agreement with other theoretical and experimental data. In future more work can be done on CO_2 which is an important molecule for the planet Mars.

VI. REFERENCES

[1] E Krishnakumar and S Srivastava *Ionization cross sections of rare gas atoms by electron impact*, J Phys. B Vol. 21, 1055 Nov. 1987

[2] H. Straub, B. Lindsay, K. Smith and R. Stebbings *Absolute partial ionization cross section for electron impact ionization of CO2 from threshold to 1000 eV*, J. Chem. Phys. Vol. 105, 4015 June 1996

[3] K. Joshipura, H. Kothari, F. Shelat, P. Bhowmik and N. Mason *Electron scattering with metastable H_2^* $(c^3\pi_u)$ molecules: ionization and other total cross sections* , J. Phys. B Vol. 43, 135207, June 2010

[4] K. Joshipura, S. Gangopadhyay, H. Kothari, F. Shelat *Total electron scattering and ionization of N, N_2 and metastable excited N_2^* $(A^3\Sigma_u^+)$: Theoretical cross sections* Phys. Lett. A Vol. 373, 2876 August 2009

[5] V. Sharma and B. Bapat, *An apparatus for studying momentum resolved electron impact dissociative and non dissociative ionization* Eur. Phys. J. D Vol. 37, 223, Oct. 2005

[6] W Wiley and I. McLaren *Time of flight mass spectrometer with improved resolution*, Rev. Sci. Instrum. Vol. 26, 1150 June 1955

[7] W. Hwang, Y Kim and M Rudd *New model for electron impact ionization cross sections of molecules*, J Chem. Phys. Vol. 104, 2956 Nov. 1995

[8] Y. Kim and M. Rudd *Binary encounter dipole model for electron impact ionization*, Phys. Rev. A Vol. 50, 3954 Nov. 1994

Effect of Solar Activity on Background of X-ray Astronomical Objects

Mr.Nirav Y Pandya

(nirav.pandya@git.org.in)

Fig. 1.Sun with a solar flare

ABSTRACT: - **We know usually that various phenomenon takes place in Sun's atmosphere due to its activity. Solar activity follows the 11 year magnetic activity cycle from solar maxima to minima or solar minima to maxima, in which number of sunspots (dark region on sun's surface) changes on the basis of activity cycle. During the Solar flare: widely explosion in Sun's atmosphere; high speed electrons hurled out into planetary space where they affect satellites, earth's atmosphere and various astronomical objects. Solar flares are always located near sunspot and occur more often when sunspots are most numerous. The aim of my work is mainly to understand "How solar flares affect the background of X-ray astronomical objects."**

To study this effect, I have taken highest X-ray flux solar flare data from GOES-10 satellite and also taken the images of background of X-ray astronomical objects for the same time period. On the base of this data, I have drawn the graph of background count rate versus flux of selected X-ray flare which clearly indicates as X-ray flux increases the background count rate also increases. Thus X-ray flux solar flare increases the background of X-ray astronomical objects.

It is necessary to study this type of effects occur in the universe because if there exists very faint sources compared to the background surrounding X-ray sources, X-ray astronomical satellite cannot detect this type of faint sources and it can be go for false prediction about that sources.

I.INTRODUCTION

We know usually that various phenomena take place in the sun's atmosphere due to its activity. Solar flare is one such violent phenomenon. During the solar flare: widely explosion in the sun's atmosphere, high speed electrons hurled out into planetary space where they affect satellites, earth's atmosphere and various astronomical objects. The aim of my project is to understand how the solar flares affect the background during the X-ray astronomical observation.

II SOLAR FLARE: BRIEF EXPLOSION IN THE SUN

A .What is a solar flare?

A solar flare is defined as a sudden and brief explosion from the active region on the sun's surface with the energy equivalent to 2.5million terrestrial nuclear bombs, each with a destructive force of 100 megatons (10^{11} kg) of TNT (trinitrotoluene).

A solar flare occurs when the magnetic energy that has built up in the solar atmosphere is suddenly released. Radiation is emitted across virtually the entire electromagnetic spectrum from radio waves at higher wavelength end to the x-ray and the gamma rays at the shorter wavelength.

B. X-ray solar flare

Since solar flares are very hot, they emit the bulk of their energy at x-ray wavelengths. For a short while large flare can outshine the entire sun in x-rays.

Fig. 2. After a solar flare

Shown here is an image of the Sun in soft x-rays. The white (brightest) region on the right hand side shows post-flare loops, hot loops that remain after a solar flare. Image from the Yohkoh Soft X-ray Telescope, from NASA's Observatories.

Solar flare can be characterized by their brightness in X-rays as observed by monitoring satellites near the earth. The biggest flares are X-class flare which has the flux of 10^{-4} and above. M-class flares have one tenth the X-ray flux of an x-class one and the c-class has one hundredth of the x-class flux.

C. Effect of solar flare in the space

During the sudden and brief outbursts protons and electrons can be accelerated to nearly the speed of light. The high speed electrons and protons are also hurled out into interplanetary space where they can threaten astronauts and satellites. During release of flare energy there is also the coronal mass ejection take place which also affect the interplanetary space and earth's atmosphere. The intense radiation from a solar flare travels to earth in eight minutes. As a result:

● The earth's upper atmosphere becomes more ionized and expands.

● Long distance radio signals can be disrupted by the resulting change in the ionosphere.

● A satellite orbit around the earth can be disturbed by the enhanced drag on the satellite from the expanded atmosphere.

● Satellite's electronic component can be damaged.

III INTRODUCTION TO X-RAY ASTRONOMY

X-rays are a form of light, but much more energetic then light detected by our eyes. The energy of an x-ray photon is ~1000 times that of a photon of visible light. They are part of the electromagnetic spectrum which is shown below in the figure.

Where as astronomical x-ray is usually imaged in a different way from normal x-rays. In astronomy we image the source of x-ray itself. Sometimes however, there is an object which does get in the way and this then can appear as a shadow on the x-ray emission.

Generally the X-ray astronomical object has million degree K temperature and X-rays are emit from the hot object. So study of the astronomy at x-ray wavelength can give us more information about astronomical object. So X-ray astronomy was started.

Today the study of x-ray astronomy to be carried out using data from a host of satellites past and present, the HEAO series, EXOSAT, Ginga, CGRO,RXTE, ROSAT, ASCA. On 20th July 1999, the CHANDRA observatory launched by NASA and on December 10, 1999 the European x-ray satellite XMM (x-ray multi mirror mission) NEWTON was launched for x-ray observation.

A wide variety of x-ray sources have been known seen since identification of the first extra solar X-ray source in 1962. The Sun,Stars,Comets,X-ray Binaries, Supernova Remnates, Quasars and Active Galactic Nuclei are most interesting X-ray sources.

Roentgen used photographic plates to detect x-rays for his experiment. Now astronomers use more modern methods of detection. Today CCD (CHARGE COUPLED DEVICE) is used as x-ray detector.

A CCD is an image sensor, consisting of an integrated circuit containing an array of linked or coupled, light sensitive capacitors. The CCD was invented in 1969 by Willard Boyle

and George E.Smith at AT&T labs. Astronomer for many years used CCD in ultraviolet bands, they are, however, new to x-ray astronomy with their first use on the Japanese-American satellite for ASCA (Advance satellite for cosmology and astrophysics) launched in 1992.

We know that X-rays are detected by earth's atmosphere and because of it the rocket flight which could left the payload in the earth's upper atmosphere were necessary. For this purpose the satellite was the good option and so X-ray astronomy satellite was developed for X-ray astronomy.

X-ray astronomy satellite: NASA's advanced x-ray astrophysics facility (AXAF), renamed the Chandra x-ray observatory in honor of Subramanian Chandrasekhar; XMM (X-ray Multi Mirror) Newton Observatory and also few new mission (ASTRO E2 "SUZAKU") were launched for the purpose of X-ray astronomy.

IV X-RAY SOLAR FLARES DATA FROM GOES

The Space Environmental Centre of the National oceanic and atmospheric administration, or NOAA provides the peak soft x-ray flux for solar flares seen from their Geostationary operational environmental satellites or GOES for short.

The satellite hovers above the points in the earth's western hemisphere, orbiting at the same rate that that earth spins. I have taken the soft x-ray flux data for solar flare from GOES Space Environmental monitor.

There are various GOES satellite provides the data of the x-ray flux for the solar flare.

GOES-5 (Jan 1, 1986-Mar 31, 1987)
GOES -6(Jan 1, 1986-nov 30, 1984)
GOES-7 (Mar 1, 1995-June 30, 2003)
GOES-8 (Mar 1, 1995-June 30, 2003)
GOES-9 (Apr 1, 1996-Aug 31, 1998)
GOES-10(Jul 1, 1998-Apr30, 2007)
GOES-11 (Aug 1, 2000-Apr 30, 2007)
GOES-12 (Jan 1, 2003-Apr 30, 2007)

Here I have taken the data of the solar x-ray flux from 2000 to 2006 using the GOES-10 satellite. Here I want to find out the date and time on which the highest X-ray flux solar flare had occurred.

For it, I have taken the curve of the solar x-ray flux in w/m^2 Versus UT (universal time) for the duration of the every five days and note down the time and flux for the different x-ray flare. In this data I have found large number of M-class solar flare and few numbers of the highest x-ray solar flare i.e. X-class solar flare. Here I got approximately hundred X-class solar flare in which the highest solar flare occurred on 28 October, 2003 at 11:00 UT with the highest X-ray flux of 0.0025 w/ m^2. This solar flare had great effect on the solar system. The curve of X-ray flux versus UTC for this highest X-ray solar flare is shown below.
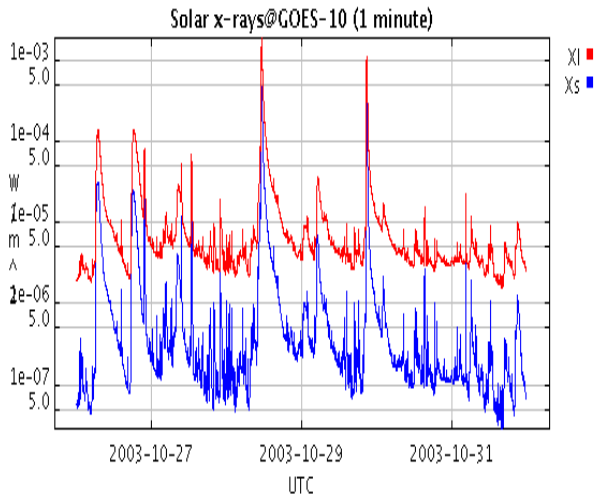
Fig. 3. XL 1-8 Ang X-ray flux (watt/m^2)
XS 0.5-3 Ang X-ray flux (watt/ m^2)

In above fig. we can see that the first and third highest flux solar flare occur within a week. The first highest and third highest solar flare occurs on 28 October, 2003 a11:00 UT and 29 October, 2003 at 22:00 UT. Due to these two highest X-ray flux solar flare, there is tremendous effect can be seen on the earth's atmosphere, Which we will see later in result.

V XMM-NEWTON DATA PREPARATION

The basic reduction of XMM-Newton data is provided by the SAS software package produced by the XMM- Newton Survey Science centre (SSC).

The SAS provides tasks to produced calibrated photon event files from the observation data format (ODF) files supplied to the user as well as some basic analysis tools. These include data filtering and extraction, production of rmfs and arfs for spectral analysis, and source detection routines.

The SAS was not designed for high level scientific analysis such as spectral fitting and temporal analysis. However, the SAS product files are designed to OGIP standards, so theoretically any high-energy is capable of processing XMM-Newton data. For example,
o HEASoft from the High Energy Astrophysics Science Archive Research Centre (HEASARC)
o CIAO from the Chandra X-ray observatory centre (CXC) can both be used for XMM-Newton data analysis.

The high energy astrophysics science archive research centre (HEASARC) is the primary archive for high-energy astronomy missions, in the extreme ultraviolet, X-ray and gamma-ray wavelengths. The HEASARC provides archival data, multi mission software and analysis tools, and information about current and past observatory missions.

We can download XMM-Newton data on a CD-ROM or from the public archive at VILSPA or also from HEASARC. HEASARC provides the data for all the observatories, data analysis tools etc.

I have download XMM-Newton data for randomly selection of 15 highest X-class solar flare. For ex: Highest solar flare

occurs on 28 October, 2003 so I have download XMM-Newton data for the duration of one day before to six days after means from 27 october,2003 to 03 November,2003. There are various type of data available in HEASARC browse archive for the XMM-Newton data. Among them I have taken it from XMMmaster (XMM master log and public archive).

Once if we got our XMM observation data, we can choose it between the observation data file (ODF) and the already processed product files created by an automatic pipeline. The advantage of the pipeline products is that you do not have to create the event files etc. yourself on your machine, which sometimes takes several hours and you can start immediately working with the scientifically data. The ODF data contains all of the observation specific data necessary for reprocessing the observation. The pipeline data contain among other things calibrated photon event files, source lists and images. Here I have used only pipeline product data.

VI XMM –NEWTON DATA ANALYSIS

A.Examine and filter an Epic data

The EPIC event lists in the EEVLIS group of the Pipeline Processing will have names of the form:

PiiiiiijjkkaaSlllcIEVLI0000.FTZ, where

iiiiiijjkk - observation number
aa - detector (M1 - MOS1, M2 - MOS2, PN - PN)
lll - exposure number within the observation
c - detector (M - MOS1 or MOS2, P - PN, T - Timing Mode)

The following sections describe the use of SAS tasks using the both the command-line and GUI interfaces, except in cases where one of the methods is particularly easy. The SAS GUI provides a very simple method for producing and displaying images, spectra, and light curves, and is the recommended method for extracting data unless large numbers of sources are being analysis.

B. Initialize SAS and Prepare the Data

(1) Gunzip the PP event list to be examined (not really necessary), and for practical purposes shorten the file name as well, e.g.:
mv P0123700101M1S001MIEVLI0000.FTZ mos1.fits.gz
gunzip mos1.fits.gz
(2) For initializing SAS GUI sasinit
(3) Invoke the sas GUI (in below fig.1)
(4) Invoke the xmmselect GUI from the SAS GUI; double click on the task name.

When here xmmselect is invoked a dialog box will first appear requesting a file name. After double click on the desired event files in the right hand column, click on file in the "EVENT" extension in the right hand column and then click on "OK." The directory GUI will then disappear and then click "RUN" on the selection GUI.

When the filename has been submitted the xmmselect GUI will appear along with a dialog box offering to display the

selection expression will include the filtering done to this point on the event file.

In xmmselect GUI we can choose the two dimensional data selecting the square boxes on the left hand side. In this case X,Y sky coordinates have been selected while one dimensional data can be selected using the round boxes.
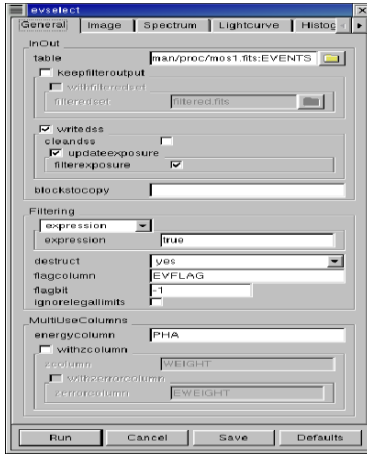

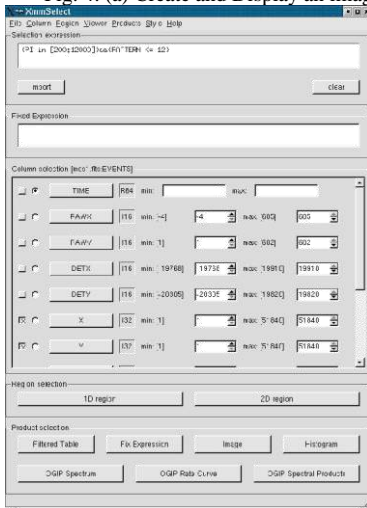Fig. 4. (a) Create and Display an image

Fig. 4. (b) Create and Display an image

C. Create and Display an Image

- To create an image of the data in sky coordinatescheck the square boxes to the left of the ``X" and ``Y" entries.

- Click on the ``Image" button near the bottom of the page. This brings up the evselect GUI.

- The default settings are reasonable for a basic image so click on the ``Run" button at the lower left corner of the evselect GUI. Different binnings and other selections can be invoked by accessing the ``Image" tab at the top of the GUI.

- The resultant image is written to the file `image.ds`, and the image is automatically displayed using ds9.
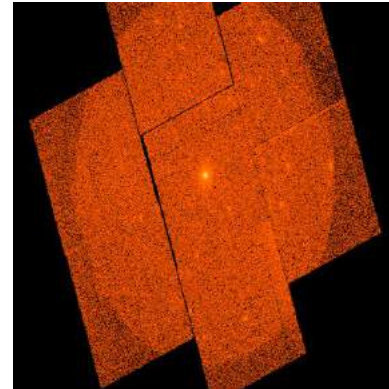

Fig. 5. (a) Image of X-ray astronomical object

Fig. 5. (b) Image of X-ray astronomical object

Two different images for EPIC MOS1 and in EPIC PN are shown in above fig. the left side fig. is for EPIC MOS with seven CCD and right side is for EPIC PN with 12 CCD.

D. Create and Display a Light Curve

- To create a light curve check the round box to the left of the ``Time" entry.

- Click on the ``OGIP Rate Curve" button near the bottom of the page. This brings up the evselect GUI.

- The default setting is for a one-second bin which is a bit fine, so access the ``Light curve" tab and change the ``timebinsize" to, e.g., 100 (100 s). Click on the ``Run" button at the lower left corner of the evselect GUI.

- The resultant light curve is written to the file rates.ds, and is displayed automatically using Grace.

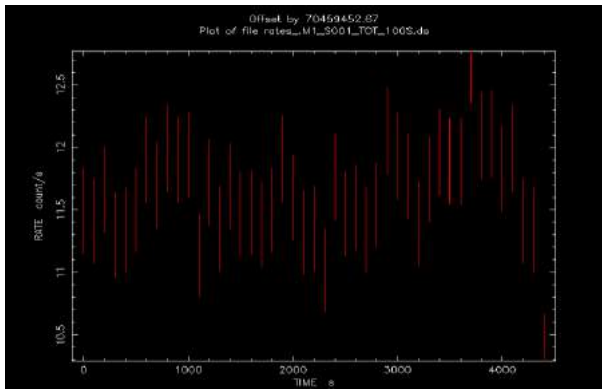Fig. 6.Total light curve with X-ray source

Fig. 7 (b) Images of background of X-ray Astronomical objects

F. Create and display a Background light curve

Above fig. shows the total light curve with the X-ray source for MOS1 which indicates that count rate for peak flare is 12.8 c/s on time 3700s for 100s background light curve.

E. Filter the Data and Create a New Event File

Filter the data using the xmmselect GUI: Here purpose of filtering is to get the background image of the MOS1 data and light curve for this background images. For it, in the image source and we want to extract the sources and we want to keep only the background area of the image.

For it, we select the each region belong to the xmmselect and then click 2D region. Doing in this way we can get the selection expression for the selected source region and then to extract it, we put "!" sign before it. So we can get only background region in the images. Then click on IMAGE and giving particular name for the background image. Thus we obtain background image. Two different background images for EPIC MOS and EPIC PN are shown as below.
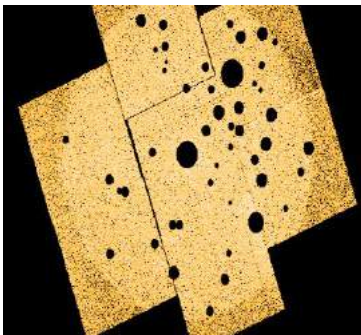
Here we got the selection expression for the background region of the images. Now in xmmselect click on OGIP rate curve and after giving particular name to it and taking particular time (here I took 100s,10s and 1s) for each light curve and then click on enter we can get the background light curve for the particular time. The background light curve for this type of selection expression in which the x-ray source region are extracted is shown in below fig.
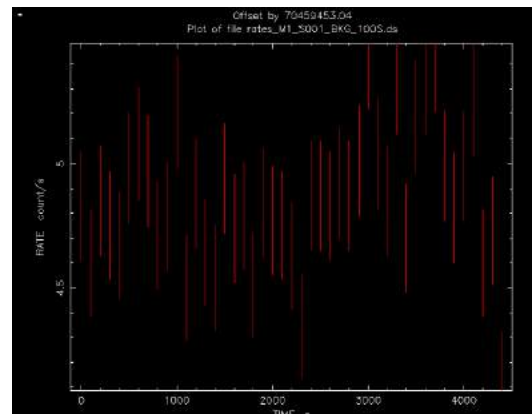

Fig. 9. Average background count rate for 100s light curve

As shown further we got background light curve for particular time and instrument containing certain observation I.D. I have used the command fplot, mo. (model), co.(constant) and then fit for find out the avg. background count rate for base level for each 100s light curve. Then I have plot the graph of avg. background count rate versus the range of the X-ray flux for selected flare. From it I have got important result which is shown below.

Fig. 7 (a) Images of background of X-ray Astronomical objects

VII RESULTS

● There are two important plots, which are shown below, describe the important result of my work. The second plot is main result of my project which is for the combined observation of both MOS1 and MOS2. It is the graph for background count rate versus flux of the selected X-ray flare. Here we can clearly see that as the flux increases the background also increases. It is not very clear result but we

GIT-Journal of Engineering and Technology   **(Sixth volume, 2013, ISSN 2249 – 6157)**

can see that background increases with the flux of X-ray solar flare.

● Now in the second fig 10. the background light curve for the duration of the highest X-ray solar flare which clearly indicates that the background clearly increases after the highest X-ray flux solar flare. Thus we can see that the emission of the outbursts during the solar flare, increase the background of the X-ray astronomical object.
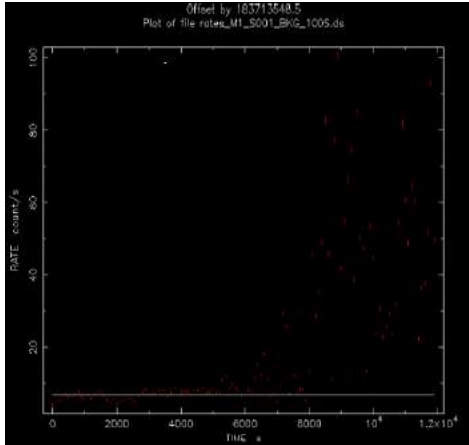

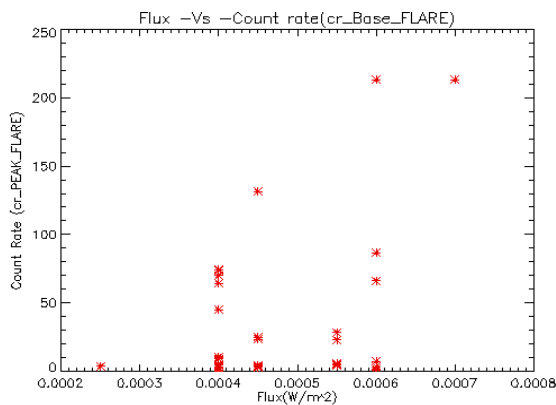Fig.10. background light curve of Highest X-ray Solar flare

Fig.11. Plot of background count rate versus x-ray flux

● Here I have observed the interesting effect of the solar flare on the XMM-Newton satellite. Before the highest X-ray flux solar flare occurs on 28, October 2003 the XMM-Newton was taking the observations but after the highest solar flare, I couldn't take my XMM-Newton data because it stops to take the observation and again it starts to take the observation on 9 November, 2003. Thus I observed the tremendous effect of it in the satellite.

VIII CONCLUSIONS

From my work on this the "effect of solar activity mainly solar flares on the background of X-ray astronomical object.",

I conclude that due to the outbursts going outside the sun, the background of the astronomical object increases.

It is necessary to study the this type of effect occurs in the universe because if there exists very faint sources compared to the background surrounding them and due to this, the X-ray astronomy satellite can't observe this type of sources and it can be go for false prediction about that sources. So it is very necessary to study this type of effect which occurs in the universe.

IX FUTURE ASPECTS

- Here I have taken the XMM-Newton data for sparsely selected highest X-class solar flare. If we take XMM-Newton data for all the X-class Solar flares, we can study the effect of solar flare on the background of the X-ray astronomical object more completely.
- I have studied the background light curve only for the 100s duration in this project. If we study the background light curve for 1s duration, then we can get understand effect of the solar flare on the temporal studies Of the X-ray astronomical objects.
- Similarly if we include the spectral analysis method, we can get more important information about the effect of solar flare on the X-ray Spectral studies of the X-ray astronomical objects.

REFERENCES

[1]   E. M. Schlegel ,The restless universe: understanding X-ray astronomy in the age of Chandra and Newton , Oxford University.

[2]   K. R. Lang :The Cambridge encyclopedia of the sun

[3]   GOES data archive: http://goes.ngdc.noaa.gov

[4]   HEASARC browse archive: http://heasarc.nasa.gov/W3Browse

[5]   XMM-Newton ABC Guide: http://heasarc.gsfc.nasa.gov/docs/xmm/abc/abc.html

[6]   XMM –Newton data cookbook: http://wave.xray.mpe.mpg.de/xmm/cookbook

Indian E-governance and It's awareness

Shruti Dilipkumar Upadhyaya, Dr. Parag Sanghani

(shrutiatnet@gmail.com, parag_sanghani@yahoo.com)

Abstract— **E – Government, also known as e-gov, digital government, transformational government ,online government, connected government is crafting a transparent, efficient, effective and comfortable interaction, between government and citizens (G2C – government to citizens), government and business enterprises (G2B –government to business enterprises) and relationship between governments (G2G – inter-agency relationship). With the help of government's SWAN (State Wide Area Network), even villages are connected with internet. So in Gujarat also, we have a better platform where Gujarat government can design, implement and utilize E-governance projects. Many Researches has been carried out for various E-Governance projects but again it is very much important to know how much effective they are. For measuring performance first step is to know how much awareness is there for various projects of Indian government. This paper in this context presents level of awareness and perceptions of citizens about online government.**

Index Terms— **E-governance, Information communication and Technology (ICT) , NeGp, Awareness about E-governance, Mission Mode Projects,**

I. INTRODUCTION

E-Government is about a process of reform in the way Governments work, share information and deliver services to external and internal clients for the benefit of both government and the citizens and businesses that they serve. (PCIP, 2002) and The OECD states that "the term e-government focuses on the use of new information and communication technologies (ICTs) by governments as applied to the full range of government functions. In particular, the networking potential offered by the Internet and related technologies has the potential to transform the structures and operation of government" (PUMA, 2001).

A more elaborate definition of governance is given by Dr. Perri in his book devoted to e-governance (2004). He defines governance as analysis and understanding of problems by elected and appointed politicians and their senior staff, the making of policy, the process of deliberation and cogitation, the process of exercising and cultivating political judgment, the making of decisions, and the oversight and scrutiny that other politicians and regulators exercise. Or, in short, the term governance is used to describe exercise of public power for steering social systems.

II. BRIEF DESCRIPTION OF THE PROJECTS

Government of India has introduced National E- governance plan (NeGp) that helps to create base for 27 Mission Mode projects, starting from small services to provide long term strategic growth to economy by e-governance. Without Information and Communication Technologies (ICT) overall growth is not possible in the concerned areas. Indeed, some of the schemes introduced in rural India have improved the government services immensely.

In NeGp, We have central MMPs like MCA21, Pensions, Income Tax, Passport and Visa, Immigration, Central Excise, Banking, MNIIC (Pilot)/ NPR, UID, e-Office (Pilot) and insurance. Integrated MMPs like CSC, e-Courts, EDI/e-Trade, India Portal, NSDG, e-Biz (Pilot), e-Procurement and then we have state MMps like Land Records (NLRMP), Road Transport, Agriculture, Police (CCTNS), Treasuries, Municipality, e-District (Pilot), Commercial Taxes, Gram Panchayat , Employment Exchange. All these projects have tentative outlay of 32488.18 Crore. NeGP(2011).

Government is spending huge amount on various E governance projects and most of the MMPs are on implementation stage, and target end date of most of the MMPs are before 2013, there is one hope latest by 2016, all E-governance projects will be on it's pick performance. When government is spending this much, one basic requirement is to make people aware and familiar with such online services. All central MMPs are managed by central government. Integrated MMPs are being managed by both Central and state government while state MMPs are responsibility of State government. However all MMPs are funded by Central government only.

Above is not exhaustive list to total E-governance program, Each state is now a days is taking challenge of providing most effective, Transparent and trustworthy governance. There are hundreds of E-governance projects in India.

III. E-GOVERNANCE INITIATIVES

National level E-governance projects

State Wide Area Network (SWAN)
State Wide Area Network (SWAN) is one of the infrastructure pillars for National E-governance Plan of Indian government. Government support for the establishment of such

infrastructure up to the block level is provided by the Department of Information Technology in accordance with the published SWAN Guidelines.

There are two Options for SWAN implementation as detailed below:

1. Public Private Partnership (PPP) Model

State identifies a suitable PPP model and selects an appropriate agency through a suitable competitive process for outsourcing the establishment, operation and maintenance of the Network.

2. NIC Model

State designates NIC (National Informatics Centre) as the prime implementation agency for SWAN for establishment, operation and maintenance of the Network.

In March 2005, Department of IT obtained Government Approval for the SWAN Scheme for an overall outlay of Rs. 3,334 Crores, with Dept of IT, Grant in Aid component of Rs. 2,005 Crores to be expended in five years, which would establish Wide Area Networks in 29 States and 6 Union territories across the country. Implementation of this Scheme is in full swing with individual project proposals have been approved for 33 States/ Union territories with total outlay of Rs. 1965 Crores1.

With SWAN project implementation, even far areas are now connected via internet, and this project has played very much vital role in overall development or rural India. As on November 2010 , SWAN is operational in 23 States/UTs.

If we focus on Gujarat, we find that Gujarat State Wide Area Network (GSWAN) has established a reliable horizontal and vertical communication corridor for within the state administration to achieve e-governance commitment and bring governance closer to public and strengthen disaster management capacity

GSWAN Network Architecture and Topology:

1. First Tier: Secretariat Center (SC) at state capital Gandhinagar, where various departments and hundreds of subordinate offices located at the state capital are connected to SC horizontally through Secretariat Campus Area Network (SCAN). All districts and Taluka offices are vertically connected with SC (the hub of wide area network).
2. Second Tier: constitutes District Centers (DCs), located at district collector's office, and multiple district level connected with DC horizontally.

Third Tier: constitutes Talukas Centers (TCs), located at Taluka Mamlatdars office, and couple of Taluka level offices horizontally connected with TC.

Mahatma Gandhi National Rural Employment Guarantee Act (MGNREGA).

MGNREGA is basically design to assist to Citizens, Workers, Gram Panchayats, Block Panchayats, Zila panchayats, Line departments executing works of NREGA, Administrator at Block and District level, State NREGA department, Ministry of Rural Development, Administrators in the Government.

Various modules of the software:

1. Beneficiary Management Module: The software captures registration, demand for work, work allocation and muster rolls on which a person worked.
2. Fund Management Module: Captures the fund transferred from States to Districts and then to Programme officers/ Panchayats and expenditure incurred by various implementing agencies on labor, material and contingency.
3. Works Management Module: Captures information about the various works undertaken under the scheme at various levels.
4. Grievance Redressal System: Allows a worker/Citizen to lodge complaint and trace the subsequent response.
5. Staffing Position Module: Captures name, telephone numbers etc. of all the officials, planning and implementing agencies from Gram Panchayat to Ministry of Rural Development involved in NREGA, thus strengthening communication and coordination among them.
6. Alerts: The software also gives alerts to implementing agencies about the various irregularities, important activities, and messages for funds to be received by the agencies.

Public Private Partnership in the implementation of NREGA is important from the following reasons:

- PPP will ensure transparency and help in information propagation
- PPP is required because the size of the programme is very large, not only from the geographical and financial perspective but from the perspective of the size of the target group of beneficiaries as well.
- PPP facilitate online monitoring and evaluation of the programme. The timely feedback will help in timely corrective actions.

There is colossal cost saving in issue of job card, pay slips etc. save amount and time in generating the registers need to keep at various locations. Rather than time saving it is mainly bringing the systems in place. Removing the bad practices like Kachha muster roll, part payments etc are the goals to be achieved. Locations where computer have reached in gram panchayat the system has helped in quickly generating the job cards and timely accepting the demand for work and issuing the acknowledgment of receipt of demand for work (Gupta et al., 2008)

Online Income Tax and Central Excise

E-payment the way to pay for something online, this scheme facilitates anytime, anywhere payment and an instant cyber receipt is generated once the transaction is complete. With this, government of India has enabled Indian citizens to file tax, central excise and service tax online.

It can be seen from the following table that every day internet users are increasing.

FORM WISE RECEIPT OF E-RETURNS UPTO 30th SEPTEMBER 2011

S.N.	FORM NAME	F.Y. 2010-11	F.Y. 2011-12	PERCENT GROWTH IN F.Y. 2011-12
1	ITR-1	13,77,444	31,03,832	125.33%
2	ITR-2	5,13,170	9,74,222	89.84%
3	ITR-3	96,315	1,79,132	85.99%
4	ITR-4& 4S	16,91,959	36,11,464	113.45%
5	ITR-5	3,49,719	5,19,505	48.55%
6	ITR-6	2,91,471	4,53,356	55.54%
Total		43,20,078	88,41,511	104.66%

Source: http://www.simpletaxindia.net/2011/10/104-increase-in-efiling-of-income-tax.html accessed on November 24, 2011.

With the help of online tax filing citizens can have the following benefits,

- Convenience – citizens can file tax at their convenient time.
- Security – System is very much secure and there is no risk of secrecy.
- Ease of use – Website gives instructions and guidelines in different languages allowing people to file returns in simple manner.
- Speed – Instead of standing in queue, tax can be filed within minutes. It saves lots of time and operational cost both citizens and government.

Automation of Central Excise and Service Tax (ACES), a Mission Mode Project of the government of India under National e-Governance Plan is widely used through website (www.aces.gov.in) having hits over 31 crores and is aimed to reduce physical interface with department with reference to:
Online registration of central excise assesses and online amendment

- Online registration of service tax assesses and online amendment
- Electronic filing of central excise returns
- Electronic filing of service tax returns
- Electronic filing of claims, permissions, intimations
- Instant e-acknowledgement of documents with unique document identification number
- View, file and track status of documents filed online

Unique ID

Unique identification project was initially conceived by the Planning Commission as an initiative that would provide identification for each resident across the country and would be used primarily as the basis for efficient delivery of welfare services. Unique ID is now known as Aadhaar which is a 12 digit individual identification number issued by the Unique Identification Authority of India on behalf of the Government of India. This number will serve as a proof of identity and address, anywhere in India.
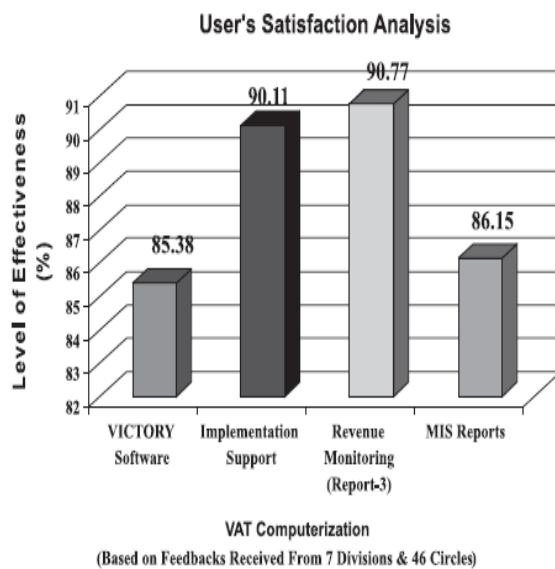
In Aadhaar the basic demographic and biometric information – photograph, ten fingerprints and iris of eye are stored, and hence, take us close to do away with multiple identities. As this can be verified online in a cost-effective manner, this can be effectively used to target various public welfare schemes. It is widely acknowledged that an electronic national databank has the potential to improve the effectiveness and efficiency of government administration. Creating an identity card based national ID system might be a first step towards this objective. (Prasad, 2007). This will help government a lot for providing government service more efficiently.

State Level E-governance Projects

- E-Seva is 'One-stop-shop' for over 66 G2C and B2C services. It facilitates citizens to avail all governmental services. E-seva centers have been established in over 200 villages and towns delivering services to citizens based on a low-cost networking model. Of the 46 bigger e-Seva Centers at mandal headquarters, E-Seva centers (with 400 service counters) spread over the Twin Cities and Ranga Reddy District. All service counters are facilitated with an electronic queuing system.Online services like eForms, eFiling, ePayments enables citizens to save time for standing in queues. Payments can be made by cash/cheque/DD/credit card/Internet. Online complaint registration allows citizens to complaint/issue online to district official. And also helps citizens to views status of complaint. With this, citizens are not required to run government offices to and fro helter-skelter. Mechanism of Online complaint registration has helped to increase transparency in government dealings. Prajavani is an e-governance initiative by the combined efforts of District Administration and National Informatics Centre in Rangareddy (Andhra Pradesh, India) in association with Web Services Division, NIC, Hyderabad, Andhra Pradesh State Center5. Prajavani is a unique public private partnership program, which gives citizens an opportunity to interact with the government without coming to any government office.

- Bihar government has taken vial initiative to provide each gazette of government online, ensuring all relevant government records in .pdf (Acrobat format) format. Now government officials and citizens can have easy reach to required information just by some click on website http://egazette.bih.nic.in/Gazette.aspx. With this website have total 2433 published gazettes available.

- "Gyan Ganga" is the finest initiatives of Gujarat government to ensure wireless Internet connectivity to all 18,000 villages in Gujarat. At the heart of "Gyan Ganga" is corDECT- A technology based on Wireless in Local Loop (WLL) - specially developed by Indian Institute of Technology (IIT) Madras.(Kokil, 2006) With the help of Gyan Ganda, citizens residing in far rural places can now view and access many online services including land records, online job application portal i.e. www.ojas.guj.nic.in,can. They can also use email services and can contact consultants and can seek help for agricultural, heath related and veterinary queries.

- State Wide Attention on Public Grievances by Application of Technology (SWAGAT), is mechanism where Gujarat's citizens can directly communicate with chief minister. In Gandhinagar, the fourth Thursday of every month is a SWAGAT day wherein the highest office in administration attends to the grievances of the man on the street. The grievances once registered, it travels the entire state online and again reply comes back within 3-4 hours. The record is then preserved in the 'SWAGAT' database and a separate log is maintained for each case6.

- SETU in Maharashtra is online portal from where citizens can have number of certificates like domicile, nationality, caste, age verification, solvency, character verification, income and occupation. SETU or the Citizen facilitation Centers act as a one-stop service centre for people who have to visit government offices for certificates, permits, authentication, affidavits and other services. It saves time of government officers and also of citizens as these services are online. It has improved transparency and efficiency both at same time.

- The Bhoomi is extraordinarily successful project of online delivery of land records in Karnataka. Farmers can have land record online and it was basically to benefit rural populations need to recognize the high level of effort that is needed to make rural population aware of the reforms that have been instituted. Earlier farmers had to ask village accountant for copy of the Record of Rights, Tenancy and Crops (RTC) – a document needed for many tasks such as obtaining bank loans. And there was huge corruption as accountants where charging from illiterate farmers for providing such documents. Again rural accountant had to travel a lot for collection and delivery of land records. Land records kiosks have been made operational in all 177 taluks and 26 special taluks. Village accountants can no more issue copies of the manual records, as only computerised records are valid. (Chawla, 2007)

- Akshaya has become weapon in rural empowerment and economic development. The project is a channel in nurturing growth and creating direct and indirect employment in the State by focusing on the various facts of e-learning, e-transaction, e- governance etc. Thus, the project is having a long-standing impact on the social, economic and political scenario of the State.

- The Information Village Research Project (IVRP) was set up in 1998 in Pondicherry (a centrally administered territory in Southern India), by the M.S. Swaminathan Research Foundation (MSSRF), a nonprofit organization# This project is basically for poor rural citizen, Information village shops are well equipped with computers, telephones, a printer, a wireless device, and a solar panel -- all latest IT infrastructure to provide rural people local news, latest prices of agricultural crops and inputs, weather reports, and government programs. This project is a huge success because the villagers attached trust and credibility to the information provided by the centers. IVRP has become a way to important information for rural people of Pondicherry.

- In the traditional manual methods the query of land record with all the related data is comparatively time consuming and backbreaking. In Tamilnadu, with the help of online land record, citizens can view Record of rights agriculture land record online. One of the important benefits in having online land records is it reduces opportunities for bribery. In addition, operators of the computerized record system are held accountable for their actions and decisions through a log of all transactions.
  - Allows easy maintenance and prompt updating of land records.
  - Allowing rural farmers easy access to their records.
  - Assembling the information related to land revenue, cropping pattern, land use, etc.
  - Utilizing the data for planning and for formulating development programs.

  This is for sure that with the help of such e-governance project, services of government have become very much trust worthy and even very much fast.

- VAT Information Computerization to Optimize Revenue Yields (VICTORY) system has facilitated

unearthing crores of tax evasion by micro and macro analysis by adopting integration of top-down and bottom-up approach. It also helped in scrutinizing of returns and validation of Input Tax Credit (ITC) from seller and purchaser data in centralized way thus speeding up the refund process. It widened the tax base in terms of Registered Dealers from 47,049 up to March 2005 (before VAT computerization) to 101,731 April 2006 to October 2006 depicting a growth rate of 116 percent. Similarly, Revenue Growth was also remarkable as it was 1604.36 in the year 2001–02 and augmented to 2389.98 in the year 2005–06 i.e. there is 785.62 crores of growth in 4 years of age of VICTORY. Saurbah Gupta,S.N. Behera, Ashok Kumar, Rajiv Ranjan, (2009)

User's Satisfaction Analysis

VAT Computerization
(Based on Feedbacks Received From 7 Divisions & 46 Circles)

If we see National Rural Employment Guarantee Service (NREGS), NREGS-AP software is a web-based end-to-end ICT solution with local language interface to ensure that the objectives and entitlements of National Rural Employment Guarantee Act (NREGA) reach the wage seeking rural households. TCS developed the software as CSR. A. Santhi Kumari, (2009)

- ➢ Transparency in all EGS transactions
- ➢ Job card data: 52,58,758 job cards are issued.
- ➢ Shelf of works: 1,96,338 no of works worth 1,71,439.46 lakhs are available in shelf
- ➢ Works Execution: 93,101 number of works are completed 1,97,520 number of works are in progress
- ➢ Payment of wages. 58901.47 amount is paid as wages to 34,08,345 wage seekers of 23,26,138 Households
- ➢ Demand satisfaction: 23,26,138 wage seekers demanded for work and are given work

- Indian Railway. IRCTC launched its official website http://www.irctc.co.in on 3 August 2002 for the purpose of railway ticket booking through Internet. Since its inception it has emerged as one of the largest online payment Internet site in India with annual growth of more than 300%, touched a daily high of 57, 000 tickets (turnover of Rs. 9 crores) and crossed 10 lakhs in ticket sales per month during several months this year. Even the average number of tickets sold through IRCTC's website in a day is more than 40,000. Sanjay Agrawal(2009).

Global E governance scenario:

- Online Parking Spot Search System (Rosenheim/Germany) : The City of Rosenheim offers an interactive search for parking spots. Users can either look for free spots in one of the garages or parking lots online or they can use their cell phone with Internet access to find out, where they can park their cars. They can also find out all the information about prices, opening hours etc either online or mobile. The site can be accessed from cell phone with Internet access (WAP). By website : http://www.rosenheim.de/parkleit/stadtplan.htm UNESCO 1(2005)

- Rindernet : Online Cattle Net (Austria) : RinderNet is a fairly successful e-governance project in Austria which aims at using Information Technology to facilitate the cattle farm owners in maintaining a comprehensive database on Cattle. All the farm cattle in the country have 'ear tags' which help in categorizing the different animals and provide background information such as vaccination details against various infectious diseases etc. With the Rindernet project, all information related to the cattle, available in ear tags and in other records has been computerised. Website : http://www.rindernet.at UNESCO 1(2005)

- Citizen Service Centers In Bahia (Brazil): The state government of Bahia has created Citizen Assistance Service Centers (SAC) that bring together federal, state and municipal agencies in a single location to offer the services that citizens most frequently need and use. The centres have been placed in locations convenient to the public, such as shopping malls and major public transportation hubs. They offer citizens tremendous time savings, while also delivering services with greater courtesy and professionalism. UNESCO 1(2005)

- Beijing E-Park (China): Beijing, the capital city of

China, began its "Digital Beijing" initiative in the year 2000. Zhongguancun E-Park, at www.zhongguancun.com.cn is a pilot project that applies the latest computer and Internet technologies to improve the efficiency and responsiveness of government. Since then, more than 6,000 businesses have been able to apply for a license, file monthly financial reports, submit tax statements and conduct 32 other G2B and G2C functions online. The system has greatly increased government transparency and efficiency, and reduced the opportunities for corruption. The mayor of Beijing announced that in five years, most government administrative functions in the city will be performed online as they are in E-Park. UNESCO 1(2005)

IV. RATIONALE OF THE STUDY

Only basic infrastructure and good E-governance programmes are not enough, there must be awareness towards these projects as well as if E governance project is not performing as per plan, there must be an assessment for it's effectiveness to choose between two i.e. either to rethink or to reset

V. RESEARCH METHODOLOGY AND SAMPLING

This is a exploratory research which tries to examine whether general public trusts online government and whether they are aware about various projects under National E-governance Plan.

Sampling design : convenience sampling

Sample size: 834 responses

Data collection : Data Collection is through both the sources, i.e from primary and secondary. In primary data collection questionnaire was used and various government websites, books, journals, government publications newspapers are studied for various concepts

Data Analysis : Analytical tools like SPSS , MS Excel are used to analyze and interpret data

VI. DATA ANALYSIS

Industry :
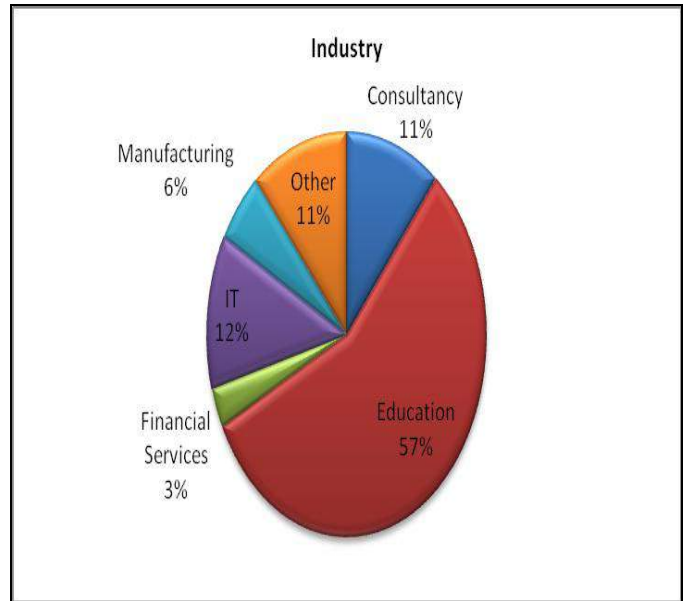
Figure No.1

Major respondets belongs to Education Industry i.e 471, followed by Information Technology, Consultacy, Other and Manufacturing

Awareness about the concept of "E-Governance"
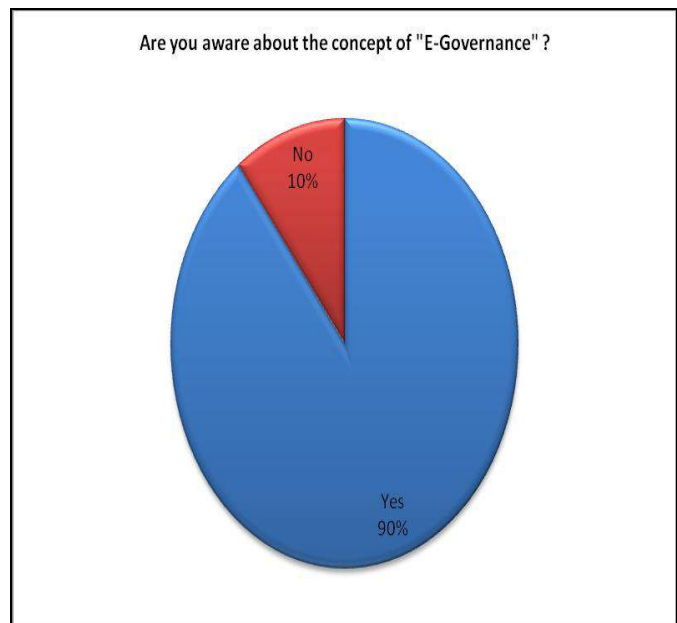
Figure No.2

As we can see only 10% respondents are not aware about the concept of E-governance.

E-governance or online government can increase transparency
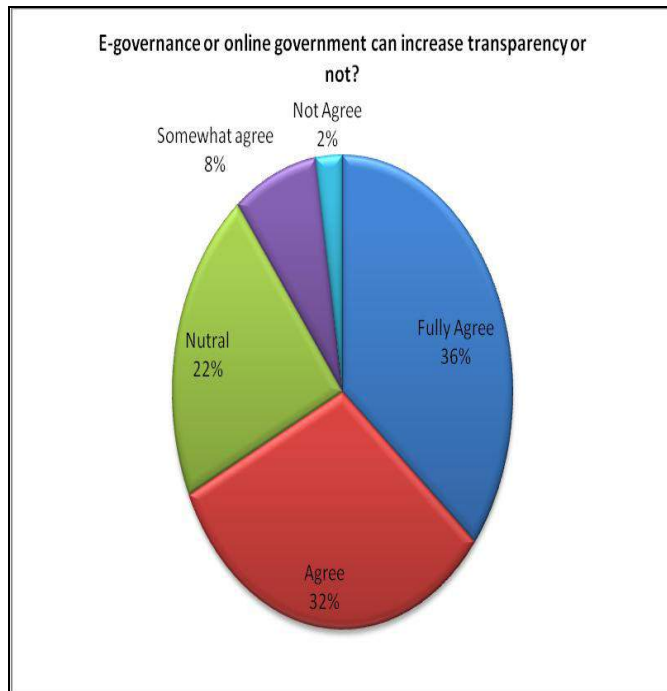
Figure No.3

We can see that 36% are fully agree and 32% respondent are sayinmg that thay are agree that with the help of E-governace trasperancy can in government operations can be achieved. Only 2% respondenta are of the openion that greater tansperancy cant be achieved.

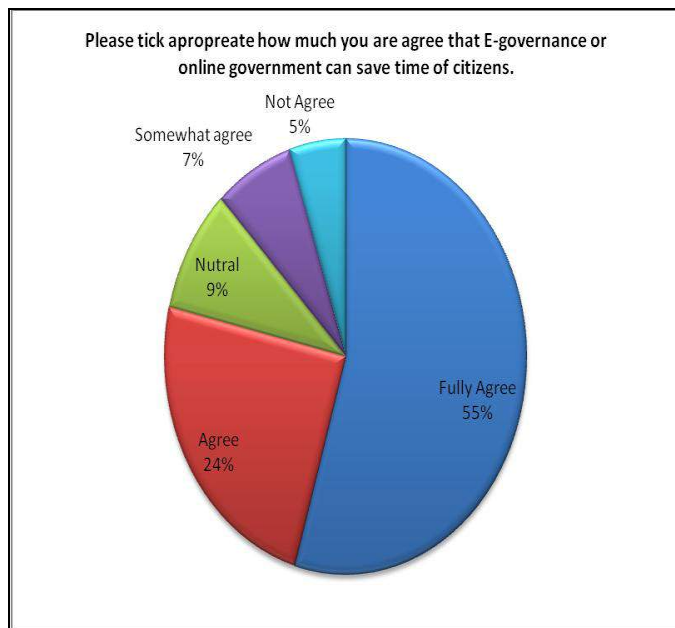*E-governance or online government can save time of citizens.*

Figure No.4

Total 55% of respondents are of openion hat online governemnt can save the time in obtaining various government services. However 9% respondents are not much confident that time can be saved

Trust on online government online services
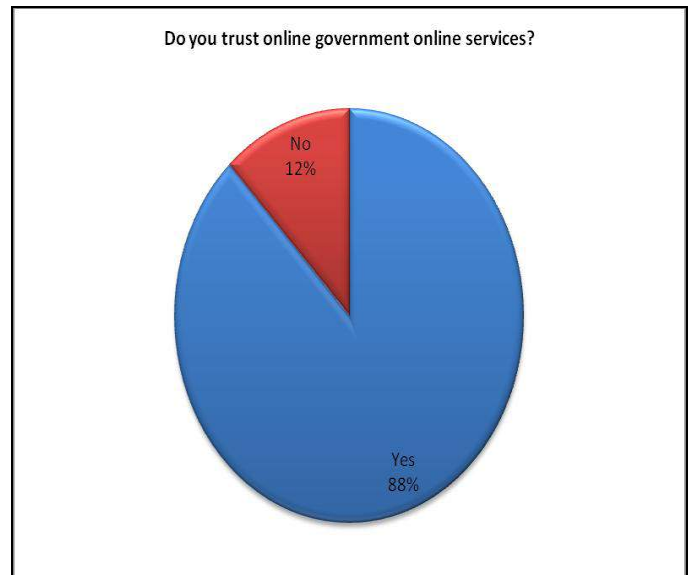
Figure No.5

Majority of respondents feels that online government operations are trustworthy. But 12% population is still not agreeing upon the same.

Awareness about National e-Governance plan
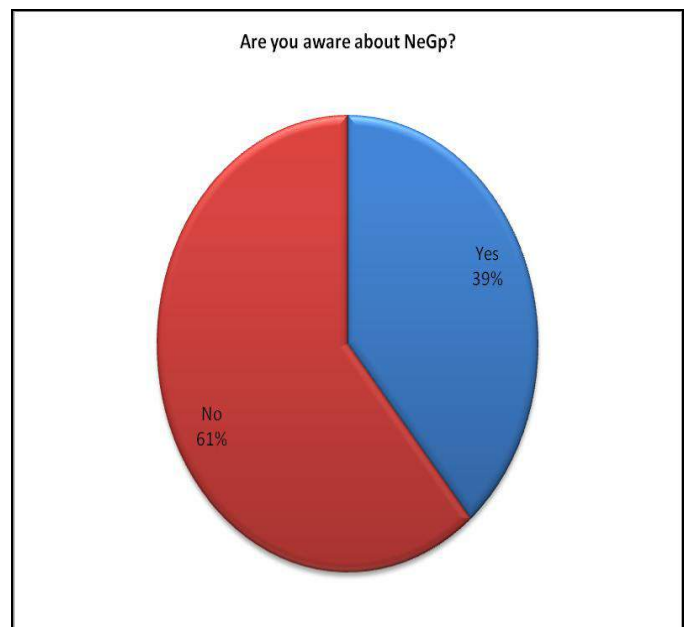
Figure No.6

As can be understood by figure No.6 that awareness about Negp is very much low. Government have outlay of Rs. 32488.18 Crore still people are not aware about such.

VI CONCLUSION

It can be observed from above facts that, awareness about E-governance is at acceptable level but government has failed me making people aware about National E-Governance plan for which there is huge outflow. Government must attempt to create awareness. One more fact is that people trust online

services offered by government and also they believe that E-governance increases transparency and it saves time of citizens as well as of government officials.

REFERENCES

[1] A compendium of mission mode projects under NeGP January 2011 Published by the National e-Governance Division, for The Department of Information Technology, Ministry of Communications and Information Technology, Government of India

[2] Annual report, 2010-11, Ministry of Rural Development Government of India

[3] Annamalai, Kuttayan and Sachin Rao. (2003). "What Works: ITC's e-Choupal and Profitable Rural Transformation Web-Based Information And Procurement Tools For Indian Farmers", Jointly published as "What Works Case Study" by World Resources Institute, Digital Dividend and University of Michigan, (August 2003) (accessed in August, 2010 from <http://www. digitaldividend.org /pdf/echoupal_case.pdf>, via Google, http://www.google.com).

[4] Background Papers, Meeting of The National e-Governance Advisory Group, 12th November, 2010,New Delhi

[5] Basu, S. (2004). E-Government and Developing Countries: An Overview. International Review of Law Computers and Technology. Vol. 18, No. 1. March 2004.

[6] Bhatnagar, Subhash and Schware Robert. (2000). Information and Communication Technology in Development: Cases from India. New Delhi, India: Sage Publications, 2000

[7] Bhatnagar, S. (2003) The Economic and Social Impact of E-government. A background technical paper for the proposed UNDESA publication -- E-government, the citizen and the state: Debating governance in the information age (World Public Sector Report for 2003: E-Government at the Crossroads), p.23

[8] BSI. (2002). Chefsache E-Government: Leitfaden für Behördenleiter. E-Government Handbuch. Bonn: Bundesamt für Sicherheit in der Informationstechnik. Retrieved from www.e-government-handbuch.de

[9] Cap Gemini, Ernst & Young (2006), Online Availability of Public Services: How is Europe Progressing Cap Gemini, Ernst & Young - Four Stages of e-Government, http://ec.europa.eu/ information_society eeurope/i2010/docs/benchmarking/online_availability_2006.pdf

[10] Cecchini, Simone and Christopher Scott. (2003). Can information and communications technology applications contribute to poverty reduction? Lessons from rural India, Information Technology for Development, Vol. 10, Issue 2 (2003): 73 – 84.

[11] CEG-IIMA (2003). Evaluation Studies by the Centre for E-Governance, Indian Institute of Management, Ahmedabad (CEG-IIMA). http://www.iimahd.ernet.in/egov/

[12] Chambers, Robert. (1983). Rural Development: Putting The Last First, Robert Chambers, 147. London: Longman, 1983.Chariar, V.M. (2005), Rejuvenating Traditional Knowledge Systems of India" (unpublished).

[13] Chawla Rajeev,(2007) Secretary, " Bhoomi: Online Delivery of Record of Rights, Tenancy and Crops to farmers in Karnataka, India", Compendium of Case Studies Published by: Universities Press (India) Pvt. Ltd.

[14] Citizen-centric Approach for e-Governance at computer society of India by Devendra Nath Gupta

[15] Computer express (2012) "E-governance will be worth Rs 41,000 crore over the next six years".[online]Availableat:http://www.expresscomputeronline.com/2004 0119/opinion02.shtml [Accessed: 24/07/2012].

[16] Compendium of mission mode projects under NeGP, January-2011, Published by the National e-Governance Division, for The Department of Information Technology, Ministry of Communications and Information Technology, Government of India.

[17] D.B.A., M. (2005) Parcticing E-governemnt : A Global Perspective. 2nd ed. London WC2E 8LU: Idea Group Publishing, p.50-55.

[18] Datar, M. (2012) Determining Priorities of E-Government: A Model Building Approach. In: Datar, M. eds. (2004) Foundations of E-government. 1st ed. Delhi: Computer Society of India, p.76-85.

[19] Deakins E and Dillon S M (2002) "E-government in New Zealand: the local authority perspective" – International Journal of Public Sector Management 15(5) pp 375 – 398

[20] E-Governance Assessment Frameworks : Prof. T. P. Rama Rao, Prof. V. Venkata Rao, Prof. S. C. Bhatnagar, Center for Electronic Governance, IIM, Ahmedabad And Shri. J. Satyanarayana, CEO, National Institute for Smart Government (NISG), Hyderabad 2004

[21] Ebrahim E, Irani Z (2005) "E-government adoption: architecture and barriers" Business Process Management Journal 11(5) pp 589-611

[22] Gartner 2002,GartnerEXP(2000) says a majority of e-Government initiatives fail or fall short of expectations, http://symposium.gartner.com/story.php.id.1367.s.5.html

[23] Gupta, Bagga, Piyush, RK, (2008). Compendium of eGovernance Initiatives in India. 1st ed. New Delhi: University Press

[24] Gupta M P and Jana D (2003) E-government evaluation: A Framework and case study, Government Information Quarterly, 20, 2003 (365-387)

[25] Gupta, P. (2012) Capacity Building for e-Governance. Computer Express, Iss. Nov-2008 p.28.

[26] Heeks, R. (2002). i-Development and not e-Development, Special Issues on ICTs and Development, Journal of International Development (2002) : 141-151.

[27] Jhunjhunwala, Ashok, Anuradha Ramachandran and Sangamitra Ramachander. (2006). Connecting Rural India: Taking a Step Back for Two Forward Information Technology in Developing Countries, Vol. 16, No. 1 (February, 2006), Telecommunications and Computer Networks Group, Madras, IIT-Madras. (accessed in December, 2006 from http://www.iimahd.ernet.in/egov/ifip/ feb2006/article1.htm).

[28] Institute for Information Systems (IWi) at DFKI (2005), Evaluating e-Government – A Process-oriented Approach, IFIP Conference 2005, Poznan (Poland), Institute for Information Systems (IWi) at DFKI, Dipl.-Kfm. Dominik Vanderhaeghen, www.kti.ae.poznan.pl / conferences / i3e / papers / bettina_kafai.pdf

[29] Irani, Z.; Al-Sebie, M.; Elliman, T. (2006) Transaction Stage of e-Government Systems: Identification of Its Location and Importance, System Sciences, 2006. HICSS Proceedings of the 39th Annual Hawaii International Conference, Volume 4, Issue, 04-07 pp. 82c - 82c.

[30] Kavikondala, S. et al. (2006) Defining e-Governance Services. Computer society of India, p.34-38.

[31] Kaushik, P.P. and Nirvikar Singh. (2004). Information Technology and Broad based development: Preliminary lessons from North India, World Development 32(4) (2004) : 591-607

[32] Kokil Priyanka,2006., Adopting E-governance "SAP-LAP Analysis: Gyan Ganga, E-Gram and Communication Information Centers (CIC)"

[33] L C Singh (2008) , "Knowledge-Driven Governance" Transforming Government e-Governance Initiatives in India

[34] Layne Karen, Lee Jungwoo (2001), Developing fully functional E-government: A four stage Model, Government Information Quarterly, 18 (2001) 122–136

[35] Madden, G. Savage, S & Simpson, M. (1997). Regional information access: the use of telecentres to meet universal service obligations, Telematics and Informatics 14(3) (1997):273-288.

[36] Malhotra, Charru, V.M. Chariar and L.K. Das. (2006). 'e' as an enabler for Shubh-Labh for Local Governance in Rural India, In National Conference on Smart Governance for Rural Development by ITM, Gurgoan at New Delhi, India on 18th February,2006.

[37] Malhotra Charru, V. M. Chariar, L.K. Das, and P. V. Ilavarasan,(2007) ICT for Rural Development: An Inclusive Framework for e-Governance.New delhi,India : computer society for India.

[38] Mutula S M(2005) "Bridging the digital divide through e-governance: A proposal for Africa's libraries and information centres" The Electronic Library 23(5) pp 591-602

[39] OECD. (2001). Project on the impact of e-government. PUMA(2001)10 REV 2. Paris: OECD.

[40] PCIP (2002). The roadmap for e-government in the developing world. The Pacific Council on International Policy, April 2002. The Working Group on E-Government in the Developing World. http:// www.pacificcouncil.org/pdfs/e-gov.paper.f.pdf

[41] Perri, (2004). E-Governance: Styles of Political Judgment in the Information Age Polity. Palgrave MacMillan, Great Britain.

[42] Perumal, S. et al. (2012) The Success Transmission Model from Governance to E-Governance. In: Unknown. eds. (2012) Critical Thinking in E-Governance. 1st ed. Delhi: p.93-96.

[43] Prasad Rajendra, (2007) DIO, NIC Mirzapur, "NISANI: National Identity Cards Scheme" 349-354 e-Governance: Case Studies

[44] Public Service Delivery: Does E-Government Help? Presented during Annual Bank Conference on Development Economics 2003 (The World Bank, South Asia Component), Bangalore, May 2003.

[45] Rama Rao T P, Bhatnagar S C, Satyanarayana J, Venkata Rao V, (2004), EAF2.0,E-Government Assessment Framework, E-Governance (Assessment and Replication) Division, E-Governance and E-Rural Group, Department of Information Technology, Government of India

[46] Rao, R. (2003). Electronic Governance: Lessons from Experiences. Information Technology in Developing Countries. Volume 13, No. 1, June 2003 http: //www.iimahd.ernet.in /egov/ifip /jun2003/article2.htm

[47] Sanjay Aggarwal (2009),General Manager (Operations), New Delhi sanjay@irctc.co.in, "Web-Based Rail Reservation (Internet Ticketing)", Compendium of e-Governance Initiatives in India, 174.

[48] Santhi Kumari, (2009) "National Rural Employment Guarantee Act (NREGS-AP Software)", Compendium of e-Governance Initiatives in India, 158-178

[49] Saurbah Gupta,S.N. Behera, Ashok Kumar, Rajiv Ranjan, (2009) "VAT Information Computerization to Optimize Revenue Yields (VICTORY)" , Compendium of e-Governance Initiatives in India, 100-106

[50] Shah Mrinalini," E-Governance in India: Dream or reality", International Journal of Education and Development using Information and Communication Technology (IJEDICT), 2007, Vol. 3, Issue 2, pp. 125-137

[51] Sheridan, W., and Riley, T.B. (2006) Commonwealth Centre for e-Governance, e-Gov Monitor, Monday, 3 July, 2006.

[52] Srinivas Yerramsetti, (2005). Role of Information Technology for Rural Development – A Case Study of Rural e-Seva Project in West Godavari District, Mphil Dissertation at Jawaharlal Nehru University (JNU), New Delhi: 126.

[53] Share, P. (1993). Telecommunication and rural remote development, Rural Society 3: 16

[54] Sharma Vinay, Seth Piyush 2009 "Effective Public Private Partnership through E-Governance Facilitation", Critical Thinking in E-Governance, 194-206

[55] The World Bank Report. (1997). Rural Development: From Vision to Action – A Sector Strategy. Washington D.

[56] Transparency and Corruption: Does E-Government Help? Paper prepared for the compilation of CHRI 2003 Report OPEN SESAME: Subhash Bhatnagar,Indian Institute of Management, Ahmedabad 3800151

[57] UNESCO (2005). E-Governance Capacity Building. http://portal.unesco.org/ci/en/ev.php-URL_ID=4404&URL_DO=DO_TOPIC&URL_SECTION=201.html

[58] UNESCO 1(2005) E-governance toolkit for developing countries, prepared by National Informatics Centre (NIC), Department of Information Technology, Ministry of Communication &IT, Government of India at the behest of UNESCO, New Delhi, Asia-Pacific Bureau for Communication and Information.

[59] Upadhyaya, Shruti Dilipkumar and Chugan, Pawan K., Sustainable Rural Development Through ICT & E-Governance in India (February 13, 2012). Global recession to global recovery: enhancing enterprise competitiveness through human capital and operations management, pp. 407-419, sameer s. Pingle, pawan k. Chugan, eds., excel india publishers, new delhi, jan. 2012. Available at ssrn: http://ssrn.com/abstract=2002673

[60] US Office of Management and Budgets (OMB), 2006 Datar, M. (2012) Determining Priorities of E-Government: A Model Building Approach. In: Datar, M. eds. (2004) Foundations of E-government. 1st ed. Delhi: Computer Society of India, p.76-85.

[61] Whinston et al. (2001). Measuring the Internet economy. Cisco Systems and University of Texas. Retrieved from http://www.internetindicators.com/jan_2001.pdf

Some Fixed Point Theorems on Hilbert Space

Mittal K. Patel and Dr. G. M. Deheri

(mittal.maths49@yahoo.com, gm.deheri@rediffmail.com)

Abstract — **An attempt has been made to extend the Banach's fixed point theorem's generalization due to Browder and Petryshyn [2]. Further, a variant of the fixed point theorem of Sangar and Waghmode [4] is presented here. Besides, incorporated in a result dealing with the product of different terms involved in the inequality, thereby, modifying and developing a variant of the well-known classical Banach's fixed point theorem.**

Index Terms—-**Hilbert space; Fixed point Theorem; Uniqueness**

I. INTRODUCTION

Towards the generalization of Browder and Petryshyn's fixed point theorem Tiwari and Lahiri [1] proved the following.

Theorem: Let E be a uniformly convex Banach space and K be a nonempty, bounded, closed convex subset of E. Let T be a continuous mapping of K into itself such that T satisfies

i) $\|Tx - Ty\| \le a_1 \|x - y\| + a_2 \|x - Tx\| + a_3 \|y - Ty\|$
$\qquad + a_4 \|x - Ty\| + a_5 \|y - Tx\|$

where x, y in K, $a_i \ge 0$ and $\sum_{i=1}^{5} a_i \le 1$.

Suppose $\lambda \in (0,1)$ be any fixed real number. Let

$$T_\lambda x = \lambda x + (1 - \lambda)Tx$$

and let there exist a $x_0 \in K$ such that the sequence $\{x_n\}$, where

$$x_n = \lambda x_{n-1} + (1 - \lambda)Tx_{n-1},$$

has a subsequence $\{x_{n_i}\}$ converging to $z \in K$. Then z is the unique fixed point of T in K and $\{x_n\} \to z$, provided

$$\|T_\lambda x - u\| < \|x - u\|$$

if u is a fixed point of T in K with $x \ne u$.

This was further extended by Sangar and Waghmode [4] to the following form, for which we need the following:

Definition: Let E be Hilbert space and K a convex set in E. Suppose T is a mapping from K into E. A mapping T is said to be monotone if $\mathrm{Re}\langle Tx - Ty, x - y \rangle \ge 0$; for all x, y in K.

Theorem: Let E be a Hilbert Space and K be a nonempty, bounded, closed and convex subset of E. Let T be a monotone and continuous mapping of K into itself such that T satisfies:

i) $\|Tx - Ty\|^2 \le a_1 \|x - y\|^2 + a_2 \|x - Tx\|^2 + a_3 \|y - Ty\|^2$
$\qquad + a_4 \|x - Ty\|^2 + a_5 \|y - Tx\|^2$

where x, y in K, $a_i \ge 0$ and $\sum_{i=1}^{5} a_i \le 1$.

ii) T has a fixed point u in K. Let $\lambda \in (0,1)$ be any fixed real number. Suppose

$$T_\lambda x = \lambda x + (1 - \lambda)Tx$$

and

iii) $\qquad \|T_\lambda x - u\| < \|x - u\| \quad if \quad x \ne u.$

iv) Let there exist a $x_0 \in K$ such that the sequence $\{x_n\}$, where

$$x_n = \lambda x_{n-1} + (1 - \lambda)Tx_{n-1}$$

has a subsequence $\{x_{n_i}\}$ converging to $z \in K$. Then z is the unique fixed point of T in K and $\{x_n\} \to z$.

Patel and Deheri [5] sharpened this result further. Here it has been sought to establish a variant of the main result of [5], where the rate of convergence is slower, precisely, we obtain the following.

Theorem: 1 Let E be a Hilbert space and K be a nonempty, bounded, closed and convex subset of E. Let T be a monotone and continuous mapping of K into itself such that T satisfies:

$$\|Tx-Ty\| \le a_1\|x-y\| + a_2\left(\|x-Tx\|+\|y-Ty\|\right)$$
$$+ a_3\left(\|x-Ty\|+\|y-Tx\|\right)$$
$$+ a_4\left(\frac{\|x-Ty\|\|y-Tx\|}{\|x-y\|} + \frac{\|x-Ty\|\|y-Tx\|}{\|Tx-Ty\|}\right)$$

where $x,\,y \in K$; $a_i \ge 0$ and

$$a_1 + 2a_2 + 2a_3 + 2a_4 \le 1$$

Then T admits a fixed point in K.

Suppose T has a fixed point u in K and satisfies the following.
i) Let $\lambda \in (0,1)$ be any fixed real number. Suppose

$$T_\lambda x = \lambda x + (1-\lambda)Tx$$

and

ii) $\qquad \|T_\lambda x - u\| \le \|x-u\| \; if \; x \ne u.$

iii) Let there be a $x_0 \in K$ such that the sequence $\{x_n\}$,

where $x_n = \lambda x_{n-1} + (1-\lambda)Tx_{n-1}$.

has a subsequence $\{x_{n_i}\}$ converging to $z \in K$. Then z is the unique fixed point of T in K and $\{x_n\} \to z$.

Proof: Let us consider $x_0 \in K$. Then we define a sequence $\{x_n\}$ of iterations of T as follows

$$x_{n+1} = Tx_n \qquad ,\forall n = 0,1,2,3,..$$

If for some n, $x_{n+1} = x_n$, then it immediately follows that x_n is a fixed point of T. Now we suppose that

$$x_{n+1} \ne x_n \qquad ,\forall n = 0,1,2,3,..$$

Then, one gets

$$\|Tx_n - Tx_{n-1}\| = \|x_{n+1}-x_n\| \qquad ,n \ge 1$$

Now, by making use of the hypothesis, we get
$$\|x_{n+1}-x_n\| \le a_1\|x_n-x_{n-1}\| + a_2\left(\|x_n-x_{n+1}\|+\|x_{n-1}-x_n\|\right)$$
$$+ a_3\|x_{n-1}-x_{n+1}\|$$

Then by Triangle inequality, one finds that

$$(1-a_2-a_3)\|x_{n+1}-x_n\| \le (a_1+a_2+a_3)\|x_n-x_{n-1}\|$$

leading to

$$\|x_{n+1}-x_n\| \le k\|x_n-x_{n-1}\|$$

where

$$k = \left(\frac{a_1+a_2+a_3}{1-a_2-a_3}\right)$$

Clearly, $k < 1$ as
$$a_1 + 2a_2 + 2a_3 + 2a_4 \le 1$$

and hence

$$\|x_{n+1}-x_n\| \to 0$$

which shows that $\{x_n\}$ is a Cauchy sequence in K. Using the completeness of K, one can find a $u \in K$ such that $x_n \to u \; as \; n \to \infty.$

Consequently,

$$x_{n+1} = Tx_n$$

is a subsequence of $\{x_n\}$ and have the same limit u. Since, T is continuous, one obtains
$$T(u) = T\left(\lim_{n\to\infty} x_n\right) = \lim_{n\to\infty} Tx_n = \lim_{n\to\infty} x_{n+1} = u$$

Hence, u is a fixed point of T in K.

Since, T has a fixed point u in K, by the definition of T_λ, it is clear that u is a fixed point of T_λ in K, because of the following relation
$$T_\lambda u = \lambda u + (1-\lambda)Tu$$
We get
$$T_\lambda u = \lambda u + (1-\lambda)u$$
which means
$$T_\lambda u = u.$$

Ishikawa [3] has proved that for any x, y, z in a Hilbert space and a real number λ, the following relation,
$$\|\lambda x + (1-\lambda)y - z\|^2 = \lambda\|x-z\|^2 + (1-\lambda)\|y-z\|^2$$
$$- \lambda(1-\lambda)\|x-y\|^2$$
$$(1.1)$$

holds. Now, by making use of (1.1) we have the following inequality,

$$\|x_n - u\|^2 = \|\lambda x_{n-1} + (1-\lambda)Tx_{n-1} - u\|^2$$
$$= \lambda\|x_{n-1}-u\|^2 + (1-\lambda)\|Tx_{n-1}-u\|^2 - \lambda(1-\lambda)\|x_{n-1}-Tx_{n-1}\|^2$$
$$< \lambda\|x_{n-1}-u\|^2 + (1-\lambda)\|Tx_{n-1}-u\|^2$$
$$(1.2)$$

Further, one can observe that,

$$\|Tx_{n-1}-u\|=\|Tx_{n-1}-Tu\|$$

$$\le a_1\|x_{n-1}-u\|+a_2\left(\|x_{n-1}-Tx_{n-1}\|+\|u-Tu\|\right)$$

$$+a_3\left(\|x_{n-1}-u\|+\|u-Tx_{n-1}\|\right)$$

$$+a_4\left(\frac{\|x_{n-1}-u\|\|u-Tx_{n-1}\|}{\|x_{n-1}-u\|}+\frac{\|x_{n-1}-u\|\|u-Tx_{n-1}\|}{\|Tx_{n-1}-u\|}\right)$$

Then by Triangle inequality, one arrive at

$$(1-a_2-a_3-a_4)\|Tx_{n-1}-u\|\le(a_1+a_2+a_3+a_4)\|x_{n-1}-u\|$$
$$(1.3)$$

Interchanging u and x_{n-1}, we get

$$\|u-Tx_{n-1}\|=\|Tu-Tx_{n-1}\|$$

$$\le a_1\|x_{n-1}-u\|+a_2\left(\|u-Tu\|+\|x_{n-1}-Tx_{n-1}\|\right)$$

$$+a_3\left(\|u-Tx_{n-1}\|+\|x_{n-1}-u\|\right)$$

$$+a_4\left(\frac{\|u-Tx_{n-1}\|\|x_{n-1}-u\|}{\|x_{n-1}-u\|}+\frac{\|u-Tx_{n-1}\|\|x_{n-1}-u\|}{\|u-Tx_{n-1}\|}\right)$$

$$(1.4)$$

Then by Triangle inequality, one can observe that

$$(1-a_2-a_3-a_4)\|Tx_{n-1}-u\|\le(a_1+a_2+a_3+a_4)\|x_{n-1}-u\|$$

Adding (1.3) and (1.4), one concludes that

$$(2-2a_2-2a_3-2a_4)\|Tx_{n-1}-u\|$$

$$\le(2a_1+2a_2+2a_3+2a_4)\|x_{n-1}-u\|$$

leading to

$$\|Tx_{n-1}-u\|\le\|x_{n-1}-u\|$$

Then by (1.2), one finds that

$$\|x_n-u\|<\|x_{n-1}-u\|$$

Observe that the sequence $\{\|x_n-u\|\}$ is strictly

monotonically decreasing and bounded and so it is convergent.
Also,

$$\|x_{n_i+1}-u\|\le\|x_{n_i+1}-T_\lambda z\|+\|T_\lambda z-u\|$$

Since T is continuous and $x_{n_i}\to z$

$$\lim_i\|x_{n_i+1}-u\|\le\|T_\lambda z-u\|$$

and

$$\lim_i\|x_n-u\|=\lim_i\|x_{n_i}-u\|=\|z-u\|$$

Hence, one obtains

$$\|z-u\|=\lim_i\|x_n-u\|=\lim_i\|x_{n_i}-u\|\le\|T_\lambda z-u\|$$

Therefore, one infers that

$$\|z-u\|\le\|T_\lambda z-u\| \qquad (1.5)$$

and by (iii) of Theorem (1), one avails

$$\|T_\lambda z-u\|<\|z-u\| \qquad (1.6)$$

From (1.5) and (1.6), one can easily conclude that

$$z=u.$$

Now, we have the following relation

$$\lim_n\|x_n-u\|=\lim_i\|x_{n_i}-u\|=\lim_i\|x_{n_i}-z\|=0,$$

which gives

$$x_n\to u=z.$$

This completes the proof.

The slower rate of convergence is exhibited in the following result.

Theorem 2: Let E, K and T be as in above theorem, but T satisfies the inequality

$$\|Tx-Ty\|\le a_1\|x-y\|+a_2\left(\|x-Tx\|+\|y-Ty\|\right)$$

$$+a_3\left(\frac{\|x-Ty\|\|y-Tx\|}{\|x-y\|}+\frac{\|x-Ty\|\|y-Tx\|}{\|Tx-Ty\|}\right)$$

where $x,y\in K; a_i\ge0$ and

$$a_1+2a_2+2a_3\le1$$

Then T admits a fixed point u in K. Suppose conditions (ii), (iii) and (iv) of the Theorem 1 are true, then T admits a unique fixed point in K.

Proof: The iterations defined in the proof of the Theorem 1 has been taken into account. It is noted that

$$\|Tx_{n-1}-u\|=\|Tx_{n-1}-Tu\|$$

$$\le a_1\|x_{n-1}-u\|+a_2\left(\|x_{n-1}-Tx_{n-1}\|+\|u-Tu\|\right)$$

$$+a_3\left(\frac{\|x_{n-1}-u\|\|u-Tx_{n-1}\|}{\|x_{n-1}-u\|}+\frac{\|x_{n-1}-u\|\|u-Tx_{n-1}\|}{\|Tx_{n-1}-u\|}\right)$$

Then by Triangle inequality

$$(1-a_2-a_3)\|Tx_{n-1}-u\|\le(a_1+a_2+a_3)\|x_{n-1}-u\|$$

$$(2.1)$$

Interchanging u and x_{n-1}, one finds that

$$\|u-Tx_{n-1}\|=\|Tu-Tx_{n-1}\|$$

$$\le a_1\|x_{n-1}-u\|+a_2\left(\|u-Tu\|+\|x_{n-1}-Tx_{n-1}\|\right)$$

$$+a_3\left(\frac{\|u-Tx_{n-1}\|\|x_{n-1}-u\|}{\|x_{n-1}-u\|}+\frac{\|u-Tx_{n-1}\|\|x_{n-1}-u\|}{\|u-Tx_{n-1}\|}\right)$$

$$\le a_1\|x_{n-1}-u\|+a_2\left(\|u-Tu\|+\|x_{n-1}-Tx_{n-1}\|\right)$$

$$+a_3\left(\frac{\|u-Tx_{n-1}\|\|x_{n-1}-u\|}{\|x_{n-1}-u\|}+\frac{\|u-Tx_{n-1}\|\|x_{n-1}-u\|}{\|u-Tx_{n-1}\|}\right)$$

Inview of Triangle inequality, one obtains

$$\left(1-a_2-a_3\right)\left\|Tx_{n-1}-u\right\| \le \left(a_1+a_2+a_3\right)\left\|x_{n-1}-u\right\|$$

(2.2)

Adding (2.1) and (2.2), one arrives at

$$\left(2-2a_2-2a_3\right)\left\|Tx_{n-1}-u\right\| \le \left(2a_1+2a_2+2a_3\right)\left\|x_{n-1}-u\right\|$$

leading to

$$\left\|Tx_{n-1}-u\right\| \le \left\|x_{n-1}-u\right\|$$

Hence, by the method of proof of Theorem 1, we get a unique fixed point of T in K.

REFERENCES

[1]   K. Tiwari and B. K. Lahiri, "Approximation of fixed points of non linear mappings", Bull .cal. Math. Soc. 81 (1989), P.427-434.

[2]   F. E. Browder and W. V. Petryshyn, "Construction of fixed points of non linear mappings in Hilbert space", J. Math. Anal. Appl. 20 (1987) P. 197-228.

[3]   S. Ishikawa, "Fixed points by a new iteration", Proc. Amer Math. Soc. 44 (1974), P. 147-150.

[4]   V. M. Sangar and B. B. Waghmode, "A fixed point theorem in Hilbert Space", Math. Ed. Vol. 23 (1993), P. 211-216.

[5]   Mittal. K. Patel and Dr. G. M. Deheri, "Some fixed point theorem on Hilbert spaces'', International Journal of Mathematical Sciences and Applications; Volume-II (2012); P. 71.

Role of Movie Review: A study with reference to Rural and Urban Youth

Dr. Raju M. Rathod, Mr. Bhautik K. Patel

rajumrathod@rediffmail.com, bhautikk29patel@gmail.com

Abstract

When movie viewers are deciding whether to go for watching movie and which movie, they should go to watch, they try to assess the likely experience of the movie. Movie viewers may worry about the risk of making a wrong selection of movie that subsequently proves disappointing. So there is a perceived risk of unsatisfactory experience, monetary loss, wasting of time, and unwanted effect on emotions. As the rate of movie tickets increase and there is uncertainty that particular movie will be offering good experience or not, youngster likes to first take the review of the movie and decide to see a particular movie. The present study attempt to study the movie consumption practice and movie selection process among the rural and urban consumers. Primary data have been collected through structure questionnaire from college going students. The study come out with useful findings.

Introduction

When movie viewers are deciding whether to go for watching movie and which movie, they should go to watch, they try to assess the likely experience of the movie. Movie viewers always have some expectation at the back of their mind. Those expectations are formed on the basis of Director of Movie, Production Banner, Star cast, Music Directors, Songs, Story line of movie etc. Because of the high proportion of experience attributes, Movie viewers may worry about the risk of making a wrong selection of movie that subsequently proves disappointing. So there is a perceived risk of unsatisfactory experience, monetary loss, wasting of time, and unwanted effect on emotions.

The worse the possible outcome and more likely it is to occur, the higher perception of risk. As it is more difficult to evaluate, perceived risk especially relevant in movie selection decision, because movie viewers always have some past good or bad experience in their mind that formed some perception about the risk. Now days because of the availability of movie ratings on the basis of detailed movie review, it helps movie viewers to minimize these perceived risks.

In our country much research is not done of impact of movie and its review. In USA, the researchers developed a database that included movie ratings and rating reasons obtained from the Motion Picture Association of America (MPAA) and information about movie content from two independent resources, Kids-in-Mind. They then assessed the relationship between movie ratings and content and trends for films released between January 1, 1992 and December 31, 2003.[i]

Pradeep K. Chintagunta, Shyam Gopinath and Sriram Venkataraman measure the impact (valence, volume, and variance) of national online user reviews on designated market area (DMA)-level local geographic box office performance of movies. In contrast with previous studies that have found that the main driver of box office performance is the volume of reviews, it has been found that it is the valence that seems to matter and not the volume.[ii]

Wenjing Duan, Bin Gu and Andrew B. Whinston examine the persuasive effect and awareness effect of online user reviews on movies' daily box office performance. In contrast to earlier studies that take online user reviews as an exogenous factor, this study consider reviews both influencing and influenced by

movie sales.[iii] Movie can be consider as mirror of society. The kind of movie made and watched by people of any country represent the socio-cultural status of entire society. It is very important that society entertains only meaningful and enriching forms of movies. Of course movies in India have been produced and seen only for entertain purpose. But for last couple of years, in India also the trend of movie making has considerably changed.

Research Methodology:

There are number of source from which movie viewers can get the review of new movie such as newspaper, television programme, internet, radio programme, magazine etc. As the rate of movie tickets increase and there is uncertainty that particular movie will be offering good experience or not, youngster likes to first take the review of the movie and decide to see a particular movie. The researcher has carried out survey method for the present study. Hence, movie review nowadays considerably influences the movie watching decision among youngsters. However the importance give to movie review would be different among rural and urban youngsters. The movie consumption practice and habit of rural and urban consumers are different.

Research Objectives

1. To study the movie consumption practice among rural and urban youth.
2. To examine the impact of review on the movie selection among rural and urban youngsters.
3. To know the perception of rural and urban youth regarding the movie review.
4. To study the opinion of rural and urban students relating to movie review.

The present study is based on primary data and secondary data. The primary data has collected from 130 respondents' of rural and urban from Anand District. Secondary data has collected from the past studies, journal, websites, books and so on.

Total numbers of undergraduate students of Anand District are the total population for the study. The researcher has conveniently selected 130 samples from rural and urban college going students' from Anand District as sample.

Findings of the study

1. The main motive for watching the movie is entertainment amongst youngsters. They also preferred to see movie as hobby and as a celebration.
2. Most of the youngsters like comedy movie. They so not much preferred off bit movie.
3. Rural and urban youngsters like almost same genre of movie except romantic movie. Rural youngsters prefer more romantic movie than urban youngsters.
4. Only negligible (1.5%) youngsters do not like to watch movie. Majority of them like to watch movie both in urban and rural area.
5. More than 85% of the youngsters have habits to watch the movie in theatre. In case of rural area, more number of youngsters would like to see movie in theatre particularly in multiplex.
6. Urban youth used to watch movie more frequently in theatre compare to rural youth. Almost 12% of the urban youth watch movie weekly. Total 42.3% youth watch movie in theatre every month.
7. Total 79.2% youngsters prefer to see Hindi movie in cinema and 87.3% rural youth like to see Hindi movie while 71.6% in case of urban. English language movie are more preferred in urban area as compared to rural area. Youngsters have very low craze for south Indian language movie.
8. 88 % of the total urban youth preferred to take review of movie and only 76.2% of the rural youth consider the review of the movie.
9. Most of the youth (41.1%) take movie review from personal reference of other after it second choice is television programme. Surprisingly more number of rural youth used internet for the movie review than the urban youth. Radio lost their importance for the movie review among urban and rural youth.
10. Majority of urban youngster (86.4%) go for movie with their friends while in rural 73% youth go with their friend for movie. Rural youngsters preferred to watch movie with the company of family members, relatives and neighbour.
11. Out of total respondents 78 % youth preferred multiplex for watch movie. But compare to urban youth, rural youth more preferred to watch movie in near by village, in small town (taluka place) single screen theatre and single screen theatre in District place.
12. There is a significance difference between the rural and urban youth regarding movie review particularly the movie review fairly work and taking movie review from multiple sources.

13. There is significance difference between urban and rural youth for watching movie to get latest trends of fashion.

14. For two statements 'I experienced that movie review fairly work' and 'I believe in taking review from multiple sources; mean scores of rural and urban youngsters have been found significantly different at 0.05 level of significance. Urban youngsters believed more in taking review from multiple sources before going to see movie as they have experience good when they took review based decision.

15. So far as the motive behind watching movie, rural youngsters have been significantly different in case of seeking information regarding fashion from movie. Rural youngster watch movie more because it gives information regarding latest fashion.

Marketing Implication

It has been found that there is a difference between urban and rural youth so far as movie consumption is concerned. They different in their preference, motives and the way they take decision to see what kind of movies and where to see a movie. Motives among youngsters for watching movies are drastically changing. More number of youngsters now would like to collect the review of movie scientifically and systematically before going to see any movie as they do not want to take any risk in terms of time and money. Now a day's consumer accepts movies of all genres provided it has entertainment values and touching their feelings. Rural consumers are searching more emotional values from movies and they also subjectively decide the movie consumption related decisions. Hence, marketers have to understand this changing phenomenon and they should creatively connect with the present urban and rural youth. More number of movies has been made with rural touch but sometimes they failed to connect with rural audience. Mere rural set up may not help to give huge hit; there should be rural heart in the movies. Marketers should also consider media consumption among rural youth to successfully market the movie among rural youth. They may not have access of contemporary media to get review of the movies. So markets should try to spread the message with the help of some innovative media which spread positive word of mouth. It has been also found that significant

Reasons	N	Mean	Std. Deviation
Entertainment	130	7.05	1.581
Stress relief	130	4.25	1.861
Hobby	130	4.97	2.260
Time pass	130	3.51	2.180
Family Entertainment	130	3.95	1.896
To know the latest fashion	130	3.92	2.006
For get together	130	3.42	2.034
Celebration	130	4.82	2.167

number of youngsters see movies as hobby and for stress reliefs. So markets should promote the movies as stress relief tool and vey exiting hobby. Movies of different genres have their own heart and soul so that markets should promote each movie differently, stereotype promotion may not help to promote different kind of movies. Rural consumers are going to be most potential customers for multiplex theatre. So, Multiplex theatre should design their marketing strategies considering sensitivity of rural youngsters.

Table 1: Motives behinds watching movie
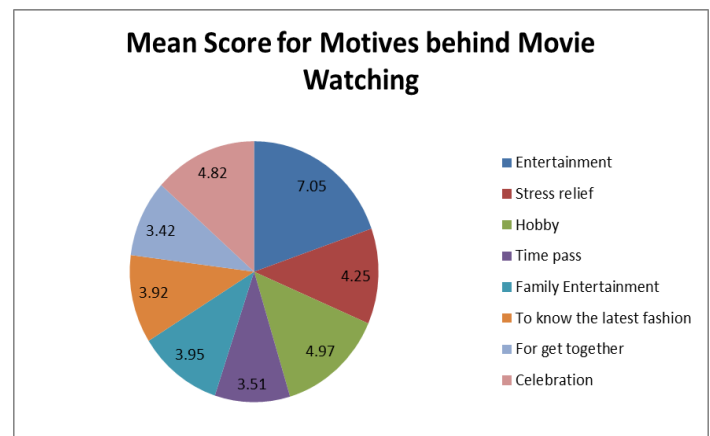
Fig. – 1

Table 2: Genre of movie

Genre of Movie	Mean	Std. Deviation
Action	4.92	1.575
Comedy	5.87	1.272
Romantic	4.75	1.997
Socio Political Issue	2.74	1.476
Off bit	2.01	1.344

Horror	3.67	1.754
Suspense	4.04	1.597

Fig. – 2

Mean Score for Genre of Movie

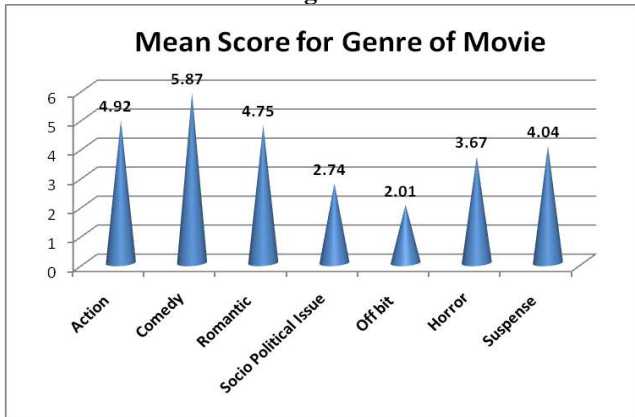**Table 3: Genre of movie by location**

Movie Genre	Location	Mean	Std. Deviation
Action	Rural	4.73	1.598
	Urban	5.09	1.545
	Total	4.92	1.575
Comedy	Rural	5.84	1.461
	Urban	5.90	1.075
	Total	5.87	1.272
Romantic	Rural	5.02	1.862
	Urban	4.49	2.099
	Total	4.75	1.997
Socio Political Issue	Rural	2.73	1.494
	Urban	2.75	1.470
	Total	2.74	1.476
Off bit	Rural	2.13	1.497
	Urban	1.90	1.182
	Total	2.01	1.344
Horror	Rural	3.46	1.664
	Urban	3.87	1.825
	Total	3.67	1.754
Suspense	Rural	4.06	1.664
	Urban	4.01	1.542

Movie Genre	Location	Mean	Std. Deviation
Action	Rural	4.73	1.598
	Urban	5.09	1.545
	Total	4.92	1.575
Comedy	Rural	5.84	1.461
	Urban	5.90	1.075
	Total	5.87	1.272
Romantic	Rural	5.02	1.862
	Urban	4.49	2.099
	Total	4.75	1.997
Socio Political Issue	Rural	2.73	1.494
	Urban	2.75	1.470
	Total	2.74	1.476
Off bit	Rural	2.13	1.497
	Urban	1.90	1.182
	Total	2.01	1.344
Horror	Rural	3.46	1.664
	Urban	3.87	1.825
	Total	3.67	1.754
Suspense	Rural	4.06	1.664
	Urban	4.01	1.542
	Total	4.04	1.597

Table 4: Movie Likings among Youngsters

Response	Location		Total
	Rural	Urban	
Yes	61	67	128
No	2	0	2
Total	63	67	130

Table 5: Movie watching habit in theatre/cinema house among Youngsters

Response		Location	
		Rural	Urban
Yes	Count	54	59
	% within Location	85.7%	88.1%

No	Count	9	8
	% within Location	14.3%	11.9%
Total	Count	63	67
	% within Location	100.0%	100.0%

Table 6: Frequency of watching habit in theatre/cinema house among Youngsters

Response		Location	
		Rural	**Urban**
Weekly	Count	**0**	**8**
	% within Location	.0%	11.9%
Fortnightly	Count	12	10
	% within Location	19.0%	14.9%
Monthly	Count	25	30
	% within Location	39.7%	44.8%
Twice in a Year	Count	18	11
	% within Location	28.6%	16.4%
Rarely	Count	8	8
	% within Location	12.7%	11.9%
Total	Count	63	67
	% within Location	100.0%	100.0%

Table 7: Language Preference among the movie viewers

Response		Location	
		Rural	**Urban**
Hindi	Count	55	48
	% within Location	87.3%	71.6%
English	Count	7	16
	% within Location	11.1%	23.9%
South Indian	Count	1	3
	% within Location	1.6%	4.5%
Total	Count	63	67
	% within Location	100.0%	100.0%

Table 8: Consideration of Movie Review

Response	Location	
	Rural	**Urban**

Yes	Count	48	59
	% within Location	76.2%	88.1%
No	Count	15	8
	% within Location	23.8%	11.9%
Total	Count	63	67

Table 9: Source used by Youngsters to get review

Response		Location	
		Rural	**Urban**
Radio	Count	0	1
	% within Location	.0%	1.7%
Television Programme	Count	18	23
	% within Location	37.5%	39.0%
Newspaper	Count	2	4
	% within Location	4.2%	6.8%
Personal Reference of others	Count	21	23
	% within Location	43.8%	39.0%
Internet	Count	7	8
	% within Location	14.6%	13.6%
Total	Count	48	59
	% within Location	100.0%	100.0%

Table 10: Preference for accompanying to see movie

Response		Location	
		Rural	**Urban**
Friends	Count	46	57
	% within Location	73.0%	86.4%
Family member	Count	9	6
	% within Location	14.3%	9.1%
Relatives	Count	2	1
	% within Location	3.2%	1.5%
Neighbour	Count	1	0
	% within Location	1.6%	.0%
Other	Count	5	2
	% within Location	7.9%	3.0%

Total	Count	63	66
	% within Location	100.0%	100.0%

Table 11: Location Preference to see movie

Response			Location	
			Rural	**Urban**
Near in my village	Count		13	5
	% within Location		20.6%	7.6%
In small town (taluka place) single screen	Count		4	1
	% within Location		6.3%	1.5%
Single screen in District place	Count		3	2
	% within Location		4.8%	3.0%
Multiplex	Count		43	58
	% within Location		68.3%	87.9%
Total	Count		63	66
	% within Location		100.0%	100.0%

Table 12: Perception of Youngsters towards movie review

| Statements	Location	Mean	t- value (Sig.)
I believe it is always good to take review before going for movie as help to reduce risk	Rural	3.94	0. 717
	Urban	3.88	
I believe that reviews are true and it gives good guidance	Rural	3.13	0.059
	Urban	3.42	
I experienced that movie review fairly work	Rural	3.21	0.011
	Urban	3.66	
I believe in taking review from multiple sources	Rural	3.35	0.038
	Urban	3.78	
I believe that review save my time and money	Rural	3.84	0.123
	Urban	4.13	

Table 12: Perception of Youngsters towards movie review

Statements	Location	Mean	t- value (Sig.)
I believe it is always good to take review before going for movie as help to reduce risk	Rural	3.94	0. 717
	Urban	3.88	
I believe that reviews are true and it gives good guidance	Rural	3.13	0.059
	Urban	3.42	
I experienced that movie review fairly work	Rural	3.21	0.011
	Urban	3.66	
I believe in taking review from multiple sources	Rural	3.35	0.038
	Urban	3.78	
I believe that review save my time and money	Rural	3.84	0.123
	Urban	4.13	

[i]Kimberly Thompson (2004), Medscape General Medicin, medical journal, http://www.hsph.harvard.edu/news/press-releases/archives/2004-releases/press07132004

[ii] Pradeep K. Chintagunta, Shyam Gopinath and Sriram Venkataraman(2009), The Effects of Online User Reviews on Movie Box Office Performance: Accounting for Sequential Rollout and Aggregation Across Local Markets, http://mktsci.journal.informs.org/content/29/5/944.short

[iii] Wenjing Duan, Bin Gu and Andrew B. Whinston (2008), Do online reviews matter? — An empirical investigation of panel data, Decision Support System, Vol. 45, no.4.

MAP: Gota Circle (N H 8 Highway) to GIT
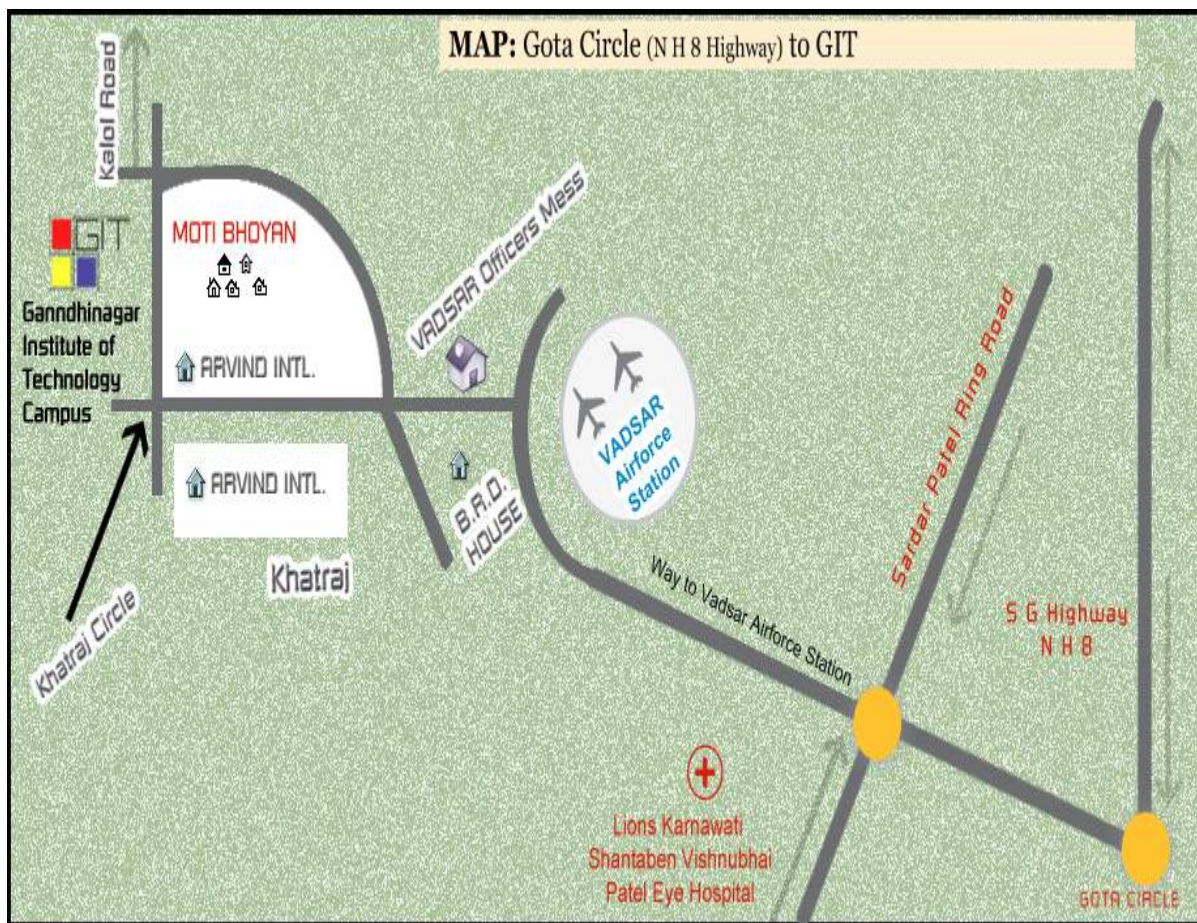
Editorial Chief

Dr N M Bhatt

Cordinator

Prof. M J Mungla

Co-Cordinators

Prof. S M Vakharia

Prof. G P Jani

Institute Address

**Gandhinagar Institute of Technology
Khatraj - Kalol Road,
Village Moti Bhoyan,
Tal. Kalol
Gandhinagar-382721**

Telephone No: +91-02764-281860/61

Fax No: +91-02764-281862

E-mail Address: director@git.org.in

Office Address:

Platinum Foundation Trust
A-201, 202, Iscon Park,
Opp, Star India Bazar,
Satellite, Ahmedabad
Gujarat, INDIA.

Telephone No: +91-079-26922627

Fax No: +91-079-26922628

E-mail Address: trustee@git.org.in